BERINGIAN ECOLOGY AS REVEALED WITH ANCIENT DNA

ANCIENT ENVIRONMENTAL DNA AS A MEANS OF UNDERSTANDING ECOLOGICAL RESTRUCTURING DURING THE PLEISTOCENE-HOLOCENE TRANSITION IN YUKON, CANADA

By TYLER JAMES MURCHIE, B.Sc., M.A.

A Thesis Submitted to the School of Graduate Studies in Partial Fulfilment of the Requirements for the Degree Doctor of Philosophy

DOCTOR OF PHILOSOPHY (2021) McMaster University
(Anthropology - Archaeology) Hamilton, Ontario, Canada

TITLE: Ancient environmental DNA as a means of understanding ecological restructuring during the Pleistocene-Holocene transition in Yukon, Canada
AUTHOR: Tyler James Murchie, B.Sc. Hons (University of Calgary), M.A. (University of Calgary).
SUPERVISOR: Professor Hendrik Nicholas Poinar
NUMBER OF PAGES: xxiv, 383

Lay abstract

A new addition to the rapidly growing field of palaeogenetics is environmental DNA (eDNA) with its immense wealth of biomolecules preserved over millennia outside of biological tissues. Organisms are constantly shedding cells, and while most of this DNA is metabolized or otherwise degraded, some small fraction is preserved through sedimentary mineral-binding. I experimentally developed new ancient eDNA methods for recovery, isolation, and analysis to maximize our access to these biomolecules and demonstrate that this novel approach outperforms alternative protocols. Thereafter, I used these methods to extract DNA from ice age permafrost samples dating between 30,000–6,000 years before present. These data demonstrate the power of ancient eDNA for reconstructing ecosystem change through time, as well as identifying evidence for the Holocene survival of caballine horse and woolly mammoth in continental North America. This late persistence of Pleistocene fauna has implications for understanding the human ecological and climatological factors involved in the Late Pleistocene mass extinction event. This effort is paralleled with megafaunal mitogenomic assembly and phylogenetics solely from sediment. This thesis demonstrates that environmental DNA can significantly augment macro-scale buried records in palaeoecology.

Abstract

Humans evolved in a world of giant creatures. Current evidence suggests that most ice age megafauna went extinct around the transition to our current Holocene epoch. The ecological reverberations associated with the loss of over 65% of Earth's largest terrestrial animals transformed ecosystems and human lifeways forever thereafter. However, there is still substantial debate as to the cause of this mass extinction. Evidence variously supports climate change and anthropogenic factors as primary drivers in the restructuring of the terrestrial biosphere. Much of the ongoing debate is driven by the insufficient resolution accessible via macro-remains.

To help fill in the gaps in our understandings of the Pleistocene-Holocene transition, I utilized the growing power of sedimentary ancient DNA (sedaDNA) to reconstruct shifting signals of plants and animals in central Yukon. To date, sedaDNA has typically been analyzed by amplifying small, taxonomically informative regions. However, this approach is not ideally suited to the degraded characteristics of sedaDNA and ignores most of the potential data. Means of isolating sedaDNA have also suffered from the use of overly aggressive purification techniques resulting in substantial loss.

To address these limitations, I first experimentally developed a novel means of releasing and isolating sedaDNA. Secondly, I developed a novel environmental bait-set designed to simultaneously capture DNA informative of macro-scale ecosystems. When combined, we identify a substantial improvement in the quantity and breadth of biomolecules recovered. These optimizations facilitated the unexpected discovery of horse and mammoth surviving thousands of years after their supposed extirpation. I followed up these results by extracting DNA from multiple permafrost cores where we confirm the late survival signal and identify a far more complex and high-resolution dataset beyond those identifiable by complementary methods. I was also able to reconstruct mitochondrial genomes from multiple megafauna simultaneously solely from sediment, demonstrating the information potential of sedaDNA.

Acknowledgements

My thanks first and foremost to Hendrik Poinar. You truly believed in me, even when I did not. Thank you for giving me this opportunity; this experience has changed who I am. You are a gentleman and a scholar, and I am forever indebted to you for all you have done for me. Thank you for always having my back. The lengths you have gone to support me are far beyond anything I could have expected. Thank you, a thousand-fold, for all that you have done for me. I will make sure I earn it and to pay it forward.

Melanie Kuch, where would I be without you? You taught me so much over the years. Thank you for your patience, thank you for your wisdom, and thank you for challenging me. Most of all, thank you for putting in the time, the sweat, and the tears. Where Hendrik was my writing and big-picture sensei, you were my wet lab sensei. I will never forget all you have done for me, all the time you gracefully sacrificed to help me in and out of the lab, and the wonderful time spent on your farm.

The mighty Ana Duggan. As far as I'm concerned, you are a bioinformatics deity. Thank you for taking the time, over and over again, to teach me and to show me the ways of the command line. I appreciate it all, and more than that, I appreciate the time I got to spend in your presence.

The McMaster Ancient DNA Centre is a special place full of special people. I'm incredibly lucky to have gotten to know such a stellar group of brilliant and kind individuals. When I first started in the lab, the old graduate student guard of Jennifer Klunk, Jonathan Hughes, Stephanie Marciniak, Matthew Emery, Emil Karpinski, and Katherine Eaton helmed an impressive and intimidating team of exceptional scientists. Jenn in particular, with her ever-trusty sidekick Toby, exuded an aura of exceptionalism. I spent my first couple of years at the Centre in equal parts awe, inspiration, and anxiety ridden imposter syndrome. Riding those emotional waves helped me gain experience in a field far from the stones, bones, and ceramics I spent most of my undergraduate and master's degrees focusing on. I owe each of those individuals, and particularly Jennifer Klunk, an immense deal of gratitude for all the lessons they taught me.

Matthew Emery, what can I say that I have not already said to you a hundred times before? You are a truly exceptional individual. A bastion of manhood. My time in the Hammer would have been entirely different without you. You helped change me as a person, making me rethink how I approach my own existence. Thank you for being exactly who you are and for all the wisdom you've imparted onto me. You've inspired me in ways you may not even realize, helping me become a better scientist, philosopher, and a better human being. You're the best friend I've ever had.

Jessica Hider, J-Blast. We have had some amazing times together over the years. I think we have both grown immensely since 2015. I would not have rather navigated these turbulent waters through the mentally treacherous lands of doctoral studies with anyone else. Your patience, kindness, and grace are exceptional. As is your grit, determination, and adaptability. Thank you for always being there and for being such a great friend. Is it time to get weird yet, or should we wait for that until after we bring our muscle-children to the church of iron to avoid social services?

Emil Karpinski, the one-eyed Polish Poet. You are a kind and brilliant man, and your confidence is infectious. Thank you for being such an amazing mentor, and a truly important friend. Our adventures in Ireland and northern Ontario will not be soon forgotten.

Katherine Eaton, the versatility of your mind is exceptional. Also, the empathy and patience you exude is unparalleled. Your presentations are consistently worthy of standing applause. You inspire me with every click of your mouse and each casual utterance of your brilliance, wisdom, humility, and kindness.

Madeline Tapson, Mad Max. I think fondly back over all the great times we've had over the years, raiding and pillaging the wastes in search of glory and plunder. May you crush your enemies in the southern lands, see them driven before you, and hear their lamentations echo across your mighty dominion.

Dirk Hackenberger, Big D. Your exuberance and drive have continuously made me want to strive all the harder. I will never forget the lion cubs, our time up north, or our adventures in Santa Cruz. Thank you for all you continue to teach me! One of the things I

have really missed over the pandemic are our squash games. I cannot wait to get back on the courts with you!

Marissa Ledger, Rose, Nancy, doctor doctor, TML. I will never forget all of the amazing times we had together while combing through your parasitic poop. You are truly great friend. You are one of the most brilliant yet humble people I've ever met. Talking to you is both so easy and comforting while also engaging and exciting. I've never had so much fun in the lab before. You continue to astound me with all that you do. I'm incredibly thankful to have you in my life.

I could go on and on, but for the sake of brevity here, I wish to thank Debi Poinar, Samantha Price, Marie-Hélène B.-Hardy, Ravneet Sidhu, Ashleigh Porter, Priyanka Gogna, Kévin Roche, and Francisco Pinilla (Pancho) for all the great times I spent with each of you, and for all that you've each taught me and helped me with over the years. I apologize if I have forgotten any Poinar lab members or visitors! But truly, each and every person who has spent time in this lab is a special person, and each of you have helped me grow and see the world just a little differently.

Thank you to Brian Golding for being on my committee and for allowing and trusting me to utilize your computer cluster! I've gained an all-new appreciation for the power of the command line; thank you for this opportunity to expand my technological capabilities. I may even eventually become a Linux convert one day soon. Your breadth of biological knowledge is inspiring. Thanks as well to Shanti Morell-Hart for being on my committee and for all your mentoring over the years, as well as your thorough and incredibly thoughtful edits on my writings. I hope there is just enough anthropology in my thesis to justify me being in this department, haha. I struggled against the co-authors to keep as much archaeology in these papers as I could. I truly appreciate the care with which you edited my dissertation. Your edits have significantly improved the quality of this work. Thanks as well to Peter Heinzman for being my external committee member and for your carefully considered critiques and comments that helped me refine many aspects of this research. Thank you Pete for taking the time to comb through this work as carefully as you did!

My thanks to Duane Froese for being an exceptional mentor. Thank you for all of your help over the years, for speaking so highly of me to others, and helping connect me with leading researchers. Thanks especially for helping facilitate the 2017 field work in the Yukon. I truly appreciate you allowing me to join the crew. Thanks as well for all the great times with other crew members: Sasiri Bandara, David Mazzucchi, and Tyler Prince. Thanks as well to Scott Cocker and Michael Pisaric for their help with this project and for the work at Crawford Lake, as well as Alistair Monteath and George S. Long for their support on the publication version of chapters 4 and 5. As well, thank you Beth Shapiro for inviting me to visit your amazing lab in Santa Cruz!

My thanks to Julio Mercader and Tristian Carter for each facilitating life changing adventures in my life. Going to Tanzania with you, Julio, was an unforgettable experience. I know climbing Kilimanjaro wasn't part of the main trip, but that experience following the workshop is one of my fondest memories. And Tristian, going to Greece felt like coming full circle with how I got into archaeology in the first place. You both enriched my life in immense ways. Thank you. Sorry I didn't find any better DNA at Naxos! Thanks Tristan for being on my committee as well for the defense. Thanks also to all the amazing people I spent time with on Naxos, especially Xara Kanarogloy and Jason Lau.

Thanks to the folks of Whiskey Club for many a thoughtful conversation and a pleasant time to de-stress after long days of reading and writing: Miriam Karrel, Peter Wallace, Christine Cluney, Taylor Smith, Tracy Prowse, Shanti Morell-Hart, and Lauren Rennie among many others. I'm sorry I got you folks sick in Sweden! It was an awesome trip, if only there was a little less vomiting, haha. Thanks as well to my fellow Misanthropes: Sarah DiBiagio, Dana Hart, and Laura Lockau. That first year feels like ages ago now. I miss our office dynamic and each of you as exceptionally unique people.

Thank you Bonnie Kahlon for many a great conversation on the 4th floor, and for being such a kind and pleasant human being. My thanks as well to John Silva, Marcia Furtado, and Delia Hutchinson for all your help with everything related to the mysterious administrative systems of the university and external funding agencies. Thank you for

always each being so kind and helpful, and for being so understanding and patient with my last-minute emails.

Rachel Axe-Thrower Hesketh—Sunshine, you have been a beacon of positivity in my life. You inspire me every time we're together. You help remind me to stay active both physically and mentally, and to keep challenging myself and experiencing all that I can. Your unwavering support, grace, passion, and exuberance has transformed me in ways I could have never anticipated. You've taught me how slow down time, if only for a moment, to see the magic. George Carlin once said, "inside every cynical person is a disappointed idealist." Sunshine, you've helped the disappointed idealist in me be reborn into a wiser, more balanced, and more appreciative person. Thank you for everything you do, and everything that you are. I love you. I can't wait to embark on our next adventure together. ❄️💔🌞

Finally, my family—Sharon and Stewart Murchie. Thank you both for always believing in me and everything you have both done to help me follow my passions. I know I've developed some peculiar interests over the years, so thank you both for always being supportive of my idiosyncrasies. I know this journey has taken me quite a long time, but I'm so immensely happy to have done it despite all the struggle. I wouldn't have rather done anything else over this past dozen or so years. Thank you for being supportive of me diving so deeply into a field of study that may otherwise seem fairly esoteric. I'm really glad we got into a weekly Sunday chat routine during my time in Ontario. It's something that has helped ground me, given me a chance to continuously reflect back over what I do with my time, and to hear both of your comforting voices, no matter the topic of conversation. I've looked forward to those chats and my visits back home the whole time I've spent out east. I can't wait to discover what the next phase of my life will bring, but I'll always know that the only reason I got to experience all that I have is because of you two. I love you mom and dad—thank you for everything.

How shall we comfort ourselves, the murderers of all murderers? What was holiest and mightiest of all that the world has yet owned has bled to death under our knives: who will wipe this blood off us? What water is there for us to clean ourselves? What festivals of atonement, what sacred games shall we have to invent? Is not the greatness of this deed too great for us? Must we ourselves not become gods simply to appear worthy of it?

—Nietzsche, *The Gay Science* (1887), sect. 125 (The madman), tr. Walter Kaufmann

Table of Contents

List of Tables

List of Figures

List of Abbreviations and Symbols

Symbol	Definition
^{14}C	Radiocarbon age (not calibrated to calendrical age)
aDNA	Ancient DNA
BLAST	Basic local alignment search tool
bp	Base pair, refers to the length of a DNA sequence
BP	Years before present (1950)
BSA	Bovine serum albumin
BWA	Burrows-wheeler aligner
Cal yr BP	Calibrated years before present (1950)
cpDNA	Chloroplast (plastid) DNA
DDT	Dithiothreitol
DNA	Deoxyribonucleic acid
DsLp	Double-stranded library preparation
eDNA	Environmental DNA
EDTA	Ethylenediaminetetraacetic Acid
ET	Extra-terrestrial
FLD	Fragment length distribution
GSSP	Global boundary stratotype section and point
GuHCl	Guanadinium hydrochloride
HTS	High-throughput Sequencing
HE	Human Era
kya	Thousand years ago
LCA	Lowest common ancestor
LGM	Last Glacial Maximum
LQE	Late Quaternary Extinctions
MEGAN	MEtaGenome ANalyzer
MIS	Marine Isotope Stage
MQ	Map quality
mya	Millions of years ago
mtDNA	Mitochondrial DNA
nDNA	Nuclear DNA
NCBI	National Center for Biotechnology Information
NGS	Next generation sequencing
PalEnDNA	Palaeo-environmental DNA
PCoA	Principal coordinates analysis
PCR	Polymerase chain reaction
PTB	N-Phenacylthiazolium
PVP	Polyvinylpyrrolidone
qPCR	Quantitative PCR
rCRS	Revised Cambridge reference sequence (mitochondrial genome)
SDS	Sodium dodecyl sulfate

Symbol	Definition
SedaDNA	Sedimentary ancient DNA
SNP	Single nucleotide polymorphism
Tris-HCl	Tris hydrochloride
UV	Ultraviolet
µL	Microliter
µM	Micromolar

Declaration of Academic Achievement

I, Tyler James Murchie, declare that this thesis titled "Ancient environmental DNA as a means of understanding ecological restructuring during the Pleistocene-Holocene transition in Yukon, Canada" and the work presented therein are my own. I confirm that this dissertation contains three primary chapters with subsequent chapters dedicated to appendices. The first manuscript was submitted and published in *Quaternary Research*. The second and third have yet to be submitted to a journal for publication. I was the lead researcher in project design, sample processing, laboratory experimentation, computational analysis, writing, and figure design for all materials in this dissertation. The co-authors listed on each paper contributed variously therein through a combination of collaborative research design, sample acquisition, wet lab assistance, computational assistance, manuscript editing, and figure design feedback. Duane Froese and his associated research teams (including Tara Sadoway and Matthew Mahony) originally collected all permafrost cores that were processed and analyzed for this dissertation.

Chapter 1 Introduction

We cannot understand how *Homo sapiens* came to populate and ultimately dominate planet Earth without a holistic integration of the physical and life sciences. Human culture is inextricably linked to the evolutionary processes that shaped our physical and mental realities, as it is to the selective pressures that formed, and were formed by, our palaeoenvironmental legacy. Understanding who we are, how we got here, and where we might consider going is fundamentally linked to the stories we tell ourselves about our role in the history of life on Earth. It is easy today to forget our inherent connectedness to the natural world in this radically unique moment in time—buttressed against the relentlessly indifferent forces of natural selection by the material, ecological, and sociocultural niches we have constructed over millennia. We are also in a unique moment insofar as our rapidly growing wealth of knowledge and technological capabilities have enabled a suite of immensely powerful methodologies allowing us to maximally exploit the information potential preserved in ancient remains hidden at the micro-scale. These innovations, hardly distinguishable from magic, have reconceptualized our relationships with other hominins (Meyer et al., 2012; Prüfer et al., 2014) and have enabled us to recover data related to past disease, biogeography, diet, evolutionary relationships, lifeways, and ecosystem composition (Fry, 2006; Hofreiter et al., 2012; Briggs and Summons, 2014; Cappellini et al., 2018; Croft et al., 2018; Swift et al., 2019). These advances have enabled far deeper glimpses behind the veil of time, but this newfound power is intractably paired with the increasing precariousness of our global situation as stressed by Ord (2020) in his work *The Precipice: Existential Risk and the Future of Humanity*.

The scope and scale of the challenges our species faces today are in many ways beyond comprehension, from anthropogenic climate change (IPCC, 2014), to an ongoing human driven ecological crisis threatening biodiversity across the entire planet (Barnosky et al., 2011; Pimm et al., 2014; Ceballos et al., 2015; De Vos et al., 2015), exponential human population growth and an associated rise in emerging infectious disease and antibiotic resistance (Nakajima, 1997; Harrison and Svec, 1998; Mah and Memish, 2000;

Jones et al., 2008; Takahashi and Tatsuma, 2014; Lindahl and Grace, 2015), rising political polarization (Carothers and O'Donohue, 2019), escalating tensions among nuclear-weapon states amidst the Coronavirus disease 2019 (COVID-19) pandemic, and growing innovations in biotechnologies and artificial intelligence of immense potential power to facilitate a paradigm shift in humanity's conceptions of ourselves and our place in the biosphere (Harari, 2016). Navigating this precipice necessitates many decisions that more than ever need to carefully consider the deep time contextual circumstances that lead to our current situation.

But, the measure of our human ecological legacy remains largely enigmatic. When humans first began dispersing from East Africa, the terrestrial world was dominated by megafauna (animals with a body mass ≥ 44 kg). This lost world of giants had persisted throughout numerous glacial-interglacial transitions over millions of years, but then came a wave of extinctions towards the end of the late Pleistocene (c. 130,000–11,700 BP) that resulted in the extinction of some 67% of megafaunal genera (~101 of 150) (Stuart, 2015; Boivin et al., 2016), which precipitated a restructuring towards contemporary Holocene biomes (Malhi et al., 2016; Stivrins et al., 2016). Status quo bias makes it easy to assume that the composition of the biosphere today is representative of relatively normal levels of biodiversity. But when we take a longer-term perspective, it becomes apparent that much of the terrestrial biosphere has substantially less diversity and animal biomass than the preceding Pleistocene epoch (Gill, 2014a; Galetti et al., 2017; Zhu et al., 2018). Much of the world today lacks the mosaic patchwork of habitats that were once built and maintained by high densities of large grazers and browsers (Zimov et al., 2012a; 2012b; Malhi et al., 2016; Smith et al., 2016). Big animals transform ecosystems by controlling wooded areas, redistribute nutrients over huge distances (Pires et al., 2018), enhance biomass turnover, and create ecotones with high edge effects on biodiversity. The ecological repercussions associated with this loss of Earth's largest terrestrial animals continues to reverberate today through Holocene ecosystems (Brault et al., 2013; Doughty et al., 2013; 2015; 2016; Lopes dos Santos et al., 2013; Smith et al., 2015; Asner et al., 2016; Bakker et al., 2016b; le Roux et al., 2018).

Unfortunately, these effects are only likely to increase with diminishing wilderness areas globally, threatening the interconnected stability of ecosystems across the planet, and potentially even reducing the carrying capacity for humans amidst our relentless population growth. Understanding the anthropogenic processes that led to our current zoological impoverishment is relevant today for informing environmental conservation efforts. How we choose to conserve these ecosystems, either as they are now, or by promoting Pleistocene flora and fauna through rewilding efforts (Svenning et al., 2015; Carey, 2016; Macias-Fauria et al., 2020), plays directly into the biospheres' long-term stability and resilience amidst our ongoing extinction crises.

Understanding the reverberating complexities of human palaeoecology is challenged by the rarity of palaeontological and archaeological remains. Direct evidence of a region's first human inhabitants and their associated lifeways would obviously be ideal, but the probability of finding the surviving remnants of highly mobile, pioneering hunter-gatherers is expectedly remote (Jaanusson, 1976; Heads, 2012)—as is the likelihood of recovering palaeontological remains from dwindling and refugial populations (Signor and Lipps, 1982; Haynes, 2013). Extinction chronologies are largely based on last appearance dates, but the rarity of these remains only allows for tenuous inferences of terminal population dynamics. These limits of visibility (compounded by a range of dating uncertainties, see Rodríguez-Rey et al., 2015) severely inhibit the accuracy of human ecological models concerning the Pleistocene-Holocene transition. The emergence of proxy based palaeoecological micro-methods (Croft et al., 2018; Swift et al., 2019)—and ancient DNA in particular—are increasingly able to fill in the holes in our records so that we might finally be able to understand how the biosphere transformed so radically as humans came to populate the continents. Sedimentary ancient DNA (SedaDNA) and related biomolecular techniques may be key for mitigating many of the visibility limitations associated with buried records. Utilizing these methods to understand the Pleistocene-Holocene transition necessitates a broad interdisciplinary effort, bringing many disparate fields together to collectively interpret the complex history that created our ecological inheritance.

The inherent interdisciplinarity of ancient DNA and Pleistocene human ecology means that this thesis is arguably not well situated within any particular discipline. I consider myself an archaeological scientist, which is why this thesis was written in a department of anthropology and is why I place an inordinate focus on humans despite not actually analyzing any archaeological remains or sites directly. But I admit that this thesis is not especially anthropological. This is not a problem in my mind as I increasingly see the disciplinary divides as being too rigid, but it does necessitate a degree of broader contextualization from many interrelated fields to properly address the topic holistically.

McGilchrist (2009) in his landmark work *The Master and His Emissary* argues that we have undergone a ratcheting cultural tilt in the western world towards a left cerebral hemispheric view of reality as characterized by denotative language, abstraction, generalization, categorization, and ultimately towards an emphasis on viewing reality as a series of individual parts or things that we have the power to manipulate and control—both physically and conceptually. While these are all inherently important aspects of cognition, survival, and the scientific method, the tilt has come in terms of de-emphasizing arguably more important right hemispheric perceptions of interconnectedness, inherent evolution/change, plasticity, uniqueness, complexity that defies simplification, and ultimately the situating of knowledge and experience within broad, holistic contexts. My aim in this chapter, and this thesis as a whole, is to help build an interdisciplinary context as to how we see our legacy within the interconnectedness of the natural world, to narrow down into the state of things in northwestern North America as the last great terrestrial giants vanished at end of the last ice age, and to zero in—through the immense growing power of ancient biomolecules—on specific slivers in time in central Yukon as humans reached the icy gateways to a New World. The data reported and discussed in this thesis are ultimately preliminary given the scope of the transformations being investigated. Spatially, my study area is limited to central Yukon for reasons of sample availability, optimal preservation, geographic relevance to the peopling of the Americas, extant collaborative networks, and my own growing passion for the eastern Beringian landscape (Yukon and Alaska) (Murchie, 2015). However, the

innovations that my colleagues and I have developed here illuminate the potential of ancient environmental DNA to increasingly augment traditional approaches to palaeoecology in a diverse range of buried contexts where biomolecular preservation is possible. The long-term goal in this case is to progressively disentangle the complexities of our human ecological past to help contextualize the contemporary biosphere and our transient human predicaments therein.

In this chapter I touch on current debates regarding the proposal that we live in an *Anthropocene* epoch, discuss environmental archaeology while highlighting theoretical notions of niche construction and its role in human history, then pivot towards a primer on the late Pleistocene in Yukon and Alaska as people first reached the Americas while megafauna disappear from the record. Then, I discuss the growing role of ancient DNA (aDNA) within archaeology, and how ancient environmental DNA (eDNA) can increasingly augment investigations at the nexus of Quaternary science. Finally, I outline the chapters in this thesis.

1.1 An alleged *Anthropocene* epoch

In August 2016, the Anthropocene Working Group (AWG; part of the Subcommission on Quaternary Stratigraphy) voted to present a formal recommendation to the International Geological Congress that we now exist in a distinct epoch from the Holocene, which they propose terming the *Anthropocene*. Waters et al. (2016) argue that the mid-20th century marks an acceleration of human activity of sufficient magnitude (e.g. radionuclides, plastics, technofossils, pesticides, greenhouse gases, metals/other modified geochemicals, changes to sedimentation and pedostratigraphy, long distance species invasions, and accelerated extirpations/extinctions) that a distinct anthropogenic signal would be geologically detectable. To date, neither the International Union of Geological Sciences nor International Commission on Stratigraphy have approved or rejected the proposal. But the *Anthropocene* concept, as first conceived by Crutzen and Stoermer (2000), has found considerable utility in a range of disciplines at the confluence of the social, earth, and life sciences. Despite the emerging range of interpretations of the *Anthropocene* concept, the AWG maintain the use of the term as a formal geologic unit

(Zalasiewicz et al., 2019b), for which they intend to submit a completed proposal to the International Commission on Stratigraphy by 2021. Zalasiewicz et al. (2019a) argue in their prelude to the AWG's formal proposal that a stratigraphic boundary around 1950 coincides with the *Great Acceleration* of human population growth, industrialization, and globalization. And despite this infinitesimally small period of geologic time, the AWG contend that this boundary marks a moment that has irrevocably changed the future of this planet in ways similar to the near instantaneous perturbation that demarcated the end of the Mesozoic.

A growing camp of archaeologists have expanded conceptions of the *Anthropocene* to better characterize the long and gradually increasing impact of humans on biotic and abiotic systems globally. Foley et al. (2013) suggest the concept of a *Palaeoanthropocene* as a diffuse transitional period marking the first, barely recognizable, hominin environmental impacts some one million years ago (mya) up to the industrial revolution. They aim to highlight that humans have been an integral and increasingly influential component of the *Earth System* since the emergence of the genus *Homo*. Malhi et al. (2016, p. 839) highlight that as early as ~1–2 mya there is evidence of abnormal megafaunal declines in Africa in proboscidean diversity (Todd, 2006), as well the extirpation of several carnivore lineages from the continent (including sabretooth cats) (Werdelin and Lewis, 2013) that otherwise continued to flourish outside of Africa until the end of the Pleistocene. Werdelin and Lewis (2013) found that large East African carnivores lost 99% of their functional richness starting around 2 mya compared to their peak Pliocene diversity between 3.6–3.0 mya. They argue that although environmental change was underway during the Pliocene-Pleistocene transition (2.6 mya) with East African forests opening into a mosaic of wooded grasslands (Cerling et al., 2011), that these carnivore extirpations lag too far behind climate induced landscape changes to be directly correlated. They instead suggest that the evolution of early hominins into a carnivore niche space significantly impacted East African megafauna during the Early Pleistocene. The evolution of anatomical features in *Homo erectus* to throw projectiles with high speed and accuracy (Roach et al., 2013), increasing use of anthropogenic fire

(James, 1989; Gowlett, 2016), and the associated metabolic demands of a growing human brain (Leonard and Robertson, 1997; Wrangham, 2008) may then have led to hominins out-competing many carnivores and placing new pressures on African megafauna (Malhi et al., 2016). From these enigmatic beginnings, the scale and scope of human-environmental influences during the *Palaeoanthropocene* gradually increased (Foley et al., 2013). Initially these were local effects in East Africa that spread as hominins and their hunter-gatherer lifeways evolved, increasing in scope and intensity with the global dispersal of the genus *Homo*, and undergoing a punctuated spike with the Neolithic revolution. The effects of humans on the *Earth System* continued to grow thereafter as we incrementally modified our environments to suit our needs, impacting terrestrial and marine ecoystems at increasingly regional scales, all of which lead up to the exponential growth spike of the industrial revolution and subsequent globalization. Foley et al. (2013) emphasize that their *Palaeoanthropocene* concept should not be temporally anchored to the geologic timescale, but rather be used to emphasize the measure and legacy of human impact on ancient environments.

In a similar vein, Boivin et al. (2016) highlight four major phases of cumulative anthropogenic influences on the biosphere: the late Pleistocene global expansion, the Neolithic advent of agriculture, island colonization, and the emergence of urbanization and commercial networks. Agriculture and urbanism are obvious forms of human environmental impact with well-documented, disproportionate influences on local ecosystems that could be considered part of a *Palaeoanthropocene*. The measure of ecological influences of nomadic, terminal Pleistocene hunter-gatherers is far more enigmatic and difficult to separate from other environmentally interconnected factors. However, the seemingly well-correlated spatiotemporal timings of mass extinctions with the progressive dispersal of humans throughout the globe is hard to discount (Martin, 1967; 1984).

It is important to be cautious and not overstate the available data as to anthropogenic impacts on palaeoecologies (Feeney, 2016). For example, Bush et al. (2015) argue against the growing trend of viewing Amazonia as anthropologically

constructed. Bush and colleagues contend that researchers are extrapolating the relatively abundant archaeological data from riverine and savanna/seasonally flooded forests out to interfluvial, terra firme ever-wet areas—90% of Amazonia—without sufficient justification. Bush et al. (2015) emphasize a spatiotemporal heterogeneity in the human ecological legacy of Amazonia where they argue that pre-Columbian human settlement patterns suggest a preference for regions with high seasonality. As such, these riverine and adjacent ecosystems were likely far more directly influenced by humans than interfluvial settings where archaeological evidence and anthropogenic fires drop substantially. Bush et al.'s charge of Erickson (2008) and likeminded colleagues of overstating the legacy of anthropogenic impacts in Amazonia reflects an overcorrection of sorts from earlier notions of a *pristine wilderness* in the Americas prior to European contact (see Denevan, 1992). So, while it is important to not discount the ecological reverberations of past human activities, it is equally important to not overstate what the data is telling us. It helps to more broadly recognize the low and biased visibility of buried records overall that can be obscured by the tendency for over-confidence and tunnel vision within theoretical schools, leading to adherents drawing too much from, and over-generalizing, the actual datasets we have available.

Stepping back to the *Palaeoanthropocene* concept, Smith and Zeder (2013) propose a sort of middle-ground insofar as rather than using the term *Palaeoanthropocene*, or searching for a *golden spike* (a Global Boundary Stratotype Section and Point [GSSP] (Remane et al., 1996; Subramanian, 2019) to demarcate the onset of significant human ecological influences, to rather reconceptualize the Holocene and Anthropocene as coeval, potentially with linked nomenclature as the *Holocene/Anthropocene* epoch. This simplifies the temporal boundary dilemma while emphasizing the magnitude and longevity of human ecological impacts that can suffer from low archaeological visibility. Zalasiewicz et al. (2019b) as leaders in the AWG argue however that the pronounced, rapid, and global scale of impacts in the mid-20th century are unambiguously human, whereas the anthropogenic component in factors

relating to the Pleistocene-Holocene transition are far more regionally diachronic as opposed to globally synchronous.

If the goal of a *Palaeoanthropocene* concept is to emphasize the deep time heritage of human history along with our legacy of disproportionate environmental impacts, I instead favor the notion of reconceptualizing our Gregorian calendar and converting it to the *Human Era* (HE) as first proposed by Emiliani (1993). In this system, 10,000 years is added to our current calendar, which would make the completion year of this dissertation 12,021 HE. This system gets around the lack of a year zero in the BC/AD (or BCE/CE) calendar system, which complicates calendrical arithmetic around the transition as 1.5 BC to 1.5 AD is a difference of one year, not three. It also recognizes human histories across the globe beyond the current calendrical focus set around the Abrahamic religions (although 1 BC would still correspond with year 10,000 HE), more closely approximates the onset of the Holocene, and just so happens to roughly correspond with the construction the earliest discovered megalithic structure Göbekli Tepe around the 10th millennium cal BC in the Southeastern Anatolia Region of present day Turkey (Schmidt, 2010; Dietrich et al., 2013). In this sense, it roughly marks the first transition from nomadic foraging lifeways towards sedentism, domestication, and the myriad other hallmarks of the Neolithic revolution. A *Human Era* calendar would accomplish many of the AWG's broader goals of underscoring our legacy of influence on the *Earth System* without presupposing the longevity that the 1950's holds in the history of life on Earth. It would seem to me that deciding the veracity of a mid-20th century Anthropocene epoch requires a degree of hindsight well beyond any of our current life-times, but I am sympathetic to the purpose of such a proposal in recognizing the disproportionate powers we now wield in transforming the *Earth System*, and the responsibility those powers must mandate if we are to navigate our current precipice. A *Human Era* system would also hopefully convey a broader sense of togetherness in our human predicament, and call attention to the need for long-term planetary stewardship. The importance of which is easily forgotten with our bias to focus on more immediately relevant timescales on the order of a human lifetime or two.

The *Anthropocene, Palaeoanthropocene,* and *Human Era* concepts are relevant to this work insofar as it remains unclear how long and how significantly humans may have been disproportionally influencing the *Earth System*. In terms of the late Quaternary extinction event as the focal point of this dissertation, if most now extinct megafauna may have otherwise persisted through the Holocene inter-glacial in the absence of *Homo sapiens,* there is reason to suspect that the roots of an *Anthropocene* may penetrate far deeper into the recesses of life's past that a mid-twentieth century onset fails to fathom. My efforts here in developing a means of disentangling the megafaunal extinctions in Beringia are aimed in part at understanding the enigmatic resonance of the *Anthropocene* in deep time.

1.2 Human ecology and environmental archaeology

Human ecology is a transdisciplinary research area concerned with the long-term relationship between humans, other organisms, and their environments. Human (also sometimes referred to as historical) ecology emphasizes a diachronic perspective in terms of the gradual evolution of ecological structure and function as related to human activities and lifeways (Crumley, 1987; 2006). Some archaeologists prefer not to be implicitly tied to ecological theory however, preferring the use of the less constrictive umbrella term *environmental archaeology* (Driver, 2001b; 2001a).

Environmental archaeology is a collection of methodological approaches originally used in conjunction with *middle range theory*—linking human behaviour and natural processes with archaeological materials through the use of ethnoarchaeology, as well as experimental and taphonomic research (Binford, 1981). In this view, the research focus is not defined by a *higher level theory*, namely ecological concepts or objectives, or other theoretical approaches (such as Systems Theory) that arose with the *New Archaeology* of the 1960s and 70s. Rather, environmental archaeology encompasses a range of theoretical and methodological schools, including largely abandoned concepts like environmental determinism and environmental possibilism, as well as a number of more active ecological approaches such as ecodynamics, ethnoecology, and cultural, human, and historical ecology (see Reitz and Schakley, 2012, pp. 6–8). Debate over

theoretical underpinnings within the discipline relates to the conceptual developments of *processual* paradigms (a positivist approach with the goal of using scientific methods to derive objective understandings of past peoples) and *post-processual* paradigms (a theoretical movement critical of the ability to derive an objective understanding of the past, emphasizing the inherent subjectivity of the discipline) (Trigger, 2006). Thomas (2001) contends that 'environmental archaeology' should be abandoned due to its ambiguity and lack of theoretical foundation in favour of 'human palaeoecology', while others do not distinguish between the two (Dincauze, 2000).

I largely agree with the conceptions used by Reitz and Schakley (2012, pp. 1–40). In this case, environmental archaeology is used as a grouping term for a range of environmentally oriented methods (principally zooarchaeology, palaeoethnobotany, and geoarchaeology) and theories, with human palaeoecology being a sub-focus that uses ecological concepts to understand human environmental interactions through time. This dissertation is an exercise in environmental archaeology using palaeogenetic methods (albeit with the anthropological component being more contextual than direct), with theoretical underpinnings rooted in ecology.

1.2.1 A legacy of constructed environments

Niche construction theory (Laland et al., 2000) is a relatively new concept in ecology with direct relevance to archaeological and palaeobiological research. Niche construction is concerned with the "…capacity of organisms to modify natural selection in their environment and thereby act as co-directors of their own, and other species', evolution" (Laland and O'Brien, 2010, p. 303). Through their activities and metabolic processes, organisms create, modify, and destroy their, and other organisms', niches (Odling-Smee et al., 1996, p. 641). Examples of this include beaver dams, nests, burrows, webs, pupal cases, modifications to atmospheric gases and nutrient cycles (e.g. photosynthesis), and decomposition. For example, earthworms and other micro-fauna dramatically affect soil chemistry and structure, exposing subsequent generations to progressively shifting sets of selective pressures through accumulative environmental modifications, which further impacts the selection of other soil-dwelling organisms such

as plants, insects, and microbes who are themselves modifying their local environment towards a niche space favorable to their own genes (Odling-Smee et al., 1996). A wide range of behaviours can also indirectly impact niche construction, such as elephant footprints in Uganda acting as habitats and dispersal routes for macroinvertebrate communities between water sources (Remmers et al., 2016), in addition to the varied behaviours of elephantids and megaherbivores that dramatically impact vegetation composition and structure (Owen-Smith, 1992; Bradshaw et al., 2003; Bakker et al., 2006; Gill et al., 2009; 2012; Johnson, 2009; Gill, 2014a). The evolutionary ramifications of niche construction may also be indirect, such as beavers transforming the edges of riparian habitats into wetlands, meadows, and lakes, which attracts a new range of fauna and flora to those ecosystems with their own effects on the beavers. Further, those wetlands may also attract (or repel) human activities, and with those encroaching humans comes a radically different evolutionary measure of fitness many steps removed from the original niche construction behaviour (Wright et al., 2002; Coles, 2006; Riede, 2012, p. 91). Progeny inherit the niches and associated sources of natural selection constructed by preceding generations, enabling a degree of co-direction in evolutionary processes. One may suspect that niche construction is driven in part by the Red Queen hypothesis (Van Valen, 1973) wherein species are under selective pressures to continuously adapt and evolve as they are pitted against other ever-evolving competitors, "…it takes all the running you can do, to keep in the same place" (Carroll, 1871, chap. 2).

Many ecologists consider niche construction theory to be a form of *ecological engineering*. Pearce (2011, p. 797) suggests that the primary difference lies in ecological engineering referring to the physical modification of an environment, with niche construction being a kind of engineering that has evolutionary feedback on the engineer. This subtle difference can be attributed to varied disciplinary objectives (Barker and Odling-Smee, 2014). Evolutionary theorists tend to favour niche construction with its diachronic evolutionary perspective (Odling-Smee et al., 1996; 2003), while ecologists can more readily operationalize models of ecological engineering with a more restrictive framework that precludes competitive and trophic interactions in their definition (as other

models already account for these factors) (Gutierrez and Jones, 2006; Wright and Jones, 2006; Berke, 2010). Biological theorists disagree on how to effectively merge these two frameworks. One suggestion is that ecological engineering be conceived as a sub-process of niche construction (Barker and Odling-Smee, 2014) and the resulting union be referred to as ecological niche construction (Kylafis and Loreau, 2008; Barker and Odling-Smee, 2014). Another camp contends that niche construction is too broadly defined to be useful, and would be better implemented as a narrower concept (Godfrey-Smith, 2000, p. 154; Sterelny, 2001, p. 333; Okasha, 2005, p. 2), such as an evolutionary subcomponent of ecosystem engineering (Pearce, 2011). While Laland and O'Brien (2010, p. 318) promote the application of niche construction for archaeological applications, they caution against it being used as another form of 'just-so' arguments filtered through an evolutionary framework. I utilize the concept here primarily to contextualize a discussion around hunter-gatherers and how we might expect them to have impacted Pleistocene ecosystems. My intention is not to operationalize the concept here in any rigorous sense.

Niche construction related conceptions go by many terms in anthropological literature, including aboriginal agronomy/land management, protoagriculture, anthropogenic ecology, humanized landscapes, and indigenous/traditional resource management (Smith, 2011, p. 838). Much of this research today falls under the umbrellas of Traditional Ecological Knowledge (commonly shorted to TEK or other similar acronyms) (Berkes et al., 2000; Huntington, 2000; Saylor et al., 2017; Lepofsky and Armstrong, 2018; Velázquez-Rosas et al., 2018; Fisher, 2020; Uchida and Kamura, 2020), ethnoecology/ethnobiology (Johnson, 2000; Barrera-Bassols and Toledo, 2005; Anderson et al., 2011; Tremblay et al., 2020) and traditional resource/land management (Fowler and Turner, 1999; Anderson, 2005; Turner and Deur, 2005; Smith, 2011). Arguably, social anthropological theory related to TEK and similar concepts is best utilized for more near-time archaeological/anthropological questions. These concepts may begin to lose some utility as the period of study recedes further into deep time, in this case over 10 millennia, where oral and historic records fade and human artifacts become scattered enigmas strewn haphazardly over immense geographic and temporal regions. As

the palaeogenetic dataset under analysis here is focused principally on the transformation of Pleistocene ecosystems, my focus throughout this work is centered on interdisciplinary theory and methods at the nexus between evolution, ecology, and archaeology.

Another concept closely related to niche construction and ecosystem engineering, and of use for discussing the late Quaternary extinctions, is the *keystone species*. This concept was coined by Paine (1969a; 1969b, p. 950) to refer to high trophic organisms with a disproportionate ecological influence. This was based on a classic experiment involving the removal of a carnivorous seastar (*Pisaster ochraceus*) from an intertidal habitat to observe the impacts of its absence on ecosystem stability (which were significant). Characteristics of keystone species include: top-down trophic effects, a prevention of monopolization in low trophic levels, and the role of stabilizing diversity (Paine, 1969a; 1969b). This makes keystones rare, functionally non-redundant, and of great ecological significance (Davic, 2002). The keystone concept has been broadly repurposed beyond this initial definition (Paine, 1995; see Davic, 2003; Valls et al., 2015), finding wide use in conservation and other ecological literature. Some scholars have critiqued this growing ambiguity that allows keystone status to be applied a range of organisms (e.g. prey, competitors, pollinators, mutualists, engineers, dominant species) (Davic, 2003, pp. 1–3), with some calling for an abandonment of the term entirely (Mills et al., 1993). Part of this concern is the synonymous use of 'key', 'keystone', and 'ecological engineer' (Higdon, 2002). For example, Davic (2002) agrees with Higdon (2002) that keystone species can be herbivores (using the broad definition of 'prey species' from Wilson and Bossert [1971, p. 127]), but contents that ecologically significant species that do not meet Paine's (1969a; 1969b) original keystone criteria are better described as 'key' or 'ecologically dominant' species, or in the case of beavers as 'ecosystem engineers', rather than 'keystones'. I use the concept here in a general sense following Davic's (2003) modification of Paine's original conceptions (1969a; 1969b) as: a strongly interactive species with disproportionate top-down effects on species diversity and competition relative to its overall biomass.

The keystone concept is relevant to the late Quaternary mass extinction of megafauna at the core of this dissertation insofar as critical losses in keystone megaherbivores (Owen-Smith, 1987; 1988; Gill et al., 2009; Gill, 2014a) may have initiated an ecological collapse akin to the historic loss of sea otters (a nearshore marine keystone critical for kelp forest maintenance) in the Commander Islands that ultimately and indirectly resulted in the extinction of Steller's sea cow (Estes and Duggins, 1995; Estes et al., 2015). The keystone concept may also continue to expand concerning *Homo sapiens* as Worm and Paine (2016) argue that humans may best be considered a *hyperkeystone species*. In this sense, human behaviors drive complex interaction chains that profoundly affect other keystones across marine and terrestrial biomes, with those interaction chains then reverberating through the food webs regulated and maintained by those keystones. Worm and Paine (2016, p. 603) suggest that although the human *hyperkeystone* role is likely not new, with humans having had disproportionate influences on other keystones since the Pleistocene, that our globalized economy today has increasingly created a ubiquitous anthropogenic noise that permeates through keystones and beyond into wider ecosystem structure and function. This noise challenges attempts to unbiasedly study non-human processes, but also highlights the importance of recognizing that our collective niche construction actions reverberate through entire food webs, changing selection pressures far beyond directly impacted organisms and their immediate environments.

If some set of Pleistocene megafaunae are best conceptualized as keystone species, the taxonomic breadth of this mass extinction event may not need to explain the loss of each species in their varied niches, but may be best understood holistically through the resonant consequences of those critical losses in inter-connected palaeo food webs, with the extirpations of woolly and Columbian mammoths (*Mammuthus* ssp.) being probable keystone candidates. Further, if humans are at least partially responsible for the extirpation of these keystones, this lends theoretical support to humans as *hyperkeystone species*, as well as notions of a *Palaeoanthropocene*.

While humans are not solitary in our capacity to profoundly modify the environment (for example, the cyanobacterial creation of an oxygen rich atmosphere), humans are uniquely potent niche constructors (Smith, 2007, p. 188; Laland and O'Brien, 2010). Our niche construction tendencies may have had profound effects on ecosystem engineers and keystones since at least the late Pleistocene. Niche construction adds another extragenetic component to the three tiered model of inheritance of use for understanding hominin evolution: genetics/epigenetics, sociocultural transmission, and now the local environment (Laland et al., 2000; Riede, 2012). Darwinian mechanisms have been applied in evolutionary archaeology to quantify and explain shifting attributes of style and function in material culture (Dunnell, 1978; Lipo, 1997; Erkens and Bettinger, 2001; Eerkens and Lipo, 2005; Lyman et al., 2008; Mesoudi and O'Brien, 2008) through the concepts of an *extended phenotype* and *memetics* (Dawkins, 1990). Proponents of niche construction in archaeology similarly extend inheritance beyond genetic and sociocultural factors to include inheritance of compounding environmental modifications that themselves confer shifting measures of fitness via natural selection. These interrelated concepts have been recently interwoven by Ellis (2015) into the metatheory of *sociocultural niche construction* which I think has utility in this thesis for contextualizing the evolutionary mechanisms that may be responsible for the late Quaternary extinctions.

1.2.2 Sociocultural niche construction and the Extended Evolutionary Synthesis

Ellis (2015, p. 293) defines sociocultural niche construction as the:

> *Alteration of sociocultural, ecological, or material patterns and processes by human individuals, groups, or populations through socially learned behaviors, exchange relations, and cooperative engineering in ways that confer heritable benefits and/or detriments to these individuals, groups, or populations.*

Sociocultural niche construction (see Fig 1.1) combines the aforementioned theoretical concepts of ecosystem engineering and niche construction with the *Extended Evolutionary Synthesis*—an expansion of the *Modern Synthesis* (Huxley, 1942) to

account for natural selection beyond vertical genetic inherence to include oblique and horizontal transmission of genetics/epigenetics (common in microbes), with the inheritance of constructed ecosystems and material culture, as well as multidirectional sociocultural inheritance (Bonduriansky and Day, 2009; Bonduriansky, 2012; Danchin, 2013; Mesoudi et al., 2013). Sociocultural niche construction also combines theories of human *ultrasociality* (the human dependence on social cooperation with non-kin as a result of biological and sociocultural adaptations) (Hill et al., 2009; Tomasello, 2014) with *cultural evolution*—the variable production, transmission, and selection of cultural information (as represented both conceptually and physically in terms of material-culture) that accumulates and changes in frequency across generations, and which confers variable adaptive fitness (Boyd and Richerson, 1982; Laland and Brown, 2002; Henrich and McElreath, 2003; Richerson and Boyd, 2005; Mesoudi et al., 2006; Richerson et al., 2010; Mesoudi, 2011; Whiten et al., 2011; Creanza et al., 2017).

The synthesis has broad utility in conceptualizing evolutionary mechanisms responsible for the human tendency to incrementally niche construct generationally. The ratcheting of cultural change as traits compound over time in this sense leads to a runaway effect in cultural evolution, increasingly driving pressures towards cultural niche derived selective mechanisms rather than far slower forms of selection at level of the gene. The concept may have the power to unite disparate elements of the social sciences, as Mesoudi (2011, chap. 10) argues in favor of, through a cultural evolutionary synthesis across the fields of anthropology/sociology, psychology, history, and so on.

The unilineal aspect of the sociocultural niche construction model (Fig 1.1) may arguably allude to early conceptions of classical social evolution as advocated by anthropologists such as Edward Burnett Tylor, Lewis Henry Morgan, and Herbert Spencer, which have been thoroughly critiqued—most notably by Franz Boas with his concepts of historical particularism and cultural relativism (see Trigger, 2006). Here though, rather than interpreting the sociocultural model as stages analogous to ‘savagery’, ‘barbarism’, and ‘civilization’, I think Ellis’ model provides a collective, positive sum accounting of how expanding cultural, material, and ecological inheritance systems

globally contributes to a ratcheting in environmental transformations from wildlands to anthro-ecosystems. The concept aids in contextualizing processes that may be responsible for some degree of the environmental transformations of the Pleistocene-Holocene transition and notions of a *Palaeoanthropocene* stretching back potentially as far as the early Pleistocene. Here, I focus on the hunter-gatherer niche construction that we might expect from humans newly arriving in Beringia from Eurasia at the end of the late Pleistocene.

1.2.3 The hunter-gatherer niche

Rowley-Conwy and Layton (2011) highlight four components of hunter-gatherer (forager) niche construction: the concentration of useable plants, small-scale cultivation, burning, and selective hunting practices. Both the concentration of wild plants in proximity to repeated habitation sites, and small-scale cultivation (the progressive increase in artificial selection practices on wild plants as manifested through reduced genetic diversity) contributes in the long-term towards the creation of a stable hunter-gatherer niche, which persisted in many regions of the world until contact with—or a transition into—agricultural populations. But these components would likely only manifest locally over long timescales and would be unexpected to contribute significantly towards the macro-vertebrate restructuring that occurred at the end of the Pleistocene. The comparatively larger-scale impacts of intentional burning (be it for landscape management or hunting) (Scherjon et al., 2015) and atypical prey-selection strategies would presumably have had a far greater impact in the short term on the development of a hunter-gatherer niche in Eurasia, Beringia, and Palaeoamerica, and the coinciding trophic restructuring of the late Quaternary extinctions. Although whether hunter-gatherer niche construction processes were short- or long-term is difficult to say as Pleistocene archaeological records in Eurasia and Beringia are characteristically sparse. Our best estimates as to the timings of the peopling may be off by thousands of years, in which time seemingly local and insignificant small-scale niche construction may have had compounding significance in reverberating human ecological transformations into shifting environmental selective pressures.

Fire. Landscape or 'off-site' burning was a widespread, well documented practice among hunter-gatherers globally (Scherjon et al., 2015). The practice is so common that Scherjon et al. (2015, p. 312) posit that it likely has considerable antiquity, alluding to the growing (but controversial) evidence of Palaeolithic Neanderthal fire-use, potentially for landscape management (Roebroeks and Villa, 2011; Roebroeks et al., 2011; Sandgathe et al., 2011; Shimelmitz et al., 2014; Pop and Bakels, 2015). Burning opens landscapes, creating diverse, parklike vegetation communities, increasing both the abundance and reliability of floral and faunal resources. Off-site fire is a relatively simple, but effective means of short- and long-term niche construction. Burning creates mosaic patches of vegetation at varied stages of regeneration. Early successional zones and the interfaces between vegetation patches typically support a higher biomass of anthropogenically useful resources than late-stage communities (Smith, 2011, p. 838). These new growth patches give food plants (used by humans and other species) a competitive advantage, which can increase the carrying capacity of browsing and grazing prey species for hunting, and can also enhance hunting for burrowing animals and birds, as well as preferentially promoting wild cultivars and many other anthropogenically useful organisms (Grayson, 2001; Bird et al., 2005; Bowman and Haberle, 2010; Bowman et al., 2011; Rowley-Conwy and Layton, 2011). For example, precontact forest burning is believed to have increased populations of white-tailed deer (*Odocoileus viginianus*) in the eastern woodlands of North America (Smith, 2009, pp. 169–171). The anthropogenic use of *fire-stick farming* (Jones, 1969) in Australia has been observed to produce a greater scale diversity of successional vegetation stages than landscapes solely under a lighting fire regime (Bliege Bird et al., 2008). Bliege Bird and colleagues used ethnographic and ecological data to argue that forager niche construction in the form of off-site burning is unlikely to have had contributed to the megafaunal extinctions in Australia (which included giant forms of marsupials, birds, and reptiles). This is in part because the anthropogenic use of fire has been observed to maintain biodiversity by reducing the local extirpation of mature habitats that can occur with large-scale natural fires. The relationship between biodiversity and fire regimes (pyrodiversity) is complex however,

particularly with the influencing role of humans in manipulating the spatial scope of fires, and hence the modulation of food webs (Bowman et al., 2016). If megafauna had been constricted to refugial habitats as a result of environmental pressures (see Haynes, 2013), one could imagine that burning these critical pockets of biodiversity could easily result in the extirpation of organisms reliant on those now infrequent niches.

Assessing the ecological impact of anthropogenic fire-use in antiquity is problematic given the low palaeoenvironmental visibility of off-site fires (namely charcoal deposits, staining, and shifting palaeoecological indicators as observed stratigraphically). Distinguishing between 'natural' and anthropogenic fire is often impossible. A range of factors can significantly impact visibility, such as the spatial scale and frequency of fire-use, human population density and mobility (as in whether certain areas are repeatedly burned as part of a seasonal round or if population density is high enough to warrant extensive local burning programs), and vegetation type (as related to the propensity to generate and preserve charcoal, and how those plants respond to fire) (Scherjon et al., 2015, p. 312). Pre-Holocene evidence of anthropogenic off-site fire-use is extremely sparse, but given the taphonomic biases in identification, and the potential for taphonomic overshadowing from a natural fire regime (especially in times of rapid climate and ecological change), an archaeological assessment of fire-use in antiquity necessarily involves a substantial degree of speculation. This is particularly true with our inherently proxy understandings of past vegetation changes (Jackson, 2012) along with spatiotemporal limits that constrain the resolution of our palaeoecological understandings and hence may mute our ability to see the influences of anthropogenic fire.

It is important however to be cautious and not overstate the available evidence as to the potential for anthropogenic fire to be a significant factor in environmental restructuring. Feeney (2016) argues that claims of hunter-gatherer land management (including fire use but also pruning, coppicing, weeding, planting/transplanting, clearing, and fertilizing) are exaggerated, and that the extant historic, ethnographic, and archaeological evidence of hunter-gatherer burning practices is too sparse to justify the alleged ubiquity of such practices into deep time. Conversely, Scherjon et al. (2015)

contends that there is good ethnographic and historic visibility for the wide-spread use of anthropogenic fires in landscape maintenance, with driving game being the most frequently cited objective for landscape burning. Scherjon and colleagues highlight that this contrasts with a comparative invisibility of such practices in much of the archaeological record. There is a general positive trend correlating humans and fire incidence in the Holocene in North America (Burney et al., 2003; Bond and Keeley, 2005; Gill et al., 2009; Rule et al., 2012; Gill, 2014a), particularly when compared to the fire regime prior to c. 16,000 cal BP (Power et al., 2008). There does seem to be a trend towards increasing fires in western and eastern North America around 15,000 BP, but charcoal data overall paints a complex, heterogenous picture of changing fire regimes.

Hunting. Likely the most impactful component of hunter-gatherer niche construction in relation to the late Quaternary extinctions, be they stable or unstable adaptions, is hunting. Viewing hunting as a form of niche construction is controversial however; Pearce (2011, p. 799) argues that predation should be considered a distinct process from niche construction as trophic influences already have their own explanatory and predictive mechanisms. A case can be made though that the decisions involved in human prey selection (at least among historic and contemporary populations that target prey of high fitness and reproductive capital) differs in important ways from other predators (Darimont et al., 2015). The creation of a stable hunter-gatherer niche involves a conscientious hunting strategy, such as Ojibwa hunters who targeted juvenile or elderly beavers rather than breeding adults to facilitate population stability and long-term exploitation for generations (Speck, 1915, pp. 294–295; Dods, 2002). In this case, with culturally inherited practices positively impacting the ecological inheritance for subsequent generations in the territory of Lake Temagami, Ontario. But such long-term planning is by no means the norm. The variability in prey-selection among hunters can have dramatic but diverse trophic impacts on food webs, and in this sense can drive changing selective pressures in heritable ecological niches.

Rowley-Coney and Layton (2011) divide hunting induced niche construction into three components. First, *competitor removal*: the displacement of competitor species

within the niche either through direct hunting or from being outcompeted. Carnivores seem to stack among the earlier wave of extinctions prior to or shortly after the Last Glacial Maximum (LGM, 26,500–19,000 BP) (Clark, 2009a). *Crocuta crocuta* (spotted hyaena), *Panthera spelaea* (cave lion), *Ursus spelaeus* (cave bear), *Homo neanderthalensis* (Neanderthals) (Estévez, 2004; Banks et al., 2008; Rozzi et al., 2009), and potentially even *Homotherium latidens* (a sabretooth cat) (Reumer et al., 2003; Paijmans et al., 2017) went extinct in this peri-LGM wave in Eurasia (see Stuart, 2015), while *Arctodus simus* (short-faced bear), *Homotherium serum* (a sabretooth cat), *Miracinonyx trumani* (American cheetah), and *Canis dirus* (dire wolf) also disappear around the same time in North America. Faith and Surovell (2009) argue that this seemingly early wave of extinctions is an artifact of an inadequate palaeontological record, driven by the *Signore-Lipps effect* (Signor and Lipps, 1982). In this principle, catastrophic mass extinctions can appear gradual due to the fossil record being spatiotemporally discontinuous, with last appearance remains among multiple faunae being randomly distributed in time prior to the extinction event (see Fig. 1.2). This would make sense in the case of late Pleistocene carnivores which we would expect to be in low abundance regardless due to their trophic position, and hence more susceptible to this effect. Faith and Surovell (2009) contend that many of these species likely went extinct closer to the window observed in more abundant herbivores, around 13,000–11,500 BP (Stuart, 2015). If an earlier loss of carnivores is accurate however, humans outcompeting in a carnivore niche space may be significant as top predators are critical for moderating herbivores and promoting diversity (Van Valkenburgh et al., 2015). As mentioned previously, multiple carnivore lineages are thought to have been extirpated from Africa as the genus *Homo* evolved into a carnivore niche space (Werdelin and Lewis, 2013). And even if dispersing humans had relatively limited direct confrontations with other predators, the *landscapes of fear* (Laundre et al., 2010; Kohl et al., 2018) (spatially distributed perceptions of increased predation risk) created by humans may have had profound effects on ecosystem functioning by indirectly impacting the top down influences of predators on Pleistocene ecosystems by altering the land use and behaviours

of those organism to avoid conflict with hominins (Van Valkenburgh et al., 2015; Clinchy et al., 2016; Smith et al., 2017; Suraci et al., 2019).

Second, *niche deterioration* (Rowley-Conwy and Layton, 2011): the overhunting of high ranked species (as per optimal foraging theory) (Winterhalder, 1981) leading to reduced prey populations, altered selective pressures, or extirpation/extinction, and consequently necessitating a widening hunter-gatherer diet breadth. Human hunting can uniquely alter an inherited niche by influencing the artificial selective pressures on prey in those habitats. For example, Africa elephants (*Loxodonta* ssp.) are currently under strong selective pressures by human poachers for their ivory, which has led to an increasing prevalence of the tusklessness trait in Mozambique (Maron, 2018). While this emerging trait is still newly under investigation, one could imagine that this will impact the ecosystem engineering capabilities of these elephants, as they use their tusks for digging (to create watering holes in dry riverbeds and to expose roots), stripping bark, defense, and display. Selective pressure for tuskless elephants is uniquely anthropogenic and may result in niche deterioration for organisms that rely on the keystone engineering characteristics of tusked elephants. Rowley-Conwy and Layton (2011) highlight an archaeological example of the over-exploitation of muskox by Palaeoeskimo populations c. 3800 ^{14}C BP that arguably led to a rapid decline in human populations (Savelle and Dyke, 2002), propelling an adaptive shift from terrestrial lifeways towards full-time marine mammal hunting thereafter (Savelle and Dyke, 2009). Evidence of salmon fishing at a 11,500 cal BP site in central Alaska may suggest a widening diet breadth as a result of fragmenting terrestrial vertebrate populations (Halffman et al., 2015). Although previous isotopic evidence had suggested that Siberian populations near Beringia may have had a long history of fishing with it being estimated that 25–50% of their diet came from freshwater aquatic sources (Richards et al., 2001, p. 6259), recent isotopic work has found that mammoths were ^{15}N-enriched compared to other terrestrial herbivores, making mammoth δ^{15}N and δ^{13}C values difficult to differentiate from freshwater fish using bulk collagen (Drucker et al., 2017). Drucker et al.'s re-analysis of phenylalanine and glutamic acid ^{15}N abundances suggests that mammoths were the predominant food source on the

late Pleistocene Crimean Peninsula, which may suggest that early Holocene fishing is an instance of widening diet breadth.

Human prey selection is atypical among predators (Darimont et al., 2015; Worm, 2015; Zeckhausera, 2017). Whereas predators typically target juveniles, elderly, or evolutionarily unfit individuals, humans today prefer large, healthy adults which happen to have high reproductive capital. Darimont et al. (2015) suggest that humans are an unsustainable super-predator, which necessitate social pressures to discourage a tendency towards over-exploitation. Still today, megafauna are most threated by human predation despite large scale conservation and legal efforts aimed at managing hunting practices (Ripple et al., 2019). The atypical preference for prey of high fitness is partly driven by contemporary factors such as hunting restrictions, trophy hunting, reduced risk as a result of high-power firearms, poverty, human over-population, and a disconnection from those landscapes, which together alter prey selection and introduce a new range of artificial selective pressures (Diekert et al., 2016). However, megaherbivores that are thought to have been keystone species in maintaining Pleistocene biomes (Owen-Smith, 1987; 1988; Gill et al., 2009; Gill, 2014a) may have naïvely thought themselves immune to predation as adults from comparatively small hominins as we suspect they were from many others in the carnivore guild (le Roux et al., 2018). If humans were uniquely able to hunt these animals in ways that other local carnivores were unable, the naiveté of megafauna to uniquely human hunting practices may have resulted in significant niche deterioration of Pleistocene biomes that had been maintained by then disappearing keystone megaherbivores. This would lend credence to the *overkill hypothesis* as first proposed by Martin (Martin, 1967; 1973; 1984; Meltzer, 2015). This is especially the case if climate change had increasingly constricted megafauna to refugial habitats as a result of ecosystem deterioration (Haynes, 2013), making then vulnerable keystone megaherbivores particularly susceptible when the new ‘super-predator’ *Homo sapiens* was rapidly added to the predator guild (Ripple and Van Valkenburgh, 2010). Even if the human predation of megafauna was just focused on juveniles, and simply added an equivalent new predatory pressure to these megaherbivores, the low fecundity of non-surviving megafauna combined with already significant top down trophic pressures from highly diverse carnivores may have made

keystone megaherbivores especially at risk of extinction from changing trophic structures (Ripple and Van Valkenburgh, 2010). This could be the case, as Ripple and Van Valkenburgh argue, even with minimal climate induced habitat deterioration.

Johnson (2002) found that the long gestation periods of megaherbivores increased their susceptibility to new trophic pressures, which they observed was strongly correlated with species that disappeared during the late Pleistocene, whereas they observed that overall body size was a comparatively minor factor. Other researchers contend however that size-selective pressure against large animals was perhaps the most significant pattern indicative of the late Quaternary extinctions with these new pressures having been unprecedented in intensity since the end-Mesozoic mass extinction, 66 mya (Smith et al., 2018). Human group size also presents a divergence from the typical predator niche space where carnivores are functionally rare in healthy ecosystems. Conversely, human adaptability allows for population growth (and hence ecological pressures) well beyond that of other organisms at equivalently high trophic positions.

The final element of hunting mediated niche construction as outlined by Rowley-Conwy and Layton (Rowley-Conwy and Layton, 2011) is *niche enhancement*: which includes strategies that act to increase the number of available prey species, such as intentionally populating islands with organisms that can be hunted, or otherwise conducting landscape management practices to increase prey species availability and predictability (Matsui et al., 2005; Swadling and Hide, 2005). This niche construction behaviour would most likely be associated during the late Pleistocene with anthropogenic burning intended to encourage early succession habitats for optimal hunting. There is a close association with the increase in human populations in eastern Beringia and the replacement of grassland grazers *Mammuthus* and *Equus* with the mixed forest browsers *Alces* and *Cervus* (Conroy et al., 2020).

Members of Cervidae tend to prefer early succession (and edge) habitats, with an increased fire regime having been observed to improve cervid (deer) populations (Carlson et al., 1999; Smith, 2009; Swanson et al., 2010; Cooley et al., 2019). Increased fire regimes have been observed in Alaska (Higuera et al., 2009), North America (Robinson et al., 2005; Gill et al., 2009), Australia (Rule et al., 2012), and Madagascar (Burney et al.,

2003) during the Pleistocene-Holocene transition, with each being spatiotemporally associated with the extinction of megafauna and the arrival of humans (Bond and Keeley, 2005; Gill, 2014a). The ordering of an increased fire regime, human dispersals, the transition of Pleistocene mosaic steppe ecosystems to shrub tundra and eventually forests, the disappearance of browsing megafauna, the Younger Dryas cold interval (Alley, 2000; Haynes, 2013; Seersholm et al., 2020), and the arrival of cervids largely overlap spatiotemporally in Beringia. However, it is probable that humans at least contributed to an increased Holocene fire regime with the aim (in part) of promoting easier access to game in their niche. Big game are costly and comparatively inefficient targets for net calorie gain to due low success rates while hunting, high pursuit time, and high butchering/transport time (Lupo and Schmitt, 2016). Big game hunting is not nearly as efficient as targeting small-to-medium sized organisms (with cervids being ideal prey for humans), which may have driven a tendency towards promoting habitats for non-megaherbivore species. However, net calorie gain is not the sole factor determining prey selection. It is likely that hunting for social, spiritual, and political reasons, such as documented among historic Aleutian whaling societies (Lantis, 1938; Black, 1987), was another significant component that drove the practice of big game hunting in the Pleistocene, even when it was suboptimal from an optimal foraging perspective (Speth, 2010).

Man the hunted. Despite increasing claims of humans being super-predators, our diet clearly indicates that we did not evolve to become apex carnivores (Bonhommeau et al., 2013). While human diets vary considerably across the globe, our human trophic levels range on average between ~2–2.6, converging globally around 2.4 today. On this scale, 1 refers to primary producers (plants), while 2 indicates herbivores (such as *Bos taurus* [cattle]). Apex predators such as *Ursus maritimus* (polar bears) and *Orcinus orca* (killer whales) have a trophic level of ~5.5. Even regions with high meat diets (Iceland, Scandinavia, Mongolia, and Mauritania) have trophic level averages between 2.5–2.8 (Bonhommeau et al., 2013, fig. 2). There are many exceptions to this trophic position, such as the Inuit who have historically subsisted on a predominantly marine mammal diet,

as well as populations who exploit a high proportion of high trophic marine food sources (Nieblas et al., 2014; Roopnarine, 2014). So while human diets do vary considerably, and in some environments occupy tertiary and even arguably apex predator positions, our omnivorous consuming practices make us more equivalent in dietary trophic position on average to Engraulidae (the anchovy family) and *Sus* ssp. (pigs) (Bonhommeau et al., 2013). These averages oversimplify the immensely adaptable complexity of the *Homo* omnivore, but it does highlight another potential reason for the seeming preponderance of megafauna at archaeological sites: we have spent most of our evolutionary history in the middle of the food chain, both as a hunter, but much longer as the hunted (Hart and Sussman, 2009). Removing the threats of large animals—be they megaherbivores or mega-carnivores/omnivores—allows us to utilize our inheritable niches more fully by being free of the *landscapes of fear* big animals can create (in this sense, by reducing the perception of risk on a landscape).

The notion of 'big game' hunting during the Pleistocene comes with an array of taphonomic and archaeological biases (Surovell and Waguespack, 2009), but there is nevertheless a pronounced trend towards big game specialization despite the high risks and non-optimal costs associated with the practice (Lupo and Schmitt, 2016). As a potential contributing factor beyond spiritual and prestige motivations, I posit that a landscape without predators and megaherbivores may have been selected for by sociocultural niche construction. Stolzenburg (2008) in his book *Where the Wild Things Were: Life, Death, and Ecological Wreckage In A Land Of Vanishing Predators* details multiple accounts wherein residents were frequently upset at even the suggestion that predators (such as wolves and coyotes) or megafauna be reintroduced to local ecosystems for rewilding efforts. As a personal anecdote to this, bobcats (*Lynx rufus*) have recently been able to re-establish themselves in my childhood community in northwest Calgary (Alberta, Canada) due to the establishment of large nature conservation areas. Since bobcat populations have increased throughout the city, there have been growing concerns among residents regarding the safety of their children and pets with even one 70-year-old woman having been mauled by one of the cats in her backyard in 2019. These concerns

are admittedly concentrated among contemporary, Eurocentrically biased populations that cannot be generalized to indigenous or ancient peoples.

Nevertheless, the presence of megacarnivores and megaherbivores on a landscape does impact one's perception of risk; "one never sleepwalks through grizzlyland" (Stolzenburg, 2008, p. 217). While many who are sympathetic to ecological science champion the reintroduction of wild animals, such as in the case of reintroducing wolves to Yellowstone National Park that resulted in surprisingly large scale ecological transformations (Smith and Ferguson, 2012), many who actually live in environments with those animals can be unsympathetic to the broader importance of those creatures when their own safety is threatened (at least among European settler populations). People are often understandably more concerned with the risks big animals pose to their families, themselves, their livestock, and their lifeways, which can result in people going out of their way to remove predators or other megafauna (such as wild horses in the Americas) from their local area. The oft-quoted exclamation from Alfred Russel Wallace (1876, p. 150) "we live in a zoologically impoverished world, from which all the hugest, and fiercest, and strangest forms have recently disappeared…" typically ignores the second half of that sentence "…and it is, no doubt, a much better world for us now they have gone." The western world today, perhaps more than ever, is cripplingly averse to the liability of any risk threatening human life. It is not hard to imagine that if our growing technological sophistication unlocks the potential for *de-extinction* to bring back Pleistocene megafauna (Shapiro, 2015) or even if rewilding efforts grow in their scale and scope, there will be immense public pushback due the dangers (both physical and economical) that big animals pose. The disproportionate positive impacts big animals (including carnivores) have on ecosystems would likely be quickly forgotten once just a few formerly safe residents are killed and eaten by the giants of the ice age. Wolves, for example, were nearly eradicated from Europe and western North America due to human persecution, and predators throughout the world are routinely shot and trapped by farmers when their livestock are threatened. This persecution is of course not universal, as indigenous peoples around the world, and notably throughout the Americas, had complex

and at times remarkably empathetic relationships with otherwise dangerous organisms in their local environments. But the degree to which historically observed compassionate and wise relationships with local organisms can be extended to highly nomadic Pleistocene hunter-foragers is far from obvious.

Despite our high-minded ideals today, and immense, disproportionate powers over the *Earth System*, humans have spent much of our evolutionary history as prey, and our fear response and behaviours echo this legacy of having evolved to live somewhere in the middle of the food chain (Hart and Sussman, 2009). The evolution of throwing (Roach et al., 2013) and the sociocultural niche system may have moved humans up trophic levels faster than our amygdala (and associated threat perception systems) had the chance to adapt to our new 'hyper-predator' role. In this sense, even if megafauna were not ideal choices from an optimal foraging perspective for net calorie gain, eliminating these organisms (directly or indirectly) helped to form our inherited ecological niche. Formerly dangerous landscapes that may have fear-limited our lifeways are now comparatively size-downgraded (Smith et al., 2018) to such a degree that few humans today in the developed world regularly concern themselves with the possibility of being killed and eaten amidst their daily activities.

Niche construction theory contributes a context to this dissertation as to how and why humans may have disproportionally accelerated the restructuring of the biosphere in deep time, and aids in understanding the potential legacy of an alleged *Anthropocene*. Hunting is but one already intricate component of the human behavioral suite that may have contributed towards the size-downgrading of terrestrial fauna at the end of the Pleistocene. Niche construction aids in conceptualizing how ancient peoples in Beringia with otherwise low archaeological visibility may have affected palaeo-ecosystems in complex and multifaceted ways that may be unseen with the data resolution derived from traditional analyses of macro-remains. This highlights the benefit of further developing higher resolution palaeo-ecological techniques, in this case via ancient biomolecules, to maximize the information potential of incomplete buried records. The inheritance of contemporary Holocene niches has had significant ramifications on the situation

humanity finds itself in today. Understanding the processes that led to our current predicament can allow us to make mindfully informed decisions moving forward as to how we wish to influence the evolution of Earth's future biosphere.

1.3 A primer on the Pleistocene-Holocene transition in eastern Beringia

The palaeoecology and archaeology of Beringia during the Pleistocene-Holocene transition is discussed in the background section of chapter 4. For the sake of non-redundancy, I will limit the discussion here to a general, big picture contextualization on the significance of the late Quaternary extinctions on our contemporary Holarctic ecosystems, of which humans are a part. Thereafter, I discuss the Younger Dryas cosmic impact hypothesis, the hyper-disease hypothesis, the visibility problems of archaeology in the northwestern subarctic, and outline a general culture-historical framework for the Beringian Period through to the Northern Archaic.

Sergey Zimov is the co-founder of Pleistocene Park (https://pleistocenepark.ru/), an initiative to experimentally restore the mammoth steppe ecosystem of the late Pleistocene in a remote region of arctic Siberia through the promotion of high densities of large herbivores (Zimov, 2005) (see Fig. 4.3). The project is intended to test the hypothesis that high animal densities lead to the high productivity phenomenon of the mammoth-steppe biome that existed throughout the Pleistocene (Zimov et al., 2012a; 2012b; Zimov and Zimov, 2014; Zhu et al., 2018). This now extinct ecosystem once stretched across Eurasia from Iberia to the Americas, supporting huge densities of animals through a mosaic of steppe grasslands and wood-pastures, which are believed to have been analogous to the modern African savannah ecosystem. The animals that engineered this ancient ecosystem seem to have thrived through as many as 52 cold and interspersed warm periods during the last 2.6 million years of the Pleistocene (Cohen and Gibbard, 2010), only to have disappeared from the record at the onset of our current Holocene epoch. This defaunation has left northern ecosystems comparatively devoid of much megafaunal biomass, with the now dense closed forests of the taiga/boreal and desert of the arctic tundra severely limiting the biological productivity that these seemingly harsh northern landscapes once supported. The high Pleistocene biomass of the

mammoth-steppe is believed to have been supported by megaherbivore ecosystem engineering and a high rate of nutrient bio-cycling that is comparatively lacking in the arctic and subarctic today. Zimov et al. (2012a) estimate that every square kilometer of Pleistocene arctic Siberia supported an animal density of approximately 1 mammoth, 5 bison, 7.5 horses, 15 reindeer, 0.25 lions, and 1 wolf. These estimates are based on dense assemblages of megafaunal bones recovered from Pleistocene permafrost, dating from >45,000–13,000 BP. Along with the other more uncommon herbivores, they estimate that each km^2 of arctic Siberia could support a herbivore biomass of 10.5 tons, which is sufficient to feed ~2 wolves. This stands in stark contrast to the biodiversity in Siberia today (Zimov et al., 2012b, p. 199):

> *If one were to travel through the entirety of Siberia from south to north… one would likely not meet any big animals. Using snowmobiles, boats, [and] helicopters, we have travelled tens of thousands of kilometers along the Siberian north, and although looking carefully we have seen only eight bears, two wolves, two lynxes and one wolverine. It could be assumed that this territory is too severe to sustain many large mammals. But that is not true.*

This last line is borne out by both the palaeontological record, as well as Sergey and his colleagues continued success with Pleistocene Park. This once seemingly inhospitable region of arctic Siberia now supports intermingled grazing herds of yakutian horse (*Equus caballus*), moose (*Alces alces*), reindeer/caribou (*Rangifer tarandus*), muskox (*Ovibos moschatus*), yak (*Bos grunniens*), European bison (*Bison bonasus*), Kalmyk steppe cattle (*Bos taurus*), and Kalmyk sheep (*Ovis aries*). Status quo bias might lead us to believe that the north is characteristically inhospitable to much animal life—that dense coniferous forests and barren tundra are expected of such northernly regions. But buried records and the ongoing experiments at Pleistocene Park demonstrate that this perception is only true in recent history. “Northern Siberia has become a desert due to human action” (Zimov et al., 2012b, p. 199). As Zimov and others contend, there is reason to suspect that humans

are the unique and ultimately responsible factor for the zoological impoverishment of our current interglacial epoch.

1.3.1 Penultimate inter-glacial

If however climate change and the resulting loss of the mammoth-steppe biome are to blame for the late Quaternary extinctions (LQE), it becomes difficult to understand the successful adaptation of megafauna to as many as 52 cold and interspersed warm periods during the last 2.6 million years of the Pleistocene (Cohen and Gibbard, 2010). There are reasons to suspect that the last glacial/interglacial transition may have been uniquely severe compared to others throughout the Pleistocene (that were each likely unique in their own ways), and that not all megafaunal lineages had experienced each of the previous transitions (Meltzer, 2020). Further, we cannot assume that these linages were unaffected by such major climatic oscillations, as perhaps pulses of expansion and contraction with cyclical ice ages were typical throughout the Pleistocene (Karpinski et al., 2020). Disentangling the climatological and anthropogenic components of the Pleistocene-Holocene transition would likely be greatly aided contextually by understanding to what degree cold-adapted megafauna were impacted during previous rises in global temperature. A key area of inquiry moving forward are palaeoecological and palaeodemographic analyses of organisms through the Eemian/penultimate interglacial or Marine Isotope Stage 5e (MIS-5e) (130,000–115,000 BP) (Shackleton et al., 2003; Dahl-Jensen et al., 2013).

The retraction of the mammoth-steppe and expansion of woody shrubs and trees is not a uniquely Pleistocene-Holocene phenomenon, as the taiga advanced substantially during MIS-5e in Siberia, transitioning local ecologies from a tundra biome (likely similar to the mammoth-steppe) towards a conifer forest that lasted the duration of the interglacial (Tarasov et al., 2005). This would suggest that the advancement of the taiga is not a Holocene phenomenon tied to the loss of megafauna, but rather a feature of interglacial periods. However, Sandom et al. (2014b) argue that forests were more mixed and semi-open during MIS-5e in Europe on the basis of beetle assemblages (used as palaeoenvironmental proxies) and contend that a mosaic of forest and wood-pasture

existed with the presence of megafauna. Likewise Kienast et al. (2011, p. 2153) suggest that the taiga during MIS-5e was more similar to early Holocene environments as open forests first began to expand throughout the mammoth-steppe, as compared to the old growth boreal that exists today. The taiga treeline has been observed to be ~270 km further north in arctic Siberia during MIS-5e than its Holocene extent, which may have been the result of megafaunal ecosystem maintenance (Doughty et al., 2015), or due to higher temperatures and precipitation during the penultimate interglacial (Turney and Jones, 2010; McKay et al., 2011). The boreal is also observed to have been more extensive during the last interglacial in Yukon and Alaska (Muhs et al., 2001). However, arctic ground squirrel nests from MIS 5e suggest that there were disjunct interglacial refugia during this period wherein steppe-tundra flora and fauna persisted until cold, arid glacial conditions returned (Zazula et al., 2011). One wonders whether similar high latitude interglacial refugia may have formed during the last glacial/interglacial transition that otherwise could have persisted until the next glacial period.

1.3.2 Extra-terrestrial impact and hyper-disease

The aptonymic Richard Firestone (Firestone et al., 2007) proposed that the Younger Dryas stadial may have been the result of extraterrestrial (ET) impacts ~12,900 years ago, contributing to both the LQE and the disappearance of the Clovis 'culture'. This was based on evidence allegedly indicative of an ET impact immediately pre-dating the Younger Dryas, including: magnetic grains with iridium, magnetic microspherules, charcoal/soot, carbon spherules, glass-like carbon containing nanodiamonds, and fullerenes with ET helium. They suggest that one or more, low-density ET objects impacted or airburst over the Laurentide ice sheets in Canada, as well as in South America, Europe, and western Asia, triggering extensive biomass burning, an impact winter due to ejected atmospheric dust that blocked solar radiation, and the abrupt return to glacial conditions with the Younger Dryas. The proposal has in large part been rejected (Pinter et al., 2011b; Pigati et al., 2012; Holliday et al., 2014; 2016; Meltzer et al., 2014; Daulton et al., 2017), with some support (Petaev et al., 2013; Wolbach et al., 2018; Pino et al., 2019; Moore et al., 2020), and others reporting mixed, but skeptical reviews

(LeCompte et al., 2012; Van Hoesel et al., 2014). Some of the main critiques revolve around reproducibility, whether the markers identified by the various authors are diagnostic of ET impacts or have other plausible explanations, and inconsistent stratigraphy and dating (Van Hoesel et al., 2014). Pinter et al. (2011b) are particularly critical of the impact hypothesis, and the shifting claims of supporting evidence. At this time, it is difficult for me to properly weigh the counterclaims without an understanding of the intricate mineralogical data being discussed. Overall, it would seem based on a series of robust critiques that the Younger Dryas ET impact hypothesis is unlikely to be the most plausible explanation for the LQE. However, ongoing research claiming to have supporting evidence of high-temperature melting and extensive biomass burning at the onset of the Younder Dryas continues to complicate the debate (Wolbach et al., 2018; Pino et al., 2019; Moore et al., 2020). Ancient environmental DNA may be able to contribute towards determining whether there were rapid shifts in the taxonomic structure of these ecosystems immediately following the alleged timing of ET impacts at the onset of the Younger Dryas. There are indications in chapter 4 that the Younger Dryas is associated with the flatlining of megafaunal sedaDNA, a result in need of further investigation to evaluate the veracity of the cosmic impact hypothesis as being a significant contributor to the LQE.

Another hypothesis proposed to account for the LQE is hyper-disease (MacPhee and Marx, 1997). In this conception, an epi- or panzootic infectious disease (or eukaryotic parasites) with a potential human or canid reservoir may have been a causative agent in the mass extinction of Pleistocene megafauna. Such a pathogen may otherwise be significantly underestimated through palaeontological records (MacPhee and Greenwood, 2013). The presence of disease in terminal populations has found some support in *Mammut americanum* faunal remains (Rothschild and Laub, 2006), and infectious disease has been identified as a partial or wholly causative agent in the historic extinction of the Christmas Island rat (*Rattus macleari*) through ancient DNA (Wyatt et al., 2008). There are multiple examples of modern and historic fauna being significantly impacted by disease (MacPhee and Greenwood, 2013), but to date the notion that disease made a

significant contribution to the LQE has little support (Lyons et al., 2004). This is in part due to the unlikelihood of finding evidence of such a pathogen in the Pleistocene, in addition to the hypothetically broad range of potential hosts with an unusually high lethality rate. It is plausible that disease was a contributing factor to the LQE to some degree and in some taxa, but currently, the proposal lacks supporting evidence. Ancient DNA is likely to be key to finding such evidence in Pleistocene faunal remains if it exists.

1.3.3 Limits of archaeological visibility in northwestern subarctic

Richard MacNeish (1959) was one of the first to culture-historically organize Yukon and Alaska's archaeological record with his creation of the British Mountain, Cordilleran, Yuma, and Northwest Microblade Traditions. But a lack of chronological structuring from this early effort limited the utility of these entities for explaining the material-culture being recovered from the area (Goebel and Buvit, 2011b, pp. 4–5). Hadleigh-West (1967) followed MacNeish with his formulation of the Denali complex, but it was not until the discovery of the deeply stratified Onion Portage site in Alaska that a degree of chronological control could be achieved in Beringian culture-history (Anderson, 1968). By the mid-1970s, there were at least fourteen archaeological complexes and six traditions classifying predominantly lithic assemblages relegated solely to the late Pleistocene and early Holocene (Goebel and Buvit, 2011b, p. 12; Wygal, 2018). This abundance of cultural-historic entities and lack of consensus regarding the region's chronology mirrored the growing realization that, by the 1970s, the record of the northwestern subarctic was far more complex than initially conceived by MacNeish (see Table 1.1 and Fig. 1.3).

There are multiple factors that contribute to the challenges in understanding the culture-history of the western subarctic (Ives, 1990, pp. 310–311). The first is poor preservation—this severely restricts the kinds of materials capable of entering the archaeological record. Subarctic soils are slightly acidic due to the percolation of water through dense coniferous litters (Fenn et al. 2006). This acidity tends to result in the degradation of organics, resulting in a taphonomic bias towards lithic tools and an absence of palaeobotanical and faunal materials. The second problem is disruptive post-

depositional processes that disturb provenience, resulting in a flattening or mixing of components. Examples of this in the subarctic include cryoturbation and bioturbation (with both floralturbation and faunalturbation being relevant factors). This is combined with the third problem—that many subarctic archaeological sites are found in low-depositional contexts (or surface finds) relative to the age and vertical distribution of artifacts. This impression may be due to a survey bias, site survival, or an actual historic tendency. Together though, post-depositional processes and a tendency towards low-deposition contexts greatly restrict the ability to stratigraphically define a chronological culture-history for the area; a few centimeters at many sites represents thousands of years. Even when datable organic remains are discovered, they are accompanied by the pervasive problem that the artifacts and radiometrically dated materials may not be contextually associated.

The final factor discussed by Ives (1990, p. 311) is the cultural tendency towards an efficient and ephemeral Athapaskan material culture that is often archaeologically invisible, and with few of those surviving tools being sensitive to cultural evolution. Ethnographic accounts for the use of minimally modified materials or those unlikely to survive and become part of buried records, such as the use of snares and deadfall as hunting traps (Wentzel, 1889; Keith, 1890), give some insight into the poor archaeological visibility of subarctic lifeways. Aspects like hearth construction were relatively expedient—they were often not excavated, rock lined, or used for long periods of time—making it difficult to differentiate these features from soils stained by otherwise commonplace natural fires. Other factors include low site visibility and a relatively small amount of work conducted to date compared with other culture areas (Holly, 2002, p. 10). This is exacerbated by geographic remoteness and sparse modern population centers that make fieldwork in Siberia, Alaska, the Yukon, western Northwest territories, and northern British Columbia/Alberta/Saskatchewan expensive and logistically challenging. A significant amount of grey literature exists that has been conducted by cultural resource management (CRM) consultants in the northern Albertan oil sands and throughout much

of the northwestern subarctic; but accessing and compiling these resources adds another layer of challenge to the analysis.

Holly (2002, p. 15) contends that a perception of environmental constraint on subarctic peoples has influenced why subarctic archaeology remains arguably ahistorical and acultural. Spaulding (1946) argued that the boreal forest was so constraining that it acted as a filter that eliminated cultural variability. This was said in regard to the actual cultural diversity of subarctic peoples in the past, but I would argue that another interpretation of the statement may be that the boreal forest acts as a homogenizing force in the archaeological record, severely muting our impressions of past diversity among subarctic peoples by limiting archaeological visibility to predominantly stone tool technologies and their minimally varying styles and functions.

This coarse record of subarctic archaeology has been greatly aided in recent years with the discovery of alpine ice patches and their remarkably well-preserved archive of archaeological and palaeontological remains (Kuzyk et al., 1999). These alpine cryospheric features form due to the gradual accumulation of snow as it is compressed into lenses (Meulendyk et al., 2012). Unlike glaciers, ice patches do not build enough mass to flow (Glen, 1955). They range from ~100–1000 m in length, ~10–80 m in width, and ~0.1–4 m in thickness (Meulendyk et al., 2012, p. 43). Caribou (reindeer, *Rangifer tarandus*) have been documented to use these features for summer thermoregulation and for relief from insect harassment (Ion and Kershaw, 1989; Anderson and Nilssen, 1998; Kuzyk et al., 1999). Humans have been aware of this behaviour since nearly the earliest concentrated occupations of eastern Beringia, which lead to the exploitation of alpine ice for caribou hunting for at least some 10,000 years. Personal items and hunting implements lost over thousands of years of caribou hunts remain preserved in these alpine ice features, which in the Yukon alone has resulted in the discoveries of over 100 dart and arrow shafts with attached sinews and feathers, over 1700 faunal remains, a moccasin, bow fragments, and more than 200 other archaeological objects (Hare et al. 2012). In contrast to the almost entirely stone assemblages of typical subarctic sites, over 95% of archaeological materials from ice patch sites have wooden components (Andrews and

MacKay, 2012). This highlights the ephemerality of Athapaskan material culture that is not well suited to archaeological preservation. Due to the effects of climate change, ice patches in the subarctic have been ablating at an increasing rate (Andrews and MacKay, 2012; Andrews et al., 2012), exposing biological materials for recovery from survey teams, but also leading to the complete degradation of many incredibly important ice patch sites. These UNESCO nominated world heritage sites have become critical and increasingly endangered archaeological archives of subarctic heritage, which will likely become increasingly important in understanding the lifeways of subarctic peoples that in many respects have been obscured by time and taphonomy.

These limits of archaeological visibility in much of the subarctic have the potential to be augmented with ancient environmental DNA wherein otherwise unbeknownst biomolecular remnants may be able to increasingly fill-in many of the cultural-historic holes of the region's buried records. Therein, allowing for a new perspective to understand when and how people lived in the seemingly severe Beringian landscape during the coldest periods of the last ice age. This context also helps inform how even if we have poor archaeological visibility of people in Beringia during the LQE, people may have still been in the region disproportionally influencing palaeoecosystems in ways that have been largely invisible to archaeologists to date.

1.3.4 The Beringian Period

Holmes (2001, p. 156) divides the earliest occupations of the eastern Beringian interior (Alaska/Yukon) into two periods (see Fig. 1.3). First, the Beringian Period (late Pleistocene to ca. 13,000 cal BP) to categorize the period when hunter-gatherers first reached Beringia—the eastern most edge of mammoth-steppe ecosystem buttressed against the Cordilleran and Laurentide ice sheets in North America—which is also a time when there remained a land (and likely cultural) connection between Alaska and Siberia. These Palaeoamerican sites tend to include burins and microblade lithics that tie these people to the Dyuktai culture of Pleistocene Siberia (Mochanov and Fedoseeva, 1996). The second, the Transitional Period (ca. 13,000–9,000 cal BP) (Holmes, 2001; 2008) follows as migrants from Siberia and potentially the northern Japanese (Hokkaido)

palaeo-peninsular area (Kobayashi, 1970; Chen, 2007; Buvit and Terry, 2015) are progressively cut-off from their east Asian contemporaries due to an inundation of the Bering land bridge. It is during this transition when the megafaunal extinctions peaked and when there was significant climate change with the return to glacial conditions during the Younger Dryas, which was followed thereafter by rapid warming and the beginnings of forestation, along with the development of regional east Beringian lithic technologies.

Within these two broad periods are a variety of cultural traditions (see Table 1.1). The East Beringian Tradition is divided into two intervals (Holmes, 2001, p. 162; 2011; Dumond, 2011, p. 351). The first, older than 13,500 BP, refers to the earliest Northeast Asian inhabitants of Alaska and Northern Yukon who used unmistakable Asian technologies—blades and microblades produced with the Dyuktai or Yubetsu techniques (Morlan, 1967; Kobayashi, 1970; Flenniken, 1987; Sato and Tsutsumi, 2007, p. 57). The second, between 13,500 BP and 11,500 BP, which includes the appearance of bifacial lithic technologies and the differential use of microblades (Holmes, 2001, p. 162). The Transitional Period is regarded as one of differentiation in Alaska. Ecological restructuring during this period may have precipitated the development of the Nenana and Mesa complexes (north Alaskan bifacial lithic sites most commonly without microblades) (Kunz and Reanier, 1994), in addition to the development of the American Palaeoarctic Tradition (northwest Alaskan sites with microblades) (Anderson, 1968; 1984), and the Denali Complex (central Alaskan sites with microblades) (West, 1967; 1975; Cook, 1969; 1996). There is still ongoing debate around the differential spatiotemporal presence of bifacial lithics (Nenana) and microblade (Denali) technocomplexes in eastern Beringia (Wygal, 2018), which have complicated Beringian culture-history and our understandings of the peopling for decades (Anderson, 1970; Clark, 2001; Dumond, 2011; Goebel and Buvit, 2011a; Wygal, 2011). This could be related to contemporaneous cohabiting groups, differences in site type (e.g., seasonality, specialization, ecozone [lowland/montane/alpine]), variable evolution in technological style and function, intra-assemblage variability obscured by recovery bias (e.g., a statistical artifact of inadequate sample sizes), or distinct populations with non-contemporaneous periods of occupation

(Goebel and Buvit, 2011b; Wygal, 2018). A historic lack of communication between Canadian, American, and Russian archaeologists has also contributed towards discontinuous chronologies and archaeological entities (e.g. phases/complexes/traditions) in Beringian archaeology.

The Cordilleran ice sheet is considered to have withdrawn from southern Yukon between 10,000 and 8000 BP (Hart and Radloff, 1990, p. 3), with the draining of proglacial lakes by 8000–7100 BP (Hughes, 1990, p. 13). Rainville and Gajewski (2013) found evidence of birch-shrub (*Betula*) tundra in the southern Yukon ca. 10,900 cal BP, and the establishment of white spruce (*Picea glauca*) by ca. 10,200 cal BP. This adds to other work in the Yukon that has found evidence of the boreal forest having established by ca. 10,400–8300 cal BP (Stuart, 1986; Cwynar, 1988; Wang, 1989; Wang and Geurts, 1991a; 1991b; Keenan and Cwynar, 1992; Lacourse and Gajewski, 2000; Whittmire, 2002; Bunbury and Gajewski, 2009a). The Cordilleran and Laurentide ice sheets merged east of the Mackenzie Mountains during the Last Glacial Maximum, which left the development of the mouth of the ice-free corridor primarily within central Yukon and the western Northwest Territories (Dyke, 2004). There is the possibility of migrations into the Americas through either a Pacific Coastal route, the ice-free corridor, or a combination thereof with some migrants potentially also using the ice sheets as highways for rapid movement (Cruikshank, 2005; Murchie, 2015; Potter et al., 2018).

Holmes (2008:71–72) defines the onset of the Taiga Period around 9500 BP with the establishment of a boreal forest. This culturally denotes a long and gradual transition towards Northern Archaic lifeways with the development of varied bifacial and notched lithics for use with atlatl and eventually bow-and-arrow technologies. However, there is very little archaeological evidence of human habitation in the northwestern subarctic once the boreal had established until around 6000 BP (Holmes, 2008). One wonders whether the extreme sparseness of archaeological sites during this early Taiga period is a result of taphonomic biases, or whether human habitation in the northwestern forests became undesirable following the disappearance of megafauna with the unchecked growth of the boreal in the wake of their functional extirpations.

1.4 Ancient environmental DNA

Ancient DNA (aDNA) has become a revolutionary method within many facets of Quaternary science. Micro-methods as a whole have come to redefine the informational potential of ancient remains far beyond their morphology and provenance (Swift et al., 2019). Ancient biomolecules can be recovered from discrete materials such as bone, teeth, and floral remains such as seeds, as well as admixed materials such as palaeo-feces, gut contents, and dental calculus (Rawlence et al., 2014). These sources of ancient biomolecules allow for investigations into the evolutionary history of long dead organisms with orders of magnitude more resolution than ever conceivable with traditional palaeontological and archaeological techniques (Shapiro et al., 2004; Gilbert et al., 2007b; Green et al., 2010; Bos et al., 2011; Meyer et al., 2012; Enk et al., 2016; Graham et al., 2016; Karpinski et al., 2020). The field continues to develop rapidly, with one of the burgeoning new subfields being ancient environmental DNA where genomic-level data from entire ecosystems can be recovered from samples as inconspicuous as soils and sediment—even in the total absence of surviving biological tissues (Taberlet et al., 2018).

One outcome of the high-throughput sequencing revolution was the recognition that environmental DNA (eDNA) recovered from water and soil could be used to monitor ecological biodiversity (Thomsen and Willerslev, 2015). eDNA—the complex mixture of degraded, metagenomic molecules from organisms at both the macro and micro-scale—is a relatively new focus in molecular ecology, and particularly within the short history of aDNA research that began in the 1980s (Hunan Medical Institute, 1980; Higuchi et al., 1984; Pääbo, 1985b; 1985a; 1989). eDNA first emerged as a subject among microbiologists in the early 2000s. They sought to identify environmental microbial taxa, understand biochemical gene function, and to assemble bacterial genomes for uncultivable microbiota (Taberlet et al., 2012). Shortly thereafter, an understanding of the broader utility of these disseminated biomolecules arose from aDNA researchers who began to discover that we can directly extract DNA from sedimentary strata (e.g. soils, sediment, palaeosols, ice, tephras) to understand past macro-ecosystems (Hofreiter et al.,

2003; Willerslev et al., 2003a; 2004a). The field has since rapidly ballooned (particularly after 2010) with increasing technological sophistication to study a variety of ecological and buried contexts, although high-latitude and high-altitude areas remain the optimal zones for eDNA preservation in deep time due to perennially cold conditions. This makes ancient environmental DNA an ideal biomarker for studying long term ecological restructuring in Beringia if we can effectively access those biomolecules. It also makes this biomarker ideal for understanding the potential legacy of the *Anthropocene* in high-latitude/altitude regions throughout the globe.

1.4.1 Terminology

Palaeoenvironmental DNA (PalEnDNA) refers to aDNA originating from multiple disseminated genetic sources as recovered from environmental (metagenomic) samples (Rawlence et al., 2014). Rawlence et al. (2014, p. 611) advocate for the use of the term 'PalEnDNA' to mitigate the growing ambiguity in metagenomic terminology. For example, the common use of 'sedimentary' ancient DNA (sedaDNA) (e.g. Alsos et al., 2015), which technically precludes tephras and palaeosols. Other examples include: the use of 'eDNA' to refer to environmental aDNA (e.g. Hebsgaard et al., 2005; Pedersen et al., 2016), which is problematic because 'eDNA' is typically reserved for modern samples; 'lake sediment DNA' (lake sedDNA), which excludes other kinds of sediment (Giguet-Covex et al., 2014); and 'dirt DNA' (Willerslev and Cooper, 2005; Hebsgaard et al., 2009) which is colloquial and technically limited to soils or palaeosols. 'PalEnDNA' is intended to include a range of environmentally 'disseminated materials'. Rawlence et al. (2014, pp. 611, 614) further argue for the inclusion of palaeofeces, gut contents, and dental calculus within the 'PalEnDNA' umbrella, as despite technically being discreet materials, the analysis is inherently metagenomic. I agree with consolidating terminology, although I think 'sedaDNA' retains utility when specifically referring to ancient sedimentary sources of environmental DNA despite the technical, and unintended exclusion of certain types of strata (namely palaeosols and tephras). Also, sedaDNA is much easier to say and read compared with PalEnDNA.

1.4.2 Authenticity

Authenticity has been a fundamental concern in aDNA since its 'childhood' (Brown and Barnes, 2015, pp. 144–147). Despite significant and rapid advances in sequencing technologies, determining whether a set of sequenced DNA reads are accurate genetic proxies of past organisms and not a result of contamination remains a substantial hurdle. This has maintained a hyper-critical perspective within aDNA since the extent and substantiveness of biomolecular degradation and contamination were first identified (e.g. Zischler et al., 1995). Both endogenous and exogenous molecules are targeted when preparing a DNA library. This has shifted means of evaluating the veracity of sequence data from a set of standard criteria (Cooper and Poinar, 2000; Willerslev et al., 2004a) in the era of PCR and Sanger sequencing, towards bioinformatic identification and exclusion in the era of high-throughput sequencing (Marciniak et al., 2015, pp. 30–31). Research targeting palaeoenvironmental DNA is further challenged in establishing authenticity without discrete materials (e.g. bone, teeth, soft tissues) for independent verification (Rawlence et al., 2014). Establishing the veracity of this data is critical; if those molecules are not reasonably demonstrated to be autochthonous (in primary context) with the host deposit, there is the pervasive chance that the analysis will succumb to false-positive results and inaccurate palaeoecological reconstructions.

Research has been carried out on the potential for leaching (Haile et al., 2007) and re-worked strata (Arnold et al., 2011) to conflate ecological signals from sedaDNA. These factors are discussed in Chapter 4 (4.2.3). In summary here, permafrost (the sample-type targeted in this dissertation), is susceptible to the erosion and redeposition of old sedaDNA in younger stratigraphic contexts, while it is thought that leaching (the vertical free movement of sedaDNA) is minimal in perennial frozen ground. However, the degree to which allochthonous sedaDNA (biomolecules in a secondary context) is problematic is likely highly contextual (Hebsgaard et al., 2009). Andersen et al. (2012, p. 1977) found strong correlations between the extent of leaching with stratigraphic structure, texture, chemistry, and particle size, as well as biotically with animal population density, biomass, and the quantity and type of primary tissue input. So while

leaching is broadly considered to not be a significant problem in permafrost conditions (D'Costa et al. 2011; Haile et al. 2009; Hansen et al. 2006; Johnson et al. 2007; Willerslev. et al. 2003, 2004), it remains important to carefully consider the potential extent of leaching. It would be a mistake to assume that certain environments are free from these processes without a sufficient local assessment. Although unfortunately the complementary optically stimulated luminescence (OSL) dating technique could not be combined with ^{14}C at the permafrost study sites under investigation here, we utilized cores from multiple sites with multiple environmental targets to aid in building a case for stratigraphic integrity (as detailed further in Chapter 4).

1.4.3 Unknowns of palaeoenvironmental DNA

There are many unknowns associated with eDNA preservation in sediment (Arnold et al., 2011, p. 418). The first is the proportion of sedaDNA molecules retained in partially degraded 'primary' tissues (e.g. leaves, roots, pollen, dung, skin), reworked 'secondary' biological sources, or those that have been otherwise been absorbed or transformed by soil microbes. Secondly, it is still in question whether sedaDNA is primarily cellular or extracellular, and whether those nucleic molecules are mostly free or particle-bound in the burial environment. It is generally thought that much of the surviving sedaDNA we can access is preserved in the absence of tissues though the formation of organo-mineral complexes as genetic material binds to sedimentary minerals (Greaves and Wilson, 1970; Lorenz and Wackernagel, 1987a; 1987b; Ogram et al., 1988; Blum et al., 1997; Arnold et al., 2011; Morrissey et al., 2015; Gardner and Gunsch, 2017). The substrate in which sedaDNA is preserved influences not only rates of preservation, but also the protocols necessary for successful DNA extraction (Slon et al., 2017, sec. Suppl. 14–19). Further, Johnson et al. (2007) found evidence of low-metabolic activity in ancient permafrost bacteria, indicating the potential long-term survival of microbes. This presents the complication of recovering a mix of ancient, damaged microbiotic DNA and viable cellular DNA with sustained active repair mechanisms that may be preferentially ligated during library preparation, or otherwise bias the

metagenomic profile. This may also facilitate the continuous degradation or transformation of sedaDNA by ancient but sustained soil microbes.

Third, factors that influence the survivability of sedaDNA over long-distance fluvial or aeolian transport are poorly understood, although the potential for long-distance transport has been demonstrated to be a significant factor for permafrost sediments in high energy erosional environments (Arnold et al., 2011). Finally, the rate of eDNA degradation by UV radiation, oxidation, hydrolysis, microbial activity, and alkylation has largely only been explored in laboratory settings that necessarily preclude many complex taphonomic variables that would be expected during erosion and deposition (Ogram et al., 1988; Willerslev et al., 2003b). Variable mechanisms for long-term preservation present a variety of shifting challenges when attempting to release those biomolecules for analysis. Saeki et al. (2010) found that the strong binding capacity of humic acids and clay minerals lead to a <2% recovery of absorbed DNA, with these humics and clays further inhibiting enzymes necessary for DNA amplification (Matheson et al., 2010). It has been demonstrated in modern soil microbiology that different extraction methodologies can bias the relative proportions of DNA from bacterial phyla, making the choice of extraction protocol an important aspect of research design that should vary based on objective (Holmsgaard et al., 2011; Knauth et al., 2013; Young et al., 2014). There has been limited testing of sedaDNA extraction protocols to improve recovery rates, to investigate variable efficiencies or taxonomic bias (Rawlence et al., 2014, p. 616), or to mitigate environmental inhibitors (Van Geel et al., 2011; Wales et al., 2014). False-negatives as a result of inhibition are a major interpretative bias for sedaDNA, with ineffective extraction protocols being a much broader problem across the field of aDNA, resulting in substantial genetic loss (Barta et al., 2014).

I experimentally address extraction related challenges (inhibitor carry-over and low DNA retention) that impacts our ability to effectively access sedaDNA from Beringian permafrost in Chapters 2 and 3. This newly optimized extraction technique (designed to minimize inhibition while maximally retaining sedaDNA) is implemented

thereafter in Chapters 4, 5, and 6 to investigate the palaeoecological transformations of terminal Pleistocene Yukon in relation to the LQE.

1.4.4 Environmental DNA targeting strategies

There are two commonly used approaches when processing sedaDNA: PCR metabarcoding and shotgun sequencing (this topic is discussed further in Chapter 2, section 2.2). PCR metabarcoding (or amplicon sequencing) targets short, taxonomically diagnostic genetic regions that are immediately flanked by deeply conserved sequences that can be amplified using short 'universal' primers (see Fig. 1.4). These regions are then PCR amplified exponentially until most of a sample consists of just those target regions. After adding adapters and sample indices (unique identifiers, usually in the same reaction), these amplicons can then be sequenced. This approach is highly effective with modern eDNA applications and has several benefits overall (including means of circumventing sedimentary inhibition and overly aggressive DNA loss). But, the technique suffers from a very limited number of genetic regions that are amenable to metabarcoding ancient DNA—which is characteristically short (fragment lengths being typically less than 50 bp) and damaged on the terminal ends (the areas that necessitate near exact identity for effective priming). As such, only a tiny and biased fraction of ecologically informative aDNA is sequenced with this approach, and because of the PCR manipulations, it is even more unclear if sequence read abundance is at all related to palaeo-biomass.

Alternatively, shotgun sequencing can be used to recover a random subset of DNA sequences from a sample with minimal bias, but will be dominated (>99.9%) by 'uninformative' (depending on the research question) bacterial sequences, *adaptemers* (chimeric artificial sequences of the adapters), and other metagenomic noise/contaminants. It is likely that molecules informative of macro-scale ecosystems (such as low abundance plants or animals) will be entirely missed with a shotgun approach unless a sample is sequenced into the hundreds of millions or billions of molecules, which is incredibly cost-ineffective, and computationally crippling.

A third underutilized technique for sedaDNA is hybridization-based capture using either arrays or in-solution enrichment (Carpenter et al., 2013; Marciniak et al., 2015, p. 29). This approach uses available genetic reference sequences to design baits/probes that can bind to target DNA of interest, which can then be isolated from the remainder of the library. Therein, complex sets of target DNA can be isolated and sequenced separately, allowing for a far greater proportion of informative sequence data retrieved from entire genomes. Enrichment can significantly reduce uninformative background/noise DNA (Steven et al., 2007; Mamanova et al., 2010b; Yergeau et al., 2010; Bartam et al., 2011; Mackelprang et al., 2011; Horn, 2012), and allow for the simultaneous sequencing of informative loci among multiple kingdoms (plants, animals, fungi) to reconstruct a holistic palaeoecological profile. Microarrays such as the GeoChip (He et al., 2007; 2010) can be used to mitigate inherent biases of single locus targeting in metabarcoding (Waugh, 2007; Piganeau et al., 2011), which has been implemented in a variety of microbiotic research (Bayer et al., 2014; Chen et al., 2014; Li et al., 2014; Tu et al., 2014; Ozen and Ussery, 2015). Success with this technique has been limited (Sadoway, 2014, chap. 2), likely due to sedimentary inhibitors impacting library preparation (the ligation of artificial adapters to the ends of DNA sequences to facilitate PCR reactions and sequencing). Developing a means of utilizing targeted enrichment with sedaDNA was the primary impetus behind this thesis. The first successful use of this technique on sedaDNA was published by Slon et al. (2017) where the authors of that study were able to recover mammalian and hominin DNA from a range of caves across Eurasia. This topic is expanded upon in Chapter 2.

1.5 Thesis layout

This thesis consists of three manuscripts, each focusing on permafrost recovered from the Klondike region of Yukon, Canada near Dawson City. These predominantly silt-rich permafrost cores were initially collected, dated, and analyzed by D'Costa et al. (2011), Mahony (2015), and Sadoway (2014), then kept in cold storage at the McMaster Ancient DNA Centre. Most are horizontal cores collected with a small portable drill (~10 cm diameter, 30 cm length) from vertical exposures opened during mining activities in

the Klondike, but subsamples from the Lucky Lady II site come from vertical cores. These permafrost materials are dated through a combination of direct ^{14}C on macro-remains and age-modeling. Other lake and permafrost cores collected during the duration of my dissertation research constitute side-projects and are not the focus of this thesis.

The first paper (Chapters 2 and 3) concerns an experimental effort untaken to refine our ability to maximally recover sedimentary DNA for a capture enrichment approach. An initial batch of experiments highlighted that inhibitory substances and DNA loss were substantial hurdles to an enrichment approach with sediments, and that the McMaster Ancient DNA Centre's standard extraction technique would be unable to successfully isolate target DNA from these permafrost cores. This led to an iterative series of experiments to determine if our silica-based guanidinium extraction protocol could be modified to maximize aDNA retention while minimizing inhibitor carry-over. This paper also involved the development of a novel bait-set (PalaeoChip Arctic-1.0) designed to capture environmental DNA from ~2100 Holarctic plant species and ~180 animals. This paper compares two extraction procedures, as well as three targeting strategies (metabarcoding, shotgun, and capture enrichment), and identifies the potential late survival of *Equus* sp. (extinct North American horse) and *Mammuthus primigenius* (woolly mammoth) in central Yukon with our optimized sedaDNA extraction technique. This paper was submitted in August 2019, published online in *Quaternary Research* in September 2020, and was in print as of January 2021 (volume 99).

The second paper (Chapters 4 and 5) utilized the methods optimized from the first manuscript to assess ecological turnover during the Pleistocene-Holocene transition with permafrost samples dating between 30,000–6000 calibrated years BP (cal BP). This paper identifies the same late survival signal of *Equus* sp. and *M. primigenius* while also observing a coeval turnover in plants and animals between 13,000–10,000 BP. We argue that this period marks the functional extripation of grazing megafauna in central Yukon, but that the declines of megafauna were gradual and iterative. Our results are contextualized with extant archaeological and palaeoecological data from the region.

The third paper (Chapter 6) details efforts to reconstruct mitochondrial genomes of *Mammuthus primigeneius*, *Equus caballus*, and *Bison priscus* from the permafrost samples processed in paper two. These mitogenomes were reconstructed solely from sediment, which we used to assess the phylogenetics of these animals at multiple time points during the Pleistocene-Holocene transition. By capturing and assembling whole mitochondrial DNA, we are able to identify subpopulations of these animals that make phylogeographic sense, and confirm that multiple distinct haplogroups co-inhabited the Klondike region around the LGM. Finally, chapter 7 summarizes the contributions of this dissertation to the interdisciplinary nexus of Quaternary science.

1.6 Tables

Table 1.1 Cultural-historic entities in Beringia.

Entity	Spatial extent	Age	Characteristics*	Literature
Dyuktai	Northeast Siberia	30,000–11,000 BP	Bifaces, burins, blades, microblades, wedge-shaped microblade cores, megafauna hunting.	(Mochanov and Fedoseeva, 1996)
Yubetsu Technique	Northern Japan	14,000 BP	Microblade manufacturing technique.	(Morlan, 1967; Kobayashi, 1970; Flenniken, 1987; Sano, 2007; Sato and Tsutsumi, 2007)
(American) Paleoarctic tradition	Beringia	13,500–2000 BP	Specialized wedge-shaped microblade cores to create regular, parallel-sided microblades and blades. Original definition encompasses many archaeological entities. Part of 'Alaskan Prodigy'.	(Anderson, 1968; Potter, 2005)
Beringian Tradition	Beringia	35,000–9500 BP	Divided into East Beringian and Late Beringian, West does not recognize Nenana, instead refers to these sites as "non-microblade" Denali.	(West, 1981; 1996; Holmes, 2001)
East Beringian Tradition	Beringia	>11,500 cal BP	Includes Dyuktai, Swan Point, Chindadn, and Nenana complexes, but not Denali.	(Holmes, 2001; 2008)
Swan Point, Healy Lake, Gerstle River	Beringia	Late Pleistocene to Holocene	Sites with microblades and burins, reminiscent of Dyuktai.	(Dumond, 2001; Holmes, 2001)
Broken Mammoth, Mead	Beringia	Late Pleistocene to Holocene	Early sites without microblades	(Dumond, 2001; Holmes, 2001)
Chindadn Complex	Beringia	13,500–11,500 cal BP	Distinctive thin, teardrop bifacial knives or points, triangular to sub-tranguloid points, microblades.	(Cook, 1969; 1996; Holmes, 2001)
Nenana Complex	Beringia	13,500–11,500 cal BP	Bifacial lithics, no microblades. Possible antecedent to Paleoindian Tradition.	(Powers and Hoffecker, 1989; Goebel et al., 1991; Holmes, 2001)
Clovis Complex/Tradition	North America	13,000 ± 200 cal BP	Distinct fluted bifacial points, blades, megafauna, continental distribution.	(Goebel et al., 1991; Haynes, 2002; Waters and Stafford Jr, 2007; Peck, 2011; Rasmussen et al., 2014)
Denali Complex	Beringia	11,500–8500 cal BP	Technological similarities to Northeast Asian and Beringian traditions, but with a novel Campus technique for microblade technologies; part of 'Alaskan Prodigy'.	(West, 1967; 1975; Holmes, 2001)
Northern Cordilleran Tradition	Southern Yukon	ca. 10,000–7100 ^{14}C BP	Large informal core and blade technology (no microblades), round and straight-based lanceolate points, bi-points, possibly burins. Likely descendent of Nenana.	(Clark, 1983; Gotthardt, 1990; Hare, 1995)
Paleoindian Tradition	The Americas	ca. 11,500–8500 ^{14}C BP	Distinctive lanceolate projectile points, high level of technological expertise, blades. Includes: Clovis, Folsom, Agate Basin, Hell Gap, Eden.	(Irwin and Wormington, 1970; Frison, 1978; Peck, 2011)
Mesa Complex	Arctic Alaska	ca. 11,700–9700 ^{14}C BP	Large unfluted lanceolate points, no blades. Part of Paleoindian Tradition.	(Kunz and Reanier, 1994; 1995; Kunz and Bever, 2003)

*Defining characteristics vary significantly by researcher, these should be taken as approximations. Holmes (2001; 2008; 2011), Hare (1995), and Clark (1991) are principle sources. Modified from Murchie (2015).

1.7 Figures

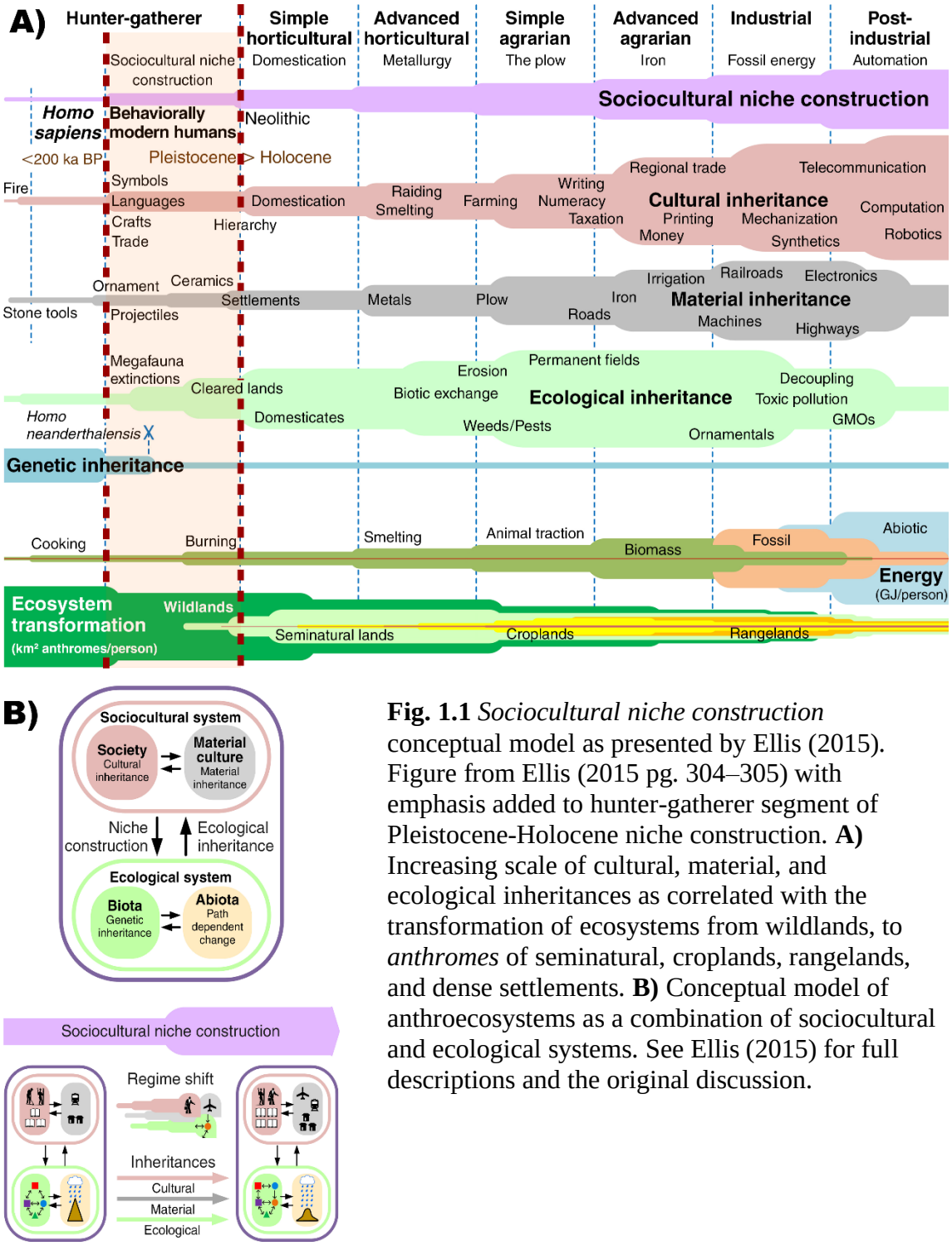

Fig. 1.1 *Sociocultural niche construction* conceptual model as presented by Ellis (2015). Figure from Ellis (2015 pg. 304–305) with emphasis added to hunter-gatherer segment of Pleistocene-Holocene niche construction. **A)** Increasing scale of cultural, material, and ecological inheritances as correlated with the transformation of ecosystems from wildlands, to *anthromes* of seminatural, croplands, rangelands, and dense settlements. **B)** Conceptual model of anthroecosystems as a combination of sociocultural and ecological systems. See Ellis (2015) for full descriptions and the original discussion.

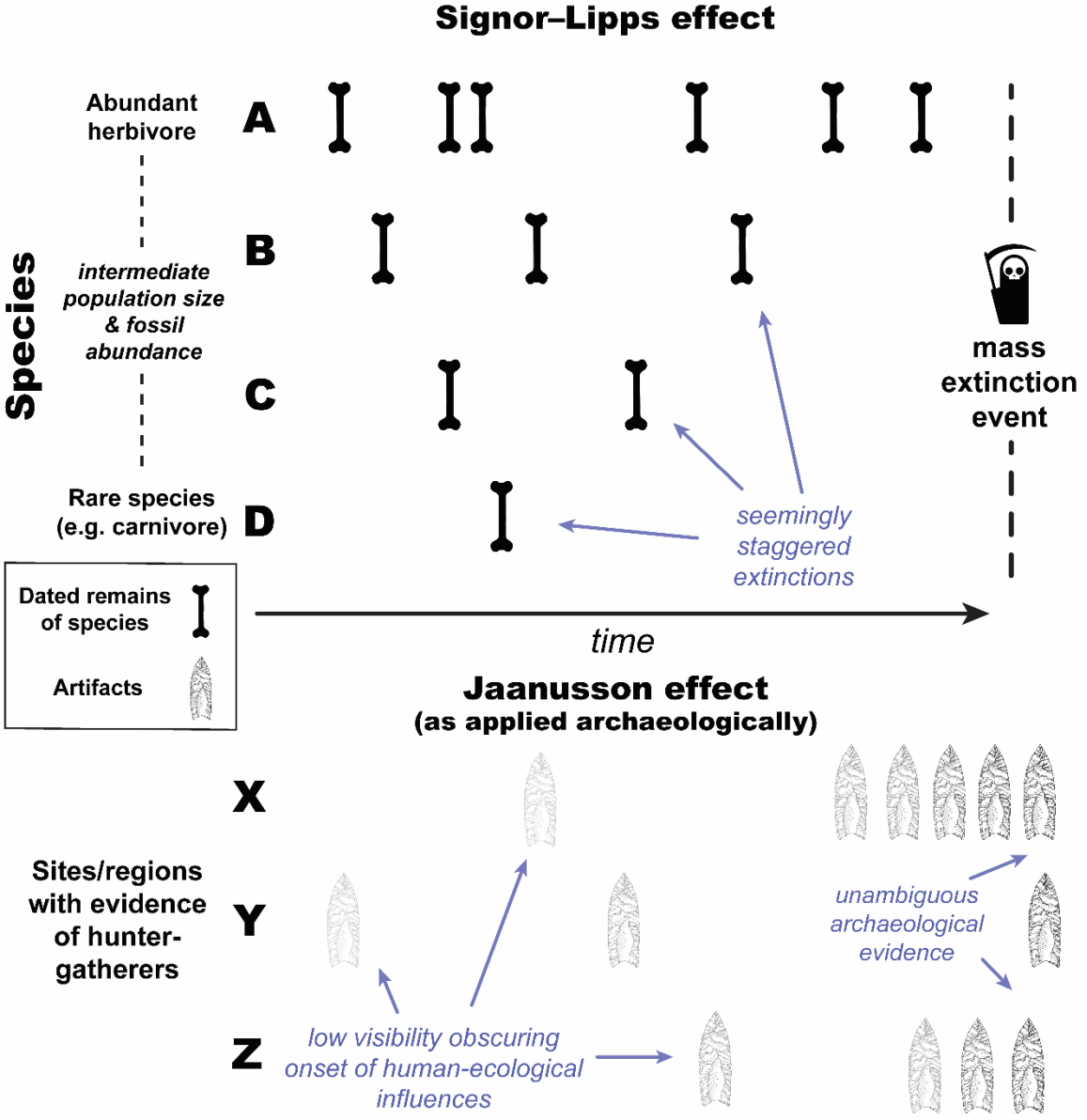

Fig. 1.2 The compounding challenges of the Signor-Lipps (1982) and Jaanusson (1976; Heads, 2012) effects in understanding the Pleistocene-Holocene extinctions and peopling of the Americas. Seemingly gradual disappearances from the fossil record could either accurately indicate a gradual loss of species or could be an artifact of inadequate sampling obscuring a more sudden mass extinction event. Likewise, the low archaeological visibility of nomadic-hunter gatherers (combined with ambiguous alleged artifacts/biofacts, such as supposed cut-marks on bone) obscures our understandings of when humans may have first started influencing palaeo-environments.

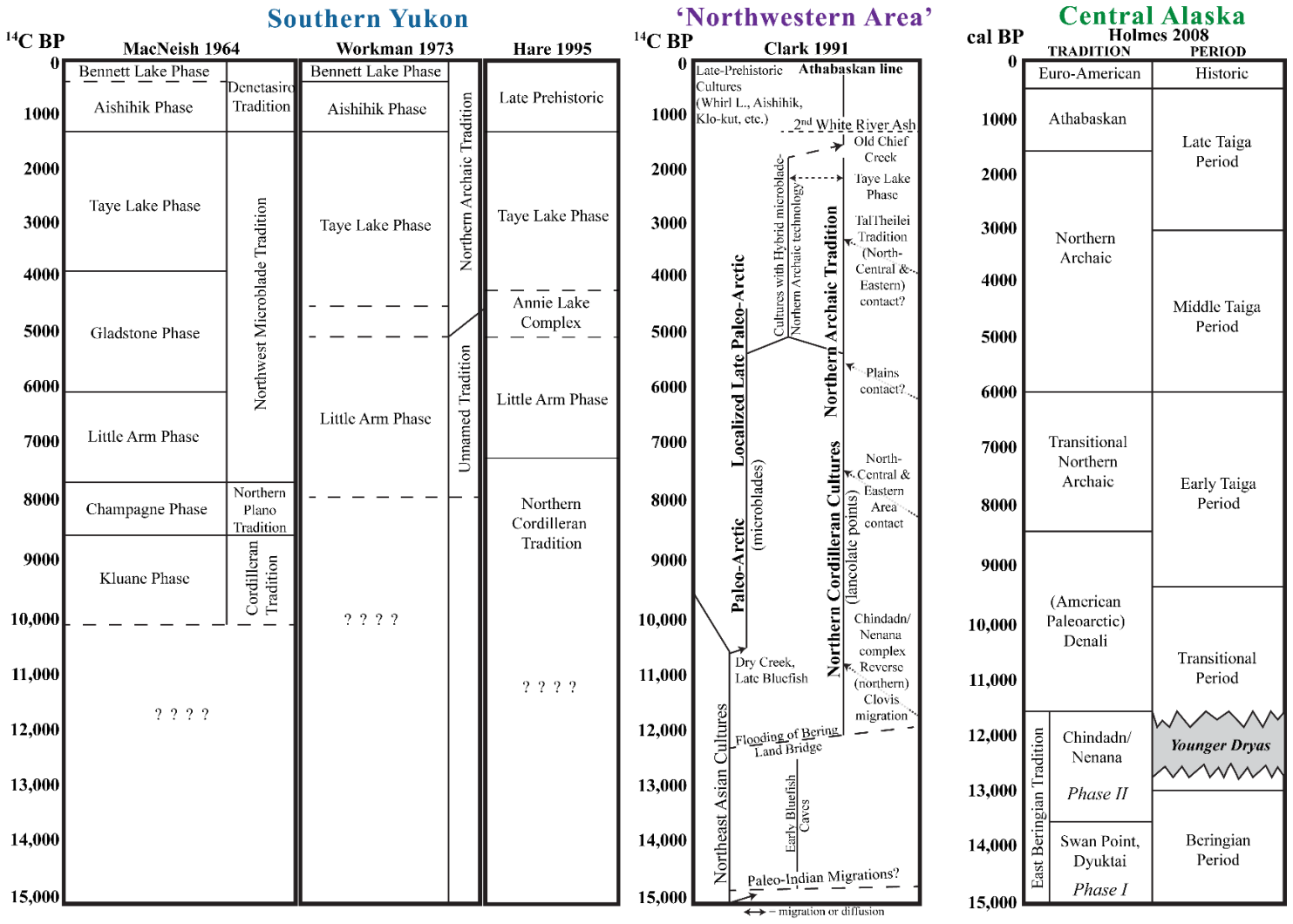

Fig. 1.3 A variety of culture-historical frameworks for the northwestern subarctic; modified compilation from Murchie et al. (2015, p. 24). **Note:** the rightmost framework is on a calibrated years BP scale, whereas the other two are on a radiocarbon scale. This makes them not directly comparable.

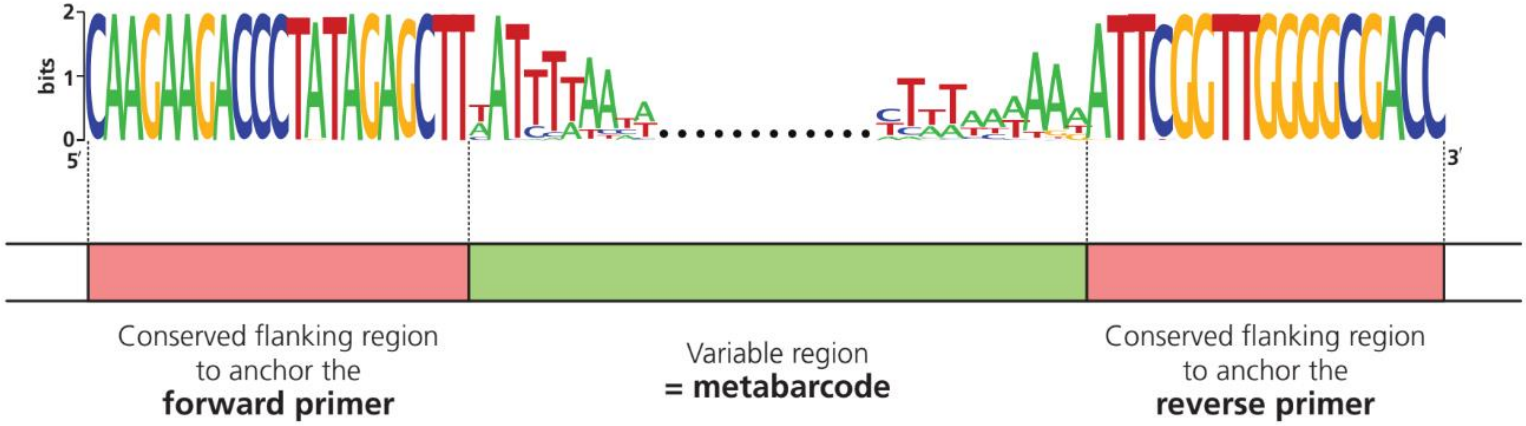

Fig. 2.1 Example of a variable metabarcode with its conserved flanking sequences. This example is based on the Lumb01 primer pair (see Bienert *et al*. 2012 and Appendix 1) targeting the suborder Lumbricina (earthworms). All Lumbricina sequences were extracted from the release 126 of EMBL using ecoPCR (1,973 sequences). Each logo consists of stacks of symbols (A, C, G, T), with one stack for each position in the nucleotide sequence. The overall height of the stack corresponds to the nucleotide conservation at that position across the Lumbricina lineage and is expressed in bits (a value of 2 indicates a perfect conservation, while 0 means the same probability for the four nucleotides). The height of each symbol within the stack indicates the relative frequency of each nucleotide at that position.

Fig. 1.4 Conception of metabarcoding captured from Taberlet et al. (2018, p. 8).

Chapter 2

Optimizing extraction and targeted capture of ancient environmental DNA for reconstructing past environments using the PalaeoChip Arctic-1.0 bait-set

Tyler J. Murchie[a,b*], Melanie Kuch[a,b], Ana T. Duggan[a,b], Marissa L. Ledger[c], Kévin Roche[d,e], Jennifer Klunk[a,f], Emil Karpinski[a,f], Dirk Hackenberger[a,g], Tara Sadoway[a,h], Ross MacPhee[i], Duane Froese[j], Hendrik Poinar[a,b,g*]

[a]McMaster Ancient DNA Centre, McMaster University, Canada
[b]Department of Anthropology, McMaster University, Canada
[c]Department of Archaeology, University of Cambridge, United Kingdom
[d]CNRS UMR 5607 Ausonius, University of Bordeaux Montaigne, France
[e]CNRS UMR 6249 Chrono-Environment, University of Bourgogne Franche-Comté, France
[f]Department of Biology, McMaster University, Canada
[g]Department of Biochemistry, McMaster University, Canada
[h]University Health Network, Toronto
[i]Division of Vertebrate Zoology/Mammalogy, American Museum of Natural History
[j]Department of Earth and Atmospheric Sciences, University of Alberta

[*]Corresponding authors: Tyler J. Murchie and Hendrik Poinar, Department of Anthropology, McMaster University, 1280 Main Street West, Hamilton, ON L8S 4L8, Canada. E-mail address: murchiet@mcmaster.ca and poinarh@mcmaster.ca

Murchie, T., Kuch, M., Duggan, A., Ledger, M., Roche, K., Klunk, J., . . . Poinar, H. (2021). Optimizing extraction and targeted capture of ancient environmental DNA for reconstructing past environments using the PalaeoChip Arctic-1.0 bait-set. *Quaternary Research,* 99, 305-328. doi:10.1017/qua.2020.59

Appendix B available at above DOI.

Abstract

Sedimentary ancient DNA (sedaDNA) has been established as a viable biomolecular proxy for tracking taxon presence through time in a local environment, even in the total absence of surviving tissues. SedaDNA is thought to survive through mineral binding, facilitating long-term biomolecular preservation, but also challenging DNA isolation. Two common limitations in sedaDNA extraction are the carryover of other substances that inhibit enzymatic reactions, and the loss of authentic sedaDNA when attempting to reduce inhibitor co-elution. Here, we present a sedaDNA extraction procedure paired with targeted enrichment intended to maximize DNA recovery. Our procedure exhibits a 7.7–19.3x increase in on-target plant and animal sedaDNA compared to a commercial soil extraction kit, and a 1.2–59.9x increase compared to a metabarcoding approach. To illustrate the effectiveness of our cold spin extraction and PalaeoChip capture enrichment approach, we present results for the diachronic presence of plants and animals from Yukon permafrost samples dating to the Pleistocene-Holocene transition, and discuss new potential evidence for the late survival (~9700 years ago) of mammoth (*Mammuthus sp.*) and horse (*Equus sp.*) in the Klondike region of Yukon, Canada. This enrichment approach translates to a more taxonomically diverse dataset and improved on-target sequencing.

Keywords:

Sedimentary ancient DNA; paleoenvironmental DNA; capture enrichment; environmental DNA; DNA extraction; PowerSoil DNA extraction kit; late quaternary extinctions; Pleistocene-Holocene transition; Yukon paleoenvironment; PalaeoChip bait-set

2.1 Introduction

Means of recovering and analyzing ecologically informative environmental DNA (eDNA) have improved substantially thanks to ongoing developments in high-throughput sequencing (HTS) technologies (Taberlet et al., 2018). Sedimentary ancient DNA molecules (sedaDNA, referring to a subset of ancient eDNA sample types; see Rawlence et al. [2014, p. 614]) have been successfully recovered from a diverse range of depositional settings to evaluate what is thought to be the local (Parducci et al., 2017, p. 930; Edwards et al., 2018) diachronic presence of animals (Haile et al., 2009; Giguet-Covex et al., 2014; Graham et al., 2016; Pedersen et al., 2016; Slon et al., 2017), plants (Anderson-Carpenter et al., 2011; Willerslev et al., 2014; Epp et al., 2015; Alsos et al., 2016; Niemeyer et al., 2017), fungi (Bellemain et al., 2013), microbiota (D'Costa et al., 2011; Ahmed et al., 2018), and eukaryotic parasites (Søe et al., 2018). It is thought that much of sedaDNA survives in the absence of tissues through the formation of organo-mineral complexes (Greaves and Wilson, 1970; Lorenz and Wackernagel, 1987a; 1987b; Ogram et al., 1988; Blum et al., 1997; Arnold et al., 2011; Morrissey et al., 2015; Gardner and Gunsch, 2017) as extracellular genetic material binds to common constituents of sediments such as humics (Crecchio and Stotzky, 1998), calcite (Cleaves et al., 2011), clays (Goring and Bartholomew, 1952; Greaves and Wilson, 1969; Cai et al., 2006), and other silicates (Lorenz and Wackernagel, 1987b; Bezanilla et al., 1995). Soil minerals have been found to stabilize a fraction of such complexes, allowing DNA molecules to resist decomposition (Morrissey et al., 2015). However, strong mineral binding can also result in poor sedaDNA mineral release when attempting to isolate these molecules during DNA extraction (Alvarez et al., 1998; Saeki et al., 2010).

Mineral-bound sedaDNA is recovered in bulk in the form of short, disseminated biomolecules from a diverse range of organisms. This generally prohibits genomic reconstructions of single individuals from eDNA samples, but it can allow for identifying the presence (and potentially relative abundance) of organisms through time. SedaDNA methods show the most promise in reconstructing palaeoflora (Anderson-Carpenter et al., 2011; Willerslev et al., 2014; Pedersen et al., 2016; Niemeyer et al., 2017; Sjögren et al.,

2017), or the variable presence of a particular taxon temporally (Graham et al., 2016). Comparative analyses using eDNA, palynology, macroremains, and vegetation surveys have argued that eDNA currently functions best as a complement to traditional palaeoecological methods (Jørgensen et al., 2012a; 2012b; Pedersen et al., 2013), as often each proxy tends to identify a partially-overlapping (complementary) set of organisms (Parducci et al., 2017, p. 932). With ongoing progress in ancient DNA (aDNA) methods, a single DNA library (DNA fragments with artificial adapter sequences attached [ligated] to allow for high-throughput sequencing [HTS]) can increasingly be used to identify a diverse range of prokaryotic and eukaryotic organisms simultaneously from a single sample with shotgun sequencing (sequencing a random subset of a DNA library to a select depth, e.g., ten million molecules) or can be targeted to amplify or enrich for specific taxa of interest. Using a targeted approach significantly improves the informative fraction of sequenced DNA reads over shotgun sequencing by reducing the proportion of off-target molecules—especially microbial DNA that otherwise tends to proportionally dominate shotgun data.

Despite rapid advances in aDNA techniques, two extraction related challenges persist that can limit the ability to fully exploit sedimentary genetic archives: 1) the presence of enzymatic inhibitors in sediment extracts, and 2) the loss of ecologically informative sedaDNA due to overly vigorous inhibitor removal. Inhibitors are substances that inhibit a broad array of enzymatic reactions necessary to prepare DNA for sequencing, such as adapter-ligation during library preparation or polymerase chain reaction (PCR) amplification during metabarcoding (described in the following subsection). Enzymatic inhibitors are often present in higher concentrations in samples that are prepared with techniques designed to maximize the recovery of aDNA (characteristically short, damaged fragments; Dabney et al., 2013a). Commercial kits have been designed with reagents that remove inhibitors from lysed samples, but these reagents can also remove potentially informative DNA that is already in low concentrations in ancient remains (Dong et al., 2006).

To address these challenges, this study evaluates various inhibitor removal treatments for their ability to reduce the carryover of enzymatic inhibitors in sedaDNA extracts while maximally retaining endogenous palaeoenvironmental DNA that can successfully undergo library adapter-ligation and targeted enrichment. Our aim is to minimize the need for excessive PCR amplifications on purified eluates by instead utilizing a capture enrichment approach (Carpenter et al., 2013) that to date has typically been applied only to discrete, rather than disseminated, materials (Rawlence et al., 2014, p. 614). We also wanted to determine whether this approach would be as viable for open-air sediments as the technique has been in cave contexts (Slon et al., 2017). Capture enrichment would theoretically aid in part to minimize the propagation of stochastic PCR biases and allow for a far greater range of targetable genetic loci that are more amenable to aDNA fragment sizes and damage characteristics.

Four previously studied sediment core samples (D'Costa et al., 2011; Sadoway, 2014; Mahony, 2015) recovered from Yukon permafrost exposures (Table 2.1, Fig 2.1) in the Klondike region were chosen to experimentally optimize a new sedaDNA extraction procedure. Further details of these iterative extraction experiments are included in the supplementary materials. We based these modifications on our in-house lysis solution and high-volume binding buffer, silica-spin column extraction method as described by Dabney et al. (2013b). Our sedaDNA modified Dabney et al. (2013b) extraction protocol is described here (Fig. 2.2) and referred to in-text as the cold spin method. Experiments with alternative inhibition removal techniques are detailed in the supplementary materials as sediment extraction/enrichment testing SET-A through SET-D (Chapter 3). The main-text experiment is referred to throughout as SET-E.

The cold spin optimized extraction protocol was used to evaluate taxonomic assignments between shotgun sequenced and target enriched datasets from four Yukon permafrost samples. These were enriched using a bait-set designed to capture mitogenomes of extinct and extant northern animals (focused on megafauna) as well as the chloroplast barcoding loci *trn*L, *rbc*L, and *mat*K from arctic and subarctic plants. This bait/probe set is referred to here as the PalaeoChip Arctic-1.0 bait-set. Results were also

compared with shotgun and enriched libraries extracted from the same samples using the DNeasy PowerSoil DNA extraction kit (QIAGEN)—one of the most commonly utilized sedaDNA extraction procedures. For each of the four permafrost core sections, sediments were subsampled and homogenized, then split into three 250 mg replicates for both extraction methods and subsequent targeting strategies in order to also assess intrasample variability. We compared our results with previously sequenced PCR metabarcoding data (Sadoway, 2014) derived also from 250 mg of the same core sections that had been extracted with a similar (but different) approach (D'Costa et al., 2011). We then used metabarcoding to amplify the chloroplast intron *trn*L (Taberlet et al., 2007) on all of the same PowerSoil and sedaDNA optimized extracts to evaluate the variation in DNA recovery between our data and the previous Sadoway (2014) metabarcoding approach.

2.2 Background: current approaches to analyzing sedaDNA

2.2.1 PCR metabarcoding

PCR metabarcoding is the most popular technique in eDNA research (Taberlet et al., 2018, chap. 2). This approach targets short, highly variable regions of the genome (regions with enough variation to identify organisms to family, genus, or species ranks) which also happen to be immediately flanked by deeply conserved regions (an identical genetic sequence region across many organisms, such as all plants). Primers are designed to bind to these two conserved flanking regions, facilitating a PCR reaction (Saiki et al., 1985; 1988; Mullis and Faloona, 1989) that amplifies the hyper-variable internal barcode at an exponential rate. A metabarcoding approach exponentially amplifies the selected metabarcode for all DNA fragments of this target region from multiple organisms simultaneously, overwhelming any other off-target eDNA left in the sample extract. After these molecules are sequenced and processed, the reads can then be identified similarly to other approaches to determine a probable host organism using algorithmic packages such as *OBITools* (Boyer et al., 2016) or *BLASTn* (Altschul et al., 1990), which compare the sequenced reads against a nucleotide reference database such as GenBank NCBI (National Center for Biotechnology Information; Benson et al., 2013; Agarwala et al., 2016) or otherwise curated references. To some degree, PCR metabarcoding can mitigate

the aforementioned challenges of inhibition through dilutions or additional purifications (McKee et al., 2015), with the addition of reagents such as bovine serum albumin (BSA) (Kreader, 1996; Garland et al., 2010), with high cycle numbers to facilitate inhibitor denaturation, and with high polymerase concentrations. The technique can also theoretically cope with substantial DNA loss from inefficient DNA purifications (in part, from overly aggressive inhibitor removal techniques) by exponentially amplifying low abundance molecules to sufficient concentrations for downstream manipulations.

PCR metabarcoding is widely used in eDNA applications to great effect (e.g., Giguet-Covex et al., 2014; Willerslev et al., 2014; Alsos et al., 2015; Epp et al., 2015; Sjögren et al., 2017), but the technique has several aspects that theoretically limit the information that can be acquired from ancient samples. Perhaps most significantly, if the few genetic regions amenable to metabarcoding fail to preserve for particular organisms in the sediment samples being tested (due to variable eDNA input as related to biomass turnover and stochastic taphonomic processes), DNA from those organisms will not be sequenced, resulting in abundant false negatives, even with a large number of PCR replicates per sample to control for stochastic amplifications (Nichols et al., 2018, p. 8). This problem is significant for palaeoenvironmental DNA applications where substantial DNA damage and loss has occurred. Regions suitable for metabarcoding often exist on the high end of the aDNA fragment spectrum (typically >100 bp [base pairs]) whereas most aDNA fragments have an average fragment length of approximately 50 bp or less. The chloroplast *trn*L intron P6 loop, used for metabarcoding plants, is a relative exception with a amplicon range of 49–188 bp (with primer landing sites added [Taberlet et al., 2007]). However even these short amplicons can exceed the typical DNA fragment sizes expected with degraded aDNA. Also, most sedaDNA does not come from suitable metabarcoding regions, but rather from a random metagenomic mixture of fragments in varying states of decay across a range of nuclear and organelle genomes. These non-barcoding regions are still useful in taxonomic identifications if they can be sequenced, either through expensive and inefficient deep shotgun sequencing (sequencing a library to near exhaustion) or another targeted approach. Metabarcoding is also vulnerable to

differential amplification rates due to variable molecular abundance per taxa, unequal damage (by region and taxa), variability in metabarcode amplification efficiency, and variably optimal PCR conditions depending on the eDNA mixture (Kanagawa, 2003; Bellemain et al., 2010; Krehenwinkel et al., 2018; Nichols et al., 2018; Sze and Schloss, 2019). These factors compound downstream biases in taxonomic determinations, especially if during inhibitor removal there was substantial loss of low-abundance molecules from taxa with comparatively low biomass turnover (Yoccoz et al., 2012, p. 3651). Metabarcoding also does not allow one to evaluate DNA damage patterns (such as cytosine deamination causing C to T base modifications on the terminal ends of aDNA fragments) due to the reliance on PCR amplifications of discrete genetic loci with intact primer landing sites. By contrast, shotgun sequencing and enrichment techniques can utilize these characteristic damage signals to build a case for ancient DNA authenticity (Ginolhac et al., 2011; Jónsson et al., 2013).

2.2.2 Capture enrichment

As an alternative to PCR metabarcoding, capture enrichment (also referred to as targeted capture) is a powerful means of increasing the fraction of target molecules that can be recovered from a DNA library (Mamanova et al., 2010a; Schuenemann et al., 2011; Carpenter et al., 2013; Marciniak et al., 2015). Capture enrichment involves designing a set of RNA probes or baits that closely match DNA sequences (including whole genomes) from organisms of interest, which are then allowed to hybridize to the predetermined target molecules that may be present in the DNA library. After hybridizing (either with in-solution biotinylated baits or on a solid-state microarray with pre-attached baits, see Marciniak et al., 2015, p. 29), the target molecules are sequestered while the non-target fraction is washed away for discard or storage for alternative use (Klunk et al., 2019). The technique allows for whole genome capture of multiple target organisms simultaneously, resulting in a huge increase in the proportion and diversity of informative sequenced DNA without the need for exponential PCR amplifications and the compounding biases therein—as well as substantially reduced costs compared to deep shotgun sequencing. Capture enrichment has been primarily utilized with discrete

materials such as bone, having seen limited use to date with eDNA sample types (Slon et al., 2016; 2017). Targeted capture has its own associated limitations such as incomplete off-target exclusion, GC biases (due to stronger hybridization of sequences rich in guanine or cytosine bases versus those that are AT rich), and limitations in finding unexpected molecules due to reference-based bait design. However, capture enrichment has the potential to allow for a far more diverse recovery of ecologically informative eDNA across entire genomes, especially in geographic regions with relatively complete nucleotide reference databases of organisms, such as the Arctic (Sønstebø et al., 2010; Willerslev et al., 2014). Being unrestricted by intact priming sites (compared to metabarcoding) can also allow for an assessment of molecular damage on an organism-by-organism basis (Ginolhac et al., 2011). Capture enrichment has the best potential when using a DNA extraction procedure intended to maximize DNA recovery. But, as discussed previously, this becomes a significant challenge with sedaDNA because of the high co-elution of inhibitory substances that inhibit enzymes used for adapter-ligation during library preparation.

2.3 Methods

2.3.1 Field sampling

The Yukon permafrost core samples (Table 2.1, Fig 2.1) used in this analysis were previously collected and analyzed by D'Costa et al. (D'Costa et al., 2011), Mahony (2015), and Sadoway (2014) from near-vertical sediment exposures, then kept in cold storage at the McMaster Ancient DNA Centre. All four samples were analyzed by Sadoway (2014) using PCR metabarcoding. Prior to core collection by all three original research teams, the sampling area was cleared of eroded materials back to frozen sediments to create a fresh coring surface for a ~10 cm diameter coring tube ~30 cm in length. Horizontal core samples were drilled with a small portable drill, recovered frozen, stored individually in plastic bags, and transported frozen to the University of Alberta or McMaster University for subsampling. Subsamples for aDNA were taken only from core interiors (described below in Methods subsection 3) as exterior and cut surfaces are more likely to contain contaminant DNA.

Bear Creek (BC 4-2B)

The Bear Creek site is located 11 km east of Dawson City, Yukon, in the Klondike mining district. Mining activities exposed a ~10 m vertical sampling surface consisting of 3 m of alluvial sediment overlain by ~7 m of ice-rich loessal silt (D'Costa et al., 2011). The Dawson tephra is prominent at the site, dating to 25,300 ^{14}C yr BP (~30,000 cal yr BP) (Froese et al., 2006), and is situated between 5.2 and 6 m from the base of the exposure. Horizontal core sample BC 4-2B was collected 50 cm below the tephra under a stratified lens of ice, likely the remnant of a surface icing similar to other sites associated with Dawson tephra in the area (Froese et al., 2006). The core sample was collected from reddish-brown ice-poor silts that extend below the tephra. These sediments are interpreted as the palaeosurface and include the palaeoactive layer that existed at the time of Dawson tephra deposition. This unit was preserved due to the rapid deposition of the tephra (~80 cm thick at this site) that shifted the active layer upward. Observations of the palaeoactive layer and preservation of the ice body indicate that there was no thawing or water migration in these relict permafrost sediments following deposition of the Dawson tephra (D'Costa et al., 2011).

Upper Goldbottom (MM12-118b)

This site is located 28 km south of Dawson along Goldbottom Creek, a tributary of Hunker Creek and the Klondike River. The 28.5 m exposure was divided by Mahony (2015, pp. 65–82) into five units, dating roughly between ~46,000 cal yr BP near the base, to ~6000 cal yr BP near the surface. The core sample MM12-118b used in this study comes from Unit 4 near the top of the exposure. The sediments consist of black and grey organic-rich silts with thin interbedded lenses of gravels and sand, as well as components of green-grey silts and interbedded humified brown organic silts. In situ graminoid and shrub macrofossils were also identified. Unit 4 is estimated to have begun deposition ca. 10,600 cal yr BP (9395 ± 25 ^{14}C yr BP, UCIAMS-114910) (Mahony, 2015, p. 77). The permafrost core used in this analysis (MM12-118b) was dated to the early Holocene at ca. 9685 cal yr BP (Mahony, 2015, p. 189).

Lucky Lady II (LL2-12-84-3 and LL12-12-217-8)

The Lucky Lady II site is located 46 km south of Dawson in the Sulphur Creek tributary of the Indian River. The site has an 11.5 m exposure that Mahony (2015, pp. 82–95) divided into two units; five vertical cores were taken at the site for high-resolution isotopic and radiocarbon analyses. The two core samples utilized in this study come from the lowermost unit, 0–3.5 m, which is estimated to have been deposited from ca. 16,500 to 13,140 cal yrs BP (13,680 ± 35 ^{14}C yr BP, UCIAMS-51324 to 11,290 ± 160 ^{14}C yr BP, UCIAMS-56390) (Mahony, 2015, p. 85). This unit consists of grey silt with a thick black organic-rich horizon (palaeosol) at 2.7 m dating from 13,410 to 13,140 cal yrs BP (11,580 ± 35 ^{14}C yr BP, UCIAMS-143308; 11,290 ± 160 ^{14}C yr BP, UCIAMS-56390) with several thinner palaeosol horizons above. The unit includes *in situ* graminoid macrofossils and multiple *Spermophilus parryii* (arctic ground squirrel) nests; several *Equus sp*. (horse) and *Bison sp*. (bison) bones were also identified. The unit is suggestive of a steppe-tundra landscape. Two core samples were selected from this site for experimental testing based on work by Sadoway (2014). Core sample LLII-12-84-3 was dated to 13,205 cal yr BP, while core sample LLII-12-217-8 was dated to 15,865 cal yr BP (Sadoway, 2014, p. 29).

2.3.2 Lab setting

Laboratory work was conducted in clean rooms at the McMaster Ancient DNA Centre. These rooms are subdivided into dedicated facilities for sample preparation, stock solution setup, and DNA extraction through library preparation. Post-indexing and enrichment clean rooms are in a physically isolated facility, while high-copy PCR workspaces are in separate building with a one-way workflow progressing from low-copy to high-copy facilities. Each dedicated workspace is physically separated with air pressure gradients between rooms to reduce exogenous airborne contamination. Prior to all phases of laboratory work, dead air hoods and workspaces were cleaned using a 6% solution of sodium hypochlorite (commercial bleach) followed by a wash with Nanopure purified water (Barnstead) and 30 minutes of UV irradiation at >100 mJ/cm^2.

2.3.3 Subsampling

Metal sampling tools were cleaned with commercial bleach, rinsed with Nanopure water immediately thereafter, and heated overnight in an oven at ~130°C. Once the tools had cooled, work surfaces were cleaned with bleach and Nanopure water and covered with sterile lab-grade tin foil. Sediment cores previously split into disks (D'Costa et al., 2011; Sadoway, 2014) and stored at −20°C had the upper ~1 mm of external sediment chiselled off to create a fresh sampling area free of exogenous contaminants for a hollow cylindrical drill bit. The drill bit (diameter 0.5 cm) was immersed in liquid nitrogen prior to sampling and a drill press was used to repeatedly subsample the disk sections (see D'Costa et al., 2011, Fig. S3). Sediment was pushed out of the drill bit using a sterile nail and the bottom 1–2 mm of sediment from the bit was removed before dislodging the remaining sample. This exterior core portion was carefully removed as it has a higher chance of containing sedaDNA from other stratigraphic contexts due to coring and core splitting. A bulk set of subsampled sediment from the same core disk was homogenized by stirring in a 50 mL falcon tube and stored at −20°C for subsequent extractions. This process was repeated individually for each core sample (Fig. 2.2).

2.3.4 Physical disruption, chemical lysis, and extraction

Subsamples from the four cores were homogenized by core and split into triplicates for each extraction method (24 extracts + 3 blanks), which were each used for shotgun, enrichment, and *trnL* metabarcoding. DNeasy PowerSoil DNA Extraction kit samples were extracted following manufacturer specifications; purified DNA was eluted twice with 25 µL EBT buffer (10 mM Tris-Cl, 0.05% Tween-20). Samples extracted with our cold spin extraction method (a sedaDNA modified version of the Dabney et al. [2013a] extraction) were processed as follows:

Lysis (DNA release)

1) 500 µL of a digestion solution (see Table 3.1) initially without proteinase K was added to PowerBead tubes (already containing garnet beads and 750 µL 181 mM NaPO4 and 121 mM guanidinium isothiocyanate from the manufacturer).
2) 250 mg of homogenized sediment was added to each PowerBead tube.

3) PowerBead tubes were vortexed at high speed for 15 minutes, then centrifuged briefly to remove liquid from the lids.
4) 15.63 µL of proteinase K (stock 20 mg/mL) was added to each tube to reach a proteinase K concentration of 0.25 mg/mL in the digestion and PowerBead solution (a total volume of 1.25 mL).
5) Tubes were finger vortexed to disrupt sediment and beads that had pelleted in step 3.
6) PowerBead tubes were securely fixed in a hybridization oven set to 35°C and rotated overnight for ~19 hours, ensuring that the digestion solution, sediment, and PowerBeads were moving with each oscillation.
7) PowerBead tubes were removed from the oven and centrifuged at 10,000 x g for 5 minutes (the maximum speed recommended for PowerBead tubes). Supernatant was transferred to a MAXYMum Recovery 2 mL tube and stored at −20°C.

Purification (DNA isolation)

8) The digestion supernatant was thawed, briefly centrifuged, and added to 16.25 mL (13 volumes) of high-volume Dabney binding buffer (see Table 3.2) in a 50 mL falcon tube and mixed by repeatedly inverting the tube by hand.
9) Falcon tubes were spun at 4500 x g in a refrigerated centrifuge set to 4°C for 20 hours overnight. (In subsequent experiments, we have found that this speed can be reduced to 2500 x g with no noticeable declines in inhibitor precipitation [data not shown].)
10) After centrifugation, falcon tubes were carefully removed and the supernatant was decanted, taking care to not disturb the darkly coloured pellet that had formed at the base of the tube during the cold spin.
11) The binding buffer was passed through a high-volume silica column (High Pure Extender Assembly, Roche Diagnostics) and extraction proceeded as per Dabney et al. (2013b).
12) Purified DNA was eluted off the silica columns with two volumes of 25 µL EBT.

Prior to all subsequent experiments, both the cold spin and PowerSoil extracts were centrifuged at 16,000 x g for 5 minutes to pellet remaining co-eluted inhibitors.

2.3.5 Library preparation

Double-stranded libraries were prepared for each extract as described in Meyer and Kircher (2010) with modifications from Kircher et al. (2012) and a modified end-repair reaction to account for the lack of uracil excision (Table 3.3). Samples were purified after blunt-end repair with a QIAquick PCR Purification Kit (QIAGEN) to maximally retain small fragments and after adapter ligation (Table 3.4) with a MinElute

PCR Purification Kit (QIAGEN), both using manufacturers protocols. Library preparation master mix concentrations can be found in Tables 3.3-3.6.

2.3.6 qPCR: Inhibition spike tests, total quantification, and indexing

Quantitative PCR (qPCR) is a technique that uses fluorescent dyes that intercalate with double-stranded DNA to monitor PCR amplifications in real-time, as opposed to at the end of the reaction with standard PCR. When paired with DNA standards at known concentrations, qPCR can be used to quantify the starting concentrations of particular DNA molecules in a sample (such as all DNA fragments derived from plants or mammals) or to quantify the total number of molecules that were successfully adapter-ligated during library preparation. The technique can also be used to assess the inhibition load of a sample as these inhibitory substances affect the rate of PCR amplification (King et al., 2009). See supplementary Appendix A (Chapter 3 section 3.1.4 and Fig. 3.6) for details on the inhibition spike test. Total library DNA quantifications reported here and in the supplementary materials used the short amplification primer sites on the library adapters to quantify total DNA copies per 1 μL with averaged PCR duplicates prior to indexing PCR (Table 3.8).

For each of the four cores and two extraction methods the subsampled triplicate with the highest total DNA concentrations (as based on the short amplification qPCR) was indexed for shotgun sequencing (8 samples + 3 blanks). All subsampled triplicates (24 samples + 3 blanks) were indexed separately thereafter for targeted enrichment and sequencing. Metabarcoded samples were processed identically, but with a *trn*L PCR amplification prior to library preparation (see section 2.3.9).

2.3.7 Targeted capture enrichment

The PalaeoChip Arctic-1.0 hybridization enrichment bait-set was designed in collaboration with Arbor Biosciences to target the mitogenomes of extinct and extant Quaternary animals (focused primarily on megafauna; number of taxa ≈ 180), and high-latitude plants based on curated reference databases developed by Sønstebø et al. (2010), Soininen et al. (2015), and Willerslev et al. (2014), initially targeting the *trn*L locus (n ≈ 2100 taxa) in the chloroplast genome with the addition of *rbc*L and *mat*K loci where

available (see Appendix B in the online supplementary materials for taxonomic list). Baits were hybridized at 55°C for 24 hours. Further details on design and wet-lab procedures can be found in the supplementary online materials (Chapter 3, Appendix A, section 3.5.1).

2.3.8 Post-indexing total quantification, pooling, size-selection, and sequencing

Post-indexed libraries were quantified using the long-amplification total library qPCR assay with averaged PCR duplicates (Table 3.10). Thereafter, those libraries were pooled to equimolar concentrations using the qPCR derived molarity estimates. This is to equalize sequencing depth between samples with wide ranges in molarity. Libraries to be enriched, shotgun sequenced, or that had been amplified with PCR metabarcoding were each pooled separately. The three pools were size-selected with gel excision following electrophoresis for molecules ranging from 150 bp to 600 bp. Gel plugs were purified using the QIAquick Gel Extraction Kit (QIAGEN), according to manufacturer's protocols, then sequenced on an Illumina HiSeq 1500 with a 2 x 90 bp paired-end protocol at the Farncombe Metagenomics Facility (McMaster University).

2.3.9 PCR metabarcoding

Sadoway (2014) previously worked with these and many other Yukon permafrost core samples using a metabarcoding approach. These libraries had been extracted in duplicate with guanidinium protocols (Boom et al., 1990; D'Costa et al., 2011) from 250 mg of the same core sections, purified with silica (Höss and Pääbo, 1993), and eluted twice (Handt et al., 1996). Further details of Sadoway's metabarcoding approach can be found in the supplement: Chapter 3, section 3.5.2.

As a follow-up to assess whether metabarcoding with PowerSoil or our cold spin extractions would produce different results than those from Sadoway, we used the same P6 loop *trn*L primers (Taberlet et al., 2007) to amplify all of the extracts from the SET-E experiments (Table 2.1). Each sample extract was PCR amplified in triplicate (PCR conditions and qPCR results are detailed in the supplement: Chapter 3, section 3.5.3), then purified with a 10K AcroPrep Pall plate using a vacuum manifold and pooled into a single 50 µL sample extract in EBT. These *trn*L metabarcoded extracts were then library

prepared, indexed, and pooled at equimolar concentrations following the same aforementioned procedures, but in a post-PCR facility. They were sequenced at the Farncombe Metagenomics Facility on an Illumina HiSeq 1500 with a 2x90 bp paired-end protocol to an approximate depth of 500,000 reads for each extraction replicate.

2.3.10 Bioinformatic processing

Additional details on the bioinformatic workflow can be found in the supplement (section 3.5.4). In brief, after trimming and merging with *leeHom* (Renaud et al., 2014), the sequenced DNA reads were mapped with *network-aware-BWA* (Li and Durbin, 2009) (https://github.com/mpieva/network-aware-bwa) to both the animal and plant baits as well as to the original plant target references (targeting *trn*L, *mat*K, *rbc*L) in order to filter out off-target molecules, hereafter referred to as map-filtering (Fig. 2.2). Two map-filtering approaches were used as we observed that while mapping to the baits is more conservative, it may unfairly bias against metabarcoding amplicons as they may not map well to the artificially tiled (and highly curated) 80 bp probes (see section 3.5.4.2). Map-filtered reads were length filtered to ≥ 24 bp (as smaller sequences generally have low support when assessing taxonomy), string de-duplicated (to remove molecules artificially duplicated during PCR) with the *NGSXRemoveDuplicates* module of *NGSeXplore* (https://github.com/ktmeaton/NGSeXplore), and then *BLASTn* (Altschul et al., 1990) aligned against a July 2018 local copy of the GenBank NCBI nucleotide database set to return the top 100 alignments (taxonomic hits) per read. Fasta and blast files (file types containing sequenced reads [fasta] and the taxonomic alignments [blast]) were passed to *MEGAN* (Huson et al., 2007; 2016) where the *BLAST* results were filtered through a lowest common ancestor (LCA) algorithm (selected parameters detailed in section 3.5.4).

MEGAN LCA

The *MEGAN LCA* algorithm determines the lowest taxonomic rank at which a set of reads can be assigned based on the assigned threshold of confidence values. For example, to call *Bison bison* as being present in this instance, at least 3 unique reads must align to a region of the *B. bison* mitogenome with ≥ 95% identical similarity, with low e-values and high bit scores (metrics used by *BLASTn* to assess the likelihood of

misalignments), and by matching or exceeding other parameters used to define confidence in the taxon identification (the rationale for selected LCA parameters are discussed further in section 3.5.4). Adjusting LCA parameters shifts the trade-off ratio of false positive to false negative assignments, although it would seem that optimal LCA parameters may only exist on a project-by-project or even sample-by-sample basis depending on the taxonomic molecular constituents present, the degree of aDNA damage, and the research question (see Huson et al., 2018). For example, if percent identity is set to 100, only exact matches will be considered, but then aDNA fragments with terminal base modifications (the majority of aDNA molecules) will be unassigned when their taxonomic classification might otherwise be obvious. Further, increasing the number of reads necessary to call a taxon node as being present can artificially bias the data to organisms that release more eDNA irrespective of actual biomass or had better organo-mineral complex preservation characteristics. For example, woody plants at boreal sites have been observed by Yoccoz et al. (2012, p. 3652) to have proportionally less DNA presence relative to above-ground biomass as compared with graminoids and forbs. This would imply that DNA recovery cannot be easily correlated with plant biomass across functional types without some form of calibration, which would likely require extensive region-specific experimentation. If minimum read counts are set too high, we might expect that some rarer woody plants would become undetectable while others would appear to be in low abundance, and that forbs would bias towards an over-representation.

Similarly, the LCA parameter top percent sets a percentage threshold of hits to be used for taxonomic classification based on the top bit-scores for a read as reported by *BLAST*. If this value is set too high (> 50%), reads that might otherwise have obviously best hits to a species or genus will instead be assigned to higher (less taxonomically useful) ranks such as family or order due to other *BLAST* hits for the same read with lower bit-scores (less sequence similarity), thus inaccurately influencing read assignment. Setting this value too low (< 5%), can likewise make taxonomic assignments inaccurately specific by artificially ignoring hits with marginally lower bit-scores that are just as likely to represent the host organism. These ambiguities in optimal LCA threshold values are

compounded by database incompleteness and the overrepresentation of certain organisms of economic or scientific interest, the unknowns of palaeo-biogeography (Jackson, 2012), variably specific genetic loci (Kress and Erickson, 2007), erroneous GenBank references (Shen et al., 2013; Lu and Salzberg, 2018), limitations of NCBI *BLASTn* and equivalent algorithms (Shah et al., 2019), and other evolutionary complexities that blur species boundaries such as introgressive hybridization (Whitworth et al., 2007; Percy et al., 2014).

Alternative approaches, such as the phylogenetic intersection analysis (PIA) recently reported by Cribdon et al. (2020), may be better suited to resolving some of these uncertainties in determining optimal criteria for taxonomic identification. These challenges are relatively typical of proxy measures of palaeobiota (e.g. Jackson, 2012; Baker et al., 2013; Fiedel, 2018) and are in need of further research. In a rough sense here, the more unique reads assigned to a taxon node (relative to similar organisms), the higher the likelihood that those taxa were indeed present. Further, relative shifts in read proportion through time (such as the ratio of graminoids and forbs to conifers and woody shrubs) can serve as a very rough estimate of past relative abundance (although this must be interpreted carefully as many stochastic processes are involved in eDNA release, degradation, preservation, and recovery). We suggest that the LCA parameters utilized here balance the challenges of false positive and false negative assignments well for these particular samples, although more research is needed to improve the criteria by which confidence parameters are selected and utilized algorithmically.

False positives

To alleviate observations of sporadic false positives in the plant data for the genus level comparisons, all plant genera were individually inspected and queried online to determine if any extinct or extant species from those clades have been observed in northern or alpine North America or northeastern Eurasia. Clades assessed to be highly improbable (those with known biogeographic extents limited to non-Holarctic regions) were added to a running list of disabled taxa in *MEGAN* that repeatedly were identified in this and parallel research (Table 3.18). We believe these false positives are driven by an

abundance of genetic research on specific taxa within these unlikely clades and an absence of data for whatever the real taxon is. Cribdon et al. (2020, pp. 2–4) refers to these false positive hits as oasis taxa. In uneven databases, sparsely populated genetic references within a clade can succumb to oases where a set of well-studied organisms drive an illusion of confidence in genetic alignments because those are the only 'good' alignments available for that read. This makes the alignment seem confident and highly specific because the wider range of organisms within those clades have yet to be sequenced. This confidence due to reference oases makes it difficult to remove false positive hits via stricter LCA parameters without also dropping a significant proportion of reads that have equally confident metrics, but are instead driven by genetically well represented clades that happen to make ecological sense. The *MEGAN* LCA algorithm has been demonstrated to be robust to false positives (Huson et al., 2007; 2018), but Cribdon et al. (2020) argue that oasis taxa can remain a problem unless addressed via manually removing so-called problematic taxa or using an approach such as their PIA algorithm. We were unaware of this software approach at the time of analysis, and instead opted for a manual removal of suspected oasis taxa. A manual exclusion approach may limit the possibility of identifying biogeographically unknown and 'rare' taxa that may otherwise have evaded detection in Quaternary records to date, but does allow for a more nuanced decision process that might otherwise be obfuscated by a set of arbitrary cut-off values. The oasis problem could also likely be alleviated with a highly curated, non-redundant, and regionally specific reference database, but this would further limit the ecological reconstruction to only organisms one expects to find. Oasis reference taxa are likely to become less problematic as reference databases are improved over time, and as alignment algorithms are better designed to cope with uneven database coverage. Increasing the *BLASTn* top hits to 500 or more, as suggested by Cribdon et al. (2020), is also something we have found in parallel research aids in combating database unevenness (data not reported here), but does often create very large blast files.

To address the probable false positive assignments here, for all genus-level plant bubble-chart comparisons (Figs. 2.6–2.7, 3.23–3.27), we used a manual exclusion

approach using a list of improbable taxa (oasis candidates) observed in these metagenomic reconstructions as well as other permafrost and lake sediments processed in parallel (Table 3.18). Other metagenomic comparisons reported here (Figs. 2.5, 3.20–3.22, 3.28–3.33) do not include these improbable taxa as disabled in *MEGAN*. Probable oasis references appear to have very low LCA-assigned read counts even when summed to high taxonomic ranks (e.g., Zingiberales) when compared with taxonomic nodes that make palaeoecological sense (Fig. 2.5). As such, these highly improbable taxa do not appear to constitute a sizable fraction of the organisms identified in this analysis.

Bubble-charts

Libraries were compared using bubble-charts with logarithmically scaled bubbles for visually proportional normalizations, but with absolute read counts retained. For the site-by-site charts reporting both animal and plant reads (Figs. 2.5, 3.20–3.22, 3.28–3.31), the plants were collapsed to higher taxonomic ranks to allow for summarized comparisons. For the plant map-filtered charts (Figs. 2.6–2.7, 3.23–3.27), all data were collapsed to the genus rank—meaning all LCA assignments to species or subspecies were pushed up to the rank genus and summed with other species within that clade. This is to mitigate species-specific resolution problems, driven in part by database incompleteness, where only a subset of species in a genus may have been sequenced for a particular locus to date. This can be seen for example with Sitka willow (*Salix sitchensis*), which has yet to be sequenced (and uploaded to GenBank) for the *trn*L locus, as compared to Arctic willow (*Salix arctica*), which is represented. This would theoretically increase the likelihood of species misassignment within that genus if the actual organism from which those DNA fragments is derived has yet to be sequenced or if that locus is not species-specific for the clade—compounded again with ancient samples by taphonomy, diachronic biogeographic shifts, and molecular evolution.

2.4 Results

2.4.1 Methodological comparison

qPCRs on the DNA libraries show an up to 7.0x increase in total adapted DNA over PowerSoil extractions among the four core samples (average 3.6x increase) with our

cold spin extraction procedure, and an up to 5.6x increase in 'endogenous' *trn*L library adapted chloroplast DNA (average 3.0x increase) (Figs. 2.3 and 3.16). Inhibition indices for our cold spin extractions were lower than PowerSoil (average = 0.75 versus 0.95 for PowerSoil, see section 3.1.4 for a description of the inhibition index), meaning that more inhibitors were retained with our cold spin extractions compared with PowerSoil. However, these inhibitors did not dramatically reduce enzymatic efficiency during adapter ligation; in post-library preparation qPCR assays (Figs. 2.3 and 3.16) these cold spin samples quantify with significantly more library adapted DNA than PowerSoil extracts, despite some inhibitor retention. When these samples were extracted following standard Dabney et al. (2013b) procedures without the cold spin, they were completely inhibited (section 3.1).

LCA-assigned reads from samples extracted using our sedaDNA modified Dabney protocol paired with PalaeoChip enrichments show a 7.7–19.3x increase in LCA assigned reads over enriched PowerSoil extracts, and a 1.2–59.9x increase compared with Sadoway's (2014) plant and animal PCR metabarcoding approach (Table 3.21). An equivalent increase is observed when comparing the *trn*L metabarcoded PowerSoil and cold spin extracts with those that were extracted with the cold spin and enriched (2.3–23.0x and 2.9–19.5x increases, respectively). Compared with shotgun, the increase in map-filtered DNA for the cold-spin enriched samples is consistently three orders of magnitude, where shotgun sequencing recovered almost no ecologically informative DNA from our plant mapping references for any of the core slices at a depth of 2 million reads each. However, several nuclear and broader chloroplast loci were identified in the non-mapped shotgun data (this is discussed further in section 3.5.4.5). LCA-assigned read count is not necessarily the most informative metric when comparing these methods however, as many reads in all variants were assigned to high taxonomic ranks with limited interpretive utility. More important is the breadth of organisms identified by being able to target multiple loci simultaneously and capture fragments too small for metabarcoding. Targeted enrichments, when paired with the cold spin extractions, recover the same predominant taxa as the two metabarcoding approaches, but with a far greater

diversity of identified organisms (Figs. 2.4–2.7, 3.20–3.27). Taxa with sufficiently high LCA-assigned read counts from the enriched libraries also show characteristic aDNA deamination patterns and fragment length distributions with *mapDamage* (Jónsson et al., 2013) (Fig. 2.9). We also observe that extraction replicates show minimal variation in terms of taxonomic assignments between homogenized subsamples, suggesting that the trends observed here are a result primarily of differences in method and not intrasample variation.

While qPCR amplifications indicate much higher starting quantities of DNA for samples extracted with the cold spin extractions compared to PowerSoil (Fig. 3.17), the downstream metagenomic comparisons show no noticeable differences in taxonomic profiles between the two extraction methods for *trn*L metabarcoded libraries (Figs. 2.6–2.7, 3.22–3.26). In multiple instances, the cold spin metabarcoded samples recovered a somewhat taxonomically broader set of eDNA across subsampled replicates, but the effect is marginal at best. We suspect that the high cycle numbers during PCR amplification compensated for the relative DNA loss of the PowerSoil extracts (observable in Fig. 3.17), amplifying the lower concentration sedaDNA of PowerSoil to the same relative taxonomic proportions. Further modifications to the cold spin extraction method may aid a metabarcoding approach. But at this time, only samples intended for enrichment or shotgun sequencing would be best served with the cold spin.

2.4.2 Palaeoecology

We observed a diverse range of molecularly identified animals and plants from well-preserved sedaDNA in these permafrost samples (Fig. 2.5). These data correspond well with palaeoecological understandings of environmental change around the Pleistocene-to-Holocene transition (Dyke, 2005; Zazula et al., 2005; 2006a), but with some notable exceptions. Our cold spin extraction method paired with targeted enrichment (using the PalaeoChip Arctic-1.0 bait-set) recovered potential sedaDNA evidence for the late survival of mammoth (*Mammuthus sp*.) and horse (*Equus sp.*) in the Klondike region of Yukon, Canada, as well as an early indication of‘low abundance pine

(*Pinus sp.*) (Fig. 2.5). The significance and means by which to interpret these data is discussed further under *Palaeoecology* (section 2.5.3) below.

2.5 Discussion

Our cold spin inhibitor removal procedure, paired with Dabney et al. (2013b) aDNA purifications and capture enrichment, consistently recovered a broader taxonomic set of on-target environmental molecules than the PowerSoil extraction kit paired with targeted enrichment, shotgun sequencing (with either extraction method), an older PCR metabarcoding approach, or a plant-specific *trn*L metabarcoding approach (with either extraction method). Over 70% of the taxon classifications identified with cold spin extractions paired with the PalaeoChip enrichments would not have been identified with alternative approaches (Figs. 2.5–2.7, 3.20–3.27). These results demonstrate the viability of targeted enrichment for taxonomically diverse environmental samples from permafrost exposures without the necessity of PCR metabarcoding and the associated compounding biases therein. These data also demonstrate the significantly improved breadth and sequencing efficiency of eDNA recovery when using capture enrichment compared with a shotgun approach. While some of the taxa identified are biogeographically implausible, most make ecological sense. The breadth of taxa identified with a capture enrichment approach (and high DNA recovery extraction method) aid in expanding the ecological scope of environmental changes that can be observed when not restricted to DNA fragments amenable to a metabarcoding approach. Deep shotgun sequencing to library exhaustion would be ideal as it is the least biased approach. However, until data storage, computational power, database completeness, and sequencing costs are significantly improved, deep sequencing strategies are largely unachievable for most users except for those with immense computational and sequencing resources.

2.5.1 Overcoming enzymatic inhibitors

Our ongoing experiments with a diverse range of sediments suggest that extracts with inhibition indices over ~0.3 are still amenable to library preparation, but with reduced adapter ligation efficiency (see section 3.4 for a discussion of extract qPCR inhibition). Solution C3 (120 mM aluminum ammonium sulfate dodecahydrate) in the

PowerSoil kit is effective at precipitating humic substances, resulting in clear, inhibitor-free extracts. However, aluminum sulfate has also been demonstrated to readily precipitate DNA along with those humic substances (Dong et al., 2006). We have found that the PowerSoil kit is effective at removing DNA inhibition, but that this approach resulted in less library adapted DNA. The kit would seem to be most effective with modern sediments and soils, where degradative processes are comparatively limited, but this inhibitor removal approach might be too aggressive at precipitating the tightly bound organo-mineral complexes in which rare fragments of sedaDNA are preserved. There seems to be an important balance between releasing enough DNA but not releasing too many inhibitors during the lysis stage, and also removing enough inhibition for enzymatic reactions, while not removing the majority of the endogenous sedaDNA during purification (Fig. 2.8). We suspect that with further optimization, the cold spin extraction procedure could be improved to better remove DNA independent inhibitors (such as humic substances) that impact enzymatic activity (Allison, 2006) in other sediment contexts. Samples with inhibitor types unaffected by the cold spin may still be best extracted with a modified PowerSoil protocol or alternative approaches. Of course, the inhibitor constituent (as well as distribution of preserved aDNA) of a site or sample likely varies considerably even at the molecular scale, making it difficult to estimate the best approach at the outset of an investigation without extensive site-specific experimentation.

Of interest for further research is how inhibitor precipitation is affected by the interaction between the lysing detergent sodium dodecyl sulfate (SDS) and the cold spin (see section 3.4.2). We suspect that the efficiency of inhibitor precipitation with the long cold spin method could be further optimized, as our experiments suggest that the presence of SDS in the lysis buffer significantly contributes to the precipitation of humics and other inhibitors, compared with extracts where sarkosyl was used as the lysing detergent. For the permafrost samples in this study, we have found that the cold spin technique is effective at removing enough inhibition for effective library preparation while maximally retaining sedaDNA. However, other samples (not in this study) with especially high concentrations of humics and other unidentified inhibitors retain much of their inhibition

despite the cold spin (with the cold spin producing thick pellets of inhibitor precipitates [$\gtrsim$ 1 cm^3], such as illustrated in Fig. 2.1), necessitating further sample-specific modifications. We have observed generally (data not reported here) that lowering the sediment input (<0.2 g), splitting the subsample into multiple low-input lysing tubes and pooling after the cold spin over a Roche column, as well as increasing the duration of the cold spin, helps further reduce the inhibitor load of especially challenging samples. Our cold spin technique is unlikely to be optimal for all forms of sedaDNA inhibition however, as it has been observed that identifying the specific inhibitory substances involved is critical to mitigating the compound-specific mechanisms that affect enzymatic reactions (Opel et al., 2010). Further research is needed to identify the inhibitor constituents of sedaDNA target samples in order to improve the inhibitor precipitation we observed while maximizing sedaDNA retention.

2.5.2 SedaDNA authenticity

DNA damage is often used as a proxy indicator for assessing whether sets of molecules are ancient or the result of modern contamination (Mitchell et al., 2005; Gilbert et al., 2007a; Ginolhac et al., 2011; Sawyer et al., 2012; Dabney et al., 2013a; Jónsson et al., 2013). Damage profiles for taxa with sufficiently high read counts ($\gtrsim$200 reads at minimum map quality 30) show characteristic aDNA deamination patterns and short fragment length distributions (Fig. 2.9). When mapping to the mitogenome, taxa with $\lesssim$200 reads typically show an insufficient overlap of fragments to identify modifications of the terminal bases. This precludes confident assessment of damage patterns and makes it difficult to authenticate rare taxa with low read counts in this dataset. Comparisons of the map-filtered with non-mapped libraries (section 3.5.4.5) suggests that our quality filtering steps are sufficiently conservative to reduce the noise characteristic of metagenomic datasets (Lu and Salzberg, 2018; Eisenhofer et al., 2019), but may also strip out some potentially informative (but less confidently assigned) reads. Our pre-*BLASTn* map-filtering approach allows for a more conservative and streamlined analysis. Using a more regionally curated *BLAST* database might alleviate some of the potential for false positives due to ecologically nonsensical oasis taxa as discussed in section 2.3.10.

However, this will also potentially come at the cost of alternative false positives and negatives due to biases in database representation that result from limitations in our proxy-driven understandings of palaeoecosystems (Jackson, 2012). This theoretically could drive taxonomic assignments towards organisms one is comfortable identifying, because the actual unexpected organism is not included as a possibility for taxonomic assignment, driving a false sense of confidence in the specificity of those reads. An approach incorporating elements from the PIA algorithm (Cribdon et al., 2020) with the interface and flexibility of the *MEGAN* software (Huson et al., 2007; 2016; Huson and Mitra, 2011) would likely be a good trajectory for moving forward with an eDNA capture enrichment or shotgun based approach.

Blank controls

Blank extraction, library, indexing, and metabarcoding reactions (used to identify buffer and cross-contaminants) in the shotgun and enriched libraries do not contain any map-filtered reads (Table 3.23). The non-mapped LCA-assigned reads for these blanks are predominantly adapter-contaminated sequences (≥ 95%) (Fig. 3.32). The map-filtered metabarcoding blanks only contain reads that could be LCA assigned to high taxonomic ranks (Fig. 3.33). This would suggest that patterns of library sequence composition observed in the sample replicates are at minimum originating from the samples themselves and are not the result of laboratory contamination.

2.5.3 Palaeoecology

This study is intended as a proof of concept to demonstrate the viability of targeted enrichment for the recovery of ecologically complex, molecular taxonomic proxies from open-air eDNA samples. Further research will utilize these methods, and complementary palaeoecological techniques, on Yukon lake sediments and permafrost cores from the Klondike area to track ecological shifts during the Pleistocene-Holocene transition. However, it is worth briefly contextualizing these broad taxonomic trends here for authenticity purposes (as summarized in Fig. 2.4).

The Bear Creek (BC 4-2B, 30,000 cal yr BP [D'Costa et al., 2011]) and the older Lucky Lady II sample (LLII 12-217-8, 15,865 cal yr BP [Mahony, 2015]) both date to a

period in which eastern Beringia is thought to have been largely a herb tundra biome, dominated by exposed mineral surfaces, prostrate willows, grasses, forbs (non-graminoid herbs), and occupied by diverse and abundant megafauna (Dyke, 2005; Zazula et al., 2005; 2006a). Our data reflect this environmental setting, particularly in the case of Bear Creek (Figs. 2.4–2.5, 3.26–3.27) (D'Costa et al., 2011). We identify a similar range of mammalian species as D'Costa et al. (D'Costa et al., 2011) using the same core sample, but with additional taxa (e.g., caribou [*Rangifer tarandus*]). More specific taxonomic assignments, especially if novel or possibly controversial, need to be treated with caution. Thus, while D'Costa et al. (2011) identified *Bos sp.*, we recovered a more specific signal for yak (with hits to both *B. grunniens* and *B. mutus* [domestic and wild yak, respectively]. Web-*BLASTing* these yak-specific reads to the top 5000 hits (rather than top 100) drops the LCA-assignment to *Bos sp.*, which is consistent with the results reported by D'Costa et al. (D'Costa et al., 2011). A follow-up investigation with deeper sequencing is intended to assess the possibility of *Bos mutus* (yak) in eastern Beringia during the Pleistocene.

Results from the younger Lucky Lady II sample (LLII 12-84-3, 13,205 cal yr BP [Sadoway, 2014]) indicate an expansion of birch shrub tundra (Dyke, 2005), reflected by a decrease in grasses and a proportional increase in birch (*Betula sp.*) and willow (*Salix sp.*) (Figs. 2.4, 3.23–3.24) relative to the earlier two core samples. The youngest core sample (MM12-118b, 9685 cal yr BP; Mahony, 2015) shows a proportional increase in conifers, particularly spruce (*Picea sp.*) but also potentially pine (*Pinus sp.*), that is consistent with pollen records in southern Yukon for the expansion of forests (Gajewski et al., 2014) and the establishment of the northern boreal forest by ~9000 cal yr BP (Dyke, 2005). Assignments to *Pinus sp.* are unexpected as previous research has found that lodgepole pine (*Pinus contorta* var. latifolia) had a northern extent of 60°N (the Yukon-B.C. border) during the early Holocene, and only reached its present-day northern limit (~63°N) by ~1790 cal yr BP (Strong and Hills, 2013). When the relevant set of pine positive samples is subjected to more stringent bioinformatic testing (section 3.5.4.4), these reads unambiguously retain their assignments to the genus *Pinus*. The stratigraphic

reliability of these sedaDNA molecules in permafrost might be questionable, but if their age is accurate, it would suggest a low-density northern expansion of pine beyond southern Yukon ~3500 years earlier than pollen and stomata records have yet indicated (Schweger et al., 2011; Strong and Hills, 2013; Edwards et al., 2015). Whereas most chloroplast sedaDNA from angiosperms is expected to be due to locally decaying tissues as pollen from these organisms does not typically contain organelle genomes (Birky, 2008), gymnosperms generally inherent their chloroplasts parentally, which has been observed specifically for pine (Chen et al., 2002). While this opens the possibility for long-distance transport of chloroplast DNA via pollen, lodgepole pine have been observed to effectively transport pollen up to 10 km (but more so in the 0.1–0.5 km range) (Perry, 1978). The southern Yukon border is some 400 km away from the study area, implying that even if this pine signal is not exactly local, it still implies the presence of pine in central Yukon some 3500 years earlier than observed in other research.

The mammalian sedaDNA constituents of these permafrost samples also display a marked change, dwindling in relative abundance and richness with time into the Holocene (Figs. 2.4, 3.20–3.22), but perhaps less sharply than commonly thought. For example, we recovered genetic evidence of both woolly mammoth (*Mammuthus primigenius*) and horse (*Equus sp.*) in the Upper Goldbottom core dated to ~9700 cal yr BP (Mahony, 2015). Previous radiocarbon dates on fossils indicate that horses disappeared from high-latitude northwestern North America relatively early, ca. 13,125 cal yr BP ("last appearance date" 11,500 ^{14}C BP, based on AMNH 134BX36 from Upper Cleary Creek [Guthrie, 2003]). This ~3400-year difference implies the existence of a substantial ghost range (i.e., a spatiotemporal range extending beyond the last appearance age, as indicated by direct dating of fossils or other associated remains; Haile et al., 2009). While this find cannot be corroborated by the macrofossil record for *Equus,* it is consistent with previous sedaDNA results from central Alaska (Haile et al., 2009).

In the absence of additional information, it is difficult to assess whether this small signal (Fig. 2.4) may be considered chronostratigraphically reliable or whether it has been affected by factors such as leaching, cryo- or bioturbation, or reworking (redeposition)

(Arnold et al., 2011), altering the relative positions of sedaDNA complexes. In the case of the mammoth reads, after merging the sequenced data from the three Upper Goldbottom core (MM12-118b) subsampled replicates, coverage was insufficient (low read counts mapping across the mitogenome) to reliably assess characteristic aDNA damage patterns (Fig. 3.38). There is arguably some indication of terminal damage with the merged *mapDamage* and short fragment length distribution (FLD), but greater sequencing depth is needed to assess their authenticity. These LCA-assigned mammoth (n=41) and horse (n=10) reads from the Upper Goldbottom core (~9700 cal yr BP) were extracted, concatenated, queried with the web-based *BLASTn*, and subjected to stricter LCA parameters (section 3.5.4.4). Despite stricter filtering, three reads were LCA-assigned to *M. primigenius, 25 to Mammuthus sp.*, and 11 were identified as Elephantidae. *Equus sp.* retained five assigned reads. A follow-up analysis with deeper sequencing of this sample will further address the veracity of this signal.

2.5.4 Limitations of comparison

There are several caveats to keep in mind when assessing our comparison of protocols and the potential of the PalaeoChip Arctic-1.0 bait-set. First, the lysis stage of our PowerSoil and of the sedaDNA modified Dabney protocols were not equivalent in duration or reagents. We followed manufacturer specifications for PowerSoil, but the lysis stage of extraction with equivalent kits can be increased in duration and augmented with additional reagents to theoretically increase DNA yield (Niemeyer et al., 2017). Further, a recently released update to the PowerSoil kit, the DNeasy PowerSoil Pro, claims to have an 8-fold increase in DNA yield compared with comparative commercial kits (it is unclear what the n-fold increase over standard PowerSoil is with this updated kit). Our experiments with the PowerSoil inhibitor removal solution C3 found consistently low DNA retention compared with our longer duration 4°C spin as an inhibitor removal technique (section 3.2). The PowerSoil inhibitor removal solution is effective at rapidly precipitating enzymatic inhibitors, but this study suggests that it is often overly aggressive and consistently precipitated viable sedaDNA in the process (Fig. 3.7). We suspect that a longer lysis stage with PowerSoil would increase overall yields,

but would not mitigate the substantial losses associated with overly aggressive humic precipitation when utilizing solution C3 (at least at manufacturer recommended concentrations). We found that the cold spin is sufficiently effective at removing enzymatic inhibition with these permafrost samples to allow for successful adapter ligation, even if the extracts were not as inhibitor free as PowerSoil. However, we have also found that samples from bogs or sites with high organic loads remained highly inhibited despite the cold spin, likely due to the high humic concentrations (among other forms of inhibition). For difficult samples such as these, further fine-tuning is needed to improve inhibitor removal.

Second, metabarcoding is not directly equivalent to enrichment when comparing taxonomic coverage and LCA-assigned read counts. Mapping our data back to the baits does strip out taxonomically informative hits—potentially to a greater degree than with metabarcoding data that might not map well to the curated bait sequences. To mitigate this, we mapped the second set of plant specific *trnL* comparisons (Figs. 2.6–2.7, 3.22–3.26) to the plant references rather than the baits sequences to increase the metabarcoding reads available for *BLAST*. We observe that mapping to the curated baits (which have low complexity and non-diagnostic regions masked or removed) substantially reduces the number of low confidence (potential false positive) spurious hits but does result in data loss (see Figs. 3.18–3.19). Map-filtering to the plant references alleviates this to some degree but in the future this strategy might be better paired with a regionally curated reference database or PIA approach (Cribdon et al., 2020) as discussed earlier.
Finally, it should be emphasized that the PCR metabarcoding data re-analyzed from Sadoway (2014) targeting multiple plant and animal loci were from samples not purified with our cold spin sedaDNA optimized extractions. The libraries that were extracted with PowerSoil and our sedaDNA modified Dabney procedure were only PCR amplified for *trn*L (rather than the suite of loci initially assessed by Sadoway [2014]). We observe that PowerSoil and cold spin extracted metabarcoding samples generally outperform their counterparts processed by Sadoway with the Boom et al. (1990) and D'Costa et al. (2011) extractions in terms of taxonomic breadth, but that these three metabarcoding approaches

do generally identify the same predominant taxa. We suspect that either of these newer extraction methods would have resulted in a wider breadth of plant and animal taxa identified for the Sadoway metabarcoded libraries. This limitation of our comparison should moderate conclusions drawn from this work.

The key observation in this study is that enrichment clearly outperforms alternative targeting strategies in this dataset, including the PowerSoil or cold spin extracted *trn*L metabarcoded libraries. We suspect this is driven in large part by the smaller fragment lengths available to an enrichment approach compared with metabarcoding. For example, in the Upper Goldbottom core (MM12-118b), LCA-assigned hits to *Betula sp.* (Figs. 2.4 and 2.7) in the enriched libraries have a FLD mode of 49 bp (n=5397), whereas hits to *Betula sp.* from the same extracts but with metabarcoded libraries have a FLD mode of 98 bp (n=500). In this case, the metabarcoding libraries were restricted to targeting much longer fragments that are comparatively rare with sedaDNA. This bias towards large fragments with metabarcoding is likely one of the main reasons why many rarer taxa are missed with this approach. Low biomass organisms would have an expectedly lower proportion of eDNA, with taphonomic processes making long fragments (those needed for metabarcoding) even more unlikely to survive. As an example where this might be driving taxonomic false negatives, *Lupinus sp.* (lupine) was identified in the Upper Goldbottom core with a combined count of 353 unique reads in the cold spin enriched libraries, but was absent from all of the metabarcoding libraries. *Lupinus sp.* enriched libraries have a FLD mode of 41 bp, with 79% of the reads being shorter than 69 bp. The *trn*L metabarcode for *L. arcticus* (Arctic lupine) is 52 bp, but with primer landing sites this fragment increases in length to 91 bp. With such a large fragment necessary for metabarcoding detection, it is not surprising that this taxon and other low biomass organisms were not detected with metabarcoding when aDNA fragments of this length are exceedingly rare. In the same way, 73% of *Betula sp.* reads in the enriched sample are shorter than 69 bp, and only 12% are 80–110 bp, whereas 83% of the metabarcoding reads for *Betula sp.* fall in the larger fragment range. Fig. 3.39 in Appendix A depicts an FLD histogram of this example.

The goal of this analysis was to establish the viability of enrichment for complex sedaDNA contexts, and to report on a new inhibitor removal technique that may yet be further optimized. Despite limitations of the comparison discussed above, the data clearly demonstrate the power of targeted enrichment for eDNA, and we intend to further expand on the PalaeoChip Arctic-1.0 bait-set with additional target sequences for regionally specific vegetation, mammals, insects, fungi, and microbiota. We also intend to optimize PalaeoChip for other non-arctic/subarctic regions.

2.6 Conclusions

The experiments outlined in this report demonstrate the utility of our cold spin inhibitor removal technique, paired with Dabney et al. (2013b) purifications, for overcoming enzymatic inhibitors in sedimentary materials. This technique utilizes the high aDNA recovery potential of Dabney purifications, while also addressing the unique challenges of sediments and soils where many inhibitory substances tend to co-elute with target sedaDNA molecules. Other extraction approaches, such as the PowerSoil kit, struggle with significant aDNA loss that ultimately limits the targeting options for maximally exploiting the genetic archives preserved in sedimentary contexts. The improved DNA retention of the cold spin inhibitor removal technique described here facilities the significantly expanded targeting scope of a capture enrichment approach for sedaDNA, in this case using the PalaeoChip Arctic-1.0 bait-set. With this approach, we were able to capture a highly complex set of plant and animal DNA from permafrost sediments that outperformed an alternative extraction strategy, shotgun sequencing, and two versions of a PCR metabarcoding approach. Many of the organisms identified here with our cold spin and enrichment strategy were entirely missed with alternative methods, including the potential late survival of woolly mammoth (*Mammuthus primigenius*) and horse (*Equus sp*.) in the Klondike of Yukon Canada, and the early Holocene appearance of pine (*Pinus sp.)*. Further work is needed to refine the potential for false positives and negatives in metagenomic datasets due to a variety of factors, but most notably database incompleteness and unevenness. Recent work reported by Cribdon et al. (2020) may serve as a viable next step towards further improving molecular taxonomic identifications to

make full use of the eDNA archives of palaeobiota being rapidly unlocked by new methods.

An enrichment approach for eDNA avoids the myriad limitations of a PCR metabarcoding strategy, and opens many new possibilities for further study, such as whole genome capture and assembly, as well as phylogenetic placement without any surviving macroremains. By increasing the taxonomic breadth of our environmental baits, and further optimizing enrichment and sedaDNA extraction conditions, this technique can continue to improve the sequenced fraction of on-target molecules without deep shotgun sequencing, or potentially biased PCR amplifications. This technique enables the recovery of a more holistic set of palaeoenvironmental DNA of widely varying molecular fragment lengths from a diverse range of genetic loci. This expanded set of captured DNA targets allows for the simultaneous molecular identification of organisms that might not have the biomass to be readily detected with other palaeoecological methods, and even in the complete absence of surviving tissues or microfossils. PCR metabarcoding is likely to remain a viable and important eDNA workhorse for the foreseeable future. As the costs of metagenomic analysis continue to decrease, and especially in situations where DNA preservation is favorable and a wide set of targets are of interest, an enrichment approach as shown here has the potential to recover a far greater diversity of molecular taxonomic identifiers to better complement traditional palaeoenvironmental approaches.

2.7 Acknowledgements

Our thanks to Alison Devault at Arbor Biosciences for her invaluable assistance with designing the bait-set, as well as Brian Golding and members of his bioinformatics research team at McMaster University for their computational resources and assistance, and all members of the McMaster Ancient DNA Centre. We also wish to thank the editors at *Quaternary Research* and peer-reviewers who provided detailed and carefully considered critiques, which significantly improved the quality of this report. We wish to thank the Arctic Institute of North America, the Garfield Weston Foundation, the Natural Sciences and Engineering Research Council of Canada, McMaster University and the Department of Anthropology, Polar Knowledge Canada (POLAR), and the Social

Sciences and Humanities Research Council of Canada for each funding various components of this research.

2.8 Tables

Table 2.1 Sample descriptions and read counts (SET-E).

Site, core, age	Sample	DNA Targeting Strategy	Extraction Method	Total Reads	Bait mapped & LCA-assigned*	Assigned of Total	Plant ref mapped & LCA-assigned**	Assigned of Total
Upper Goldbottom MM12-118b 9685 cal yr BP	GB1	Metabarcoding	D'Costa et al., 2011	109,233	311	0.3%	1,937	1.8%
	SET256-MB	Metabarcoding (*trn*L only)	PowerSoil	493,220			1,855	0.4%
	SET257-MB			335,392			1,529	0.5%
	SET258-MB			424,696			1,911	0.4%
	SET256-En	Enrichment		6,292,874	12,812	0.2%	63,562	1.0%
	SET257-En			675,550	4,105	0.6%	18,541	2.7%
	SET258-En			820,382	4,354	0.5%	17,695	2.2%
	SET256-SG	Shotgun		1,717,174	5	0.0%	48	0.0%
	SET268-MB	Metabarcoding (*trn*L only)	Cold Spin (sedaDNA modified Dabney)	373,049			1,959	0.5%
	SET269-MB			442,926			2,417	0.5%
	SET270-MB			330,692			1,942	0.6%
	SET268-En	Enrichment		1,704,149	122,282	**7.2%**	176,221	**10.3%**
	SET269-En			1,782,291	104,760	**5.9%**	143,800	**8.1%**
	SET270-En			1,269,901	102,542	**8.1%**	140,495	**11.1%**
	SET268-SG	Shotgun		2,202,687	133	0.0%	153	0.0%
Lucky Lady II LLII 12-84-3 13,205 cal yr BP	LL3	Metabarcoding	D'Costa et al., 2011	738,708	971	0.1%	5,615	0.8%
	SET259-MB	Metabarcoding (*trn*L only)	PowerSoil	452,855			2,115	0.5%
	SET260-MB			272,395			1,399	0.5%
	SET261-MB			386,793			1,655	0.4%
	SET259-En	Enrichment		515,685	2,563	0.5%	7,056	1.4%
	SET260-En			692,434	3,470	0.5%	8,285	1.2%
	SET261-En			1,060,105	2,368	0.2%	6,463	0.6%
	SET259-SG	Shotgun		1,517,583	17	0.0%	21	0.0%
	SET271-MB	Metabarcoding (*trn*L only)	Cold Spin	565,986			2,449	0.4%
	SET272-MB			437,902			2,269	0.5%
	SET273-MB			483,637			2,583	0.5%
	SET271-En	Enrichment		1,837,939	119,031	**6.5%**	146,562	**8.0%**
	SET272-En			1,343,928	110,609	**8.2%**	134,102	**10.0%**
	SET273-En			1,267,881	112,855	**8.9%**	139,643	**11.0%**
	SET272-SG	Shotgun		2,122,805	145	0.0%	150	0.0%
Lucky Lady II LLII 12-217-8 15,865 cal yr BP	LL1	Metabarcoding	D'Costa et al., 2011	77,373	448	0.6%	2,359	3.0%
	SET262-MB	Metabarcoding (*trn*L only)	PowerSoil	459,492			2,140	0.5%
	SET263-MB			295,806			1,675	0.6%
	SET264-MB			552,797			2,082	0.4%
	SET262-En	Enrichment		534,677	452	0.1%	2,119	0.4%
	SET263-En			873,741	312	0.0%	1,634	0.2%
	SET264-En			418,730	648	0.2%	2,721	0.6%
	SET264-SG	Shotgun		1,497,940	6	0.0%	14	0.0%
	SET274-MB	Metabarcoding (*trn*L only)	Cold Spin	358,119			1,320	0.4%
	SET275-MB			448,934			1,720	0.4%
	SET276-MB			458,110			1,579	0.3%
	SET274-En	Enrichment		867,275	6,600	**0.8%**	10,223	**1.2%**
	SET275-En			996,802	5,614	**0.6%**	8,541	**0.9%**
	SET276-En			352,658	2,802	**0.8%**	4,019	**1.1%**
	SET274-SG	Shotgun		1,992,150	40	0.0%	50	0.0%

Site, core, age	Sample	DNA Targeting Strategy	Extraction Method	Total Reads	Bait mapped & LCA-assigned*	Assigned of Total	Plant ref mapped & LCA-assigned**	Assigned of Total
Bear Creek BC 4-2B 30,000 cal yr BP	BC	Metabarcoding	D'Costa et al., 2011	172,330	1348	0.8%	8,554	5.0%
	SET265-MB	Metabarcoding (*trn*L only)	PowerSoil	427,087			2,486	0.6%
	SET266-MB			333,002			2,664	0.8%
	SET267-MB			325,894			2,204	0.7%
	SET265-En	Enrichment		682,544	1,590	0.23%	4,340	0.6%
	SET266-En			868,112	1,770	0.20%	4,392	0.5%
	SET267-En			857,863	2,249	0.26%	5,533	0.6%
	SET265-SG	Shotgun		1,338,467	5	0.00%	0	0.0%
	SET277-MB	Metabarcoding (*trn*L only)	Cold Spin	547,884			4,176	0.8%
	SET278-MB			475,359			3,398	0.7%
	SET279-MB			634,490			4,852	0.8%
	SET277-En	Enrichment		1,254,744	62,778	**5.0%**	73,276	**5.8%**
	SET278-En			1,294,040	37,878	**2.9%**	45,323	**3.5%**
	SET279-En			1,544,949	47,613	**3.1%**	57,484	**3.7%**
	SET279-SG	Shotgun		8,593,408	133	0.0%	131	0.0%

*Reads map-filtered to animal and plant baits, size filtered to ≥ 24 bp, de-duplicated, *BLASTn* aligned, and *MEGAN LCA* assigned. **Reads map-filtered to plant references, with the same subsequent filtering parameters. Core section ages as per D'Costa et al. (D'Costa et al., 2011), Mahony (2015), and Sadoway (2014).

2.9 Figures

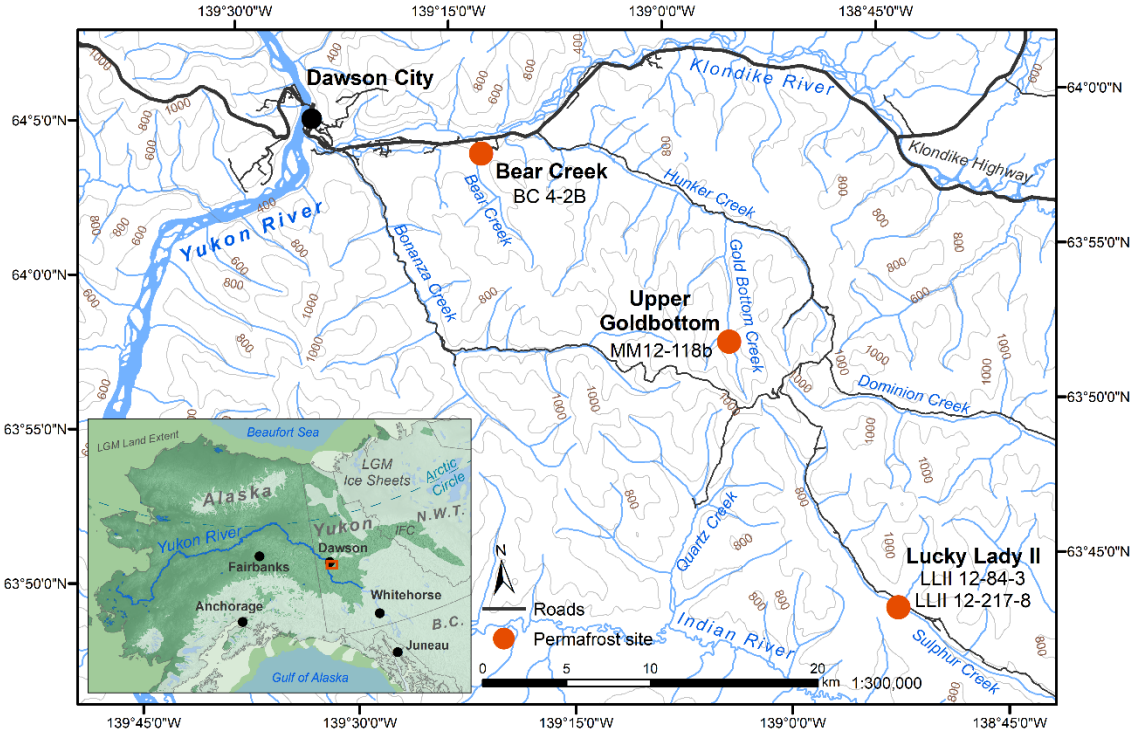

Fig. 2.1 Permafrost sampling sites in the Klondike region of Yukon, Canada (Table 2.1). Ice sheet data from Dyke (2004). Sea level at last glacial maximum (LGM, 26.5–19 ka BP) (Clark, 2009b) set to 126 meters below sea level (m bsl) based on midpoint between maximum and minimum eustatic sea level estimation models in Clark and Mix (2002). IFC = ice-free corridor. Base map data retrieved from GeoYukon (https://mapservices.gov.yk.ca/GeoYukon/, hosted by the Government of Yukon); contours elevation unit: meters above sea level.

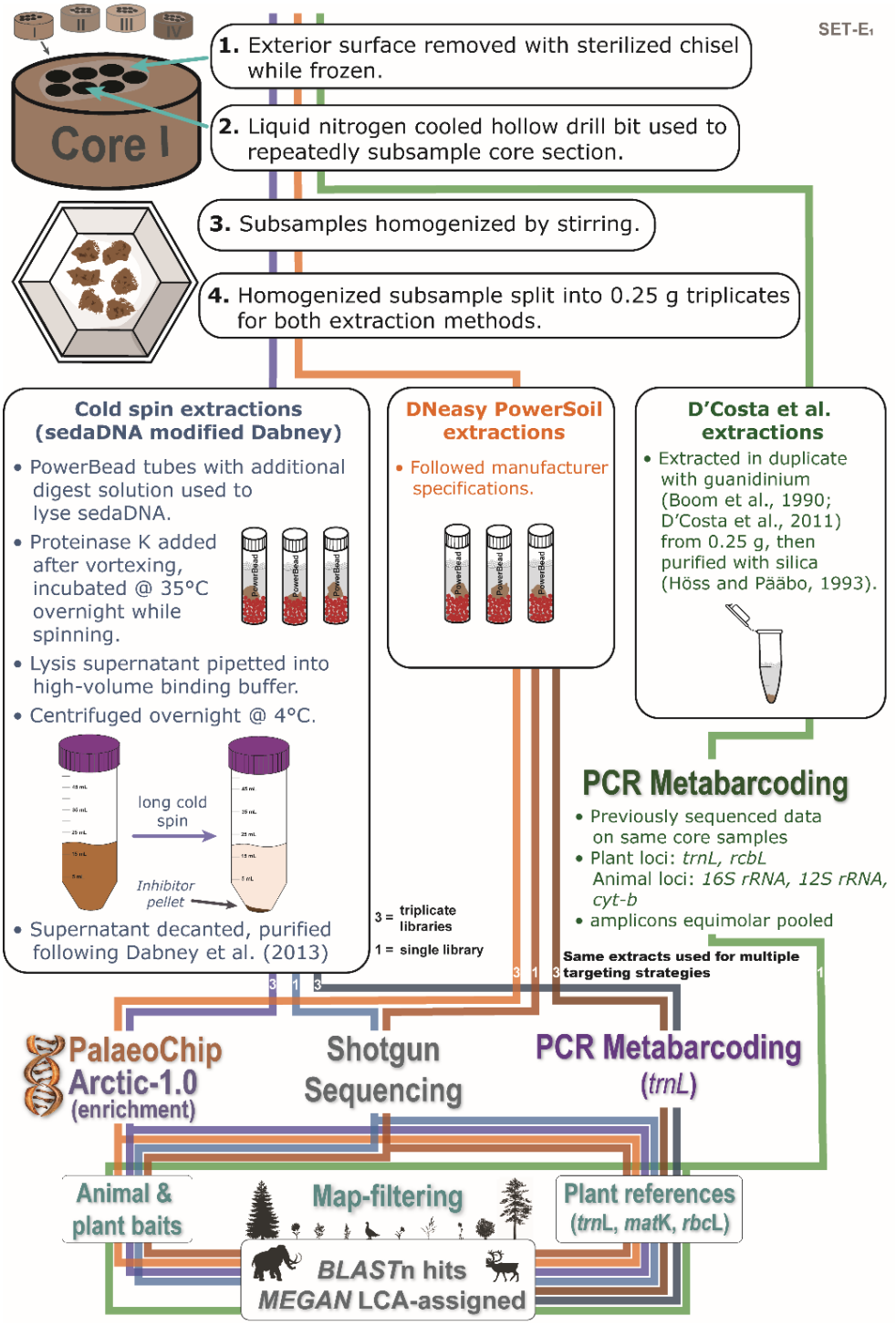

Fig. 2.2 Subsampling to taxon assignment schematic comparing extraction, targeting, and bioinformatic filtering strategies. See the methods section for further details on extraction, double-stranded library preparation, capture enrichment, qPCR assays, and the bioinformatic workflow.

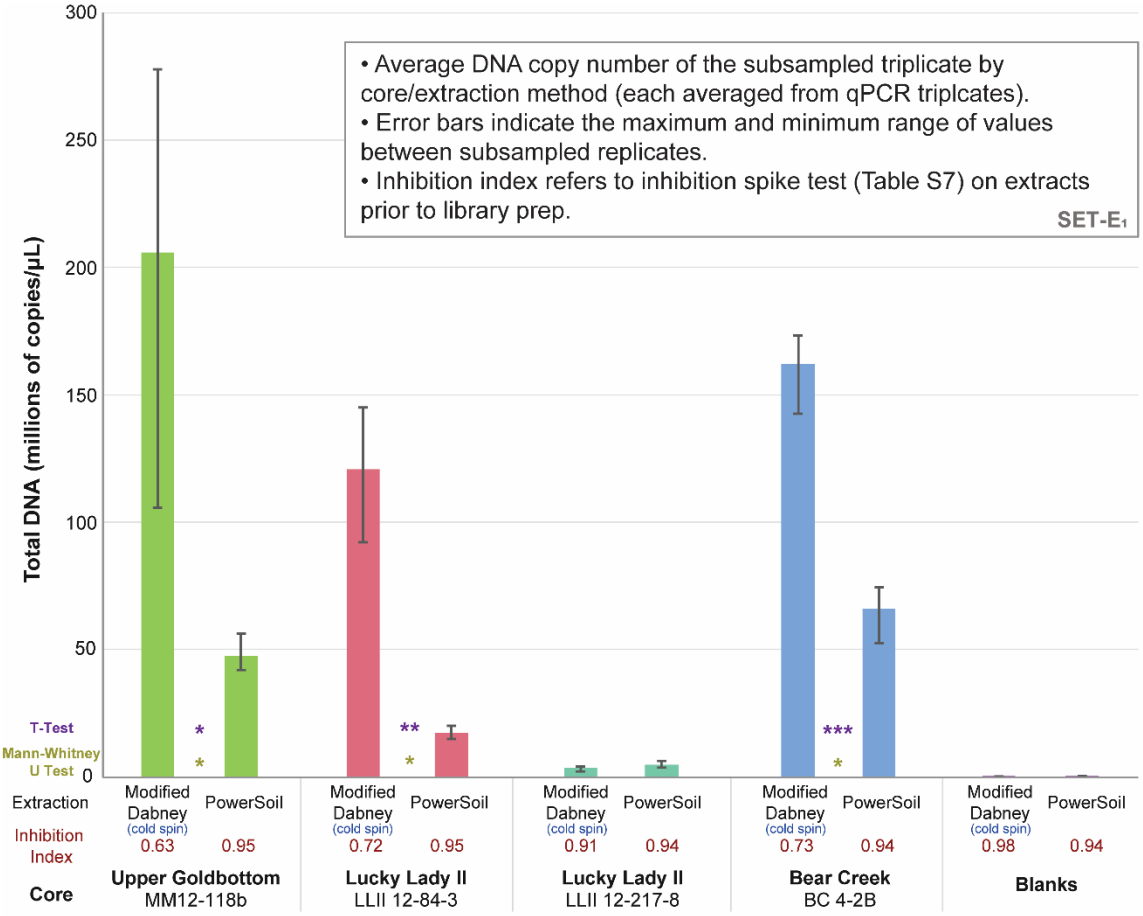

p-values: * ≤ 0.05, ** ≤ 0.01, *** ≤ 0.001

QPCR standard curves (plates 1 and plate 2 respectively): E = 97.6% and 95.1%, R^2 = 0.999 and 0.999, slope = −3.382 and -3.446.

Fig. 2.3 Total DNA quantification of library-adapted molecules comparing both extraction methods by core sample (see Table 3.8 for qPCR specifications). The large range for modified Dabney extraction on core MM12-118B is driven by a single extraction replicate with a lower copy number. Core LLII 12-217-8 consistently has low DNA recovery but also a low co-elution of DNA-independent inhibition. Core LLII 12-127-8 likely contains predominantly highly degraded sedaDNA compared with the other three samples (discussed further in section 3.4).

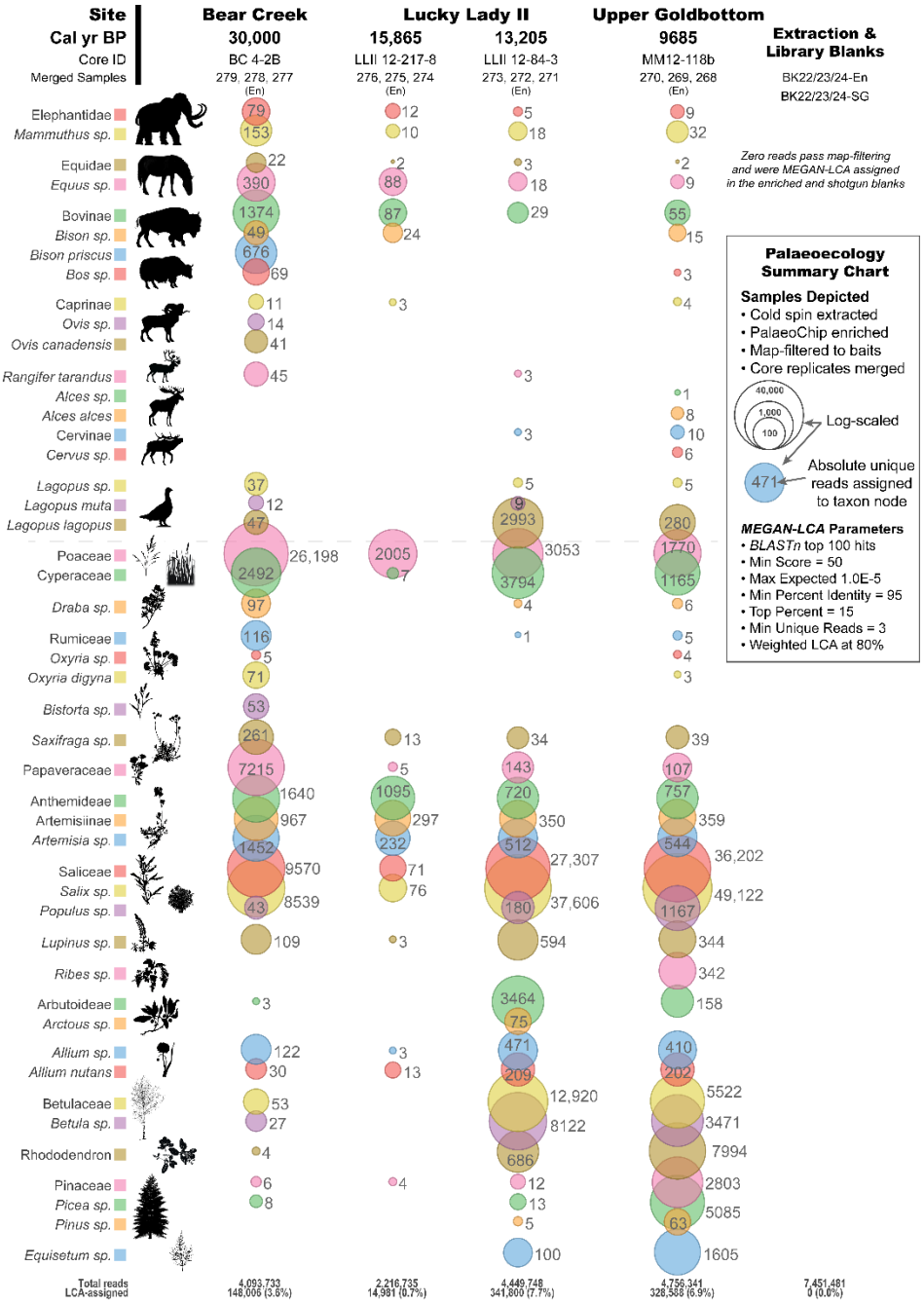

Fig. 2.4 Metagenomic summary comparison of all four permafrost core samples that were extracted with the sedaDNA modified Dabney (cold spin) method, capture-enriched with the PalaeoChip baits, and map-filtered to the target bait sequences. Metabarcoding and PowerSoil libraries are not depicted. Subsampled replicates merged in *MEGAN*. Only select organisms depicted.

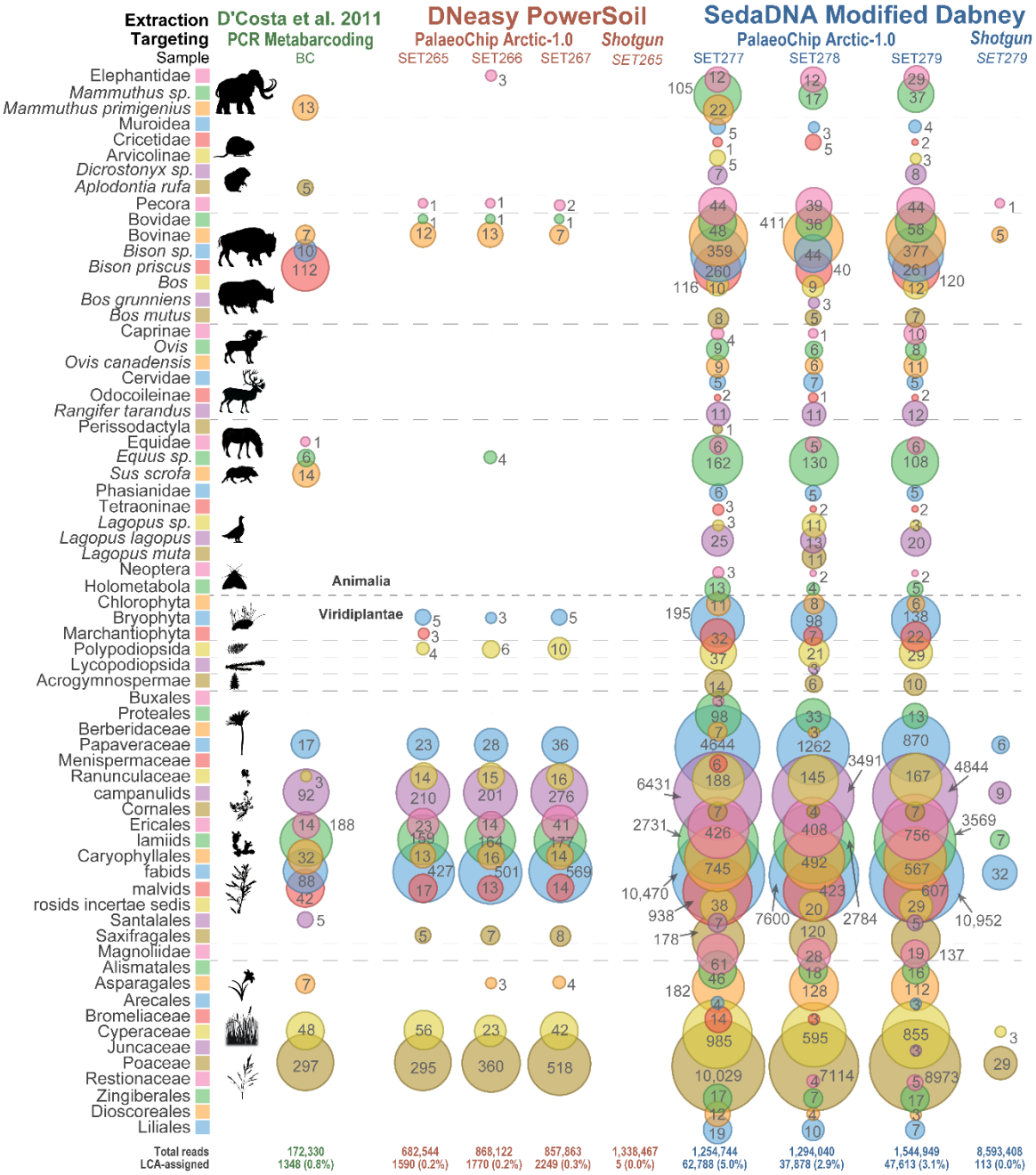

Fig. 2.5 Metagenomic comparison of the Bear Creek core sample (BC 4-2B). Reads map-filtered to the baits and compared with absolute counts and logarithmically scaled bubbles. Sample dated to ~30,000 cal yr BP (D'Costa et al., 2011; Sadoway, 2014; Mahony, 2015). Values indicate total reads assigned to that taxon node for Animalia, and a clade summation of reads for Viridiplantae. Note: hits to Arecales, Bromeliaceae, Restionaceae, Zingiberales, and Diosoreales are likely false positives driven by uneven reference coverages within Commelinids.

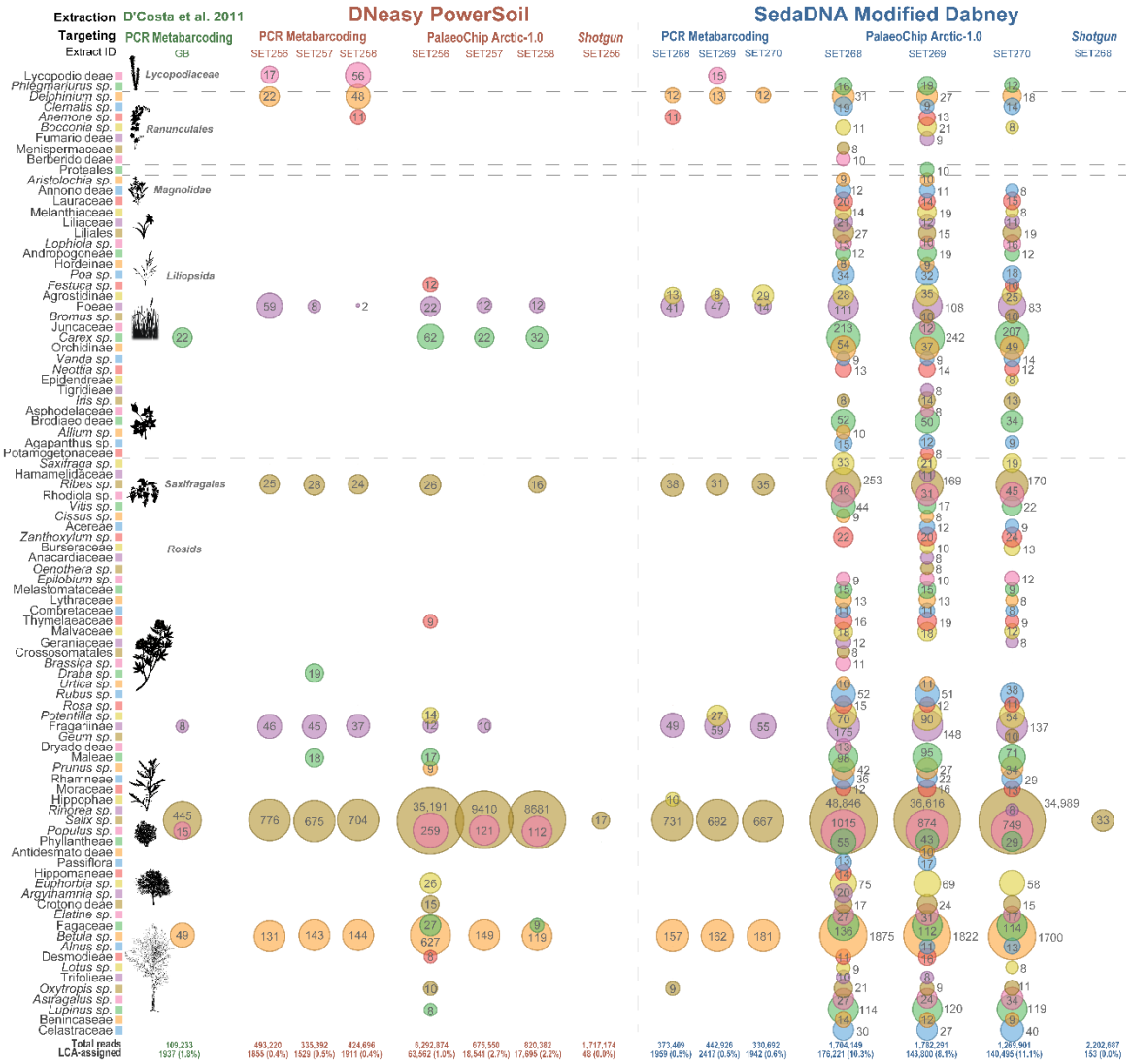

Fig. 2.6 Metagenomic comparison of Upper Goldbottom core MM12-118b with reads map-filtered to the plant references, part 1 of 2. Compared with absolute counts and logarithmically scaled bubbles. Core slice dated to 9685 cal yr BP (Sadoway, 2014; Mahony, 2015). Values indicate total reads assigned to that taxon node.

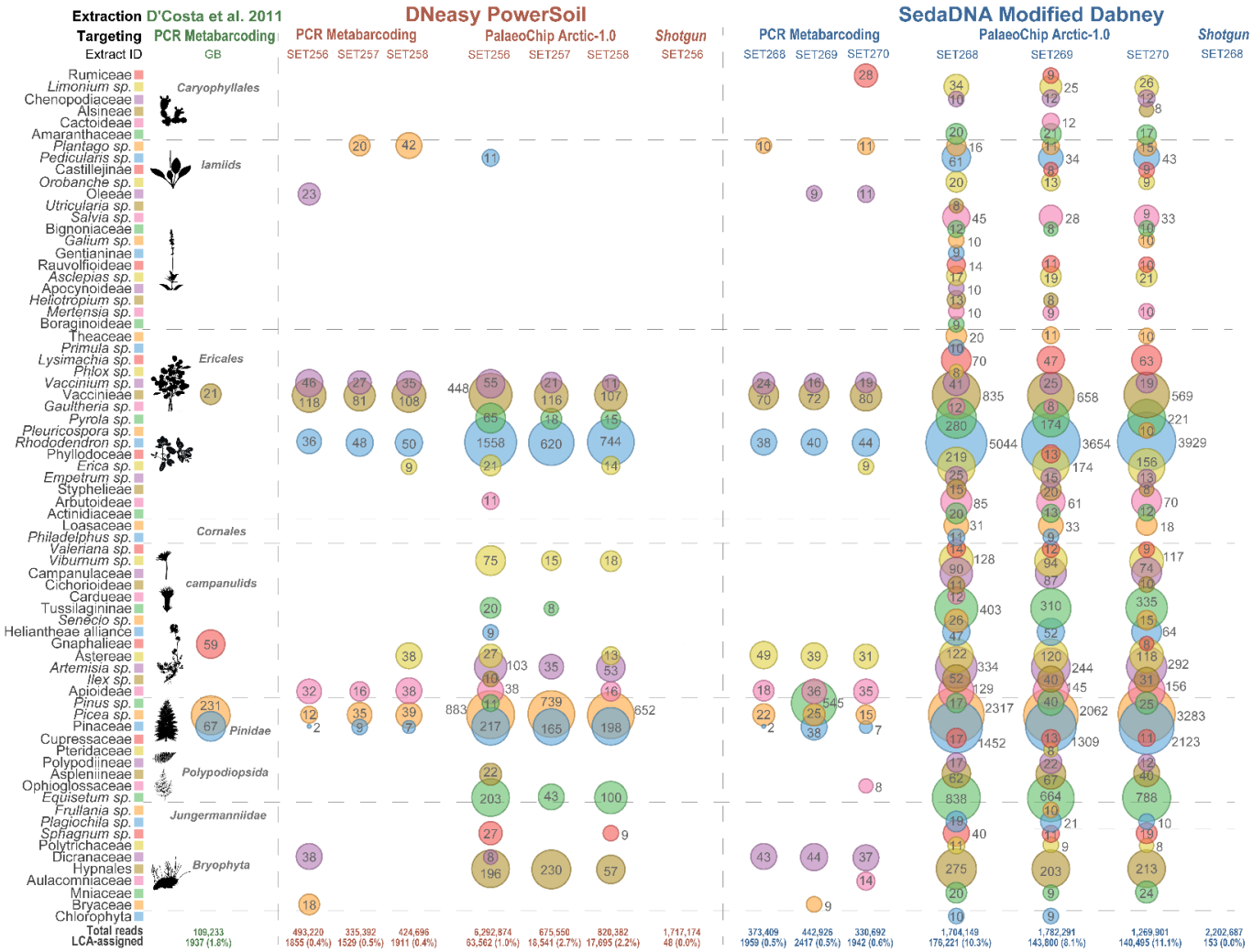

Fig 2.7 Metagenomic comparison of Upper Goldbottom permafrost core MM12-118b with reads map-filtered to the plant references, part 2 of 2. Compared with absolute counts and logarithmically scaled bubbles. Core slice dated to 9685 cal yr BP (Sadoway, 2014; Mahony, 2015). Values indicate total reads assigned to that taxon node.

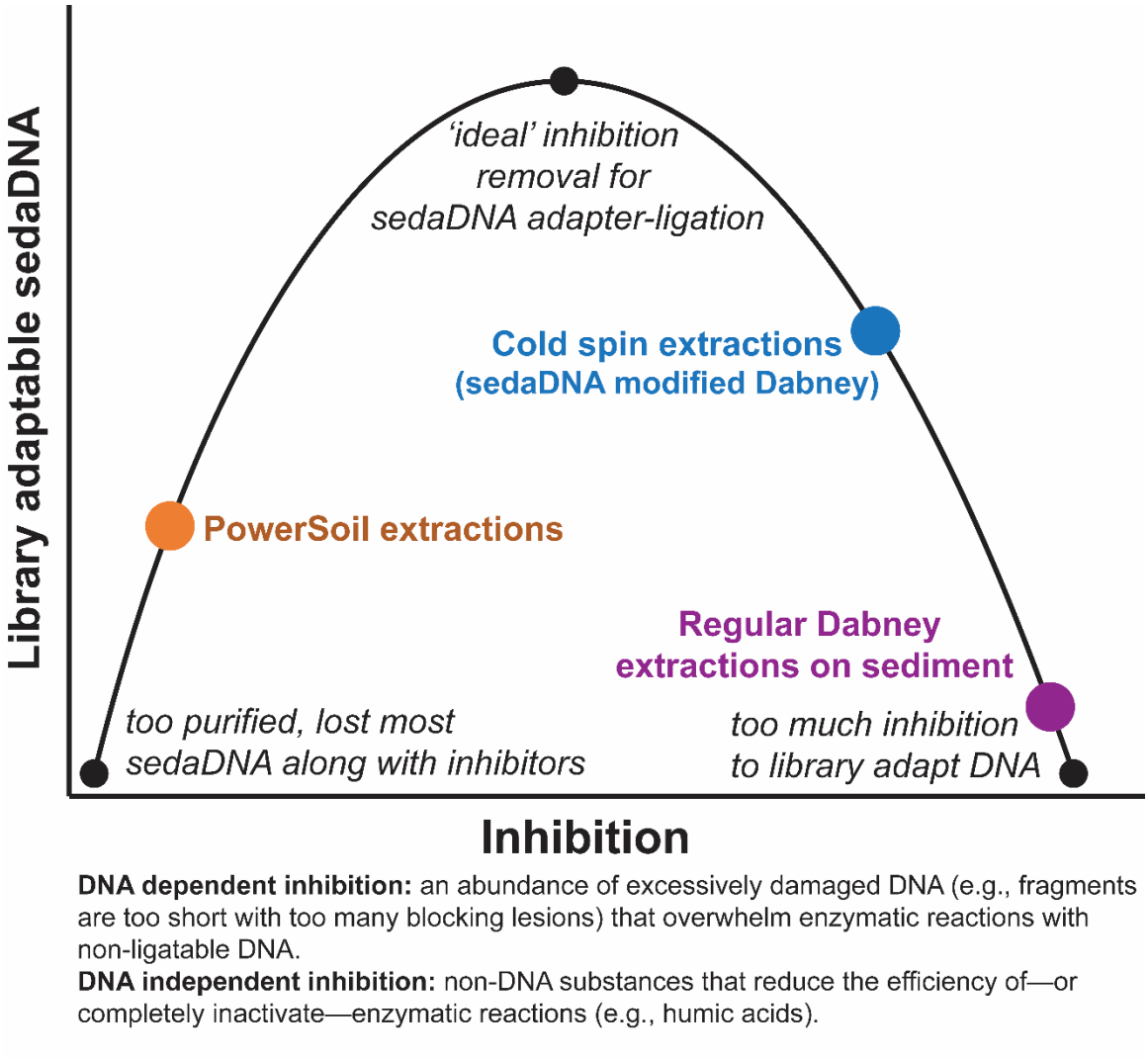

Fig. 2.8 Conceptual representation of the balance needed to overcome sedaDNA inhibition.

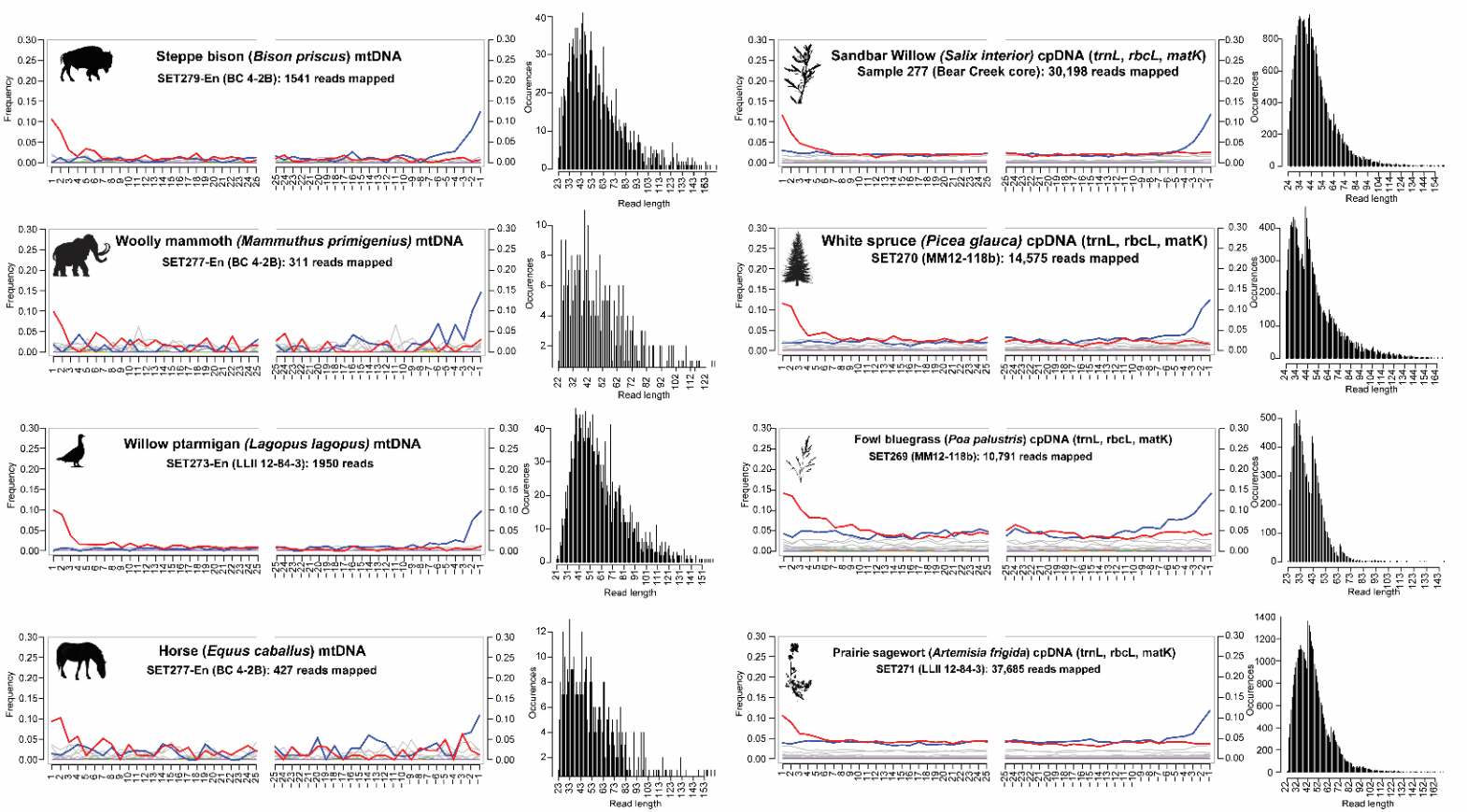

Fig. 2.9 Example *mapDamage* plots showing aDNA characteristic terminal deamination patterns and short fragment length distributions (FLD) (length filter ≥ 24 bp, mapping quality filter ≥ 30). We suspect that the bimodal distributions in some of the plant FLDs is due to non-specific mapping of closely related taxa. Taxa chosen for mapping are not necessarily accurate species of the ancient molecules, such as in this case *Equus caballus*, but rather a closely related organism with an available NCBI-RefSeq organelle genome.

Chapter 3

Supplementary Materials, Appendix A

Optimizing extraction and targeted capture of ancient environmental DNA for reconstructing past environments using the PalaeoChip Arctic-1.0 bait-set

Appendix B (list of taxa in PalaeoChip baits) available online at DOI below.

Murchie, T., Kuch, M., Duggan, A., Ledger, M., Roche, K., Klunk, J., . . . Poinar, H. (2020). Optimizing extraction and targeted capture of ancient environmental DNA for reconstructing past environments using the PalaeoChip Arctic-1.0 bait-set. *Quaternary Research,* 1-24. doi:10.1017/qua.2020.59

Each of the following sets of experiments followed the same protocols for subsampling, library preparation, indexing, qPCR inhibition spike tests, and qPCR total quantifications as described in the main paper. Master mix concentrations for each of the aforementioned reactions can be found in Tables 3.1–3.9. Variations in extraction protocols for testing inhibition clean-up techniques are detailed with the description of that experimental sediment extraction/enrichment test (SET) below, from SET-A to SET-D_2. See the table of contents for an outline of sections in this appendix.

3.1 SET-A: Initial explorations

Our first set of experiments was intended to determine the best sedaDNA extraction strategy to compare shotgun and targeted enrichment sequencing strategies with previously sequenced PCR metabarcoding data collected by Sadoway (2014) on four Yukon sediment cores. However, SET-A informed us that inhibition was a substantial problem with these sediments using our typical in-house demineralization-digestion and Dabney et al. (2013b) extraction protocol (hereafter referred to as Dabney), whereas the DNeasy PowerSoil DNA Extraction Kit (hereafter referred to as PowerSoil) only successfully recovered sedaDNA in one of the four cores (with a successful positive control amplification). We felt that this necessitated further experimentation to see if we

could overcome enzymatic inhibition and library adapt our target environmental DNA (eDNA) molecules with a high DNA retention purification method. Permafrost core disks from two strata at Lucky Lady II as well as Bear Creek and Upper Goldbottom Creek (Figure 1, main text) were tested to compare a kit-based sediment DNA extraction strategy (PowerSoil) with our in-house Dabney extraction method.

3.1.1 SET-A. Extraction

Samples processed with PowerSoil were extracted following manufacturer specifications. Samples processed using Dabney were first subjected to a two-stage lysis buffer: 1) samples were demineralized in 1 mL of 0.5M EDTA, then rotated continuously for 18 hours at 25°C; 2) samples were then spun down, supernatants were removed, and a proteinase K buffer (Table 3.1) was added to the sediments to digest overnight at 25°C. The demineralization-digestion supernatants were extracted using a high-volume binding buffer and silica columns following Dabney et al.(2013b).

3.1.2 SET-A. Bioanalyzer, inhibitor clean-up, and indexing

Straight and 1/10 diluted extracts were run on an Agilent 2100 Bioanalyzer as a high sensitivity DNA assay (see Fig. 3.1 and Fig. 3.2). Straight extracts from Dabney samples were darkly coloured and failed to produce a detectable DNA signal on the Bioanalyzer (the baseline was unable to be determined), which we suspected was indicative of abundant co-eluted substances that would adversely affect library preparation. We tested whether a 1/10 dilution or additional purification step prior to blunt end repair would sufficiently remove inhibitors for library preparation in the Dabney extracts, or whether the straight uninhibited PowerSoil extracts would perform better (Table 3.12). In a qPCR indexing reaction (Table 3.6) following double-stranded library preparation (DsLp) (Meyer and Kircher, 2010; Kircher et al., 2012), only the positive controls and a single PowerSoil extract from Bear Creek clearly amplified (see Fig. 3.3) despite all samples previously producing positive amplifications and sequence data with a PCR metabarcoding approach (Sadoway, 2014). We suspected that the Dabney extracts were highly inhibited rather than lacking in endogenous DNA. We also suspected that while the PowerSoil kit was effective at removing sedimentary inhibitors,

it was ineffective at retaining the kinds of low abundance and highly degraded molecules characteristic of ancient DNA (aDNA).

3.1.3 SET-A. Inhibition, qPCR, and DsLp

In SET-A, a subset of straight, 1/10 and 1/100 diluted extracts, as well as library adapted samples were spiked with a E^3 49 bp oligo. Straight and 1/10 extracts prepared with Dabney were completely inhibited (Fig. 3.4). Even library adapted samples that had two purification steps and 1/100 diluted extracts were partially inhibited during the inhibition spike test. To determine whether these inhibitors were causing library preparation to fail, we spiked our positive control into each of the Dabney extracts and brought the samples through DsLp. The only samples with positive indexing qPCR amplifications were the positive control and the partially inhibited reaction from LLII 12-127-8 (Fig. 3.5). All other spiked reactions flatlined, which indicates that inhibition was a significant problem when attempting to convert these extracts into libraries using our in-house lysis and extraction techniques. Compared with the kit however, DNeasy PowerSoil was only sporadically successful at retaining sedaDNA despite all of these core samples previously having been found to contain ancient environmental DNA with PCR metabarcoding (D'Costa et al., 2011; Sadoway, 2014). Our follow-up set of experiments was designed to test various inhibitor removal treatments from the PowerSoil kit and other associated methods to minimize inhibition while maximizing the retention of sedaDNA with our in-house extraction protocols.

Most total DNA quantifications in SET-A to SET-D_2 used the short amplification primer sites on the library adapters and were compared against the same library prepared 49-bp oligo standard used in the spike tests (Table 3.8). The total adapted DNA assay was also modified in some instances to quantify the 'endogenous' chloroplast constituent of adapted molecules by pairing the *trn*L P6-loop forward primer-g (Taberlet et al., 2007) with the reverse P7R library adapter primer (IS8, see Table 3.9). Enk et al. (2013) demonstrated that a single-locus qPCR assay can be used to predict on-target ancient DNA high-throughput sequencing read counts. Previous analyses (D'Costa et al., 2011; Sadoway, 2014) indicated that ancient vegetation was the most consistently abundant

fraction of the biomolecules in these cores, and as such could serve as a rough proxy for assessing aDNA retention for successfully library adapted molecules between various inhibitor removal strategies. For all qPCR results reported here, standard curve metrics are included in the associated captions. Ideal standard curve values are: $R^2 = 1$, slope = -3.3 (or between -3.1 and -3.5), efficiency = 90–105%.

3.1.4 SET-A. Inhibition Index

A positive control spike qPCR assay (King et al., 2009; Enk et al., 2016) was used to assess the relative impact of DNA independent inhibitors (co-eluted substances such as humics that inhibit enzyme function) on the enzymatic amplification efficiency of a spiked amplicon in the presence of template sedaDNA derived from variable lysing and extraction methods (Table 3.7, Fig. 3.6). We suspected that enzymes in library preparation would be inhibited similarly to AmpliTaq Gold polymerase in qPCR. Shifts in the qPCR amplification slope of our spiked oligo with AmpliTaq Gold (due to co-eluted inhibitors in sedaDNA extracts) could then be quantified and used to infer the likelihood of failed adapter ligation due to enzymatic inhibitors (rather than a lack of sedaDNA). Admittedly, AmpliTaq Gold is not a 1:1 stand-in for inhibition sensitivity during blunt-end repair and adapter ligation, as AmpliTaq is among the most sensitive polymerases to inhibition induced reductions in amplification efficiency (Al-Soud and Radstrom, 1998), and due to qPCR specific inhibition such as the reduction in florescence despite successful amplification (Sidstedt et al., 2015). Our experiments do suggest that these enzymes have a very roughly commensurate inhibition sensitivity, insofar as eluates completely inhibited during this spike test are unlikely to successfully undergo library adapter ligation.

To quantify the co-eluted inhibition affecting each spiked amplification, we compared the qPCR slope of an oligo-spiked sedaDNA extract (1 µL of sample eluate spiked with 1 µL of a 49-bp oligo [1000 copies {E^3}], see Table 3.7) with the qPCR slope of 1 µL E^3 oligo standard in 1 µL of EBT. Average C_q and max relative fluorescence units (RFU) for each PCR replicate (processed in triplicates) were calculated, as was the hill slope of the amplification curve by fitting a variable-slope sigmoidal dose-response

curve to the raw fluorescence data using GraphPad Prism v. 7.04 (https://www.graphpad.com/) (based on King et al. [2009]). The E^3 oligo-spiked averages (C_q, RFU, and sigmoidal hillslope) were divided by the corresponding E^3 oligo standard amplification value, then averaged together to generate an 'inhibition index' per PCR replicate, which were averaged again across PCR replicates to determine an extract's inhibition index, ranging from 0–1. In this case, 0 indicates a completely inhibited reaction (no measurable increase in RFU), and 1 indicates a completely uninhibited reaction relative to the spiked E^3 oligo-standard (see Fig. 3.6). Anything above 0.9 (the bottom range for blanks and standards of differing starting quantities) is considered essentially uninhibited insofar as *Taq* polymerase inhibition is concerned (NOTE: Figure 4 [main text] / Figure S8 depicts inhibition as increasing from left to right on the x-axis, which is opposite of how the inhibition index is depicted).

3.2 SET-B: Comparing inhibition removal strategies

The second set of experiments tested the following inhibitor removal augmentations to a digestion and Dabney extraction protocol:

1) Physical disruption with PowerBeads (vortexing for 10 minutes) and a proteinase K digestion buffer (see Table 3.1) (proteinase K was added to each sample individually after vortexing so as to not damage the enzyme, but prior to overnight incubation with continuous oscillation) to release bound DNA.
2) The addition of solution C3 (120 mM aluminum ammonium sulfate dodecahydrate) from the PowerSoil kit prior to Dabney purifications to precipitate inhibitors (maintaining the 1/3 volumes of solution C3 to digest supernatant).
3) A 1 hour 4°C centrifuge at 3900 x *g* with the high-volume Dabney binding buffer in 50 mL tubes to precipitate inhibitors prior to DNA isolation.
4) Sonication with and without a post-sonication purification to disrupt bonds between inhibitors and 'endogenous' sedaDNA (Table 3.14).

Each combination of these inhibitor removal treatments was used on three cores, subsampled from homogenized triplicates. See Table 3.13 for the SET-B sample list. The extracts were assayed with a qPCR inhibition spike test (Table 3.7) then brought through double-stranded library preparation (DsLp) and quantified using P5/P7 adapter primers (Table 3.8). A subset of these were also indexed to confirm that the qPCR indexing reaction correlates with our short amplification observations (Fig. 3.9).

SET-B. Results and interpretations

The 4°C centrifuge samples (and sonicated derivatives) outperformed other inhibitor removal treatments in terms of DNA retention (Fig. 3.7). All other treatment variations had low DNA retention, but frequently outperformed the 1 hour 4°C centrifuge variant in the inhibition spike test. Sonication and post-sonication purifications (to re-concentrate DNA) seemed to help with reducing polymerase inhibition in the qPCR spike test, but also resulted in DNA loss compared to their non-sonicated counterparts. The use of PowerSoil beads for physical disruption resulted in visually clearer extracts and less inhibition than an EDTA based demineralization. Overall, the more treatments utilized, the less inhibition observed, but also the less DNA retained. Solution C3 from the PowerSoil kit was effective at reducing inhibition (both visually in terms of eluate colour retention and in the subsequent inhibition assay), but also resulted in substantial DNA loss. This may explain the results of SET-A where the PowerSoil kit was observed to be effective at removing DNA inhibition but had low DNA retention. The kit is effective with modern sediments and soils, but might precipitate tightly bound organo-mineral complexes (Haile, 2008, p. 18; Arnold et al., 2011, p. 418) in which sedaDNA is preserved. There seems to be an important balance between releasing enough DNA, but not releasing too many inhibitors, as well as removing enough inhibition for enzymatic reactions, while not removing the majority of the 'endogenous' sedaDNA (Fig. 3.8). We also wanted to verify that our short amplification assay roughly correlates with amplification during the qPCR indexing reaction (Fig. 3.9). In this assay we can see that sonication results in fewer adaptable molecules during indexing, which is a trend also apparent in the short amplification assay in Fig. 3.7.

3.3 SET-C: Fine-tuning the cold spin

The only viable treatment from SET-B appears to be the 4°C spin. Our follow-up goal was to determine whether we could maximize the inhibitor removal of the spin at various timings, in this case testing 1, 6, and 19 hours (Table 3.15). We found that increasing the duration of the 4°C spin reduced the polymerase inhibition observed during the qPCR spike test (Fig. 3.10), which correlated with higher quantifications following

library adapter ligation (Fig. 3.9). We also attempted to quantify 'endogenous' sedaDNA in extracts prior to adapter ligation using two chloroplast barcoding primer sets, *rbc*L-H1a/H1b (Poinar et al., 1998) and *trn*L P6-loop g/h (Taberlet et al., 2007). However, we found that even in extracts with an inhibition index of ~0.6–0.8 that these assays were uninformative for quantifying pre-DsLp DNA concentrations because the amplification curves were non-standard (the exponential and linear phases had shallower slopes [see Fig. 3.6 for examples]). This was likely due to both DNA-dependent and DNA-independent inhibition. We found that varying the polymerase concentration dramatically changed the extract quantifications on chloroplast amplicons, which will be elaborated on further in section SET-D.

The final experiment with SET-C samples was to assess whether varying the extract input or enzymatic concentration during blunt-end repair (the first phase of DsLp) would affect the total number of adapter ligated molecules between a highly inhibited sample (BC 4-2B) and an uninhibited sample (LLII 12-217-8) (Fig. 3.11). While there was a reduction in the extraction range of total quantified DNA between replicates of the inhibited core (BC 4-2B) using double the blunt-end repair enzymatic concentrations (T4 polynucleotide kinase and T4 DNA polymerase, see Table 3.3 for standard concentrations), the effect was marginal. There was also no improvement in halving the extract input in terms of reducing inhibition load on the blunt-end repair enzymes beyond reducing the total adapted DNA by half. Increasing blunt-end repair enzyme concentrations is only recommended for critically important samples where the additional cost is not a concern, as our results suggest that the improvement is marginal.

3.4 SET-D: Optimizing our modified Dabney extraction protocol

This final optimization experimental set was intended to fine-tune components of our modified Dabney protocol (Table 3.16). We wanted to determine whether a physical disruption with PowerBeads is necessary, or if a straight digestion or combined demineralization and digestion buffer is best for releasing sedaDNA (SET-B led us to suspect that EDTA might be releasing too many inhibitors). We also wanted to determine whether the duration of the lysis stage was significant, so 6- and 19-hour lysis variants

were tested. Finally, we were interested whether increasing the 4°C spin to two days would plateau our inhibition removal procedure, or if we could further improve the amount of library adapted molecules in highly inhibited cores without losing 'endogenous' sedaDNA. Part-way though this experiment, we also discovered an interesting (initially, admittedly, very frustrating) variable effect on inhibitor retention linked to the lysis detergent. For the first set of samples (SET-D_1) sarkosyl was used as the detergent during lysis instead of SDS. Once this unintended reagent change was discovered (after a series of experiments where the long cold spin was unexpectedly no longer removing inhibition in our most inhibited core sample, BC 4-2B) a second set of homogenized subsamples was taken (SET-D_2) for our highly inhibited core where we switched back to SDS as the lysis detergent. We also conducted tests to quantify 'endogenous' chloroplast sedaDNA on extracts (prior to DsLp) from SET-C and -D samples (as alluded to in section SET-C). However, we are unsatisfied with these assays on purified extracts as they still contain co-eluted inhibition (likely both DNA independent and dependent inhibitors), and as such remain unconvinced by their quantifications. Further work developing these specific extract assays (by improving florescence detection, improving inhibition removal, increasing polymerase concentrations, or by size selecting out 'viable' DNA fragments) is recommended.

3.4.1 SET-D. Results and interpretations

SET-D experiments yielded five results of interest as observed in Fig. 3.12. First, in column I, there is some indication that increasing the duration of lysis from 9 hours to 19 hours increases inhibitor release (likely as well as DNA release). Inhibitors were not effectively removed during the long cold spin in this instance as sarkosyl appears to be an ineffective detergent to pair with this inhibitor removal technique. This is the only glimpse we observed into the variation of lysis time spans. The optimal interval for our workflow is 19 hours (leaving the samples to oscillate overnight at 35°C). The long cold spin is effective at removing additional inhibition when paired with SDS as observed with columns IV and V in Fig. 3.12. We did not investigate variation in lysis period further as

19 hours is most effective with our workflow and has higher DNA release (as observed in SET-E in the main paper).

Second, the proteinase K buffer with sarkosyl—without either EDTA for demineralization or PowerBeads for physical disruption—has the lowest inhibitor retention (inhibition indices ≳0.9) as observed in column II. However, subsequent experiments (detailed in the last SET-D subsection) found that this method also has the worst DNA release.

Third, the detergent used during lysis makes a significant difference in inhibitor retention. All extraction replicates of the inhibited core (BC 4-2B) lysed with the detergent sarkosyl in the proteinase K buffer (with a PowerBead disruption) remain highly inhibited (all failed the inhibition spike test) despite the 4°C inhibition precipitation spin as observed with the inhibition indices in columns III. This is starkly contrasted with column IV where the only experimental change was the use of SDS in the lysing buffer rather than sarkosyl. This was also visually observed in the sarkosyl samples with the lack of a 'dark inhibitor pellet' following the cold spin and much more darkly stained silica-columns and brown-to-black eluates. Our hypothesis for this detergent interaction is detailed in the subsequent SET-D subsection *SDS and sarkosyl*.

Fourth, columns IV and V have equivalent inhibition indices. Subsequent library preparations and short amp quantifications found that increasing the cold spin to 48 hours does slightly increase adapter ligated DNA for both methods (Fig. 3.12). Further, EDTA and PowerBeads as a means of disrupting organo-mineral sedaDNA complexes have roughly equivalent DNA yields, but PowerBeads do release more DNA on average.

Fifth, there appears to be a saturation point for inhibitor removal (at least qPCR polymerase sensitive inhibitors) after approximately 24 hours with the cold spin with our current reagent concentrations. The cold spin at 48 hours show no difference in inhibition indices. This could potentially be modified with higher concentrations of SDS (discussed further in the following subsection on SDS), but this variant was not tested in our optimizations.

3.4.2 SET-D. SDS and sarkosyl

The most unexpected result of this project was the effect of unintentionally switching detergents on inhibitor precipitation during the 4°C spin. While there is some degree of precipitation during cold centrifugation with a sarkosyl lysing buffer, or even when spinning low-volume purified extracts at room temperature prior to adapter ligation, the marked increase in precipitation with SDS is visually distinct with thick inhibitor pellets forming during the 4°C spin. SDS (sodium dodecyl sulfate) is an anionic surfactant. Surfactants form self-aggregates (micelles) as their concentration increases (Tanford, 1980). These micelles arrange to have exterior hydrophilic heads, and interior hydrophobic tails. Typically, surfactants are present in submicellar concentrations, but these self-aggregate structures can form at sufficiently high concentrations, particularly with constant mixing. Micelles can also co-aggregate with other amphiphilic compounds (those with hydrophobic and hydrophilic domains) such as humic substances (Otto et al., 2003; Koopal et al., 2004), which we suspect is one of the main DNA independent inhibitors in these sediments due to dark colouration (Alaeddini, 2012). SDS precipitates at 4°C and calcium has been found to increase the precipitation of SDS micelles. We hypothesize that our cold spin with high guanidinium concentrations and SDS based digestion buffer (also containing $CaCl_2$ intended for improving proteinase K efficiency) might have created some form of optimal conditions for micelle formation and the subsequent precipitation of humics and other amphiphilic compounds that bound to SDS micelles. It is also possible that pH is involved in humic acid solubility and is affecting this precipitate reaction (Shaban and Mikulaj, 1998), or that proteins also play some role (Schlager et al., 2012), potentially as related to disentangling sedaDNA from its protective organo-mineral complex (Greaves and Wilson, 1969; 1970; Lorenz and Wackernagel, 1987b; Ogram et al., 1988; Taylor and Parkinson, 1988; Bezanilla et al., 1995; Blum et al., 1997; Crecchio and Stotzky, 1998; Khanna et al., 2005; Cleaves et al., 2011). The interaction we have observed here would be of benefit for investigation to further improve the purification of palaeoenvironmental DNA. It is likely that components of the binding or lysing buffers, mixing strategy, or temperature could be

tweaked further to improve inhibitor precipitation, thus increasing sedaDNA yield from highly inhibited materials.

3.4.3 SET-D. Chloroplast assay of 'purified' extracts with variable Taq

As discussed in section SET-C, we had intended to test 'endogenous' cpDNA retention and release through our procedure before and after library preparation. However, we found that this assay, either with *rbc*L or *trn*L primers, was not a reliable means of assessing 'endogenous' sedaDNA retention through our inhibition removal technique or library adapter ligation efficiency. We found that even our uninhibited core (LLII 12-217-8) had inconsistent DNA quantifications (Fig. 3.14), largely due to non-standard (shallow) amplification slopes affecting the starting quantity metric in our qPCR assay. It is possible that co-eluted humics not removed during the cold-spin may impact florescence detection with these qPCR assays on extracts (Sidstedt et al., 2015), in addition to directly affecting the polymerase. We found substantial quantification increases when doubling *Taq* concentrations (Fig. 3.15). Despite the overall unreliability of these extract assays however, there are two important pieces of information that can be gleaned. First, there is almost no DNA release during lysis when utilizing just a proteinase K digestion buffer with sarkosyl—meaning, without EDTA or physical disruption from PowerBeads. This complete lack of amplifiable DNA rules out column II (Fig. 3.13) as a viable extraction strategy. We found the least inhibition with this method-core combination (both in terms of its inhibition indices [Fig. 3.14] and visually non-coloured elutes). Second, despite the qPCR inhibition assay detecting minimal inhibition in this core overall with any method, there is still some sort of inhibition in the extracts affecting the efficiency of AmpliTaq Gold polymerase. This might indicate that while this sample has low DNA independent inhibition (humics and other enzymatically inhibitory substances) that do not impact the amplification of spiked, undamaged synthetic amplicons, this sample likely has high DNA dependent inhibition (Fig. 2.8). Meaning, there might be substantial aDNA damage (such as blocking lesions) or an abundance of extremely short molecules that the *Taq* polymerase is either getting stuck on or stuck amplifying repeatedly, which ultimately leads to poor florescence. This core also had the

lowest DNA recovery (Table 2.1 and Fig. 3.17), which when paired with this assay, suggests that the sedaDNA in this core is more fragmentary and damaged than the other permafrost samples.

Potentially spiking lysing buffers with a known quantity of aDNA sized and damage characteristic non-target DNA, then assaying those synthetic molecules after library preparation with a dual adapter/synthetic target-specific primer set (such as described in Table S9), would be a more reliable means of assessing DNA loss from the cold spin and DNA independent inhibitor effects on library preparation efficiency. However, this assay would not assess DNA dependent inhibition specific to the sedaDNA constituents of the sample. The polymerases used in qPCR amplifications are not directly equivalent to those used in library preparation. Extracts or libraries with florescence inhibition (Sidstedt et al., 2015) might yet be amenable to adapter and indexing ligations, as well as potentially sequencing, but be largely undetectable with *Taq* based qPCR assays unless the reaction is maximally saturated with polymerase to mitigate various forms of inhibition. While potentially feasible with small sample-sets, this strategy would be costly, and likely difficult to standardize across highly variable molecular constituents even within the 'same' homogenized sedimentary sample (however 'homogenized' a sediment sample could be on a molecular scale).

3.5 SET-E: Additional data for main-text experiment.

This section reports on details not included in the main-text, including: PalaeoChip Arctic-1.0 bait design and enrichment wet-lab procedures, metabarcoding parameters, a comprehensive bioinformatic workflow, and other supplementary data of use for evaluating the main-text experiment.

3.5.1 SET-E. Enrichment: PalaeoChip bait-set design and wet lab procedures.

The PalaeoChip Arctic-1.0 hybridization enrichment bait-set was designed in collaboration with Arbor Biosciences to target whole mtDNA of extinct and extant Quaternary animals (focused primarily on megafauna; number of taxa ≈ 180), and high latitude plant cpDNA based on curated reference databases developed by Sønstebø et al. (2010), Soininen et al. (2015), and Willerslev et al. (2014), initially targeting *trn*L (n ≈

2100 taxa) (see Appendix B for taxonomic list [https://doi.org/10.1017/qua.2020.59]). This list was queried with the *NCBI Mass Sequence Downloader* software (Pina-Martins and Paulo, 2015) to recover additional nucleotide data from GenBank (Benson et al., 2018) for *trn*L, as well as adding targets for *mat*K and *rbc*L. These three regions were selected as they are among the most sequenced and taxonomically informative portions of the chloroplast genome (Hollingsworth et al., 2011). Baits were designed in collaboration with Arbor Biosciences to 80 bp with ~3x flexible tiling density, clustered with >96% identity and >83% overlap, and baits were removed with >25% soft-masking (to reduce low complexity baits with a high chance of being off-target in complex environmental samples). Bait sequences were queried with *BLASTn* against the NCBI database on a local computer cluster using a July 2018 database, then inspected in *MEGAN* (Huson et al., 2007; 2016). Baits with a mismatched taxonomic target and *BLASTn* alignment were queried again using a web-blast script (Camacho et al., 2009; NCBI Resource Coordinators, 2018) to determine if these mismatches were due to local database incongruities with the web-based NCBI database. Mismatches were again extracted with *MEGAN*, individually inspected, then removed from the bait-set if determined to be insufficiently specific.

Enrichment: wet lab. Hybridization and bait mixes were prepared to the concentrations in Table 3.11. For each library, 7 µL of template was combined with 2.95µL of Bloligos (blocking oligos which prevent the hybridization between library adapter sequences). The hybridization and bait mixes were combined and pre-warmed to 60°C, before being combined with the library-Bloligo mixture. The final reaction was incubated for 24 hours at 55°C for bait-library hybridization.

The next day, beads were dispensed (540 µL total between two tubes), washed three times with 200 µL of binding buffer for each tube, then suspended in 270 µL of binding buffer per tube and aliquoted into PCR strips. Baits were captured using 20 µL of the bead suspension per library, incubated at 55°C for 2.5 minutes, finger vortexed and spun down, and incubated for another 2.5 minutes. Beads were pelleted and the supernatant (the non-captured library fraction) was removed and stored at −20°C. The

beads were resuspended in 180 µL of 55°C Wash Buffer X and washed four times following the MYbaits V4 protocol. Beads were eluted in 15 µL EBT, PCR reamplified for 12 cycles (Table 3.6), then purified with MinElute columns following manufacturer's protocols in 15 µL EBT.

3.5.2 SET-E. Sadoway (2014) PCR metabarcoding

Extensive inhibition was observed in the extracts at the time by Sadoway (2014, chap. 8), which was detected using qPCR spike tests similar to those developed by King et al. (2009). This necessitated a tenfold extract dilution, which were then amplified in duplicate for each primer set, targeting: *rbc*L (Willerslev et al., 2003b; CBOL Plant Working Group, 2009; Hollingsworth, 2011), *trn*L (Taberlet et al., 2007), *16S rRNA* (Höss et al., 1996), *and 12S rRNA* (Kuch et al., 2002), each following cited PCR conditions. The locus *cytochrome b* (*cyt-b*) was also targeted using a set of degenerate primers designed with FastPCR (Kalendar et al., 2011; Sadoway, 2014). *Cyt-b* amplifications were found to be most efficient in 20 µL reactions using AmpliTaq Gold (0.05U/µL), 1X PCR Buffer II, 2.5 mM MgCl2, 0.25 mM dNTPs, 0.5X Evagreen, 250 nM (forward/reverse primers) when cycled with a 3 minute denaturation at 95°C, 45 cycles of 95°C for 30 seconds, and 60°C for 30 seconds (Sadoway, 2014). QPCR products were purified with 10K AcroPrep Pall plates (Pall Canada Direct Ltd., Mississauga, ON, Canada) using a vacuum manifold. QPCR assays were used to pool each amplicon set in equimolar concentrations, which were library prepared and dual-indexed following the same Illumina protocols as described above (Meyer and Kircher, 2010; Kircher et al., 2012). Samples were sequenced on a HiSeq 1500 Rapid Run (2 x 100bp, Illumina Cambridge Ltd, Essex, UK) at the Farncombe Metagenomics Facility (McMaster University, ON) to an approximate target depth of 100,000 reads each.

3.5.3 SET-E. PCR metabarcoding *trnL*

Components of the *trn*L metabarcoding reaction are detailed in Table 3.17. Each extract was run in PCR triplicate and purified using a 10K AcroPrep Pall plate and vacuum manifold in a post-PCR facility. Each well of the AcroPrep membrane was pre-wet with 50 µL EB and the vacuum was applied for ~10 minutes until almost dry. Post-

PCR products were mixed with 100 µL EB per well, added with a multichannel pipette to the AcroPrep plate, and the vacuum manifold was applied until dry (~10 minutes). Wells were washed with another 100 µL EB and vacuumed until dry. 17 µL EBT was added per well and the plate was gently vortexed for 30 minutes. Each well was mixed thoroughly via pipetting, then wells were combined to make a single metabarcoded product from the PCR triplicates for a final volume of ~50 µL. qPCR DNA concentration estimates are reported in Fig. 3.17. Thereafter, these PCR products were library prepared identically to the other samples, but all in a post-PCR facility.

3.5.4 SET-E. Bioinformatic workflow

Reads from all library sets (enriched, shotgun sequenced, and both versions of PCR metabarcoding) were demultiplexed with *bcl2fastq* (v 1.8.4), converted to bam files with *fastq2bam* (https://github.com/grenaud/BCL2BAM2FASTQ), then trimmed and merged with *leeHom* (Renaud et al., 2014) using ancient DNA specific parameters (--ancientdna). Reads were then either aligned to a concatenated reference of the animal and plant probes or to a concatenated reference of just the plant target sequences with *network-aware-BWA* (Li and Durbin, 2009) (https://github.com/mpieva/network-aware-bwa) with a maximum edit distance of 0.01 (-n 0.01), allowing for a maximum two gap openings (-o 2), and with seeding effectively disabled (-l 16500). Mapped reads that were merged or unmerged but properly paired were extracted with *libbam* (https://github.com/grenaud/libbam), collapsed based on unique 5' and 3' positions with *biohazard* (https://bitbucket.org/ustenzel/biohazard), and restricted to a minimum length of 24 bp. Mapped reads were string deduplicated using the *NGSXRemoveDuplicates* module of *NGSeXplore* (https://github.com/ktmeaton/NGSeXplore), then queried with *BLASTn* to return the top 100 alignments (-num_alignments 100 -max_hsps 1) against a July 2018 version of the NCBI Nucleotide database on a local computer cluster. Libraries that were not map-filtered to our reference targets (either with the baits or original plant references) were treated identically, although only returned the top 10 alignments to mitigate unwieldy (>20 Gb) file sizes. Sequencing summary counts are in Table 2.1.

Blast and fasta files for each sample (unmapped and mapped variants) were passed to *MEGAN* (Huson et al., 2007; 2016) using the following LCA parameters: min-score = 50 (default), max expected (e-value) = 1.0E-5, minimum percent identity = 95% (allows 1 base mismatch at 24 bp, 2 at 50 bp, and 3 at 60 bp to account for cytosine deamination and other aDNA characteristic damage or sequencing errors), top percent consideration of hits based on bit-score = 15% (allows for slightly more conservative taxonomic assignments than the 10% default based on trial and error), minimum read support = 3 or 8 (number of unique reads aligning to an NCBI sequence for that taxon to be considered for LCA, 3 used when mapping to the animal and plant baits, 8 when mapping to the plant references), minimum complexity = 0.3 (default minimum complexity filter), and utilizing the LCA weighted algorithm at 80% (two rounds of analysis that purportedly increases taxon specificity but doubles run time over the native algorithm). Metagenomic profiles were compared in *MEGAN* using absolute read counts. Libraries were not subsampled to an equal depth prior to processing; McMurdie and Holmes (2014) have demonstrated that this rarefying approach is the most ineffective means of accounting for unequally sequenced metagenomic data. Instead, we logarithmically scaled our bubble charts to visually normalize between samples proportionally but retained raw read counts. There are more sophisticated (and arguably fairer) means of normalizing unequally sequenced libraries, but we feel that this approach does visually normalize well between such variable methodological variants, and streamlines effectively with the *MEGAN* software.

3.5.4.1 SET-E. Map-filtered to animal and plant baits.

To visualize the taxonomic variability between these replicates, comparative trees in *MEGAN* were summed to the rank of ‘order’; Animalia was then fully uncollapsed (as the read counts were more manageable compared with plant assignments). Viridiplantae clades were collapsed to higher ranks (higher than ‘order’) in some cases for summarized visualizations (otherwise there were too many leaves to display at once in a single figure, even when only showing summaries by ‘order’). Thereafter, all leaves were selected and visualized with logarithmically scaled bubble charts; additional higher LCA-assigned

Animalia ranks were also selected where taxonomically informative (for example, reads that could only be conservatively LCA-assigned to Elephantidae or *Mammuthus sp.*, but which in this context likely represent hits to *Mammuthus primigenius* [woolly mammoth]). Low abundance (<3 reads), non-informative and non-target clades (e.g. bacteria, fungi, or LCA-assignments to high ranks) were excluded for visualization purposes.

3.5.4.2 SET-E. Map-filtered to plant reference sequences.

For the bubble charts mapped to the plant references, the same procedures were followed, although the LCA stringency was increased from a minimum of three unique reads to eight. These libraries were mapped to the plant references to reduce the potential false negatives that might result from the metabarcoding data not mapping well to 80 bp probes. We found that when comparing these two map-filtering strategies, metabarcoded libraries had fewer taxa identified when mapping to the baits compared with mapping to the original plant references (see Figs. 3.18–3.19), which might unfairly bias the data against a metabarcoding approach. To address this limitation, we map-filtered the follow-up *trn*L metabarcoding comparison to the original plant references. We observed that all libraries had increased read counts when using a less restrictive map-filtering strategy.

Probable false positives (e.g. clades with a solely tropical distribution) were excluded from LCA-assignment. This was done to reduce the possibility of database incompleteness (somewhat closely related but as yet unsequenced organisms, either currently present in the target region or having been extirpated from Beringia), compounded by genetic conservation and/or convergence, driving off-target identifications. See section 2.3.10 in the main paper for a discussion of ‘oasis taxa’ and the problems of false positives and negatives. Our approach of manually removing ‘nonsensical’ organisms presumes that distributions of plants are roughly comparable to how we have observed them in recent history or through palaeoecological proxies, which is of course a false assumption. These false positive identifications are likely the result of database incompleteness combined with taxonomically non-specific genetic regions, post-mortem DNA modifications, and imperfect alignments. False positives can be somewhat

mitigated by using a highly curated local reference database for taxonomic assignment rather than the entire NCBI database, but this also succumbs to *a priori* limitations where one will only find organisms that they intend to find, resulting in false negatives and potentially an over-confidence in taxonomic identifications due to a reverse 'oasis' effect. There is no perfect solution, but we believe our approach strikes a reasonable enough balance to fairly compare between methods here. In retrospect, using a regionally curated, or at least non-redundant *BLAST* database combined with map-filtering to the target organisms (rather than to the baits, or perhaps to the baits but with reference padding to aid with *bwa* mapping) may have been a better approach. Also, the strategy reported by Cribdon et al. (2020) is likely of particular use in similar shotgun or target enriched libraries moving forward, as is increasing *BLAST* top hits to 500 or more.

3.5.4.3 SET-E. MapDamage.

Taxa with high blast and LCA-assigned read-counts were selected to evaluate damage patterns and fragment length distributions (FLD) (see Table 3.19 and Figs. 3.33–3.37). Enriched libraries were mapped to reference genomes of either the LCA-assigned organism itself (e.g. *Mammuthus primigenius*) or a phylogenetically closely related organism (e.g. *Equus caballus*) if there was no species call or if a reliable reference genome for the probable ancient organism does not yet exist. Mapping followed the aforementioned parameters and software, with an additional map-quality filter to ≥ 30 with *samtools* (https://github.com/samtools/samtools) and passed to *mapDamage* (Jónsson et al., 2013) (v 2.0.3, https://ginolhac.github.io/mapDamage/). Plant chloroplast DNA references were reduced to the target barcoding loci (*trn*L, *rbc*L, and *mat*K), each separated by 100 Ns. Mitochondrial reference genomes were used for animal taxa of interest.

3.5.4.4 SET-E. Stringent LCA filtering for unexpected taxa

Pine. For sample SET269-MB and a concatenation of samples SET268-En, 269-En, and 270-En, LCA-assignments to *Pinus sp.* are retained (245/545 and 10/42 respectively) when web-*BLASTing* to the top 5000 hits and increasing the *MEGAN*-LCA

stringency to 100% identity, a top bit-score consideration of 40%, maximum e-score of 1.0E-8, and minimum 90% read coverage.

Mammoth and horse. LCA-assigned mammoth (n=41) and horse (n=10) reads from the Upper Goldbottom core (~9700 cal yr BP, Fig. 2.4) were extracted, concatenated, and queried with the web-based *BLASTn* to the top 20,000 hits on the NCBI GenBank nuceotide database to assess the reliability of their taxon assignments. LCA parameters were increased to 100% identity and 25% top bit-score consideration. With these more stringent parameters and effectively unlimited alignment references, 3 reads were LCA-assigned to *Mammuthus primigenius, 25 to Mammuthus sp.*, and 11 were identified as Elephantidae. *Equus sp.* retained 5 assigned reads.

3.5.4.5 SET-E. Other additional data.

The following list details the additional SET-E data included in this appendix.

1. Map-filtering reference comparisons: Figures 3.18–3.19.
2. Bait-mapped bubble chart extension from main text: Figures 3.20–3.22.
3. Plant metabarcoding (*trn*L) bubble chart extension from main text, Figures 3.23–3.27. A list of 'disabled' taxa in MEGAN is included in Table 3.18.
4. Non map-filtered comparison of enriched, shotgun, and Sadoway metabarcoding samples: Figures 3.28–3.31.
5. Blanks comparison, non map-filtered: Figure 3.32; Metabarcoding blanks bubble chart, mapped to plant references: Fig. 3.33. See also Table 3.23 for blank sample summaries.
6. *mapDamage* plots: Figures 3.34–3.38. See also Table 3.19 for *bwa* mapped reference counts.
7. A summation of major clade *MEGAN* LCA-assignments from the main text: Table 3.20 and Table 3.21.
8. A summary of fold-increases in LCA-assigned DNA comparing the cold spin enriched libraries with alternative approaches: Table 3.22.
9. Histogram of FLDs between *trn*L metabarcoding and enriched hits to *Betula sp:* Fig. 3.39.

Non map-filtered variants of the enriched, shotgun, and Sadoway metabarcoding samples are included as Figures 3.28–3.31. These were generated identically to the metagenomic bubble charts in the main text, except only the top 10 alignments (rather than top 100) were kept for the non-map filtered blasts to reduce unwieldy file sizes. This is potentially problematic as false positives have a higher chance of aligning with so few

top hits (due to over-representation of well-studied taxa when using the public NCBI nucleotide database); these non-map filtered charts should be interpreted with caution. Only major prokaryotes are depicted, and within the eukaryotes, only chordates and Viridiplantae shown (to be able to visualize these comparisons relatively succinctly). Additional potentially 'authentic' sedaDNA taxa are identified in the non-map filtered bubble charts. However, most of these potentially authentic taxa are in the curated baits (such as moose, *Alces alces*). So, either 1) those taxa are identified with nuclear or otherwise non-target genetic loci, 2) those reference sequences regions had been clustered or masked in the curated baits (due to being relatively non-specific), which is why they did not map during initial filtering, or 3) the low top alignments (10 versus 100) resulted in less conservative LCA-assignments when not map-filtering the reads, which is why they are not present in the map-filtered, top 100 hits comparison. They might align well to moose (in this example), but also align relatively well to other cervids. This may be why in the map-filtered variant where more top hits are retained, the LCA more conservatively classifies these reads at a higher (less informative) taxonomic rank (e.g. Cervidae or Pecora). It is also worth noting that common sequencing contaminants and adapter-contaminated genomes on NCBI (e.g. camel, carp, wheat) remain in the non-map filtered metagenomic profiles despite attempts to filter out adaptamers (chimeric adapter sequences created during PCR)—whereas these problematic hits are filtered out early in processing by map-filtering. These false positives inflate the read counts in the non-mapped comparisons, particularly with taxa collapsed at such high ranks to allow for the entire metagenomic profile of each core to be easily visualized. These problems make all of the bubble charts for the non map-filtered libraries seem identical; however, this is certainly not the case when carefully observing the reads and their alignments by taxon node in *MEGAN*. For this reason, the non map-filtered comparisons are of minimal interpretive utility overall.

The false positive problem is most obviously apparent with the non-map filtered shotgun data (Figures 3.28–3.31). These shotgun samples appear to recapitulate much of the same ecological profile with plant clades collapsed at high taxonomic ranks. This is in

part due to an over-abundance of probable false positives, but also reads aligning to regions of the chloroplast and nuclear genomes with few available reference sequences to discriminate between taxonomically specific and deeply conserved loci (in part due to the 'oasis' reference problem as discussed in the main text in reference to Cribdon et al. [2020]). The chloroplast loci *trn*L, *rbc*L, and *mat*K were selected for targeting (and map-filtering) because of the abundance of reference data available for a wide variety of plants in these loci (particularly arctic species) as a result of concerted barcoding efforts (Ratnasignham and Hebert, 2007; CBOL Plant Working Group, 2009; Hollingsworth, 2011). But as the huge discrepancies between shotgun data illustrate—insofar as having almost no data when map-filtered to barcoding loci, versus tens of thousands of aligned reads in the non-mapped variants—loci amenable to barcoding efforts constitute an extremely tiny proportion of the nuclear and organelle genetic material released by plants and other organisms into the environment. Despite constant cellular shedding, a tiny fraction of DNA avoids being metabolized by bacteria, incorporated into microbial genomes, or otherwise degraded through a range of chemical and physical processes. Those few surviving molecules (likely far less than 1%) are subsequently preserved through mineral binding and other processes for a time, making them amenable to sedaDNA research. But with eDNA release and rare preservation mechanisms, very few molecules survive overall; fewer still are represented in extant genetic reference databases, fewer are targeted by our baits, and even fewer still can be detected by metabarcoding. Surely much of this shotgun data has utility as the same broad taxonomic trends are observed without any targeting. And this will increasingly be the case moving forward as reference databases are expanded to include genomic-level data from many more species. But at this time, it is difficult to authenticate many of these reads when they only have a handful of hits to poorly sequenced regions of the nuclear genome. These shotgun samples illustrate that a bait-set including a broader suite of informative nuclear and organelle loci (along with a robust regional reference database for expected taxa) is likely to be one of the next best steps when designing a targeting strategy to make full use of the sedimentary genetic archives available for Quaternary research. Currently, it is

difficult to trust most of these shotgun reads when they do not map to our curated reference data and contain very few (1–3) *BLAST* hits.

3.6 Tables

Table 3.1 Final concentrations of components in the proteinase K digestion solution.

Proteinase K Digestion Solution	
Component	Final Concentration
Tris-Cl (pH 9.0)	0.02 M
SDS	0.5 %
Proteinase K	0.25 mg/ml
CaCl2	0.01 M
DTT	100 mM
PVP	2.5 %
PTB	5 mM

Samples were digested overnight at 35°C with rotation. Nanopure Barnstead water was used to bring up the volume to the desired concentration. Concentrations based on Karpinski et al. (2016). For samples where sarkosyl was used instead of SDS, the final detergent concentration was unchanged. Sediment input: 0.25 g.

Table 3.2 Final concentrations of components in the Dabney binding buffer.

Dabney Binding Buffer	
Component	Final Concentration
Guanidine Hydrochloride	5 M
Isopropanol (100%)	40 %
Tween-20	0.05 %
3 M Sodium Acetate (pH 5.2)	0.09 M

Nanopure Barnstead water was used to bring up the volume to the desired concentration. Concentrations based on Dabney et al. (2013b).

Table 3.3 Final concentrations of components in the blunt-end repair mixture.

Blunt-End Repair Mixture	
Component	Final Concentration
NE Buffer 2.1	1X
DTT	1 mM
dNTP mix	100 µM
ATP	1 mM
T4 polynucleotide kinase	0.5 U/µL
T4 DNA polymerase	0.1 U/µL

A final volume of 40 µL was used for the mixture and template DNA. Nanopure Barnstead water was used to bring up the volume to the desired concentration. Extract template: 10 µL.

Table 3.4 Final concentrations of all components in the adapter ligation mixture.

3. Adapter Ligation Mixture	
Component	Final Concentration
T4 DNA Ligase Buffer	1X
PEG-4000	5%
Adapter Mix	0.5 µM
T4 DNA Ligase	0.125 U/µl
2. Adapter Mix	
IS1_adapter_P5.F	200 µM
IS2_adapter_P7.F	200 µM
IS3_adapter_P5+P7.R	200 µM
Oligo Hybridization Buffer	1X
1. Oligo Hybridization Buffer	
NaCl	500 mM
Tris-Cl, pH 8.0	10 mM
EDTA, pH 8.0	1 mM

Oligo Hybridization Buffer was prepared prior to the Adapter Mix, which was prepared separately for IS1_adapter_P5.F and IS2_adapter_P7.F. These two mixes were then combined after an incubation at 95°C for 10 seconds, and a ramp from 95°C to 12°C at a rate of 0.1°C/sec. A final volume of 40 µl was used for the mixture and template DNA. Nanopure Barnstead water (not listed) was used to bring the volume up to the desired concentration.

Table 3.5 Final concentrations of components in the adapter fill-in mixture.

Adapter Fill-In Mixture	
Component	Final Concentration
ThermoPol Reaction Buffer	1X
dNTP Mix	250 µM
BST Polymerase (large fragment)	0.4 U/µl

A final volume of 40 µl was used for the mixture and template DNA with the addition of Nanopure Barnstead water to bring the mix up to the desired concentration and volume.

Table 3.6 Primer sequences, PCR master mix, and cycling protocol for indexing amplification.

Indexing PCR Master Mix			
Component		Final Concentration	
KAPA SYBR®FAST qPCR Master Mix (2X)		1X	
Forward primer		750 nM	
Reverse primer		750 nM	
Primer Sequences			
Forward Primer	AATGATACGGCGACCACCGAGATCTACAC***NNNNNNN***ACACTCTTTCCCTACACGACGCTCTT		
Reverse Primer	CAAGCAGAAGACGGCATACGAGATTAT***NNNNNNN***ACTGGAGTTCAGACGTGT		
Indexing PCR Protocol			
Phase	Temperature (°C)	Time	Cycles
Initial Denaturation	98	3 min	
Denaturation	98	20 sec	Repeated for 8-12 cycles
Annealing	*60*	*20 sec*	
Extension	72	25 sec	
Final Extension	72	3 min	

The N in each primer sequence represents the 7 bp index specific to each primer. A final reaction volume of 40 µl was used for the assay, with 12.5 µl of the adapter ligated DNA libraries. Nanopure Barnstead water (not listed) was used to bring the volume up to the desired concentration.
Fluorescence readings were recorded post-annealing as indicated above with asterisks.

Table 3.7 Inhibition spike test qPCR assay.

PCR Master Mix			
Component	Final Concentration		
10X PCR Buffer II	1X		
MgCl2	2.5 mM		
dNTP mix	250 µM		
BSA	1 mg/ml		
Forward primer (971)	0.25 µM		
Reverse primer (1040)	0.25 µM		
EvaGreen	0.5X		
AmpliTaq Gold	0.05 U/µL		
Oligo	Sequence (5'–3')		
Forward primer (971_Mamm_Fwd)	CCCTAAACTTTGATAGCTACC		
Reverse primer (1040_Mamm_Rev)	GTAGTTCTCTGGCGGATAGC		
Double stranded 49 bp amplicon based on the mammoth *12S* mitochondrial gene	CCCTAAACTTTGATAGCTACCT TTACAAAGCTATCCGCCAGAGA ACTAC		
Input*	Volume		
PCR master mix	8 µL		
sedaDNA extract template	1 µL		
49 bp amplicon spike	1 µL		
PCR Protocol			
Phase	Temperature (^{o}C)	Time	Cycles
Initial Denaturation	95	5 min	
Denaturation	95	30 sec	Repeated for 50 cycles
Annealing	54	30 sec	
Extension	**72**	50 sec	
Final Extension	72	1 min	
Melt Curve	**55–95**	**5 sec per degree**	

*Sample wells = 1 µL template + 1 µL spike. QPCR standard wells = 1 µL spike, 1 µL 0.1X TE. Non-template controls = 2 µL 0.1X TE.
**Fluorescence readings were recorded post-annealing and during the melt curve as indicated above with asterisks.
Assay from Enk et al. (2016)**.** Nanopure Barnstead water was used to bring the master mix up to the desired concentration and volume.

Table 3.8 Library adapted short amp total quantification PCR.

PCR Master Mix			
Component	Final Concentration		
KAPA SYBR®FAST qPCR Master Mix (2X)	1X		
Forward primer	0.2 µM		
Reverse primer	0.2 µM		
Oligos	Sequence (5'–3')		
Forward primer (ILPr_shortampP5F_MeyerIS7)	ACACTCTTTCCCTACACGAC		
Reverse primer (ILPr_shortampP7R_MeyerIS8)	GTGACTGGAGTTCAGACGTGT		
Library adapted oligo based on the mammoth *12S* mitochondrial gene. *(Priming sites with reverse-complement bolded.)*	**ACACTCTTTCCCTACACGAC**GCTCTTCCGAT CTCCCTAAACTTTGATAGCTACCTTTACAAAG CTATCCGCCAGAGAACTACAGATCGGAAGAG C**ACACGTCTGAACTCCAGTCAC**		
Input	Volume		
PCR master mix	6 µL		
Library adapted template	4 µL		
PCR Protocol			
Phase	Temperature (ºC)	Time	Cycles
Initial Denaturation	95	5 min	
Denaturation	95	30 sec	Repeated for 30 cycles
Annealing + Extension	60	45 sec	
Melt Curve	**65–95**	**5 sec per degree**	

Nanopure Barnstead water was used to bring the mix up to the desired concentration and volume. Oligo based on Enk et al. (2016); primers based Meyer and Kircher (2010).

Table 3.9 Library adapted *trnL* short amp total quantification PCR.

PCR Master Mix			
Component	Final Concentration		
10X PCR Buffer II	1X		
MgCl2	2.5 mM		
dNTP mix	250 µM		
BSA	1 mg/ml		
Forward primer	0.25 µM		
Reverse primer	0.75 µM		
EvaGreen	0.5X		
AmpliTaq Gold	0.05 U/µL		
Oligos	Sequence (5'–3')		
Forward primer (trnL_P6-g_F)	GGGCAATCCTGAGCCAA		
Reverse primer (ILPr_shortampP7R_MeyerIS8)	GTGACTGGAGTTCAGACGTGT		
Oligo with binding sites for library adapter primers and *trnL* primers from Taberlet et al. (2007). Oligo insert shows no significant similarity with blastn and a top blast hit to Staphylococcus aureus with an E-value of 0.056 using megablast at the time of publication. *(Priming sites with reverse-complement bolded.)*	GTGACACTCTTTCCCTACACGACT**GG GCAATCCTGAGCCAA**ATGATATGATT TGAGATATTGATAGAATTGAATGCAT AGTGATAAAAGGATGATATATTAGGA TAGGTGCAGAGACTCAATGGA**ACACG TCTGAACTCCAGTCAC**GTA		
Input	Volume		
PCR master mix	8 µL		
Library adapted template	1 µL		
PCR Protocol			
Phase	Temperature (^{o}C)	Time	Cycles
Initial Denaturation	95	5 min	
Denaturation	95	30 sec	Repeated for 50 cycles
Annealing	51	30 sec	
Extension	*72*	50 sec	
Final Extension	72	1 min	
Melt Curve	*55–95*	*1 sec per degree*	

*Fluorescence readings were recorded post-annealing and during the melt curve as indicated above with asterisks.

Nanopure Barnstead water was used to bring the master mix up to the desired concentration and volume.

Library adapter primer based on Meyer and Kircher (2010); primer *trnL*-g targets the P6 loop of the *trnL* cpDNA intron, and is based on Taberlet et al. (2007).

Table 3.10 Library adapted and indexed long amp total quantification PCR.

PCR Master Mix			
Component		Final Concentration	
KAPA SYBR®FAST qPCR Master Mix (2X)		1X	
Forward primer		0.2 µM	
Reverse primer		0.2 µM	
Oligos		Sequence (5'–3')	
Forward primer (ILPr_shortampP5F_MeyerIS5)		AATGATACGGCGACCACCGA	
Reverse primer (ILPr_shortampP7R_MeyerIS6)		CAAGCAGAAGACGGCATACGA	
PhiX library adapted control standard from 100 pM to 62.6 fM		AATGATACGGCGACCACCGA *ADAPTER INSERT* TCGTATGCCGTCTTCTGCTTG	
Input		Volume	
PCR master mix		6 µL	
Library adapted and indexed template		4 µL	
PCR Protocol			
Phase	Temperature (°C)	Time	Cycles
Initial Denaturation	95	5 min	1
Denaturation	95	30 sec	Repeated for 35 cycles
Annealing + Extension	60	45 sec	
Cooldown	8	30 sec	1

Nanopure Barnstead water was used to bring the mix up to the desired concentration and volume. Primers from Meyer and Kircher (2010).

Table 3.11 Enrichment mastermixes.

Hybridization MasterMix	
Component	Final Concentration
Hyb N (19.46X SSPE, 13.5 mM EDTA)	9X, 6.25mM
Hyb D (50X Denhardt's Solution)	8.75X
Hyb S (10% SDS)	0.25%
Hyb R RNAsecure	1.56X
Bait Mixture (200 ng baits per reaction)	11.11 ng/µL
Bait Mixture	
Component	Final Concentration
Plant: 18,672 baits	83.33 ng/rxn
Animal: 57,588 baits	138.89 ng/rxn
Library MasterMix	
Component	Final Concentration
Block A (Illumina bloligos xGens)	0.04 ng/µL
Block C (Human COt-1 DNA)	0.19 ng/µL
Block O (Salmon Sperm DNA)	0.19 ng/µL
Library template input	7 µL
Wash Buffer X (0.2X WB)	
Component	Final Concentration
HYB S (10% SDS)	0.08 %
Wash Buffer (0.1X SSC; 0.1% SDS; 1mM EDTA)	0.2X

Nanopure Barnstead water was used to bring mixes up to the desired concentration and volume.

Table 3.12 SET-A sample list.

SET ID	Extraction method	Extract clean-up prior to DsLp	Core/sample	Previous ID	Site	Sample Type
SET2	PowerSoil		MM12-118b	GB1	Upper Goldbottom	Permafrost
SET4	DD-Dabney		MM12-118b	GB1	Upper Goldbottom	Permafrost
SET5	DD-Dabney	1/10 dilution	MM12-118b	GB1	Upper Goldbottom	Permafrost
SET6	DD-Dabney	QiaQuick Purification	MM12-118b	GB1	Upper Goldbottom	Permafrost
SET9	PowerSoil		LLII 12-84-3	LL3	Lucky Lady II	Permafrost
SET10	PowerSoil	1/10 dilution	LLII 12-84-3	LL3	Lucky Lady II	Permafrost
SET13	DD-Dabney		LLII 12-84-3	LL3	Lucky Lady II	Permafrost
SET14	DD-Dabney	1/10 dilution	LLII 12-84-3	LL3	Lucky Lady II	Permafrost
SET15	DD-Dabney	QiaQuick purification	LLII 12-84-3	LL3	Lucky Lady II	Permafrost
SET17	PowerSoil		LLII 12-217-8	LL1	Lucky Lady II	Permafrost
SET19	DD-Dabney		LLII 12-217-8	LL1	Lucky Lady II	Permafrost
SET20	DD-Dabney	1/10 dilution	LLII 12-217-8	LL1	Lucky Lady II	Permafrost
SET21	DD-Dabney	QiaQuick purification	LLII 12-217-8	LL1	Lucky Lady II	Permafrost
SET23	PowerSoil		BC 4-2B	BC	Bear Creek	Permafrost
SET25	DD-Dabney		BC 4-2B	BC	Bear Creek	Permafrost
SET26	DD-Dabney	1/10 dilution	BC 4-2B	BC	Bear Creek	Permafrost
SET27	DD-Dabney	QiaQuick purification	BC 4-2B	BC	Bear Creek	Permafrost
SETPC1	PowerSoil		*N. shastensis*	089	Gypsum Cave, Nevada	Palaeofeces
SETPC2	DD-Dabney		*N. shastensis*	089	Gypsum Cave, Nevada	Palaeofeces
SETBK1	PowerSoil	**Extraction Blanks**				
SETBK2	DD-Dabney					

Core/previous ID as per Sadoway (2014). All sediment cores from the Yukon.
PowerSoil: DNeasy PowerSoil extraction kit.
DD-Dabney: a two-stage demineralization (0.5 M EDTA) and digestion (proteinase K buffer, Table 3.1) (each overnight) followed by purification with a high-volume binding buffer and Roche Diagnostics silica-spin column following Dabney et al.(2013b).
DsLp: Double-stranded library preparation (Meyer and Kircher, 2010; Kircher et al., 2012).
PC1/2: Positive control 089, *Nothrotheriops shastensis (*Shasta ground sloth) palaeofeces (Poinar et al., 1998).
Pre-DsLp clean-up with a QiaQuick PCR Purification Kit, or the extract was diluted to 1/10 prior to DsLp.
Observations: Dabney extracts without an additional clean-up were very darkly coloured compared to the clear PowerSoil extracts.

Table 3.13 SET-B sample list.

Sample Information					Treatment			Sample Information					Treatment				
SET ID	Extract ID	Core	Previous ID	Sample Type	PowerBeads	Solution C3	4°C Spin	SET ID	Extract ID	Core	Previous ID	Sample Type	PowerBeads	Solution C3	4°C Spin	Sonication	Post-sonication purification
SET28	D7a	LLII 12-84-3	LL3	Pf	Y	-	-	**SET73**	D7a	LLII 12-84-3	LL3	Pf	Y	-	-	Y	Y
SET29	D8a	LLII 12-84-3	LL3	Pf	Y	-	Y	**SET74**	D8a	LLII 12-84-3	LL3	Pf	Y	-	Y	Y	Y
SET30	D9a	LLII 12-84-3	LL3	Pf	Y	Y	-	**SET75**	D9a	LLII 12-84-3	LL3	Pf	Y	Y	-	Y	Y
SET31	D10a	LLII 12-84-3	LL3	Pf	Y	Y	Y	**SET76**	D10a	LLII 12-84-3	LL3	Pf	Y	Y	Y	Y	Y
SET32	D11a	LLII 12-84-3	LL3	Pf	-DD	Y	Y	**SET77**	D11a	LLII 12-84-3	LL3	Pf	-DD	Y	Y	Y	Y
SET33	D7b	LLII 12-84-3	LL3	Pf	Y	-	-	**SET78**	D7b	LLII 12-84-3	LL3	Pf	Y	-	-	Y	-
SET34	D8b	LLII 12-84-3	LL3	Pf	Y	-	Y	**SET79**	D8b	LLII 12-84-3	LL3	Pf	Y	-	Y	Y	-
SET35	D9b	LLII 12-84-3	LL3	Pf	Y	Y	-	**SET80**	D9b	LLII 12-84-3	LL3	Pf	Y	Y	-	Y	-
SET36	D10b	LLII 12-84-3	LL3	Pf	Y	Y	Y	**SET81**	D10b	LLII 12-84-3	LL3	Pf	Y	Y	Y	Y	-
SET37	D11b	LLII 12-84-3	LL3	Pf	-Dig	Y	Y	**SET82**	D11b	LLII 12-84-3	LL3	Pf	-Dig	Y	Y	Y	-
SET38	D7c	LLII 12-84-3	LL3	Pf	Y	-	-	**SET83**	D7c	LLII 12-84-3	LL3	Pf	Y	-	-	Y	Y
SET39	D8c	LLII 12-84-3	LL3	Pf	Y	-	Y	**SET84**	D8c	LLII 12-84-3	LL3	Pf	Y	-	Y	Y	-
SET40	D9c	LLII 12-84-3	LL3	Pf	Y	Y	-	**SET85**	D9c	LLII 12-84-3	LL3	Pf	Y	Y	-	Y	-
SET41	D10c	LLII 12-84-3	LL3	Pf	Y	Y	Y	**SET86**	D10c	LLII 12-84-3	LL3	Pf	Y	Y	Y	Y	Y
SET43	D12a	LLII 12-217-8	LL1	Pf	Y	-	-	**SET88**	D12a	LLII 12-217-8	LL1	Pf	Y	-	-	Y	Y
SET44	D13a	LLII 12-217-8	LL1	Pf	Y	-	Y	**SET89**	D13a	LLII 12-217-8	LL1	Pf	Y	-	Y	Y	Y
SET45	D14a	LLII 12-217-8	LL1	Pf	Y	Y	-	**SET90**	D14a	LLII 12-217-8	LL1	Pf	Y	Y	-	Y	Y
SET46	D15a	LLII 12-217-8	LL1	Pf	Y	Y	Y	**SET91**	D15a	LLII 12-217-8	LL1	Pf	Y	Y	Y	Y	Y
SET47	D16a	LLII 12-217-8	LL1	Pf	-DD	Y	Y	**SET92**	D16a	LLII 12-217-8	LL1	Pf	-DD	Y	Y	Y	Y
SET48	D12b	LLII 12-217-8	LL1	Pf	Y	-	-	**SET93**	D12b	LLII 12-217-8	LL1	Pf	Y	-	-	Y	-
SET49	D13b	LLII 12-217-8	LL1	Pf	Y	-	Y	**SET94**	D13b	LLII 12-217-8	LL1	Pf	Y	-	Y	Y	-
SET50	D14b	LLII 12-217-8	LL1	Pf	Y	Y	-	**SET95**	D14b	LLII 12-217-8	LL1	Pf	Y	Y	-	Y	-
SET51	D15b	LLII 12-217-8	LL1	Pf	Y	Y	Y	**SET96**	D15b	LLII 12-217-8	LL1	Pf	Y	Y	Y	Y	-
SET52	D16b	LLII 12-217-8	LL1	Pf	-Dig	Y	Y	**SET97**	D16b	LLII 12-217-8	LL1	Pf	-Dig	Y	Y	Y	-
SET53	D12c	LLII 12-217-8	LL1	Pf	Y	-	-	**SET98**	D12c	LLII 12-217-8	LL1	Pf	Y	-	-	Y	Y
SET54	D13c	LLII 12-217-8	LL1	Pf	Y	-	Y	**SET99**	D13c	LLII 12-217-8	LL1	Pf	Y	-	Y	Y	-
SET55	D14c	LLII 12-217-8	LL1	Pf	Y	Y	-	**SET100**	D14c	LLII 12-217-8	LL1	Pf	Y	Y	-	Y	-
SET56	D15c	LLII 12-217-8	LL1	Pf	Y	Y	Y	**SET101**	D15c	LLII 12-217-8	LL1	Pf	Y	Y	Y	Y	Y
SET58	D17a	BC 4-2B	BC	Pf	Y	-	-	**SET103**	D17a	BC 4-2B	BC	Pf	Y	-	-	Y	Y
SET59	D18a	BC 4-2B	BC	Pf	Y	-	Y	**SET104**	D18a	BC 4-2B	BC	Pf	Y	-	Y	Y	Y
SET60	D19a	BC 4-2B	BC	Pf	Y	Y	-	**SET105**	D19a	BC 4-2B	BC	Pf	Y	Y	-	Y	Y
SET61	D20a	BC 4-2B	BC	Pf	Y	Y	Y	**SET106**	D20a	BC 4-2B	BC	Pf	Y	Y	Y	Y	Y
SET62	D21a	BC 4-2B	BC	Pf	-DD	Y	Y	**SET107**	D21a	BC 4-2B	BC	Pf	-DD	Y	Y	Y	Y
SET63	D17b	BC 4-2B	BC	Pf	Y	-	-	**SET108**	D17b	BC 4-2B	BC	Pf	Y	-	-	Y	-
SET64	D18b	BC 4-2B	BC	Pf	Y	-	Y	**SET109**	D18b	BC 4-2B	BC	Pf	Y	-	Y	Y	-
SET65	D19b	BC 4-2B	BC	Pf	Y	Y	-	**SET110**	D19b	BC 4-2B	BC	Pf	Y	Y	-	Y	-
SET66	D20b	BC 4-2B	BC	Pf	Y	Y	Y	**SET111**	D20b	BC 4-2B	BC	Pf	Y	Y	Y	Y	-
SET67	D21b	BC 4-2B	BC	Pf	-Dig	Y	Y	**SET112**	D21b	BC 4-2B	BC	Pf	-Dig	Y	Y	Y	-
SET68	D17c	BC 4-2B	BC	Pf	Y	-	-	**SET113**	D17c	BC 4-2B	BC	Pf	Y	-	-	Y	Y
SET69	D18c	BC 4-2B	BC	Pf	Y	-	Y	**SET114**	D18c	BC 4-2B	BC	Pf	Y	-	Y	Y	-
SET70	D19c	BC 4-2B	BC	Pf	Y	Y	-	**SET115**	D19c	BC 4-2B	BC	Pf	Y	Y	-	Y	-
SET71	D20c	BC 4-2B	BC	Pf	Y	Y	Y	**SET116**	D20c	BC 4-2B	BC	Pf	Y	Y	Y	Y	Y
SETBK3	D23	Extraction blank			-DD	-	-	**SETBK3-S**	D23	Extraction blank			-DD	-	-	Y	-
SETBK4	D24	Extraction blank			Y	Y	Y	**SETBK4-S**	D24	Extraction blank			Y	Y	Y	Y	-
SETBK5	D25	Extraction blank			Y	Y	Y	**SETBK5-S**	D25	Extraction blank			Y	Y	Y	Y	Y

Core and previous ID as per core slice designation in Sadoway (2014). Pf = permafrost; Y = treatment was used on sample; -DD = 1M EDTA demineralization overnight followed by proteinase K digestion buffer; -Dig = Same as DD without EDTA phase. SET samples on the left half of the divide were not sonicated. For samples on the right half that were, 25 µL of extract was added to 25 µL of EBT (see Table S14 for sonication run parameters). For samples that were sonicated, a subset was purified/concentrated with QiaQuick PCR purification kit back to 25 µL.

Table 3.14 Sonication run parameters.

Target bp (Peak)	50–150
Peak Incident Power (W)	175
Duty Factor	10%
Cycles per burst	200
Treatment Time (s)	480
Temp (C) (+/-2)	7

Minimum input volume is 50 µL, so 25 µL extracts were diluted with 25 µL EBT to bring up to volume.

Table 3.15 SET-C sample list.

SET ID	Core	Previous ID	4°C Spin	4°C Timing (hours)
SET118	LLII 12-84-3	LL3	-	-
SET119	LLII 12-84-3	LL3	-	-
SET120	LLII 12-84-3	LL3	-	-
SET121	LLII 12-84-3	LL3	Y	1
SET122	LLII 12-84-3	LL3	Y	1
SET123	LLII 12-84-3	LL3	Y	1
SET124	LLII 12-84-3	LL3	Y	6
SET125	LLII 12-84-3	LL3	Y	6
SET126	LLII 12-84-3	LL3	Y	6
SET127	LLII 12-84-3	LL3	Y	19
SET128	LLII 12-84-3	LL3	Y	19
SET129	LLII 12-84-3	LL3	Y	19
SET130	LLII 12-217-8	LL1	-	-
SET131	LLII 12-217-8	LL1	-	-
SET132	LLII 12-217-8	LL1	-	-
SET133	LLII 12-217-8	LL1	Y	1
SET134	LLII 12-217-8	LL1	Y	1
SET135	LLII 12-217-8	LL1	Y	1
SET136	LLII 12-217-8	LL1	Y	6
SET137	LLII 12-217-8	LL1	Y	6
SET138	LLII 12-217-8	LL1	Y	6
SET139	LLII 12-217-8	LL1	Y	19
SET140	LLII 12-217-8	LL1	Y	19
SET141	LLII 12-217-8	LL1	Y	19
SET142	BC 4-2B	BC	-	-
SET143	BC 4-2B	BC	-	-
SET144	BC 4-2B	BC	-	-
SET145	BC 4-2B	BC	Y	1
SET146	BC 4-2B	BC	Y	1
SET147	BC 4-2B	BC	Y	1
SET148	BC 4-2B	BC	Y	6
SET149	BC 4-2B	BC	Y	6
SET150	BC 4-2B	BC	Y	6
SET151	BC 4-2B	BC	Y	19
SET152	BC 4-2B	BC	Y	19
SET153	BC 4-2B	BC	Y	19
SETBK9	Extraction Blank		Y	1
SETBK10	Extraction Blank		Y	6
SETBK11	Extraction Blank		Y	19
SETLBK12	Library Blank			

All samples were physically disrupted with PowerBeads.

Table 3.16 SET-D sample list.

Sample Information				Extraction Variants			
SET ID	Core	Previous ID	Sample Type	Lysing Method	Detergent	Lysing Timing (hours)	4°C Timing (hours)
SET160	LLII 12-217-8	LL1	Pf	PowerBead+Digest	Sarkosyl	9	24
SET161	LLII 12-217-8	LL1	Pf	PowerBead+Digest	Sarkosyl	9	24
SET162	LLII 12-217-8	LL1	Pf	PowerBead+Digest	Sarkosyl	9	24
SET163	LLII 12-217-8	LL1	Pf	PowerBead+Digest	Sarkosyl	19	24
SET164	LLII 12-217-8	LL1	Pf	PowerBead+Digest	Sarkosyl	19	24
SET165	LLII 12-217-8	LL1	Pf	PowerBead+Digest	Sarkosyl	19	24
SET166	LLII 12-217-8	LL1	Pf	PowerBead+Digest	Sarkosyl	9	48
SET167	LLII 12-217-8	LL1	Pf	PowerBead+Digest	Sarkosyl	9	48
SET168	LLII 12-217-8	LL1	Pf	PowerBead+Digest	Sarkosyl	9	48
SET169	LLII 12-217-8	LL1	Pf	PowerBead+Digest	Sarkosyl	19	48
SET170	LLII 12-217-8	LL1	Pf	PowerBead+Digest	Sarkosyl	19	48
SET171	LLII 12-217-8	LL1	Pf	PowerBead+Digest	Sarkosyl	19	48
SET172	LLII 12-217-8	LL1	Pf	Digest	Sarkosyl	9	24
SET173	LLII 12-217-8	LL1	Pf	Digest	Sarkosyl	9	24
SET174	LLII 12-217-8	LL1	Pf	Digest	Sarkosyl	9	24
SET175	LLII 12-217-8	LL1	Pf	Digest	Sarkosyl	19	24
SET176	LLII 12-217-8	LL1	Pf	Digest	Sarkosyl	19	24
SET177	LLII 12-217-8	LL1	Pf	Digest	Sarkosyl	19	24
SET178	LLII 12-217-8	LL1	Pf	Digest	Sarkosyl	9	48
SET179	LLII 12-217-8	LL1	Pf	Digest	Sarkosyl	9	48
SET180	LLII 12-217-8	LL1	Pf	Digest	Sarkosyl	9	48
SET181	LLII 12-217-8	LL1	Pf	Digest	Sarkosyl	19	48
SET182	LLII 12-217-8	LL1	Pf	Digest	Sarkosyl	19	48
SET183	LLII 12-217-8	LL1	Pf	Digest	Sarkosyl	19	48
SET184	LLII 12-217-8	LL1	Pf	EDTA-Digest	Sarkosyl	9	24
SET185	LLII 12-217-8	LL1	Pf	EDTA-Digest	Sarkosyl	9	24
SET186	LLII 12-217-8	LL1	Pf	EDTA-Digest	Sarkosyl	9	24
SET187	LLII 12-217-8	LL1	Pf	EDTA-Digest	Sarkosyl	19	24
SET188	LLII 12-217-8	LL1	Pf	EDTA-Digest	Sarkosyl	19	24
SET189	LLII 12-217-8	LL1	Pf	EDTA-Digest	Sarkosyl	19	24
SET190	LLII 12-217-8	LL1	Pf	EDTA-Digest	Sarkosyl	9	48
SET191	LLII 12-217-8	LL1	Pf	EDTA-Digest	Sarkosyl	9	48
SET192	LLII 12-217-8	LL1	Pf	EDTA-Digest	Sarkosyl	9	48
SET193	LLII 12-217-8	LL1	Pf	EDTA-Digest	Sarkosyl	19	48
SET194	LLII 12-217-8	LL1	Pf	EDTA-Digest	Sarkosyl	19	48
SET195	LLII 12-217-8	LL1	Pf	EDTA-Digest	Sarkosyl	19	48
SET196	BC 4-2B	BC	Pf	PowerBead+Digest	Sarkosyl	9	24
SET197	BC 4-2B	BC	Pf	PowerBead+Digest	Sarkosyl	9	24
SET198	BC 4-2B	BC	Pf	PowerBead+Digest	Sarkosyl	9	24
SET199	BC 4-2B	BC	Pf	PowerBead+Digest	Sarkosyl	19	24
SET200	BC 4-2B	BC	Pf	PowerBead+Digest	Sarkosyl	19	24
SET201	BC 4-2B	BC	Pf	PowerBead+Digest	Sarkosyl	19	24
SET202	BC 4-2B	BC	Pf	PowerBead+Digest	Sarkosyl	9	48
SET203	BC 4-2B	BC	Pf	PowerBead+Digest	Sarkosyl	9	48
SET204	BC 4-2B	BC	Pf	PowerBead+Digest	Sarkosyl	9	48
SET205	BC 4-2B	BC	Pf	PowerBead+Digest	Sarkosyl	19	48
SET206	BC 4-2B	BC	Pf	PowerBead+Digest	Sarkosyl	19	48
SET207	BC 4-2B	BC	Pf	PowerBead+Digest	Sarkosyl	19	48
SET208	BC 4-2B	BC	Pf	Digest	Sarkosyl	9	24
SET209	BC 4-2B	BC	Pf	Digest	Sarkosyl	9	24
SET210	BC 4-2B	BC	Pf	Digest	Sarkosyl	9	24
SET211	BC 4-2B	BC	Pf	Digest	Sarkosyl	19	24
SET212	BC 4-2B	BC	Pf	Digest	Sarkosyl	19	24
SET213	BC 4-2B	BC	Pf	Digest	Sarkosyl	19	24
SET214	BC 4-2B	BC	Pf	Digest	Sarkosyl	9	48
SET215	BC 4-2B	BC	Pf	Digest	Sarkosyl	9	48
SET216	BC 4-2B	BC	Pf	Digest	Sarkosyl	9	48
SET217	BC 4-2B	BC	Pf	Digest	Sarkosyl	19	48
SET218	BC 4-2B	BC	Pf	Digest	Sarkosyl	19	48
SET219	BC 4-2B	BC	Pf	Digest	Sarkosyl	19	48
SET220	BC 4-2B	BC	Pf	EDTA-Digest	Sarkosyl	9	24
SET221	BC 4-2B	BC	Pf	EDTA-Digest	Sarkosyl	9	24
SET222	BC 4-2B	BC	Pf	EDTA-Digest	Sarkosyl	9	24
SET223	BC 4-2B	BC	Pf	EDTA-Digest	Sarkosyl	19	24
SET224	BC 4-2B	BC	Pf	EDTA-Digest	Sarkosyl	19	24
SET225	BC 4-2B	BC	Pf	EDTA-Digest	Sarkosyl	19	24
SET226	BC 4-2B	BC	Pf	EDTA-Digest	Sarkosyl	9	48
SET227	BC 4-2B	BC	Pf	EDTA-Digest	Sarkosyl	9	48
SET228	BC 4-2B	BC	Pf	EDTA-Digest	Sarkosyl	9	48
SET229	BC 4-2B	BC	Pf	EDTA-Digest	Sarkosyl	19	48
SET230	BC 4-2B	BC	Pf	EDTA-Digest	Sarkosyl	19	48
SET231	BC 4-2B	BC	Pf	EDTA-Digest	Sarkosyl	19	48
BK15			E-B	PowerBead+Digest	Sarkosyl	9	
BK16			E-B	EDTA-Digest	Sarkosyl	9	
BK17			E-B	PowerBead+Digest	Sarkosyl	19	
BK18			E-B	EDTA-Digest	Sarkosyl	19	
SET244	BC 4-2B	BC	Pf	PowerBead+Digest	SDS	19	24
SET245	BC 4-2B	BC	Pf	PowerBead+Digest	SDS	19	24
SET246	BC 4-2B	BC	Pf	PowerBead+Digest	SDS	19	24
SET247	BC 4-2B	BC	Pf	PowerBead+Digest	SDS	19	48
SET248	BC 4-2B	BC	Pf	PowerBead+Digest	SDS	19	48
SET249	BC 4-2B	BC	Pf	PowerBead+Digest	SDS	19	48
SET250	BC 4-2B	BC	Pf	EDTA-Digest	SDS	19	24
SET251	BC 4-2B	BC	Pf	EDTA-Digest	SDS	19	24
SET252	BC 4-2B	BC	Pf	EDTA-Digest	SDS	19	24
SET253	BC 4-2B	BC	Pf	EDTA-Digest	SDS	19	48
SET254	BC 4-2B	BC	Pf	EDTA-Digest	SDS	19	48
SET255	BC 4-2B	BC	Pf	EDTA-Digest	SDS	19	48
BK19			E-B	PowerBead+Digest	SDS	19	24
BK20			E-B	EDTA-Digest	SDS	19	48

Pf = permafrost; E-B = extraction blank. SET-D_1 in grey (left and upper right sections), SET-D_2 in blue (bottom right section).

Table 3.17 Metabarcoding qPCR amplification, *trnL*.

PCR Master Mix			
Component	Final Concentration		
10X PCR Buffer II	1X		
MgCl2	1.5 mM		
dNTP mix	250 µM		
BSA	1 mg/ml		
Forward primer	0.25 µM		
Reverse primer	0.25 µM		
EvaGreen	1X		
AmpliTaq Gold	0.65 U/µL		
Oligos	Sequence (5'–3')		
Forward primer (trnL_P6-g_F)	GGGCAATCCTGAGCCAA		
Reverse primer (trnL_P6-h_R)	CCATTGAGTCTCTGCACCTATC		
Oligo with binding sites for library adapter primers and *trnL* primers from Taberlet et al. (2007). Oligo insert shows no significant similarity with BLASTn and a top blast hit to Staphylococcus aureus with an E-value of 0.056 using megablast at the time of publication. *(Priming sites with reverse-complement bolded.)*	GTGACACTCTTTCCCTACACGACT**GG GCAATCCTGAGCCAA**ATGATATGATT TGAGATATTGATAGAATTGAATGCAT AGTGATAAAAGGATGATATATTAG**GA TAGGTGCAGAGACTCAATGG**AACAC GTCTGAACTCCAGTCACGTA		
Input	Volume		
PCR master mix	24 µL		
Extract template	1 µL		
PCR Protocol			
Phase	Temperature (^{o}C)	Time	Cycles
Initial Denaturation	95	5 min	
Denaturation	95	30 sec	Repeated for 45 cycles
Annealing	52	30 sec	
Extension	*72*	50 sec	
Final Extension	72	1 min	

*Fluorescence readings were recorded post-annealing as indicated above with asterisks.

Nanopure Barnstead water was used to bring the master mix up to the desired concentration and volume. T*rnL*-g/h targets the P6 loop of the *trnL* cpDNA intron, and is based on Taberlet et al. (2007) with a custom in-house standard for quantification (SET-E).

Table 3.18 Disabled taxa in MEGAN with NCBI ID.

[2323] unclassified Bacteria	[78725] Cleistes
[2706] Citrus	[78760] Epistephium
[3298] Zamiaceae	[79318] Irvingia
[3520] Casuarinaceae	[85234] Oncotheca
[3642] Lecythidaceae	[85241] Plagiopteron
[3680] Begoniaceae	[93758] Corchorus
[3733] Moringaceae	[100370] Croton
[3737] Sapotaceae	[102805] Barnadesioideae
[3805] Bauhinia	[106722] Dorstenia
[4268] Malpighiaceae	[112800] Achariaceae
[4328] Proteaceae	[112827] Lacistemataceae
[4420] Victoria	[112836] Paropsia
[4441] Camellia	[124867] Pandaceae
[4527] Oryza	[126560] Picconia
[4613] Bromeliaceae	[134367] hybrid subtypes
[4618] Zingiberales	[142700] Pimelea
[4672] Dioscorea	[149357] Cissus
[4710] Arecaceae	[156614] environmental samples <viruses,unclassified bacterial viruses>
[12908] unclassified sequences	[163724] Crotalarieae
[13394] Capparis	[163736] Podalyrieae
[13484] Dianella	[169618] Ixoroideae
[13669] Sarcandra	[169619] Cinchonoideae
[14107] Restionaceae	[169659] Psychotrieae
[16472] Goodeniaceae	[173686] Santiria
[16739] Piperaceae	[179710] Homalium
[19955] Ebenaceae	[180118] Mammea
[21910] Verbenaceae	[186616] environmental samples <viruses,superkingdom Viruses>
[22063] Monimiaceae	[214912] Sterculioideae
[22973] Chrysobalanaceae	[225222] Platysace
[23808] Simaroubaceae	[226089] Elatostema
[24942] Dilleniaceae	[233879] Putranjivaceae
[26000] Elaeocarpaceae	[235594] Bridelieae
[26122] Gesneriaceae	[238071] Samydeae
[26778] Nothofagaceae	[238073] Scolopieae
[28384] other sequences	[238074] Prockieae
[37820] Hydrostachys	[238075] Abatieae
[39173] Ocimum	[239467] Phyteuma
[39613] Loeseneriella	[246513] Coldenia
[40029] Rhizophoraceae	[256812] Pera
[41867] Stilbaceae	[261082] Goniothalamus
[42220] Curtisiaceae	[324786] Pomaderreae
[43690] Canarium	[325293] Phyliceae
[43707] Meliaceae	[367897] environmental samples <viruses,unclassified DNA viruses>
[44985] Hyacinthaceae	[494674] Gypothamnium
[47936] environmental samples <proteobacteria,phylum Proteobacteria>	[768725] Prunus hybrid cultivar
[48479] environmental samples <bacteria,superkingdom Bacteria>	[1003877] Benincaseae
[48510] environmental samples <archaea,superkingdom Archaea>	[1445966] Gnetidae
[53907] Ormosia	[1446378] Araucariales
[55234] Monotoca	[1504452] Osmelia
[55390] Adinandra	[1525719] Palicoureeae
[56627] Ochnaceae	[1648022] Parapholiinae
[58436] Argostemma	[1699513] Myrtoideae
[58963] Moraea	[1895897] Pombalia
[60092] Vinca	[1978182] Detarioideae

[61964] environmental samples <eukaryotes,superkingdom Eukaryota>	[2060783] Scyphostegioideae
[65009] Dipterocarpoideae	[2231387] dalbergioids sensu lato
[69062] Globularia	[2233854] mirbelioid clade
[72403] Clusia	[2233855] indigoferoid/millettioid clade
[77014] Melicope	[2304098] Cayratieae
[77071] Cecropia	[2508080] Crocoideae

This list is a combination of *MEGANs* default and intentionally disabled taxa. Sporadic mishits to some species within these families or genera were identified in this work and parallel Beringian analyses. It is believed much of this is driven by an abundance of genetic research on specific organisms (what Cribdon et al. [2020] refers to as 'oasis taxa'), compounded by database incompleteness for some Quaternary Holarctic plant taxa. The highest possible rank at which no taxa within the clade have a Holarctic distribution were selected to be disabled for simplicity (rather than individually disabling a wide set of species due to robust genetic research on those clades).

Table 3.19 Taxon specific mapping summary at a minimum length of 24 bp and mapping quality of 30.

Library	Core	Extraction	*Bison priscus* NC_027233	*Equus caballus* NC_001640	*Mammuthus primigenius* NC_007596	*Lagopus lagopus* NC_035568	*Picea glauca* NC_028594	*Poa palustris* NC_027484	*Salix interior* NC_024681	*Artemisia frigida* NC_020607
L-SET-256-En	MM12-118b	PowerSoil	6	0	3	14	1,723	0	37,569	3,645
L-SET-257-En			1	0	0	7	1,279	298	15,097	1,371
L-SET-258-En			2	0	1	24	1,212	263	14,894	1,495
L-SET-259-En	LLII 12-84-3	PowerSoil	2	4	2	110	130	218	4,236	1,023
L-SET-260-En			5	1	5	74	196	294	5,214	1,209
L-SET-261-En			1	0	1	63	136	196	3,419	917
L-SET-262-En	LLII 12-217-8	PowerSoil	5	4	3	3	17	227	113	1,080
L-SET-263-En			6	2	0	1	20	106	93	850
L-SET-264-En			9	7	3	1	33	171	169	1,671
L-SET-265-En	BC 4-2B	PowerSoil	37	4	2	7	52	920	1,518	939
L-SET-266-En			35	8	8	10	95	953	1,453	977
L-SET-267-En			26	7	2	13	79	1,477	1,864	1,149
L-SET-268-En	MM12-118b	Modified Dabney	103	47	44	**245**	13,524	11,502	**141,195**	34,802
L-SET-269-En			106	45	83	201	12,396	**10,791**	113,197	29,313
L-SET-270-En			104	32	37	178	**14,575**	10,480	112,797	30,262
L-SET-271-En	LLII 12-84-3	Modified Dabney	74	49	59	1,798	**10,170**	13,523	92,828	**37,685**
L-SET-272-En			82	59	67	**1,611**	9,921	12,811	85,995	36,168
L-SET-273-En			78	51	61	**1,950**	9,718	12,694	**96,063**	36,377
L-SET-274-En	LLII 12-217-8	Modified Dabney	89	58	17	21	533	**1,551**	1,731	**6,462**
L-SET-275-En			80	81	31	21	444	1,484	1,426	4,455
L-SET-276-En			74	43	13	14	231	727	745	2,226
L-SET-277-En	BC 4-2B	Modified Dabney	**1,466**	**427**	**311**	127	**4,907**	**20,006**	**30,198**	**26,042**
L-SET-278-En			**1,034**	**338**	**131**	123	3,082	13,724	20,619	15,035
L-SET-279-En			**1,541**	**370**	**221**	113	3,770	16,781	26,821	18,734
L-SET-BK22-En	Ext. Blank	PowerSoil	0	0	0	0	0	0	0	0
L-SET-BK23-En	Ext. Blank	Modified Dabney	0	0	0	1	0	0	0	0
L-SET-Bk24-En	Library Blank		0	0	0	0	0	0	0	0

Figures 3.34–3.38 report *MapDamage* profiles for highlighted cells. Note: these reads are not filtered to those that solely map to their associated reference. Mapping to each reference was done independently (SET-E).

Table 3.20 Bait map-filtered reads *MEGAN* LCA-assignment summary, SET-E.

SedaDNA Extraction	Targeting Strategy	Total reads	Map-filtered summation				Map-filtered select major clade summations (reads mapped-to-baits, string de-duplicated, ≥ 24bp)											
			Mapped-to-baits*		*BLASTn* aligned & *MEGAN* assigned		Bacteria and Archaea		Fungi		Metazoa		Virdiplantae		No *BLASTn* hits		Not LCA-assigned	
PowerSoil	Enrichment	14,292,697	41,592	**0.3%**	36,693	***0.3%***	15	**0.0%**	0	**0.0%**	143	**0.3%**	36,507	**87.8%**	2,149	**5.2%**	2,750	**6.6%**
Modified Dabney	Enrichment	15,516,557	961,734	**6.4%**	835,364	***5.6%***	282	**0.0%**	56	**0.0%**	8,152	**0.8%**	826,203	**85.9%**	68,228	**7.1%**	58,132	**6.0%**
PowerSoil	Shotgun	6,071,164	161	**0.0%**	50	***0.0%***	0	**0.0%**	0	**0.0%**	0	**0.0%**	50	**31.1%**	103	**64.0%**	8	**5.0%**
Modified Dabney	Shotgun	14,911,050	2,216	**0.0%**	470	***0.0%***	4	**0.2%**	0	**0.0%**	8	**0.4%**	449	**20.3%**	1,642	**74.1%**	104	**4.7%**
D'Costa et al.	Metabarcoding	1,097,644	3176	**0.3%**	3078	***0.3%***	0	**0.0%**	0	**0.0%**	463	**14.6%**	2,608	**82.1%**	57	**1.8%**	41	**1.3%**

Map-filtered summation: percent of total reads.
Map-filtered major clade summations: percent of mapped-to-baits*.

Table 3.21 Non-map-filtered reads *MEGAN* LCA-assignment summary, SET-E.

SedaDNA Extraction	Targeting Strategy	Total reads	Non-map-filtered select major clade summations (string de-duplicated and ≥ 24bp)											
			Bacteria & Archea		Fungi		Metazoa		Virdiplantae		No *BLASTn* hits		Not LCA-assigned	
PowerSoil	Enrichment	14,292,697	243,941	**1.7%**	3,234	**0.0%**	40,345	**0.3%**	462,592	**3.2%**	9,178,308	**64.2%**	877,851	**6.1%**
Modified Dabney	Enrichment	15,516,557	127,382	**0.8%**	11,354	**0.1%**	93,089	**0.6%**	1,685,455	**10.9%**	9,368,011	**60.4%**	526,480	**3.4%**
PowerSoil	Shotgun	6,071,164	113,216	**1.9%**	728	**0.0%**	24,177	**0.4%**	44,852	**0.7%**	4,997,565	**82.3%**	488,337	**8.0%**
Modified Dabney	Shotgun	14,911,050	150,986	**1.0%**	3,141	**0.0%**	87,745	**0.6%**	233,197	**1.6%**	11,863,278	**79.6%**	499,037	**3.3%**
D'Costa et al.	Metabarcoding	1,097,644	43	**0.0%**	0	**0.0%**	20,245	**1.8%**	76,953	**7.0%**	14,097	**1.3%**	17,690	**1.6%**

Non-map-filtered major clade summations: percent of total reads.

Table 3.22 Comparative fold increase in LCA-assigned reads of cold spin extracts with PalaeoChip enrichments over alternative approaches.

Mapped-to-baits, LCA-assigned					
	Extraction Method: Targeting Strategy:	PowerSoil		SedaDNA modified Dabney	D'Costa et al. 2001
		Enrichment	Shotgun	Shotgun	Metabarcoding
SedaDNA modified Dabney extraction paired with targeted enrichment	MM12-118b	15.7x	5,497.1x	1,020.6x	24.7x
	LLII 12-84-3	19.3x	7,024.8x	1,152.1x	59.9x
	LLII 12-217-8	7.7x	1,763.2x	351.7x	1.2x
	BC 4-2B	15.8x	9,826.3x	2,371.7x	4.7x
	Average	**14.6x**	**6,027.9x**	**1,224.0x**	**22.6x**

Mapped-to-plant references, LCA-assigned							
	Extraction Method: Targeting Strategy:	PowerSoil			SedaDNA modified Dabney		D'Costa et al. 2001
		Metabarcoding	Enrichment	Shotgun	Metabarcoding	Shotgun	Metabarcoding
SedaDNA modified Dabney extraction paired with targeted enrichment	MM12-118b	23.0x	5.0x	3,514.5x	17.8x	1,414.3x	5.5x
	LLII 12-84-3	20.6x	9.1x	6,977.6x	19.5x	1,366.4x	12.7x
	LLII 12-217-8	2.3x	2.6x	1,132.5x	2.9x	421.7x	0.3x
	BC 4-2B	6.3x	7.3x	58,281.9x	5.8x	2,856.4x	0.9x
	Average	**13.0x**	**6.0x**	**17,476.6x**	**11.5x**	**1,514.7x**	**4.9x**

SET-E.

Table 3.23 Summary of blank samples and map-filtering counts.

Sample Type	Sample	DNA Targeting Strategy	Extraction Method	Total Reads	Bait mapped & LCA-assigned*	LCA-Assigned of Total	Plant ref mapped & LCA-assigned**	LCA-Assigned of Total
Extraction Blank	SETBK22-SG	Shotgun	PowerSoil	2,756,360	0	0.0%	0	0.0%
	SETBK22-En	Enrichment		102,752	0	0.0%	0	0.0%
	SETBK22-MB	Metabarcoding		628,453	*nm*		156	0.0%
Extraction Blank	SETBK23-SG	Shotgun	SedaDNA Modified Dabney	1,748,595	0	0.0%	0	0.0%
	SETBK23-En	Enrichment		1,186	0	0.0%	0	0.0%
	SETBK23-MB	Metabarcoding		987,906		0.0%	50	0.0%
Library Blank	SETBK24-SG	Shotgun	*NA*	2,841,911	0	0.0%	0	0.0%
	SETBK24-En	Enrichment		677	0	0.0%	0	0.0%
	SETBK24-MB	Metabarcoding		578,123	*nm*		16	0.0%
PCR blank	SETBK25-MB	Metabarcoding		973,729	*nm*		41	0.0%

*Reads map-filtered to animal and plant baits, size filtered to ≥ 24 bp, de-duplicated, *BLASTn* aligned, and MEGAN LCA assigned.
**Reads map-filtered to plant references, with the same subsequent filtering parameters. *Nm* = not mapped to animal/plant baits. Enriched has low total read counts due to off-target exclusion expected with targeted capture, combined with equimolar pooling with samples.
See Figures 3.32–3.33 for blank bubble charts, *SET-E.*

3.7 Figures

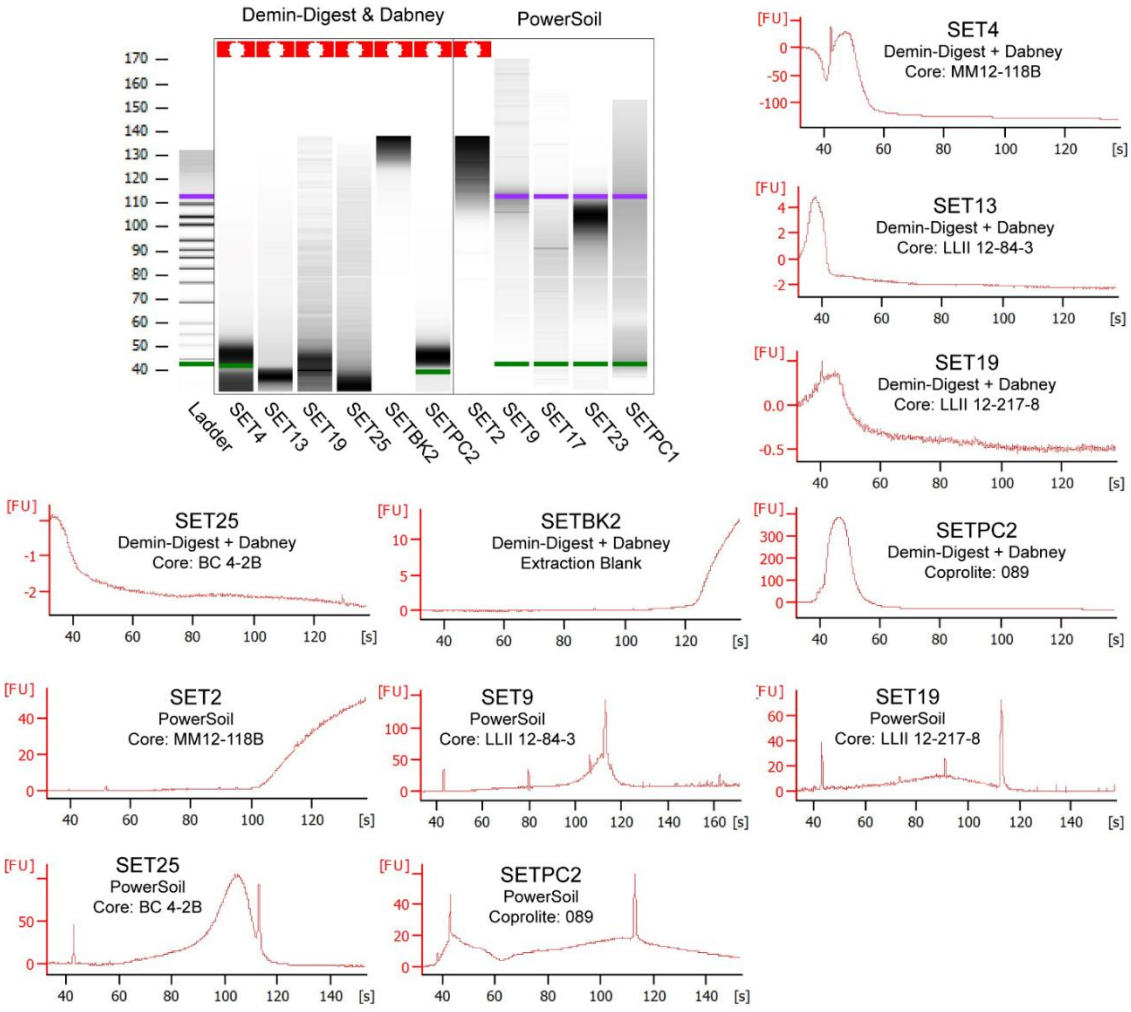

Fig. 3.1 Bioanalyzer, high sensitive DNA assay, SET-A.

Run on an Agilent 2100 Bioanalyzer. Note that lanes 2-8 failed (too darkly coloured to detect baseline florescence), likely due to a high inhibition (humic) load.

PowerSoil: DNeasy PowerSoil extraction kit.
Demin-Digest + Dabney: demineralization (0.5 M EDTA) and digestion (proteinase K buffer, see Table 2) (each overnight separately) followed by purification with a high-volume binding buffer and silica column following Dabney et al. (2013b).
089: *N. shastensis* palaeofeces from (Poinar et al., 1998).
Core ID as per Sadoway (2014).

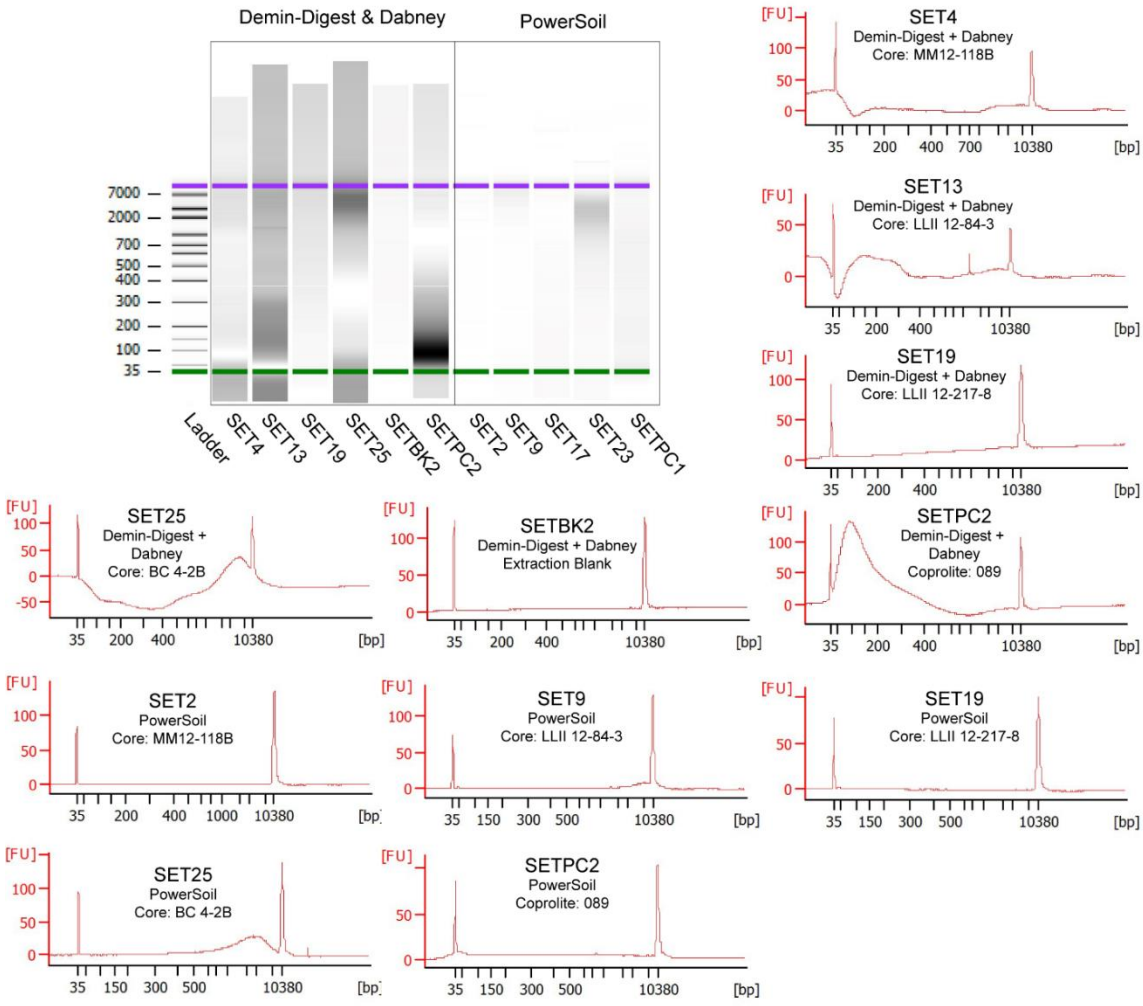

Fig. 3.2 Bioanalyzer, high sensitive DNA assay, SET-A with a 1/10 dilution.

Run on an Agilent 2100 Bioanalyzer.
PowerSoil: DNeasy PowerSoil extraction kit.
Demin-Digest + Dabney: demineralization (0.5 M EDTA) and digestion (proteinase K buffer, see Table 2) (each overnight separately) followed by purification with a high-volume binding buffer and silica column following Dabney et al. (2013b).
089: *N. shastensis* palaeofeces from (Poinar et al., 1998).
Core ID as per Sadoway (2014).

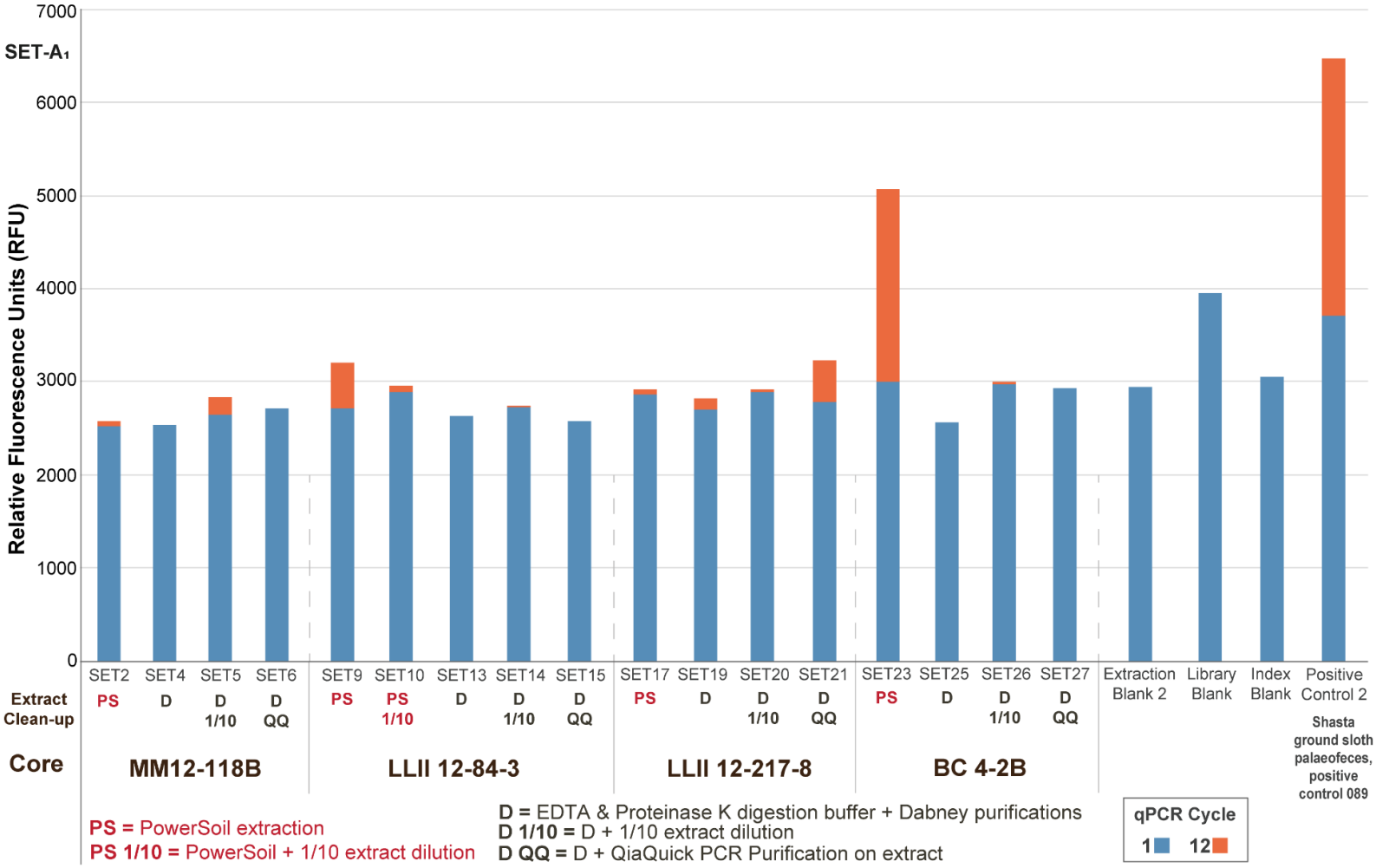

Fig. 3.3 SET-A, indexing RFU bar chart for qPCR cycles 1 and 12.

Extract clean-up: purification strategy prior to double stranded library preparation

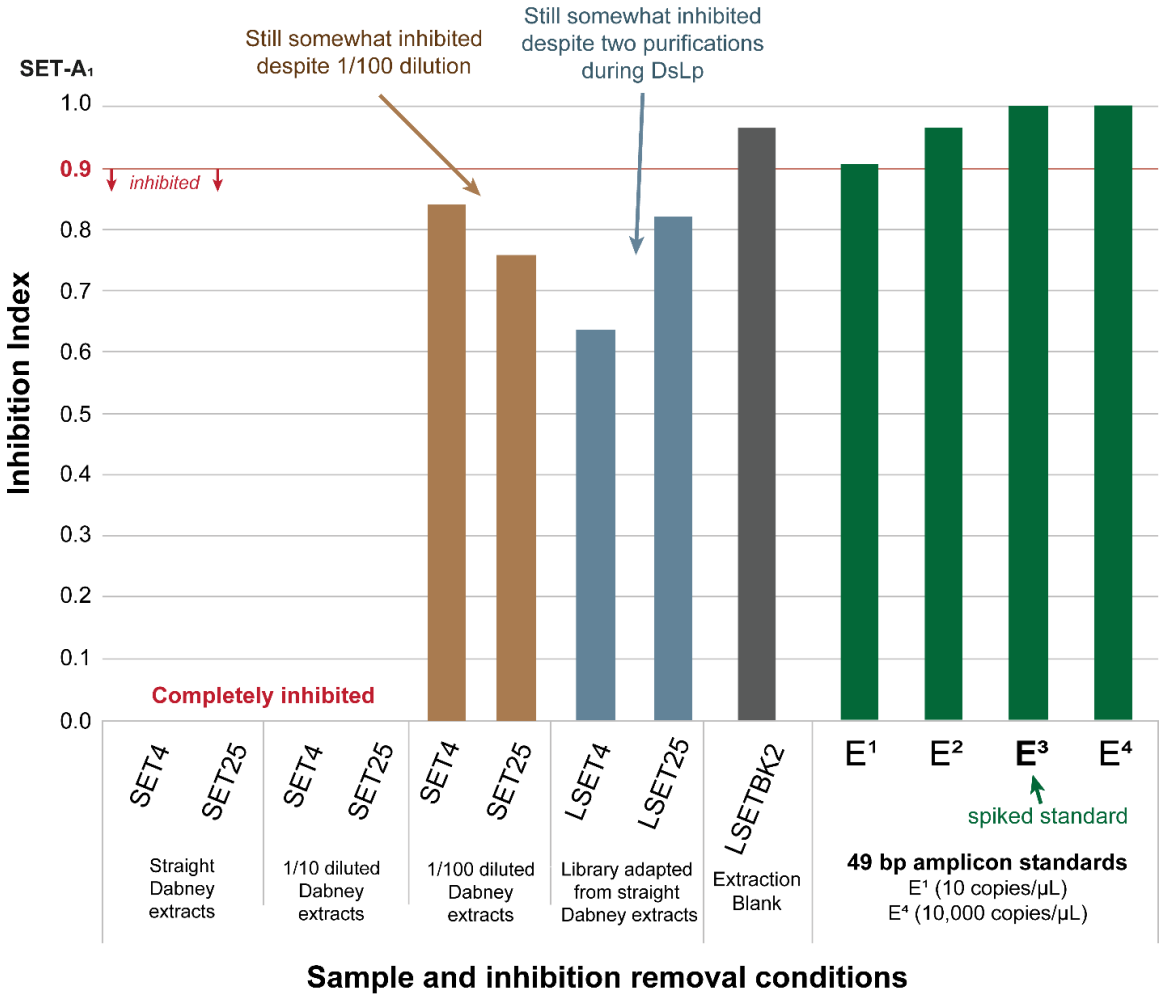

Fig. 3.4 SET-A, Inhibition indices of inhibitor clean-up strategies.

First three column sets are extracts that were spiked for the assay. SET samples with an 'L' prefix denote libraries that were assayed for inhibition.

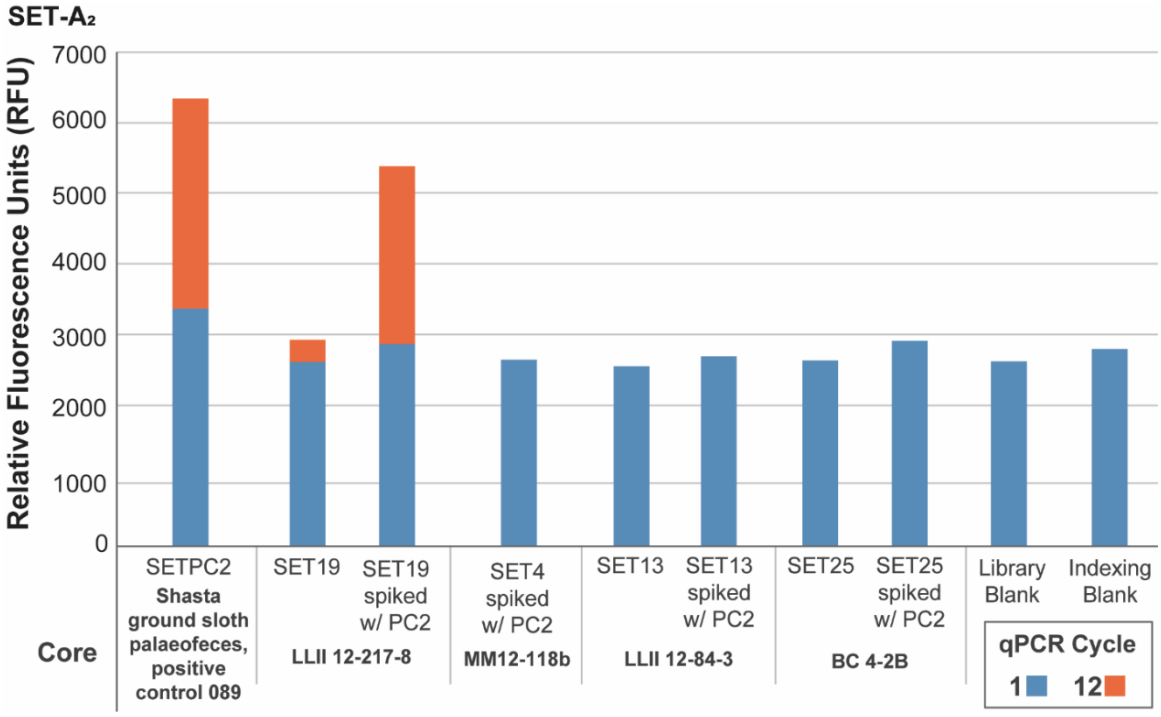

Fig. 3.5 SET-A, Indexing qPCR reaction of positive control spiked extracts prior to library preparation.

The SET4 extract was exhausted; only SET4 with a positive control spike was tested in this experiment.

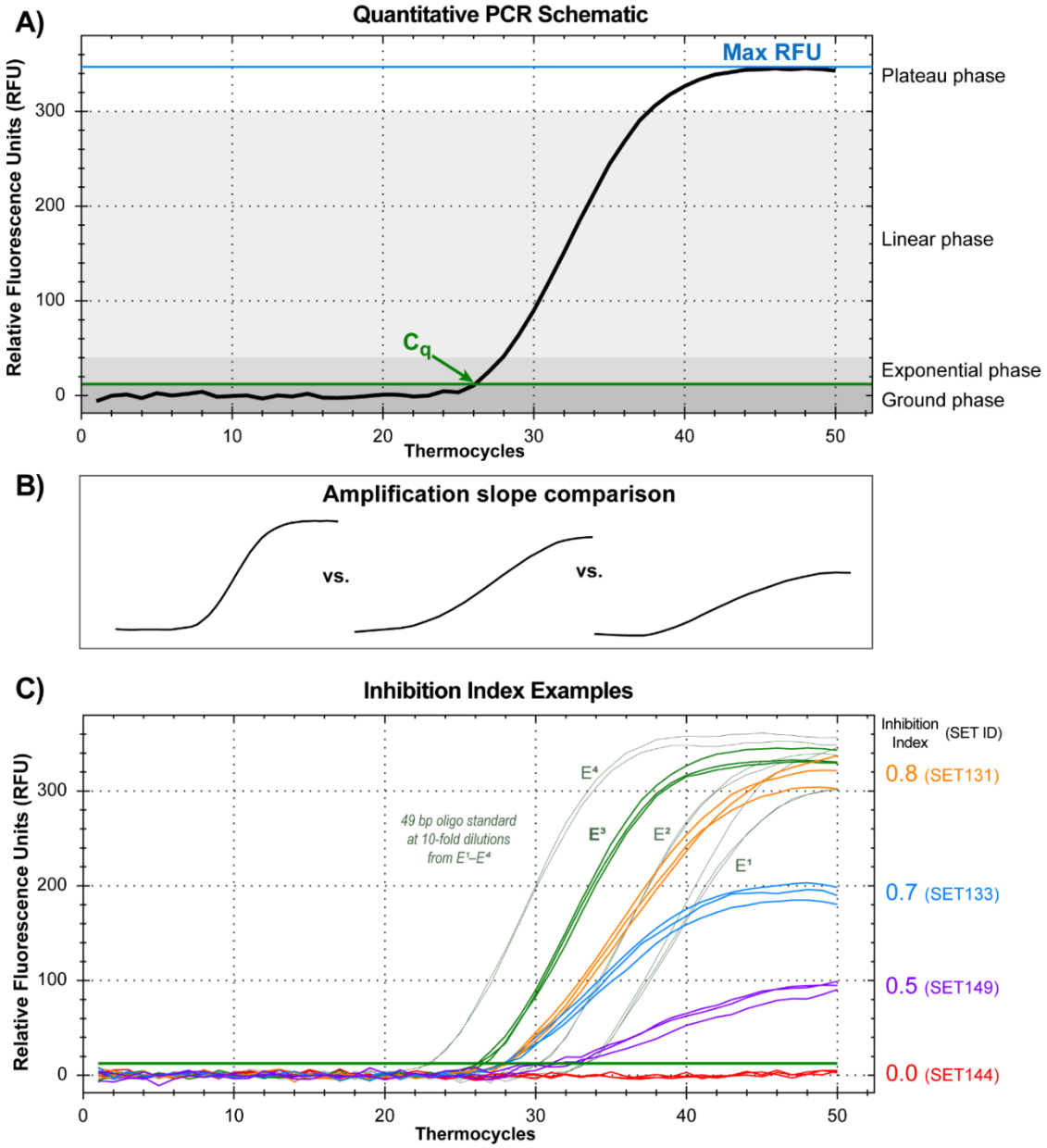

Fig. 3.6 Components of the inhibition index.
A) A standard qPCR reaction showing C_q and max RFU. **B)** A comparison of various amplification slopes from a typical reaction (left), towards increasingly inhibited reactions (right). **C)** Example inhibition indices derived from averaging the C_q, max RFU, and by fitting a variable-slope sigmoidal dose-response curve to the raw fluorescence data (using GraphPad Prism v. 7.04) based on King et al.(2009) for each PCR replicate by sample against the spiked E^3 standard. Inhibition index values <0.5 tend to occur when individual PCR replicates fail in a triplicate series; blanks and standard serial dilutions E^2 and E^1 tend to have inhibition indices >0.9 despite their 10- and 100-fold reduction in starting DNA causing a 3 or 6 cycle C_q shift. QPCR standard curve: E = 94.2%, R^2 = 0.997, slope = −3.469. See Table 3.7 for PCR assay specifications.

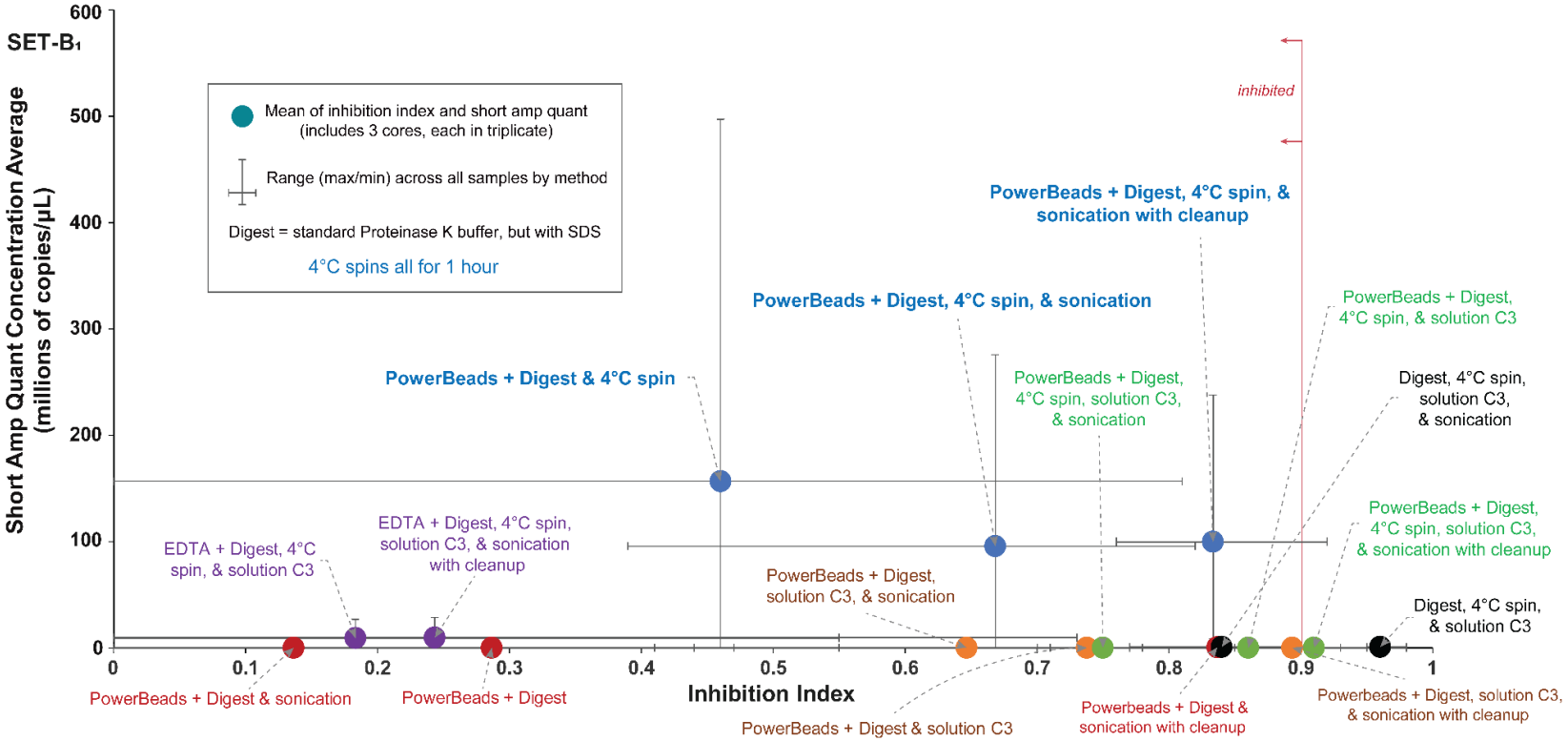

Fig. 3.7 SET-B, comparing treatments for enzymatic inhibitor removal by their DNA retention.

Details for the short amp DNA quantification can be found in Table 3.8. See Table 3.7 and Fig. 3.6 for details on the inhibition index. See Table 3.13 for SET-B sample list. Short amp qPCR standard curves for plates 1 and 2 respectively: E = 103.8% and 92.4%, R^2= 0.999 and 0.995, slope = −3.234 and −3.519.

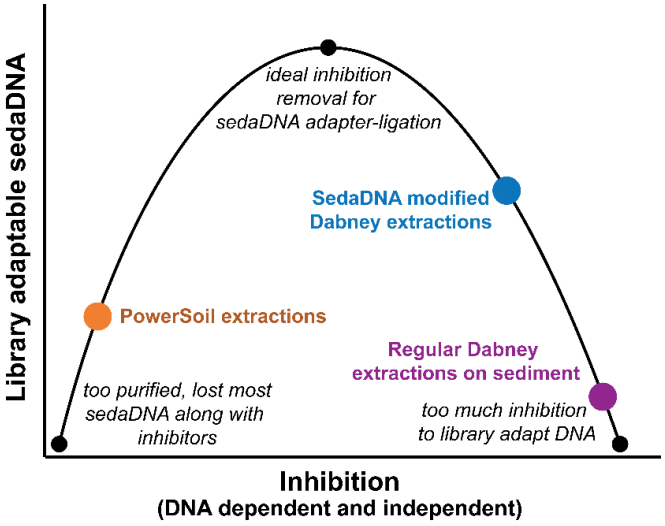

Fig. 3.8 Conceptual balance of overcoming sedaDNA inhibitor co-elution.

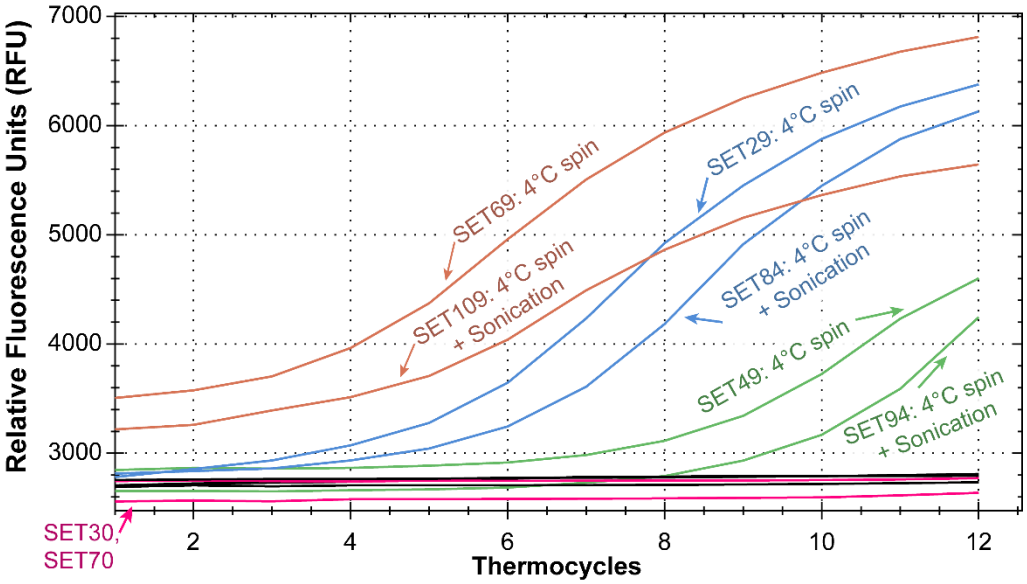

SET-B1

SET ID	Core	PowerBeads	PowerSoil Solution	1 hour 4°C Spin	Sonication	Post-Sonication Purification
SET69	BC 4-2B	Y	-	Y	-	-
SET109	BC 4-2B	Y	-	Y	Y	-
SET29	LLII 12-84-3	Y	-	Y	-	-
SET84	LLII 12-84-3	Y	-	Y	Y	-
SET49	LLII 12-217-8	Y	-	Y	-	-
SET94	LLII 12-217-8	Y	-	Y	Y	-
SET30	LLII 12-84-3	Y	Y	-	-	-
SET70	BC 4-2B	Y	Y	-	-	-

Fig. 3.9 SET-B, qPCR indexing reaction to confirm correlation with short amp quantification. See Table 3.6 for indexing qPCR specifications. See Table 3.13 for SET-B sample list.

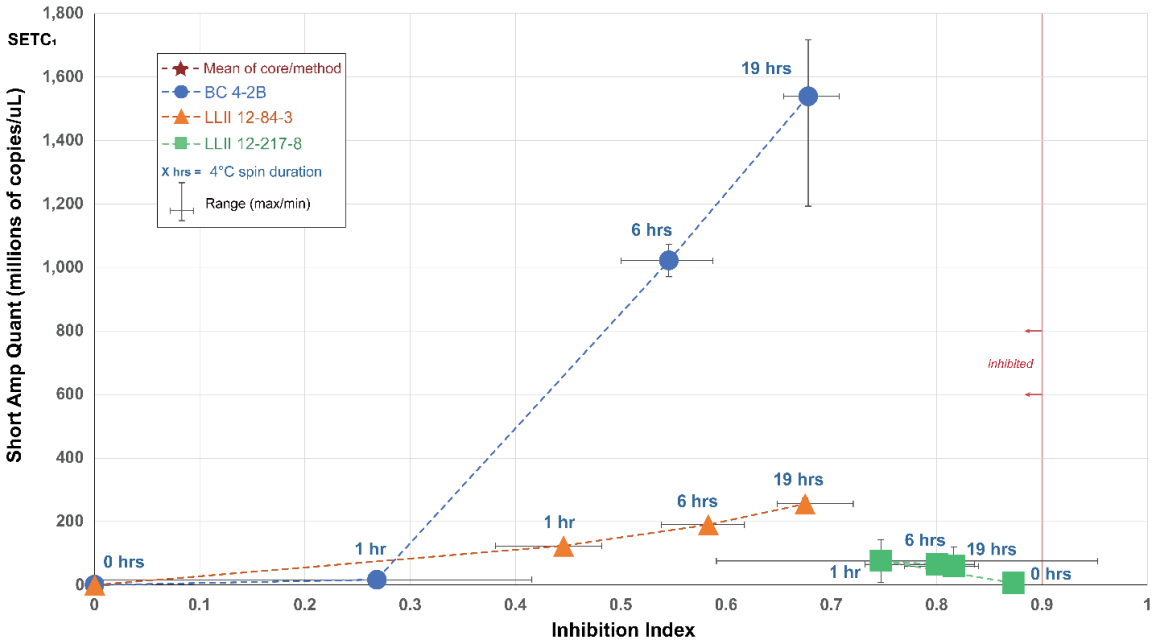

Fig. 3.10 Variable duration 4°C centrifuge on the carryover of enzymatic inhibitors and library adapted DNA, SET-C.

Short amp qPCR standard curve: E = 100.7%, R^2= 0.998, slope = −3.306. See Table 3.15 for sample list.

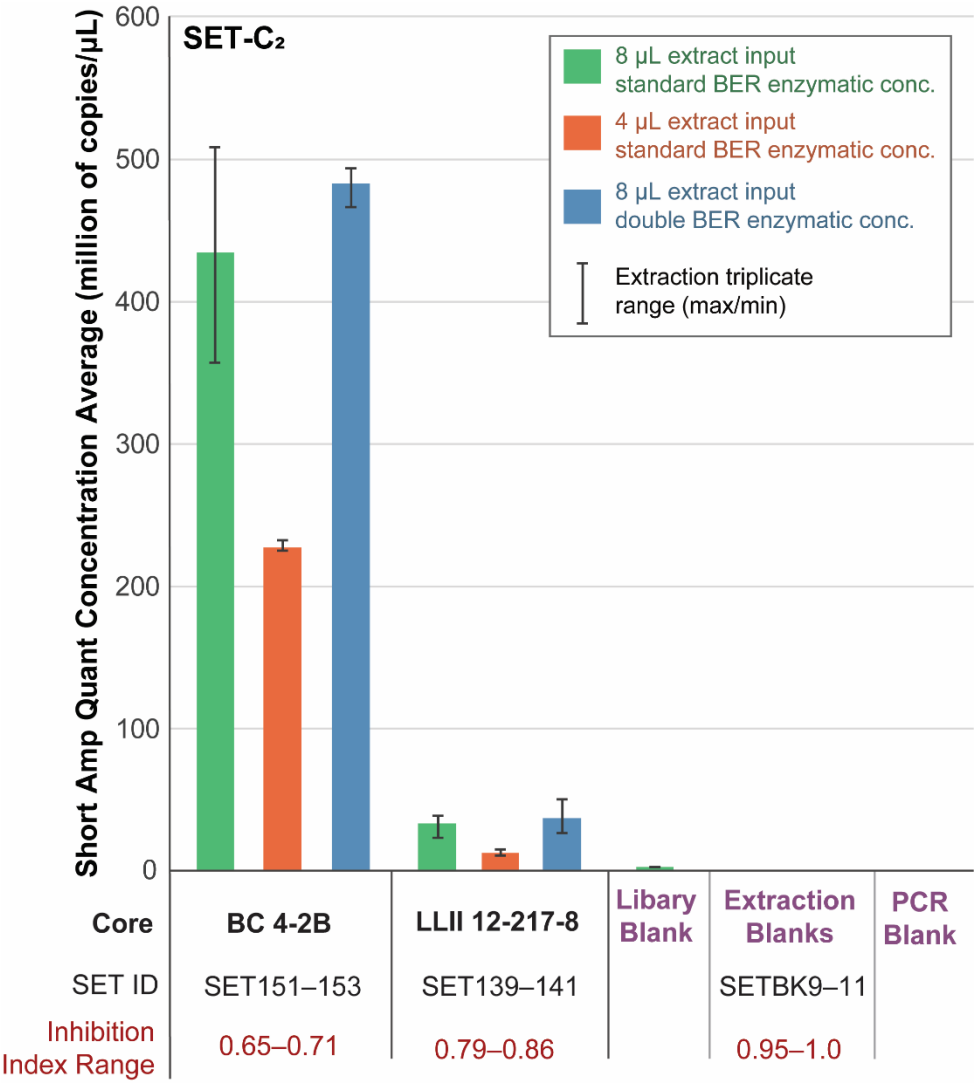

Fig. 3.11 Total double stranded DNA with variable extract input and blunt-end repair (BER) enzymatic concentrations, SET-C.
BER enzymatic conc. = blunt-end repair enzymatic concentrations.
PCR triplicate used to determine DNA concentration average per SET sample. Extraction triplicate used to determine mean and range of DNA concentration average by method and core. Short amp qPCR standard curve: E = 100.3%, R^2= 0.992, slope = −3.314. An inhibition index < 0.9 is considered inhibited (to some degree).

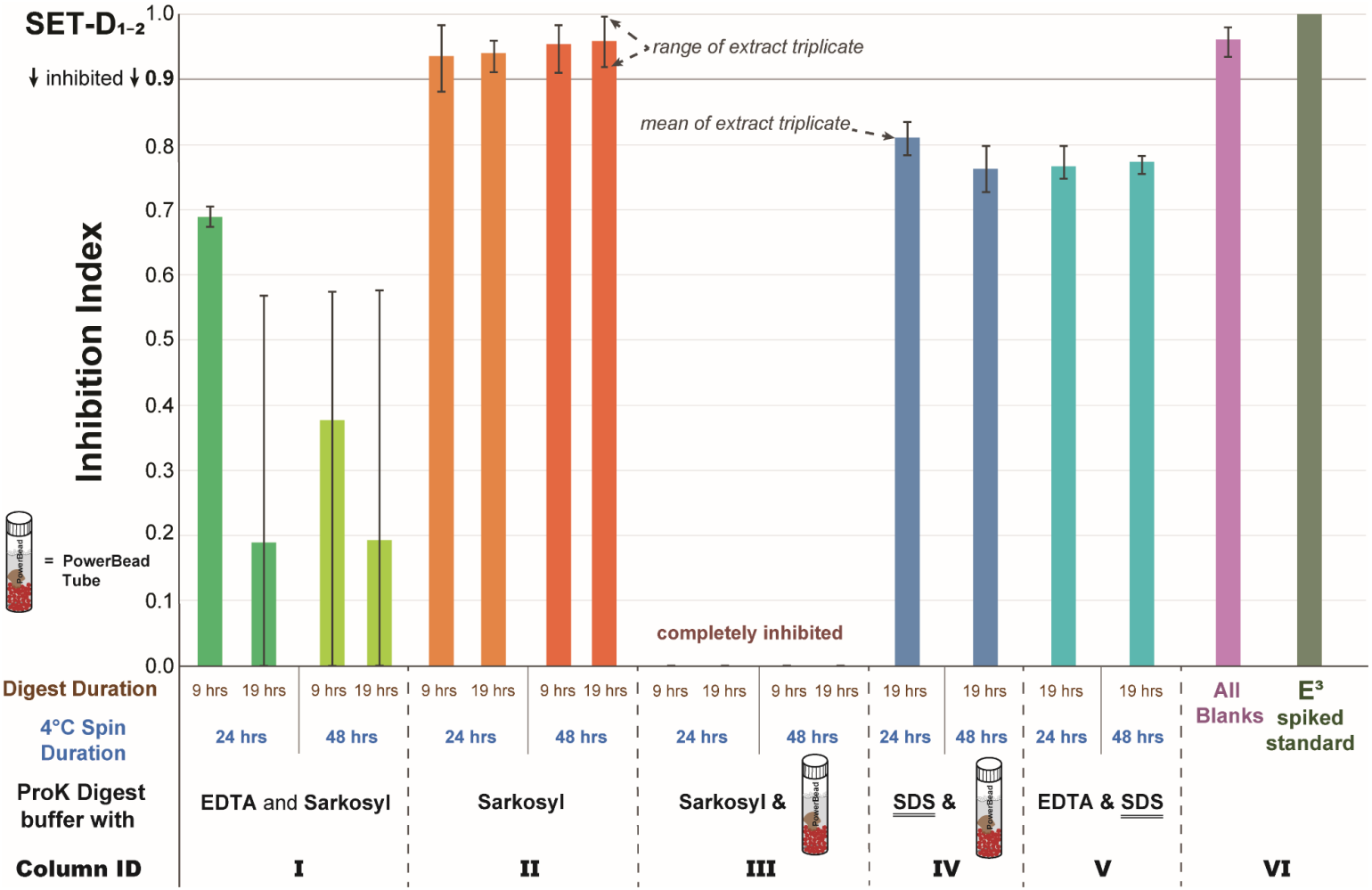

Fig. 3.12 SET-D, core BC 4-2B, variation in co-eluate inhibitor retention by lysing method and inhibitor removal procedure. PCR triplicate used to determine inhibition index per SET sample. Extraction triplicate used to determine mean and range of inhibition indices by method and core. See Table 3.16 for sample list.

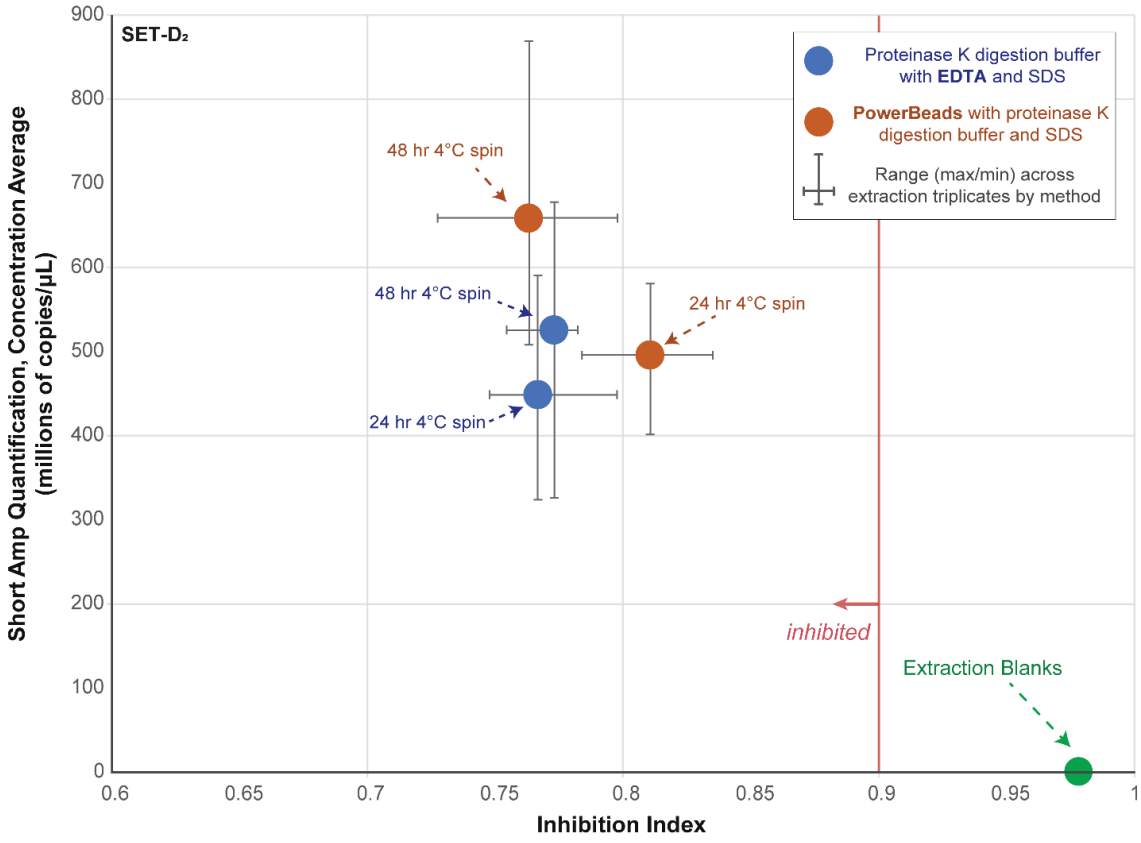

Fig. 3.13 SET-D Variable lysis disruption and cold spin duration for core BC 4-2B. Details for the short amp DNA quantification can be found in Table 3.8. See Table 3.7 and Fig. 3.6 for details on the inhibition index. See Table 3.16 for SET-D sample list. PCR triplicates used to determine average copies per µL per SET sample. Extraction triplicates used to determine mean and range of inhibition indices and short amp quantifications by method. Short amp qPCR standard curve: E = 100.5%, R^2= 0.998, slope = −3.310.

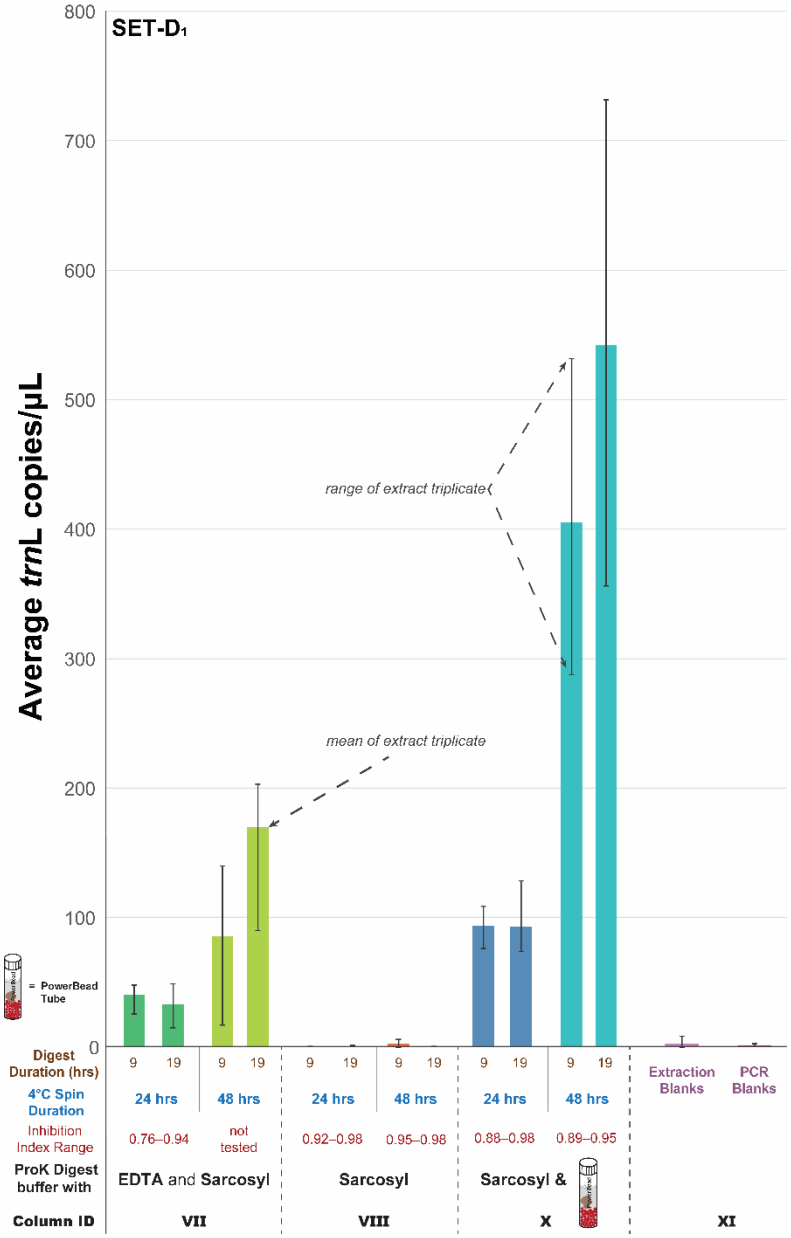

Fig. 3.14 Variable extract amplification of core LLII 12-217-8, *trn*L 'endogenous' qPCR.

This core sample had low inhibition in all experiments, regardless of the inhibition removal technique used. It was the only "uninhibited" sample in the SET-A positive control spike test (Fig. 3.5). The wide variation in DNA concentrations is due to non-standard PCR amplification curves. As such, *these values are unreliable indicators of actual DNA concentration in the extracts*. This data was included despite being unreliable because it shows that column VIII has no amplifiable DNA and no inhibition, ruling it out as a potential lysis option (as related to column II in Fig. 3.12). PCR triplicates used to determine average *trn*L copies per µL per SET sample. Extraction triplicate used to determine mean and range of inhibition indices by method. See Table 3.16 for sample list. QPCR standard curves for plates 1 and 2 respectively: E = 97.5% and 101.1%, R^2= 0.983 and 0.985, slope = −3.373 and −3.296. Column IDs correlated with Fig. 3.11 and Fig. 3.15.

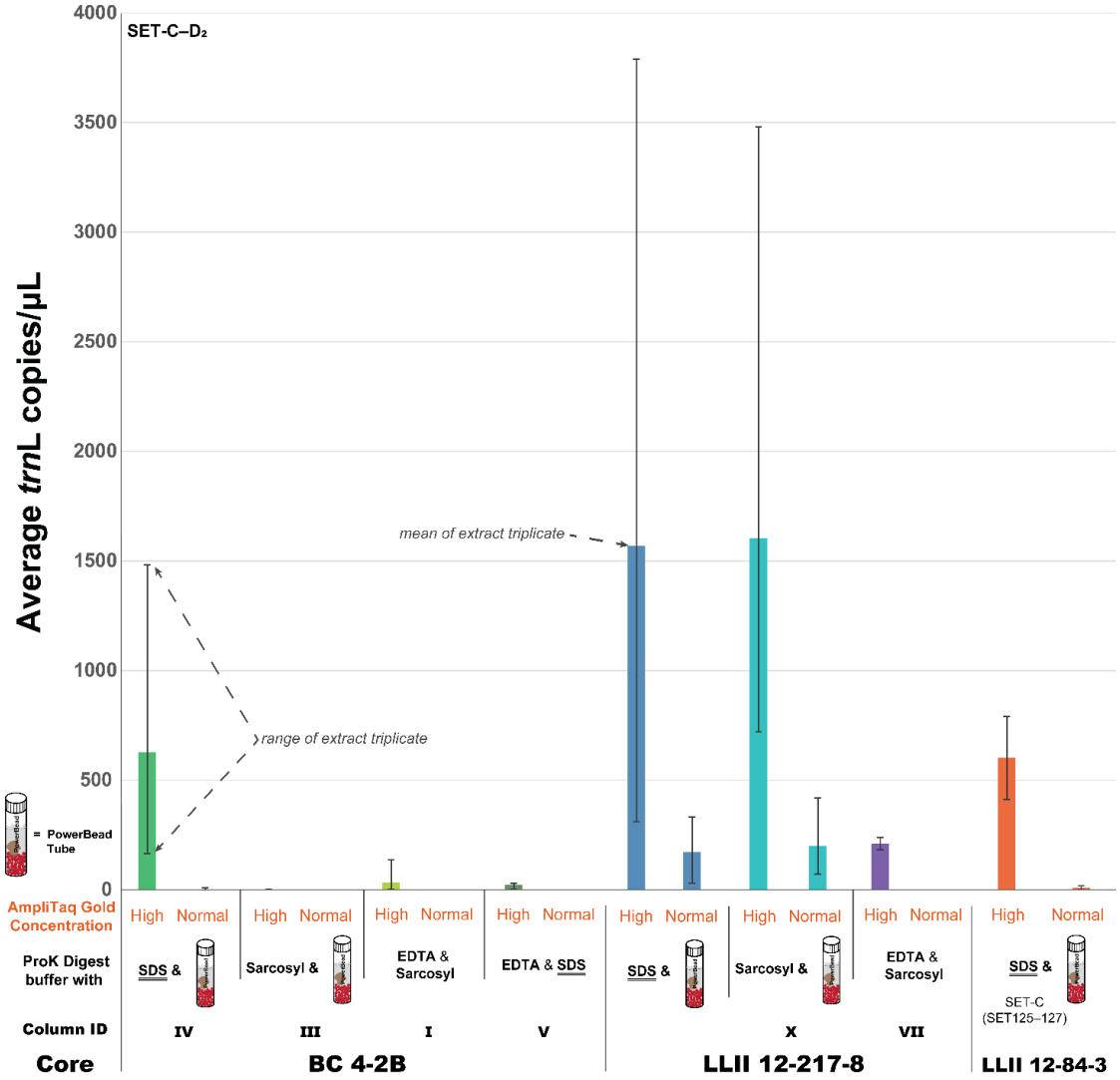

Fig. 3.15 Variable AmpliTaq Gold concentrations on *trn*L 'endogenous' sedaDNA qPCR amplifications.

The wide variation in DNA concentration is due to non-standard PCR amplification curves. As such, *these values are unreliable indicators of actual DNA concentration in the extracts.* This data was included despite being unreliable because it shows that there is some sort of inhibition affecting these extracts, even for the core with low levels of inhibition (LLII 12-217-8, e.g. Fig. 3.5). PCR triplicates used to determine average *trn*L copies per µL per SET sample. Extraction triplicate used to determine mean and range of inhibition indices by method. QPCR standard curve: E = 103.8%, R^2= 0.983 and 0.992, slope = −3.234. Column IDs correlated with Fig. 3.12 and Fig. 3.14.

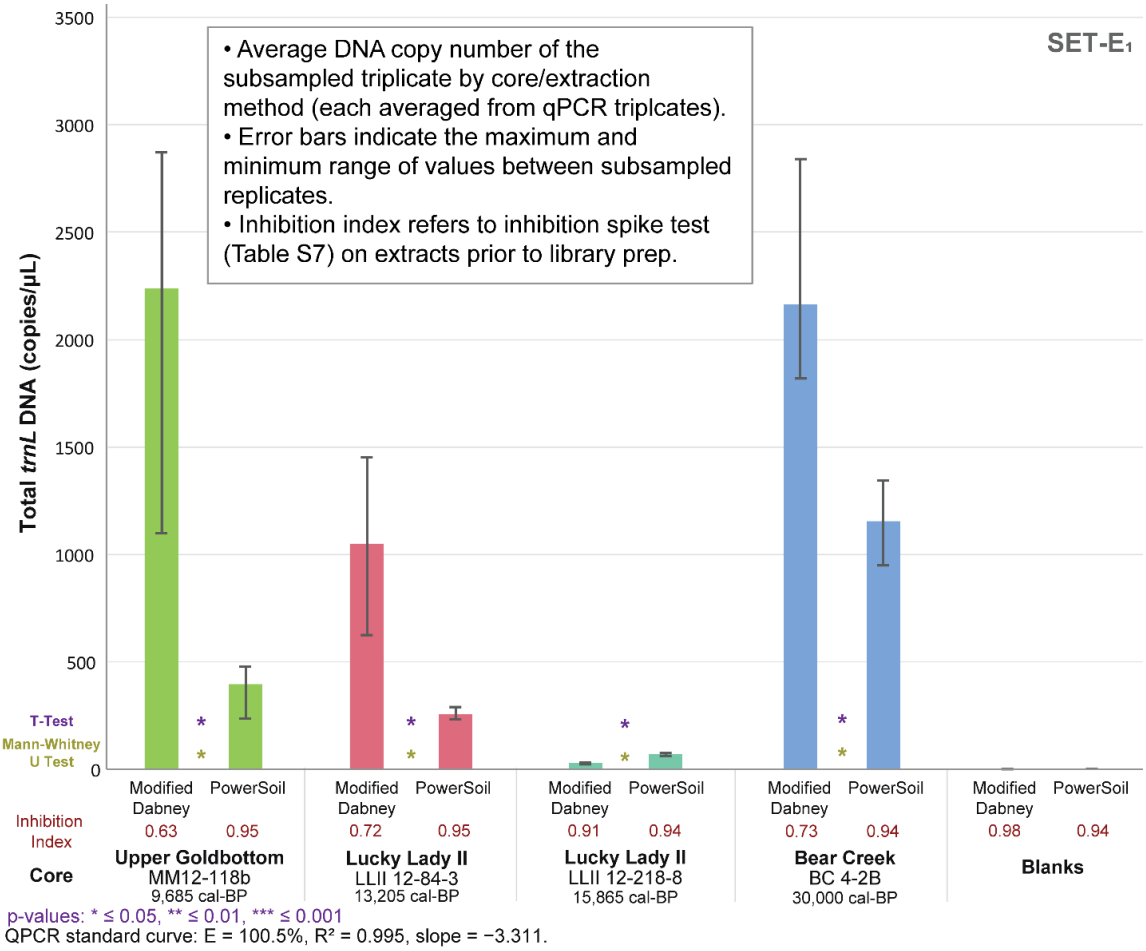

Fig. 3.16 DNA quantification of *trn*L specific library adapted molecules comparing both extraction methods by core (see Table 3.9 for qPCR specifications). Core LLII 12-217-8 consistently has low DNA recovery, but also a low co-elution of DNA independent inhibition.

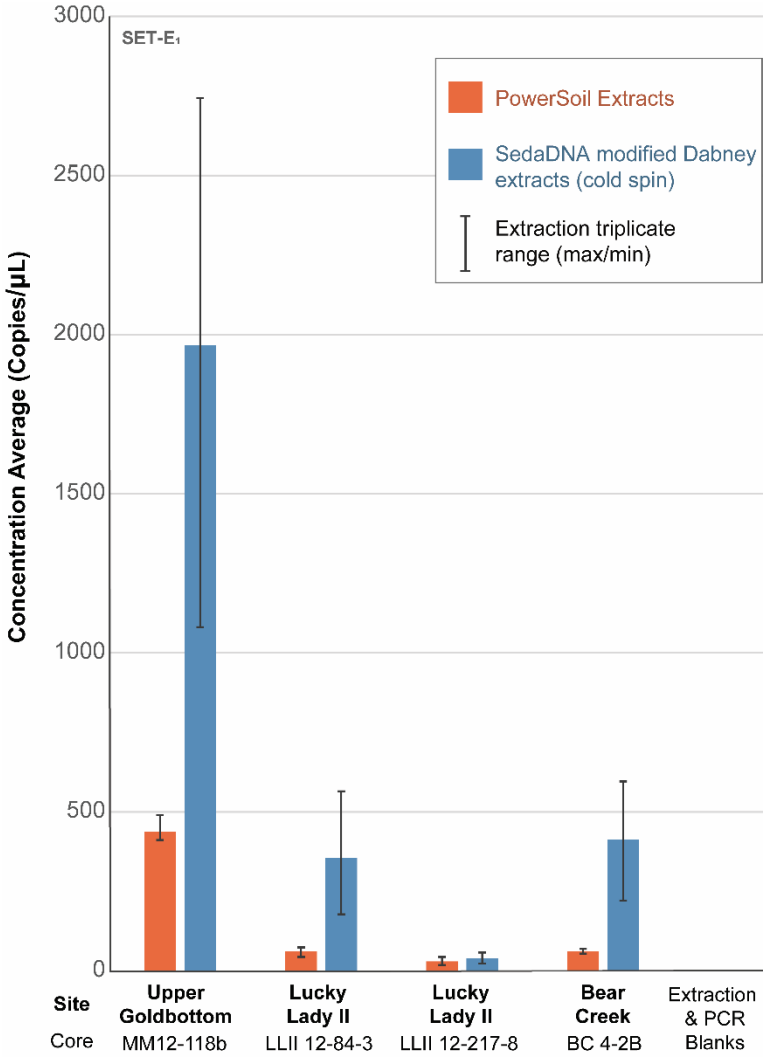

Fig. 3.17 QPCR estimated starting concentration averages by extraction type and site for *trn*L metabarcoded extracts. QPCR standard curve: E = 97.6%, R^2 = 0.998, slope = −3.381.

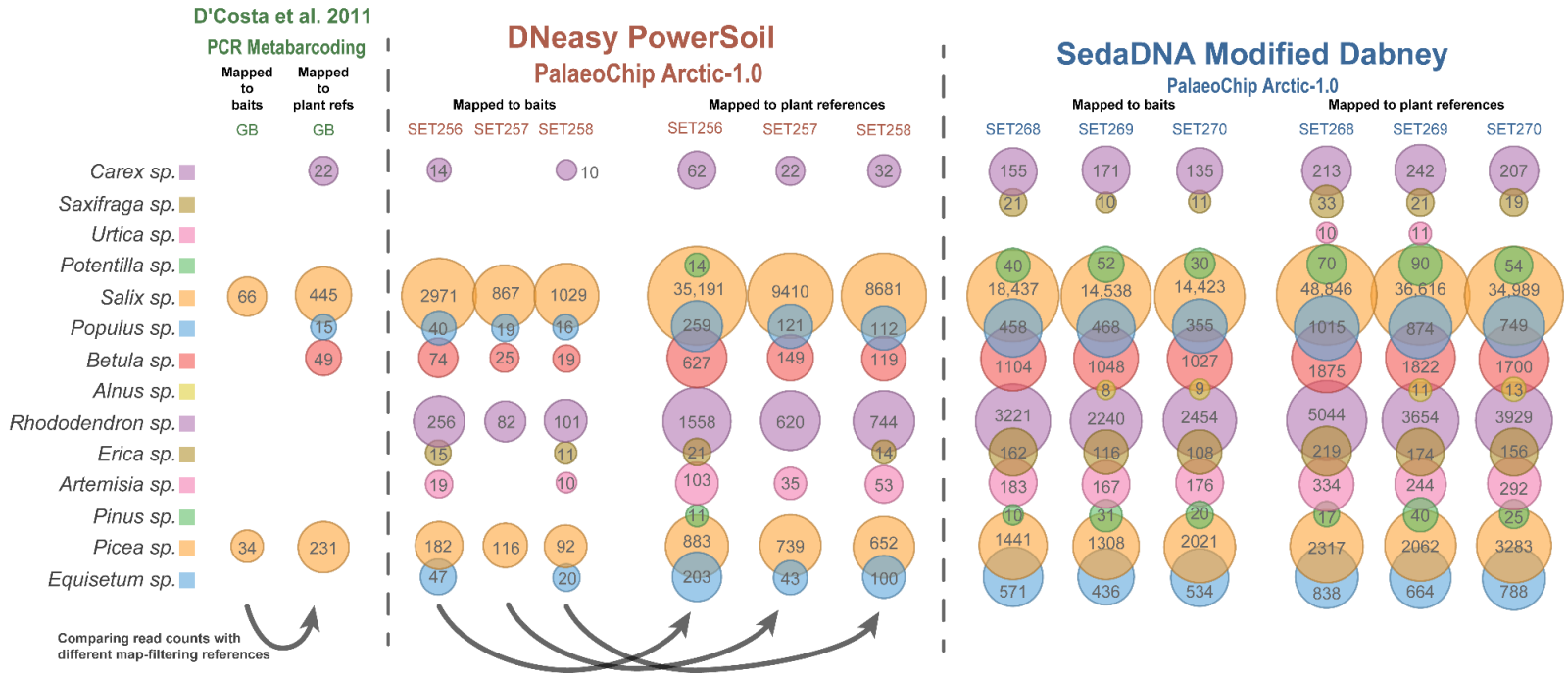

Fig. 3.18 Comparing LCA-assignments between Upper Goldbottom (MM12-118b) libraries map-filtered to the plant and animal baits, and those map-filtered to the plant references. The baits are more conservative for map-filtering, but also might be more biased against metabarcoding reads that do not map well against tiled baits. This can be seen in the first two columns where some taxa are absent from the bait map-filtered variants (SET-E).

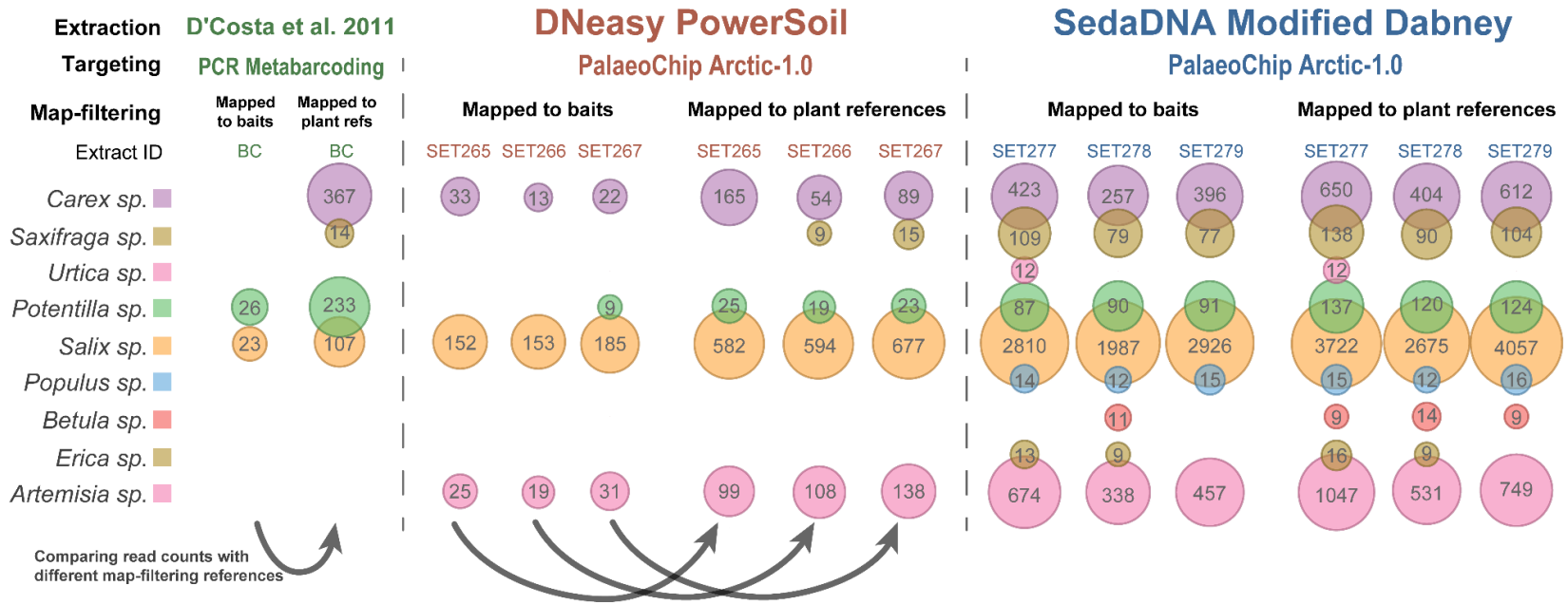

Fig. 3.19 Comparing LCA-assignments between Bear Creek (BC 4-2B) libraries map-filtered to the plant and animal baits, and those map-filtered to the plant references. The baits are more conservative for map-filtering, but also might be more biased against metabarcoding reads that do not map well against tiled baits. This can be seen in the first two columns where some taxa are absent from the bait map-filtered variants (SET-E).

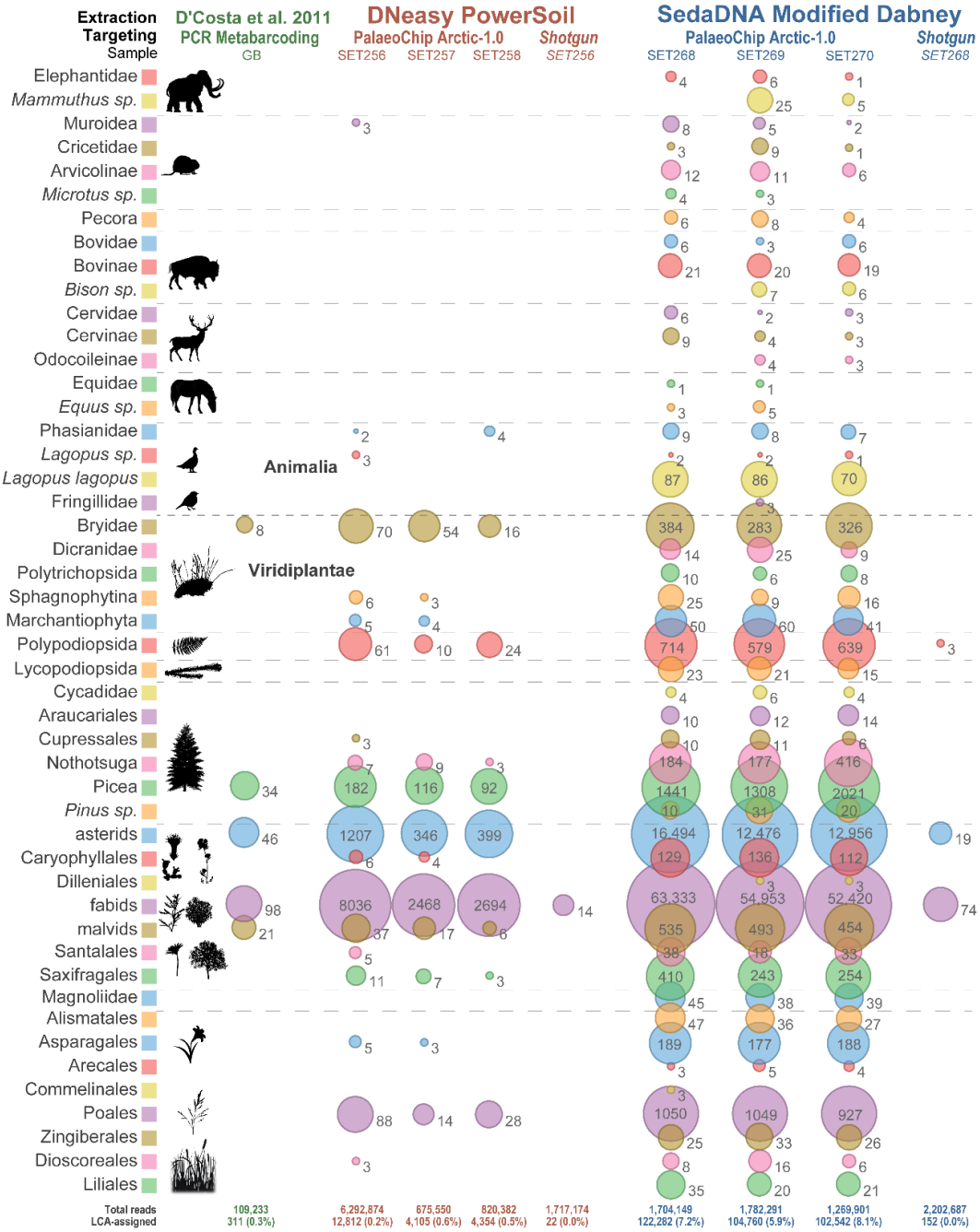

Fig. 3.20 Metagenomic comparison of Upper Goldbottom permafrost core MM12-118b. Reads mapped to animal and plant baits and compared with absolute counts and logarithmically scaled bubbles. Core slice dated to 9,685 cal yr BP (Sadoway, 2014; Mahony, 2015). Values indicate total reads assigned to that taxon node for Animalia, and a clade summation of reads for Viridiplantae. See Table 2.1 for read summaries (SET-E). Note: hits to Arecales, Zingiberales, and Diosoreales are likely false positives driven by uneven reference coverages within Commelinids.

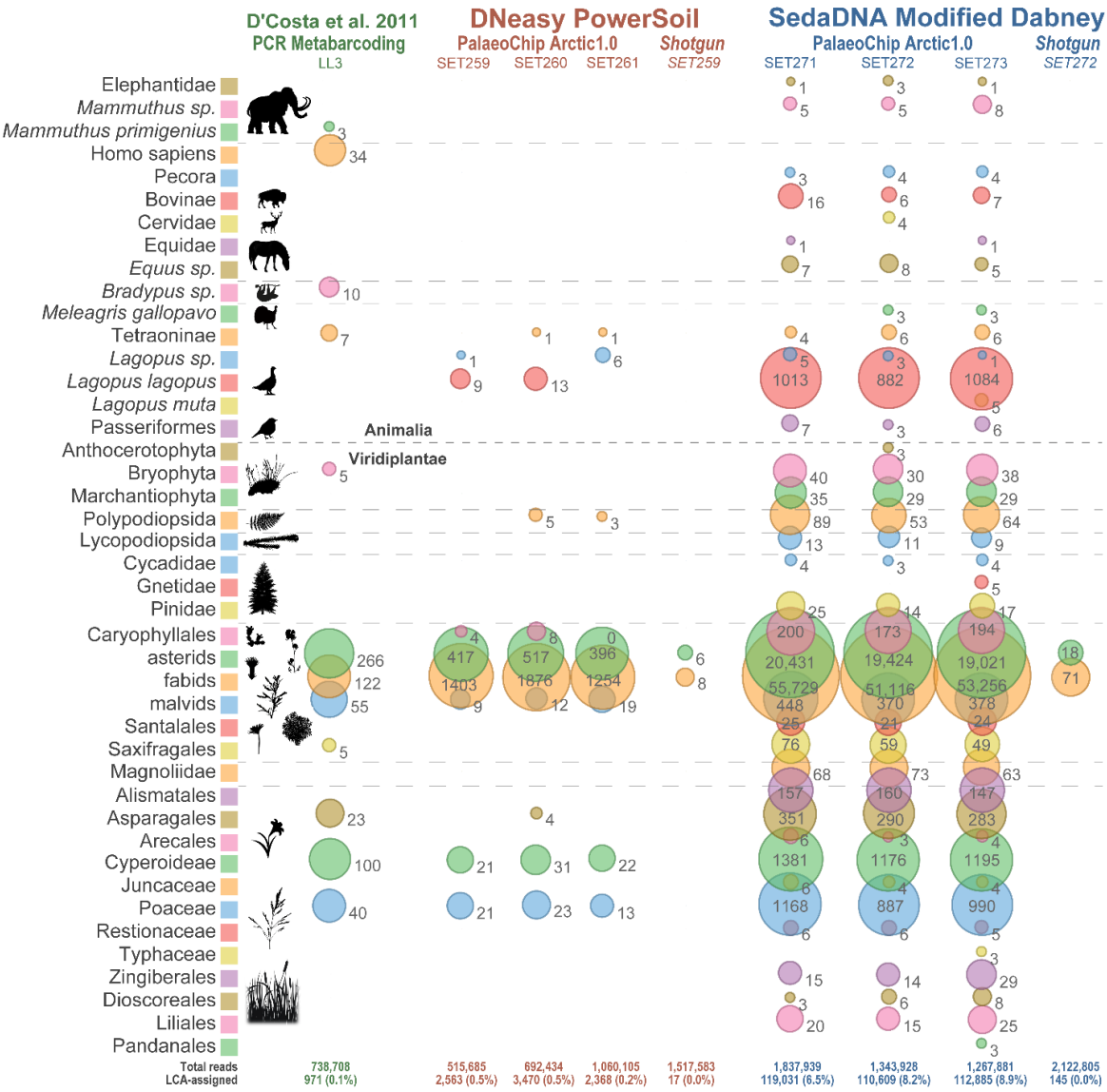

Fig. 3.21 Metagenomic comparison of Lucky Lady II permafrost core LLII-12-84-3, reads mapped to baits, logarithmically scaled bubbles. Core slice dated to 13,205 cal yr BP (Sadoway, 2014). Values indicate total reads assigned to that taxon node for Animalia, and a clade summation of reads for Viridiplantae. See Table 2.1 for read summaries (SET-E). Note: hits to Arecales, Zingiberales, and Diosoreales are likely false positives driven by uneven reference coverages within Commelinids.

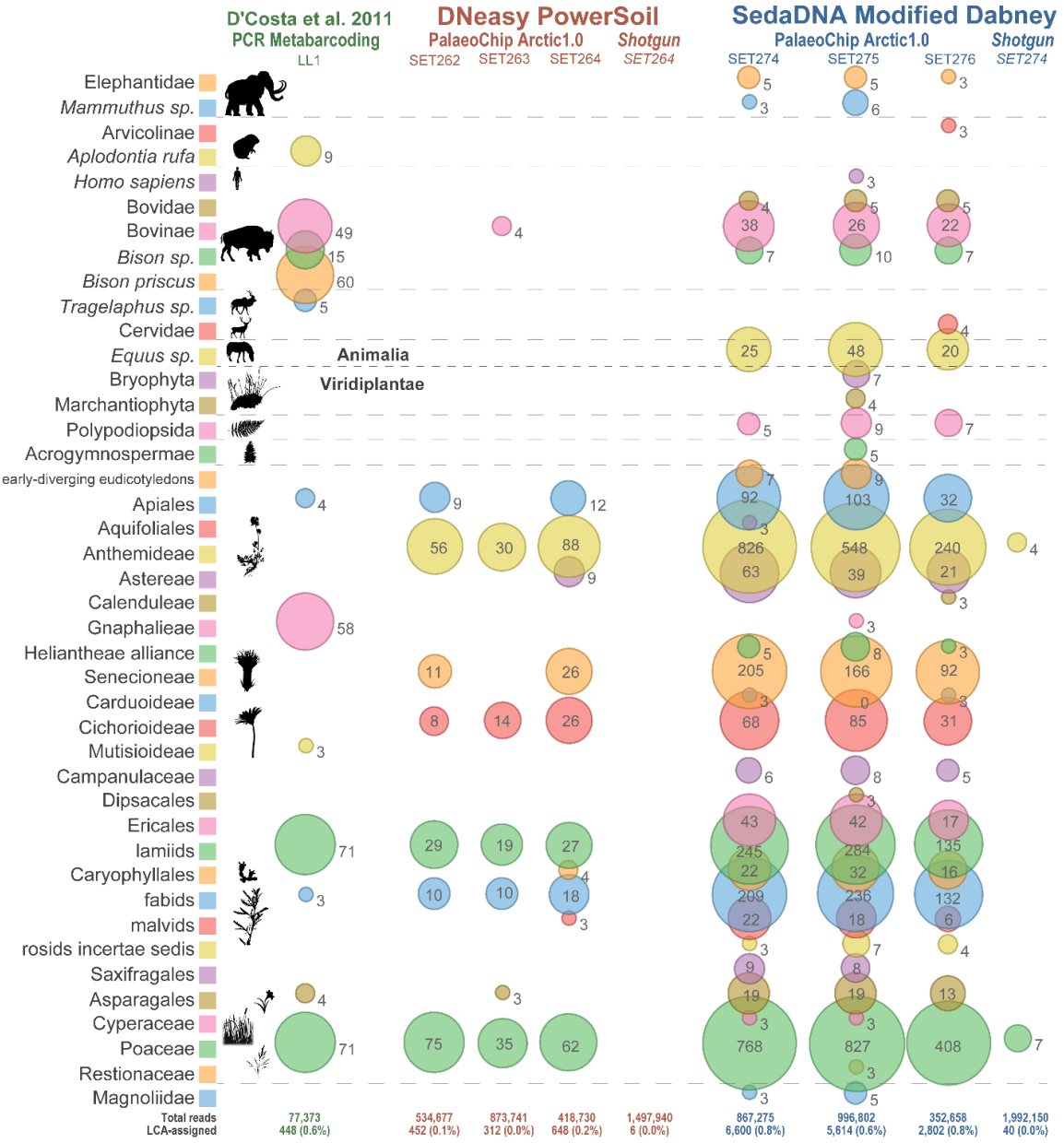

Fig. 3.22 Metagenomic comparison of Lucky Lady II permafrost core LLII-12-217-8, reads mapped to baits, logarithmically scaled bubbles. Core slice dated to 15,865 cal yr BP (Sadoway, 2014). Values indicate total reads assigned to that taxon node for Animalia, and a clade summation of reads for Viridiplantae. See Table 2.1 for read summaries (SET-E). Note: hits to Arecales, Zingiberales, and Diosoreales are likely false positives driven by uneven reference coverages within Commelinids.

.

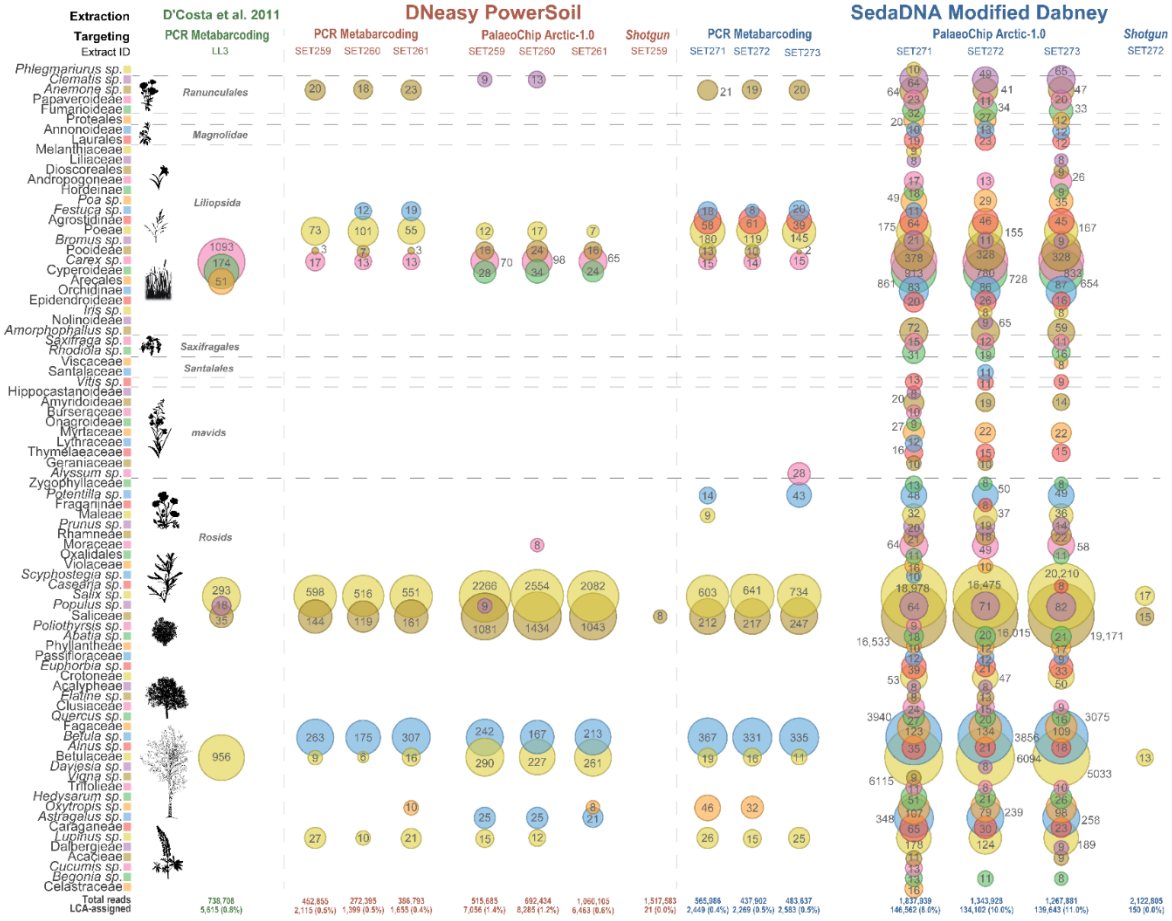

Fig. 3.23 Metagenomic comparison of Lucky Lady II permafrost core LLII-12-84-3 with reads mapped to plant references, 1 of 2. Compared with absolute counts and logarithmically scaled bubbles. Core slice dated to 13,205 cal yr BP (Sadoway, 2014). Values indicate total reads assigned to that taxon node (SET-E).

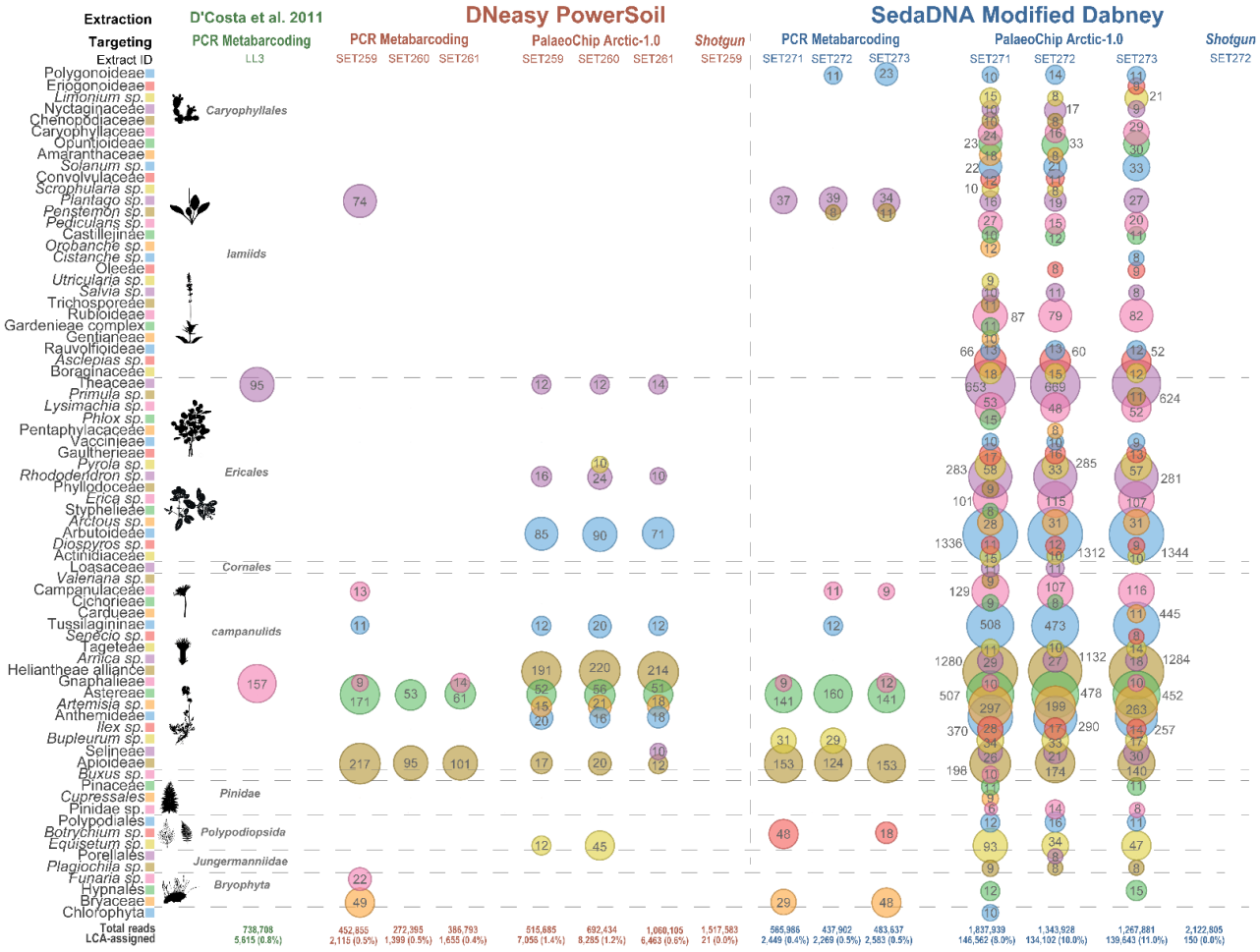

Fig. 3.24 Metagenomic comparison of Lucky Lady II permafrost core LLII-12-84-3 with reads mapped to plant references, 2 of 2. Compared with absolute counts and logarithmically scaled bubbles. Core slice dated to 13,205 cal yr BP (Sadoway, 2014). Values indicate total reads assigned to that taxon node (SET-E).

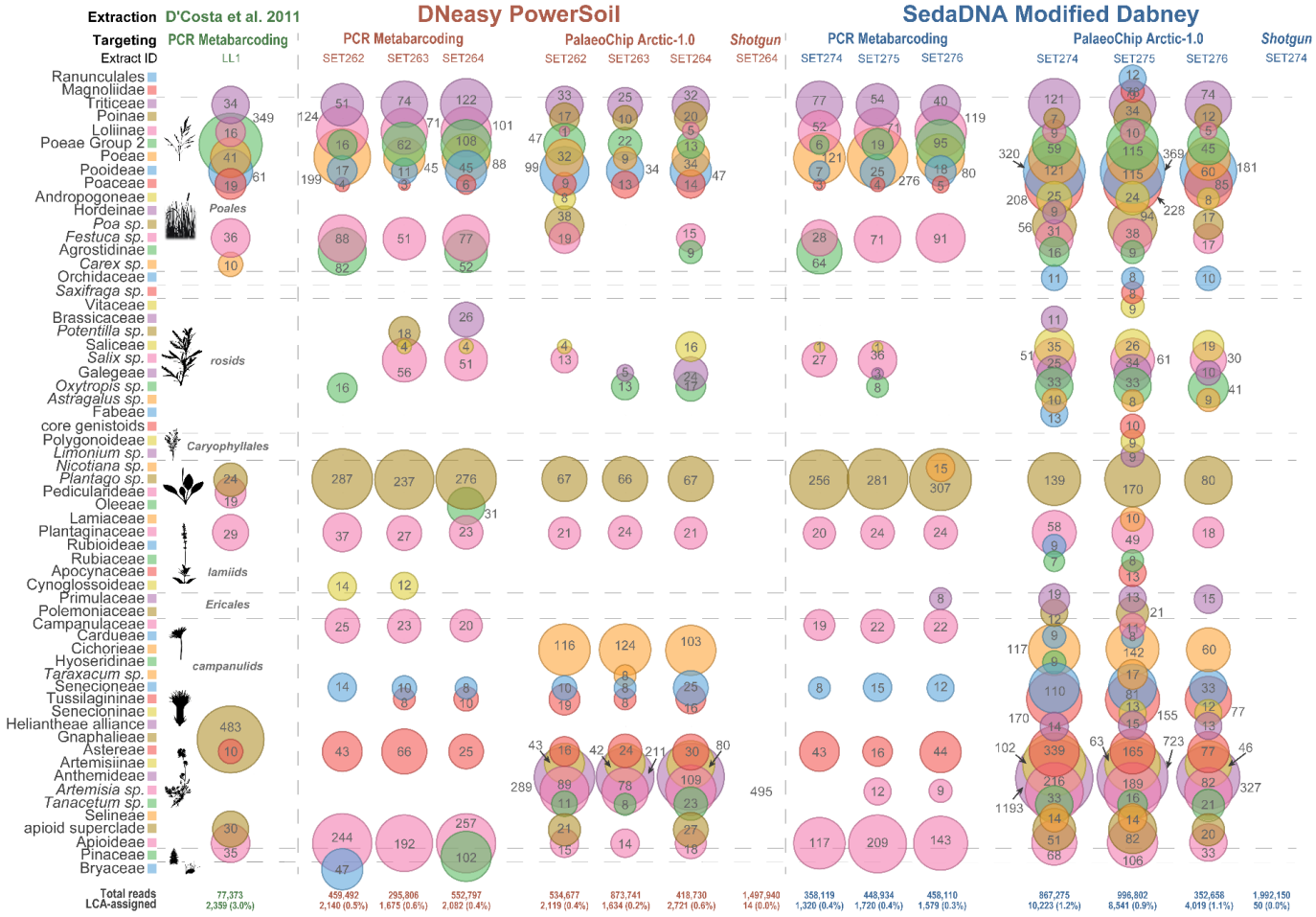

Fig. 3.25 Metagenomic comparison of Lucky Lady II permafrost core LLII-12-217-8 with reads mapped to plant references, 1 of 1. Compared with absolute counts and logarithmically scaled bubbles. Core slice dated to 15,865 cal yr BP (Sadoway, 2014). Values indicate total reads assigned to that taxon node (SET-E). Note: this is the routinely poorly performing core, which we believe contains and abundance of highly degraded DNA and minimal DNA independent inhibition.

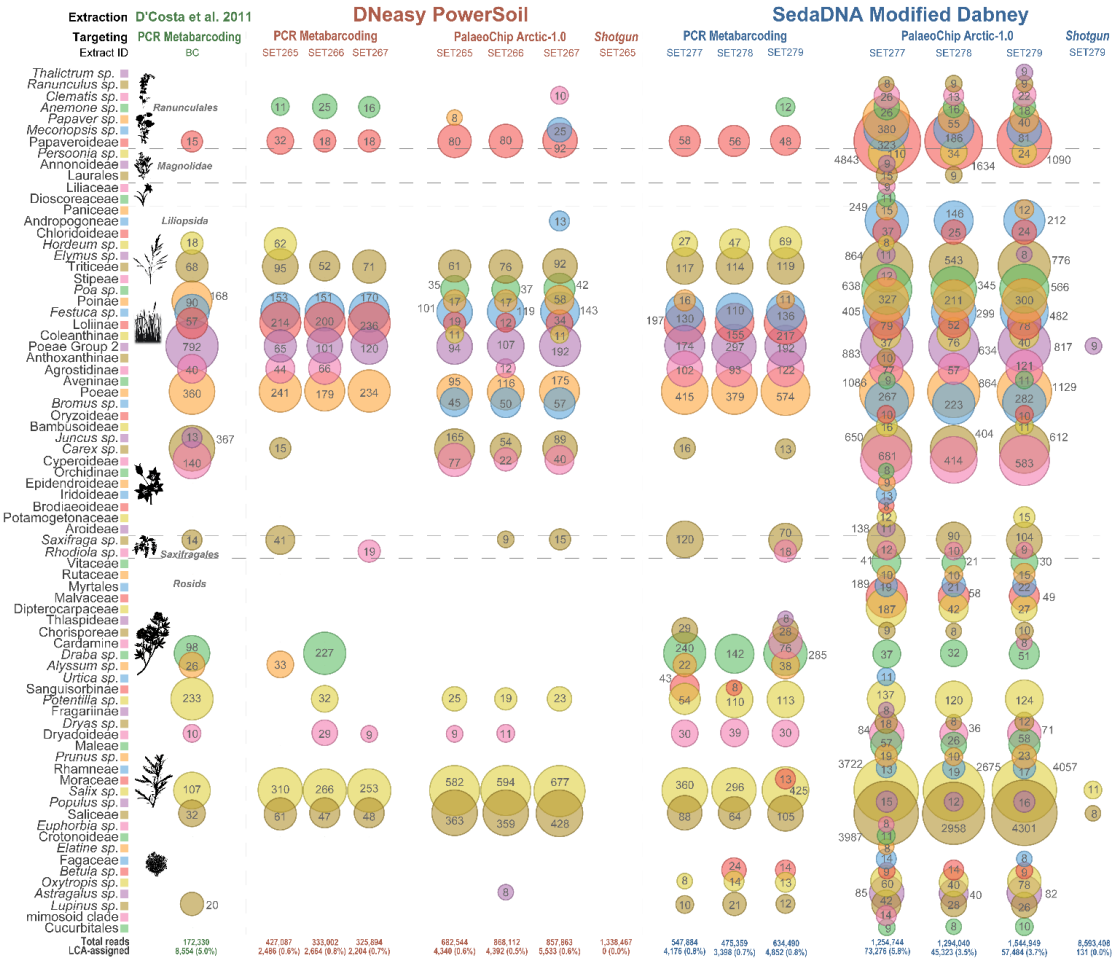

Fig. 3.26 Metagenomic comparison of Bear Creek permafrost core BC 4-2B with reads mapped to plant references, 1 of 2. Compared with absolute counts and logarithmically scaled bubbles. Core slice dated to ~30,000 cal yr BP (D'Costa et al., 2011; Sadoway, 2014; Mahony, 2015). Values indicate total reads assigned to that taxon node (SET-E).

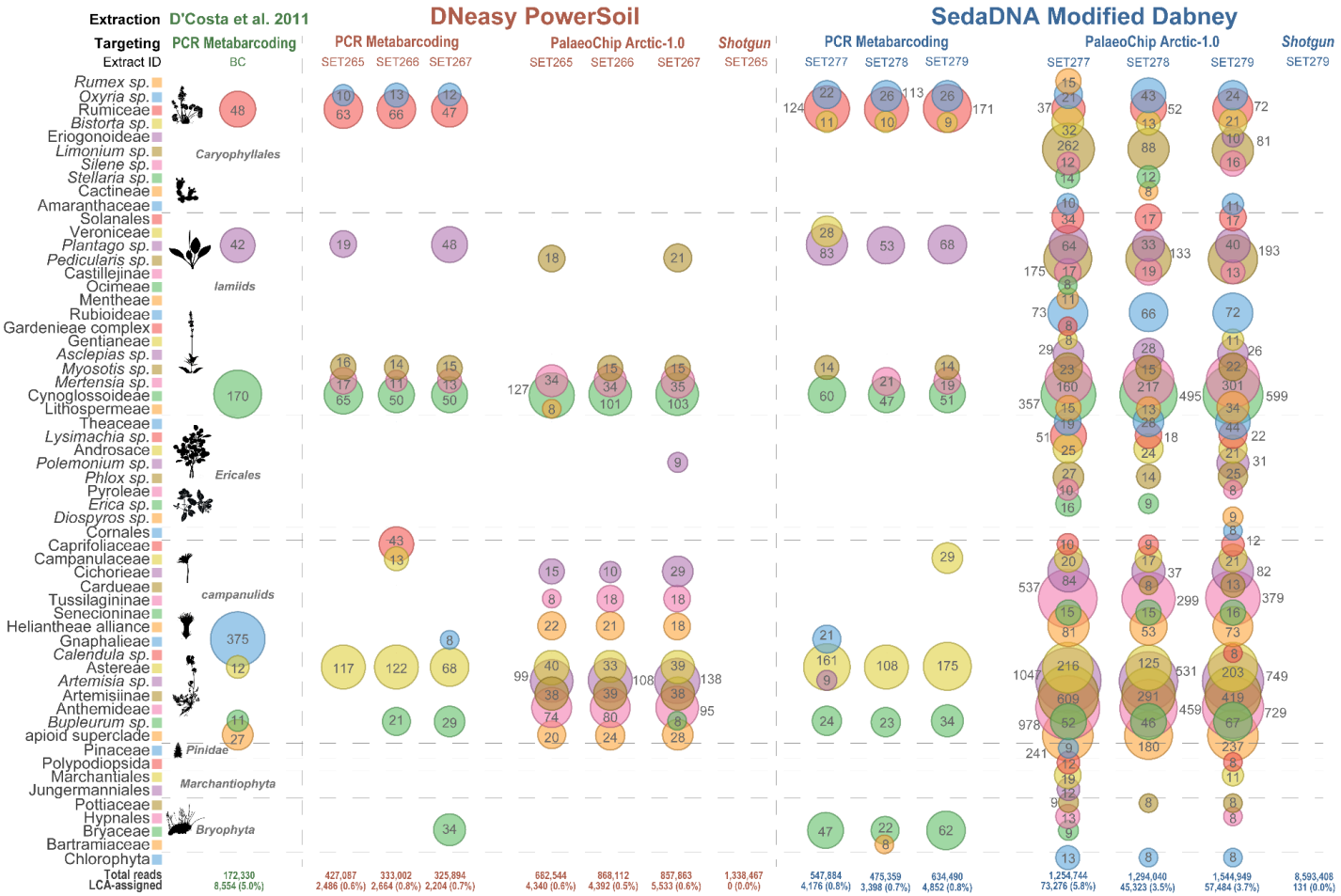

Fig. 3.27 Metagenomic comparison of Bear Creek permafrost core BC 4-2B with reads mapped to plant references, 2 of 2. Compared with absolute counts and logarithmically scaled bubbles. Core slice dated to ~30,000 cal yr BP (D'Costa et al., 2011; Sadoway, 2014; Mahony, 2015). Values indicate total reads assigned to that taxon node (SET-E).

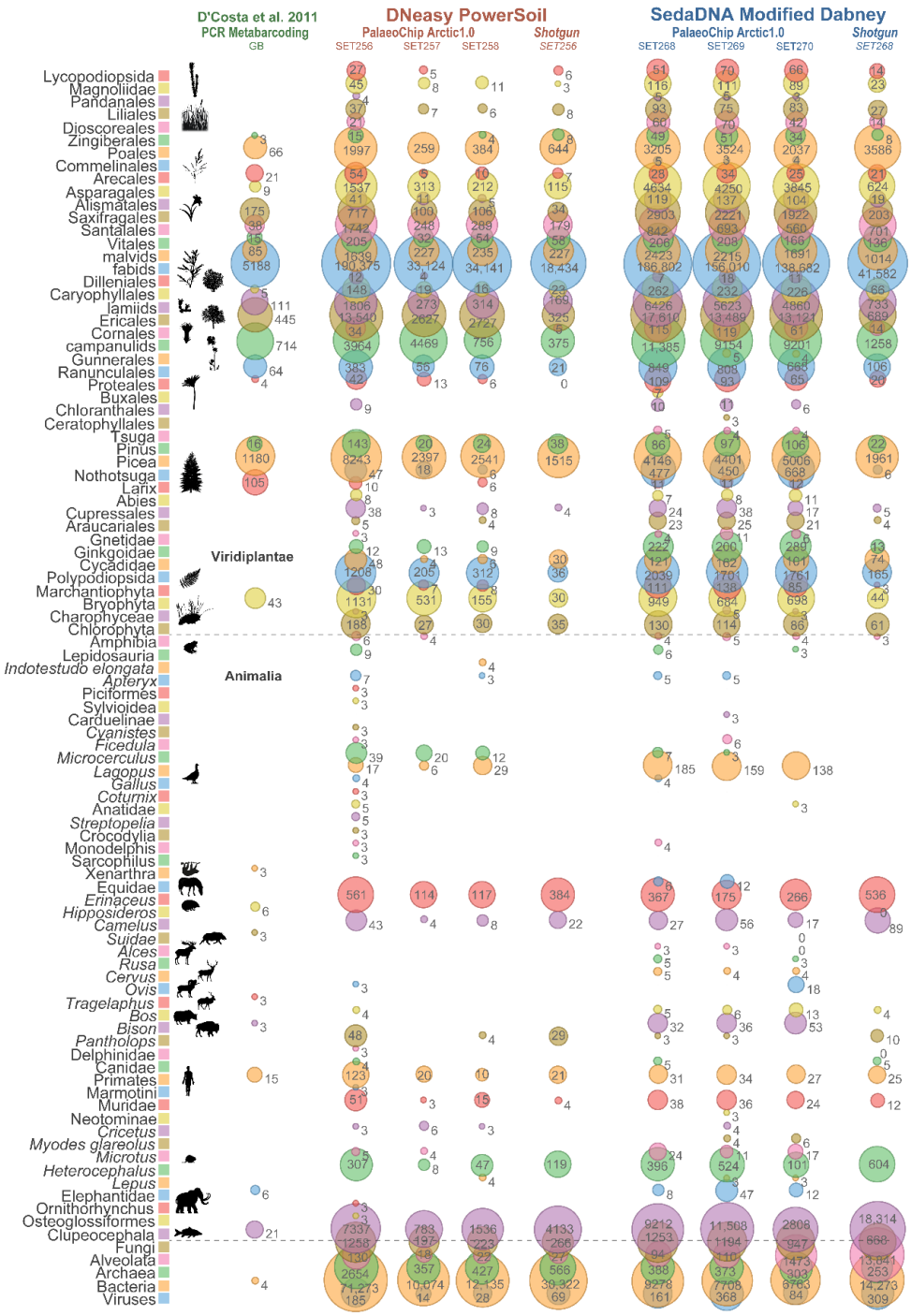

Fig. 3.28 Metagenomic comparison of Upper Goldbottom permafrost core MM12-118b, all reads (not map-filtered), absolute counts, bubbles log-scaled. Core slice dated to 9,685 cal yr BP (Sadoway, 2014; Mahony, 2015). Values indicate total reads assigned to that taxon node for Animalia, and a clade summation of reads for Viridiplantae (SET-E).

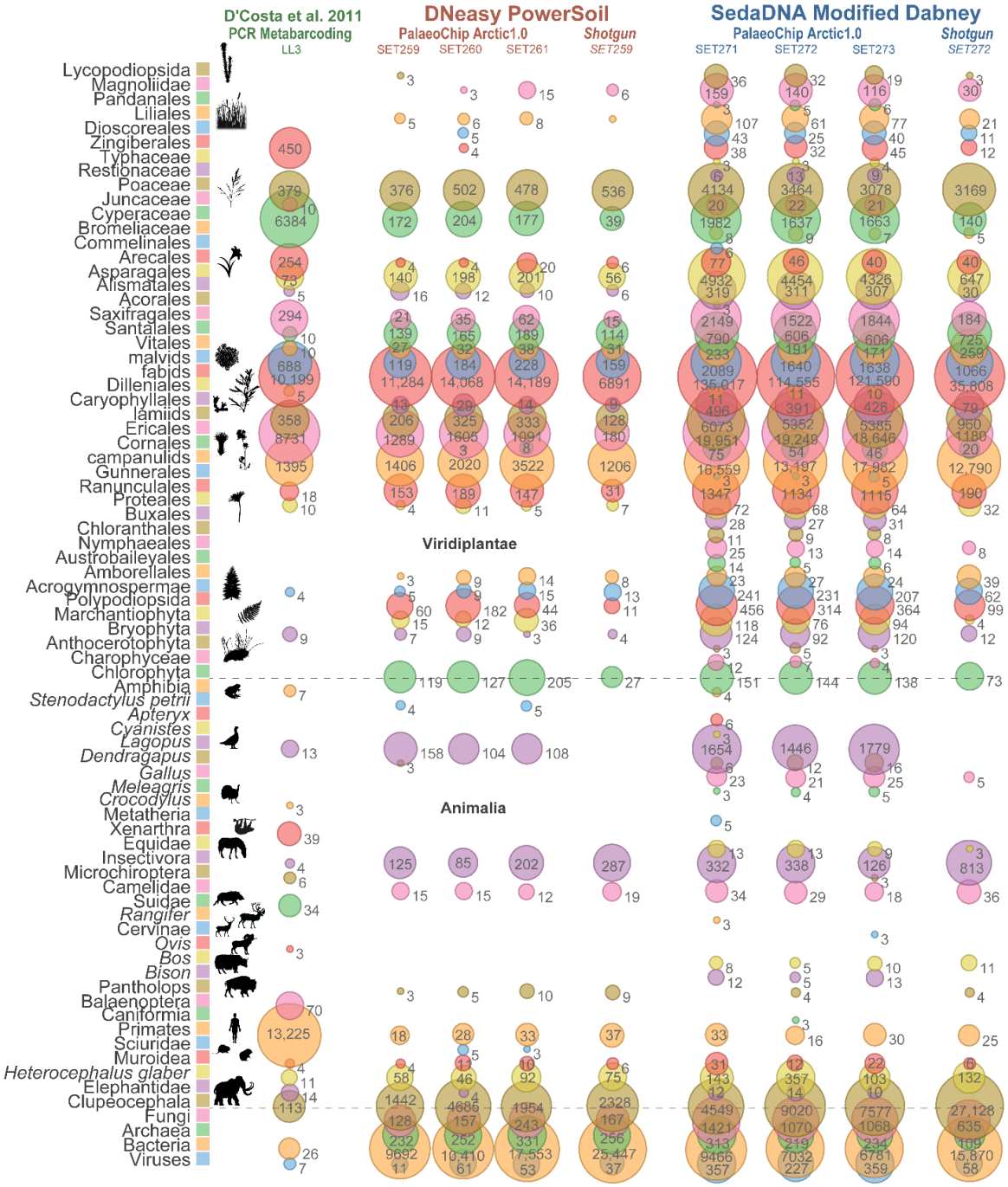

Fig. 3.29 Metagenomic comparison of Lucky Lady II permafrost core LLII-12-84-3, all reads (not map-filtered), absolute counts, bubbles log-scaled. Core slice dated to 13,205 cal yr BP (Sadoway, 2014). Values indicate total reads assigned to that taxon node for Animalia, and a clade summation of reads for Viridiplantae (SET-E).

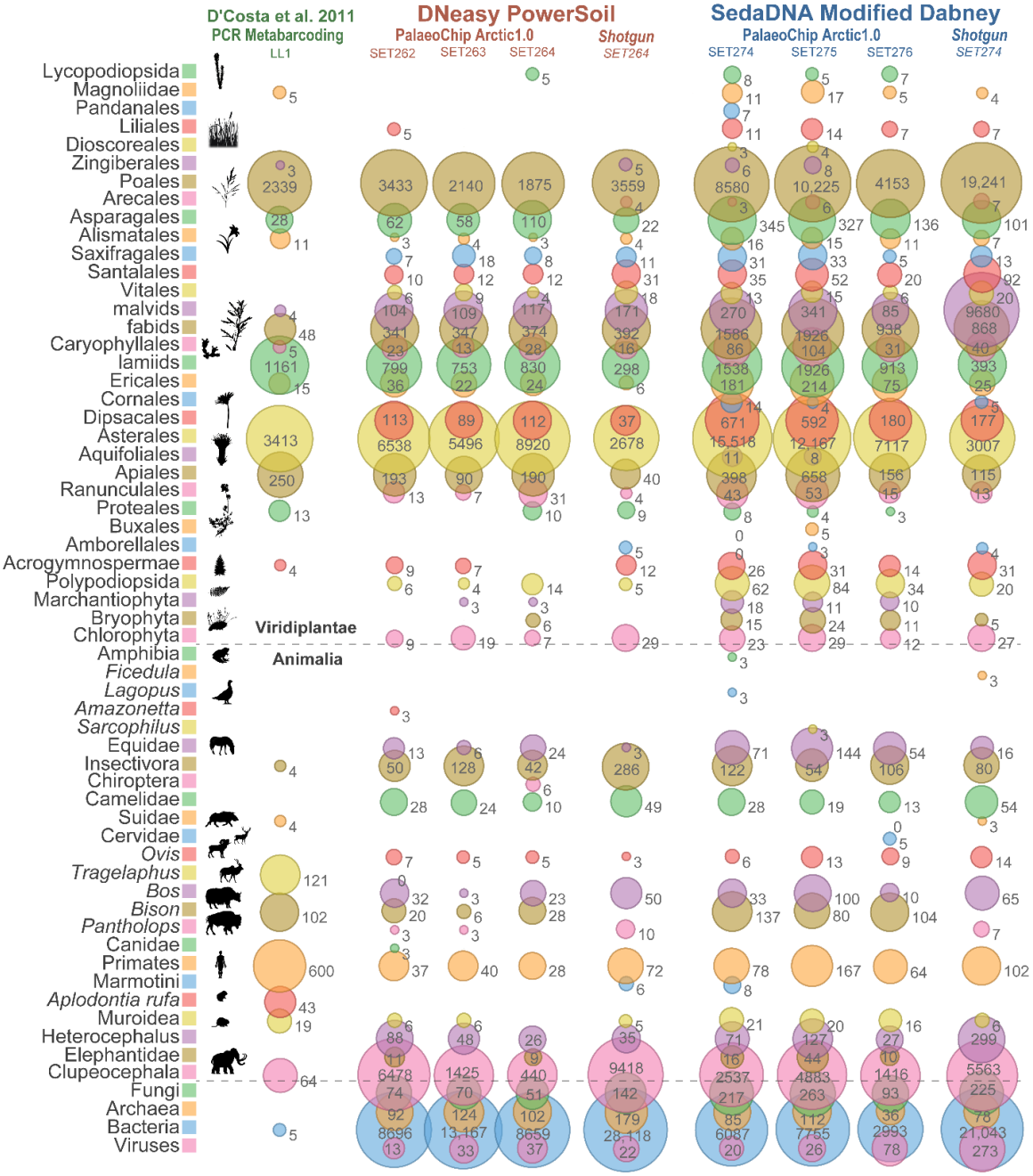

Fig. 3.30 Metagenomic comparison of Lucky Lady II permafrost core LLII-12-217-8, all reads (not map-filtered), absolute counts, bubbles log-scaled. Core slice dated to 15,865 cal yr BP (Sadoway, 2014). Values indicate total reads assigned to that taxon node for Animalia, and a clade summation of reads for Viridiplantae (SET-E).

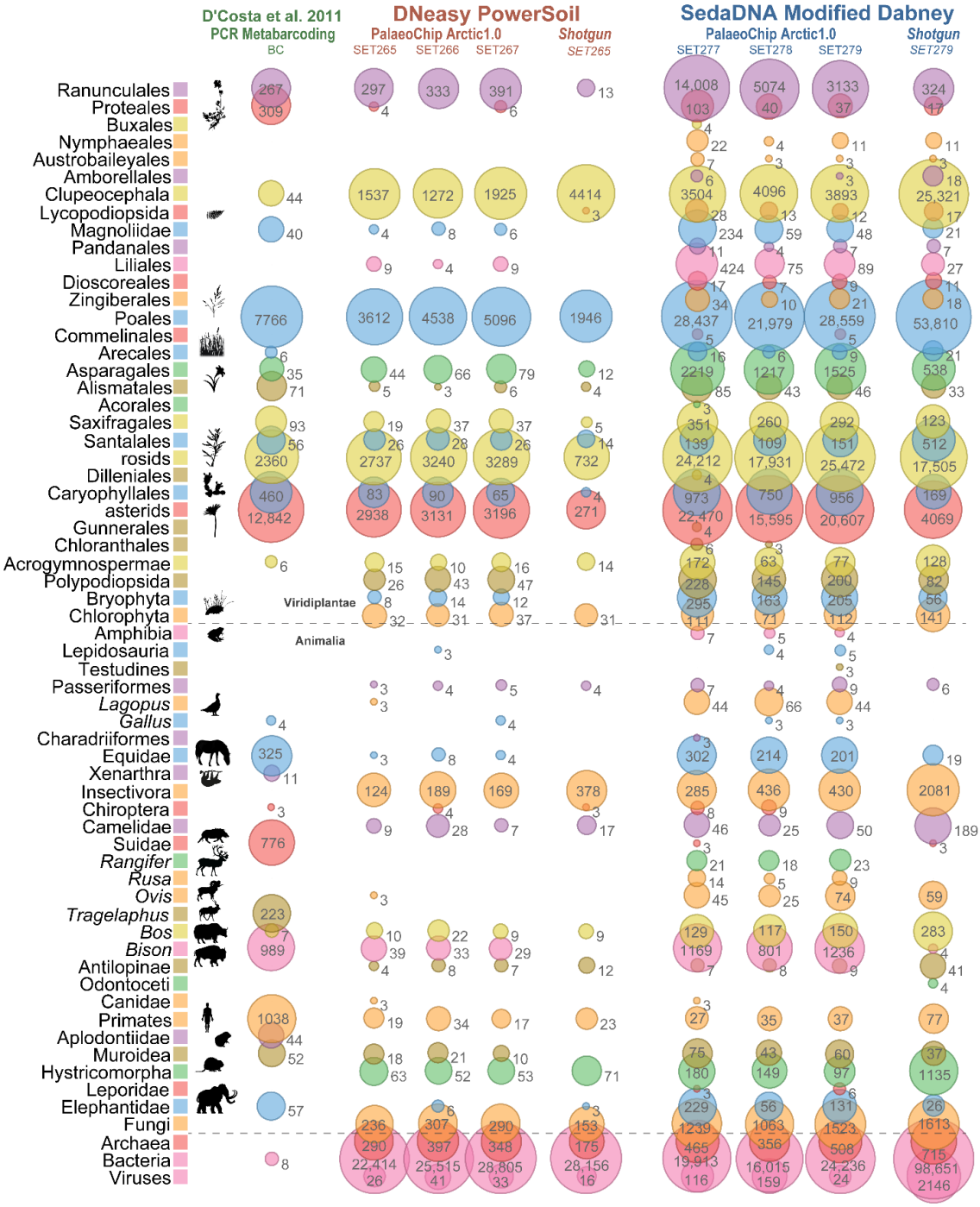

Fig. 3.31 Metagenomic comparison of Bear Creek permafrost core BC 4-2B, all reads (not map-filtered), absolute counts, bubbles log-scaled. Core slice dated to ~30,000 cal yr BP (D'Costa et al., 2011; Sadoway, 2014; Mahony, 2015). Values indicate total reads assigned to that taxon node for Animalia, and a clade summation of reads for Viridiplantae (SET-E).

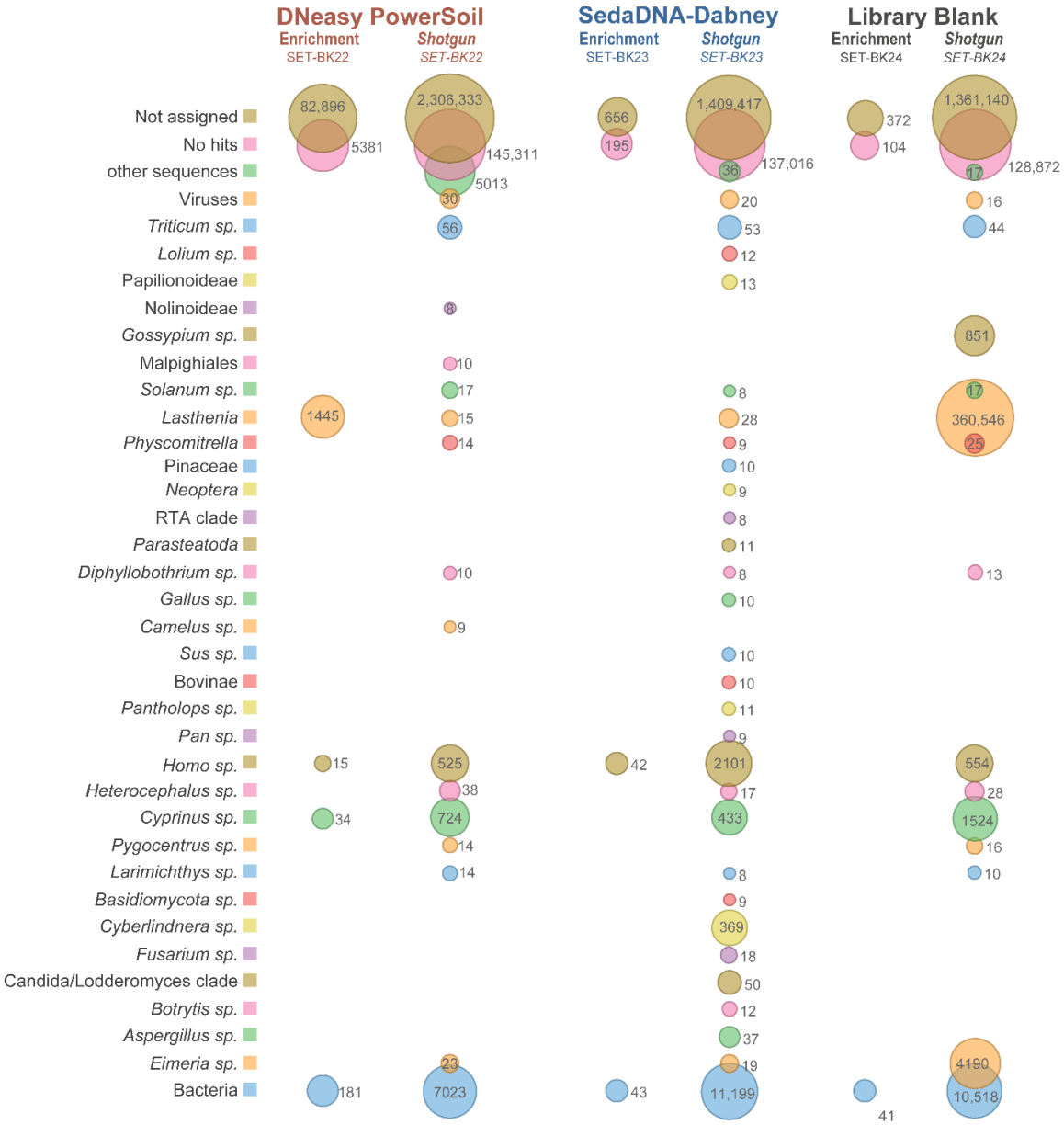

Fig. 3.32 Metagenomic comparison of extraction and library blanks, all reads (not map filtered), absolute counts, bubbles log-scaled. Values indicate total reads assigned to that taxon node; uncollapsed to genera (SET-E).

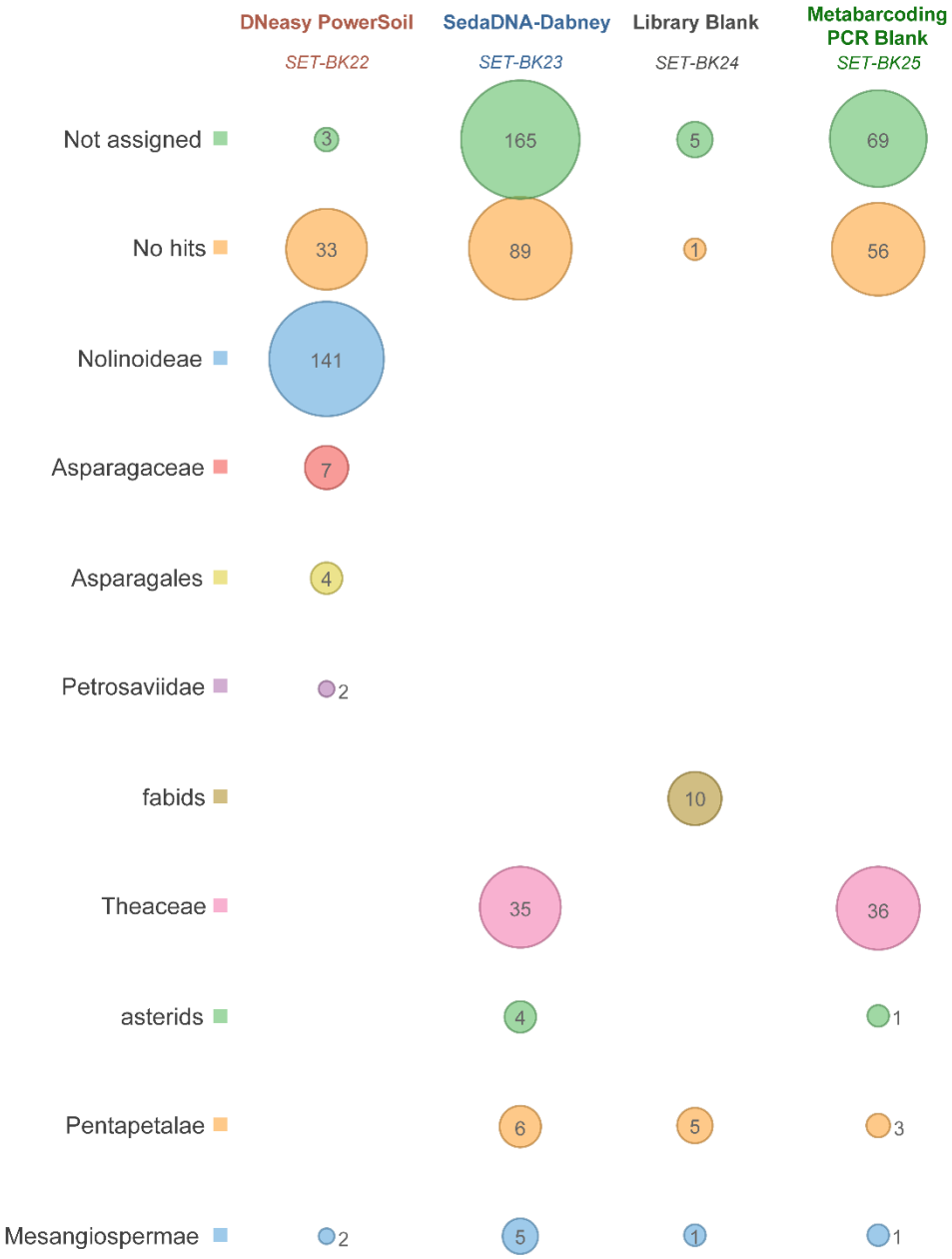

Fig. 3.33 Metagenomic comparison of the metabarcoding blanks from extraction, library preparation, and PCR map-filtered to the plant references (*rbc*L, *mat*K, *trn*L) displaying all reads fully uncollapsed to the lowest LCA assigned nodes with log-scaled bubbles for visual normalization. Values indicate total reads assigned to that taxon node (fully uncollapsed) (SET-E). Enriched and shotgun blank controls mapped to the plant references had 0 reads that passed map-filtering (see Table 3.23).

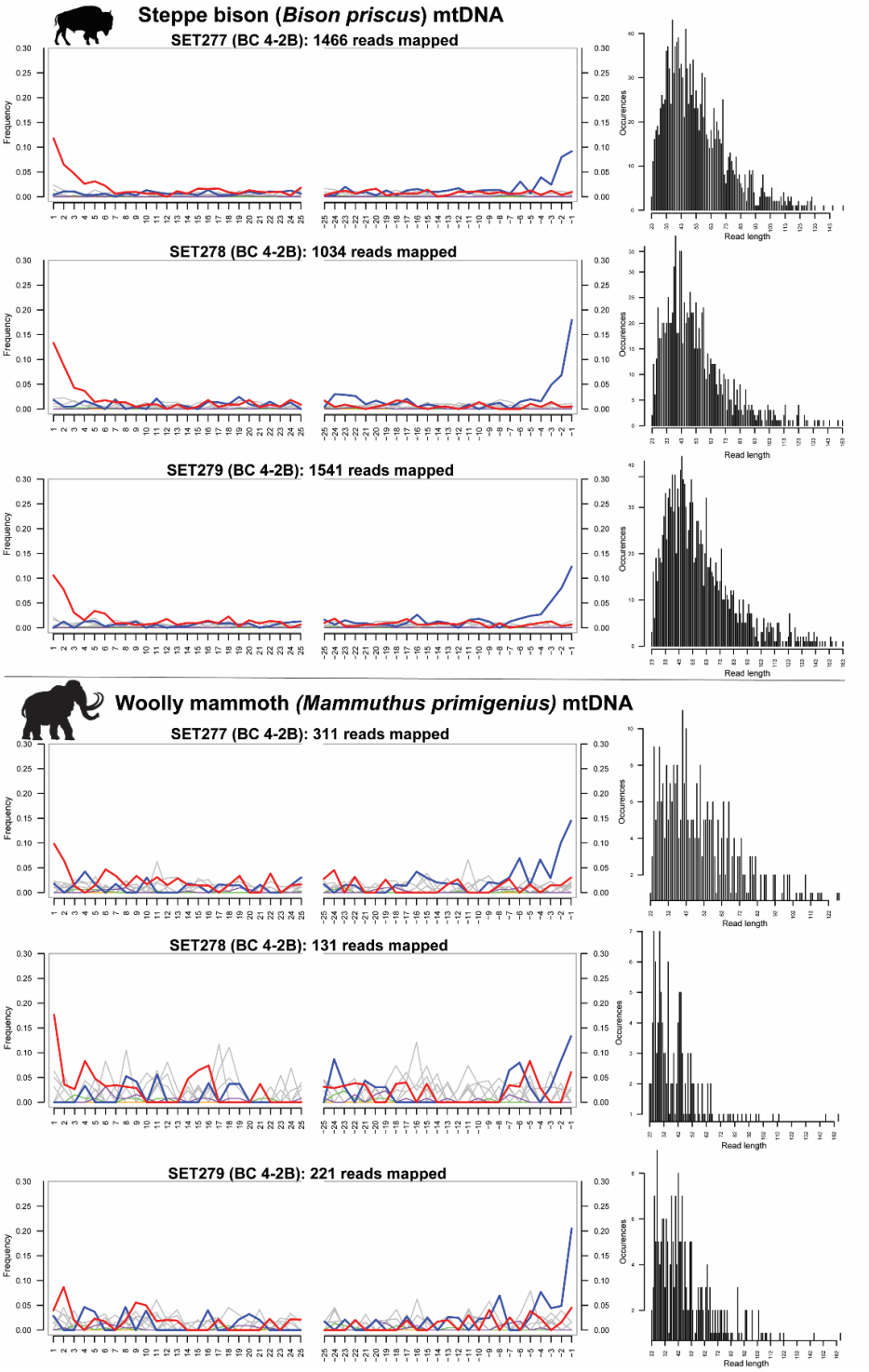

Fig. 3.34 *MapDamage* plots for *Bison priscus* and *Mammuthus primigenius.* Minimum length = 24 bp, minimum mapping quality = 30 (SET-E).

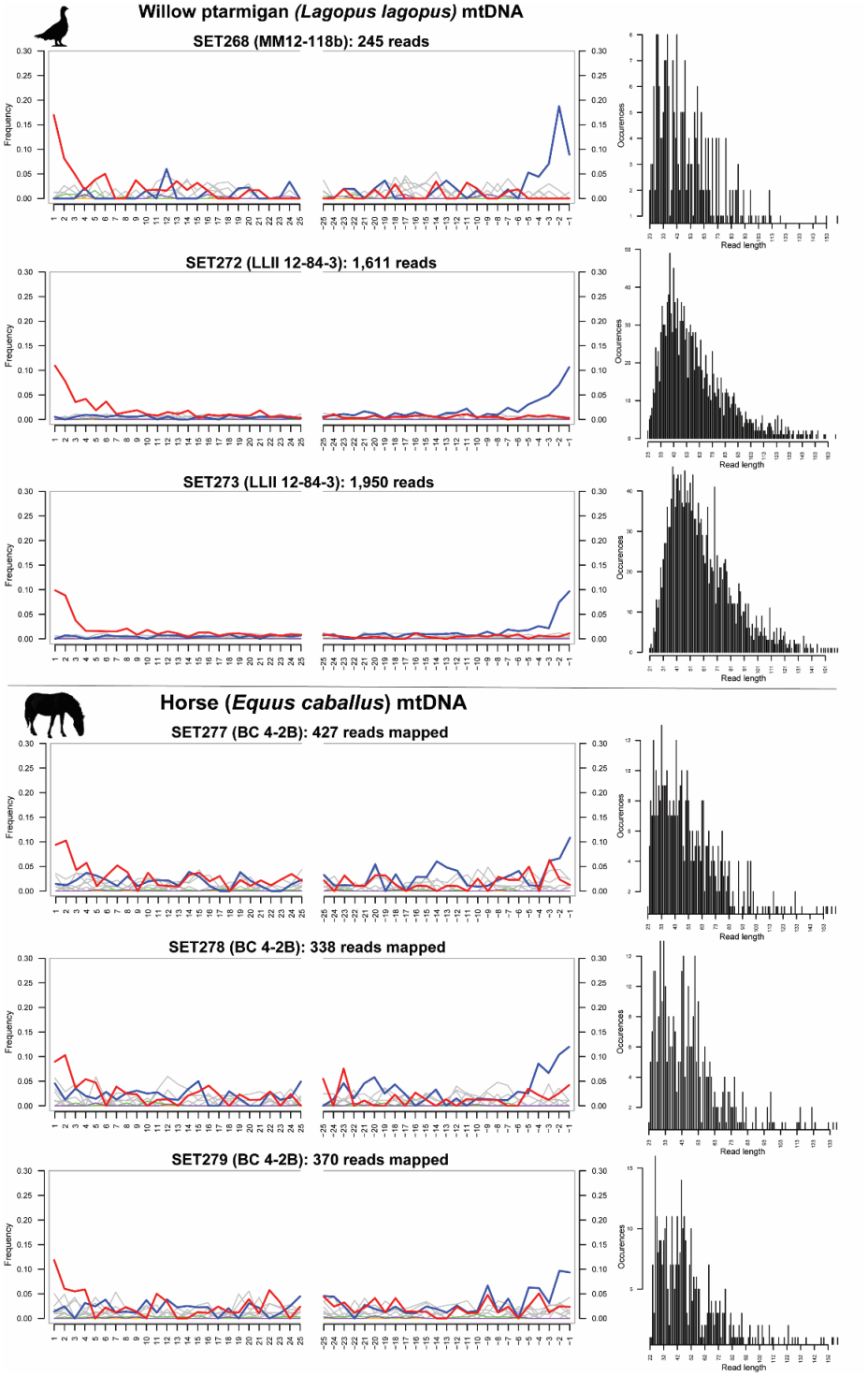

Fig. 3.35 *MapDamage* plots for *Lagopus lagopus* and *Equus caballus.* Minimum length = 24 bp, minimum mapping quality = 30 (SET-E).

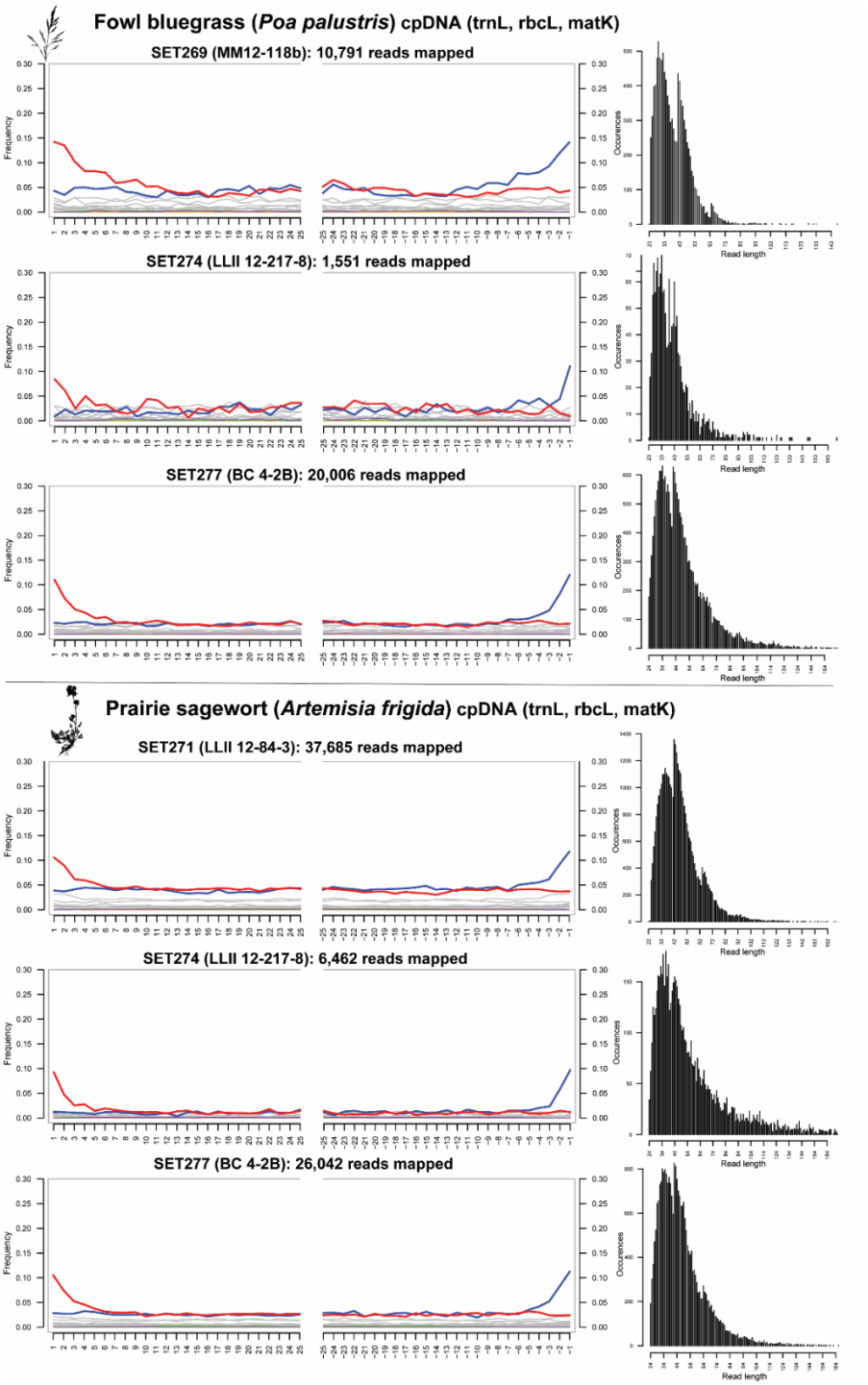

Fig. 3.36 *MapDamage* plots for *Poa palustris and Artemisia figida.* Minimum length = 24 bp, minimum mapping quality = 30. We suspect that the biomodial distribution of the fragment length distributions is due to non-specific mapping of closely related taxa in conserved regions of these cpDNA barcoding loci (SET-E).

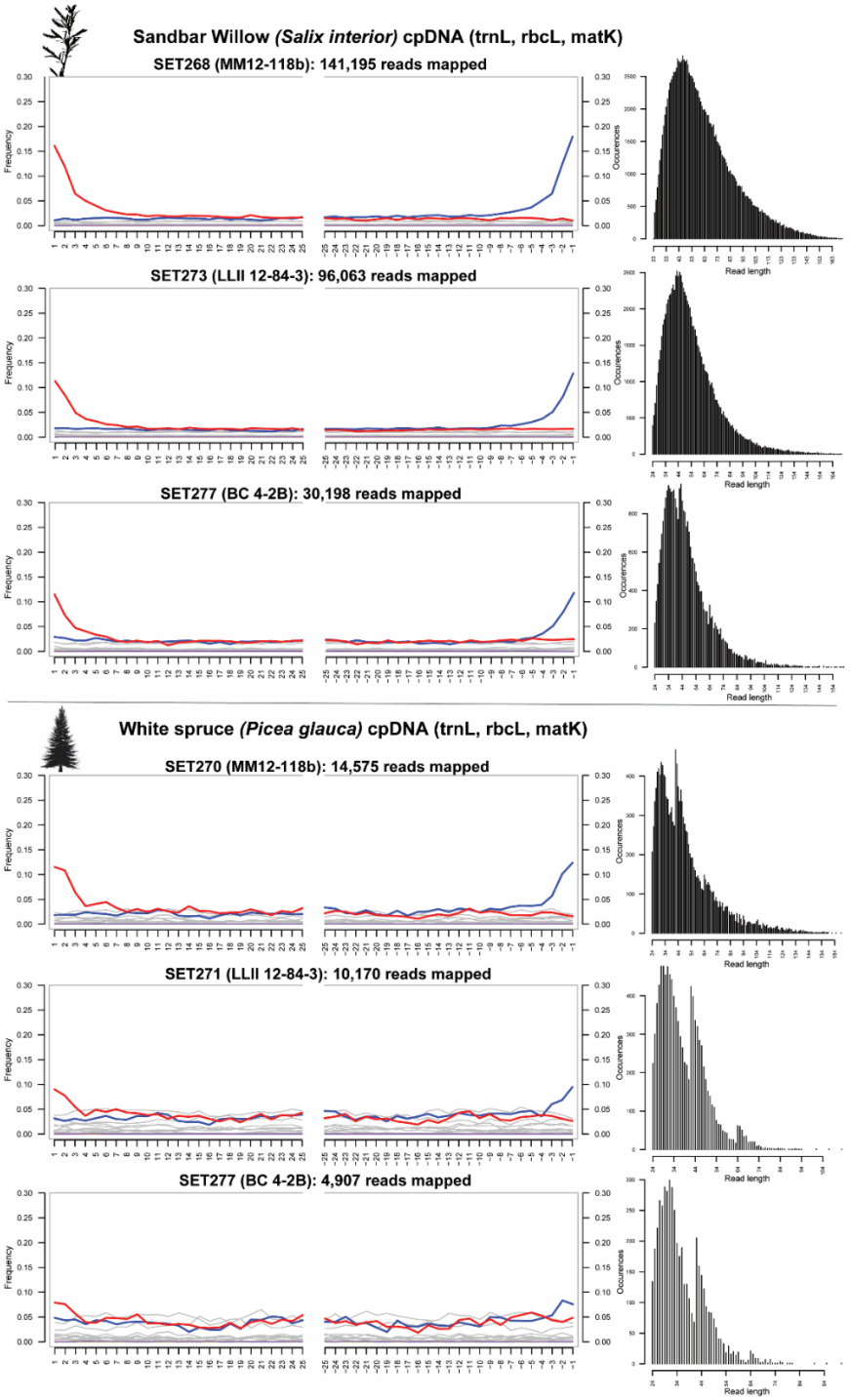

Fig. 3.37 *MapDamage* plots for *Salix interior* and *Picea glauca.* Minimum length = 24 bp, minimum mapping quality = 30. We suspect that the biomodial distribution of the fragment length distributions is due to non-specific mapping of closely related taxa in conserved regions of these cpDNA barcoding loci (SET-E).

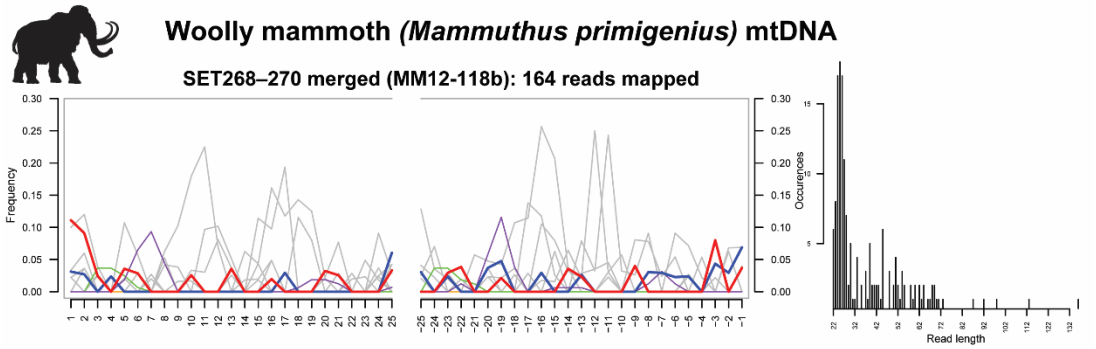

Fig. 3.38 *MapDamage* MM12-118b merged replicates plot for *Mammuthus primigenius*. Minimum length = 24 bp, minimum mapping quality = 30. Read counts are too low (not enough overlap on the mitogenome to assess termini deamination) despite concatenating the 3 extractions to assess damage. However, fragments are characteristically short and map well to multiple loci across the mitogenome. Greater sequencing depth is needed to better assess this signal (SET-E).

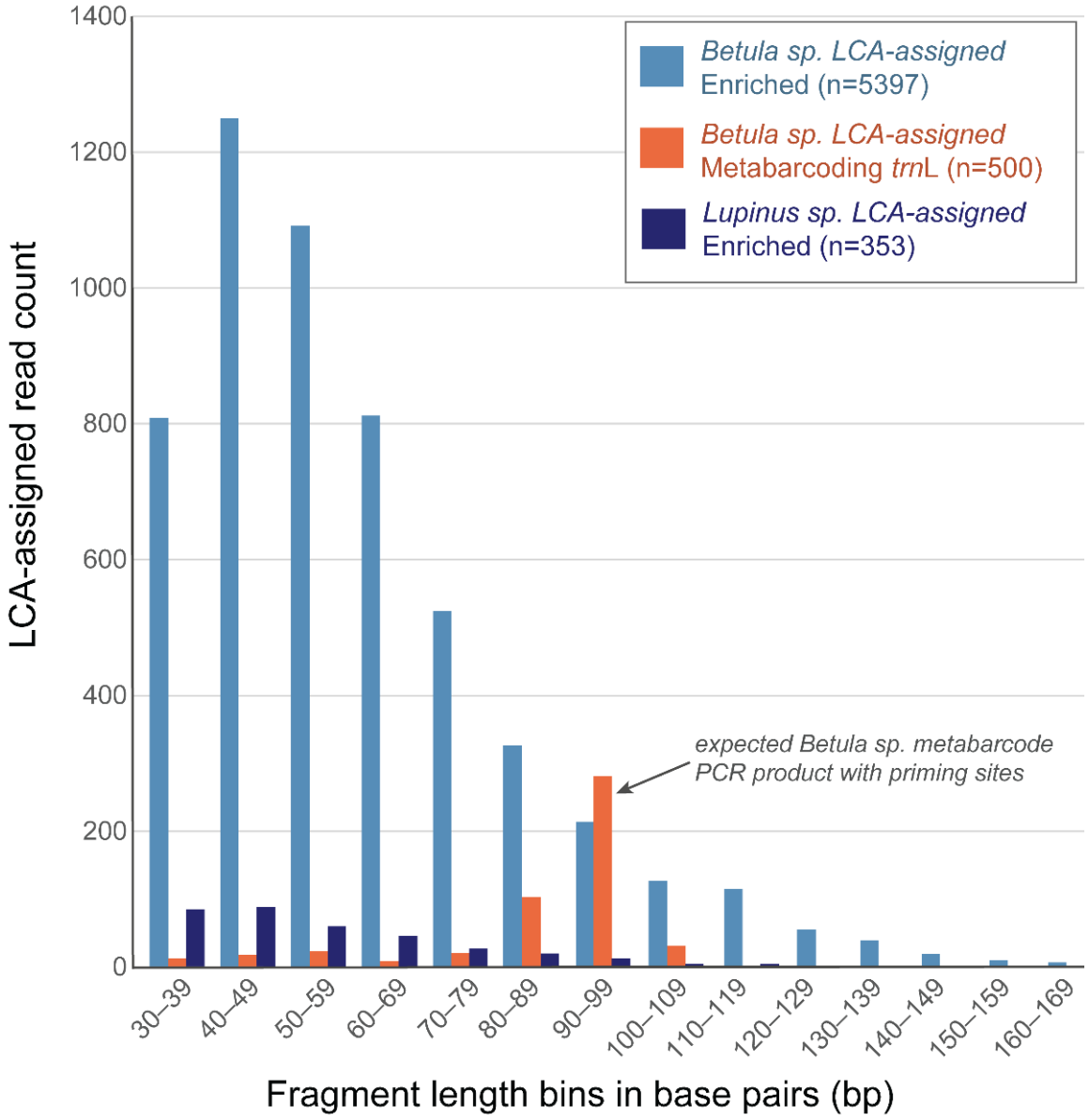

Fig. 3.39 Histogram of fragment lengths for reads assigned to *Betula sp.* with enrichment and metabarcoding, as well those assigned to *Lupinus sp.* with enrichment for the Upper Goldbottom core (MM12-118b). The abnormally short metabarcode amplicons (30–70 bp) for *Betula sp.* might be some form of PCR artefacts or unmerged reads. Inspecting a subset of these short reads still return assignments of *Betula sp.* (100% identity) even with the top 20,000 hits on web-*BLASTn* (SET-E).

Chapter 4

Ecological turnover and megafaunal ghost ranges as revealed by palaeoenvironmental DNA

Tyler J. Murchie[a,b*], Alistair J. Monteath[c,d], George S. Long[e], Emil Karpinski[a,e], Scott Cocker[d], Grant Zazula[f], Ross MacPhee[g], Duane Froese[c*], Hendrik Poinar[a,b,h*]

[a]McMaster Ancient DNA Centre, McMaster University, Canada.
[b]Department of Anthropology, McMaster University, Canada.
[c]Department of Earth and Atmospheric Sciences, University of Alberta, Canada.
[d]School of Geography and Environmental Science, University of Southampton, Southampton, UK
[e]Department of Biology, McMaster University, Canada.
[f]Yukon Government, Palaeontology Program, Department of Tourism and Culture, Whitehorse, Canada.
[g]Division of Vertebrate Zoology/Mammalogy, American Museum of Natural History
[h]Department of Biochemistry, McMaster University, Canada

[*]Corresponding authors: Tyler J. Murchie and Hendrik Poinar, Department of Anthropology, McMaster University, 1280 Main Street West, Hamilton, ON L8S 4L8, Canada; Duane Froese, Department of Earth and Atmospheric Sciences, University of Alberta, 116 St & 85 Ave, Edmonton, AB T6G 2R3, Canada.
E-mail address: murchiet@mcmaster.ca, duane@ualberta.ca, and poinarh@mcmaster.ca

Abstract

The multitude of factors alleged to have contributed to the late Quaternary mass extinction of some two-thirds of Earth's megafauna is complicated by the coarse record of buried macro-fossils. In response, micro-methods such as ancient DNA have been increasingly able to augment discontinuous palaeontological records. The scope and information potential of ancient environmental DNA have expanded dramatically in recent years, having undergone continuous methodological improvements in the analysis of biomolecules preserved for millennia in the absence of biological tissues. Here, we present sedimentary ancient DNA data diachronically identifying fauna and flora from permafrost cores recovered from the Klondike of Yukon, Canada. We observe a substantial turnover in ecosystem composition between 13,000–10,000 calendar years BP with the rise of woody shrubs and the disappearance of steppe-tundra vegetation. We also identify a lingering signal of *Equus sp.* (North American horse) and *Mammuthus primigenius* (woolly mammoth) from multiple samples thousands of years after their last dated macro-fossils.

Keywords

Late Quaternary extinctions, Beringia, ancient environmental DNA, PalaeoChip capture enrichment, Pleistocene-Holocene transition, ghost range, permafrost, shrub expansion, mammoth-steppe, woolly mammoth

4.1 Introduction

Humans evolved and dispersed throughout the continents in an epoch dominated by giant animals. Megafauna (body mass ≥ 44 kg) only exist in comparable densities today in small refugia of our globe (mainly Africa), with most now being in a state of decline, and many being either threatened or endangered (Dirzo et al., 2014; Pimm et al., 2014). The ecological reverberations associated with the late Pleistocene loss of approximately 101 of 150 genera (Boivin et al., 2016, p. 6390) of Earth's largest terrestrial animals continues to reverberate through contemporary ecosystems, impacting vegetation composition and diversity, ecosystem biochemistry, as well as regional and global climate feedback systems (Brault et al., 2013; Doughty et al., 2013; 2015; 2016; Smith et al., 2015; Asner et al., 2016; Bakker et al., 2016b; 2016a; Malhi et al., 2016; le Roux et al., 2018). The mass extinction of primarily large animals is argued by some to be the direct result of rapid climate change and attendant environmental feedbacks during the climatologically tumultuous late Pleistocene (Guthrie, 2006; Boulanger and Lyman, 2013; Rozas-Dávila et al., 2016; Meltzer, 2020). Others contend (Martin, 1984; Zimov et al., 1995; Barnosky et al., 2004; Braje and Erlandson, 2013; Sandom et al., 2014a; Smith et al., 2018) that factors unique to the last glacial period must be sought, such as the coincident dispersal of a new predator—*Homo sapiens*—or with growing (but controversial and widely criticized) evidence of a terminal Pleistocene, extra-terrestrial impact (Firestone et al., 2007; Pinter et al., 2011b; Van Hoesel et al., 2014; Wolbach et al., 2018; Pino et al., 2019; Moore et al., 2020). It is likely that no single factor can account for the staggered magnitude of such losses globally, but rather that each ecosystem experienced a variable set of locally compounding pressures (Lorenzen et al., 2011; Meltzer, 2020).

In the case of eastern Beringia (Yukon and Alaska), Guthrie (2006), Mann et al. (2013; 2015), and Rabanus-Wallace et al. (2017) argue that the expansion of woody shrubs (*Betula* and *Salix*) and peatlands with an increased moisture-regime during the Pleistocene-Holocene transition explains the loss of grazing megafauna. Whereas Zimov et al. (1995) contend that megafaunal extirpations preceded a rise in woody shrubs, with

the loss of keystone megaherbivores having led to the disappearance of the graminoid and forb dominated, mammoth-steppe biome (Owen-Smith, 1987; Zimov et al., 2012a; Willerslev et al., 2014; Bakker et al., 2016b). To date, robustly disentangling the relative timings of ecological restructuring versus megafaunal population declines has largely exceeded the resolution of Quaternary records.

There has been a drive to understand the late Pleistocene-to-Holocene mass extinction event since it became recognized by scientists of the mid-19 century (Lund, 1841; Wallace, 1876). The topic has undergone a resurgence in recent years in part due to our ecologically uncertain future amidst projections of incipient and rapid climate change driven by anthropogenic factors (IPCC, 2014). Extinction rates today are estimated to be 1000 times the background rate (Pimm et al., 2014) and are projected to increase to 10,000 times (Alroy, 2015; De Vos et al., 2015). It has been estimated that some one million species face the risk of extinction within decades unless anthropogenic drivers of biodiversity loss are reduced in intensity (IPBES, 2019). Understanding our most recent 'near-time' example highlighting the consequences of a rapid climate change and increasing anthropogenic pressures on biotic systems can aid in historically contextualizing efforts aimed at mitigating our multiple ongoing ecological crises (Barnosky et al., 2011; Ceballos et al., 2015).

Taphonomy challenges our attempts to tease apart the palaeoecological nuances of the late Quaternary extinctions (LQE), necessitating relatively precise estimates for megafaunal population declines and last appearance dates (Zazula et al., 2014; Stuart, 2015), timings of ecological shifts (e.g. changes in plant community structure), as well as robust archaeological evidence of human mobility. Extinction chronologies have been traditionally based on last appearance dates of macro-remains, but the rarity of these fossils only allows for tenuous inferences of terminal population dynamics. The probability of finding evidence for dwindling or refugial populations is remote, which is compounded in species with otherwise low population densities, resulting in a blurring of multi-species extirpations (Signor and Lipps, 1982). Attempts to cross this impasse have generated abundant research, but taphonomic limitations continue to undermine our

understandings of this complex period of restructuring in the terrestrial biosphere. As such, while directly dated macro-remains can provide the most confident temporal evidence for the presence of a taxon at a particular moment in the past, other measures can aid in complementing these palaeontological datasets by filling in some of the knowledge gaps to be expected with buried remains. Two micro-methods are increasingly being used in Quaternary research to help refine our estimates as to the timings of the LQE: coprophilic spores and sedimentary ancient DNA (sedaDNA).

Here, we present PalaeoChip enriched sedaDNA data derived from 21 permafrost cores (Table 4.1) recovered from the Klondike goldfields (Fig. 4.1)—the unglaciated region of west-central Yukon Territory, Canada (Froese et al., 2009)—dating between 30,000–6000 calibrated (calendar) years before present (cal yr BP). This work builds on the results reported in Murchie et al. (2021b) where *Equus* sp. (North American horse) and *Mammuthus primigenius* (woolly mammoth) were identified in permafrost sediments dating to ~9700 calibrated years before present (cal BP), which is indicative of a substantial *ghost range*—an extended spatio-temporal range derived from palaeoecological proxies beyond the last dated macro-remains (Haile et al., 2009).

Our aims here are two-fold. First, to assess whether a permafrost sedaDNA dataset (Fig. 4.2) would support either the shrub and peatland expansion driven extinction model as argued by Guthrie (2006) and Mann et al. (2013; 2015; Rabanus-Wallace et al., 2017). Or whether megafaunal declines preceded the rise in woody shrubs, supporting the keystone megaherbivore model that the loss of ecological engineers resulted in the disappearance of the mammoth-steppe (Zimov et al., 1995; Bakker et al., 2016b). Secondly, to assess whether the sedaDNA ghost range identified in Murchie et al. (2021b) was an anomaly or is also observed in other coring sites, and whether this correlates with the lingering coprophilous fungal signal as reported by Conroy et al. (2020).

4.2 Background

4.2.1 Late Quaternary extinctions on the eastern mammoth-steppe

Late Pleistocene extinctions after 40,000 BP in Eurasia, Beringia, and North America arguably followed a two-stage extinction pattern (Stuart, 2015) (see Table 5.1 and Fig. 5.1). The first wave seems to have occurred shortly prior to or during the Last Glacial Maximum (LGM, 26,500–19,000 BP) (Clark, 2009a) which in eastern Beringia included the extinctions of *Homotherium latidens* (scimitar-toothed cat) and *Arctodus simus* (short-faced bear). The second pulse occurred between 15,000–10,000 BP, which in mainland Beringia included Equidae (caballine and stilt-legged horses), *Mammuthus primigenius* (woolly mammoth), *Panthera spelaea* (cave lion), and *Saiga tatarica* (saiga antelope), while at least 20 genera went extinct in North America south of the continental ice sheets. Other species such as *Bison priscus* (steppe bison) survived until at least ~6000 years ago in southern Yukon (Zazula et al., 2017b) with genetic data indicating a survival of *B. priscus* in southern Yukon and interior Alaska as recently as ~325–490 years ago (Heintzman et al., 2016). *M. primigenius* (woolly mammoth) survived on St. Paul (Alaska) and Wrangel (Russia) islands until about 5500 and 4000 cal yrs BP respectively (Vartanyan et al., 2008; Graham et al., 2016). Many of these faunal assemblages, particularly those of predators, species with small populations, or in understudied regions, are expectedly sparse. This has led some to argue that these two late Pleistocene extinction pulses are likely just an artifact of the inadequate record of dated macro-remains (Faith and Surovell, 2009), and that the true extinction occurred around the onset of the Younger Dryas, c. 12,900 cal BP (Fiedel, 2009).

Beringia's environment during the late Pleistocene is characterized as being a graminoid and forb-dominated steppe-tundra mosaic often referred to as the *mammoth-steppe* (Guthrie, 2001; Zazula et al., 2003; Graf, 2008; Froese et al., 2009; Kuzmina et al., 2011; Zimov et al., 2012a; Hoffecker et al., 2014; Willerslev et al., 2014). The mammoth-steppe was the most extensive biome on Earth during the late Pleistocene stretching from the Iberian Peninsula eastward across Eurasia into Canada and the continental United States (Guthrie, 2001; Zimov et al., 2012a; Pavelková Řičánková et al., 2014; Bocherens,

2015). And despite its size, the mammoth-steppe had a surprisingly large-scale homogeneity of mosaic vegetation and fauna across the northern hemisphere (Guthrie, 2001; Zimov et al., 2012a; Bocherens, 2015) that facilitated high biotic productivity (higher energy and nutrient turnover than contemporary northern environments). This supported a diverse biomass of large bodied organisms, comparable to the modern Africa Savannah (Zimov et al., 2012a). Pavelková Řičánková et al. (2014) argue that the Altai-Sayan Range of Central Eurasia represents a refugial analog of this now extinct biome, and efforts by Sergey Zimov and his team in arctic Siberia have been working towards experimentally creating a modern version of the mammoth-steppe in Pleistocene Park (https://pleistocenepark.ru/) (Fig. 1).

Owen-Smith (1987) proposed the 'keystone herbivore' hypothesis to explain the role of megaherbivores in radically transforming vegetation structure and composition (Owen-Smith, 1992; Bradshaw et al., 2003; Bakker et al., 2006; Gill et al., 2009; 2012; Johnson, 2009; Gill, 2014b). Nutrients can become locked in leaves and stems, but are liberated for use by fauna, accelerating biogeochemical cycling (Malhi et al., 2016, pp. 842–843). In this model, megafauna are critical for maintaining and promoting diversity in open-mosaic environments, and for controlling the abundance of woody vegetation that can limit biodiversity in old-growth zones (Bakker et al., 2016b). A severe reduction of these megafaunal engineers (Gutierrez and Jones, 2006; Wright and Jones, 2006; Berke, 2010) would have resulted in the conversion of mosaic, steppe grasslands and wood pastures to more uniform forests and prairies, shrinking mosaic ecotones—high productivity transition areas between biological communities (Ries et al., 2004)—thereby reducing the carrying capacity of terminal Pleistocene environments. This in turn could have led to a positive-feedback loop wherein diminishing megafauna were increasingly unable to control woody shrub expansion, further reducing the biotic productivity of the mammoth-steppe.

Alternatively, an increasing moisture regime during the Bølling–Allerød interstadial (c. 14,690–12,890 cal BP) (Rasmussen et al., 2006) may have resulted in the paludification of Beringia (the spread of peatlands) along with the rise of mesic-adapted

woody shrubs that were highly defended against herbivory, replacing the herbaceous diet of Pleistocene grazers (woolly mammoth, steppe bison, horse) (Guthrie, 2006; Mann et al., 2013; 2015; Rabanus-Wallace et al., 2017). In this line of argument, rapidly oscillating climate change and attendant environmental feedbacks were the proximate cause in the disappearance of the mammoth-steppe in eastern Beringia, along with the megafauna it supported.

4.2.2 Palaeoamericans in eastern Beringia

The first people to inhabit the northwestern portions of unglaciated North America (eastern Beringia: Alaska and Yukon) arrived from Siberia following dispersal across the exposed Bering Isthmus. Humans may have reached the Siberian arctic coast, west of the Yenisey River as early as ~45,000 cal BP (Pitulko et al., 2016; Maschenko et al., 2017) (Figs. 3 and S2). Evidence during this period is fragmentary, but these first northern peoples had sophisticated Upper Palaeolithic technologies, including prepared lithic blade-cores and abundant bone tools (Pitulko et al., 2004; Graf, 2014, pp. 65–69). The earliest evidence of humans in western Beringia, east of the Lena River (Hoffecker and Elias, 2007, pp. 4–5), is ~32,000 cal yr BP (Nikolskiy and Pitulko, 2013, p. 4191). This site has an abundance of faunal remains, including lithic and osseous tools, and projectile point fragments embedded in two differently-aged woolly mammoths (*M. primigenius*) (Nikolskiy and Pitulko, 2013, p. 4191).

Humans appear to have thrived in Siberia until the peak of the Last Glacial Maximum (LGM, 26,500–19,000 BP) (Clark, 2009a), although to date it appears as if these populations largely remained in western Beringia (Hoffecker and Elias, 2007, p. 95). A series of alleged archaeological components at Bluefish Caves I and II in northern Yukon date to as early as ~23,800 years ago (Bourgeon, 2015; Bourgeon et al., 2017) based on bones that have been debatably interpreted to exhibit human-made “cut-marks” and other modifications. Sedimentary biomarkers of faecal sterols and polycyclic aromatic hydrocarbons have also been interpreted to be suggestive of a human presence on the Alaskan North Slope from 34,000–16,000 cal BP, along with a rise in fire activity (Vachula et al., 2020). However, the strongest evidence of sustained human occupations

in eastern Beringia comes from sites in the Tanana River Valley, Alaska, chiefly at Swan Point CZ_4 (Holmes, 2001; 2011) dating as early as ~14,000 years ago (Potter et al., 2018, sec. Suppl.).

Middle Upper Palaeolithic occupations around Lake Baikal and the Yenisey and Lena drainages in Siberia have evidence of semi-subterranean dwellings, storage pits, diverse faunal remains (large-to-small mammals, birds), and a substantial quantity of lithic debris and other artifacts (Ermolova, 1978, pp. 15–29; Abramova, 1989; Abramova et al., 1991; Goebel, 2002a; Hoffecker and Elias, 2007, pp. 93–96). These people hunted a variety of megafauna, including: *Mammuthus primigenius* (woolly mammoth), *Coelodonta antiquitatis* (woolly rhinoceros), *Bison priscus* (steppe bison), *Rangifer tarandus* (reindeer), and horse (*Equus* sp.) (Goebel, 1999, pp. 214–214; Hoffecker and Elias, 2007, p. 90). There may have been an abandonment of much of Siberia and Beringia during the LGM due to the extreme cold climatic conditions (Davis and Ranov, 1999; Goebel, 1999; 2002a; Dolukhanov et al., 2002; Graf, 2005; 2009; 2010; 2014), although this is contested by Kuzmin and others (Kuzmin and Keates, 2005; Fiedel and Kuzmin, 2007; Kuzmin, 2008). It has been hypothesized that people may have taken refuge farther south in the Russian Far East and on the Palaeo-Sakhalin-Hokkaido-Kuril Peninsula in present day northern Japan (Graf, 2014, sec. 74; Izuho, 2014; Buvit and Terry, 2016).

The people who came to reoccupy Beringia after the LGM seem to have had substantially different lifeways from their predecessors. Late Upper Palaeolithic populations in Siberia had developed a mobile settlement system technologically based on a highly economical and portable use of lithic raw material: microblades (Goebel, 2002b). Sites after ~21,000 cal BP lack semi-subterranean dwellings and storage pits (Hoffecker and Elias, 2007, p. 97) and have thin occupation layers with single taxon dominant faunal assemblages (Graf, 2014, p. 75). This shift in lifeways towards high residential mobility seems to have been adapted to perusing mobile herd fauna that were becoming increasingly dispersed as the mammoth-steppe began to shrink and be replaced by shrub forests and tundra (Goebel, 2002a; Graf, 2005).

4.2.3 Sedimentary ancient DNA

Ultimately, much of the LQE debate comes down to the inability of rare macro-fossils to convey the temporal resolution necessary to untangle the complexities of the Pleistocene-Holocene transition. Micro-methods (Swift et al., 2019) are increasingly able to fill in the holes in our records to augment discontinuous fossil records, which can aid in identifying ghost ranges (Comandini and Rinaldi, 2004; Haile et al., 2009; Andersen et al., 2012), for independently assessing population declines, and to estimate the timings of *functional extinctions* (Säterberg et al., 2013; Rozas-Dávila et al., 2016)—the point at which a species disappears from fossil or historical records, no longer significantly contributes to ecosystem functioning, and when population size has reduced to the degree that inbreeding depression and genetic drift results in an increasing loss of fitness.

Ancient environmental DNA (eDNA) (Taberlet et al., 2018) has been demonstrated to be a powerful method for directly assessing the local (Edwards et al., 2018) diachronic presence of animals, plants, fungi, and microbiota (Haile et al., 2009; Anderson-Carpenter et al., 2011; Bellemain et al., 2013; Willerslev et al., 2014; Graham et al., 2016; Niemeyer et al., 2017; Slon et al., 2017; Ahmed et al., 2018; Murchie et al., 2021b). SedaDNA (referring to a subset of ancient eDNA sample types; see Rawlence et al. [2014, p. 614]) is thought to survive in the absence of macro-tissues as cellular material binds to sedimentary minerals (Greaves and Wilson, 1970; Lorenz and Wackernagel, 1987b; 1987a; Ogram et al., 1988; Blum et al., 1997; Arnold et al., 2011; Morrissey et al., 2015; Gardner and Gunsch, 2017). Much of eDNA is likely to be quickly metabolized by bacteria or otherwise degraded through a range of chemical and physical processes. However, a small fraction can absorb into the sedimentary matrix, protecting these molecular fragments for millennia, especially when consistently frozen. Sediment samples as small as 100 mg contain tens of billions of DNA fragments from all forms of life in a local ecosystem. However, there are several sedaDNA challenges to be aware of: 1) whether sedaDNA is in a stratigraphically accurate context, 2) whether the targeting strategy, reference databases, and taxon assignment approach can accurately assess the breadth of sequenced eDNA, and 3) the degree to which sedimentary inhibitors or

differential degradation may bias a sedaDNA signal (Murchie et al., 2021b). Of particular importance for the kinds of permafrost sedaDNA analyzed in this report are the factors of reworked sedaDNA and leaching.

Reworked sedaDNA. The potential for the preservation and transport of sedaDNA complexes presents the possibility that molecules from a sediment sample may be allochthonous (in secondary context). Arnold et al. (2011) found considerable evidence of reworked strata in their periglacial sediments by combining optically stimulated luminescence (OSL) dating with radiocarbon. Permafrost sedaDNA was found to survive over longer time periods and through more disruptive post-depositional processes. Dating inconsistencies at a portion of their sites indicated that some sediments with dated macro-remains had been eroded and redeposited. As such, permafrost in high-energy erosional environments, or depositional settings with large catchment areas, could facilitate the preservation of sedaDNA during erosion and transport, and their subsequent re-deposition within younger strata.

Leaching. The vertical movement of free DNA has been alleged to be "demonstrably negligible... in high-latitude, low-energy, perennial frozen settings" (Arnold et al., 2011, p. 18). A number of studies have found synchronous palaeoecological shifts when comparing complementary palynological and macro-remain evidence with permafrost sedaDNA reconstructions (Willerslev et al., 2003b; Lydolph et al., 2005), in addition to 'age-dependent' damage patterns (Willerslev et al., 2004a; Hansen et al., 2006; Haile et al., 2007). Leaching is considered to not be a significant problem in permafrost conditions (Willerslev et al., 2003b; 2014; Johnson et al., 2007; Haile et al., 2009; Hebsgaard et al., 2009; D'Costa et al., 2011).

4.3 Results

4.3.1 Palaeoecology

We observe a diverse range of plant and animal sedaDNA; *Bison priscus* (steppe bison), *Mammuthus primigenius* (woolly mammoth), *Equus* sp. (caballine horse), and *Lagopus lagopus* (willow ptarmigan) constitute most of the assignable reads within Animalia (Fig. 4.4), in addition to less abundant organisms such as *Rangifer tarandus*

(caribou/reindeer), *Ovis sp.* (likely Dall sheep), and potentially *Bos* sp. (bovins). Many reads expectedly lack taxonomic specificity at species and genus ranks (as many regions of the mitochondrial genome are variably conserved) and as such a large portion of reads could only be confidently assigned to higher ranks such as Caprinae, Pecora, Perissodactyla, and Elephantidae. In some cases, such as with hits to order Perissodactyla and superorder Afrotheria, we can be confident that they represent *Equus* (or its familial relative, *Haringtonhippus* [stilt-legged horses]) and *Mammuthus* respectively as unique members of their clades in the late Quaternary record of this region. There is also a low biomolecular signal from ecologically rare animals in this dataset including *Canis lupus* (grey wolf) and *Martes* sp. (marten). A variety of rodents were identified, including *Urocitellus sp.* (likely arctic ground squirrel), *Microtus xanthognathus* (taiga vole), and *Dicrostonyx groenlandicus* (northern collared lemming). Human was identified despite not being present in the PalaeoChip baits but is also observed in the negative controls. These human reads are likely contaminants but hint at the possibility of targeting ancient human DNA from Beringian permafrost.

Overall, this rich sedaDNA dataset reflects a gradual decline in megafauna through time (Fig. 4.5). Elephantidae is one of the first to decrease in sedaDNA abundance around 17,000 cal BP. This is followed by shrinking signals for Bovidae and Equidae, until a punctuated decrease occurs around the Pleistocene-Holocene transition, during which the animal sedaDNA signal comparatively flatlines as *Alces alces* (moose) and *Cervus sp.* (deer) enter our sedaDNA record in abundance. Our admittedly coarse set of permafrost samples suggests an extirpation timing between 13,000–10,000 cal BP, but we do also observe a lag in the final disappearance of *Equus* and *Mammuthus*. Cores from Lucky Lady II, Upper Goldbottom, and Upper Quartz retain 100+ reads assignable to those taxa well beyond their last dated macro-remains (Fig. 4.4).

Trends of major environmental turnover are also reflected by plant taxa (Figs. 4.5–4.6). Pleistocene graminoids such as Poaceae (grasses), Cyperaceae (sedges), and a variety of forbs (herbaceous [non-woody] flowering plants) such as *Artemesia* (sagebrush), *Lupinus* (lupine), *Saxifraga* (rockfoil), *Papaver* (poppy), and *Ranunculus*

(buttercup) were identified in abundance. Woody taxa such as *Salix* (willow), *Populus* (poplar), *Betula* (birch), *Rhododendron*, *Arctous* (bearberry), and *Picea* (spruce) were identified with increasing abundances after ~13,200 cal BP, along with ferns (*Equisetum* and *Gymnocarpium*) and *Sphagnum* (peat moss). Our data suggests that forbs and graminoids (in this case Poaceae and Asteraceae) were dominant until the late Bølling–Allerød (Fig. 4.5, see also section 5.6.3 for a breakdown by site). The rise of woody plants also marks the growing abundance of Pinaceae (pine family, in this case *Picea*). The pronounced shift from forb and grassland environments towards woody shrubs and boreal forest is coeval with a diminishing signal of megafaunal sedaDNA.

4.3.2 Assessing ancient authenticity

The 13 negative controls (9 extraction blanks and 4 library blanks) had negligible library adapted molecules prior to indexing (Fig. 5.3) and had minuscule molarities after targeted enrichment (Fig. 5.4). Despite using the entire post-enrichment eluate for each of the 13 negative controls during equimolar pooling, these blanks received minimal sequenced reads (102,440) and even fewer reads that could be taxonomically binned (81, 0.08%). Shotgun sequencing blanks processed with a subset of these libraries in Murchie et al. (2021b) were almost entirely (>95%) *adaptemers* (adapter chimeric DNA), and contained no signal of the ecologically relevant organisms under investigation here or in that previous work. As all thirteen negative controls were processed identically in parallel with the permafrost subsamples, and yet contain none of the same sedaDNA signal, we can conclude that the trends observed here originate at minimum from the original sediments themselves and are not in any substantive way the result of cross-contamination.

We also observe ancient DNA characteristic damage profiles where sufficient reads could be mapped to *MEGAN* and *PIA* identified references (Fig. 4.7, see also section 5.6.4). When mapping to a specific reference, *mapDamage* (Jónsson et al., 2013) (v 2.0.3) quantifies the proportion of polymorphic nucleotides to assess whether reads are characteristically damaged on their ends (and as such, are more likely to be ancient), which rarely occurs with modern contaminants. This trend is observed consistently where

sufficient read depth is achieved, supporting the argument that these reads are ancient and originate from the samples themselves.

The taxonomic constituents of these samples are also more clearly correlated with age than site, suggesting that reworking and leaching have contributed minimally (if at all) to the ecological reconstructions (Fig. 4.8). Approximately 90% of the variance observed can be explained by principal coordinates 1 and 2, with the proportion of Pinaceae, Asteraceae, and Salicaceae being the primary taxon nodes driving inter-sample disparities. This is also reflected in the site-specific proportional charts (section 5.6.3).

4.4 Discussion

We observe three main trends within this dataset. 1) Forbs and graminoids characteristic of the mammoth-steppe ecosystem are genetically coeval with grazing megafauna. The transition towards woody shrubs and trees between 13,000–10,000 cal BP is associated with the disappearance of a megafaunal signal, which is when we suggest grazing megafauna in the Klondike region likely became functionally extinct. 2) For certain megafauna, there is a small lingering sedaDNA signal that persists into the Holocene. These ghost ranges are indicative, but not dispositive, of their continued persistence with a high latitude refugium subsequent to the loss of other continental populations and the functional extinction of these taxa. 3) The megafaunal DNA signal decays gradually after the LGM, with *Mammuthus primigenius* reads being the first to decline, followed thereafter by *Bison priscus* and *Equus* sp.

4.4.1 Ecological turnover and the disappearance of the mammoth-steppe

Mammuthus, Equus, and *Bison* are closely associated in our dataset with forbs and graminoids, whereas cores dominated genetically by woody shrub taxa such as *Salix* and *Betula* are correlated with a reduced sedaDNA signal for these grazers. It is during the early Holocene spike in *Salix* and *Betula* ~10,340 cal BP where *Asteraceae* and *Poaceae* correspondingly reduce significantly in abundance and grazing megafauna largely disappear from our record. Chronologically, our sedaDNA dataset suggests that *Mammuthus primigenius* may have been the first megafaunal species in the Klondike to undergo a population reduction as indicated by a decreasing sedaDNA signal for this

taxon after ~17,000 cal BP. It is difficult to say whether signal decay reflects an actual reduction in the regional abundance of animals or is reflective of other factors unique to this genetic proxy (such as stochastic eDNA release, preservation, or recovery). We discuss the relative changes in taxonomically identified sedaDNA sequences as being a very rough approximation of local palaeo-abundance, although this association is largely unknown and needs further research. *Mammuthus primigenius* macro-fossils are comparatively rare in central Yukon relative to more northerly sites around Old Crow (Fig. 5.1), but few of those have been successfully radiocarbon dated and many likely originate beyond radiocarbon time. Our faunal sedaDNA data somewhat conflicts with abundances of radiocarbon dated macro-remains insofar as we observe the most DNA reads identified as *Mammuthus*, *Equus*, and *Bison* frontloaded between 30,000–16,000 cal BP. Conversely, dated faunal remains of *Mammuthus* and *Bison* in eastern Beringia have modes around 15,000 cal BP, with only *Equus* remains being predominant nearer to 25,000 cal BP (Fig. 5.1).

Biomolecules identified as *Bison* sp. and *Equus* sp. are the next to decrease in read counts after ~15,000 cal BP. However, there is a subsequent spike in their signals at 12,800 cal BP that may be associated with previously described dispersals through the ice-free corridor (Shapiro et al., 2004; Heintzman et al., 2016) or other local factors. Despite these apparent declines, *Bison*, *Equus*, and *Mammuthus* all seem to have persisted until the Younger Dryas (ca. 12,900–11,700 cal BP) at which point their DNA signals flatline. This is correlated with a reduction of graminoids and forbs in the local environment and their replacement by woody shrubs, predominantly *Salix* sp. This is also associated with a rise in *Lagopus lagopus* (willow ptarmigan), rodents, and the browsers *Alces alces* and *Cervus* sp. (likely *Cervus canadensis* [elk/wapiti]). We observe a seesawing in the ecological signal between forbs/graminoids and woody shrubs in the Lucky Lady 2 cores between 13,800–12,800 BP, with rises in *Salix* ssp. (willow) reads being tightly associated with the explosion of *Lagopus lagopus* (willow ptarmigan) sedaDNA—a grouse that subsists largely on woody shrubs. Periods of forb/graminoid expansion (shrub reduction) are also associated with rises in *Bison* and *Equus* signals,

lending weight to the megaherbivore engineering model of woody plant control (Owen-Smith, 1987; 1988; Asner et al., 2016; Bakker et al., 2016b). Keesing and Young (2014) observed on the African savanna that when large grazing mammals were removed from an area, the rodent populations doubled, which increased the populations of predators that target small-bodied animals. We too observe a spike in rodent sedaDNA at ~10,340 BP that persists through our Holocene samples, along with the low-abundance appearance of *Martes* (martens). These sedaDNA macro-ecological reconstructions imply that *Mammuthus primigenius, Equus* sp., and *Bison priscus* had reduced in local population size, having become largely functionally extirpated within the Klondike between 12,800–10,300 BP, after which the local ecosystem fully transitioned towards woody shrubs with an associated rise in mosses, *Picea* (spruce), and other boreal flora (Fig. 4.6). Despite flatlining overall, reads for these grazing taxa extend beyond their last dated macro-remains, perhaps even as far as the mid-Holocene, which has already been observed for *Bison priscus* (Heintzman et al., 2016; Zazula et al., 2017b).

It has been argued that interpreting relative floral abundances with eDNA requires a degree of calibration. Yoccoz et al. (2012), for example, observed that their above-ground vegetation surveys were accurately mirrored in modern environmental soil DNA, but they found that functional groups (woody plants, graminoids, and forbs) varied in their proportional eDNA representation. Woody plants were most affected by this eDNA trend, being proportionally under-represented compared to above ground biomass by ~1:5 (Yoccoz et al., 2012, fig. 2), while graminoids (grass-like herbaceous plants) were under-represented by ~1:1.5. Conversely, forbs (herbaceous flowering plants that are not grass-like) were observed to be genetically over-represented by ~2.5:1. We have attempted to roughly calibrate our floral metagenomic dataset to better conceptually account for this observation (Fig. 5.46). However, even without calibrating read counts based on growth habit, the taxa observed make biogeographical and temporal sense in the context of central Yukon, and their presence is consistent with both palynological records and other ancient eDNA research. Our dataset mirrors that of Willerslev et al. (2014) in which forbs were found to proportionally dominate their metabarcoded sedaDNA during the LGM up

until the Holocene. We suspect that this is at least in part due to eDNA release and preservation characteristics of forbs with higher rates of biomass turnover compared to woody taxa, leading to some degree of genetic over-representative bias. But, the substantial abundance of forbs even when cut by half likely reflects the abundance of flowering herbs on the Pleistocene mammoth-steppe, which may be under-represented palynologically.

The rise in Pinaceae (spruce) around ~10,000 BP, and its growing dominance through our ~6,000 BP samples is consistent with other records from the Yukon that have demonstrated an early development of the boreal forest beginning around 10,000 BP (Wang and Geurts, 1991b; 1991a; Lacourse and Gajewski, 2000; Bunbury and Gajewski, 2009b; Rainville and Gajewski, 2013; Gajewski et al., 2014). We observe similar trends in most plant taxa, albeit with a comparatively less abundant signal for *Betula*. Palynological studies frequently report an abundance of *Betula* with a comparatively small initial influx of *Salix* in the Alaskan-Yukon interior during the terminal Pleistocene shrub expansion and decline of the mammoth-steppe (Wang and Geurts, 1991a; Guthrie, 2006). While we observe a distinct rise in *Betula* at ~13,205 cal BP that persists into the Holocene (Fig. 4.6), the number of *Betula* sedaDNA molecules are comparatively dwarfed by the extreme abundances of Salicaceae (*Salix* [willow] and *Populus* [poplar]). *Betula* is known to be over-represented by pollen, whereas *Salix* is often under-represented palynologically (Pennington and Tutin, 1980; Bradshaw, 1981; Schofield et al., 2007; Roy et al., 2018). The sedaDNA data in this sense may either reflect a more accurate local signature of *Salix* and *Betula* proportionally or may instead be biased in the reverse—questioning the *Betula* driven shrub expansion model typically observed palynologically.

The over-abundance of *Salix* as compared to *Betula* is relevant to the shrub-expansion based extinction model as argued by Guthrie (2006) who contends that an increasing moisture regime and rise of mesic-hydric vegetation with chemical defenses against herbivory (notably *Betula nana* [dwarf birch]) is likely to have driven regional extirpations of grazing megafauna in eastern Beringia. However, if the over-abundance of

Salix compared to *Betula* in this dataset better mirrors palaeo-biomass relative to palynological records, this questions the rise of defensive vegetation as being a driver in the extirpations, as *Salix* is the most preferred food source among contemporary subarctic browsers (Bryant and Kuropat, 1980). While *Bison* and *Equus* are generally considered closer towards the obligate grazer end of dietary guilds (Guthrie, 2001; Fox-Dobbs et al., 2008), both have been observed to exhibit variable grazing and even mixed feeding (Gardner et al., 2007; Jiménez-Hidalgo et al., 2019). *Mammuthus, Equus,* and *Bison* coprolites have also been observed to have a diet variably rich in forbs, and graminoids, with a smaller but notable proportion of shrubs (van Geel et al., 2008; 2011; Willerslev et al., 2014). Further, it is unclear why the 15,000 BP signal decline in *Mammuthus* and *Bison* are associated with a mammoth-steppe ecosystem, predating the rise of woody shrubs in this dataset by some 2,000 years (Fig. 4.5), and predating the Bølling warming by some 500 years (Fig. 4.9). *Equus* sedaDNA persists after this initial decline during early phases of shrub expansion until also flatlining between 13,000–10,000 BP.

Guthrie (2003) observed that horses had undergone body-size declines after the LGM up until their extirpation from Beringia. Mann et al. (2013; 2015) and Rabanus-Wallace et al. (2017) contend that a shifting moisture gradient from xeric to mesic-hydric with the paludification of eastern Beringia best accounts for the loss of dryland-specialists (*Equus*, *Mammuthus*) whereas mesic and mixed feeding seasonal fauna (*Rangifer*, *Cervus*, *Ovibos*) retained suitable habitats and hydric specialists (*Alces*, *Homo sapiens*) were able to invade new Beringian niches. While warming, an increasing moisture regime, the arrival of newly competitive cervid browsers, and the rise of woody shrubs may explain much of the terminal signal decay observed for grazing specialists, this does not explain the relative declines of *Mammuthus* and *Bison* sedaDNA prior to the Bølling–Allerød chronozone—to the degree that sedaDNA abundance is at all correlated with palaeo-biomass. The rise of woody shrubs in this case may be partially explained by the gradual reduction in *Mammuthus* and *Bison* ecosystem engineering. Notably, these animals only appear to have become functionally extirpated from the Klondike following the Younger Dryas—a period characterized by rapid cooling, drought, an alleged extra-

terrestrial impact, and a pronounced rise in archaeological visibility in eastern Beringia (Fig. 4.9 and Fig. 5.1) (Graf and Bigelow, 2011). The Younger Dryas may have been the punctuated spike after an already protracted period of population declines. Seersholm et al. (2020) observed a similar punctuated shift in flora and fauna during the Younger Dryas with sedaDNA from Halls Cave in Texas. They found that while floral diversity recovered following the abrupt return to glacial conditions, faunal diversity did not. Although, how this chronozone may have been so ecologically severe is unclear as it has been observed elsewhere in Beringia that shifts in vegetation were subtle during the Younger Dryas (Bigelow and Edwards, 2001).

The degree to which humans may have been involved in a portion of these transformations depends in part on the believability of the arguably anthropogenic cutmarks at Bluefish Caves, and as to whether those intermittent occurrences from 24,000–15,000 BP (Cinq-Mars, 1979; Cinq-Mars and Morlan, 1999; Harington, 2011; Bourgeon et al., 2017) represent an ecologically significant and sustained human presence in eastern Beringia. This is potentially supported by the identification of fecal biomarkers on the Alaskan North Slope (Vachula et al., 2020), but the lack of evidence for semi-subterranean dwellings and other characteristic features of middle Upper Palaeolithic assemblages as seen in western Beringia and Lake Baikal (Ermolova, 1978, pp. 15–29; Abramova, 1989; Abramova et al., 1991; Goebel, 2002a; Hoffecker and Elias, 2007, pp. 93–96) casts doubt as to whether there was an ecologically significant human presence in eastern Beringia prior to 14,000 BP. Thereafter, megafauna who had already undergone millennia of oscillating climatological and ecological pressures may have been especially vulnerable to novel anthropogenic forces. Post-LGM high mobility lifeways would have been particularly well suited to progressing along stepping stone refugia into the Americas (Haynes, 2013). Therein, even minimal human hunting and niche construction practises such as burning (Laland and O'Brien, 2010; Pinter et al., 2011a; Riede, 2011; Roos et al., 2018) could have increased mortality rates among low fecundity megafauna (Johnson, 2002; Säterberg et al., 2013) to the degree that they were unable to recover from the tumultuous climatic oscillations of the late Pleistocene. In this case,

anthropogenic contributions are at most a contributing factor to the final extirpations in eastern Beringia, which remains difficult to differentiate from the Younger Dryas chronozone. SedaDNA analyses of Pleistocene permafrost targeting human DNA may be key to addressing lingering unknowns in the peopling of Beringia. As is a sedaDNA investigation of the critical 2500-year gap between 12,800 BP and 10,300 BP.

4.4.2 Megafaunal ghost ranges

We observe a persistence of *Equus* and *Mammuthus* sedaDNA until ~10,000 cal BP, perhaps as late as 6,000 cal BP (Fig. 4.4), far beyond the last dated macro-remains for these taxa (*Equus*: 12,558 cal BP in Alaska, 15,421 cal BP in Yukon; *Mammuthus*: 13,211 cal BP in Alaska, 13,784 cal BP in Yukon). However, interpreting ghost ranges with sedaDNA necessitates caution. Arnold et al. (2011) found that although permafrost contains a wealth of well-preserved eDNA, the favorable characteristics of perennially frozen ground increases the likelihood for allochthonous organics being redeposited within younger strata. They argue that while reworked strata are of less concern when assessing first appearance dates and "abundant" sedaDNA signals, reworked strata are an inherent problem when assessing LQE last appearance dates. They highlight the careful analysis of loess sediments from the Stevens Village site in central Alaska where Haile et al. (2009) utilized ^{14}C, OSL, extensive eDNA sampling on and off site, and careful sedimentological analyses to plausibly infer the late survival of *Mammuthus* and *Equus* to as late as ~10,000 BP. The cores we used to construct our sample set were not recovered with ancient DNA in mind, but were instead selected to expediently follow up on results presented by Murchie et al. (2021b). Although we acknowledge that the signals for late megafaunal persistence should be interpreted with careful skepticism, and require additional supporting evidence, they are not implausible on their face, for the following reasons.

First, the ghost range signal observed for *Mammuthus* and *Equus* is observed at three different sites in 6–9 separate permafrost cores, and is correlated with substantial, consistent changes in vegetation. In samples younger than 13,000 cal BP there is a complete restructuring of vegetation; many new plant species appear while others are

substantially reduced in abundance. To our knowledge, no plant taxa completely disappeared during the transition, which limits our ability to utilize the plant data to chronologically test for allochthonous sedaDNA. However, the megafaunal read counts observed in the alleged ghost range samples are comparable to those observed during periods of known presence. It is reasonable to ask how many reads are sufficient to say an organism was truly present, but there cannot be any single answer to that question. At the same time, *Mammuthus* counts as high as 56 or 61 unique sedaDNA molecules at ~10,000 cal BP seem relatively high considering the substantial turnover in vegetation.

Certainly in the case of cores with sediments younger than 13,000 cal BP, the presence of *Mammuthus* and *Equus* extending to ~10,000 cal BP is highly consistent with other investigations (Vartanyan et al., 2008; Haile et al., 2009; Graham et al., 2016; Pečnerová et al., 2017). Furthermore, reads for these megafaunal taxa are observed at two sites across all subsampled replicates and are associated with a completely different plant ecological signature. Here the point is that it would be expected that both floral and animal sedaDNA would be reworked at similar rates, which is not what is observed. Graminoids and forbs do persist, as would be expected, but there is no obviously mixed ecological signal.

The youngest signatures for *Equus* and *Mammuthus*, ca. ~6000 cal BP, are of great interest because they imply local survival of these taxa long after the Pleistocene-Holocene transition. If very late insular occurrences of mammoths are ignored (Graham et al., 2016), there are no accepted radiocarbon dates on mammoth or horse macrofossils in Beringia that fall anywhere close to the mid-Holocene. Although the authenticity of the identifications is not in question, the wide temporal gap between these late samples and all others is concerning. However, this point needs to be evaluated in context. Palaeontological and archaeological records across much of the Arctic and Subarctic are notably sparse. Small refugial populations, already functionally extinct, might have survived in remote pockets at sizes too small to be readily detectable by random fossil collecting. The case of *Mammuthus* survival on St. Paul and Wrangel islands in the Bering and Chukchi Seas until 5500 and 4000 cal years BP respectively (Vartanyan et al.,

2008; Graham et al., 2016) is especially interesting, because until recent decades neither population was known to have lasted into the mid-Holocene. *Bison priscus* was likewise discovered to have survived throughout the Holocene in southern Yukon (Heintzman et al., 2016; Zazula et al., 2017b). Conroy et al. (2020) observe a persistence of coprophilous fungi in the Alaskan interior at Windmill and Jan Lakes until ~9000 cal BP and 4500 cal BP. This consistent spore accumulation may be related to biomass replacement by browsing cervids, but may also serve as supporting evidence of a high-latitude refugium of Pleistocene megafauna until the mid-Holocene. The way forward is through further testing and confirmation, which can be achieved by sampling a broader range of high latitude sites where reworking is negligible and taxon spectra can be recovered for the widest possible range of organisms.

4.5 Conclusion

The late Pleistocene palaeontological record of Beringian megafauna is robust compared to many other areas of Eurasia and the Americas (Stuart, 2015), but it is nevertheless too sparse to effectively tease apart the complexity of factors involved in the Pleistocene-Holocene transition and the coeval collapse of the megafauna. While our sample set here is also coarse, the data retrieved highlight the power of environmental DNA for the recovery of highly complex signals of ecological change from exceptionally small sediment inputs, and in the absence of any macro-scale biological tissues. Utilizing targeted enrichment for sedaDNA is also far more efficient for high-throughput sequencing applications compared to a shotgun approach where Murchie et al. (2021b) had 0.002% macro-ecological on-target sequence data out of ~21 million reads with shotgun sequenced versions of the samples processed here, compared to as much as ~10% on-target with PalaeoChip enrichments. If this sedaDNA approach were paired with a robust sampling effort targeting sites with clear evidence of stratigraphic integrity across multiple regions and with tight temporal control, these records could prove to be key to unraveling the ambiguities of this extinction event that has confounded Quaternary science since the 1800s.

4.6 Acknowledgements

Thanks to Ana T. Duggan for the development and maintenance of her exceptional ancient DNA pipeline. Further, thanks to Brian Golding for providing access to his computational resources, which were invaluable to the processing of these datasets. Thanks to all members and affiliates of the McMaster Ancient DNA Centre for their ongoing support, as well as the admin and faculty of the Anthropology department at McMaster University. Special thanks to Melanie Kuch, Jennifer Klunk, Marissa L. Ledger, and Kévin Roche for their wet-lab assistance. Thanks to CANA foundation for their support as well as our colleagues in the Future Arctic Ecosystems (FATE) research consortium. We wish to also thank McMaster University, the Arctic Institute of North America, the Garfield Weston Foundation, the Natural Sciences and Engineering Research Council of Canada, McMaster University, Polar Knowledge Canada (POLAR), and the Social Sciences and Humanities Research Council of Canada for each funding various components of this research. Thank you to the placer gold mining community of the Klondike and the Tr'ondëk Hwëch'in for their continued support of our research and access to study sites in the central Yukon.

4.7 Materials and Methods

A detailed description of sampling sites as well as wet lab procedures from subsampling to sequencing and bioinformatic processing are in the supplementary online materials (sections 5.3.1–5.3.8).

4.7.1 Summary

Subsamples of 21 permafrost cores recovered from the Klondike region of Yukon, Canada (Fig. 4.1, Table 4.1)—dating between 30,000–6,000 calibrated years before present (BP)—were processed for sedimentary ancient DNA (sedaDNA) to evaluate changing biomolecular signals of plants and animals during the late Pleistocene-Holocene transition in eastern Beringia near the mouth of the ice-free corridor. We utilized a sedaDNA modified Dabney et al. (2013b) extraction procedure with the long cold spin inhibitor removal technique as described in Murchie et al. (2020), and prepared double

stranded, dual-indexed libraries (Meyer and Kircher, 2010; Kircher et al., 2012) for targeted enrichment (Fig. 4.2). We used the PalaeoChip Arctic-1.0 plant and animal baits (Murchie et al., 2021b) to capture enrich these libraries for chloroplast barcoding loci (*trn*L, *mat*K, *rbc*L) of arctic/subarctic plants and for whole mitochondrial genomes (or singular loci where mitogenomes were unavailable at the time of bait-design in 2017) of extinct and extant northern animals (focused on megafauna). Libraries were sequenced on an Illumina HiSeq 1500 with 2x90 paired-end read chemistry.

After trimming, merging, and filtering the sequenced reads (detailed in the supplement, section 5.3.8), *BLASTn* (Altschul et al., 1990) was used to taxonomically identify the reads to the top 600 hits against a July 2019 local copy of the GenBank database (Benson et al., 2013; Agarwala et al., 2016), which was used as the input for *MEGAN Community Edition* (Huson et al., 2007; 2016) (v6.19.7, https://github.com/husonlab/megan-ce) and *PIA* (Phylogenetic Intersection Analysis; Cribdon et al., 2020) (v 5.3, https://github.com/Allaby-lab/PIA). The outputs from *MEGAN* are plotted in the main text, while plots of individual extraction replicates from both *MEGAN* and *PIA* are included in the supplement. *MapDamage* (Jónsson et al., 2013) (v2.0.3, https://ginolhac.github.io/mapDamage/) was used to assess the aDNA damage signals of taxonomically identified taxa, which are included in the supplement (section 5.6.4). All other analyses are detailed further in the supplement.

4.7.2 Field sampling

The permafrost samples used in this analysis were previously collected, dated, and analyzed by D'Costa et al. (D'Costa et al., 2011), Mahony (2015), and Sadoway (2014), then kept in cold storage at the McMaster Ancient DNA Centre. Prior to core collection by all three original research teams, the sampling area was cleared of eroded materials back to frozen sediments to create a fresh coring surface for a ~10 cm diameter coring tube ~30 cm in length. Horizontal core samples were drilled with a small portable drill, recovered frozen, stored individually in plastic bags, and transported frozen to the University of Alberta or McMaster University for subsampling. Horizontal permafrost cores were collected from Bear Creek, Upper Quartz, and Upper Goldbottom. Vertical

cores were taken from Lucky Lady II. See Fig. 4.1 for site locations within the Klondike region of Yukon, Canada. See Table 1 for a list of sample information. Site descriptions can be found in the supplement (section 5.3.1).

4.8 Tables

Table 4.1 Permafrost cores analyzed for sedaDNA.

Site	Core ID	DNA ID	Age (BP)[1]	Input (grams)[2]	Total raw reads	PalaeoChip Mapped & *MEGAN* assigned[3]
Bear Creek	BC 4-2B	PHP-1	30,000	1.05	5,650,809	241,143 *(4.27%)*
Lucky Lady II	LL2S-189-E	PHP-2	10,220	0.9	8,667,496	9,908 *(0.11%)*
	LL2S-253-D1	PHP-3	10,340	0.6	9,303,528	491,487 *(5.28%)*
	LL2C-118-C	PHP-4	13,105	0.6	7,749,177	178,973 *(2.31%)*
	LL2C-205-B	PHP-5	13,150	0.6	4,997,824	48,226 *(0.96%)*
	LLII 12-84-3	PHP-6	13,205	1.35	10,235,721	806, 601 *(7.88%)*
	LL2C-243-A2	PHP-7	13,870	0.6	5,820,472	54,700 *(0.94%)*
	LLII 12-170-6	PHP-8	15,405	0.3	1,331,181	17,628 *(1.32%)*
	LLII 12-217-8	PHP-9	15,865	1.05	3,115,296	38, 566 *(1.24%)*
Upper Goldbottom	MM12-118B	PHP-11	9,685	1.35	7,983,085	541,521 *(6.78%)*
	MM12-119B	PHP-12	10,340	1.5	18,409,441	1,823,618 *(9.91%)*
	MM12-116b	PHP-13	17,500	0.3	1,624,580	174,890 *(10.77%)*
	MM12-115b	PHP-14	18,510	0.3	2,320,965	35,539 *(1.53%)*
	MM12-117b	PHP-15	21,775	0.3	1,910,387	164,997 *(8.64%)*
Upper Quartz	MM12-QC-10	PHP-19	5,765	0.6	9,244,928	190,555 *(2.06%)*
	MM12-QC-9	PHP-20	5,840	0.6	5,913,447	312,597 *(5.29%)*
	MM12-QC-8	PHP-21	5,915	0.6	5,142,454	265889 *(5.17%)*
	MM12-QC-6	PHP-22	12,805	0.6	6,080,182	114,978 *(1.89%)*
	MM12-QC-4	PHP-23	14,925	0.9	14,729,646	68,186 *(0.46%)*
	MM12-QC-3	PHP-24	15,745	0.3	1,129,623	17,162 *(1.52%)*
	MM12-QC-2	PHP-25	16,560	0.3	1,568,411	29,419 *(1.88%)*
Blanks	Extraction (9) & library (4) negative controls				102,440	81 *(0.08%)*
			TOTAL		133,031,093	5,626,664 *(4.23%)*

Core identifications (ID) and age estimates (years before present) as per D'Costa et al. (2011) for Bear Creek, Sadoway (2014) for Lucky Lady II, and Mahony (2015) for Upper Goldbottom and Upper Quartz. See Table 5.13 in the supplementary online materials for a full breakdown of sedaDNA replicates per core.
PHP = Pleistocene-Holocene Permafrost.
[1]Mean age estimates from original sources.
[2]Input across extract replicates.
[3]Sequenced reads that pass quality filters for de-duplication, adaptemer removal, minimum size (24 bp), and map to the PalaeoChip references that could then also be *BLASTn* aligned and taxonomically binned in *MEGAN*. Percent on-target reads (those that map to the PalaeoChip references) of total raw sequenced reads.

4.9 Figures

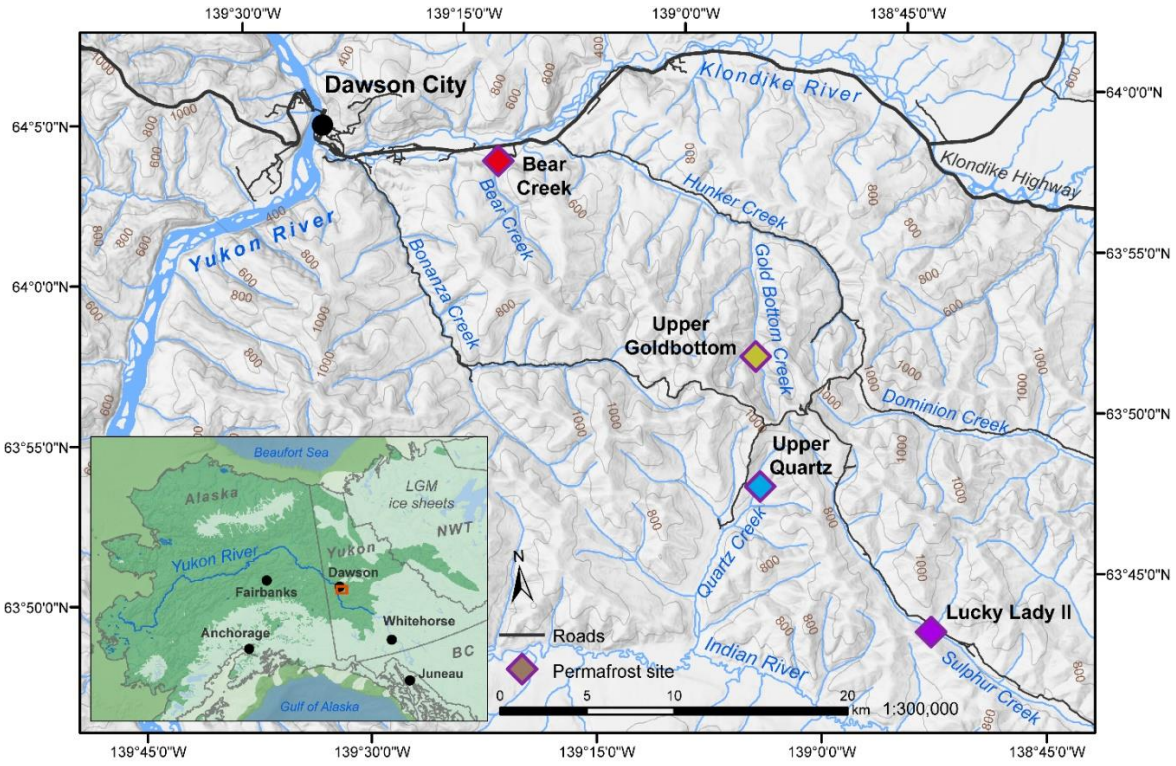

Fig. 4.1 Permafrost sites from the Klondike region of Yukon, Canada. Base map data retrieved from GeoYukon; contours elevation unit: meters above sea level. See Fig. 4.3 for description of inset map data sources.

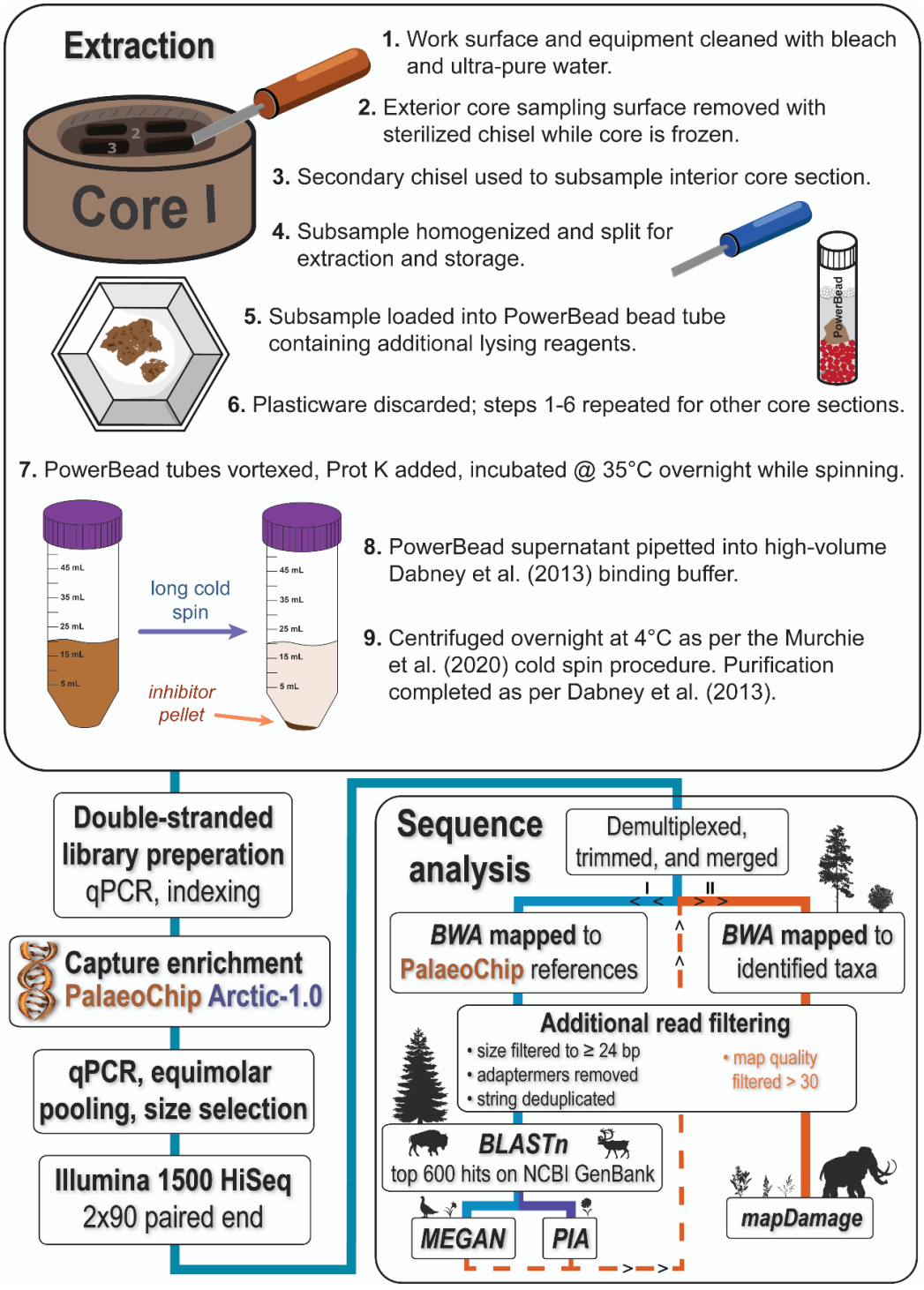

Fig. 4.2 Workflow schematic from wet-lab procedures (extraction to sequencing) to *in silico* sequence analysis.

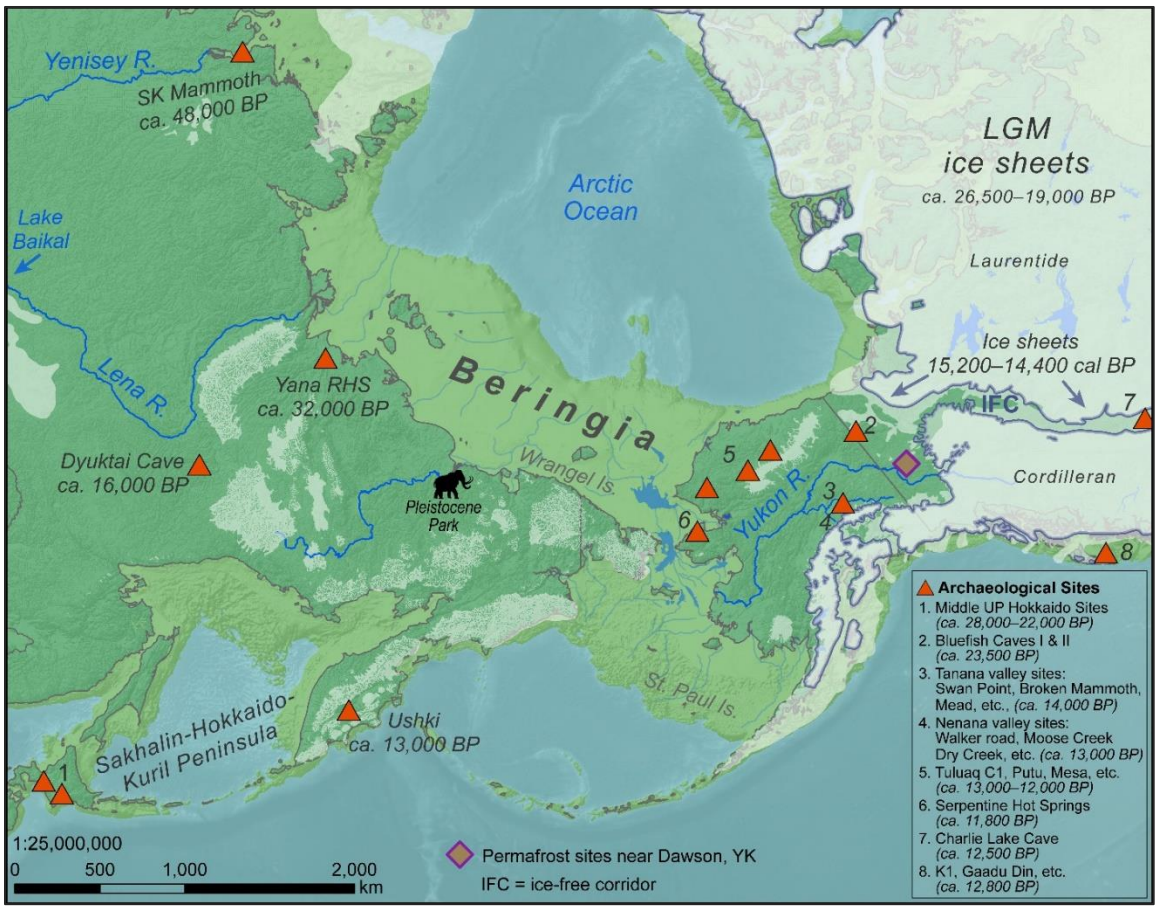

Fig. 4.3 Beringia during the Late Pleistocene. Includes select archaeological sites and geographic areas discussed in text. Ice sheet data at Last Glacial Maximum (LGM, 26.5–19 ka BP) (Clark, 2009) and 12.5 ^{14}C ka BP (15.2–14.4 cal ka BP) from Dyke (2004). Sea level during LGM set to 126 meters below sea level (m bsl) based on midpoint between maximum and minimum eustatic sea level estimation models in Clark and Mix (2002). Beringian palaeodrainage data from Bond (2019) (http://data.geology.gov.yk.ca/). Archaeological sites and ages from (Potter et al., 2018).

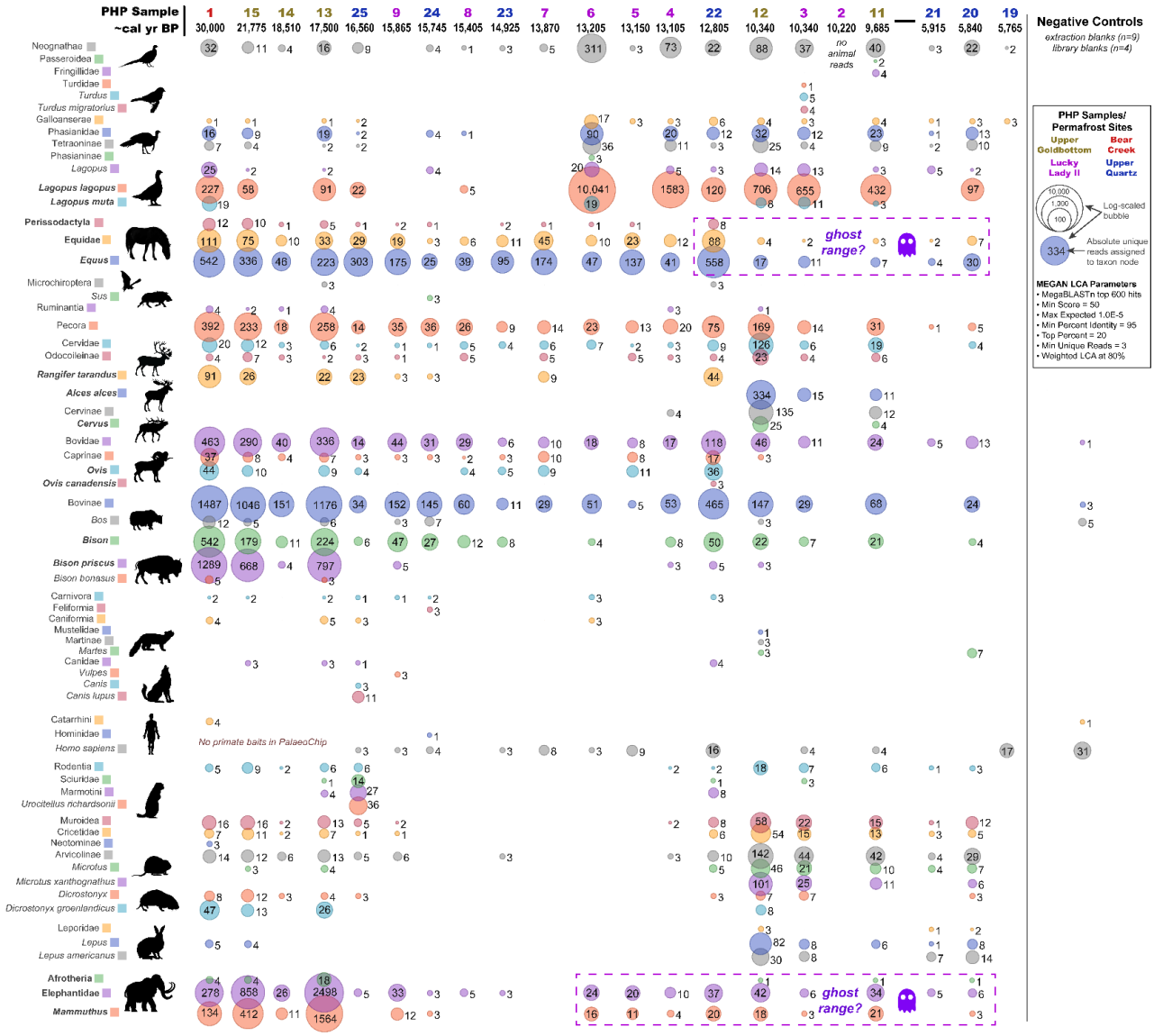

Fig. 4.4 Animalia metagenomic comparison of permafrost core subsamples analyzed using *BLASTn* to *MEGAN-LCA* assigned reads. Values indicate unique reads assigned to that taxon node.

Last dated remains of *Equus*: 12,558 cal BP (Alaska), 15,421 cal BP (Yukon).
Last dated remains of *Mammuthus*: 13,211 cal BP (Alaska), 13,784 cal BP (Yukon).

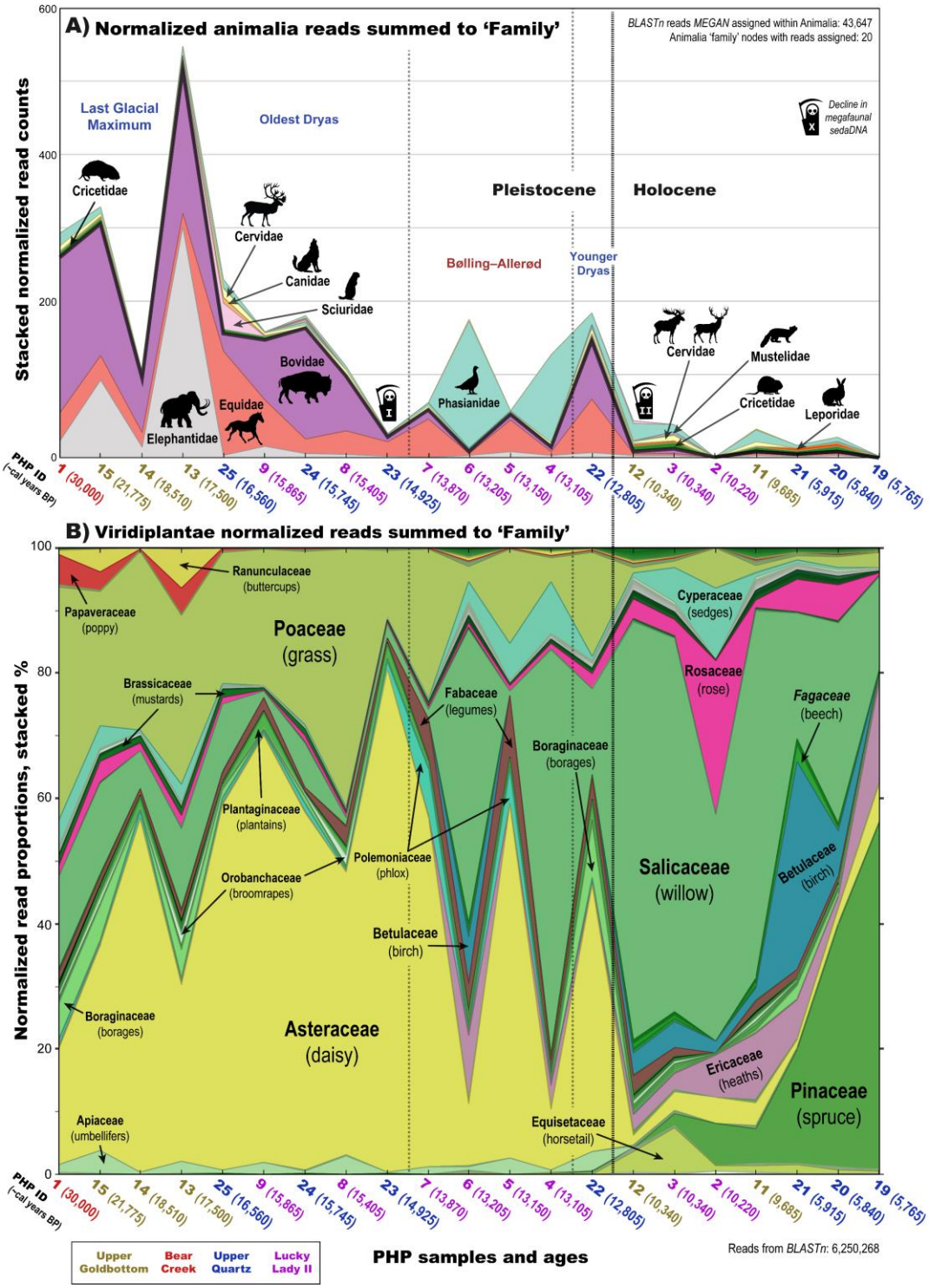

Fig. 4.5 Stacked normalized reads assigned to the 'family' rank in **A)** Animalia (insects excluded) with read counts, and **B)** Viridiplantae with stacked percentage proportions. See Fig. 4.4 and Fig. 4.6 for absolute read counts.

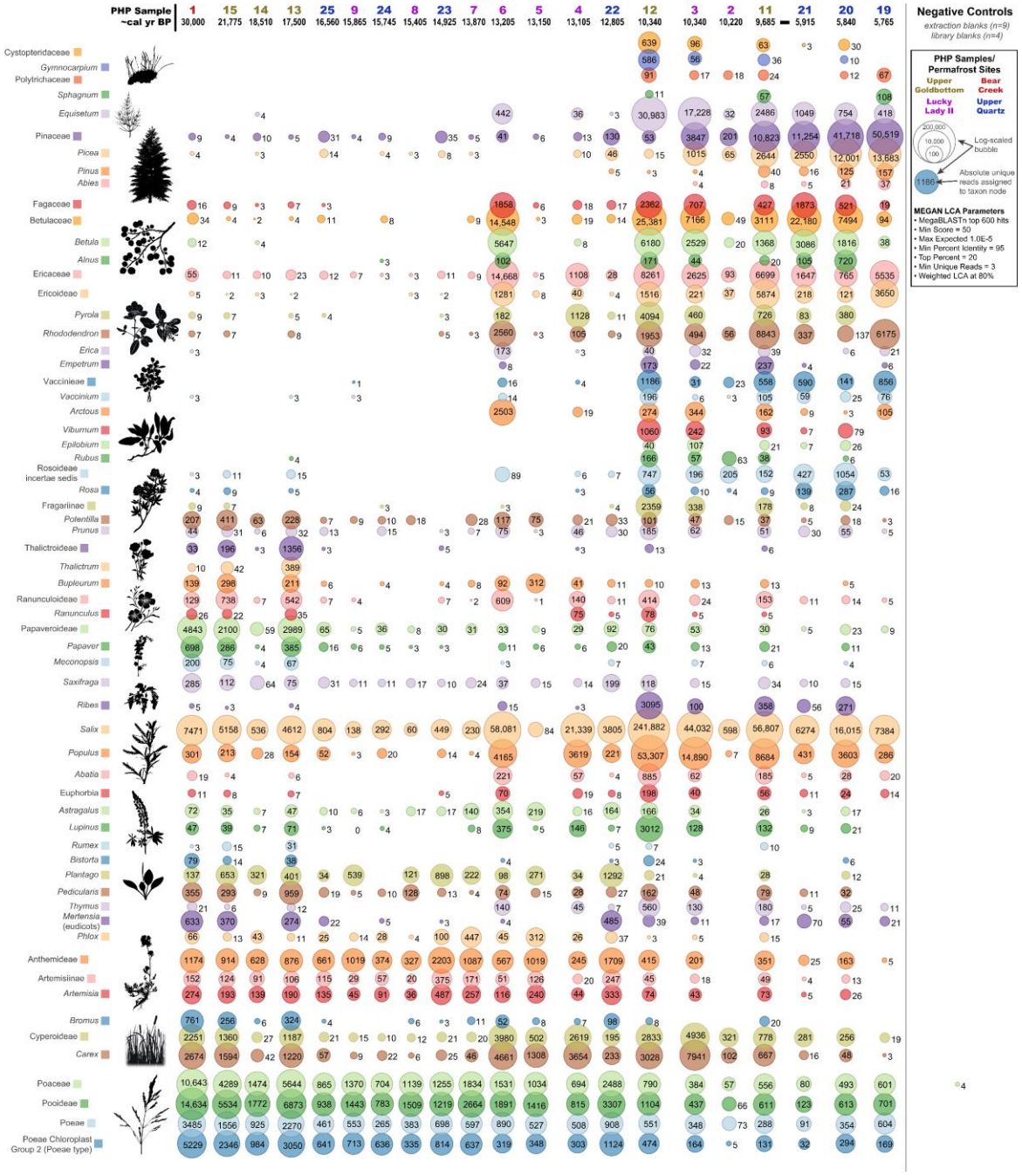

Fig. 4.6 Viridiplantae metagenomic comparison of permafrost core subsamples analyzed using *BLAST*n to *MEGAN* assigned reads. Values indicate unique reads assigned to that taxon node. Select taxon nodes depicted.

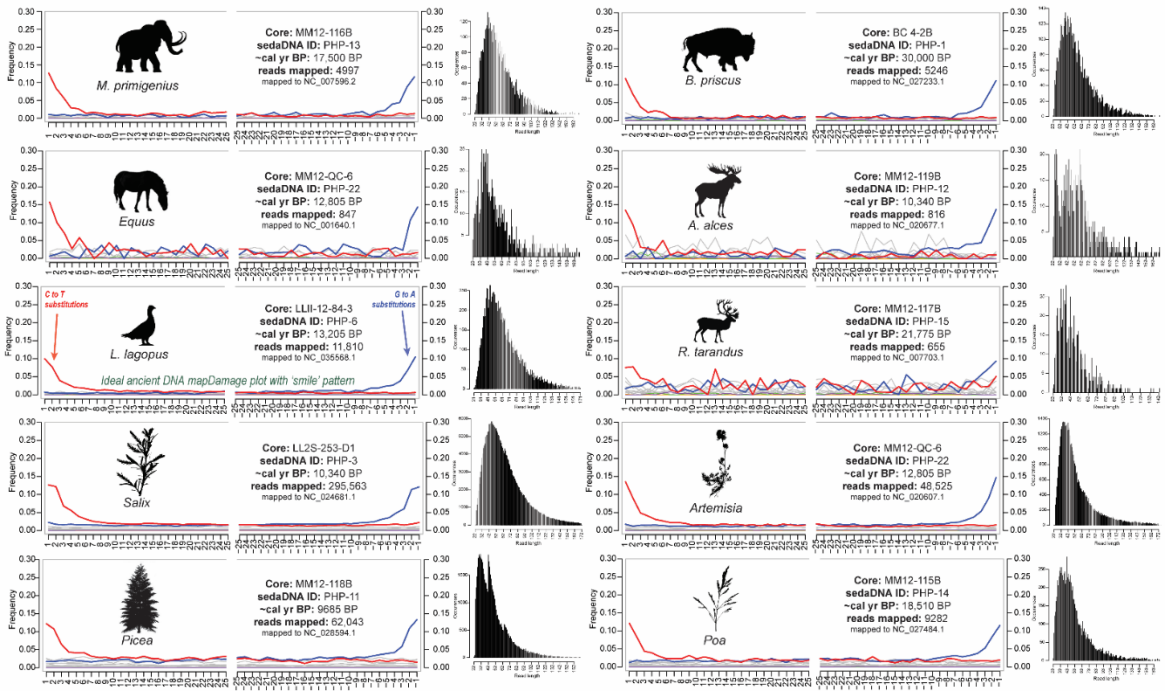

Fig. 4.7 Example *mapDamage* plots. Minimum size 24 bp, minimum map quality 30. See section 5.6.4 (Figs. 5.8–5.21) for a full breakdown of fragment misincorporation plots by taxa and core.

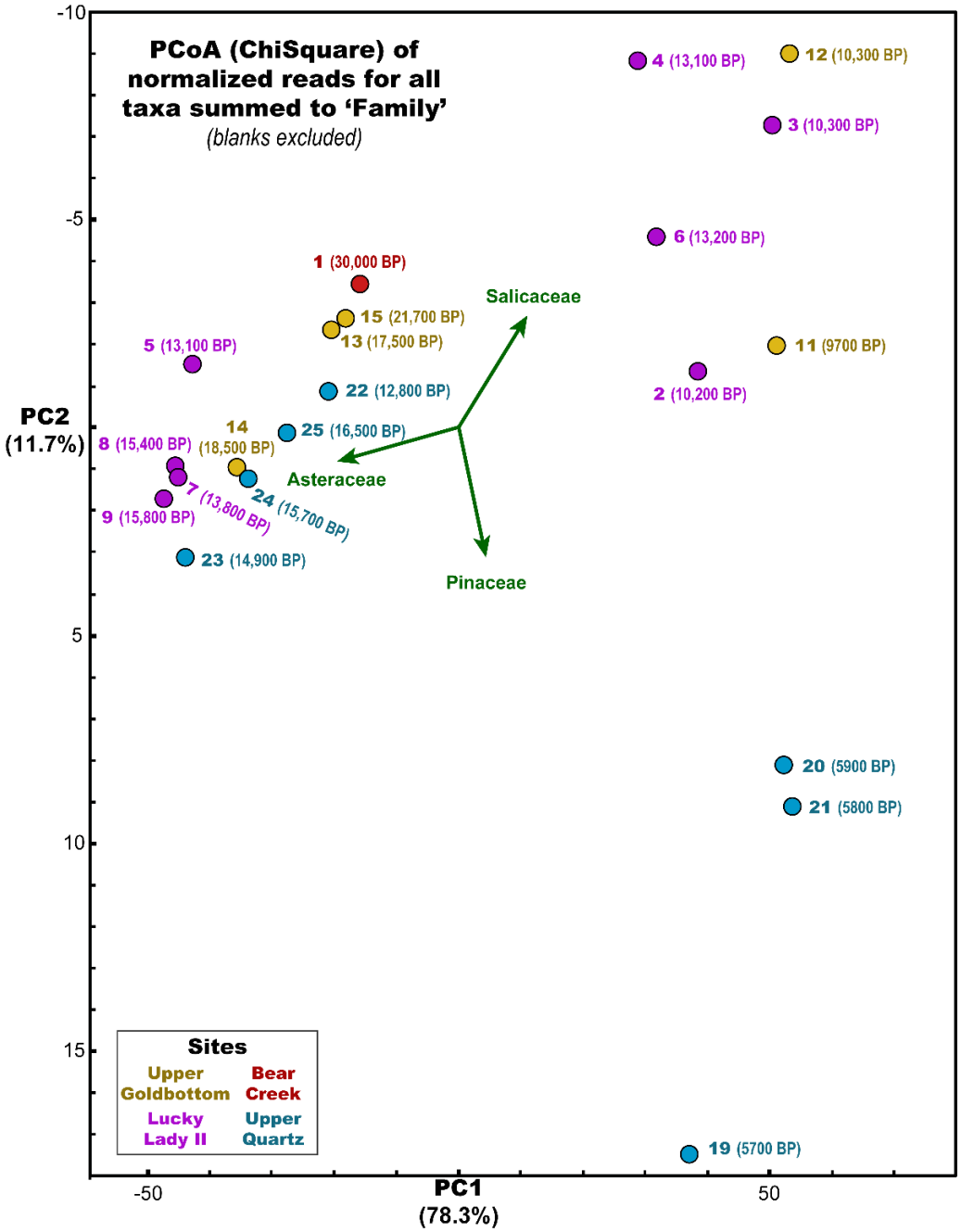

Fig. 4.8 Metagenomic principal coordinates analysis (PCoA) produced in *MEGAN* (Huson et al., 2016) using a chi-square ecological index (Lebart et al., 1977).

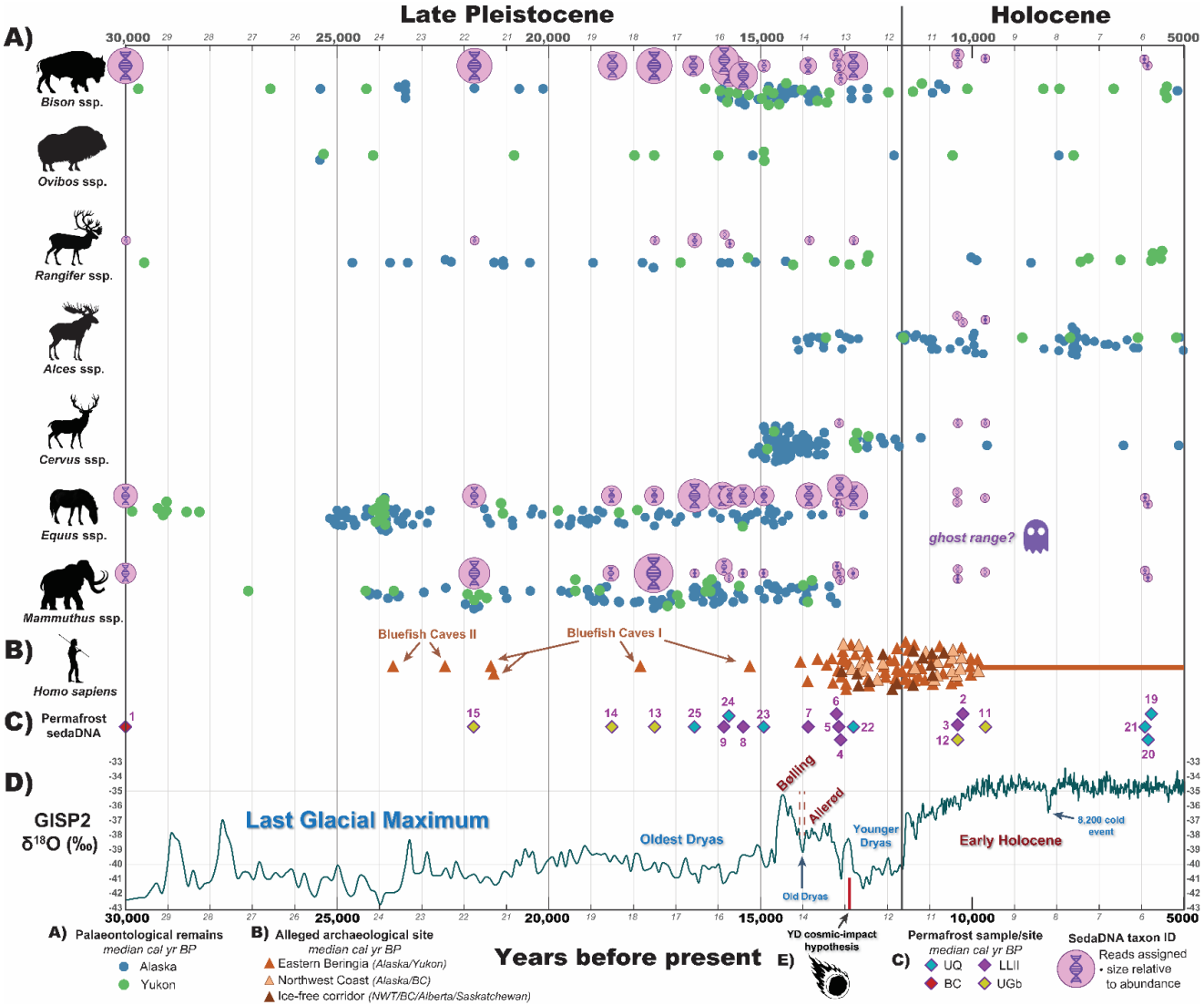

Fig. 4.9 Synthesis of palaeontological, archaeological, climatological, and megafaunal sedaDNA data.
A) Dated macro-remains of select megafaunal taxa in eastern Beringia (Conroy et al., 2020).
B) Earliest archaeological sites in northwestern North America (Potter et al., 2018).
C) Central Yukon permafrost samples analyzed in this study.
D) Greenland Ice Sheet Project 2 (GISP2) oxygen isotope profiles at 2 meter intervals (Grootes and Stuiver, 1997).
E) Onset of the Younger Dryas, and alleged (highly controversial) cosmic impact hypothesis (Wolbach et al., 2018).

Chapter 5

Supplemental materials for "Ecological turnover and megafaunal ghost ranges as revealed by palaeoenvironmental DNA"

5.1 Palaeontology additional data

Table 5.1 Bestiary of Pleistocene-Holocene extripations based on Stuart (2015).

Peri-LGM phase (40,000–15,000 cal BP)		
Eurasia	**Beringia**	**North America south of ice sheets**
Ursus spelaeus (cave bear)	*Arctodus simus* (short-faced bear)	*Eremotherium rusconii* (E. laurillardi sloth)
Crocuta crocuta (spotted hyaena)	*Homotherium serum* (a sabretooth cat)	*Glyptotherium floridanum* (a glyptodont)
Panthera spelaea (cave lion)		*Holmesina septentrionalis* ('giant armadillo')
Megaloceros giganteus (giant deer)		*Paramylodon* (*Glossotherium*) *harlani* (Harlan's ground sloth)
Palaeoloxodon naumanni (Naumann's elephant)		*Miracinonyx trumani* (American cheetah)
Homotherium latidens (a sabretooth cat)		*Homotherium serum* (a sabretooth)
		Canis dirus (dire wolf)
Pleistocene-Holocene transition (after 15,000 BP) to mid-Holocene		
Eurasia	**Beringia**	**North America south of ice sheets**
Coelodonta antiquitatis (woolly rhino)	*Mammuthus primigenius* (woolly mammoth)	*Panthera atrox* (American lion)
Panthera spelaea (cave lion)	*Panthera spelaea* (cave lion)	*Arctodus simus* (short-faced bear)
Mammuthus primigenius (woolly mammoth)	*Saiga tatarica* (saiga antelope)	*Megalonyx jeffersonii* (Jefferson's ground sloth)
Bison priscus (steppe bison)	*Equus caballus* (caballine horse)	*Mammuthus columbi* (Columbian mammoth)
Megaloceros giganteus (giant deer)	*Haringtonhippus francisci* (New World stilt-legged horse)	*Mammuthus primigenius* (woolly mammoth)
	Bootherium bombifrons (Harlan's musk ox)	*Mammut am*ericanum (mastodon)
	Bison priscus (steppe bison) (DNA evidence suggests persistence until ~400 yrs BP)	Equidae (horses)
		Platygonus compressus and *Mylohyus nasutus* (extinct peccaries)
		Palaeolama mirifica (extinct lama)
		Hemiauchenia macrocephala (large-headed lama)
		Cervalces scotti (extinct moose)
		Bootherium bombifrons (Harlan's musk ox)
		Navahoceros fricki (American mountain deer)
		Stockoceros onusrosagris (a pronghorn)
		Camelops hesternus (western camel)
		Castoroides ohioensis (giant beaver)
		Smilodon fatalis (a sabretooth)
		Nothrotheriops shastensis (Shasta ground sloth)
		Oreamnos harringtoni (extinct mountain goat)
		Bison priscus (steppe bison)

*List is not exhaustive.

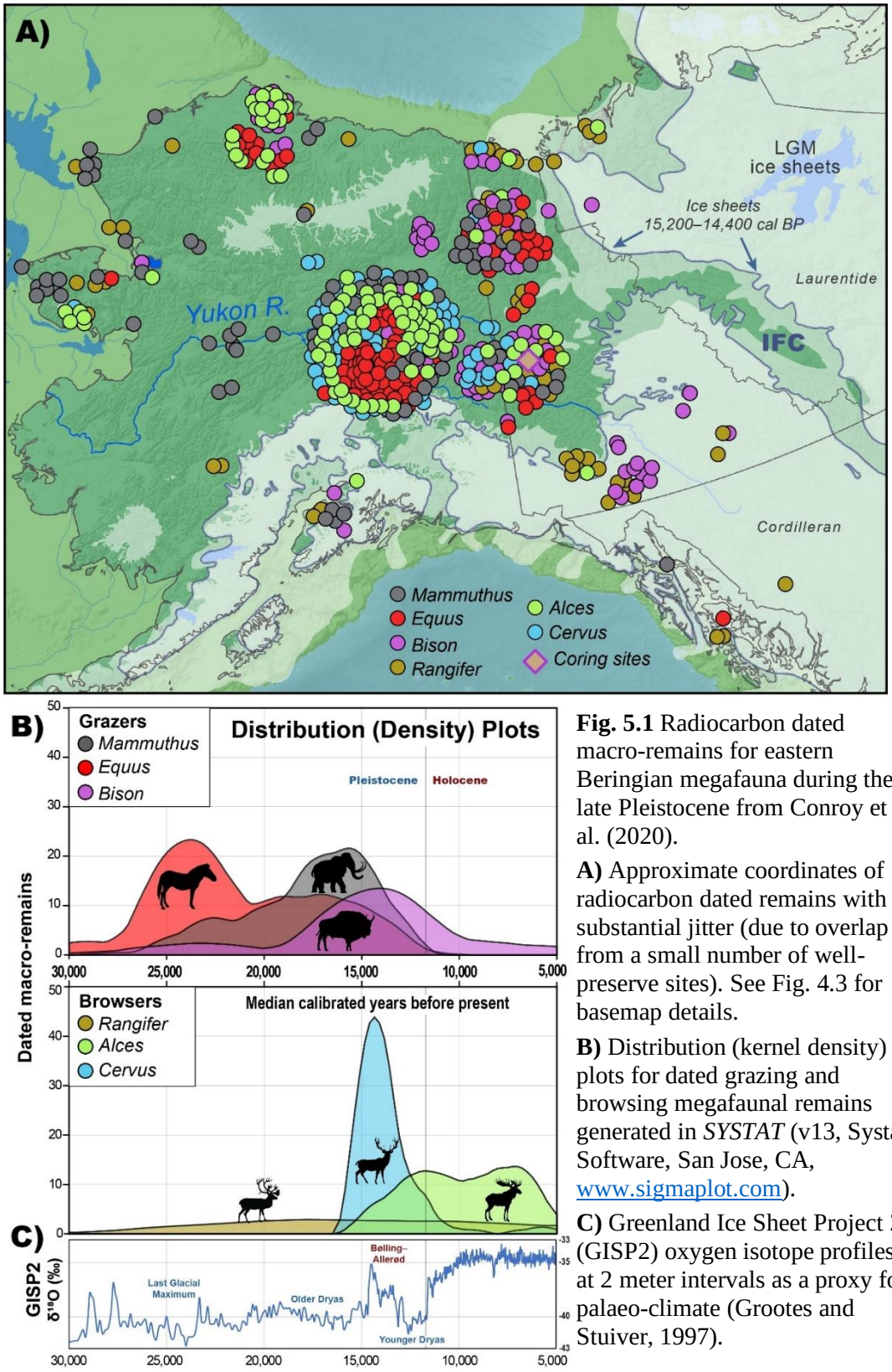

Fig. 5.1 Radiocarbon dated macro-remains for eastern Beringian megafauna during the late Pleistocene from Conroy et al. (2020).

A) Approximate coordinates of radiocarbon dated remains with substantial jitter (due to overlap from a small number of well-preserve sites). See Fig. 4.3 for basemap details.

B) Distribution (kernel density) plots for dated grazing and browsing megafaunal remains generated in *SYSTAT* (v13, Systat Software, San Jose, CA, www.sigmaplot.com).

C) Greenland Ice Sheet Project 2 (GISP2) oxygen isotope profiles at 2 meter intervals as a proxy for palaeo-climate (Grootes and Stuiver, 1997).

5.2 Beringian archaeology additional data

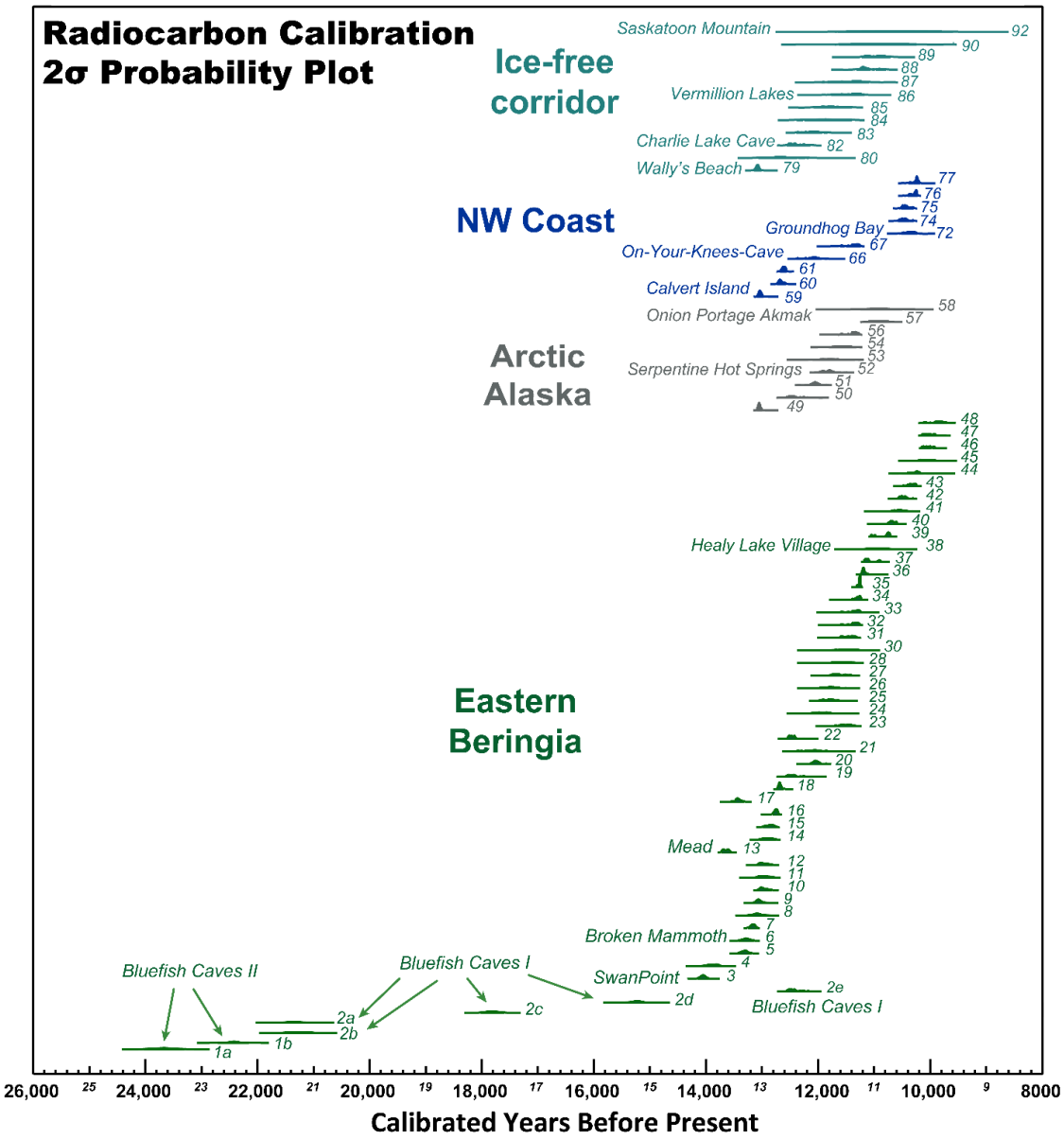

Fig. 5.2 Radiocarbon calibration plot of the earliest alleged archaeological sites in northwestern North America. Data compiled by Potter et al. (2018). Calibrated using Calib Rev 7.0.4 with IntCal13 (Stuiver and Reimer, 1993; Reimer et al., 2013; Stuiver et al., 2020) (http://calib.org/). See the supplementary materials of Potter et al. (2018) for the original data, and Table 5.2 for calibration data.

Table 5.2 Potter et al. (2018) data of earliest archaeological sites in northwestern North America.

Intcal ID	Site/Component	Ages				Area	Ref
		^{14}C yr BP[1]	±	n of dates	Median cal yr BP		
1a	Bluefish Caves II	19,650	130	7	**23674**	BI	49
1b	Bluefish Caves II	18570	110	7	**22441**	BI	49
2a	Bluefish Caves I	17,610	100	7	**21290**	BI	49
2b	Bluefish Caves I	17,660	100	7	**21361**	BI	49
2c	Bluefish Caves I	14,645	75	7	**17826**	BI	49
2d	Bluefish Caves I	12,790	65	7	**15241**	BI	49
2e	Bluefish Caves I	10,490	55	7	**12449**	BI	49
3	Swan Point CZ4	12,160	20	8	**14053**	BI	83
4	Little John sub-paleosol	12,020	70	1	**13879**	BI	84
5	Mead CZ5	11,460	50	1	**13308**	BI	75
6	Broken Mammoth CZ4	11,440	60	2	**13283**	BI	85
7	Upward Sun River C1	11,320	30	3	**13163**	BI	86
8	Walker Road C1	11,220	90	3	**13086**	BI	87
9	Moose Creek C1	11,190	60	1	**13060**	BI	88
10	Linda's Point	11,100	40	2	**12980**	BI	89
11	Dry Creek C1	11,120	90	1	**12971**	BI	90
12	Owl Ridge C1	11,110	60	2	**12975**	BI	91-92
13	Mead CZ4	11,808	20	5	**13646**	BI	75
14	Bachner C1	11,030	70	1	**12897**	BI	93
15	Teklanika West C1	11,000	40	2	**12857**	BI	94
16	Eroadaway	10,890	40	1	**12753**	BI	95
17	MacDonald Creek (FAI-2043)	11,600	50	1	**13430**	BI	96-97
18	MacDonald Creek (FAI-2043)	10,730	40	1	**12683**	BI	96-97
19	Moose Creek C2	10,500	60	1	**12457**	BI	88
20	Mead CZ3	10,270	20	5	**12039**	BI	98
21	Broken Mammoth CZ3	10,290	70	1	**12082**	BI	85
22	Owl Ridge C2	10,490	30	7	**12473**	BI	91-92
23	Owl Ridge C2	10,020	40	6	**11508**	BI	91-92
24	Phipps	10,230	70	1	**11948**	BI	99
25	Upward Sun River C2	10,140	40	2	**11804**	BI	86
26	FAI-2077	10,130	50	1	**11774**	BI	96-97
27	Swan Point CZ3	10,080	40	3	**11650**	BI	83
28	XBD-308	10,050	70	1	**11576**	BI	100
29	XBD-338 C1	>10000	80*	1	**11478**	BI	100
30	XBD-338 C2	10,000	80	1	**11502**	BI	100
31	Upward Sun River C3	9,990	30	3	**11446**	BI	101
32	Whitmore Ridge C1	9,950	40	3	**11356**	BI	102
33	Little Delta River #3	9,920	60	1	**11341**	BI	100
34	Panguingue Creek C1	9,890	50	3	**11291**	BI	103
35	Carlo Creek C1	9,880	20	6	**11259**	BI	104
36	Gerstle River C1	9,740	40	1	**11188**	BI	105
37	Dry Creek C2	9,660	30	9	**11111**	BI	90
38	Healy Lake Village Chindadn (2 hearths)	9,580	110	2	**10923**	BI	106
39	Little John Paleosol	9,510	20	6	**10763**	BI	84
40	Gerstle River	9,450	40	2	**10685**	BI	105
41	XBD-303	9,340	80	1	**10547**	BI	100
42	XBD-312	9,290	40	1	**10487**	BI	100
43	Sparks Point	9,170	50	3	**10336**	BI	107
44	Chugwater C2	9,080	90	2	**10249**	BI	108-109
45	XBD-306	8,930	90	1	**10025**	BI	100
46	Gerstle River C3	8880	20	9	**10037**	BI	105
47	Upward Sun River C4	8,870	30	2	**10028**	BI	86
48	Teklanika West C2	8,820	40	1	**9867**	BI	94
49	Tuluaq C1	11,160	20	5	**13051**	NA	110
50	Putu	10,490	70	1	**12433**	NA	111
51	Raven Bluff	10,280	30	7	**12049**	NA	112
52	Serpentine Hot Springs	10,150	30	3	**11828**	NA	113
53	HAR-006	10,140	90	1	**11769**	NA	114
54	Irwin Sluiceway	10,050	50	2	**11565**	NA	115
55	Mesa	10,000	80*		**12106**	NA	116
56	Nat Pass	9,960	30	2	**11360**	NA	117

Intcal ID	Site/Component	Ages				Area	Ref
		^{14}C yr BP[1]	±	n of dates	Median cal yr BP		
57	NR-5	9,570	60	2	**10930**	NA	118
58	Onion Portage Akmak	9,570	150	1	**10900**	NA	119
59	Calvert Island (EjTa-4)	11,140	25	1	**13036**	NWC	39
60	Calvert Island (EjTa-4)	10,720	60	5	**12669**	NWC	39
61	Calvert Island (EjTa-4)	10,625	20	1	**12614**	NWC	39
62	K1 Cave	10,960	80*		**12837**	NWC	120
63	Gaadu Din 1 Cave	10,620	80*	6	**12592**	NWC	121
64	Gaadu Din 2 Cave	10,530	80*	12	**12478**	NWC	122
65	Cardinalis Creek	10,370	80*		**12235**	NWC	123
66	On-Your-Knees Cave	10,300	50	1	**12106**	NWC	124
67	Hunter Island	9,940	50	1	**11355**	NWC	125
68	Namu	9,700	80*		**11091**	NWC	126
69	Kilgii Gwaay	8,540	80*	12	**10890**	NWC	121
70	Hidden Falls	9,500	80*		**10818**	NWC	127-128
71	Arrow Creek 2	9,500	80*		**10818**	NWC	129
72	Ground Hog Bay	9,200	70	2	**10371**	NWC	130
73	Richardson Island	9,290	80*	8	**10474**	NWC	131
74	Irish Creek	9,280	40		**10468**	NWC	132
75	Neck Creek	9,260	30		**10446**	NWC	133
76	Trout Creek	9,130	40		**10275**	NWC	132
77	Rice Creek	9,090	50		**10243**	NWC	132
78	Arrow Creek 1	8,800	80*		**9849**	NWC	129
79	Wally's Beach	11,210	40	4	**13081**	IFC	53
80	Vermilion Lakes Loc A, C9b	10,770	180	3	**12677**	IFC	134
81	Lake Minnewanka	10,800	80*		**12711**	IFC	135
82	Charlie Lake Cave	10,470	50	3	**12419**	IFC	137
83	Vermilion Lakes Loc A, C9a	10,300	60	4	**12101**	IFC	134
84	Vermilion Lakes Loc A, C6b	10,200	110	2	**11881**	IFC	134
85	Twin Pines Layer 2	10,140	80		**11775**	IFC	138
86	Vermilion Lakes Loc B, C4	9,910	100	3	**11386**	IFC	134
87	Lindoe (EaOp9)	9,900	120		**11391**	IFC	139
88	Twin Pines Layer 3	9,750	80		**11163**	IFC	138
89	Vermilion Lakes Loc A, C6a	9,640	100	2	**10967**	IFC	135
90	Gap site (DlPo20)	9,600	240		**10930**	IFC	140
91	J-Crossing (DjPm-16)	9,600	80*		**10944**	IFC	141
92	Saskatoon Mountain, Level 11	9,380	360	1	**10660**	IFC	138

BI= Beringian interior, NA = North Alaska, NWC= Northwest Coast, IFC=Ice-free Corridor

[1]Oldest date from site.

*^{14}C date with error range not supplied; used median age with ± 80 for calibration using Calib Rev 7.0.4 with IntCal13 (Stuiver and Reimer, 1993; Reimer et al., 2013; Stuiver et al., 2020) (http://calib.org).

5.3 Materials and Methods

5.3.1 Field site descriptions

Bear Creek (n=1). The Bear Creek site is located 11 km east of Dawson City, Yukon, in the Klondike placer mining district. Mining activities had exposed a ~10 m vertical surface consisting of 3 m of alluvial sediment overlain by 7 m of ice-rich loessal silt (D'Costa et al., 2011). The Dawson tephra is prominent at the site, dating to 25,300 ^{14}C yr BP (~30,000 cal yr BP) (Froese et al., 2006), and is situated between 5.2 and 6 m from the base of the exposure. Horizontal core sample BC 4-2B was collected 50 cm below the tephra under a stratified lens of ice, likely the remnant of a surface icing similar to other sites associated with Dawson tephra in the area (Froese et al., 2006). The singular core sample used in this analysis from Bear Creek (BC 4-2B) was collected from reddish-brown ice-poor silts that extend below the tephra. These sediments are interpreted as the palaeosurface and include the palaeo-active layer that existed at the time of Dawson tephra deposition. This unit was preserved due to the rapid deposition of the tephra (~80 cm thick at this site) that shifted the active layer upward. Observations of the palaeoactive layer and preservation of the ice body indicate that there was no thawing or water migration in these relict permafrost sediments following deposition of the Dawson tephra (D'Costa et al., 2011).

Upper Goldbottom (n=5). This site is located 28 km southeast of Dawson along Gold bottom Creek, a tributary of Hunker Creek and the Klondike River. The 28.5 m exposure was divided by Mahony (2015, pp. 65–82) into five units, dating roughly between 46 ka cal yr BP near the base, to 6 ka cal yr BP near the surface. Unit 3 (18.0–22.5 m) is the oldest unit included in this sample set, which consists of grey silts with *in situ* graminoid macrofossils and a few lenses of thin gravels. Four arctic ground squirrel nests were recovered dating between 25,285 to 20,375 cal yrs BP (20,960 ± 150, UCIAMS-131095; 16,895 ± 45, UCIAMS-114712) (Mahony, 2015, p. 73). The three permafrost samples from Unit 3 used in this analysis date to 21,775 cal BP (MM12-117B), 21,000 cal BP (MM12-116B), and 18,510 cal BP (MM12-115B) (Mahony, 2015, p. 189).

Unit 4 (22.5–26.5 m) consist of black and grey organic rich silts with thin (5–15 cm) interbedded lenses of gravels and sand, as well as components of green-grey silts and interbedded humified brown organic silts. *In situ* graminoid and shrub macrofossils were also identified. Unit 4 is estimated to have begun deposition ca. 10,600 cal yr BP (9,395 ± 25, UCIAMS-114910) (Mahony, 2015, p. 77). Aggregation rates could not be assessed at the time as radiocarbon dated samples were laterally-offset. Core samples MM12-118B and MM12-119B date to 9,685 and 10,340 cal BP respectively (Mahony, 2015, p. 189).

Upper Quartz (n=7). The Upper Quartz site is located 33 km southeast of Dawson in the narrow valley of Quartz Creek, a tributary to the Indian River. Mahony (2015, pp. 44–59) divided the 7 m vertical section into three units. The lowermost unit (0–2.8 m) consists of grey and brown silts with several thin (1–3 cm) discontinuous black organic lenses in the upper ~1 m with abundant *in situ* macroremains of graminoid vegetation and rare detrital woody macroremains. Radiocarbon dates from this unit indicate a deposition between 16,560–13,510 cal yrs BP (13,680 ± 390, UCIAMS-114710; 11,680 ± 35, UCIAMS-131100). Two arctic ground squirrel nests were identified at 0 and 0.75 m from the base in this unit, with ^{14}C dates of 16,270 and 15,740 cal yrs BP respectively (13,510 ± 45, UCIAMS-131096; 13,110 ± 35, UCIAMS-142195). Aggradation rates for this unit were estimated by Mahony (2015, p. 48) to range from 0.06–0.14 cm/year. Permafrost cores MM12-QC-2, MM12-QC-3, and MM12-QC-4 were sampled from this unit, and were dated to 16,560 cal yr BP (13,680 ± 390, UCIAMS-114710), 15,745 cal yr BP, and 14,925 cal yr BP respectively (Mahony, 2015, pp. 181, 190).

The second unit (2.8–3.8 m) consists of grey and black silts, a laterally continuous black organic rich layer with *in situ* macroremains of shrubby roots and graminoid vegetation. The unit also contains several aggregational ice lenses (2 cm thick), one syngenetic ice wedge, and abundant non-parallel, wavy microlenticular cryostructures (Mahony, 2015, p. 52). Shrub macroremains had date ranges between 13,685 and 13,160 cal yrs BP (11,885±35, UCIAMS-142206; 11,315±35, UCIAMS-142205), although

aggradation rates could not be estimated. Core MM12-QC-6 was sampled from this unit, and was ^{14}C dated to 12,805 cal yr BP (10,960 ± 35, UCIAMS-114733).

The uppermost unit (3.7–7.0 m), consists of organic-rich black and grey silts, interbedded discontinuous diamict and sand lenses (10–15 cm thick) with *in situ* macroremains of fibrous organics and wood. Cryostructures are generally non-parallel wavy lenticular (2–6 mm) with microlenticular ice, crustal ice, and a syngenetic ice wedge (~50 cm wide). Aggradation rates were estimated at 2.0 cm/year (Mahony, 2015, p. 55). Radiocarbon samples have dates ranging from 5,925 to 5,165 cal yrs BP (5,160 ± 20, UCIAMS-114899; 4,520 ± 25, UCIAMS-142207). Permafrost cores MM12-QC-8, MM12-QC-9, and MM12-QC-10 were sampled from this unit, dating to 5,915, 5,840, and 5,765 cal yr BP (Mahony, 2015, p. 190).

Lucky Lady II (n=8). The Lucky Lady II site is located 46 km southeast of Dawson along the Sulphur Creek tributary of the Indian River. Core samples from this site were previously analyzed by both Mahony (2015, pp. 82–95) and Sadoway (2014, pp. 8, 29), with Sadoway using PCR metabarcoding and targeted enrichment techniques. Dating of the permafrost samples from Lucky Lady II is in reference to Sadoway (2014, p. 29).

A 11.5 m section of Lady Lady II permafrost exposure was sampled by Mahony (2015, pp. 82–95), which was divided into two units; five vertical cores were taken at the site for high-resolution isotopic and radiocarbon analyses. The lowermost unit (0–3.5 m) unit consists of grey silts with a thick black-organic rich horizon (palaeosol) at 2.7 m from the base dating from 13,410 to 13,140 cal yrs BP (11,580 ± 35 ^{14}C yr BP, UCIAMS-143308; 11,290 ± 160 ^{14}C yr BP, UCIAMS-56390) with several thinner palaeosol horizons above. The unit includes *in situ* graminoid macrofossils and multiple arctic ground squirrel nests; several horse and bison bones were also identified. The unit is suggestive of a steppe-tundra landscape, which is estimated to have been deposited from ca. 16,500 to 13,140 cal yrs BP (13,680 ± 35 ^{14}C yr BP, UCIAMS-51324 to 11,290 ± 160 ^{14}C yr BP, UCIAMS-56390), with an aggradation rate of 0.12–0.62 cm/year (Mahony, 2015, p. 85) and with deep active layers. Samples PHP-4 through PHP-9 were recovered

from this unit, dating between 15,865 and 13,105 (11,250 ± 20 ^{14}C BP) cal yrs BP (Sadoway, 2014, p. 29).

The uppermost unit (3.5–11.5 m) consists of organic-rich grey and black silts with more organic-rich sediments towards the top of the unit exposure. Several black organic-rich horizons (2–6 cm thick) are interspersed throughout the unit. The defining contact between the upper and lower units at Lucky Lady II is the appearance of shrub vegetation macrofossils in the uppermost unit. This upper unit contains abundant *in situ* shrub and graminoid macroremains, but no *in situ* animal remains were identified. The unit was deposited between 13,150 and 8,525 cal yrs BP (11,300 ± 35, UCIAMS-142197; 7,750 ± 25, UCIAMS-143296) at an aggradation rate of ~0.12–0.19 cm/year (Mahony, 2015, p. 90). This unit suggests a shift away from a Pleistocene steppe-tundra landscape towards one with an abundance of shrub vegetation. Permafrost samples PHP-2 and PHP-3 were recovered from this unit, dating to 10,220 and 10,340 (9195 ± 20 ^{14}C BP) cal yrs BP respectively (Sadoway, 2014, p. 29).

5.3.2 Lab setting

Laboratory work was conducted in clean rooms at the McMaster Ancient DNA Centre, which are subdivided into dedicated facilities for sample preparation (separate facilities for subsampling eDNA and discrete materials), stock solution setup, and DNA extraction through library preparation (collectively "pre-amplification rooms"). The post-indexing amplification clean room (enrichment) is in a physically isolated facility from the Centre's standard aDNA labs, while the subsequent high-copy PCR workspace is in a separate building; the centre has a unidirectional workflow progressing from low-copy to high-copy facilities to reduce the chance of cross-contamination. Each dedicated workspace is physically separated with air pressure gradients between rooms to reduce exogenous airborne contamination. Prior to all phases of laboratory work, dead air hoods and workspaces were cleaned using a 6% solution of sodium hypochlorite (commercial bleach) followed by a wash with Nanopure purified water (Barnstead) and 30 minutes of UV irradiation at >100 mJ/cm^2.

5.3.3 Subsampling

Permafrost sedaDNA subsamples were only taken from core interiors and care was taken to ensure that none of the sampling tools or interior surfaces were exposed any materials that had come in physical contact with the core exteriors. Permafrost samples from Lucky Lady II had been previously subsampled by Sadoway (2014) at the University of Alberta. These subsamples were homogenized by core and transported to McMaster University by T. Sadoway where they have remained in cold storage. All other subsamples (see Table 4.1 in the main-text or Table 5.13 here) were processed as follows.

Metal sampling tools were cleaned with commercial bleach, rinsed with Nanopure water immediately thereafter, UV irritated on both sides for >30 min, then heated overnight in an oven at ~130°C. Once the tools had cooled the next day, work surfaces were cleaned with bleach and Nanopure water and covered with sterile lab-grade tin foil. Sediment cores previously split into disks (D'Costa et al., 2011; Sadoway, 2014) and stored at −20°C had the upper ~1 mm of external sediment chiselled off to create a fresh sampling area free of exogenous contaminants. For those cores that had not yet been split, a bleach and UV decontaminated handsaw was used to create a groove ~1–2 cm deep around the circumference of the core. A ~1 inch chisel was placed into the groove and a hammer was used to gradually split the core through percussion around the circumference. Once split, this opened a fresh interior surface previously unexposed to sampling equipment. For both the previously split and newly split cores, a small (~1/4 inch) decontaminated chisel was then used to carefully remove interior sediment from the core, which was collected in a weigh boat. After enough material was acquired for multiple extractions (~2–5 g), the core was covered in sterile tin foil and re-frozen. The subsampled material in the weigh boat was homogenized by manually stirring using a small metal chisel as the sediment thawed. This sediment was transferred to a 50 mL falcon tube and refrozen. Thereafter, the work area was thoroughly cleaned with bleach and Nanopure water, all plastic-ware was discarded, and metal tools were placed across the room for decontamination. The now decontaminated workspace was prepared again with sterile tin foil and another core sample. Gloves were changed frequently throughout

subsampling (multiple times per core) to minimize cross and exogenous contamination. New metal tools that had been treated with bleach, UV, and heat decontaminated from the previous day were used for each new core and all sterile tools remained isolated in the oven during subsampling. The homogenized sediments for each core were later subsampled for subsequent DNA extractions.

5.3.4 Lysis and purification

We followed the lysing and sedaDNA extraction procedure described in Murchie et al. (2021b). The first round of sediments (PHP) were lysed with an input of 0.3 g. Subsequent experiments determined that this resulted in a higher inhibitor load for certain samples leading to ~10-20% failed or suboptimal adapter ligation efficiencies during library preparations (see Figs. 5.3–5.4 in section 5.6.2). For the second round of extractions (PHP_{ii}), we reduced the input to 0.15 g, but used two PowerBead lysing tubes per sample that were pooled on the same Roche column following the long cold spin.

Subsamples were lysed with a digest solution (Table 5.3) preloaded into DNeasy PowerBead tubes, then vortexed for 20 minutes using a TissueLyser II. Thereafter, the tubes were briefly centrifuged to remove liquid from the lids, and proteinase K was pipetted into each tube individually. The tubes were then briefly finger vortexed to disturb the sediment-bead pellets that had formed at the base and the tubes and were loaded in an incubator to oscillate overnight at 35°C. The next day, the PowerBead tubes were centrifuged at 10,000 x g for 5 minutes and the supernatant was transferred to a 2 mL MAXYMum Recovery tube and stored at −20°C for later purifications.

For sedaDNA purification, the digestion supernatant (≈1.25 mL) was thawed, briefly centrifuged, and added to ≳16.25 mL (13 volumes) of high-volume guanidinium binding buffer (see Table 5.4) in a 50 mL falcon tube and mixed by repeated inversion. The 50 mL tubes were loaded into a refrigerated centrifuge for the Murchie et al. (2021b) long cold spin, where they were centrifuged at 2500 x g at 4°C for ~20 hours overnight. Thereafter, the falcon tubes were carefully removed from the centrifuge buckets, and the supernatant was decanted, taking care to not disturb the darkly coloured pellet that had formed during the cold spin. The binding buffer was passed through a high-volume silica-

column (High Pure Extender Assembly, Roche Diagnostics) over multiple rounds of centrifugation and extraction proceeded as per Dabney et al. (2013b) with binding and wash centrifugation at 3300 x g, two rounds of PE wash, followed by two 30 second dry spins at 16,000 x g with the tubes rotated 180° between spins to minimize the chance of ethanol retention. Purified DNA was eluted off the silica columns with two volumes of 25 µL EBT (each while waiting 5 minutes after EBT loading to maximize elution, then centrifuging at 16,000 x g for 1 minute). Prior to all subsequent experiments the extracts were centrifuged at 16,000 x g for ≳5 minutes to pellet any remaining co-eluted inhibitors. Care was taken when subsampling these extracts to avoid disturbing any pellet precipitates.

5.3.5 Library preparation, quantitative PCR, and indexing

Doubled stranded libraries were prepared for each extract as described in Meyer and Kircher (2010) with modifications from Kircher et al. (2012) and a modified end-repair reaction to account for the lack of uracil excision (Table 5.5). Samples were purified after blunt-end repair with a QIAquick Nucleotide Removal Kit (QIAGEN) (to maximally retain small fragments) and after adapter ligation (Table 5.6) and indexing (Table 5.8) with a MinElute PCR Purification Kit (QIAGEN). Pre-indexing total library adapted DNA concentrations were estimated with the short amplification qPCR assay (Table 5.9).

5.3.6 Targeted capture with PalaeoChip

Probe design. In-solution enrichments were carried out using the previously designed PalaeoChip Arctic v1.0 bait set (Murchie et al., 2021b). This bait set targets whole mitochondrial genomes from approximately 180 extinct and extant Holarctic fauna, and the chloroplast barcoding loci (*trn*L, *rbc*L, and *mat*K) from approximately 2100 species of plants. See Murchie et al. (2021b Supp. 15–16) for further details on the design of PalaeoChip Arctic-1.0.

Enrichment Wet lab. In solution enrichments were carried out using a modified version of the myBaits v4.1 protocol (Daicel Arbor Biosciences). In summary, hybridization and bait mixes were prepared to the concentrations in Table 5.10. For each

library, 7 µL of template was combined with 5 µL of the library block master mix (using xGens, Human COt-1 DNA, and Salmon Sperm). Hybridization and bait mixes were combined and pre-warmed to 60°C before being combined with the library-block mixture. The final reaction for batch 1 (PHP) was incubated for 48 hours at 55°C for bait-library hybridization. The second round of libraries (PHP_{ii}) were enriched with a hybridization temperature of 60°C over ~72 hours to improve off-target exclusion.

After the hybridization, beads were dispensed (20 µL per reaction), washed with 200 µL of binding buffer per reaction, then resuspended in 20 µL binding buffer per reaction and aliquoted into PCR strips. Baits were captured using 20 µL of the bead binding buffer suspension per library, incubated at 55°C for 2.5 minutes (60°C for the second round), finger vortexed and spun down, then incubated for another 2.5 minutes. Beads were pelleted and the supernatant (the non-captured library fraction) was removed and stored at −20°C as per Klunk et al. (2019). The beads were resuspended in 180 µL of 60°C Wash Buffer X per tube and washed four times following the MYbaits v4.2 protocol. Beads were resuspended in 18.8 µL EBT, PCR reamplified for 12 cycles (Table S7), then purified with MinElute columns following manufacturer's protocols and eluted in 15 µL EBT.

5.3.7 Total quantification, pooling, size selection, and sequencing

Libraries were quantified using the long-amplification total library qPCR assay (Table 5.11) and pooled to equimolar concentrations. Pools were size-selected with gel excision following electrophoresis for molecules ranging between 150–500 bp. Gel plugs were purified using the QIAquick Gel Extraction Kit (QIAGEN), according to manufacturer's protocol, then sequenced on an Illumina HiSeq 1500 with a 2x90 bp paired-end protocol at the Farncombe Metagenomics Facility (McMaster University, ON).

5.3.8 Bioinformatic workflow

Reads were demultiplexed with *bcl2fastq* (v 1.8.4), converted to bam files with *fastq2bam* (https://github.com/grenaud/BCL2BAM2FASTQ), then trimmed and merged with *leeHom* (Renaud et al., 2014) using ancient DNA specific parameters (--ancientdna).

Reads were mapped to a concatenation of the PalaeoChip Arctic-1.0 plant and animal probe references with *network-aware-BWA* (Li and Durbin, 2009) (https://github.com/mpieva/network-aware-bwa) with a maximum edit distance of 0.01 (-n 0.01), allowing for a maximum two gap openings (-o 2), and with seeding effectively disabled (-l 16500). Mapped reads that were merged or unmerged but properly paired were extracted with *libbam* (https://github.com/grenaud/libbam), collapsed based on unique 5' and 3' positions with *biohazard* (https://bitbucket.org/ustenzel/biohazard) (for PCR deduplication), and converted to fasta files and restricted to a minimum length of 24 bp. Fasta files were additionally filtered to remove any reads with lingering sequence similarity to the Illumina adapter sequences (…/fasta2oneline.pl input.fasta | agrep -v -1 AGATCGGAA | agrep -v -1 TTCCGATCT | tr "\t" "\n" | tail -n+2 > output.fasta) and were string deduplicated using the *NGSXRemoveDuplicates* module of *NGSeXplore* (https://github.com/ktmeaton/NGSeXplore).

These filtered fastas were used as the input for *BLASTn* (Altschul et al., 1990) against a July 2019 local copy of the GenBank NCBI (National Center for Biotechnology Information; Benson et al., 2013; Agarwala et al., 2016) nucleotide database and set up to return the top 600 alignments (unique accession hits) per read with e-values less than 1.0E-5 (flags: -num_alignments 600 -max_hsps 1 -evalue 0.00001). The *BLASTn* outputs were then passed to *MEGAN* (Community Edition, v.6.19.7, https://github.com/husonlab/megan-ce) (Huson et al., 2007; 2016) where the *BLASTn* results were filtered through a lowest common ancestor (LCA) algorithm using the following parameters:

- Min-score = 50 (default)
- Max expected (e-value) = 1.0E-5;
- Minimum percent identity = 95%
    - Allows 1 base mismatch at 24 bp, 2 at 50 bp, and 3 at 60 bp to account for deamination and other aDNA characteristic damage or sequencing errors.
- Top percent consideration of hits based on bit-score = 20%.
    - More conservative taxonomic assignments than the 10% default by taking more of the top hits into consideration for LCA assignment.
- Minimum read support = 3
    - Number of unique reads aligning to an NCBI accession sequence for that taxon to be considered for LCA.

- Minimum complexity = 0.3
    - Default minimum complexity filter.
- LCA weighted algorithm at 80%.
    - Two rounds of analysis that increases LCA specificity by taking all taxonomic assignments of a library into consideration.

A second set of *BLASTn* files, identical to those utilized in *MEGAN* except for being in a different output format (-outfmt "6 std staxids") were passed to *PIA* (Phylogenetic Intersection Analysis; Cribdon et al., 2020) (https://github.com/Allaby-lab/PIA) using default inputs. The *PIA* output was converted to a *MEGAN* readable format using scripts available on the *PIA-accessories GitHub* (https://github.com/Allaby-lab/PIA-accessories). All libraries from both the *MEGAN-LCA* and *PIA* taxonomic binning approaches were then compiled using *MEGAN's* compare feature with absolute read counts. Plant and animal sequences were inspected separately; taxonomic nodes deemed to be ecologically informative (through data exploration prioritizing taxa with high read counts, distinct changes in read abundance through time, or are otherwise known to be ecologically significant organisms) were selected and plotted using *MEGAN*'s built-in bubble chart feature. In these inter-sample comparative charts, absolute assigned read counts are retained, but the bubble sizes are scaled (either square-root or logarithmic) to visually normalize between samples of differing sequence depths. As these logarithmically scaled bubbles make it difficult to see change through time (whereas linearly scaled bubbles obscure all but the most abundant taxon nodes), a normalized set of *MEGAN* libraries was used to create stacked proportional charts to more clearly observe changing sedaDNA taxon assignments through time. A PCoA was also created through *MEGAN* with these normalized libraries. All *MEGAN* charts were exported as EPS files and were cosmetically fine-tuned in *Adobe Illustrator* (Adobe Inc., 2020) (https://adobe.com/products/illustrator).

Thereafter, the closest available genetic references were obtained for notable taxa identified with the *MEGAN-LCA* and *PIA* taxonomic binning approaches. All samples were mapped to these references using the same aforementioned procedures but with an additional map-quality filter set to ≥ 30 with *samtools* (https://github.com/samtools/samtools), then assessed for ancient DNA typical damage

signals using *mapDamage* (Jónsson et al., 2013) (v 2.0.3, https://ginolhac.github.io/mapDamage/). The *mapDamage* misincorporation plot outputs were compiled and cosmetically fine-tuned in *Adobe Illustrator* (Adobe Inc., 2020), and are included in the supplemental materials.

5.4 Master mix recipe tables

Table 5.3 Final concentrations of components in the proteinase K digestion solution.

Proteinase K Digestion Solution	
Component	Final Concentration
Tris-Cl (pH 9.0)	0.02 M
SDS	0.5 %
Proteinase K	0.25 mg/ml
CaCl2	0.01 M
DTT	100 mM
PVP	2.5 %
PTB	5 mM
Volume per rxn	0.5 mL

These are the buffer concentrations once combined with the 0.75 mL of the pre-loaded PowerBead solution (Bead tubes with garnet beads and 750 µL 181 mM NaPO4, 121 mM guanidinium isothiocyanate). Protenaise K added individually (15.53 µL) after vortexing for >20 minutes. Samples digested overnight at 35°C with rotation. Nanopure Barnstead water was used to bring up the volume to the desired concentration. Concentrations based on Karpinski et al. (2016).

Table 5.4 Final concentrations of components in the guanidinium binding buffer.

Guanidinium Binding Buffer	
Component	Final Concentration
Guanidine Hydrochloride	5 M
Isopropanol (100%)	40 %
Tween-20	0.05 %
3 M Sodium Acetate (pH 5.2)	0.09 M

Nanopure Barnstead water was used to bring up the volume to the desired concentration. Concentrations based on Dabney et al. (2013b). Utilized a ratio of 13 volumes of binding buffer to 1 volume of lysis supernatant. With a typical expected volume of 1.25 mL of lysis, 16.25 mL of binding buffer was used.

Table 5.5 Final concentrations of components in the blunt-end repair mixture.

Blunt-End Repair Mixture	
Component	Final Concentration
NE Buffer 2.1	1X
DTT	1 mM
dNTP mix	100 µM
ATP	1 mM
T4 polynucleotide kinase	0.5 U/µL
T4 DNA polymerase	0.1 U/µL

A final volume of 40 µL per rxn was used for the mixture and template DNA. Nanopure Barnstead water was used to bring up the volume to the desired concentration. Extract input: 10 µL.

Table 5.6 Final concentrations of all components in the adapter ligation mixture.

3. Adapter Ligation Mixture	
Component	Final Concentration
T4 DNA Ligase Buffer	1X
PEG-4000	5%
Adapter Mix	0.5 µM
T4 DNA Ligase	0.125 U/µl
2. Adapter Mix	
IS1_adapter_P5.F	200 µM
IS2_adapter_P7.F	200 µM
IS3_adapter_P5+P7.R	200 µM
Oligo Hybridization Buffer	1X
2. Oligo Hybridization Buffer	
NaCl	500 mM
Tris-Cl, pH 8.0	10 mM
EDTA, pH 8.0	1 mM

Oligo Hybridization Buffer was prepared prior to the Adapter Mix, which was prepared separately for IS1_adapter_P5.F and IS2_adapter_P7.F. These two mixes were then combined after an incubation at 95°C for 10 seconds, and a ramp from 95°C to 12°C at a rate of 0.1°C/sec. A final volume of 40 µl was used for the mixture and template DNA. Nanopure Barnstead water (not listed) was used to bring the volume up to the desired concentration.

Table 5.7 Final concentrations of components in the adapter fill-in mixture.

Adapter Fill-In Mixture	
Component	Final Concentration
ThermoPol Reaction Buffer	1X
dNTP Mix	250 µM
BST Polymerase (large fragment)	0.4 U/µl

A final volume of 40 µl was used for the mixture and template DNA with the addition of Nanopure Barnstead water to bring the mix up to the desired concentration and volume.

Table 5.8 Primer sequences, PCR master mix, and cycling protocol for indexing amplification.

Indexing PCR Master Mix			
Component		Final Concentration	
KAPA SYBR®FAST qPCR Master Mix (2X)		1X	
Forward primer		750 nM	
Reverse primer		750 nM	
Primer Sequences			
Forward Primer	AATGATACGGCGACCACCGAGATCTACAC***NNNNNNN***ACACTCTTTCCCTACACGACGCTCTT		
Reverse Primer	CAAGCAGAAGACGGCATACGAGATTAT***NNNNNNN***ACTGGAGTTCAGACGTGT		
Indexing PCR Protocol			
Phase	Temperature (°C)	Time	Cycles
Initial Denaturation	98	3 min	
Denaturation	98	20 sec	Repeated for 8-12 cycles
Annealing	*60*	*20 sec*	
Extension	72	25 sec	
Final Extension	72	3 min	

The N in each primer sequence represents the 7 bp index specific to each primer. A final reaction volume of 40 µl was used for the assay, with 12.5 µl of the adapter ligated DNA libraries. Nanopure Barnstead water (not listed) was used to bring the volume up to the desired concentration.

Fluorescence readings were recorded post-annealing as indicated above with asterisks.

Table 5.9 Library adapted short amp total quantification PCR.

PCR Master Mix			
Component		Final Concentration	
KAPA SYBR®FAST qPCR Master Mix (2X)		1X	
Forward primer		0.2 µM	
Reverse primer		0.2 µM	
Oligos		Sequence (5'–3')	
Forward primer (ILPr_shortampP5F_MeyerIS7)		ACACTCTTTCCCTACACGAC	
Reverse primer (ILPr_shortampP7R_MeyerIS8)		GTGACTGGAGTTCAGACGTGT	
Library adapted oligo based on the mammoth *12S* mitochondrial gene. *(Priming sites with reverse-complement bolded.)*		**ACACTCTTTCCCTACACGAC**GCTCTTCCGAT CTCCCTAAACTTTGATAGCTACCTTTACAAAG CTATCCGCCAGAGAACTACAGATCGGAAGAG C**ACACGTCTGAACTCCAGTCAC**	
Input		Volume	
PCR master mix		6 µL	
Library adapted template		4 µL	
PCR Protocol			
Phase	Temperature (°C)	Time	Cycles
Initial Denaturation	95	5 min	
Denaturation	95	30 sec	Repeated for 30 cycles
Annealing + Extension	60	45 sec	
Melt Curve	**65–95**	**5 sec per degree**	

Nanopure Barnstead water was used to bring the mix up to the desired concentration and volume. Oligo based on Enk et al. (2016); primers based Meyer and Kircher (2010).

Table 5.10 Enrichment master-mixes.

Hybridization MasterMix	
Component	Final Concentration
Hyb N (19.46X SSPE, 13.5 mM EDTA)	9X, 6.25mM
Hyb D (50X Denhardt's Solution)	8.75X
Hyb S (10% SDS)	0.25%
Hyb R RNAsecure	1.56X
Bait Mixture (200 ng baits per reaction)	11.11 ng/µL
Bait Mixture	
Component	Final Concentration
Plant: 18,672 baits	83.33 ng/rxn
Animal: 57,588 baits	138.89 ng/rxn
Library MasterMix (blocks)	
Component	Final Concentration
Block A (xGens)	0.04 ng/µL
Block C (Human COt-1 DNA)	0.19 ng/µL
Block O (Salmon Sperm DNA)	0.19 ng/µL
Library template input	7 µL
Wash Buffer X (0.2X WB)	
Component	Final Concentration
HYB S (10% SDS)	0.08 %
Wash Buffer (0.1X SSC; 0.1% SDS; 1mM EDTA)	0.2X

Nanopure Barnstead water was used to bring mixes up to the desired concentration and volume.

Table 5.11 Library adapted and indexed long amp total quantification PCR.

PCR Master Mix			
Component		Final Concentration	
KAPA SYBR®FAST qPCR Master Mix (2X)		1X	
Forward primer		0.2 µM	
Reverse primer		0.2 µM	
Oligos		Sequence (5'–3')	
Forward primer (ILPr_shortampP5F_MeyerIS5)		AATGATACGGCGACCACCGA	
Reverse primer (ILPr_shortampP7R_MeyerIS6)		CAAGCAGAAGACGGCATACGA	
PhiX library adapted control standard from 100 pM to 62.6 fM		AATGATACGGCGACCACCGA *ADAPTER INSERT* TCGTATGCCGTCTTCTGCTTG	
Input		Volume	
PCR master mix		6 µL	
Library adapted and indexed template		4 µL	
PCR Protocol			
Phase	Temperature (^{o}C)	Time	Cycles
Initial Denaturation	95	5 min	1
Denaturation	95	30 sec	Repeated for 35 cycles
Annealing + Extension	60	45 sec	
Cooldown	8	30 sec	1

Nanopure Barnstead water was used to bring the mix up to the desired concentration and volume. Primers from Meyer and Kircher (2010).

5.5 *MEGAN* disabled taxa

Table 5.12 Disabled taxa in MEGAN with NCBI ID.

[2323] unclassified Bacteria	[78725] Cleistes
[2706] Citrus	[78760] Epistephium
[3298] Zamiaceae	[79318] Irvingia
[3520] Casuarinaceae	[85234] Oncotheca
[3642] Lecythidaceae	[85241] Plagiopteron
[3680] Begoniaceae	[93758] Corchorus
[3733] Moringaceae	[100370] Croton
[3737] Sapotaceae	[102805] Barnadesioideae
[3805] Bauhinia	[106722] Dorstenia
[4268] Malpighiaceae	[112800] Achariaceae
[4328] Proteaceae	[112827] Lacistemataceae
[4420] Victoria	[112836] Paropsia
[4441] Camellia	[124867] Pandaceae
[4527] Oryza	[126560] Picconia
[4613] Bromeliaceae	[134367] hybrid subtypes
[4618] Zingiberales	[142700] Pimelea
[4672] Dioscorea	[149357] Cissus
[4710] Arecaceae	[156614] environmental samples <viruses,unclassified bacterial viruses>
[12908] unclassified sequences	[163724] Crotalarieae
[13394] Capparis	[163736] Podalyrieae
[13484] Dianella	[169618] Ixoroideae
[13669] Sarcandra	[169619] Cinchonoideae
[14107] Restionaceae	[169659] Psychotrieae
[16472] Goodeniaceae	[173686] Santiria
[16739] Piperaceae	[179710] Homalium
[19955] Ebenaceae	[180118] Mammea
[21910] Verbenaceae	[186616] environmental samples <viruses,superkingdom Viruses>
[22063] Monimiaceae	[214912] Sterculioideae
[22973] Chrysobalanaceae	[225222] Platysace
[23808] Simaroubaceae	[226089] Elatostema
[24942] Dilleniaceae	[233879] Putranjivaceae
[26000] Elaeocarpaceae	[235594] Bridelieae
[26122] Gesneriaceae	[238071] Samydeae
[26778] Nothofagaceae	[238073] Scolopieae
[28384] other sequences	[238074] Prockieae
[37820] Hydrostachys	[238075] Abatieae
[39173] Ocimum	[239467] Phyteuma
[39613] Loeseneriella	[246513] Coldenia
[40029] Rhizophoraceae	[256812] Pera
[41867] Stilbaceae	[261082] Goniothalamus
[42220] Curtisiaceae	[324786] Pomaderreae
[43690] Canarium	[325293] Phyliceae
[43707] Meliaceae	[367897] environmental samples <viruses,unclassified DNA viruses>
[44985] Hyacinthaceae	[494674] Gypothamnium
[47936] environmental samples <proteobacteria,phylum Proteobacteria>	[768725] Prunus hybrid cultivar
[48479] environmental samples <bacteria,superkingdom Bacteria>	[1003877] Benincaseae
[48510] environmental samples <archaea,superkingdom Archaea>	[1445966] Gnetidae
[53907] Ormosia	[1446378] Araucariales
[55234] Monotoca	[1504452] Osmelia
[55390] Adinandra	[1525719] Palicoureeae

[56627] Ochnaceae	[1648022] Parapholiinae
[58436] Argostemma	[1699513] Myrtoideae
[58963] Moraea	[1895897] Pombalia
[60092] Vinca	[1978182] Detarioideae
[61964] environmental samples <eukaryotes,superkingdom Eukaryota>	[2060783] Scyphostegioideae
[65009] Dipterocarpoideae	[2231387] dalbergioids sensu lato
[69062] Globularia	[2233854] mirbelioid clade
[72403] Clusia	[2233855] indigoferoid/millettioid clade
[77014] Melicope	[2304098] Cayratieae
[77071] Cecropia	[2508080] Crocoideae

This list is a combination of *MEGANs* default taxa and some intentionally disabled taxa. Sporadic mishits to some species within these families or genera were identified in parallel analyses (see Murchie et al., 2021b). It is believed much of this is driven by an abundance of genetic research on specific organisms (what Cribdon et al. [2020] refers to as ‘oasis taxa’), compounded by database incompleteness for some Quaternary Holarctic plant taxa. The highest possible rank at which no taxa within the clade have a Holarctic distribution were selected to be disabled for simplicity.

5.6 SedaDNA additional data

5.6.1 Full sample list with core replicates

Table 5.13 Permafrost cores analyzed for sedaDNA with expanded core replicates.

Site	Core ID	SedaDNA ID	Age	Input (grams)	Total Raw Reads	PalaeoChip Mapped & MEGAN assigned
Bear Creek (D'Costa et al., 2011)	BC 4-2B	PHP-1	30,000	0.25	1,619,859	58,020 (3.58%)
		SET-277		0.25	1,235,759	76,001 (6.15%)
		SET-278		0.25	1,275,219	47,127 (3.70%)
		SET-279		0.25	1,519,972	59,995 (3.95%)
Lucky Lady II (Sadoway, 2014)	LL2S-189-E	PHP-2	10,220	0.3	63,685	250 (0.39%)
		PHPii-2		0.3	4,141,976	8716 (0.21%)
		PHPii-2cd		0.3	4,461,835	942 (0.02%)
	LL2S-253-D1	PHP-3	10,340	0.3	*not sequenced*	
		PHPii-3		0.3	5,445,860	111,232 (2.04%)
		PHPii-3cd		0.3	3,857,668	380,255 (9.86%)
	LL2C-118-C	PHP-4	13,105	0.3	1,619,858	83,631 (5.16%)
		PHPii-4		0.3	6,129,319	95,342 (1.56%)
	LL2C-205-B	PHP-5	13,150	0.3	1,126,060	25,222 (2.24%)
		PHPii-5		0.3	3,871,764	23,004 (0.60%)
	LLII 12-84-3	PHP-6	13,205	0.3	1,571,297	127,515 (8.12%)
		PHPii-6		0.3	4,287,316	246,751 (5.76%)
		SET-271		0.25	1,807,078	150,779 (8.34%)
		SET-272		0.25	1,322,559	137,744 (10.42%)
		SET-273		0.25	1,247,471	143,812 (11.53%)
	LL2C-243-A2	PHP-7	13,870	0.3	1,449,830	6395 (0.44%)
		PHPii-7		0.3	4,370,642	48,305 (1.11%)
	LLII 12-170-6	PHP-8	15,405	0.3	1,331,181	17,628 (1.33%)
	LLII 12-217-8	PHP-9	15,865	0.3	958,126	15,200 (1.59%)
		SET-274		0.25	845,348	10,397 (1.23%)
		SET-275		0.25	970,115	8778 (0.91%)
		SET-276		0.25	341,707	4191 (1.28%)
Upper Goldbottom (Mahony, 2015)	MM12-118B	PHP-11	9685	0.3	79,090	6035 (7.63%)
		PHPii-11		0.3	3,221,976	60,152 (1.87%)
		SET-268		0.25	1,678,166	182,089 (10.85%)
		SET-269		0.25	1,754,121	148,670 (8.48%)
		SET-270		0.25	1,249,732	144,575 (11.57%)
	MM12-119B	PHP-12	10,340	0.3	*not sequenced*	
		PHPii-12		0.3	61,637	296 (0.48%)
		CSMii-PHP-12a		0.3	5,234,065	587,919 (11.23%)
		CSMii-PHP-12b		0.3	3,464,073	441,102 (12.73%)
		CSMii-PHP-12c		0.3	4,649,222	366,785 (7.89%)
		CSMii-PHP-12d		0.3	5,000,444	427,516 (8.55%)
	MM12-116b	PHP-13	17,500	0.3	1,624,580	174,890 (10.77%)
	MM12-115b	PHP-14	18,510	0.3	2,320,965	35,539 (1.53%)
	MM12-117b	PHP-15	21,775	0.3	1,910,387	164,997 (8.64%)
Upper Quartz	MM12-QC-10	PHP-19	5765	0.3	2,279,133	168,768 (7.41%)
		PHPii-19		0.3	6,965,795	21,787 (0.31%)
	MM12-QC-9	PHP-20	5840	0.3	1,883,409	186,238 (9.89%)
		PHPii-20		0.3	4,030,038	126,359 (3.14%)
	MM12-QC-8	PHP-21	5915	0.3	1,590,777	229,319 (14.42%)
		PHPii-21		0.3	3,551,677	36,570 (1.03%)

Site	Core ID	SedaDNA ID	Age	Input (grams)	Total Raw Reads	PalaeoChip Mapped & MEGAN assigned
Upper Quartz (Mahony, 2015)	MM12-QC-6	PHP-22	12,805	0.3	1,135,493	41,668 (3.67%)
		PHPii-22		0.3	4,944,689	73,310 (1.48%)
	MM12-QC-4	PHP-23	14,925	0.3	1,207,782	26,776 (2.22%)
		PHPii-23a		0.3	5,380,376	17,206 (0.32%)
		PHPii-23b		0.3	8,141,488	24,204 (0.30%)
	MM12-QC-3	PHP-24	15,745	0.3	1,129,623	17,162 (1.52%)
	MM12-QC-2	PHP-25	16,560	0.3	1,568,411	29,419 (1.87%)
Blanks	Extraction Blanks (Batch 1)	PHP-10-BK	*na*		9,882	81 (0.82%)
		PHP-18-BK	na		1,495	
		PHP-26-BK	na		7,351	
	Library Blanks (Batch 1)	LibBK-PHP_CL	na		4,451	
	Extraction Blanks (Batch 2)	PHPii-BK27	na		2,316	
		PHPii-BK28	na		4,045	
		PHPii-BK29	na		2,170	
		CSMii-BK2	na		8,681	
	Library Blanks (Batch 2)	PHPii-LB	na		4,570	
		CSMii-LB	na		275	
	Extraction Blanks (Batch 3)	SET-BK22	na		55,877	
		SET-BK23	na		852	
	Library Blanks (Batch 3)	SET-BK24	na		475	

5.6.2 Pre-sequencing qPCR concentration estimates

In the initial batch of subsamples (PHP; Table 5.13) sedaDNA recovery and isolation was high, although success was somewhat inconsistent. For example, PHP-2, PHP-3, and PHP-12 had less than 1,000,000 total library adapted DNA molecules (based on a quantitative PCR [qPCR] assay prior to indexing) (Fig. 5.3). Generally, low pre-indexing estimates are suggestive of poor ligation success during library preparation—likely as a result of co-eluted inhibitory substances during extraction (Murchie et al., 2021b)—or poor aDNA preservation. This pattern was observed again in the post-enrichment qPCR where almost no PalaeoChip Arctic-1.0 on-target DNA could be isolated from those challenging libraries (Fig. 5.4), whereas most other libraries retained sufficient concentrations for pooling and sequencing. A subsequent batch of subsamples (PHP_{ii}) with lower sediment inputs (0.15 g x 2 PowerBead tubes) improved the DNA isolation of those challenging samples, which enabled the recovery of sedaDNA from all targeted permafrost cores.

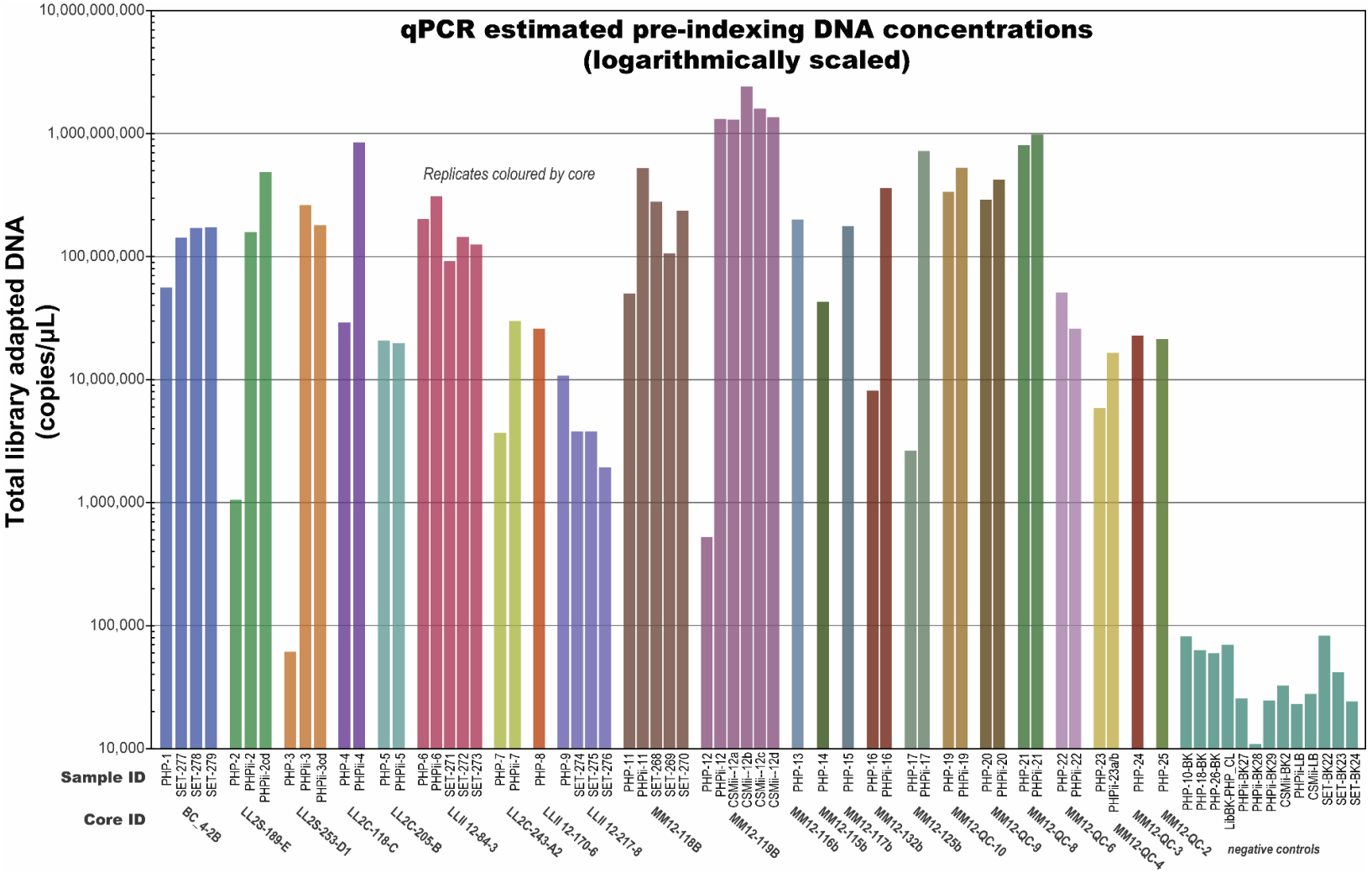

Fig. 5.3 Pre-indexing short amplification qPCR assay for estimating total adapted DNA concentrations. See Table 5.9 for assay specifications.

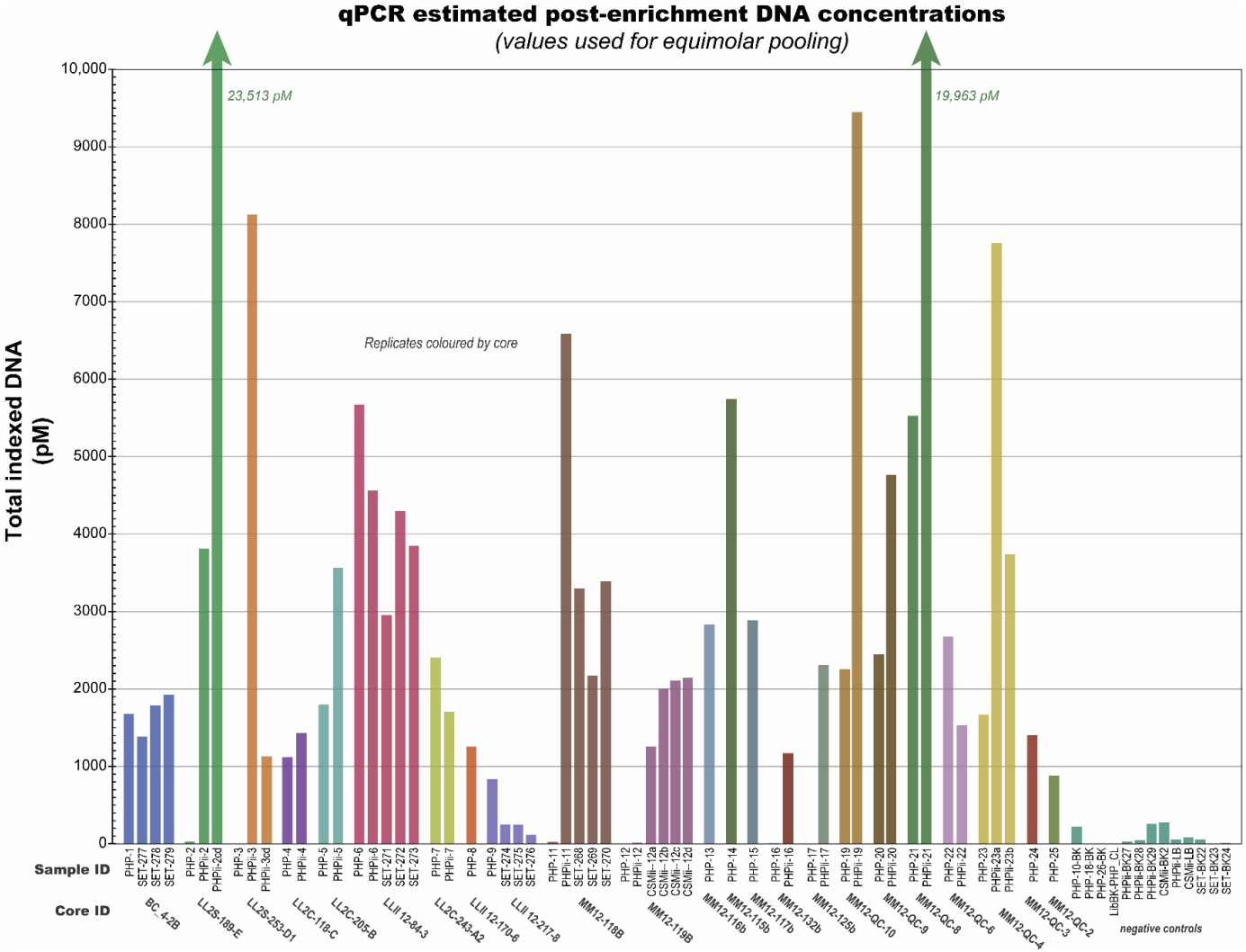

Fig. 5.4 Post-enrichment long amplification qPCR assay for estimating total adapted DNA concentrations following targeted capture for equimolar pooling. See Table 5.11 for assay specifications.

5.6.3 Normalized read proportions by site

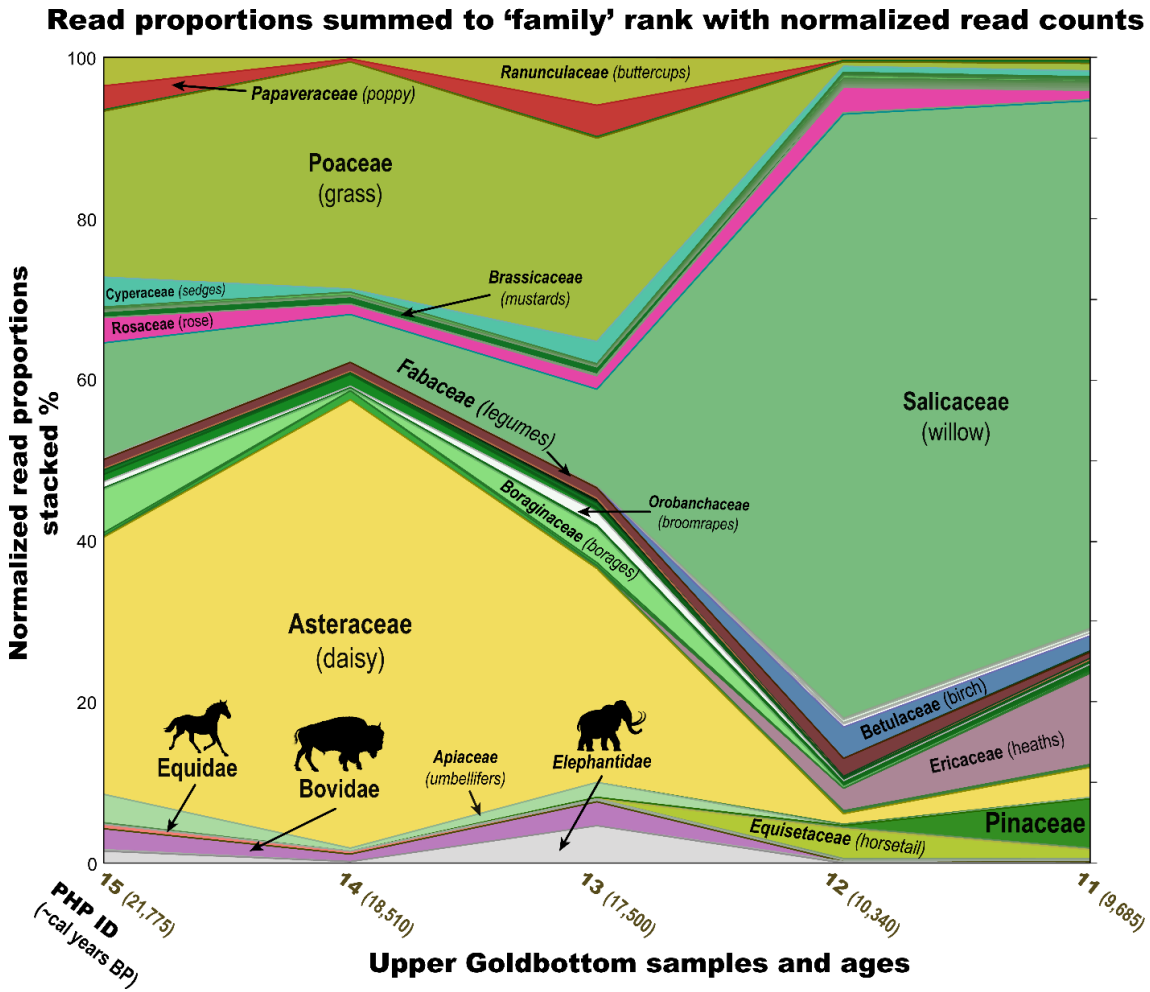

Fig. 5.5 Upper Goldbottom stacked percentage line chart of normalized read counts for all eukaryotic 'Family' nodes.

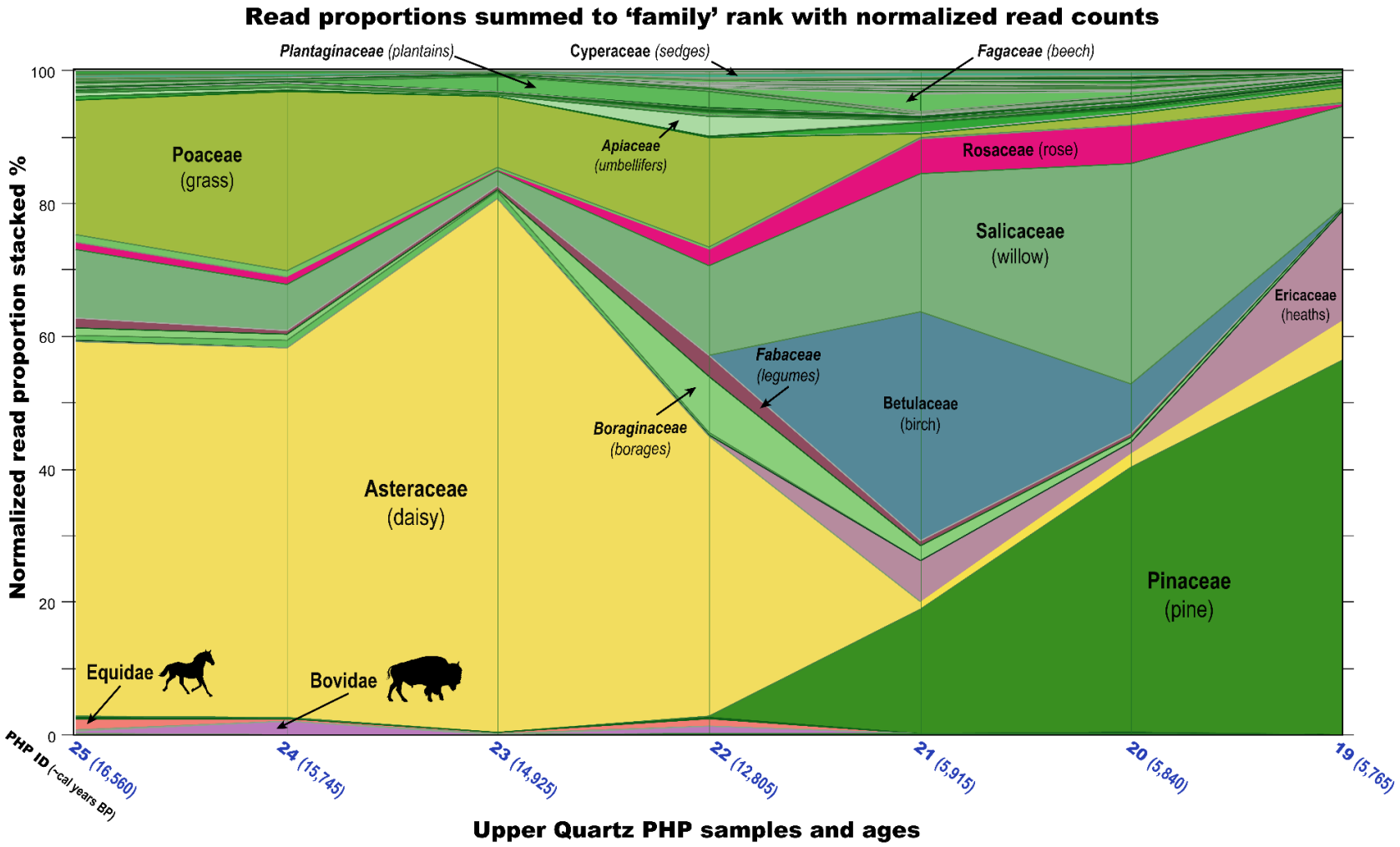

Fig. 5.6 Upper Quartz stacked percentage line chart of normalized read counts for all eukaryotic 'Family' nodes.

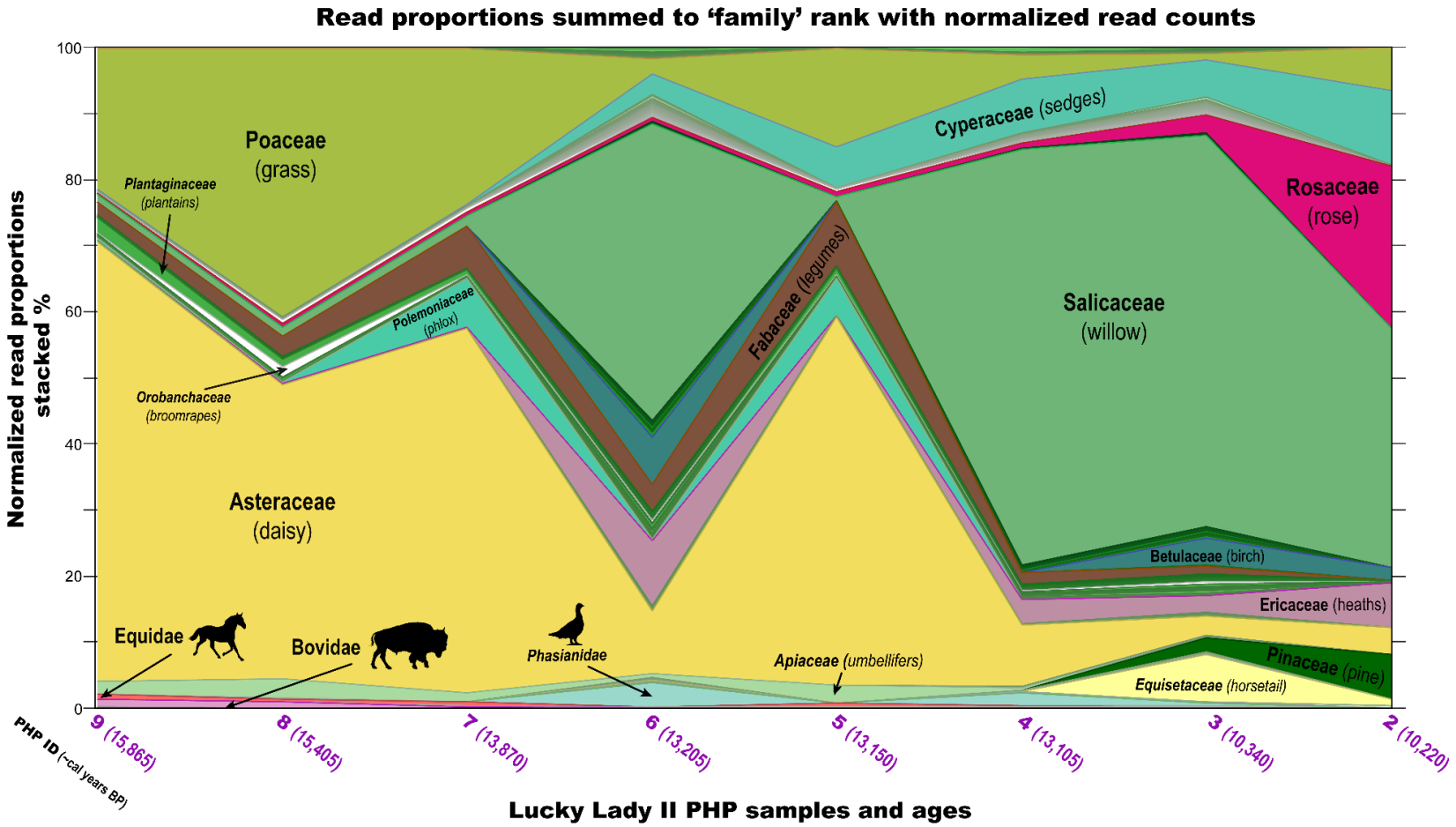

Fig. 5.7 Lucky Lady II stacked percentage line chart of normalized read counts for all eukaryotic 'Family' nodes.

5.6.4 *mapDamage* plots

The following section details the *mapDamage* plots for a range of taxa bimolecularly identified via *BLASTn/MEGAN*. Approximately ~200 reads are necessary to see a clear deamination signal indicative of terminal nucleotide misincorporations that are characteristic of ancient DNA. Plots generated with less than 200 reads tend to be very jagged as there is insufficient overlap of reads on the reference sequence for terminal damage to become apparent. Further, mapped read counts are inflated when mapping to a specific organism compared with taxonomically binned read counts that can be confidently *MEGAN* or *PIA* assigned. This is due to a degree of non-specific mapping of conserved regions of the mitochondrial and chloroplast genomes. This, in some instances, results in stacks of non-specific mapped reads at these conserved sites that contain internal polymorphisms, which can cause some jagged misincorporation plots and fragment length distributions. Conversely, reads that can be *BLASTn* and *MEGAN/PIA* assigned are individually diagnostic of the identified organism, and hence have smaller counts. Regardless of whether all of the mapped reads utilized for *mapDamage* originate from the specific organism to which they were mapped, or more likely originate from closely related species in the same genus or family (as often there is no complete genomic reference for the exact species that these reads likely originated from), these damage plots for samples with >200 mapped reads contain terminal deamination patterns in both plant and animal sequences that are characteristic of ancient DNA. This again suggests that these molecules originate from the samples themselves and are not the result of contamination. Figs. 5.22–5.23 in section 5.6.5 provide an example of this observation of non-specific mapping that can cause messy *mapDamage* plots.

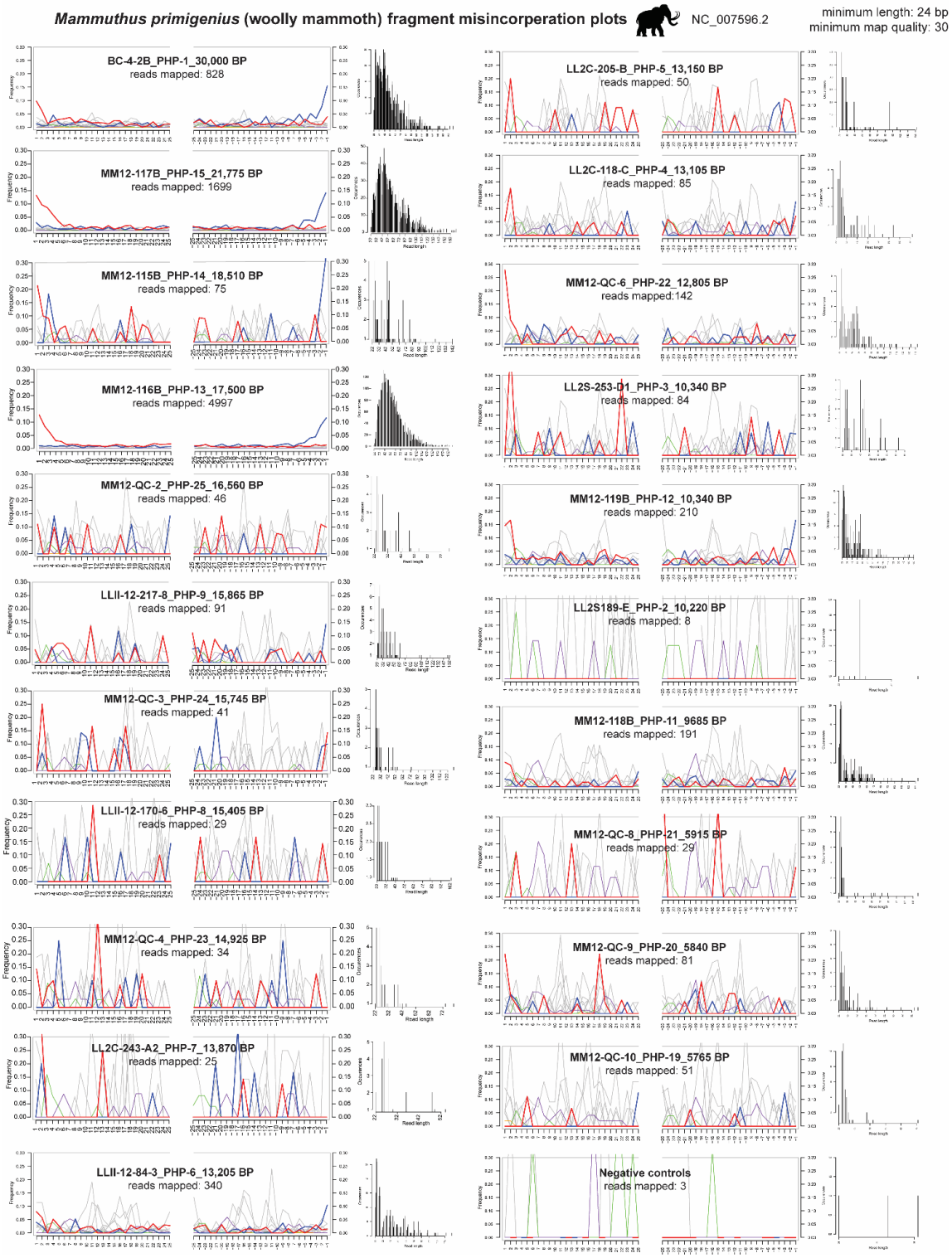

Fig. 5.8 *Mammuthus primigenius mapDamage* plots and fragment length distributions.

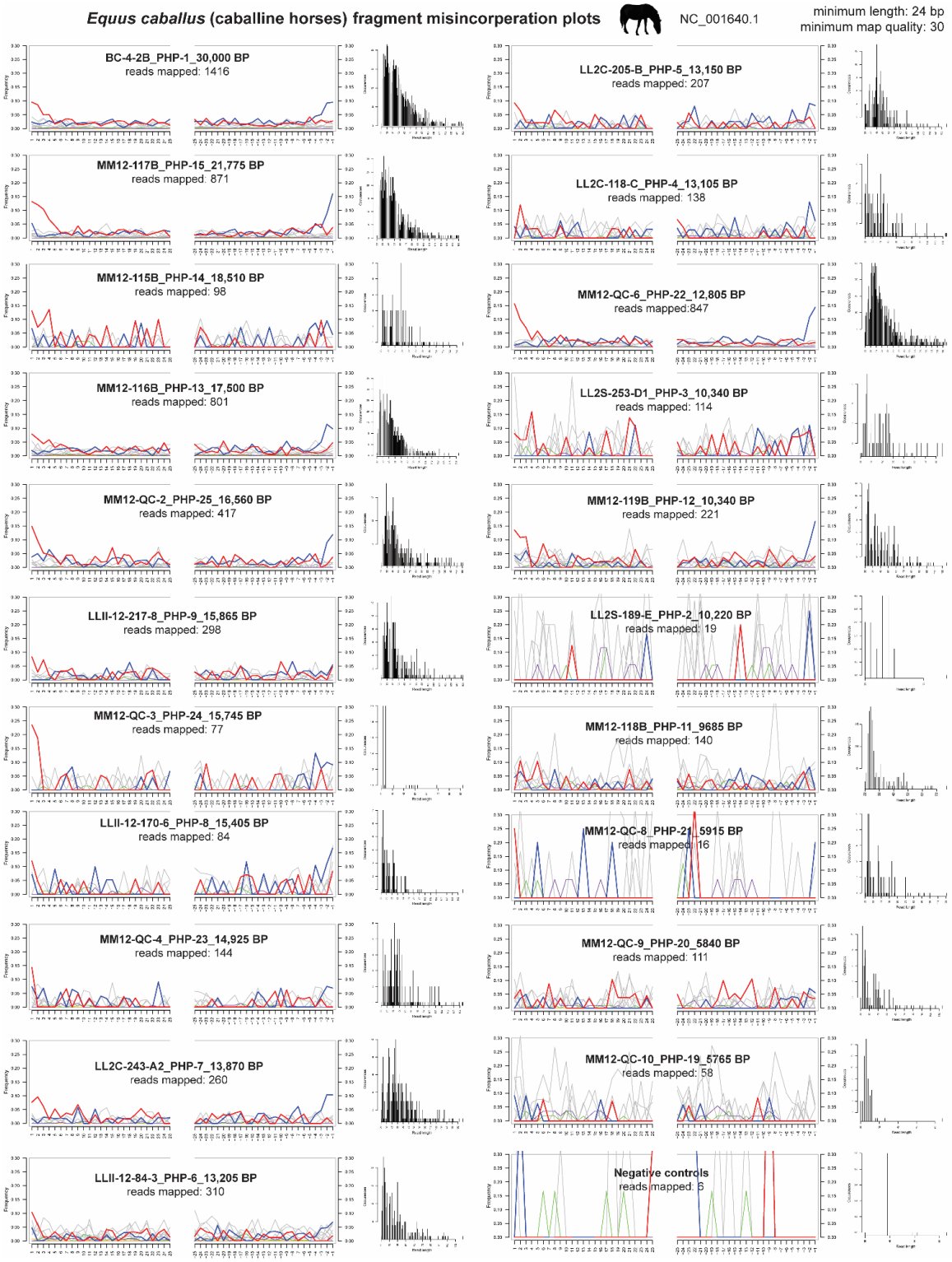

Fig. 5.9 *Equus mapDamage* plots and fragment length distributions.

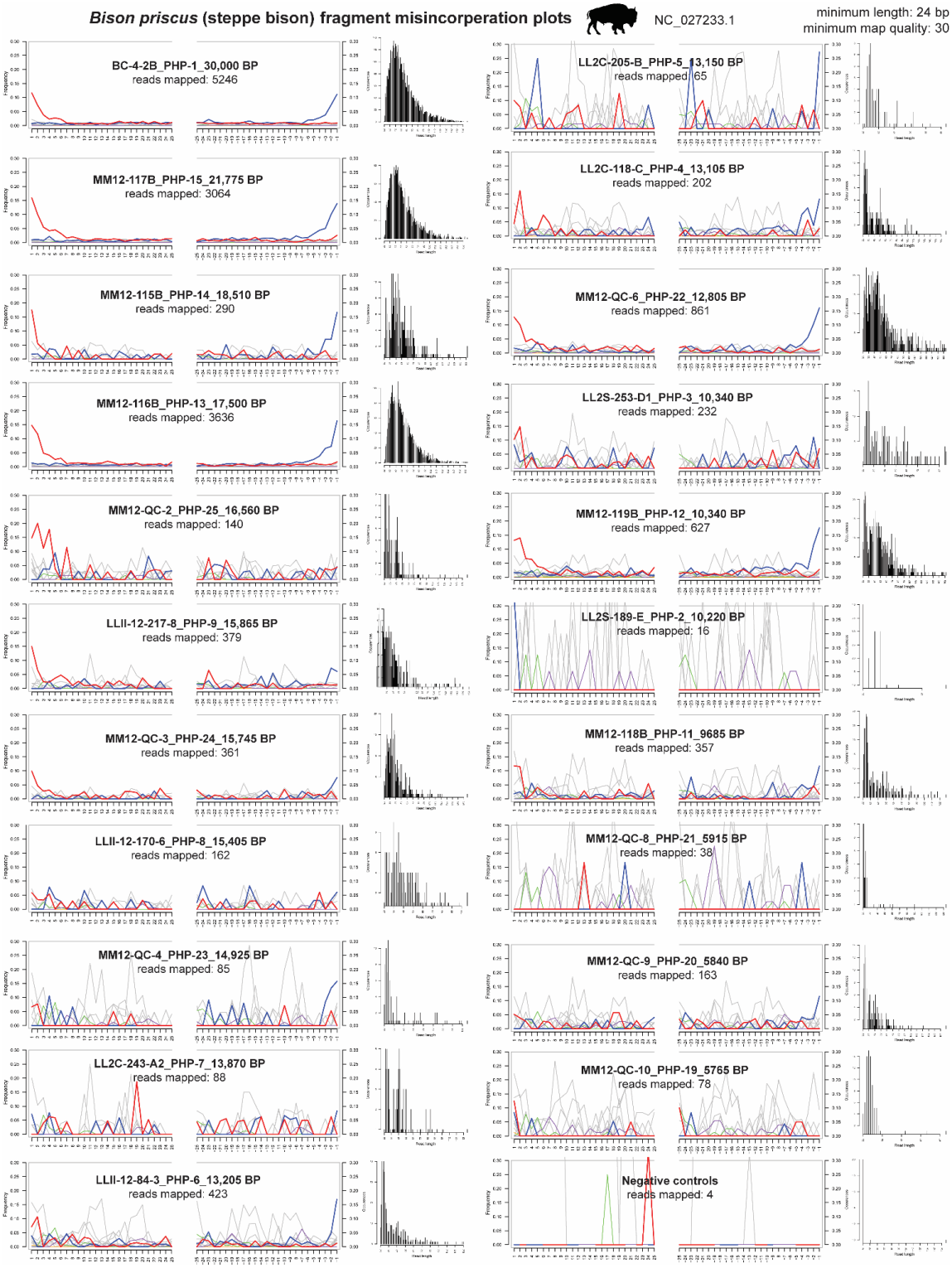

Fig. 5.10 *Bison priscus mapDamage* plots and fragment length distributions.

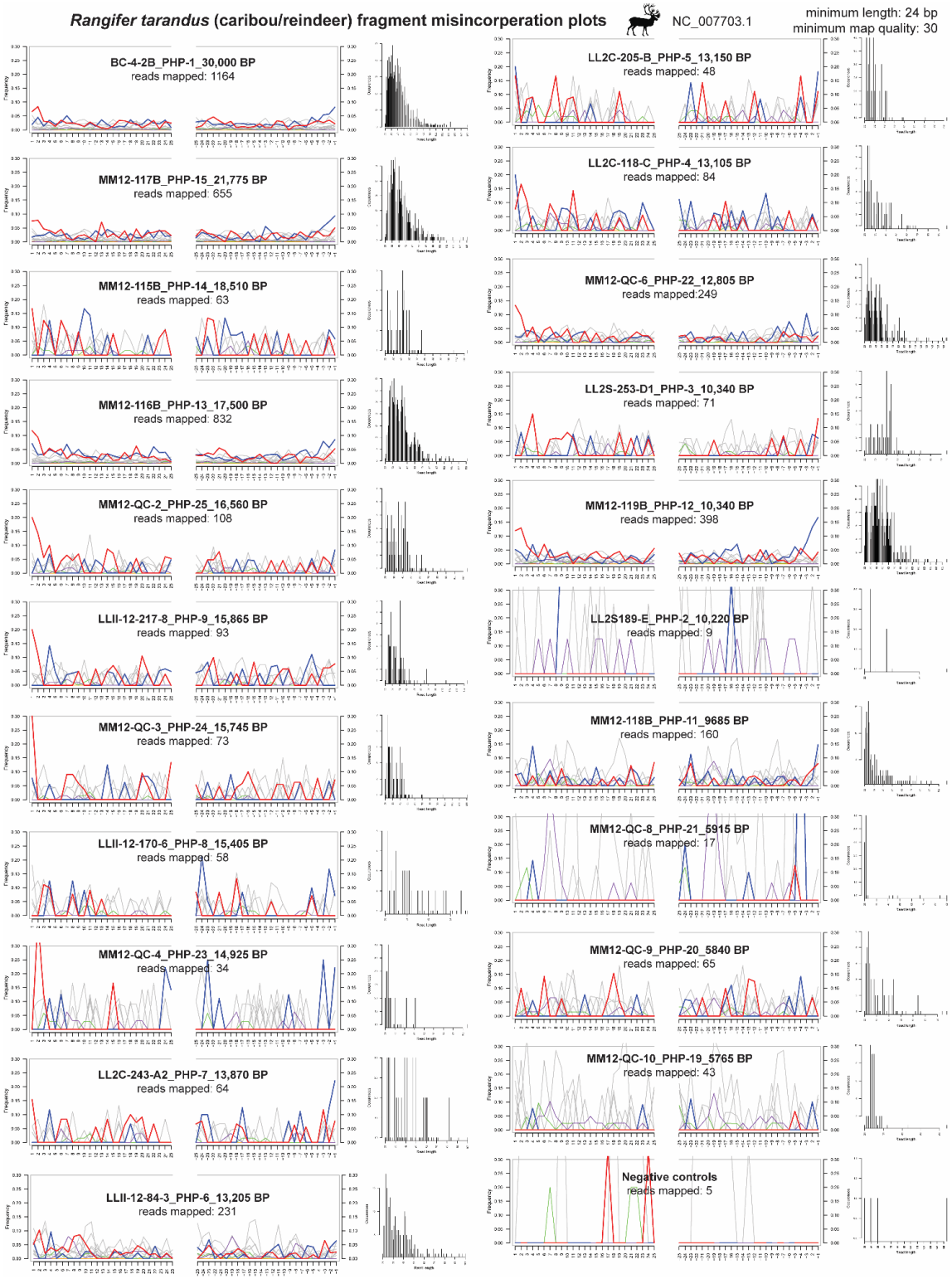

Fig. 5.11 *Rangifer tarandus mapDamage* plots and fragment length distributions.

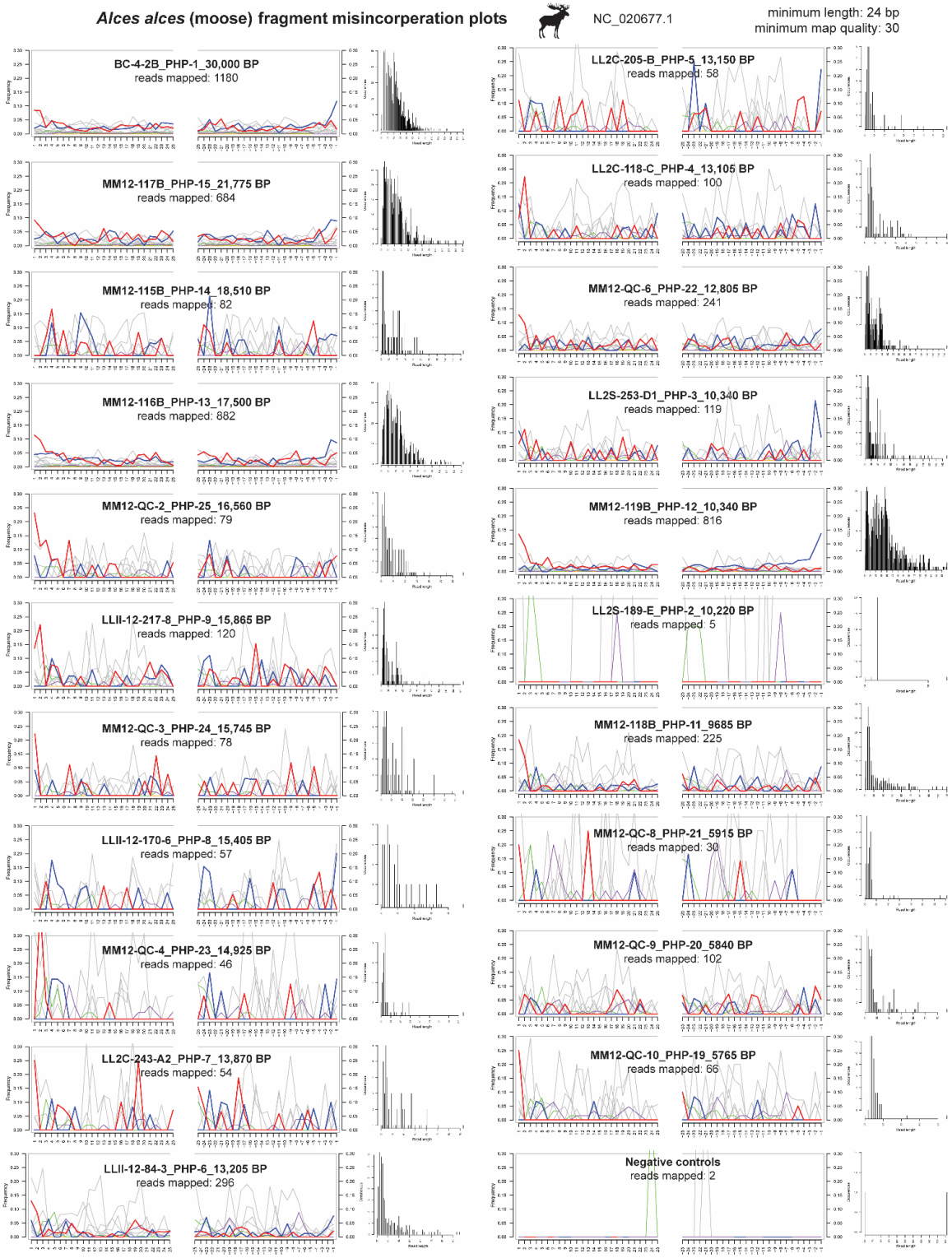

Fig. 5.12 *Alces alces mapDamage* plots and fragment length distributions.

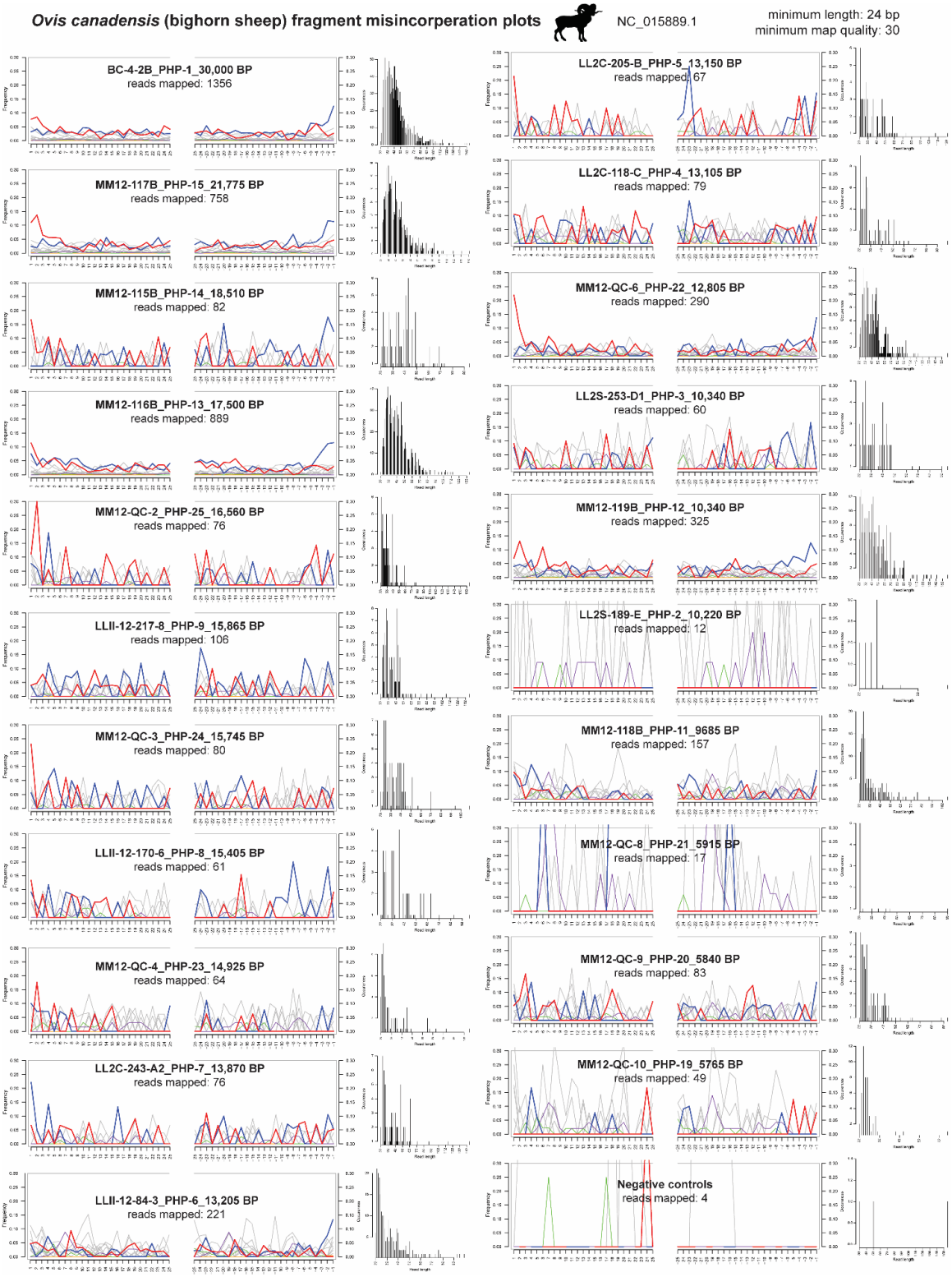

Fig. 5.13 *Ovis canadensis mapDamage* plots and fragment length distributions.

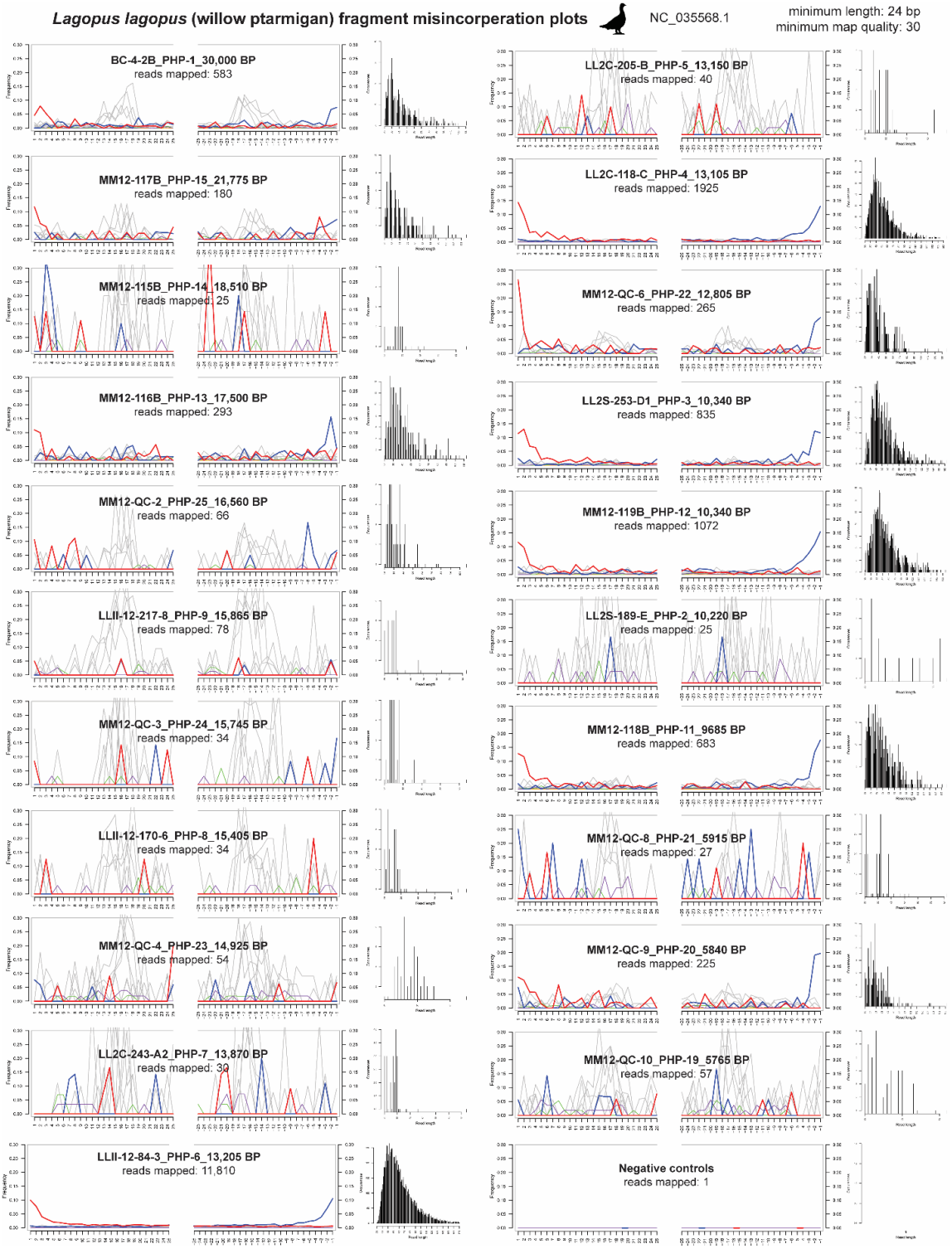

Fig. 5.14 *Lagopus lagopus mapDamage* plots and fragment length distributions.

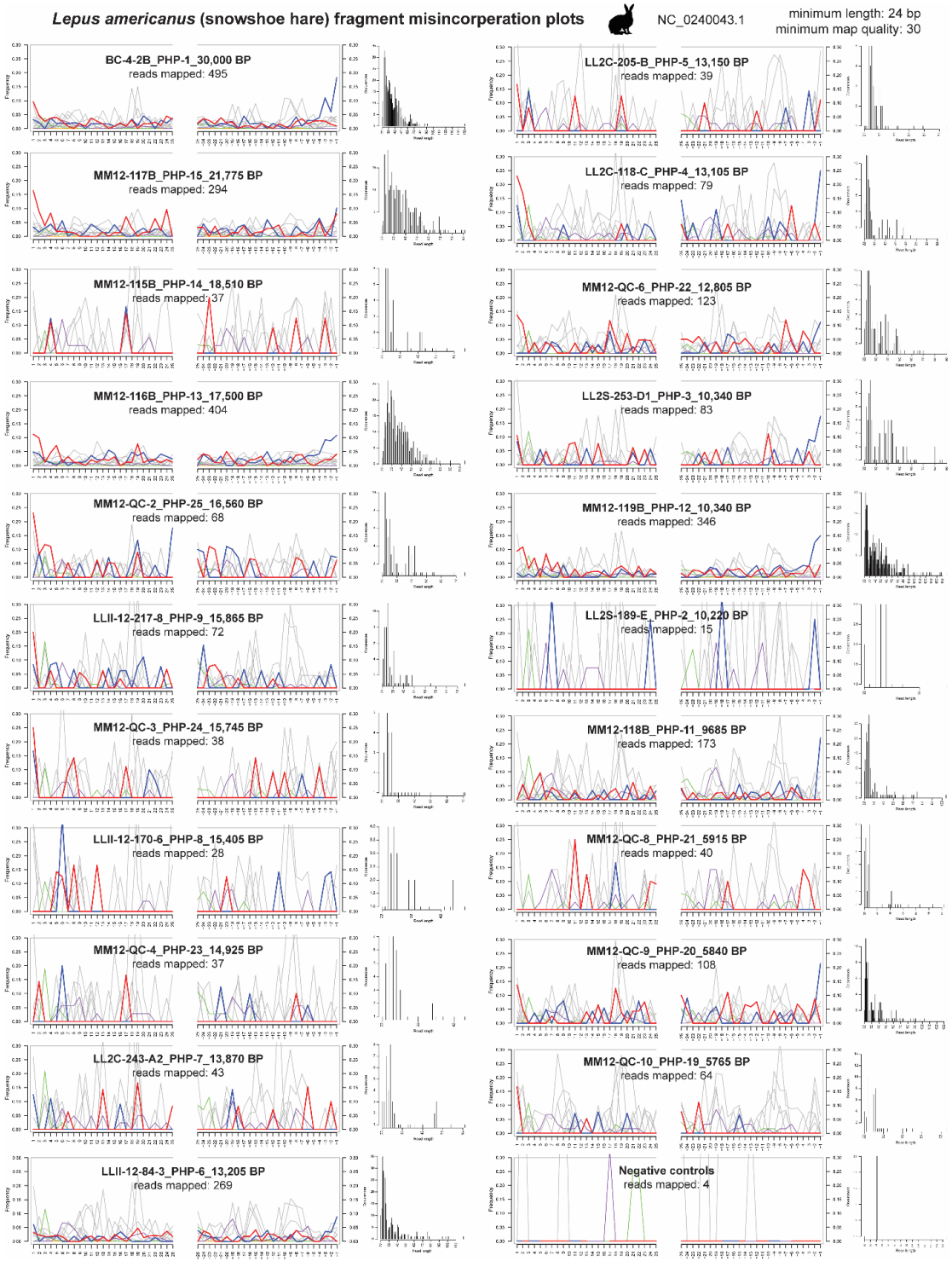

Fig. 5.15 *Lepus americanus mapDamage* plots and fragment length distributions.

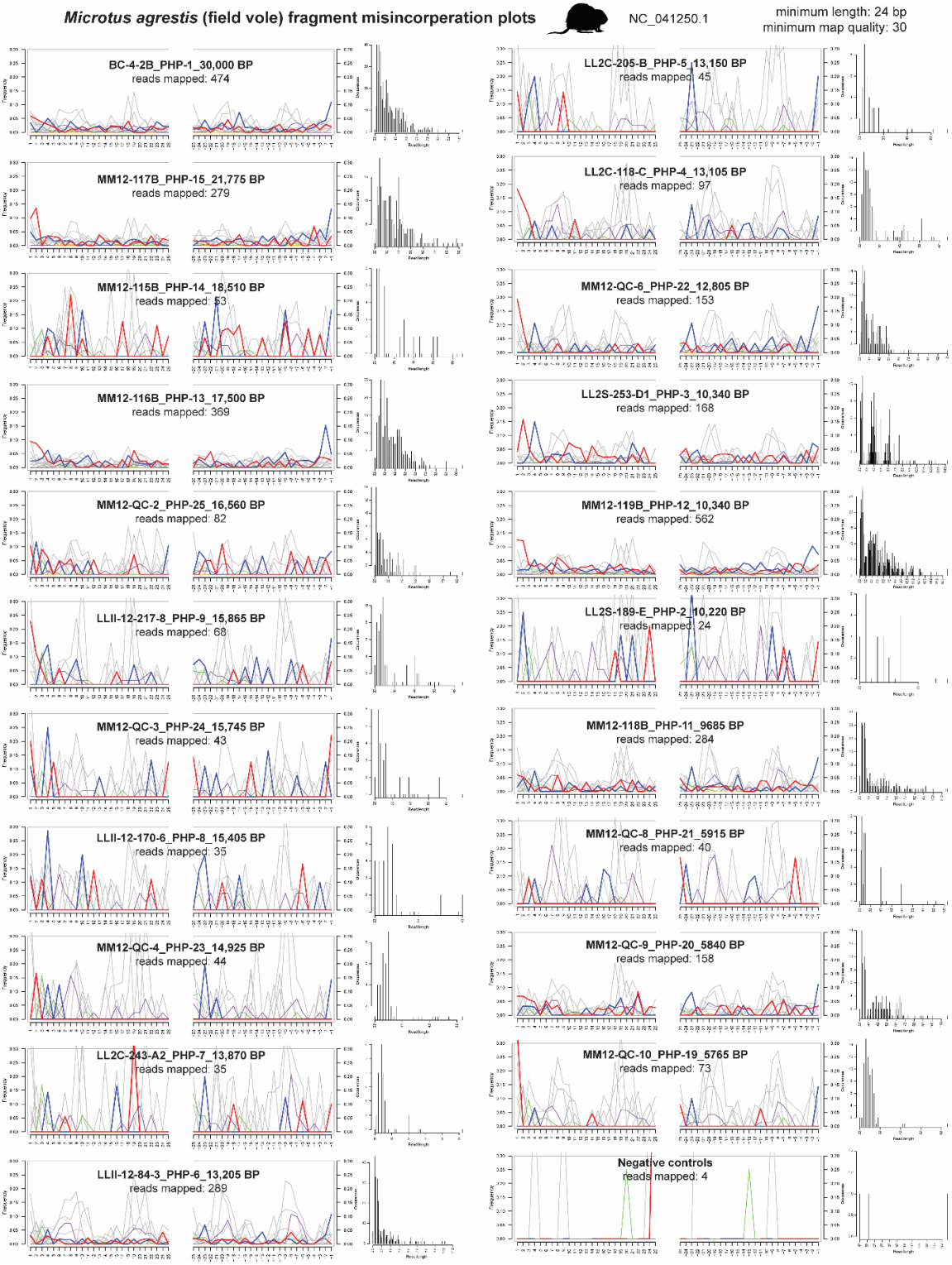

Fig. 5.16 *Microtus agrestis mapDamage* plots and fragment length distributions.

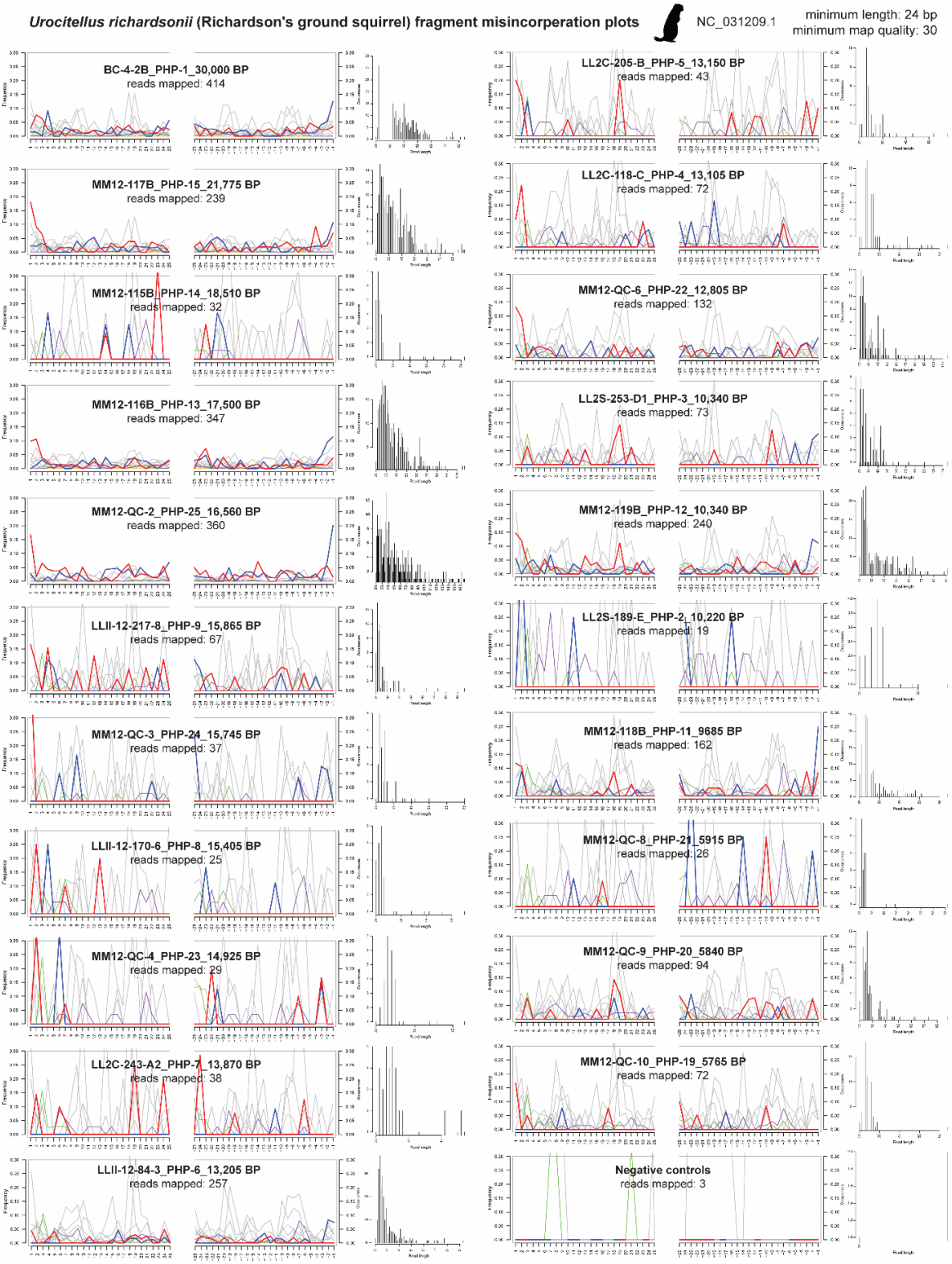

Fig. 5.17 *Uroitellus richardsonii mapDamage* plots and fragment length distributions.

Fig. 5.18 *Poa palustris mapDamage* plots and fragment length distributions.

Fig. 5.19 *Artemisia frigida mapDamage* plots and fragment length distributions.

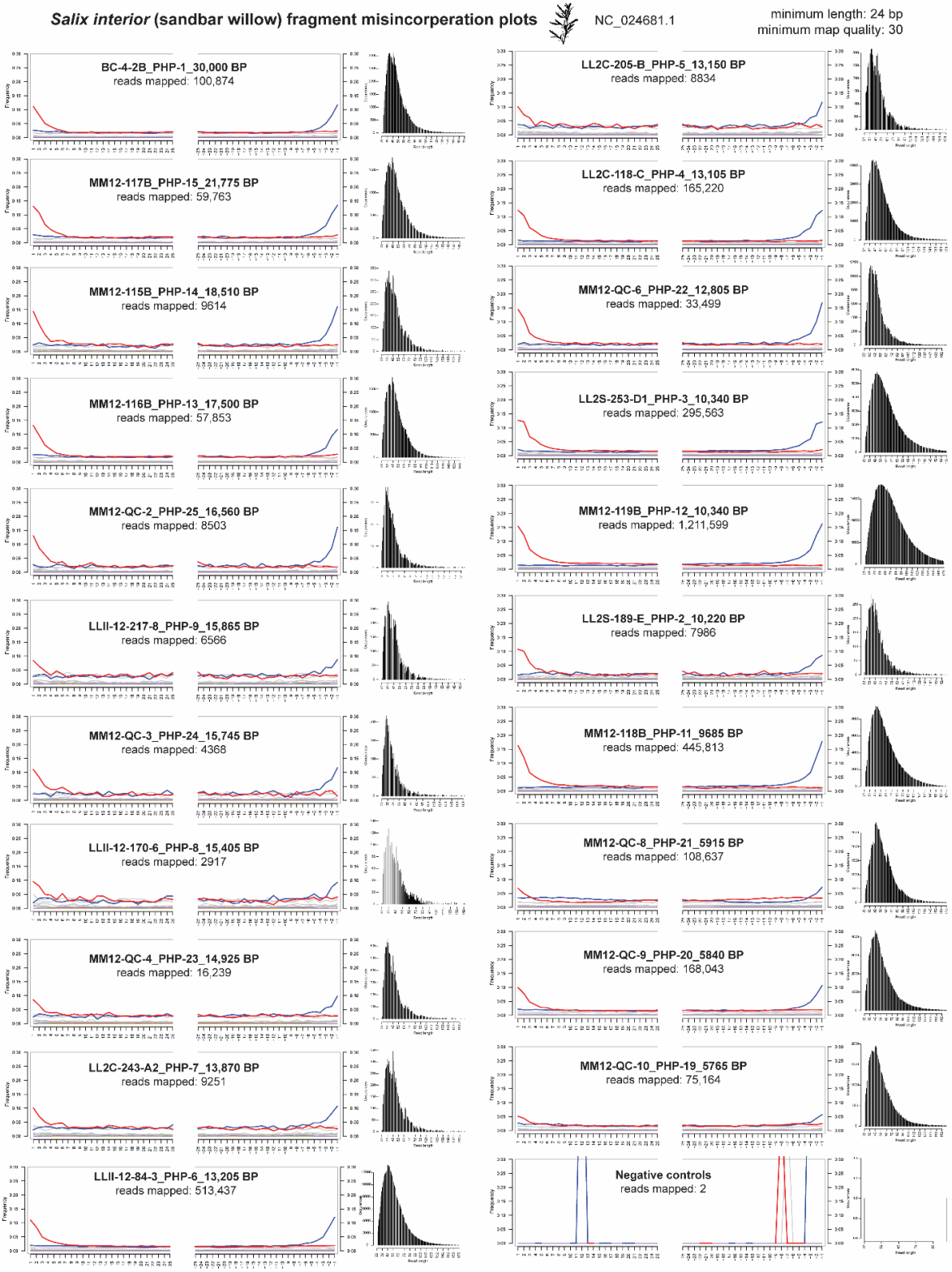

Fig. 5.20 *Salix interior mapDamage* plots and fragment length distributions.

Fig. 5.21 *Picea glauca mapDamage* plots and fragment length distributions.

5.6.5 Specific versus non-specific mapping example

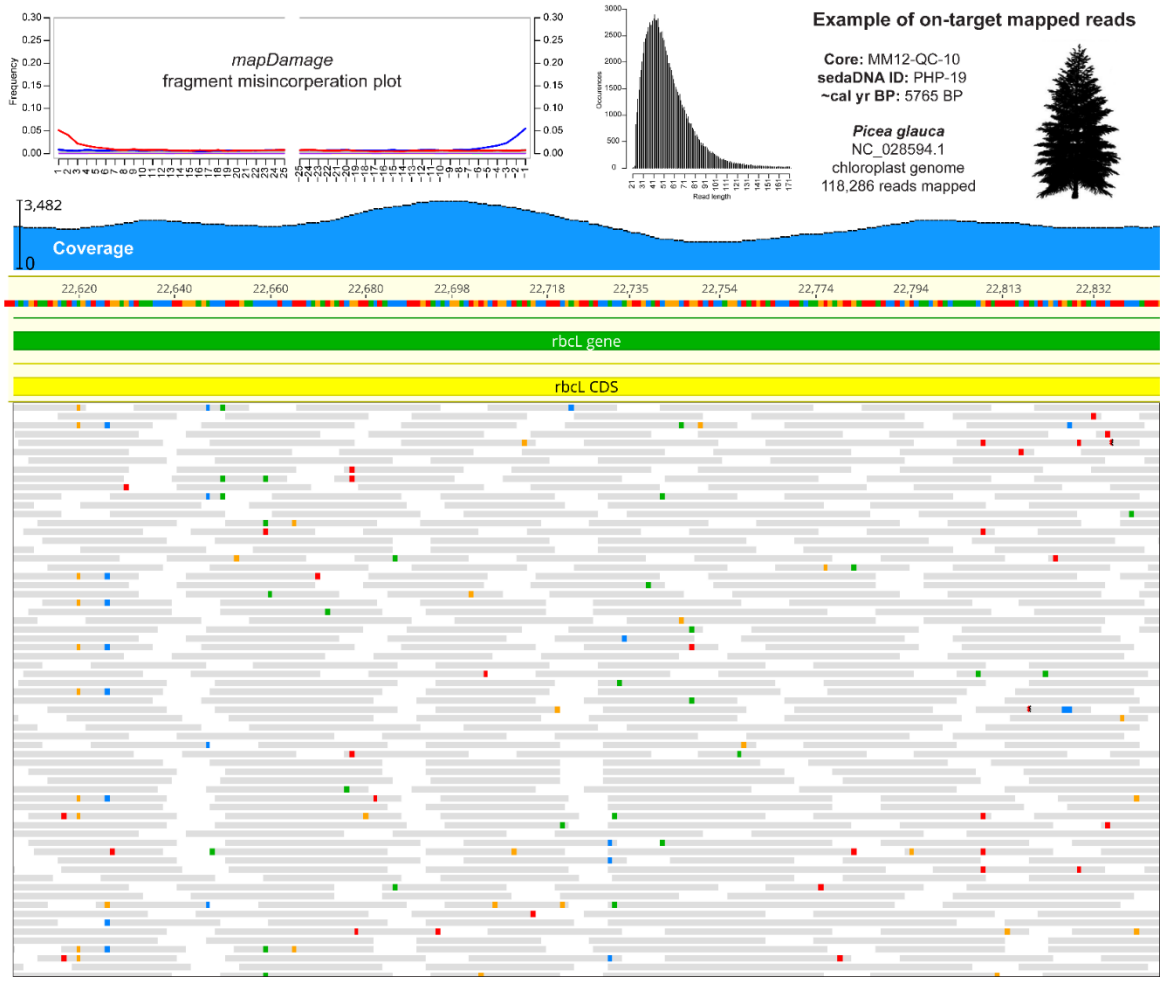

Fig. 5.22 Example of on-target mapped reads for *Picea*.

Fragment misincorporation plot and fragment length distribution generated with *mapDamage* (Jónsson et al., 2013) (v 2.0.3, https://ginolhac.github.io/mapDamage/). Visualization of mapped reads in Geneious Prime (2019.2.3, www.geneious.com).

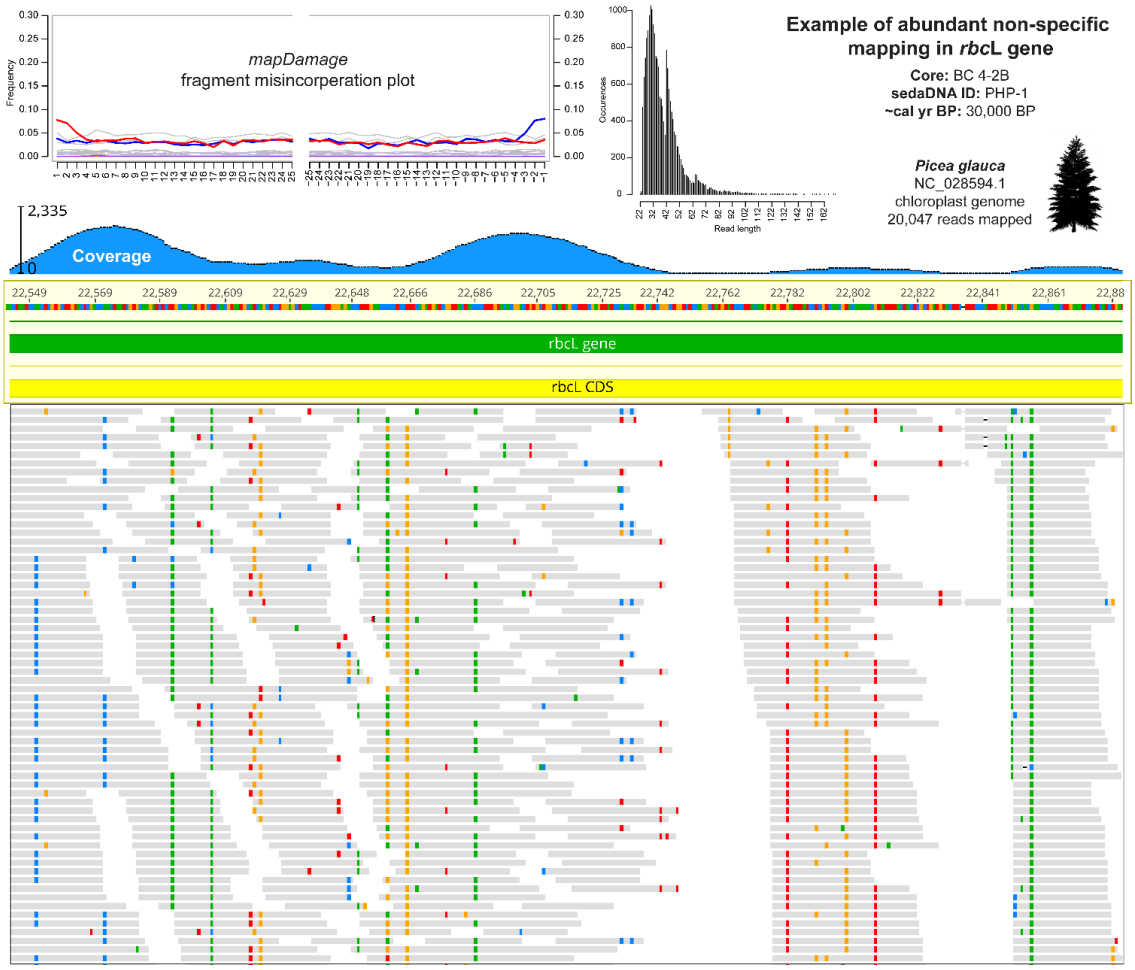

Fig. 5.23 Example of abundant off-target mapped reads for *Picea*.

Fragment misincorporation plot and fragment length distribution generated with *mapDamage* (Jónsson et al., 2013) (v 2.0.3, https://ginolhac.github.io/mapDamage/). Visualization of mapped reads in Geneious Prime (2019.2.3, www.geneious.com).

Note: this off-target mapping does not affect the *BLASTn* to *MEGAN* assignments. However, it does inflate the number of reads that map to a reference when assessing *mapDamage* plots (also causing the jagged baseline). Regardless of off-target reads, there is still a pronounced signal of damage on the ends of these molecules even with the polymorphic interior sites. The number of mapped reads here should not be used to infer taxonomic presence, but rather as a gauge for assessing terminal base damage.

5.6.6 *MEGAN* and *PIA*: Taxonomic binning replicate comparisons

This section includes a taxonomic binning breakdown of subsampled replicates across batches. We observe a consistency between replicates in terms of their taxonomic compositions. We also observe that while the *PIA* taxonomic binning approach may be effective in reducing the potential for false-positive hits, it is too conservative to be of direct utility with this dataset. We utilized the top 600 *BLASTn* hits (100 more hits retained than recommended by the *PIA* developers [Cribdon et al., 2020]), but still observe in many instances that all 600 hits are for the same or very closely related organisms. In these instances, *PIA* drops the read entirely assuming that this portion of the database is lacking in references aside from a set of over-represented 'oasis' taxa, irrespective of the taxonomic accuracy. Overall, this results in substantial data loss compared with *MEGAN*. We suspect that this limitation could be avoided by returning as many as the top 1500+ hits, but our blast files were already almost unwieldy with 600 hits. Some individual blast files are over 200 gigabytes, and in total the post-filtering dataset is approximately 3 terabytes in size. These limitations could likely be avoided by utilizing a non-redundant or otherwise manually curated reference database, but these options may bias taxonomic binning to only organisms one expects to find. A *BLASTn* or similar alignment approach that had the option to collapse accession hits based on Taxonomy ID up to a certain threshold and could instead return the top 500+ Taxonomic ID hits would help alleviate the challenges of metagenomic noise observed here and in Murchie et al. (2021b). We also observed that there is utility in an ensemble *PIA* and *MEGAN* approach insofar as it provides a sanity check for taxonomic binning of rare or unexpected taxa. The flexibility and power of *MEGAN* with its customizable LCA and comprehensive GUI was found to be highly effective with this dataset, with limitations in *BLASTn* customization being the limiting factor.

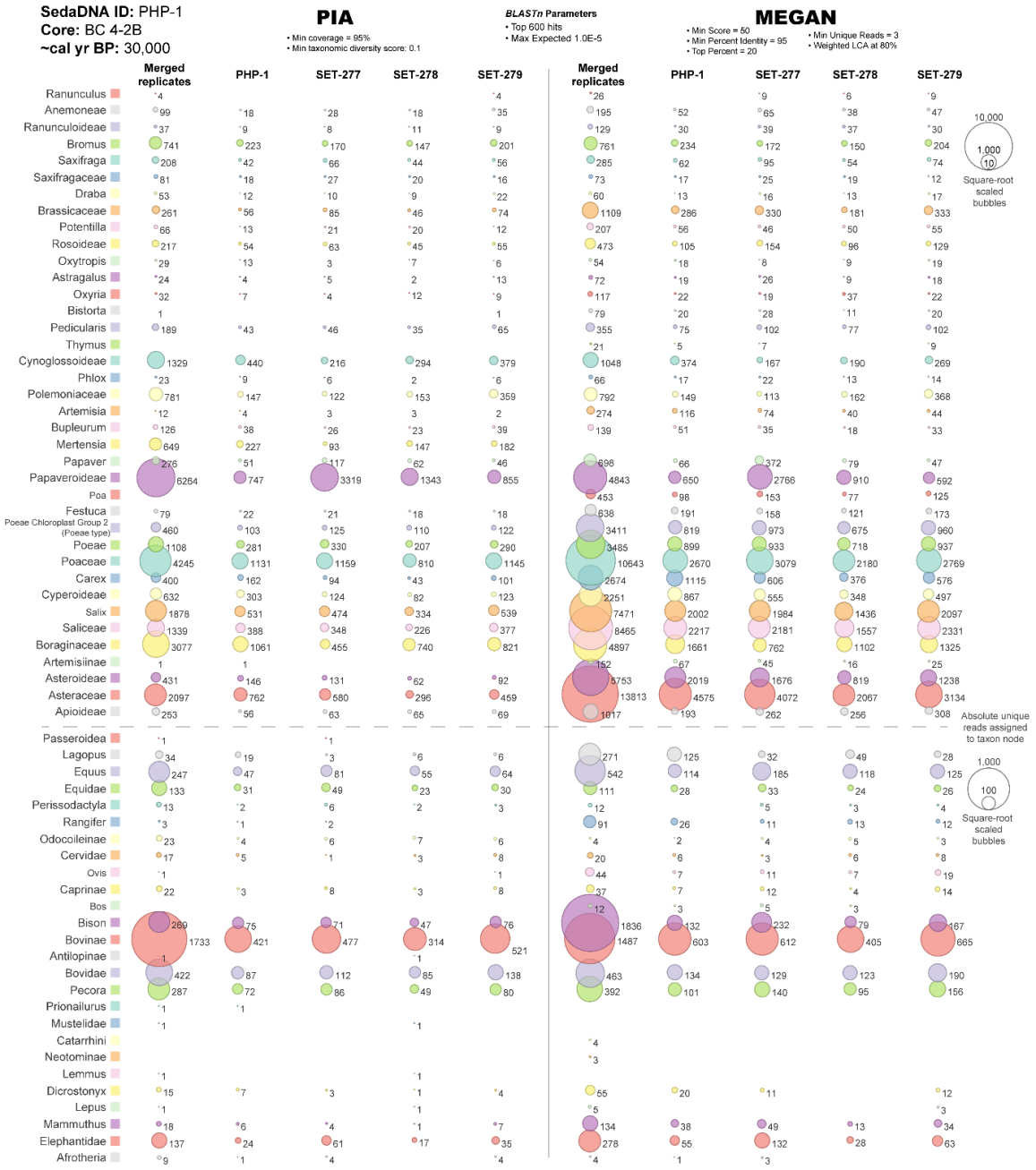

Fig. 5.24 PHP-1 replicates comparison with *PIA* and *MEGAN* taxonomic binning. Select nodes depicted.

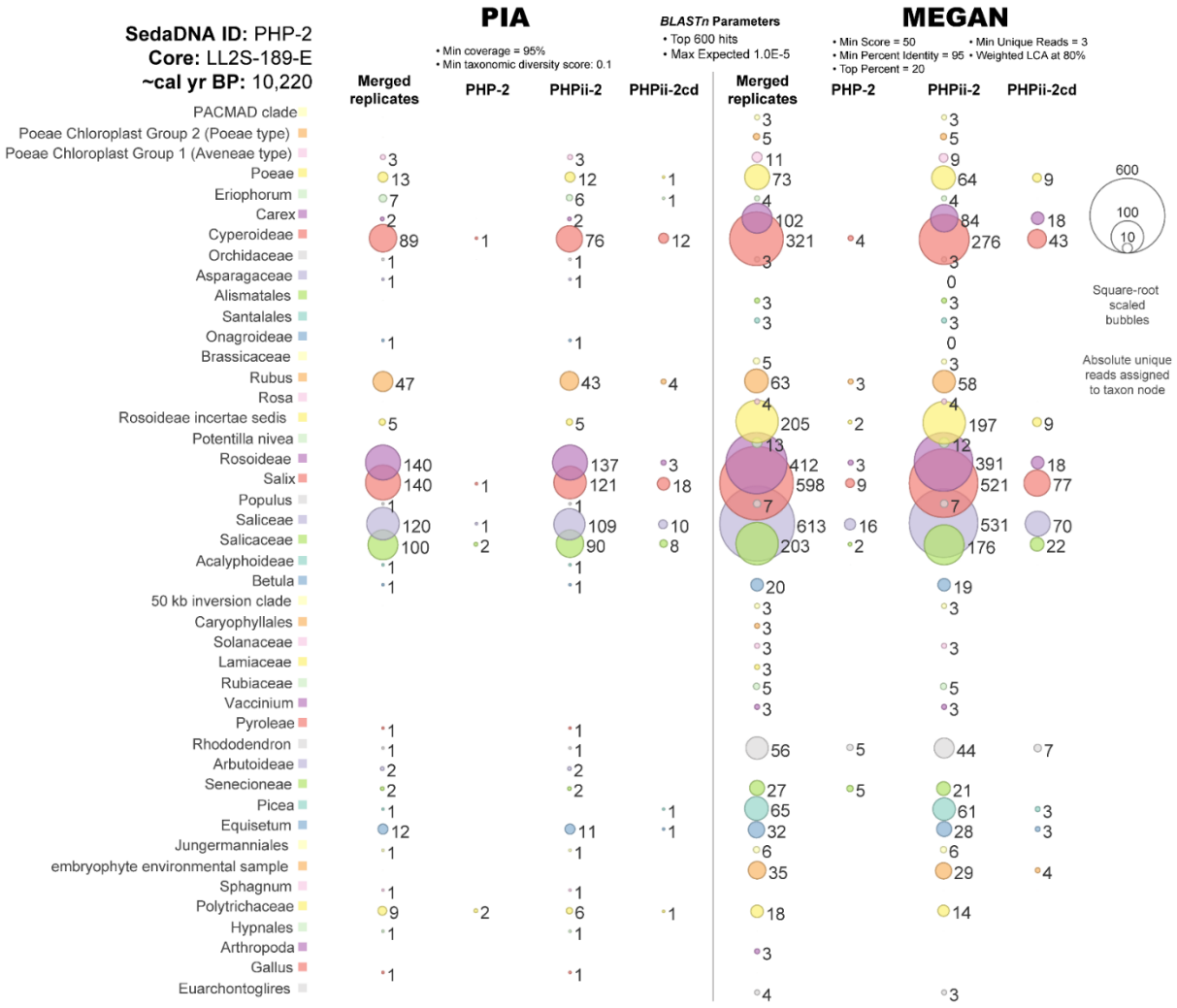

Fig. 5.25 PHP-2 replicates comparison with *PIA* and *MEGAN* taxonomic binning. Select nodes depicted.

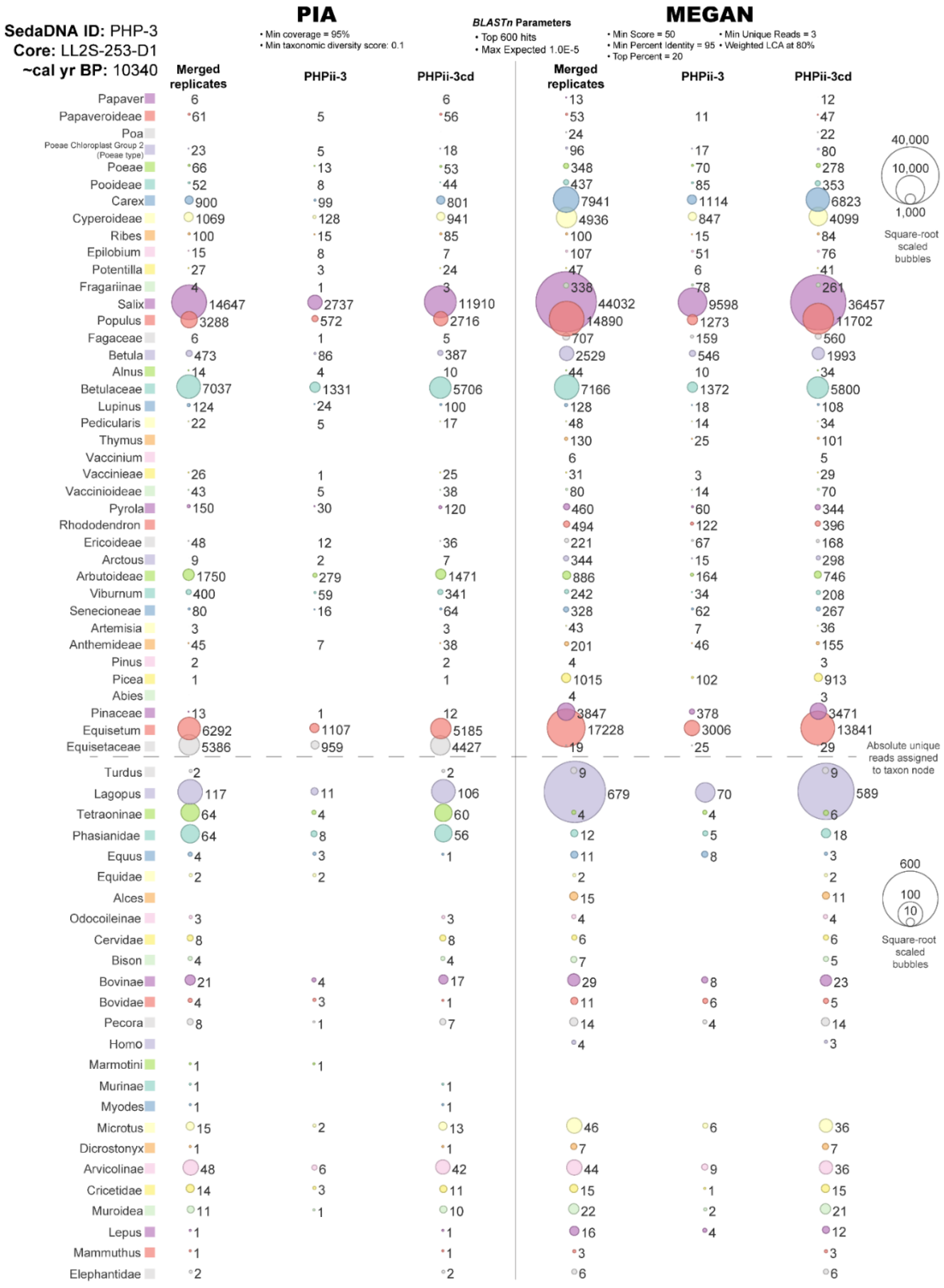

Fig. 5.26 PHP-3 replicates comparison with *PIA* and *MEGAN* taxonomic binning. Select nodes depicted.

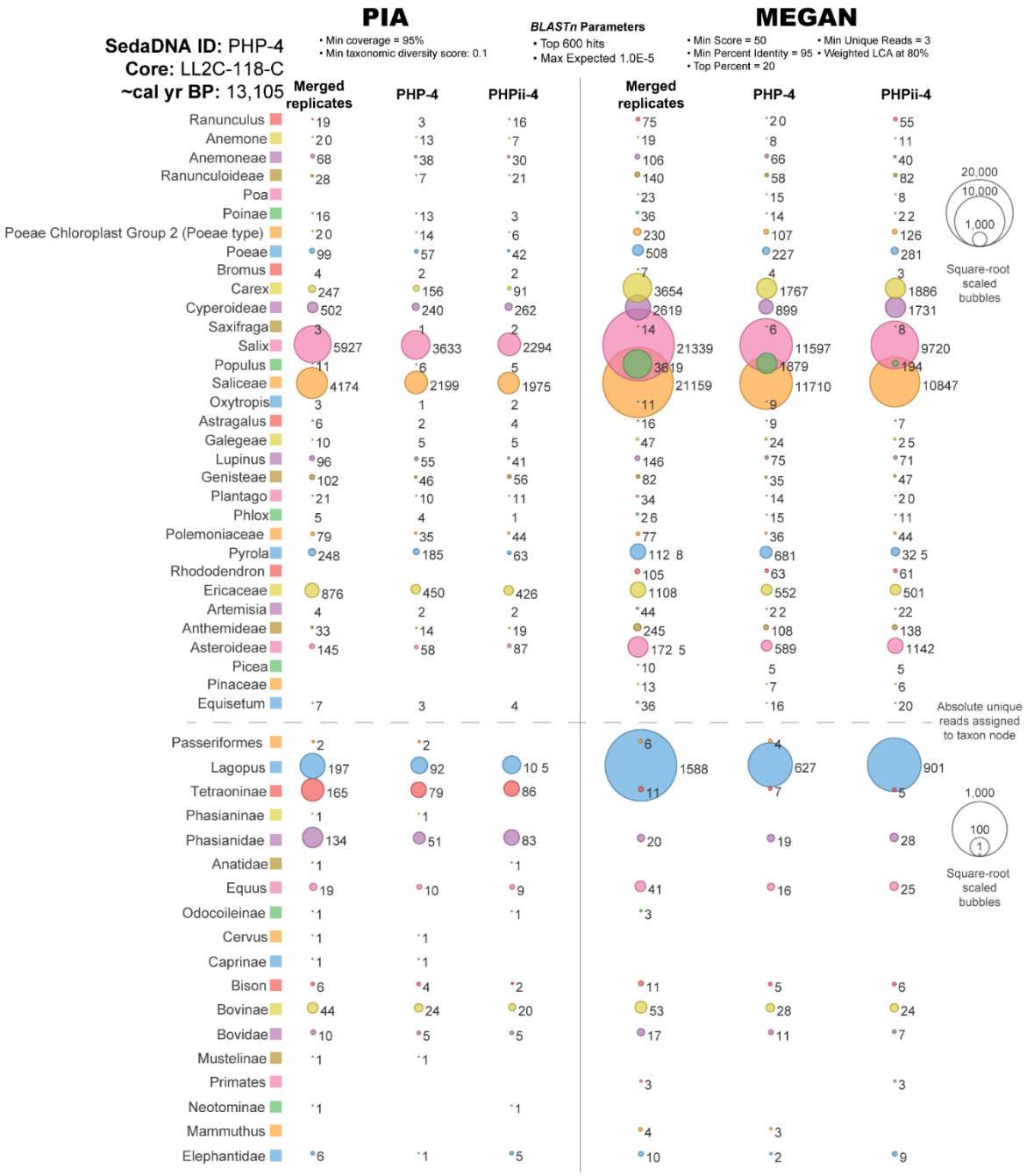

Fig. 5.27 PHP-4 replicates comparison with *PIA* and *MEGAN* taxonomic binning. Select nodes depicted.

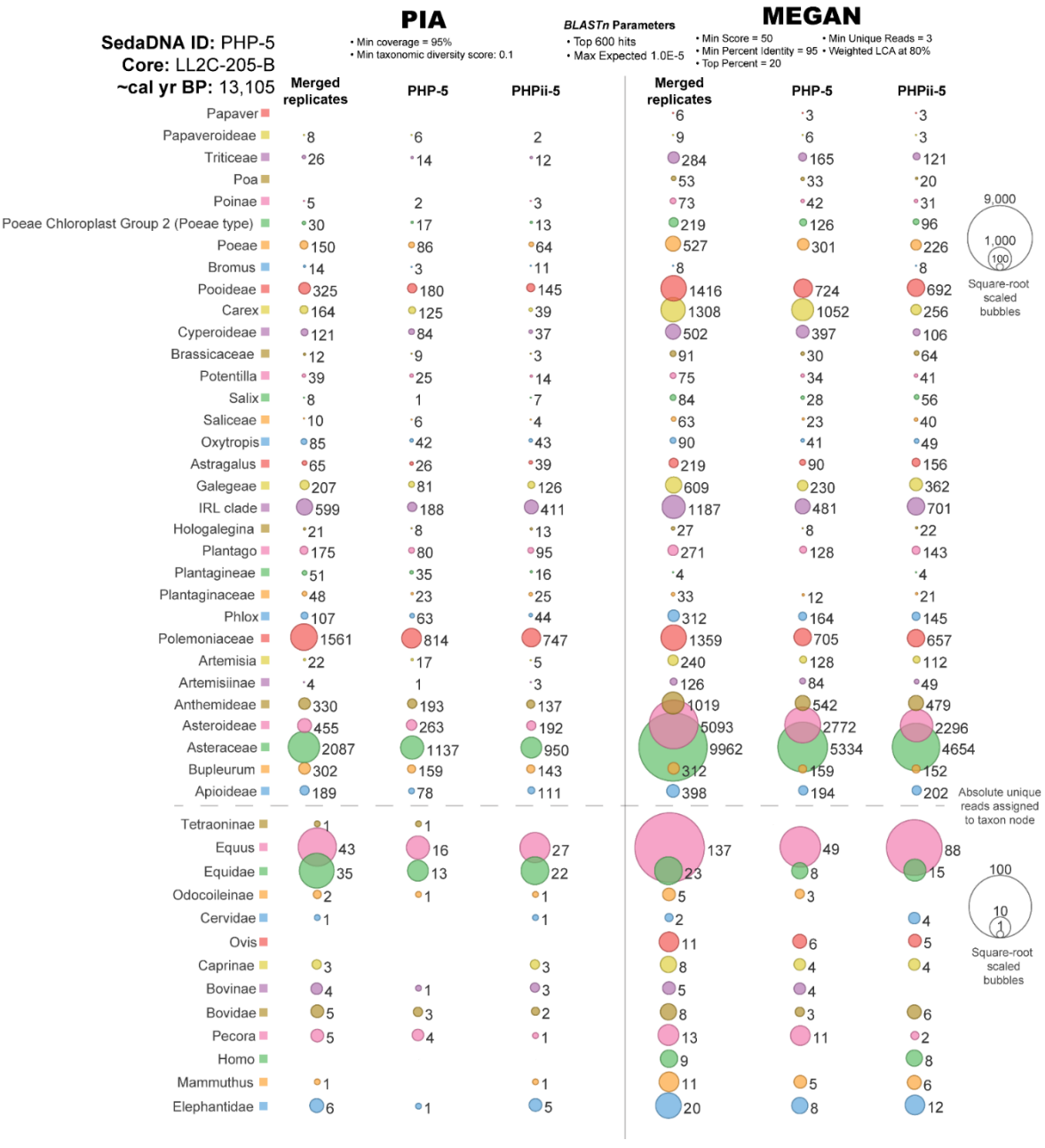

Fig. 5.28 PHP-5 replicates comparison with *PIA* and *MEGAN* taxonomic binning. Select nodes depicted.

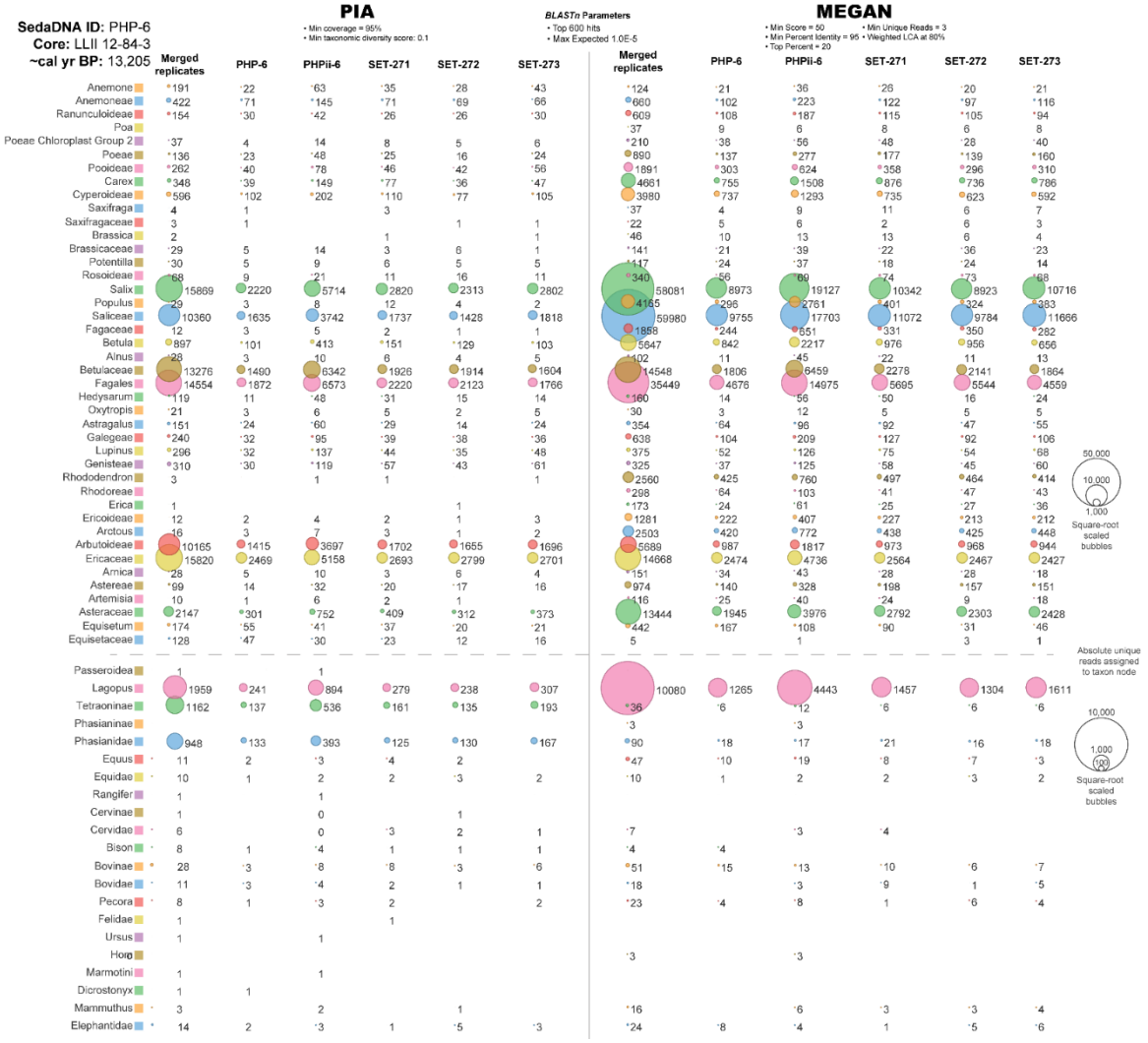

Fig. 5.29 PHP-6 replicates comparison with *PIA* and *MEGAN* taxonomic binning. Select nodes depicted.

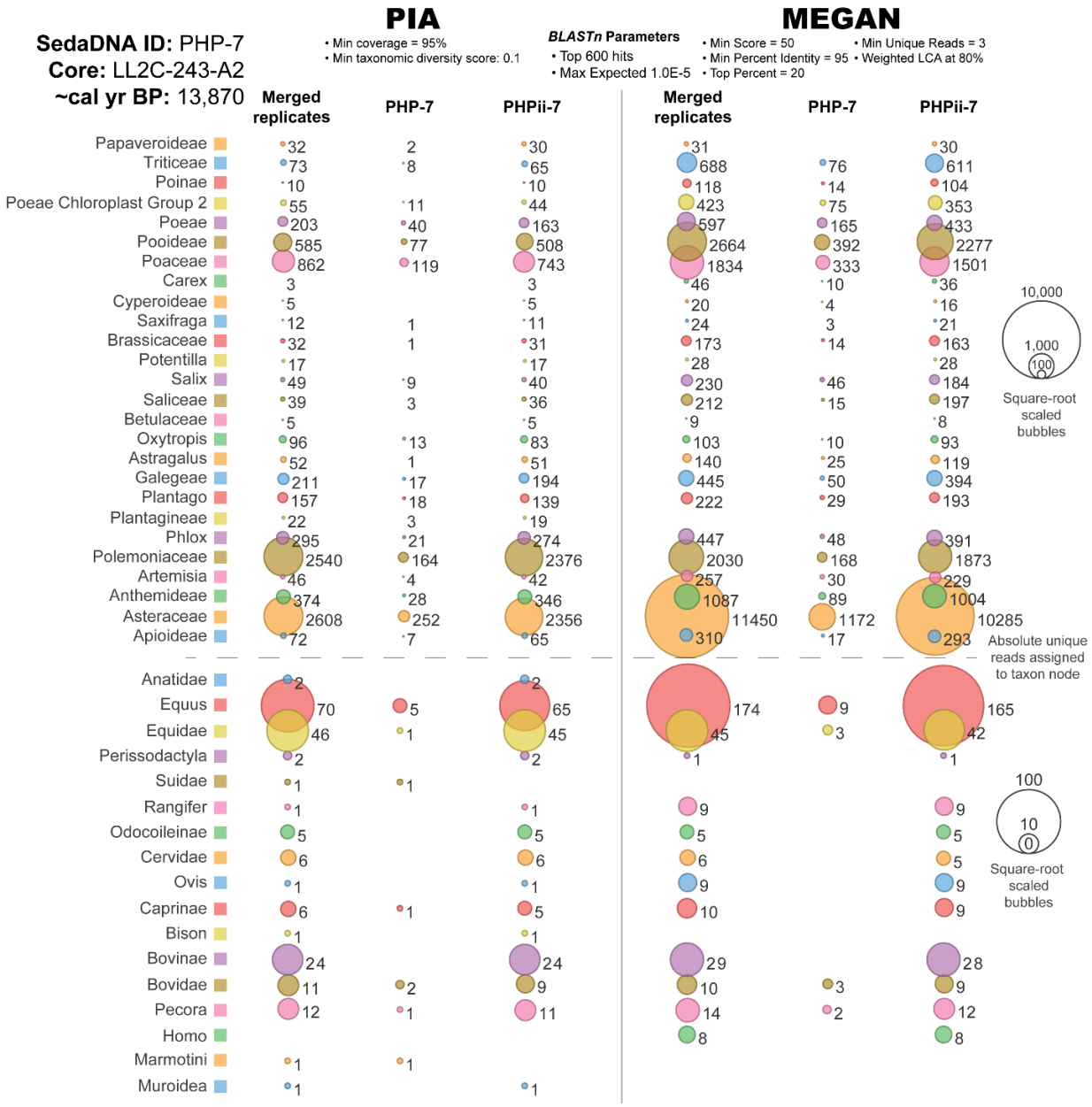

Fig. 5.30 PHP-7 replicates comparison with *PIA* and *MEGAN* taxonomic binning. Select nodes depicted.

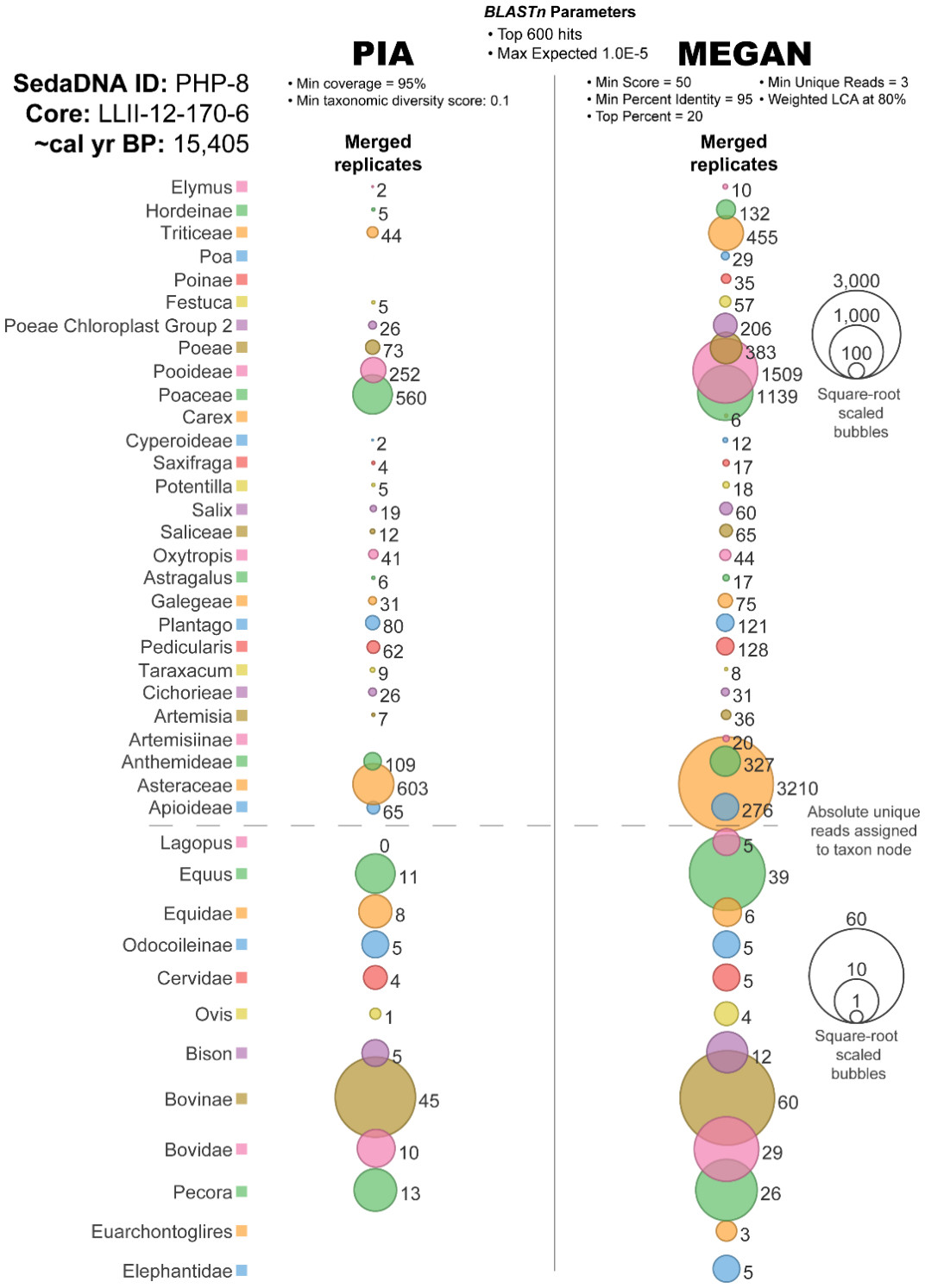

Fig. 5.31 PHP-8 replicates comparison with *PIA* and *MEGAN* taxonomic binning. Select nodes depicted.

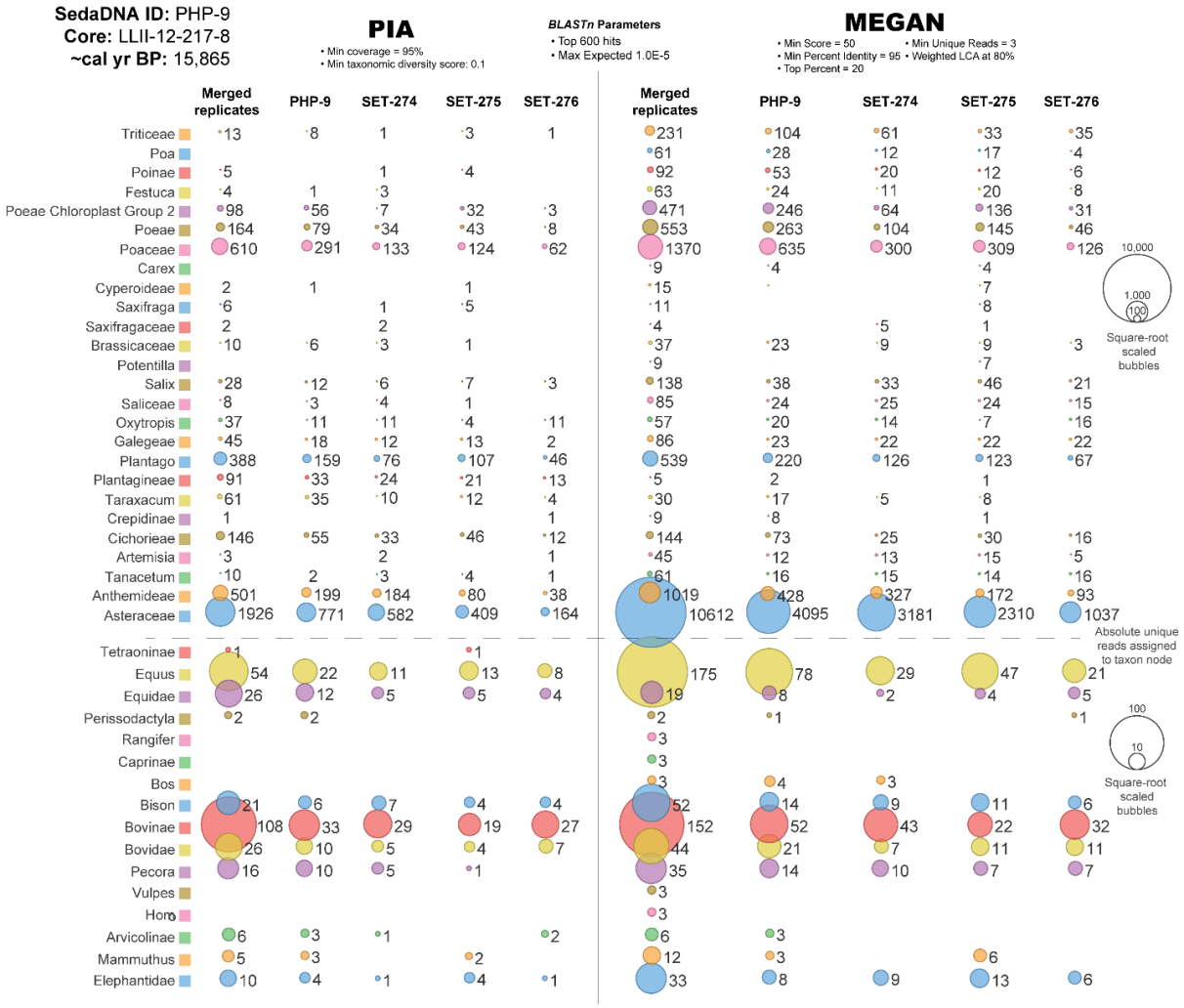

Fig. 5.32 PHP-9 replicates comparison with *PIA* and *MEGAN* taxonomic binning. Select nodes depicted.

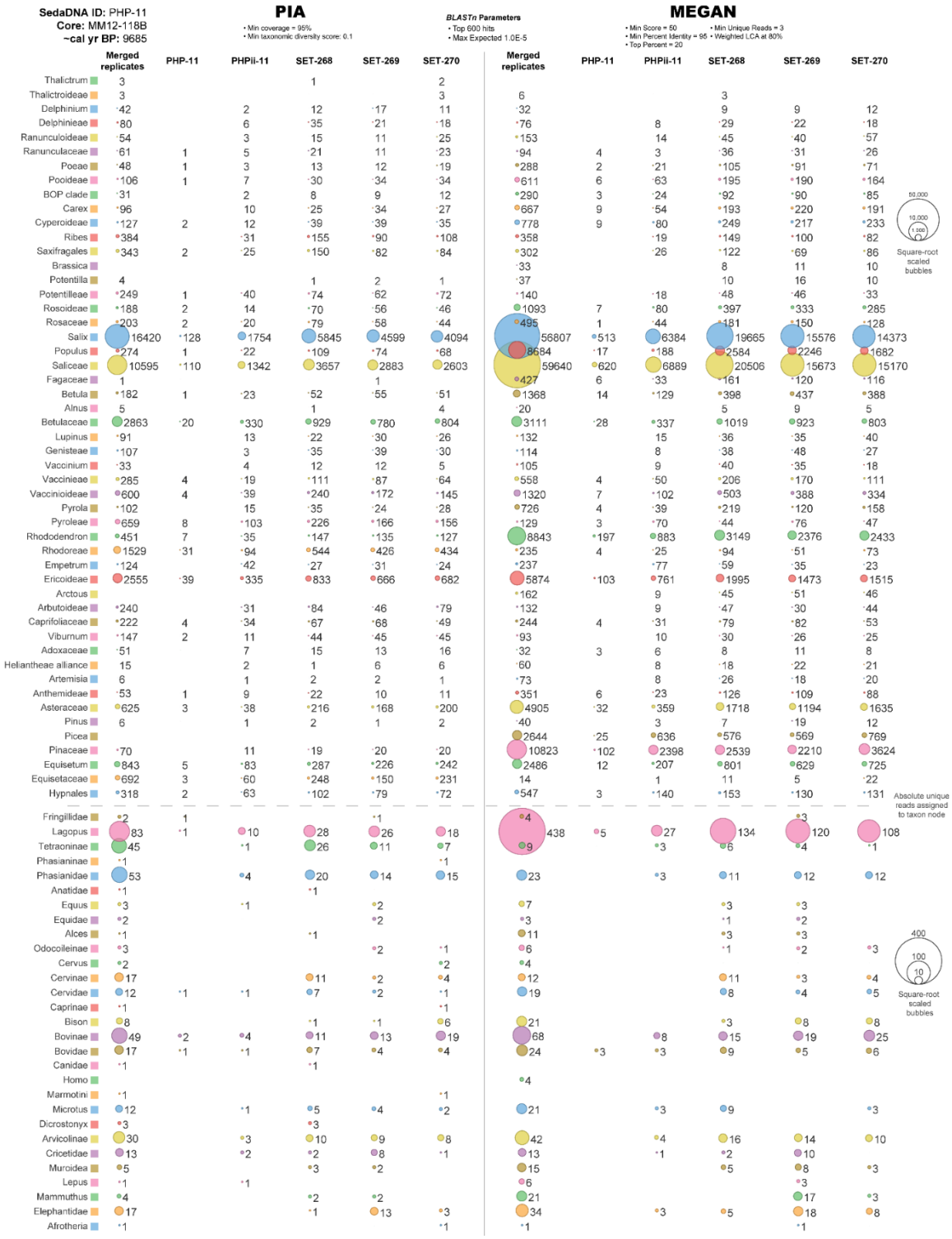

Fig. 5.33 PHP-11 replicates comparison with *PIA* and *MEGAN* taxonomic binning. Select nodes depicted.

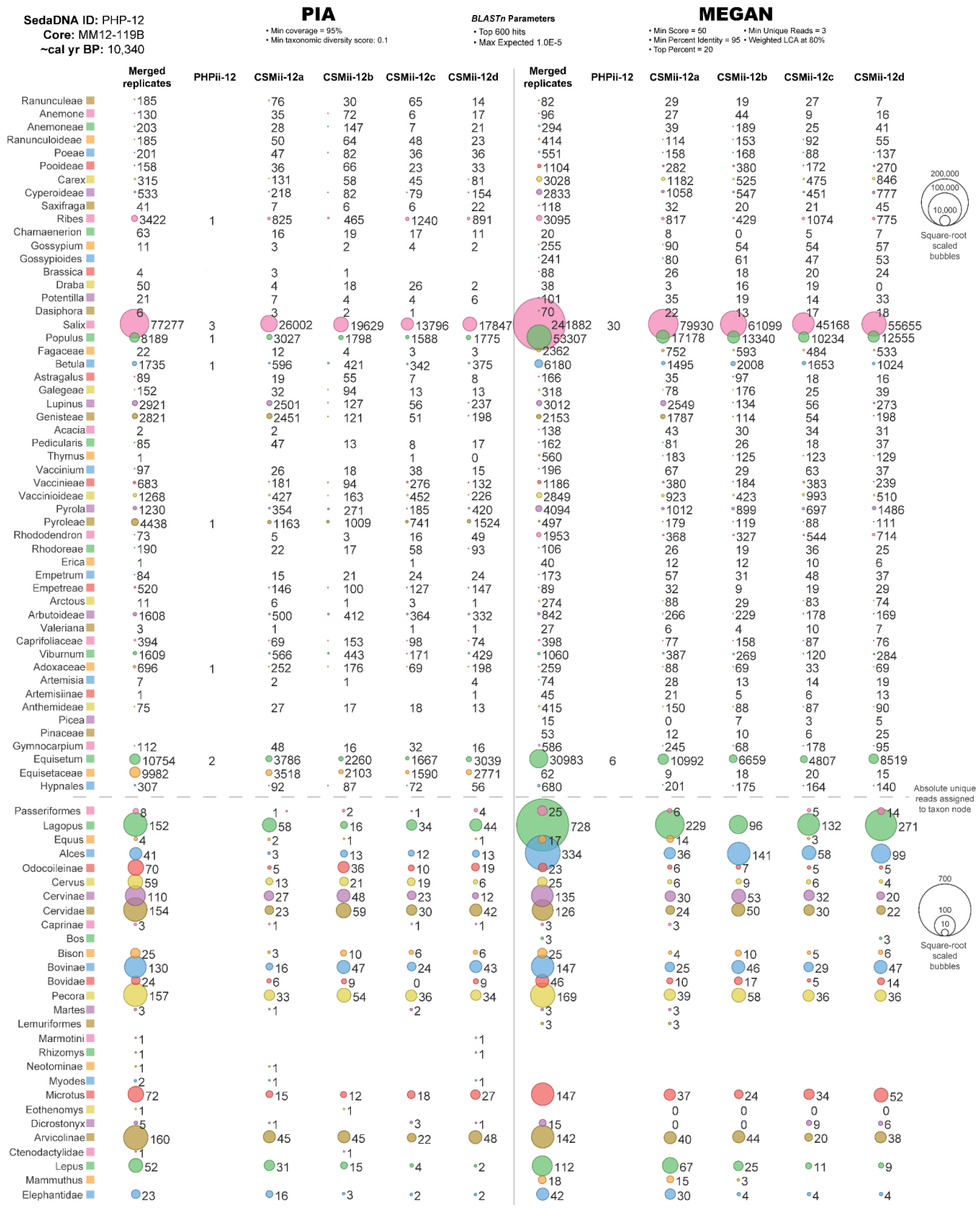

Fig. 5.34 PHP-12 replicates comparison with *PIA* and *MEGAN* taxonomic binning. Select nodes depicted.

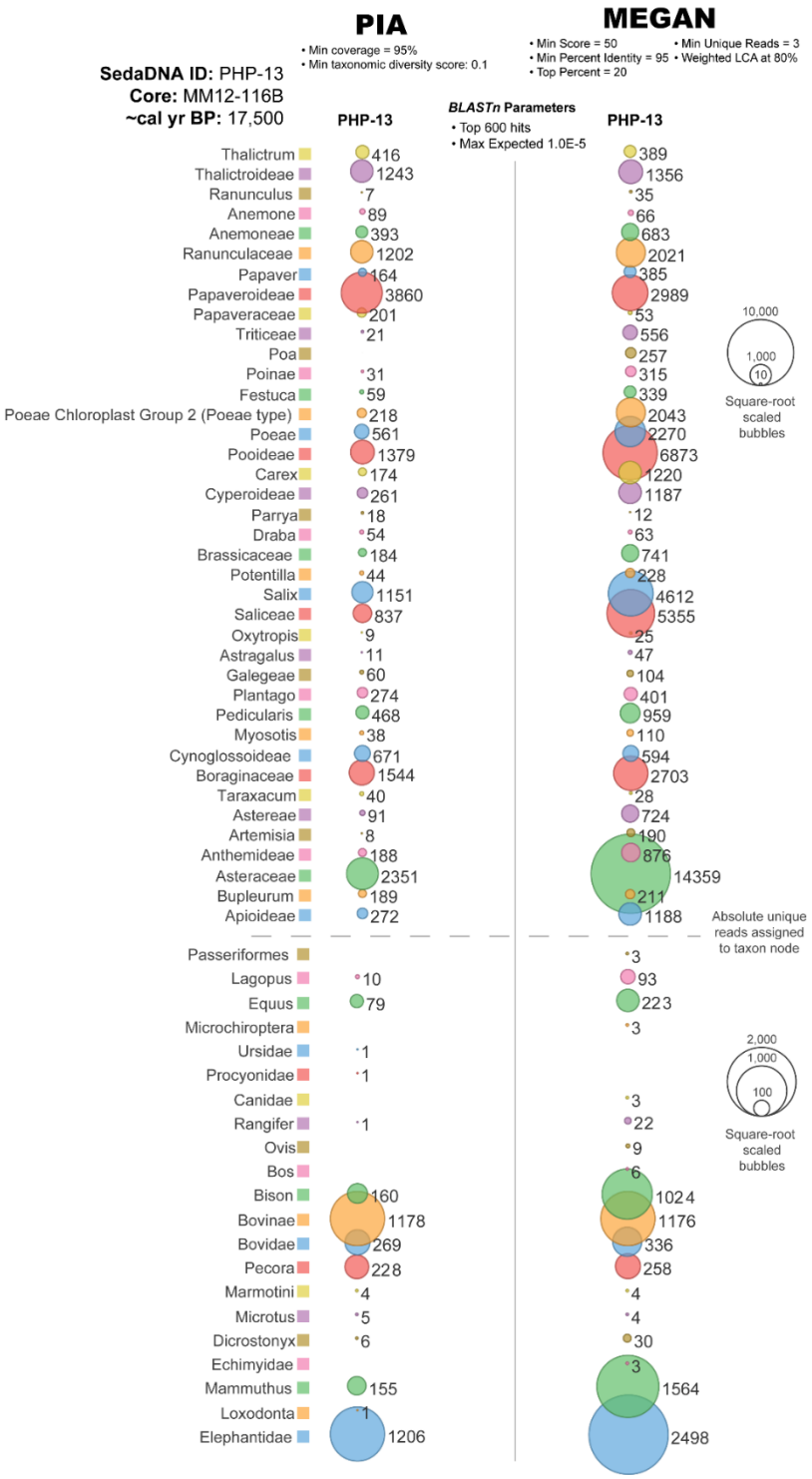

Fig. 5.35 PHP-13 replicates comparison with *PIA* and *MEGAN* taxonomic binning. Select nodes depicted.

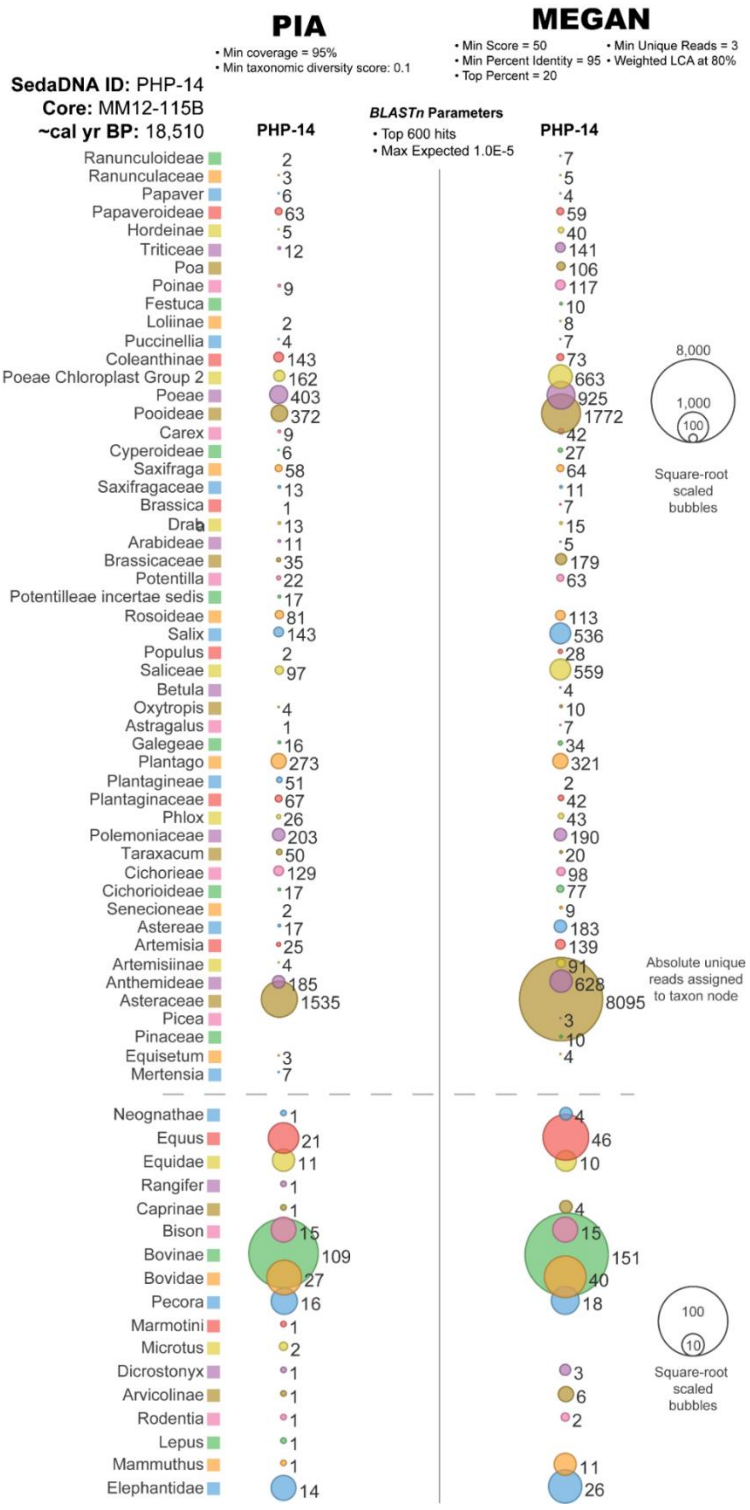

Fig. 5.36 PHP-14 replicates comparison with *PIA* and *MEGAN* taxonomic binning. Select nodes depicted.

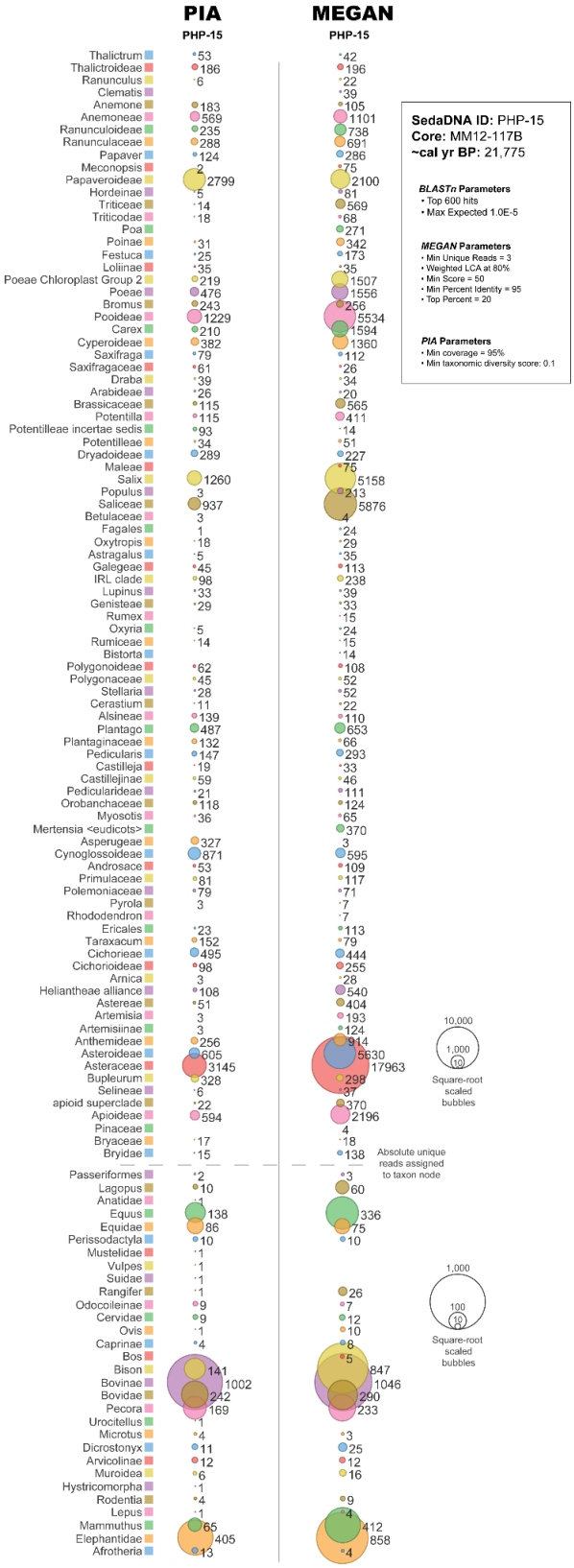

Fig. 5.37 PHP-15 replicates comparison with *PIA* and *MEGAN* taxonomic binning.

Select nodes depicted.

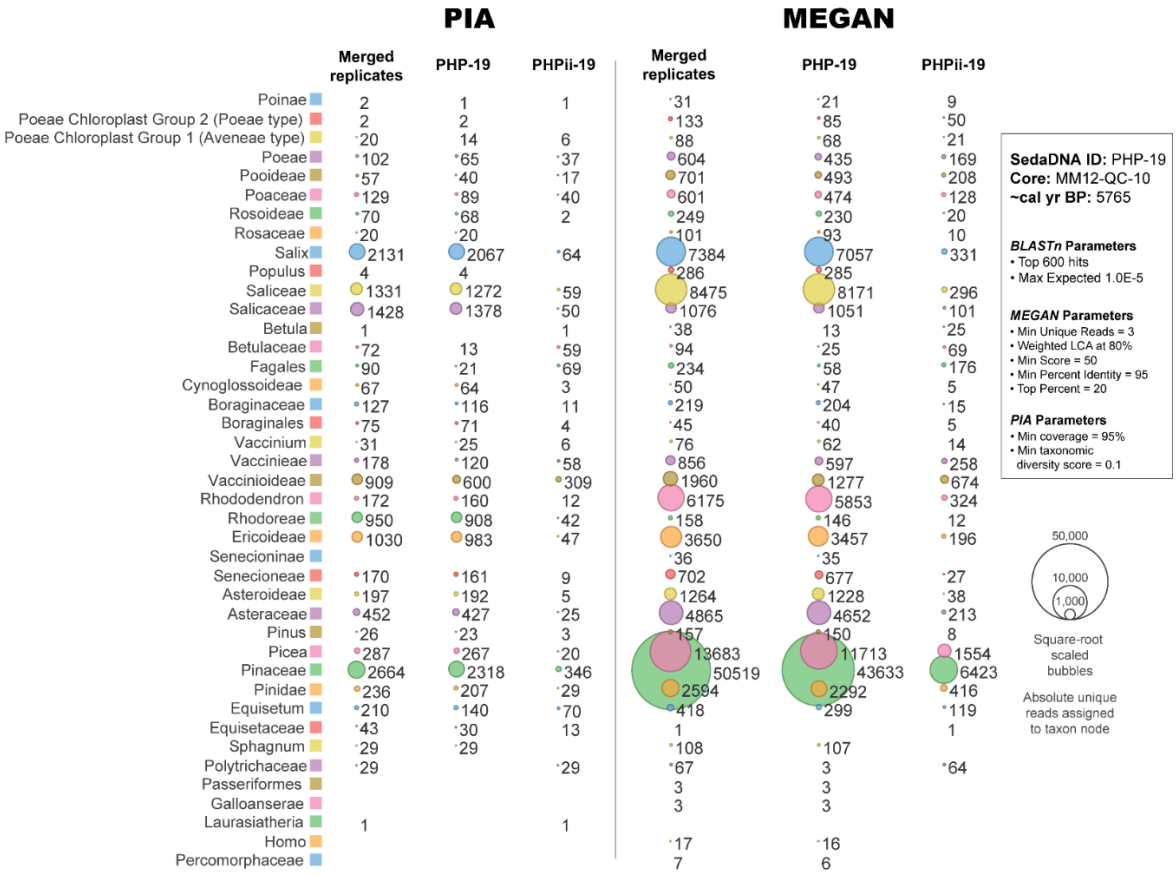

Fig. 5.38 PHP-19 replicates comparison with *PIA* and *MEGAN* taxonomic binning. Select nodes depicted.

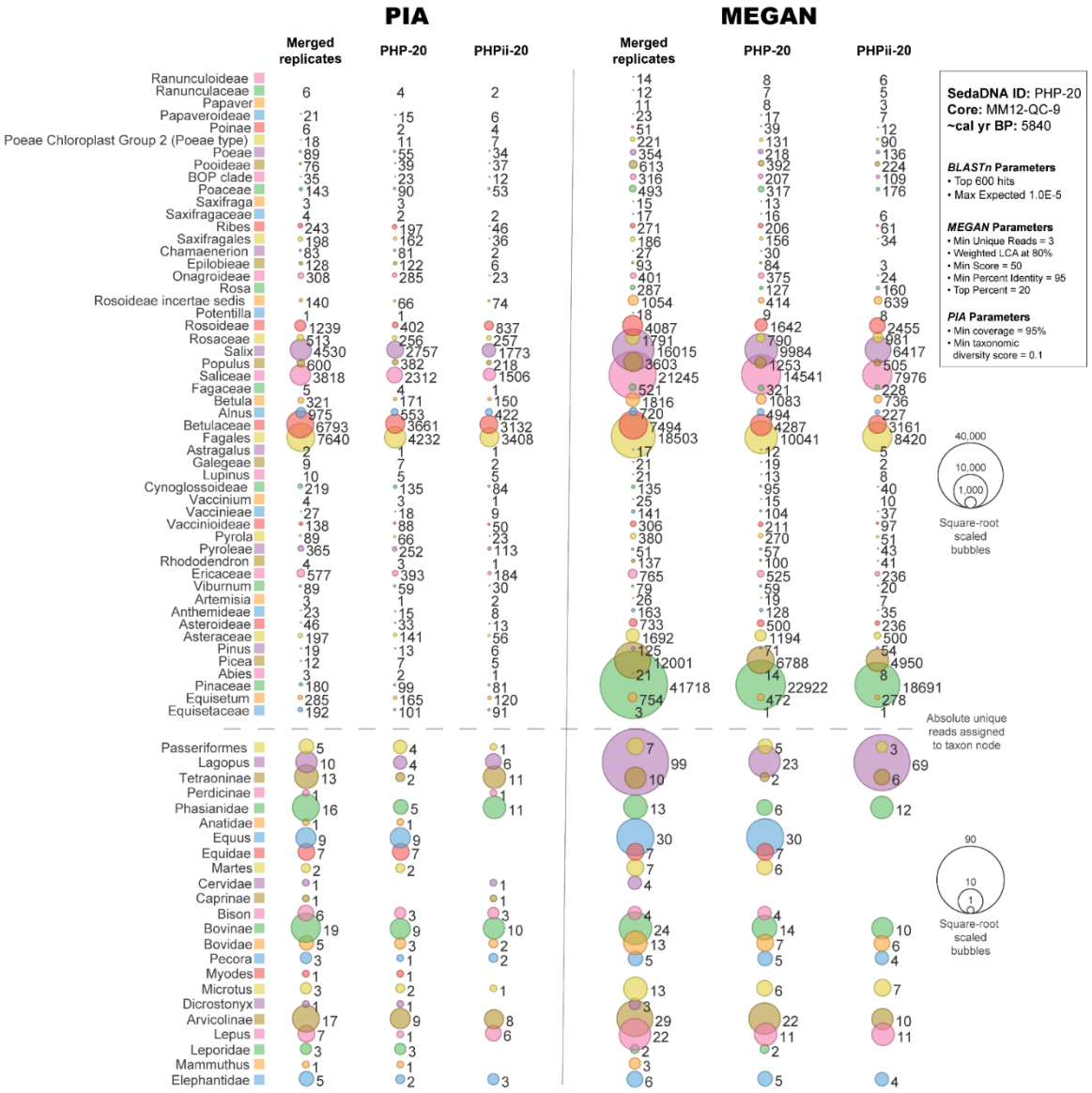

Fig. 5.39 PHP-20 replicates comparison with *PIA* and *MEGAN* taxonomic binning. Select nodes depicted.

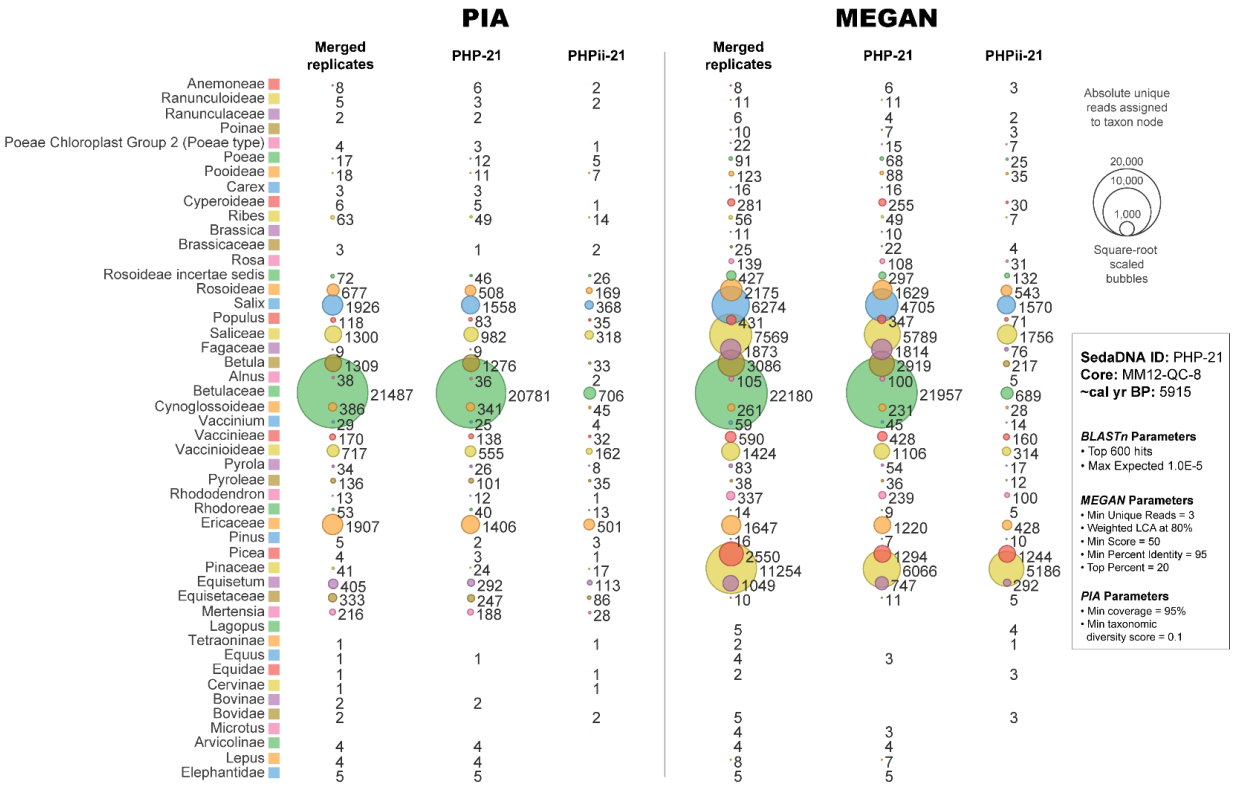

Fig. 5.40 PHP-21 replicates comparison with *PIA* and *MEGAN* taxonomic binning. Select nodes depicted.

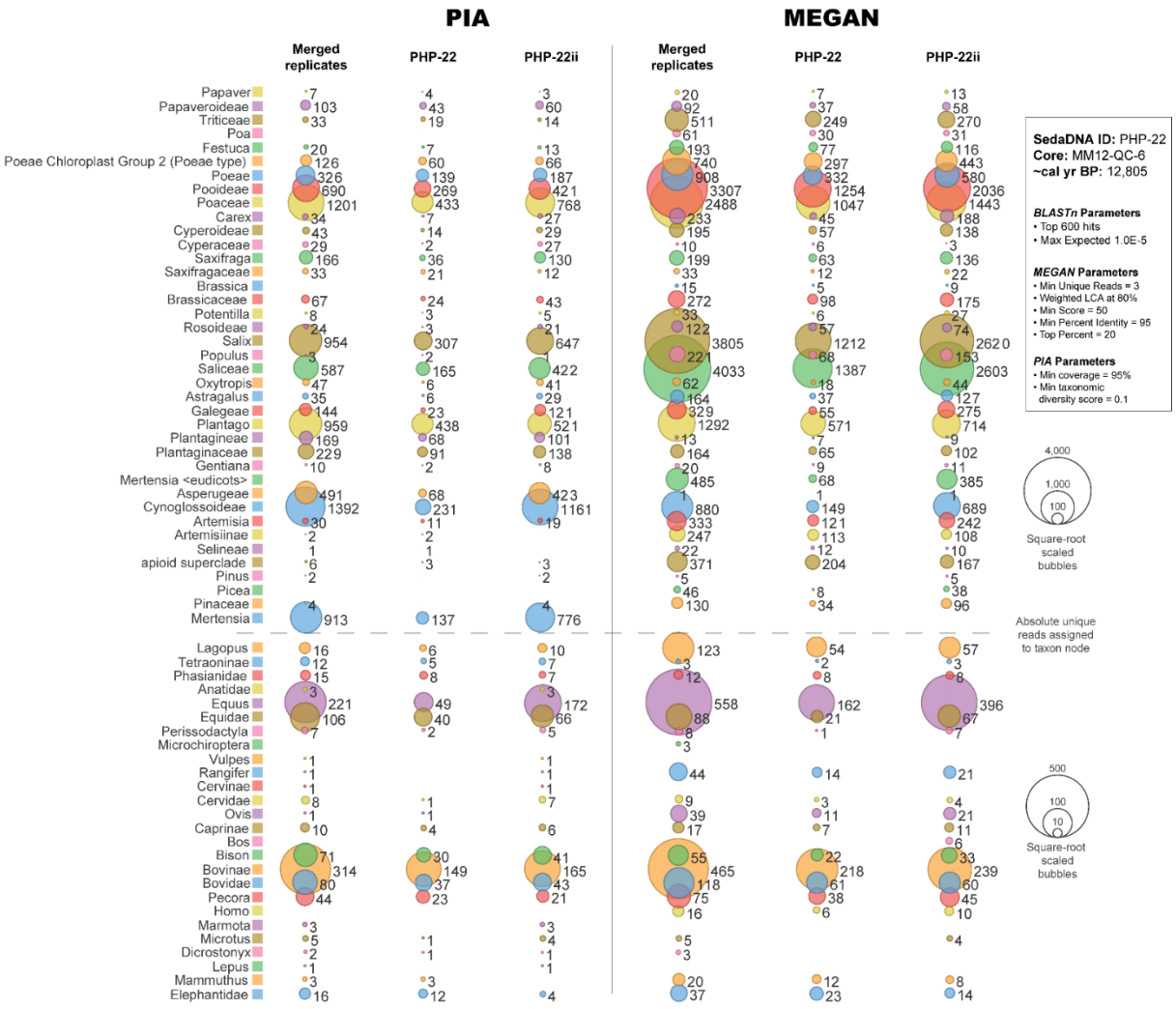

Fig. 5.41 PHP-22 replicates comparison with *PIA* and *MEGAN* taxonomic binning. Select nodes depicted.

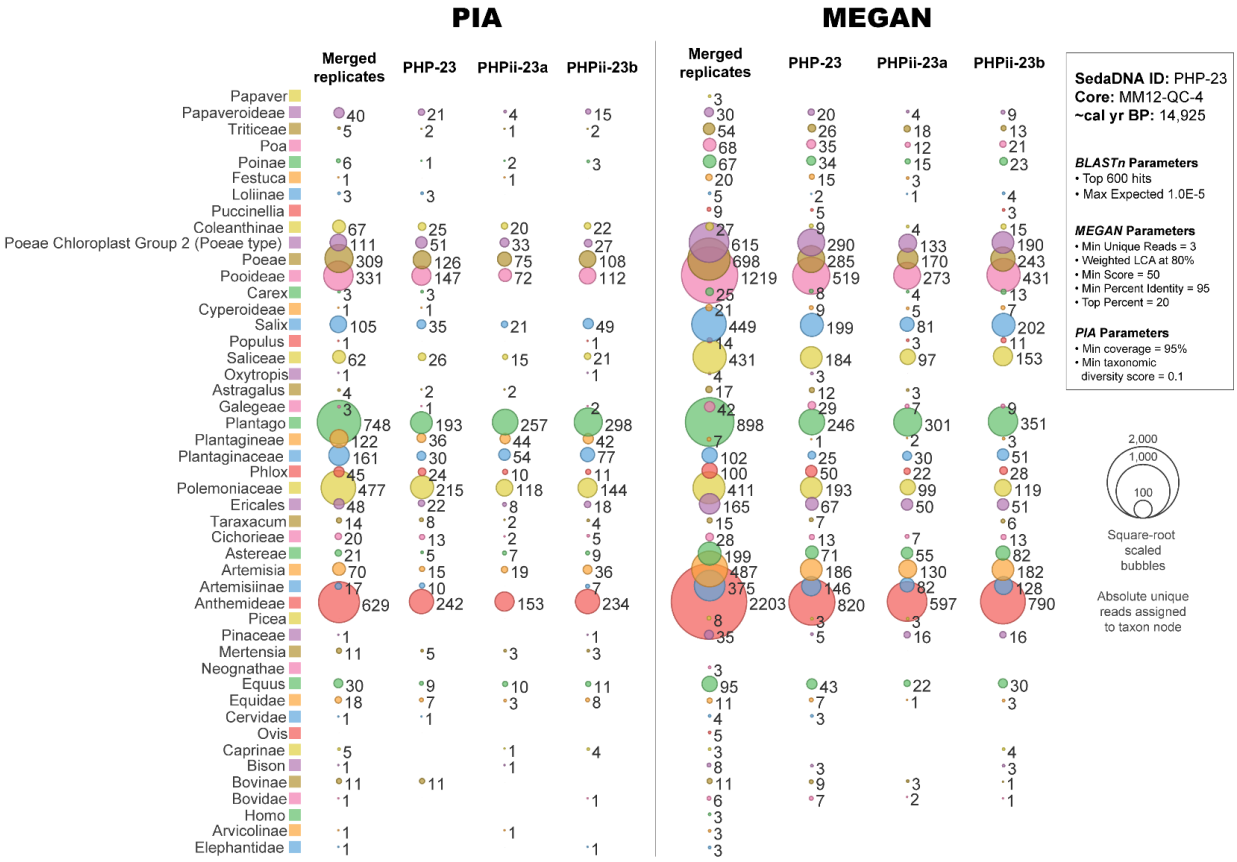

Fig. 5.42 PHP-23 replicates comparison with *PIA* and *MEGAN* taxonomic binning. Select nodes depicted.

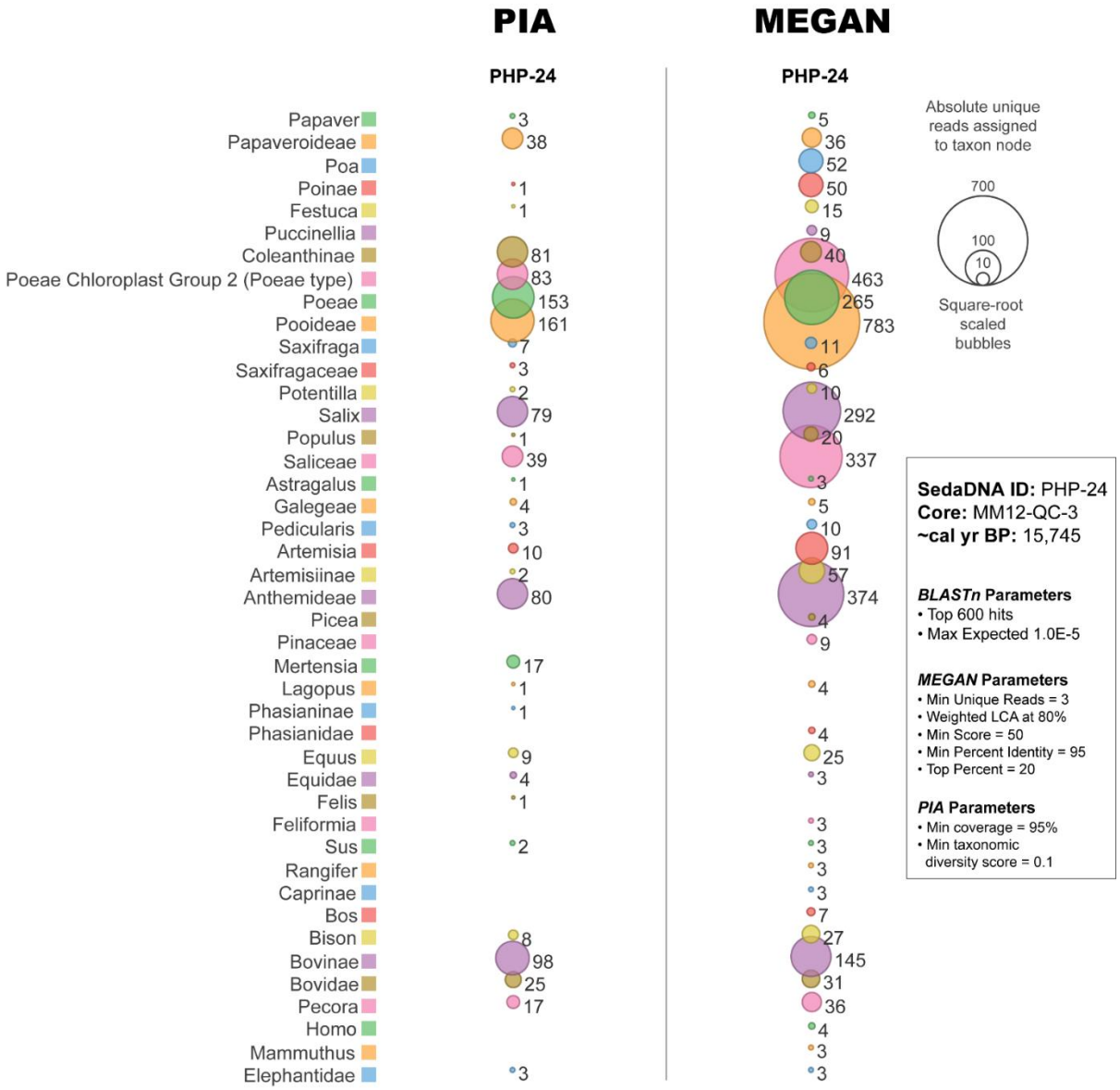

Fig. 5.43 PHP-24 replicates comparison with *PIA* and *MEGAN* taxonomic binning. Select nodes depicted.

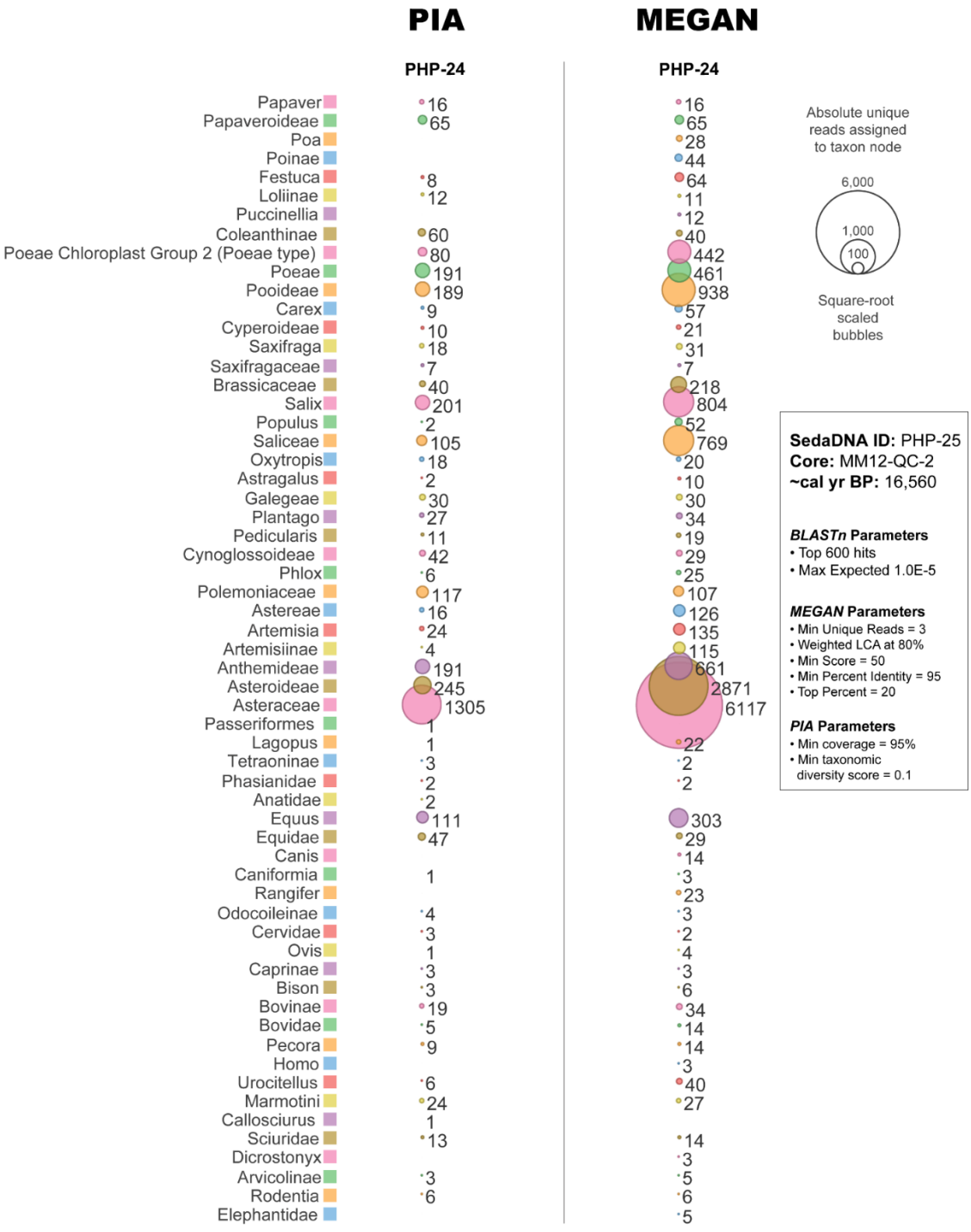

Fig. 5.44 PHP-24 replicates comparison with *PIA* and *MEGAN* taxonomic binning. Select nodes depicted.

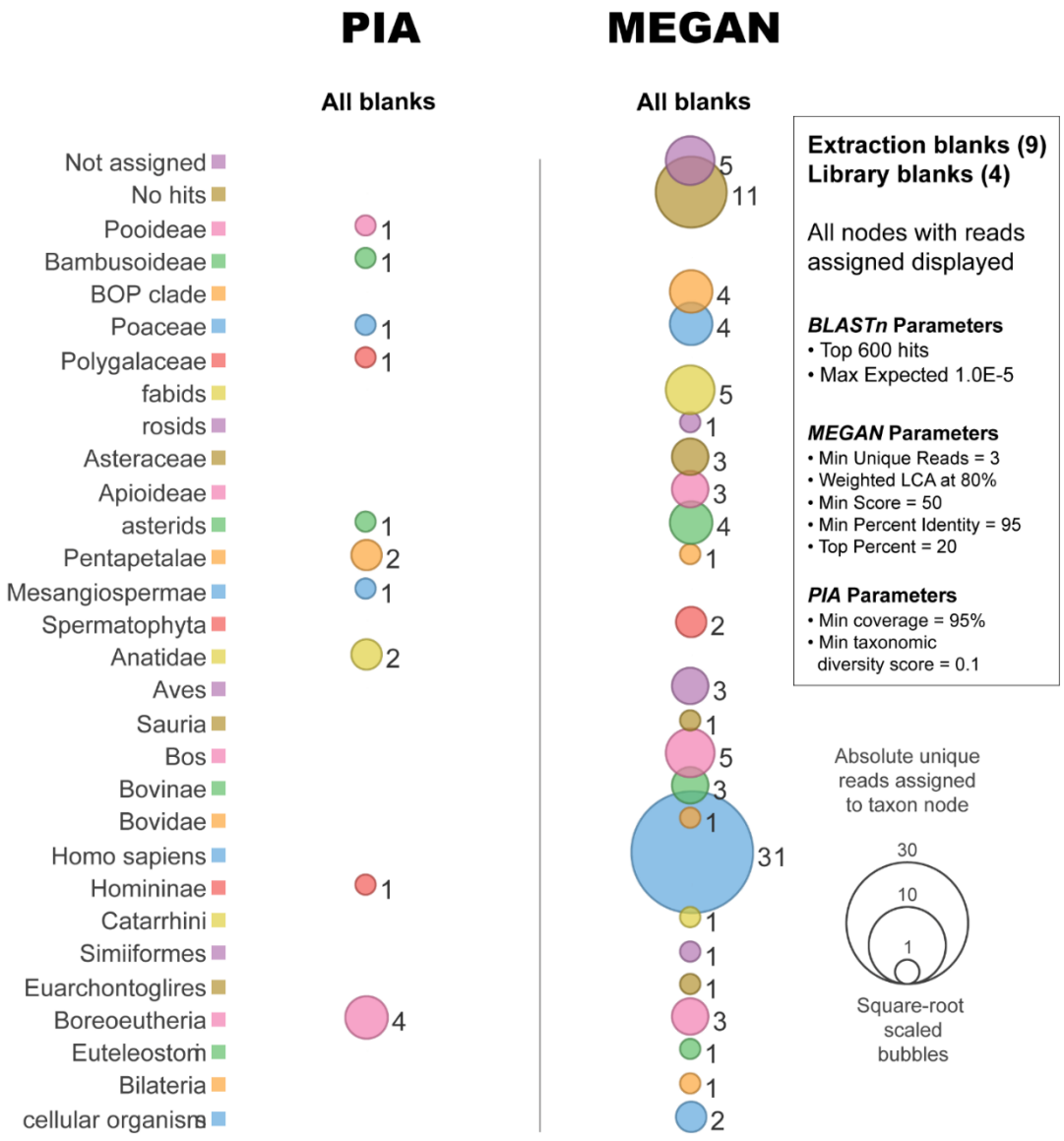

Fig. 5.45 Blanks comparison with *PIA* and *MEGAN* taxonomic binning.

Select nodes depicted.

5.6.7 Calibrated floral DNA

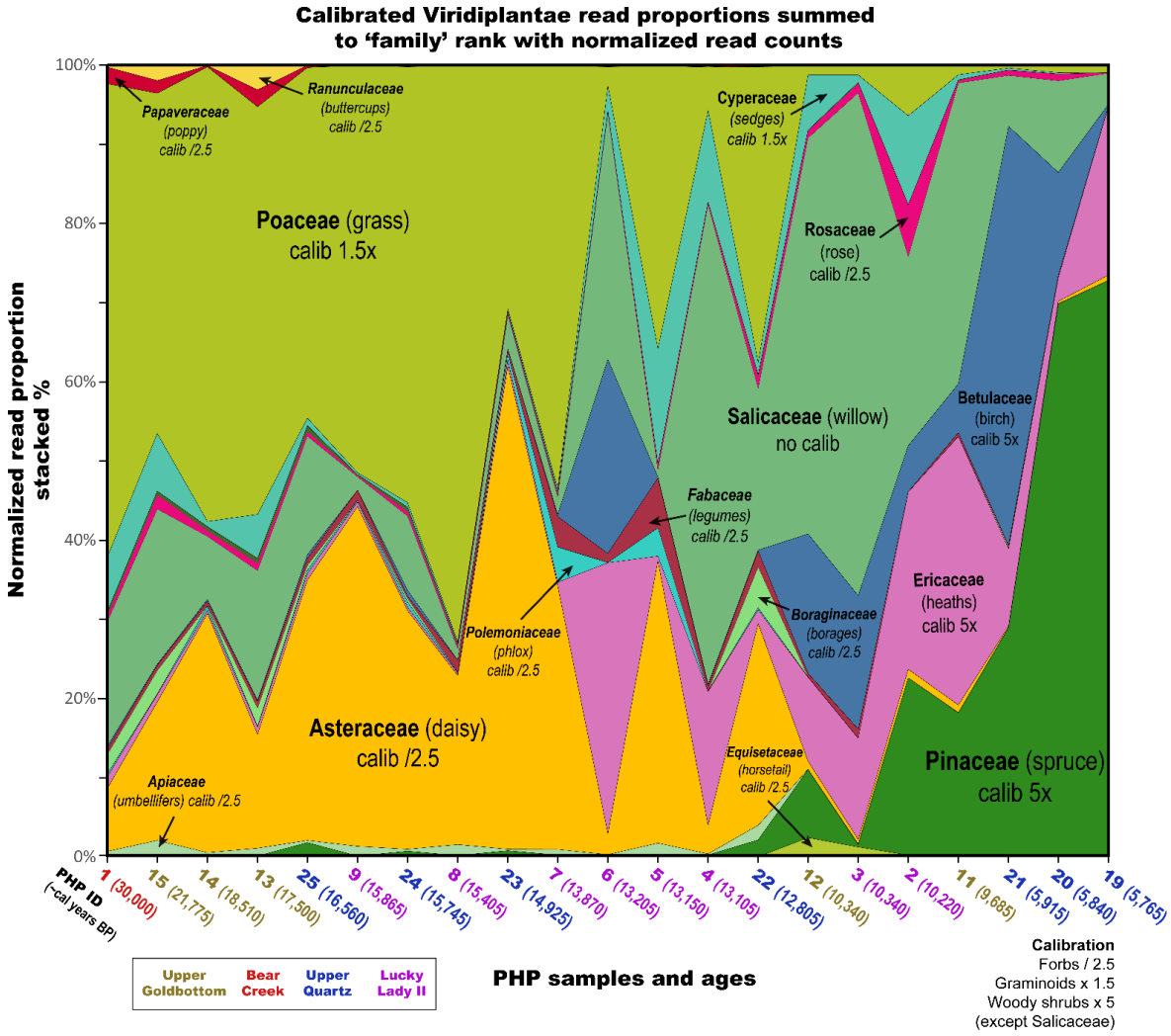

Fig. 5.46 Calibrated read proportions of abundant plant families as per Fig. 8 in the main text. These families include many growth forms, but those deemed most probable were used to calibrate the normalized read proportions per family.

Chapter 6

Reassembling mitochondrial genomes of extinct megafauna using environmental DNA

Authors

Tyler J. Murchie[a,b*], Ana T. Duggan[c], Emil Karpinski[a,d], Grant Zazula[e], Ross MacPhee[f], Beth Shapiro[g,i], Duane Froese[h*], Hendrik Poinar[a,b,j*]

[a]McMaster Ancient DNA Centre, McMaster University, Canada.
[b]Department of Anthropology, McMaster University, Canada.
[c]Public Health Agency of Canada, Winnipeg, Canada
[d]Department of Biology, McMaster University, Canada.
[e]Yukon Government, Palaeontology Program, Department of Tourism and Culture, Whitehorse, Canada.
[f]Division of Vertebrate Zoology/Mammalogy, American Museum of Natural History, USA.
[g]Paleogenomics Lab, University of California Santa Cruz, USA.
[i]Ecology & Evolutionary Biology Department, University of California Santa Cruz, USA.
[j]Department of Biochemistry, McMaster University, Canada

[*]Corresponding authors: Tyler J. Murchie and Hendrik Poinar, Department of Anthropology, McMaster University, 1280 Main Street West, Hamilton, ON L8S 4L8, Canada; Duane Froese, Department of Earth and Atmospheric Sciences, University of Alberta, 116 St & 85 Ave, Edmonton, AB T6G 2R3, Canada.
E-mail address: murchiet@mcmaster.ca, duane@ualberta.ca, and poinarh@mcmaster.ca

Abstract

Phylogenetically placing extinct organisms is relegated almost entirely to sequence data recovered from discrete macro-tissues such as bones and teeth. However, the growing sophistication of environmental DNA methods now permit the recovery of whole organelle genomes from multiple organisms simultaneously using disseminated environmental samples such as soils and sediment, and in the total absence of macro-tissues. Here, we present mitochondrial genomes assembled from late Pleistocene Yukon permafrost wherein we phylogenetically assess *Mammuthus primigenius* (woolly mammoth), *Equus caballus* (North American caballine horse), and *Bison priscus* (steppe bison) sedimentary ancient DNA to infer haplotype diversity at multiple time-points during the late Pleistocene.

6.1 Introduction

Environmental DNA (eDNA) is principally used for taxon identification in terrestrial and aquatic ecosystem reconstructions (Anderson-Carpenter et al., 2011; Willerslev et al., 2014; Graham et al., 2016; Pedersen et al., 2016; Sjögren et al., 2017; Slon et al., 2017; Murchie et al., 2021b) as well as in palaeodietary reconstructions with palaeofeces, dental calculus, or gut contents (Poinar et al., 1998; Warinner et al., 2015; Weyrich et al., 2015; 2017; Karpinski et al., 2016; Ozga et al., 2016; Søe et al., 2018). To a lesser extent, the method has been used as a rough means of estimating the population biomass of organisms in an ecosystem (Takahara et al., 2012; Yoccoz et al., 2012; Doi et al., 2015; 2017; Wei et al., 2018; Matesanz et al., 2019), although how eDNA input and organo-mineral preservation influences the relationship between disseminated genetic abundances and macro-biomass needs further research. Assessing evolutionary relationships with phylogenetics has been predominantly relegated to discrete tissues such as bones and teeth where morphology can independently infer taxonomy, as well as to a lesser extent with hair and palaeofeces—drawing assumptions about what species may have been present at a given locality. Genetically admixed environmental materials (Rawlence et al., 2014) such as sediments, palaeosols/soils, and water/ice would seem to be inappropriate sample types for genomic reconstructions of palaeo-fauna (which enable well-resolved phylogenies, as well as phylogeographic or haplotype reconstructions) as these materials have not been generally observed to contain genome-scale DNA preservation, and as they are expected to contain a complex mixture of eukaryotic and prokaryotic biomolecules. However, Slon et al. (2017) demonstrated that sufficient quantities of hominin sedimentary ancient DNA (sedaDNA) can be selectively captured in cave contexts from strata without osteological remains, which can be used to assemble mitochondrial genomes along with their phylogenetic placement.

A similar capture enrichment approach was utilized by Murchie et al. (2021b; 2021a) to selectively sequence mitochondrial and chloroplast DNA of Holoarctic fauna and flora recovered from permafrost sediments deposited in an open-air context during the Pleistocene-Holocene transition in central Yukon, Canada. Murchie and colleagues

observed that a substantial abundance of sequence data was recovered that could be used to assemble whole mitochondrial genomes from *Equus* sp. (extinct North American horse), *Bison priscus* (extinct steppe bison), *Mammuthus primigenius* (extinct woolly mammoth), *Rangifer tarandus* (caribou/reindeer), and *Lagopus lagopus* (willow ptarmigan). Here, we report on the sedaDNA mitogenomic assembly and phylogenetic analysis of Pleistocene fauna from multiple timepoints during the last glacial/interglacial transition (Fig. 6.1, Table 6.1). This dataset is augmented from Murchie et al. (2021a) to include a set of UDG-treated libraries for the Bear Creek core wherein terminal deamination-derived polymorphisms on the ends of DNA fragments are repaired to improve single nucleotide polymorphism (SNP) identification and mapped read coverage.

6.2 Results and discussion

Sufficient on-target sedaDNA sequence data (≳ 3x coverage of at least 80% of the reference genome) was acquired to reconstruct 11 mitochondrial genomes from the three targeted families—Elephantidae, Equidae, Bovidae (Tables E6.2–E6.4 in section 6.6). All non-UDG treated libraries contain distinctive terminal deamination patterns on reads mapped to these taxa, and the negative controls contain no reads that could be *BLASTn* identified or mapped to the reference genomes. Combined with the temporally distinctive palaeoecological reconstructions detailed in Murchie et al. (2021b; 2021a), there is strong support that these sequenced reads originate from the samples themselves and are characteristically ancient.

6.2.1 *Mammuthus*

Our expanded Murchie et al. (2021a) dataset had sufficient *Mammuthus* reads to reconstruct mitogenomes in samples PHP-1, PHP-13, and PHP-15 (Fig. 6.2, Table E6.2). These sedaDNA genomes fall within Clade I (haplotype C) as per Enk et al. (2016) as *Mammuthus primigenius* (woolly mammoth), which is believed have been distributed from eastern Beringia southeast to the Great Lakes and Atlantic Coast along the southern margin of the Laurentide ice sheet. This population was genetically distinct from haplogroup I-F (*Mammuthus columbi* [Columbian mammoth] and *M. jeffersonii* [a likely hybrid between *M. primigenius/columbi*]) that occupied the Great

Plains and West Coast regions of North America (Enk et al., 2016, fig. 2). Multiple haplogroups have been observed among Beringian woolly mammoths where it is thought that *M. primigenius* phenotypes from Eurasia were introduced to American *Mammuthus* lineages (Enk et al., 2016; Chang et al., 2017). When we investigate segregating SNPs in the *Mammuthus* ssp. alignment compared to the mapped reads and our consensus sequences, it becomes clear that there are *M. primigenius* inputs in the same sample from both haplogroup I-C (American) and haplogroups I-D&E (Eurasian) in PHP-1, which dates to ~30,000 cal BP (Fig. 6.3). We observe evidence of an at least near-synchronous overlap of distinct *Mammuthus* populations in the Klondike at this timepoint (relative to how much time each core sample might represent). This makes phylogeographical sense for peri-LGM *Mammuthus* in Beringia and supports the proposition that interbreeding was possible in eastern Beringia due to cohabiting Eurasian and American populations. In this case, the consensus for PHP-1 called ambiguous bases at most segregating sites, creating a non-committal chimeric or 'franken-genome' of multiple *Mammuthus primigenius* subpopulations. This explains the low internal haplotype I-C bootstrap support in the placement of these sedaDNA genomes where they occupy a pseudo-ancestral position due to the ambiguous base calls at segregating sites. While these chimeric genomes preclude Bayesian phylogenetics, they nevertheless identify the extended at least near co-habitation of multiple *M. primigenius* populations in the Klondike through the terminal late Pleistocene. We identified >50 segregating SNPs illustrating a conflation of I-C and I-D&E alleles in PHP-1. A similar pattern was observed in samples PHP-15 (21,775 cal BP) and PHP-13 (17,500 cal BP), although the SNPs in these temporally later samples are predominantly associated with *M. primigenius* haplotype I-C.

6.2.2 *Equus*

Three equid mitogenomes also had sufficient read coverage to call consensus sequences (Table E6.3). Unlike *Mammuthus, w*e did not observe mitochondrial allelic diversity within the reads mapped to *Equus caballus,* although the reads are clearly distinct from the Eurasian lineage of *E. caballus* utilized for the reference genome

(GenBank accession: NC_001640.1). These sedaDNA genomes contain a unique set of linked SNPs most closely associated with *E. caballus* var. *lambei* (Yukon wild horse) (Fig. 6.4). These sedaDNA mitogenomes fall within the known diversity of caballine horses in Eurasia and the Americas, being distinct from *Haringtonhippus francisci* (New World stilt-legged horse) and other extinct (*Hippidon* ssp., *E. ovodovi*) and extant (*E. zebra, E. asinus, E. kiang*) equids. The *BLASTn* to *MEGAN/PIA* approach reported in Murchie et al. (2021b; 2021a) was only able to identify reads to the genus *Equus* sp, in part due to the ongoing systematics debate regarding the genus *Equus* (Barrón-Ortiz et al., 2019). In contrast here however, our sedaDNA mitogenome assembly and phylogenetics approach can confidently identify the *lambei* subpopulation of *Equus caballus*, even in libraries bordering the minimum read coverage cut-off (~3X) with ~800 mapped reads.

6.2.3 *Bison*

Five mitogenomes could be reconstructed from the augmented Murchie et al. (2021a) sedaDNA dataset (Figs. 6.5, E6.7; Table E6.4). All are clearly associated with *Bison priscus* (steppe bison) with four falling into an eastern Beringia clade and the fifth falling within the diversity of Eurasian steppe bison (Shapiro et al., 2004; Heintzman et al., 2016; Froese et al., 2017). As with *Mammuthus*, multiple instances of linked SNPs were observed in the mapped reads wherein both clades were seemingly represented with segregating sites, leading the consensus sequence to call ambiguous bases at these positions (Fig. E6.7). The youngest sample (PHP-22; 12,805 cal BP) is most clearly associated with American *B. priscus* whereas the oldest sample (PHP-16; 40,410 cal BP) falls within the known diversity of Eurasian populations (Fig. 6.5). Samples of intermediate age (PHP-1, PHP-13, PHP-15) contain reads associated with both populations. The overlap of these populations makes phylogeographic sense for Beringian bison. Following the last inter-glacial (MIS 5e, 130,000–115,000 BP) (Shackleton et al., 2003) a land bridge is believed to have formed in the Bering sea between 70,000–60,000 BP, which was intermittently connected from 60,000–30,000 BP until reaching its maximum extent during the LGM (~21,000 BP) before the Bering seaway reopened by c. 11,000 BP (Elias and Crocker, 2008; Hu et al., 2010; Meiri et al., 2013). The ~40,000 cal

BP Upper Goldbottom core would appear to correspond with a movement of bison into eastern Beringia during periods of at least a partial land bridge connection. This is consistent with previous research that identified *B. priscus* gene flow from Eurasia into Beringia nearer to the LGM (Shapiro et al., 2004; Froese et al., 2017), a trend also observed with in our *Mammuthus* dataset where both Siberian and eastern Beringian clades are identified as co-inhabiting central Yukon during the terminal late Pleistocene.

Identifying such evidence for the cohabitation of distinct Eurasian and American lineages of *Bison* and *Mammuthus* would only have been possible with ancient DNA analyses of individual bones from faunal assemblages from the same site or region with tightly overlapping radiometric ages. Here however, we observe evidence for the near-synchronous occupation of regionally distinct populations in the Klondike solely through sedaDNA. The breadth of time each sedaDNA core sample may represent is unclear, but even if these populations had staggered, near overlapping presence in the Klondike, this data suggests that Eurasian and American lineages were present around the same time in the same place, enough so that it is reasonable to suppose that inter-breeding was possible.

6.2.4 Augmented palaeo-faunal reconstruction at Bear Creek (30,000 cal BP)

The augmented Bear Creek UDG-treated libraries enriched with both PalaeoChip and *Bison* ssp. baits improves the faunal resolution reported by Murchie et al. (2021b; 2021a) and D'Costa et al. (D'Costa et al., 2011) at the 30,000 cal BP timepoint below the Dawson tephra (Westgate et al., 2000; Froese et al., 2002; Zazula et al., 2006b). While most reads that were taxonomically binned are still assigned to the same predominant taxa as Murchie et al. (2021b; 2021a) (*Mammuthus, Equus, Bison,* and *Rangifer*) we see an increased richness in the diversity of lower abundance fauna with deeper sequencing. Newly identified taxa include: *Ochotona collaris* (Collared pika), more specific hits to *Ovis dalli* (dall sheep), *Bootherium bombifrons* (helmeted muskox), potentially *Bos primigenius* (aurochs), *Mustela nivalis* (least weasel), *Vulpes* sp. (fox), *Canis* sp. (wolf), Feliformia (suborder containing "cat-like" carnivorans), Eulipotyphla (order containing hedgehog/mole/shrew), more specific assignments within Equidae to *Equus*

caballus/przewalskii, as well as Corvoidae (superfamily of oscine passerine birds that contains crows, ravens, and magpies) and Antidae (family of water birds that includes ducks and geese). No faunae were identified in the negative controls despite being processed identically in parallel and being pooled to equimolar concentrations.

There are two notable peculiarities in this enhanced faunal dataset. First, D'Costa et al. (D'Costa et al., 2011) and Murchie et al. (2021b; 2021a) both observed hits to the genus *Bos*, with Murchie et al. identifying *Bos mutus/grunniens* (yak) in their *BLASTn* data initially, which return to *Bos* sp. after increasing the LCA stringency. Here, 76 reads are retained to *Bos* sp. (aligning across the mitogenome) with 6 being specifically called as *Bos primigenius* (aurochs). This consistent *Bos* signal may suggest that one of the Eurasian *Bos* species (*Bos primigenius* or *Bos mutus*) was present in eastern Beringia at some low population density. These hits retain their *Bos* binning when percent identity is increased to 100%. *Bos* was one of the few taxa identified in the negative controls in Murchie et al. (2021a); this blank contamination was entirely absent in the augmented negative control dataset here. However, there is reason to doubt this taxonomic identification—some number of these *Bos* reads are potentially false positives within Bovidae due to database bias, mitogenomic conservation, and close phylogenetic association. *Bos* is highly over-represented on GenBank, which raises the question as to whether 1000 top hits is sufficient to classify these reads when there are 1000+ *Bos* ssp. mitochondrial GenBank entries capable of swamping the BLAST results for conserved regions of the bovid mitogenome. When *bwa* mapping to *Bos mutus*, *Bison* reads overwhelm the dataset, returning a *Bison priscus* consensus sequence, which challenges attempts to isolate this enigmatic *Bos* signal from other bovid DNA. *Bos* faunal remains have never been found in eastern Beringia (Stuart, 2015), making this consistent signal both very interesting and challenging to authenticate. Further experimentation is needed to resolve this oddly persistent signal, potentially with competitive mapping, a custom reference database, *BLASTn* top hits to 10,000+, and SNP phasing. At this time, it is our suspicion that hits to *Bos* are likely misidentified reads within Bovidae driven by database biases.

Second, human is also identified in this dataset in abundance despite neither bait-set specifically targeting human DNA. When mapping to the rCRS (NC_012920.1) we can assemble a 56.2X mitochondrial genome with 91.8% reference coverage. After curation, *Mitomaster* (Lott et al., 2013) was used to identify this consensuses genome as haplogroup T2b5 with 86.99% quality as per *HaploGrep2* (Weissensteiner et al., 2016) (Table E6.7). These libraries were UDG treated, so we cannot use *mapDamage* to evaluate deamination. However, haplogroup T2b is only considered to have diverged around 10,000 years BP and is predominantly a Near Eastern and European lineage (Pala et al., 2012, p. 920). In this case, we can conclude that this human signal is very likely the result of contamination. Approximately 9500 reads came from a single indexed replicate of a library that otherwise had minimal human reads mapping in other sequenced index combinations, suggesting that one of the index primer aliquots may be contaminated. The negative controls run with this batch only contain 6 reads that map to the rCRS, suggesting that this contamination is specific to this indexed library. My (Tyler Murchie) mitochondrial haplogroup is H1, suggesting that this human contamination originates from a third-party source. In terms of the palaeo-faunal reconstruction of Bear Creek some 30,000 years ago, we can dismiss the human signal observed in Fig. 6.6.

6.2.5 Moving forward

To date, PCR metabarcoding remains the predominant method for eDNA research (Taberlet et al., 2018), with shotgun sequencing being a viable but rarely utilized approach (Pedersen et al., 2016). While metabarcoding ensures highly efficient sequencing of ecologically informative genetic loci (compared to highly inefficient shotgun sequencing), it comparatively lacks the genomic resolution and associated capabilities of targeted enrichment or shotgun sequencing. Metabarcoding necessitates intact priming sites and fragment lengths (>100 bp) that are rare with sedaDNA (fragment length modes ≈ 30–50 bp). By instead utilizing the PalaeoChip Arctic-1.0 capture enrichment bait-set, whole organelle genomes can be captured from a highly diverse range of faunal targets, while also simultaneously capturing plant chloroplast DNA to facilitate floral ecological reconstructions (Murchie et al., 2021b; 2021a). Capture

enrichment also significantly improves the eukaryotic data efficiency of environmental DNA compared to shotgun sequencing, while retaining the ability to selectively capture any nuclear or organelle region of interest, from any number of organisms, simultaneously.

The next obvious application of capture enrichment techniques with sedaDNA is targeting ancient human mitochondrial genomes. The first version of PalaeoChip was intentionally designed to not capture hominin DNA as there was a concern that modern human contaminants may overwhelm the faunal and floral sequence data. However, with separate sequence indices for human enrichments, a large batch of non-UDG treated libraries to evaluate ancient DNA damage signals, and carefully selected permafrost sites, human sedaDNA from open-air permafrost sites is poised to become a viable and powerful new tool in biomolecular archaeology. In the case of permafrost sediments such as those detailed here from eastern Beringia, this data would have the ability to not only selectively recover human sedaDNA, but also authenticate that it is ancient, date the organic and mineral matrices from which those sedaDNA molecules are derived using a combination of OSL and radiocarbon methods (Haile et al., 2009), and to identify haplotypes associated with the peopling of Beringia and the Americas—all without any macro-remains. While directly dated archaeological evidence of osteological remains, artifacts, or other macro-identifiers would constitute the strongest evidence for the spatiotemporal dispersals of hominins throughout the continents, Pleistocene archaeological sites are rare and seldom contain incontrovertible evidence. Micro-methods may prove key here to augmenting the expected limitations of buried records. While this approach has the potential to revolutionize the palaeo-ecological resolution of environmental samples, this imminent advancement is intractably paired with growing ethical concerns in the sequencing of human DNA from environmental sources where haplotypes can be identified (Handsley-Davis et al., 2020). Further, as demonstrated here, human contamination can be notoriously difficult to separate from authentically ancient DNA. Unambiguously demonstrating that human DNA originates from a set of ancient environmental samples will necessitate especially rigorous wet-lab (and bioinformatic)

procedures to rule out the potential for contamination that can originate from third-party sources well-beyond the individuals processing the samples.

Irrespective of the human contamination observed here, this study demonstrates the genomic resolution potential of sedaDNA wherein population genetic questions can be addressed for multiple organisms simultaneously as ecosystems evolved through time, and in the total absence of any surviving biological tissues. The growing sophistication of sedaDNA and recognition of the immense genetic archives preserved in the north are paired with the growing realization that perennial frozen ground is increasingly poised to undergo widespread, accelerating, and irreversible permafrost thaw across much of the arctic and subarctic (Kokelj et al., 2015; 2017; Nitze et al., 2018; Lewkowicz and Way, 2019; Ward Jones et al., 2019). As this permafrost thaws it is likely to lose much of its contextual association as it slumps, as well as undergoing mass degradation of the innumerable biomolecules that have been cold preserved therein for tens, to likely hundreds, of thousands of years. These palaeogenetic repositories of the north's ecological heritage will not survive indefinitely given current projections of a warming arctic. This underscores the growing urgency in archiving permafrost materials for future biomolecular research wherein genomes of long extinct organisms can be reassembled solely from the submicroscopic remains left behind on ancient landscapes.

6.3 Tables

Table 6.1 Permafrost samples re-analyzed from Murchie et al. (2021).

Site	Core	Age	SedaDNA ID	Input (grams)	UDG Treatment	Enrichment target	Total raw reads
Bear Creek *D'Costa et al. (2011)*	BC 4-2B	30,000	PHP-1	2.05	UDG & non-UDG	Combined pools	104,717,062
				1.00	*UDG*	*PalaeoChip (animals)*	*34,161,498*
					UDG	*Bison bison/priscus*	*64,904,755*
				1.05	*non-UDG*	*PalaeoChip (plants/animals)*	*5,650,809*
Lucky Lady II *Sadoway (2014)*	LL2S-189-E	10,220	PHP-2	0.90	*non-UDG*	PalaeoChip Arctic-1.0 (Holarctic plants/animals)	8,667,496
	LL2S-253-D1	10,340	PHP-3	0.60	*non-UDG*		9,303,528
	LL2C-118-C	13,105	PHP-4	0.60	*non-UDG*		7,749,177
	LL2C-205-B	13,150	PHP-5	0.60	*non-UDG*		4,997,824
	LLII 12-84-3	13,205	PHP-6	1.35	*non-UDG*		10,235,721
	LL2C-243-A2	13,870	PHP-7	0.60	*non-UDG*		5,820,472
	LLII 12-170-6	15,405	PHP-8	0.30	*non-UDG*		1,331,181
	LLII 12-217-8	15,865	PHP-9	1.05	*non-UDG*		3,115,296
Upper Goldbottom *Mahony (2015)*	MM12-118B	9,685	PHP-11	1.35	*non-UDG*	PalaeoChip Arctic-1.0 (Holarctic plants/animals)	7,983,085
	MM12-119B	10,340	PHP-12	1.50	*non-UDG*		18,409,441
	MM12-116b	21,000	PHP-13	0.30	*non-UDG*		1,624,580
	MM12-115b	18,510	PHP-14	0.30	*non-UDG*		2,320,965
	MM12-117b	21,775	PHP-15	0.30	*non-UDG*		1,910,387
	MM12-132b	40,410	PHP-16	0.60	*non-UDG*		1,756,829
	MM12-125b	42,100	PHP-17	0.60	*non-UDG*		2,383,139
Upper Quartz *Mahony (2015)*	MM12-QC-10	5,765	PHP-19	0.60	*non-UDG*	PalaeoChip Arctic-1.0 (Holarctic plants/animals)	9,244,928
	MM12-QC-9	5,840	PHP-20	0.60	*non-UDG*		5,913,447
	MM12-QC-8	5,915	PHP-21	0.60	*non-UDG*		5,142,454
	MM12-QC-6	12,805	PHP-22	0.60	*non-UDG*		6,080,182
	MM12-QC-4	14,925	PHP-23	0.90	*non-UDG*		14,729,646
	MM12-QC-3	15,745	PHP-24	0.30	*non-UDG*		1,129,623
	MM12-QC-2	16,560	PHP-25	0.30	*non-UDG*		1,568,411
Blanks	Extraction (16) & library (7) negative controls				UDG & non-UDG	PalaeoChip (plants/animals) + PalaeoChip (animals) + Bison ssp.	115,890

Total sequenced reads in augmented dataset: 236,250,764.

6.4 Figures

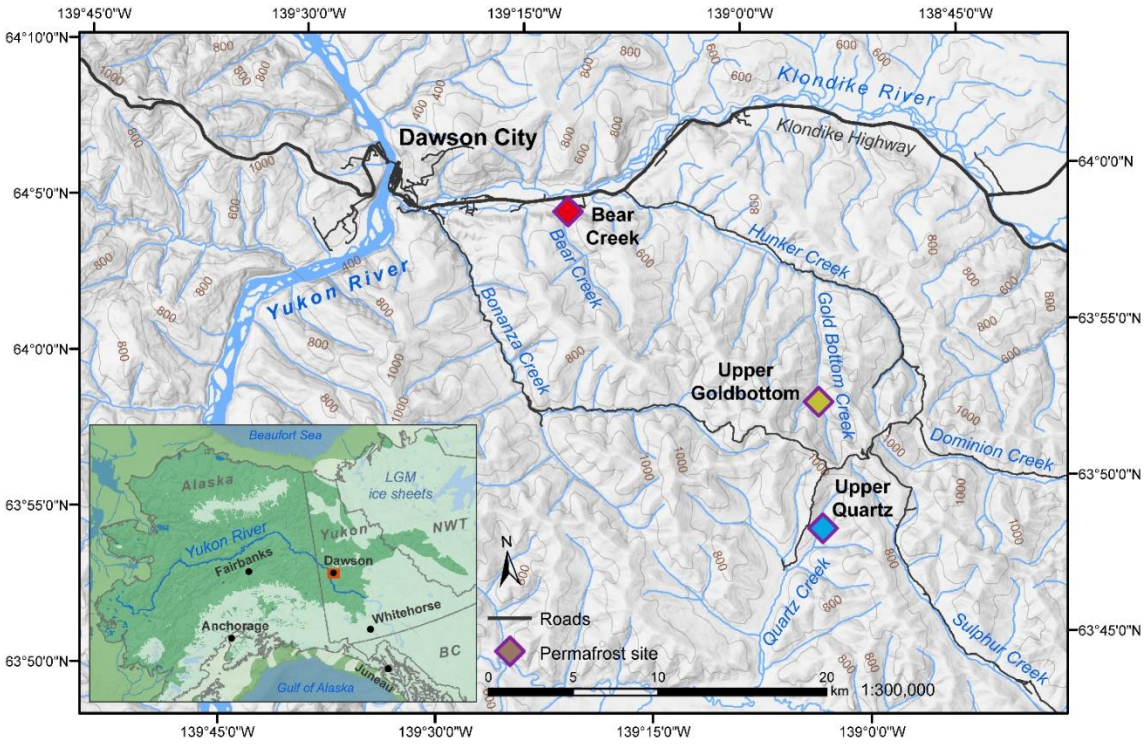

Fig. 6.1 Permafrost sites from the Klondike region of Yukon, Canada with sedaDNA reconstructed mitogenomes. Base map data retrieved from GeoYukon; contours elevation unit: meters above sea level (m bsl). Inset ice sheet data at Last Glacial Maximum (LGM, 26.5–19 ka BP) (Clark, 2009) from Dyke (2004). Sea level during LGM set to 126 m bsl based on Clark and Mix (2002). Beringian palaeodrainage data from Bond (2019) (http://data.geology.gov.yk.ca/).

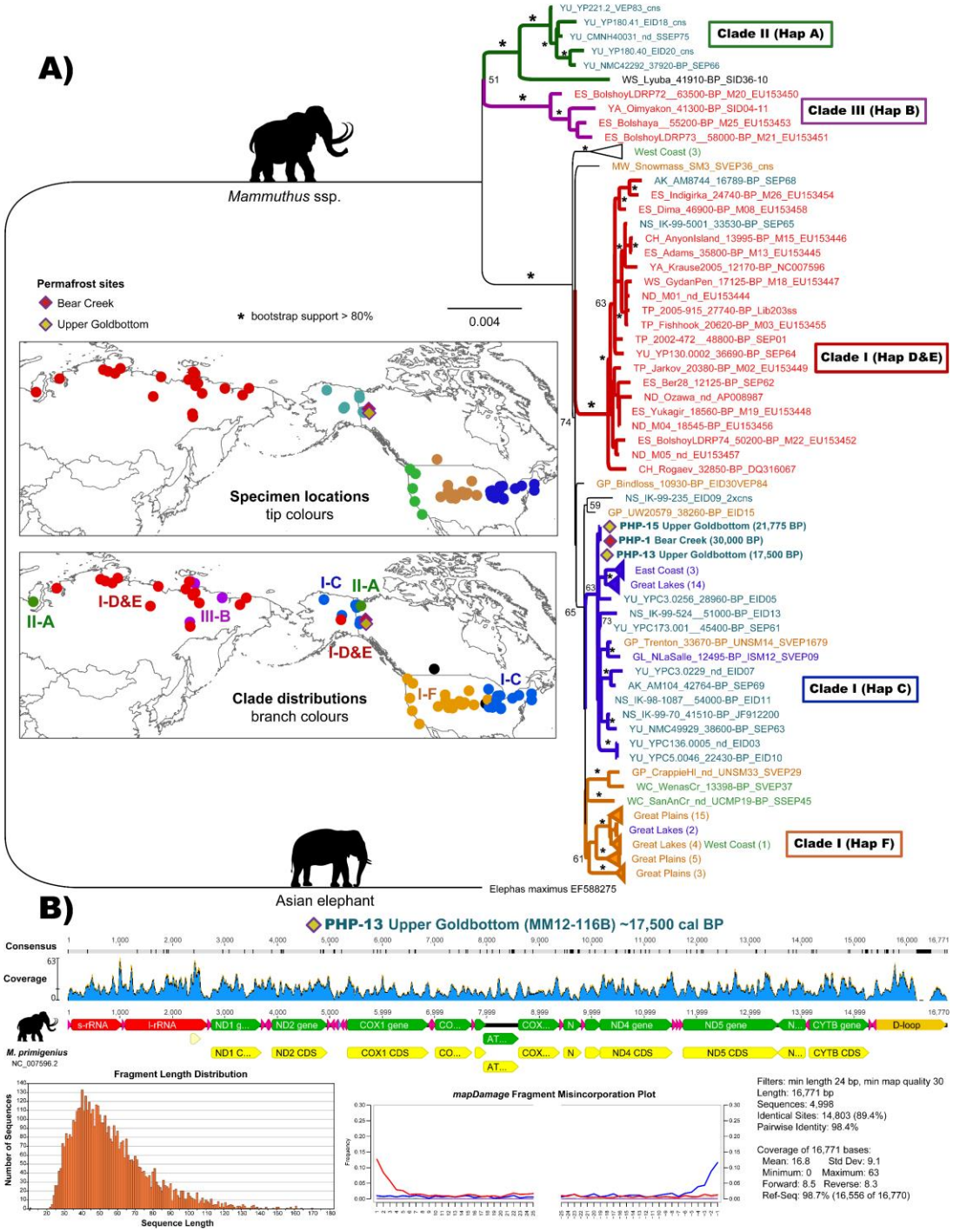

Fig. 6.2 Maximum likelihood tree of *Mammuthus* ssp. Generated in *IQ-Tree* (Nguyen et al., 2015) with 200-bootstrap support and *IQ-Tree* model test (best-fit model: TN+F+I+G4). Complete and partial mitogenomes, clade/haplogroup designations, and colour coding as per Enk et al. (2016). Tips are colour coded based on specimen locations (upper inset map), and branches are coloured based on clades (lower inset map) as per Enk et al. (2016). **B)** Example mitogenome coverage of sample PHP-13 generated with Geneious Prime (2019.2.3) and *mapDamage.*

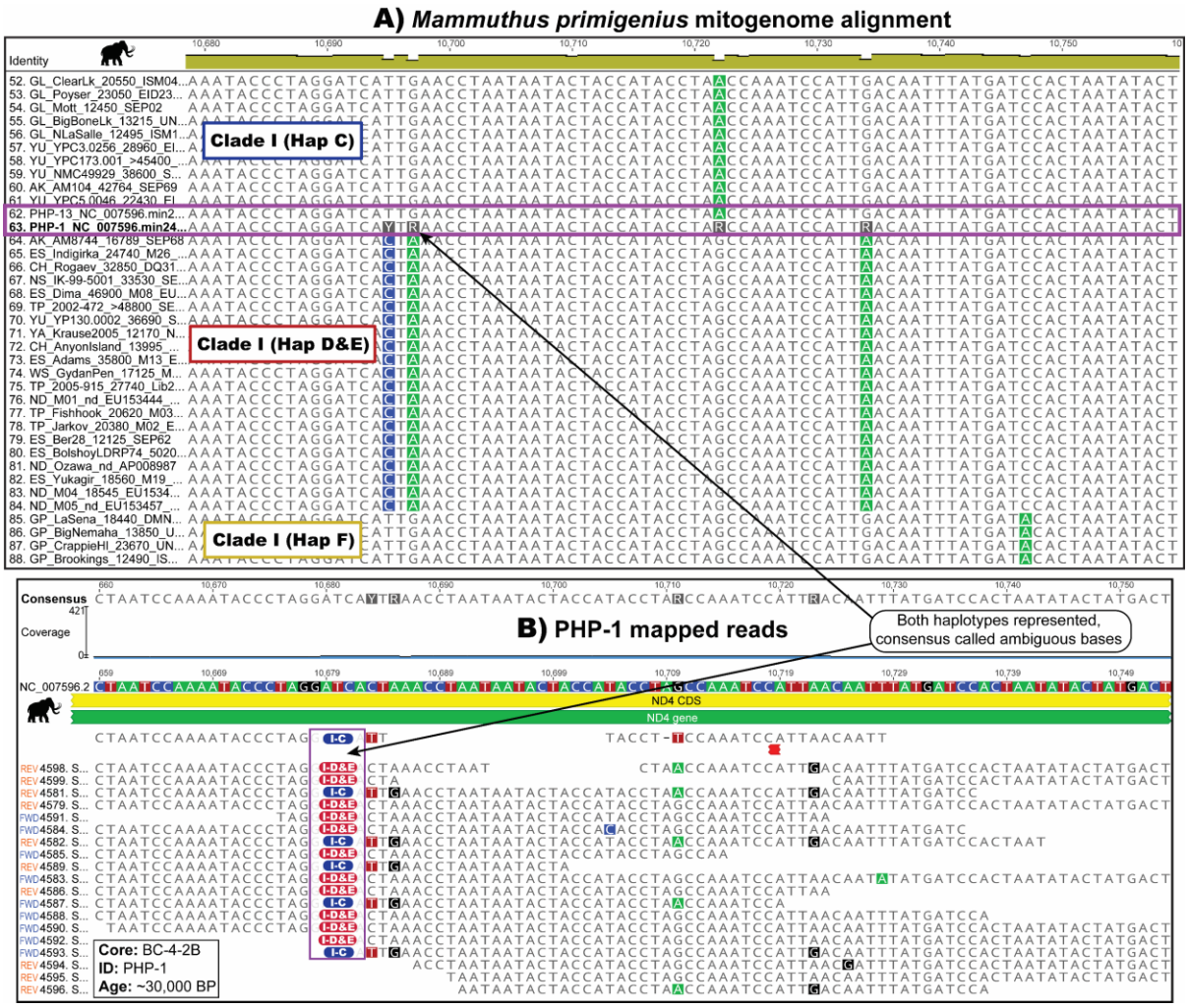

Fig. 6.3 Multi-allelic segregating sites of *M. primigenius* mitogenomes.
A) Multiple alignment generated with *muscle* v3.8.425 (Edgar, 2004) and visualized in Geneious Prime (2019.2.3). Sequence order modified from *muscle*. Clade/haplotype designations as per Enk et al. (2016).
B) Mapped reads in the ND4 gene with allelic variability indicative of both haplotypes I-C and I-D&E.

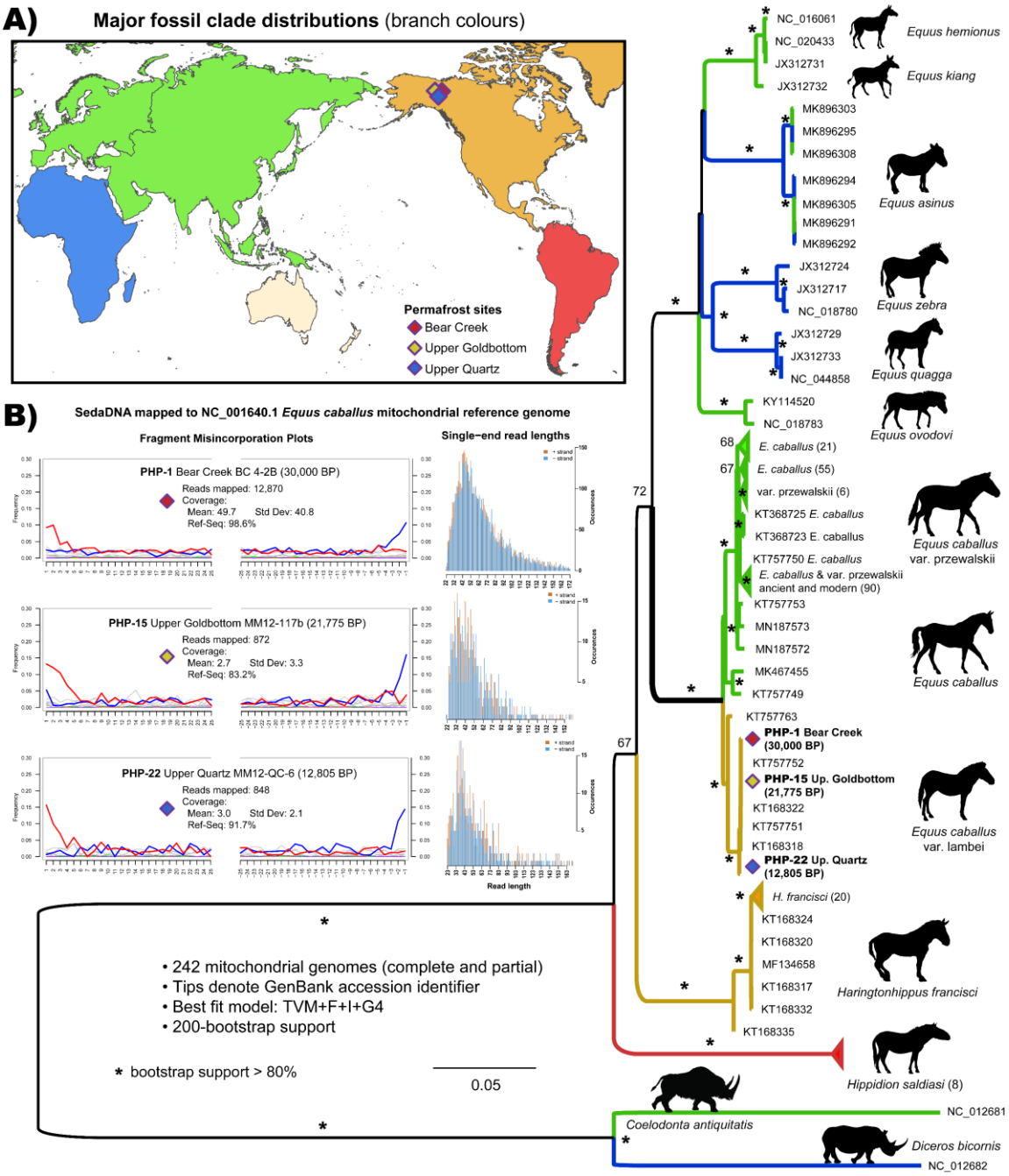

Fig. 6.4 Maximum likelihood tree of Equidae with emphasis on *Equus caballus* (extinct and extant caballine horses). Generated in *IQ-Tree* (Nguyen et al., 2015). Colour coded branches as per Heintzman et al. (2017). **A)** Major equid clade distributions in the fossil record. **B)** *MapDamage* plots depicting aDNA typical terminal deamination patterns and fragment length distributions with mapping statistics.

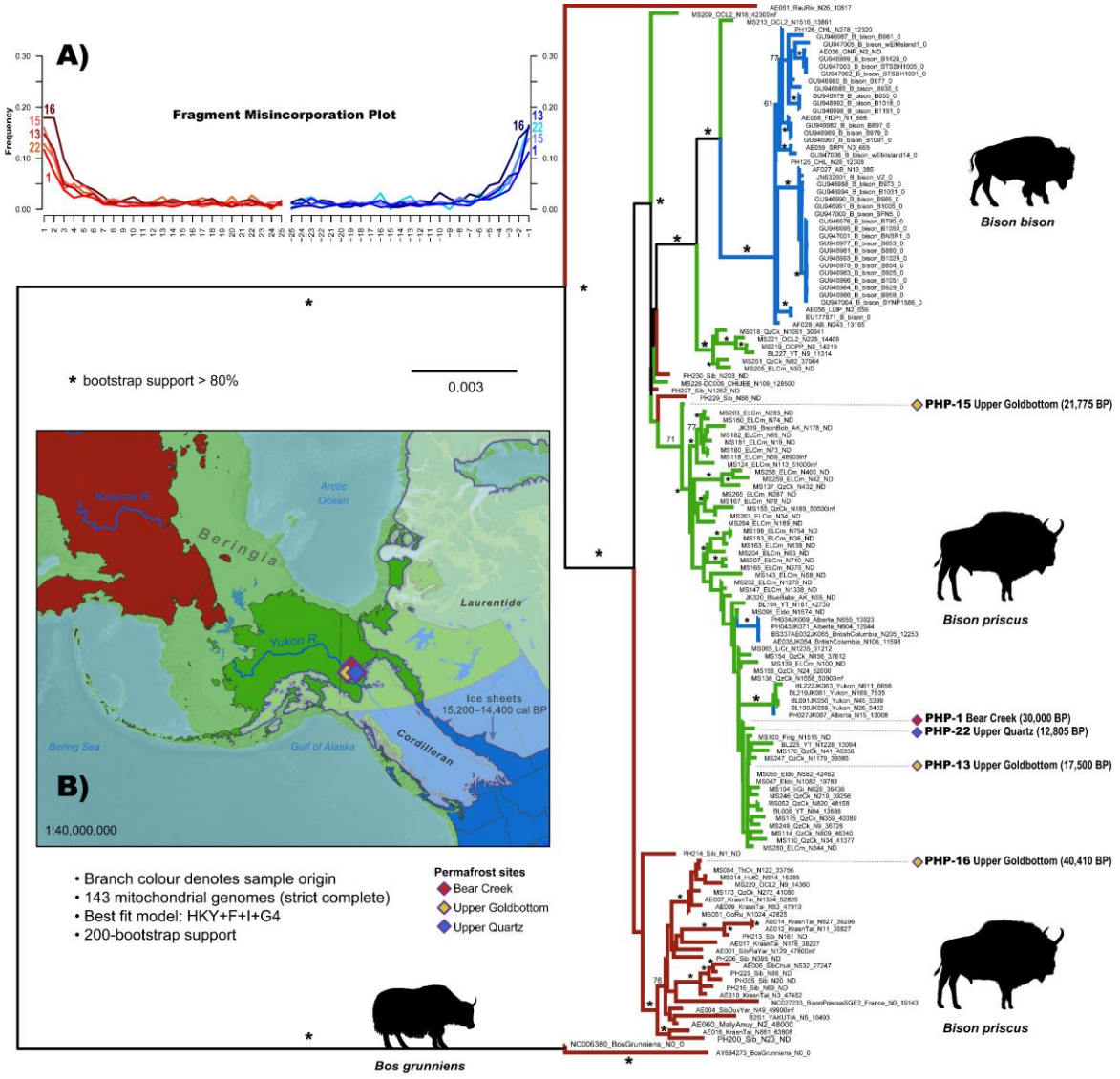

Fig. 6.5 Maximum likelihood tree of *Bison* with emphasis on extinct *Bison priscus*. Generated in *IQ-Tree* (Nguyen et al., 2015). **A)** *MapDamage* plots depicting aDNA typical terminal deamination patterns for reconstructed mitogenomes. **B)** Specimen recovery locations split between Siberia (red), Beringia (Green), and areas south of the ice-free corridor (blue).

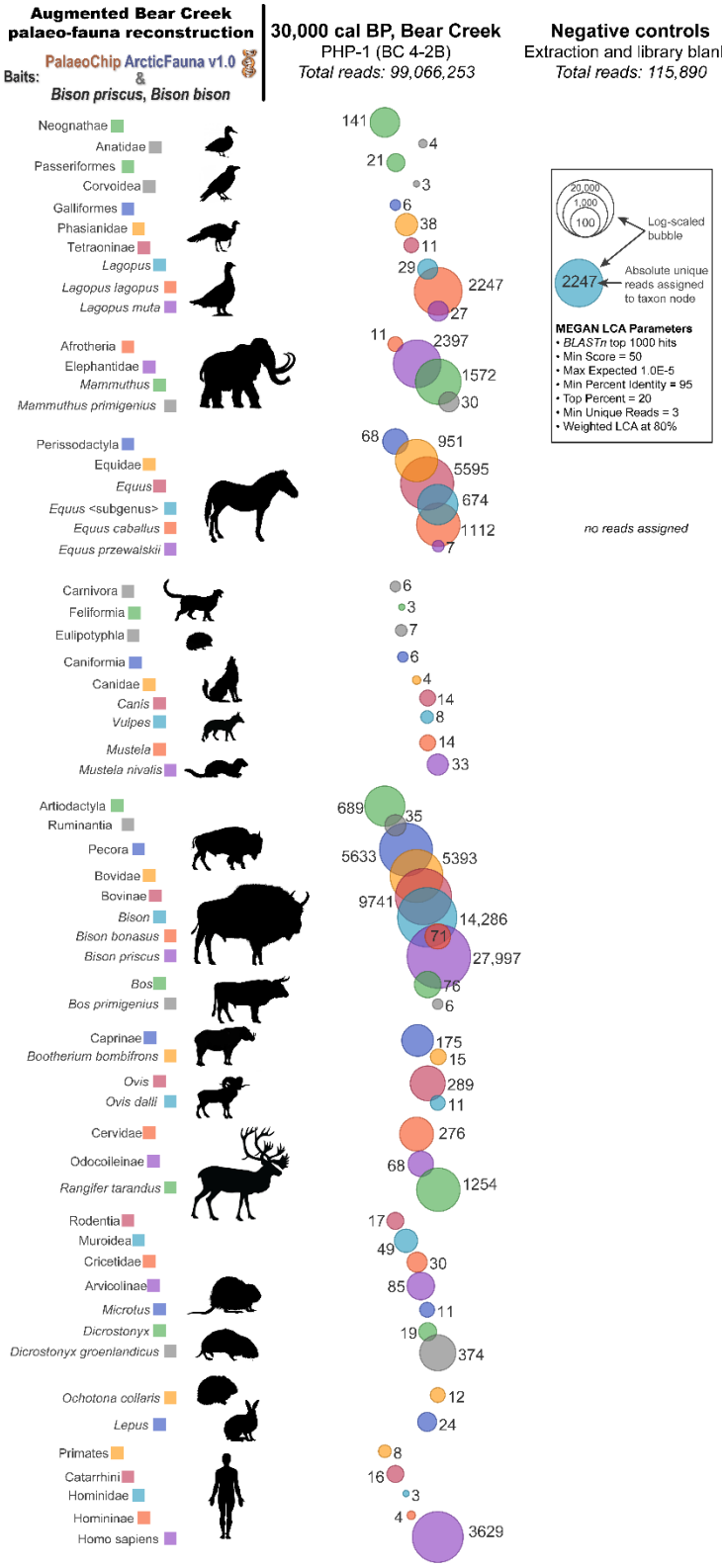

Fig. 6.6 Augmented Bear Creek palaeo-faunal reconstruction with additional UDG-treated libraries.

z

6.5 Materials and methods

6.5.1 Summary

Permafrost sedaDNA data reported by Murchie et al. (2021a) was re-analyzed for mitogenomic and phylogenetic applications, and was augmented with a set of uracil–DNA–glycosylase (UDG) treated double-stranded libraries (Briggs et al., 2009; Meyer and Kircher, 2010; Kircher et al., 2012) for core sample PHP-1 from Bear Creek (BC 4-2B), Yukon dated to ~30,000 cal yr BP (D'Costa et al., 2011). In Murchie et al. (2021a), 23 permafrost cores recovered from the Klondike region of Yukon, Canada—dating between ~30,000–6,000 years before present (BP)—were processed for sedimentary ancient DNA (sedaDNA) to evaluate changing biomolecular signals of plants and animals during the late Pleistocene-Holocene transition. Here and in Murchie et al. (2021a), lysed sedaDNA was purified using the Dabney et al. (2013b) high-volume silica-spin column extraction procedure paired with the long cold spin inhibitor removal technique as described by Murchie et al. (2021b). Double stranded, dual-indexed libraries (Meyer and Kircher, 2010; Kircher et al., 2012) were used for targeted enrichment where the PalaeoChip Arctic-1.0 plant and animal bait-set was used to capture enrich these libraries for Holarctic floral (chloroplast barcoding loci: *trn*L, *mat*K, *rbc*L) and fauna (whole mitochondrial genomes with an emphasis on megafauna). An Illumina HiSeq 1500 was used for 2x75 paired-end sequencing. After trimming, merging, and filtering the sequenced reads, *BLASTn* (Altschul et al., 1990) was used to taxonomically identify the reads to the top 1000 hits against a July 2019 local copy of the GenBank database (Benson et al., 2013; Agarwala et al., 2016), which was used as the input for *MEGAN* (Huson et al., 2007; 2016) (https://github.com/husonlab/megan-ce). *MEGAN* Identified taxa with sufficiently high read counts were selected for targeted read mapping using *network-aware-BWA* (Li and Durbin, 2009) (https://github.com/mpieva/network-aware-bwa). Geneious Prime 2019.2.3 (https://www.geneious.com) was used to curate reads mapped to select taxa, while *muscle* v3.8.425 (Edgar, 2004) (http://www.drive5.com/muscle/) was used for multiple alignments prior to phylogenetic analyses with *IQ-Tree* v1.4.0 (Nguyen et al., 2015) (http://www.iqtree.org/). *mapDamage*

(Jónsson et al., 2013) (v 2.0.3, https://ginolhac.github.io/mapDamage/) was used to assess the aDNA damage signals. Site descriptions can be found in Murchie et al. (2021a).

6.5.2 Lab setting

Laboratory work was conducted in clean rooms at the McMaster Ancient DNA Centre, which are subdivided into dedicated facilities for sample preparation (separate facilities for subsampling eDNA versus discrete materials), stock solution setup, and DNA extraction through library preparation. The post-indexing and capture enrichment clean room is in a physically isolated facility from the centre's standard aDNA labs, while the subsequent high-copy post-PCR workspace is in a separate building; the centre has a unidirectional workflow progressing from low-copy to high-copy facilities to reduce the chance of cross-contamination. Each dedicated workspace is physically separated with air pressure gradients between rooms to reduce exogenous airborne contamination. Prior to all phases of laboratory work, dead air hoods and workspaces were cleaned using a 6% solution of sodium hypochlorite (commercial bleach) followed by a wash with Nanopure purified water (Barnstead) and 30 minutes of UV irradiation at >100 mJ/cm^2.

6.5.3 Lysing, purification, library preparation, quantitative PCR, and indexing

Most samples were lysed and extracted by Murchie et al. (2021a), although 4 new extracts (0.25 g input each) from core BC 4-2B were added for UDG treatment, which were processed identically, but with the extracts subdivided into multiple replicates. Doubled stranded libraries were prepared as described in Meyer and Kircher (2010) with modifications from Kircher et al. (2012). Samples were purified after blunt-end repair with a QIAquick PCR Purification Kit (QIAGEN) (to maximally retain small fragments) and after adapter ligation and indexing with a MinElute PCR Purification Kit (QIAGEN). This augmented set of subsamples from core BC 4-2B was library prepared with UDG treatment for improved mitogenomic assembly, which was split into multiple library replicates for downstream processing. See Murchie et al. (2021a) for all master mix recipes, and Table E6.6 for the blunt-end repair UDG master mix concentrations.

6.5.4 Targeted capture with PalaeoChip Arctic-1.0

Probe design. In-solution enrichments were carried out using the previously designed PalaeoChip Arctic v1.0 bait set (Murchie et al., 2021b). This bait set targets whole mitochondrial genomes from approximately 180 extinct and extant Holarctic fauna, and the chloroplast barcoding loci (*trn*L, *rbc*L, and *mat*K) from approximately 2100 species of plants. See Murchie et al. (2021b Supp. pg. 15–16) for further details on the design of PalaeoChip Arctic-1.0.

Enrichment Wet lab. In solution enrichments were carried out using a modified version of the myBaits v4.1 protocol (Daicel Arbor Biosciences). In summary, hybridization and bait mixes were prepared to the concentrations in Table S9. For each library, 7 µL of template was combined with 5 µL of the library block master mix (using xGens, Human COt-1 DNA, and Salmon Sperm). Hybridization and bait mixes were combined and pre-warmed to 60°C before being combined with the library-block mixture. The first batch of samples (PHP) was incubated for 48 hours at 55°C for bait-library hybridization. The second round of libraries (PHP_{ii}) were enriched with a hybridization temperature of 60°C over ~72 hours to improve off-target exclusion.

After the hybridization, beads were dispensed (20 µL per reaction), washed with 200 µL of binding buffer per reaction, then resuspended in 20 µL binding buffer per reaction and aliquoted into PCR strips. Baits were captured using 20 µL of the bead binding buffer suspension per library, incubated at 55°C for 2.5 minutes (60°C for the second round), finger vortexed and spun down, then incubated for another 2.5 minutes. Beads were pelleted and the supernatant (the non-captured library fraction) was removed and stored at −20°C as per Klunk et al. (2019). The beads were resuspended in 180 µL of 60°C Wash Buffer X per tube and washed four times following the MYbaits v4.2 protocol. Beads were resuspended in 18.8 µL EBT, PCR reamplified for 12 cycles (Table S7), then purified with MinElute columns following manufacturer's protocols and eluted in 15 µL EBT.

6.5.5 Total quantification, pooling, size selection, and sequencing

Enriched and indexed libraries were quantified using the long-amplification total library qPCR assay and pooled to equimolar concentrations (Murchie et al., 2021a). Pools were size-selected with gel excision following electrophoresis for molecules ranging between 150–500 bp. Gel plugs were purified using the QIAquick Gel Extraction Kit (QIAGEN), according to the manufacturer's protocol, then sequenced on an Illumina HiSeq 1500 with a 2x75 bp paired-end protocol at the Farncombe Metagenomics Facility (McMaster University, ON).

6.5.6 Bioinformatic workflow

Reads were demultiplexed with *bcl2fastq* (v 1.8.4), converted to bam files with *fastq2bam* (https://github.com/grenaud/BCL2BAM2FASTQ), then trimmed and merged with *leeHom* (Renaud et al., 2014) using ancient DNA specific parameters (--ancientdna). Initially for *BLASTn* identification, reads were mapped (map-filtered) to a concatenation of the PalaeoChip Arctic-1.0 plant and animal probe references with *network-aware-BWA* (Li and Durbin, 2009) (https://github.com/mpieva/network-aware-bwa) with a maximum edit distance of 0.01 (-n 0.01), allowing for a maximum two gap openings (-o 2), and with seeding effectively disabled (-l 16500). Mapped reads that were merged or unmerged but properly paired were extracted with *libbam* (https://github.com/grenaud/libbam), collapsed based on unique 5' and 3' positions with *biohazard* (https://bitbucket.org/ustenzel/biohazard) (for PCR deduplication), and converted to fasta files and restricted to a minimum length of 24 bp. Subsequent fasta files were additionally filtered to remove any reads with lingering sequence similarity to the Illumina adapter sequences (…/fasta2oneline.pl input.fasta | agrep -v -1 AGATCGGAA | agrep -v -1 TTCCGATCT | tr "\t" "\n" | tail -n+2 > output.fasta) and were string deduplicated using the *NGSXRemoveDuplicates* module of *NGSeXplore* (https://github.com/ktmeaton/NGSeXplore).

These filtered fastas were used as the input for *BLASTn* (Altschul et al., 1990), which were aligned against a July 2019 local copy of the GenBank NCBI (National Center for Biotechnology Information; Benson et al., 2013; Agarwala et al., 2016)

nucleotide database set to return the top 600 alignments (unique accession hits) per read with e-values less than 1.0E-5 (flags: -num_alignments 600 -max_hsps 1 -evalue 0.00001). The *BLASTn* outputs were then passed to *MEGAN* (Community Edition, v.6.19.7, https://github.com/husonlab/megan-ce) (Huson et al., 2007; 2016) where the *BLASTn* results were filtered through a lowest common ancestor (LCA) algorithm using the following parameters:

- Min-score = 50 (default)
- Max expected (e-value) = 1.0E-5;
- Minimum percent identity = 95%
    - Allows 1 base mismatch at 24 bp, 2 at 50 bp, and 3 at 60 bp to account for cytosine deamination and other aDNA characteristic damage or sequencing errors.
- Top percent consideration of hits based on bit-score = 20%.
    - More conservative taxonomic assignments than the 10% default by taking more of the top hits into consideration for LCA assignment.
- Minimum read support = 3
    - Number of unique reads aligning to an NCBI accession sequence for that taxon to be considered for LCA.
- Minimum complexity = 0.3
    - Default minimum complexity filter.
- LCA weighted algorithm at 80%.
    - Two rounds of analysis that increases LCA specificity by taking all taxonomic assignments of a library into consideration.

All libraries were then compiled using *MEGAN's* compare feature with absolute read counts but with bubble size logarithmically scaled to proportionally normalize visually between samples of differing sequence depths. Thereafter, the closest available genetic references were obtained for notable taxa identified with the *MEGAN-LCA* taxonomic binning approach. All samples were mapped to these references using the same aforementioned procedures but with an additional map-quality filter set to ≥ 30 with *samtools* (https://github.com/samtools/samtools), then assessed for ancient DNA typical damage signals using *mapDamage* (Jónsson et al., 2013) (v 2.0.3, http://https//ginolhac.github.io/mapDamage/).

Finally, *bwa* mapped reads from the *mapDamage* workflow were imported into Geneious Prime 2019.2.3 (https://www.geneious.com/) where the contigs were manually curated using pre-assembled alignments and NCBI references as guides. Spurious-indels

were manually removed, nucleotides with a read coverage less than 3 were 'N' masked, and regions with high coverage (>3 standard deviations from the coverage mean) were carefully inspected for non-specific mapping—all polymorphisms relative to the reference in these high coverage regions were N-masked. Consensus sequences were called at either a 65% (*Equus*) or 75% (*Bison* and *Mammuthus*) nucleotide identity threshold depending on the abundance of allelic diversity, otherwise ambiguous bases were called in those positions. These reconstructed mitochondrial genomes were then aligned with *muscle* v3.8.425 (Edgar, 2004) (http://www.iqtree.org/http://www.drive5.com/muscle/) against other publicly available mitogenomes on GenBank NCBI (National Center for Biotechnology Information; Benson et al., 2013; Agarwala et al., 2016). A maximum likelihood phylogenetic analysis was conducted using *IQ-Tree* v1.4.0 (Nguyen et al., 2015) (http://www.iqtree.org/) (flags: -m TEST -b 1000 -nt AUTO). Trees were analyzed in FigTree v1.4.4 (http://tree.bio.ed.ac.uk/software/figtree/). All figures were cosmetically fine-tuned in *Adobe Illustrator* (Adobe Inc., 2020) (https://adobe.com/products/illustrator).

6.6 Extended data

Table E6.2 Reads mapped to *Mammuthus primigenius* (NC_007596.2)

Core	SedaDNA ID	UDG vs. non-UDG	mean coverage	Ref seq coverage	# of reads	GC	Pairwise identity
BC-4-2B	**PHP-1**	**All reads (UDG + non-UDG)**	**23.2**	**99.1%**	**6334**	**40.2%**	**97.1%**
BC-4-2B	*PHP-1*	*UDG*	*18.0*	*99.1%*	*4778*	*40.1%*	*97.3%*
BC-4-2B	*PHP-1*	*non-UDG*	*5.1*	*95.2%*	*1557*	*40.4%*	*96.6%*
MM12-116b	**PHP-13**	**non-UDG**	**16.8**	**98.7%**	**4998**	**38.9%**	**98.4%**
MM12-117b	**PHP-15**	**non-UDG**	**5.7**	**96.4%**	**1700**	**39.3%**	**97.8%**
LLII-12-84-3	PHP-6	non-UDG	0.8	21.1%	341	45.3%	97.7%
MM12-119B	PHP-12	non-UDG	0.6	27.1%	211	42.9%	95.9%
MM12-132b	PHP-16	non-UDG	0.5	32.3%	139	39.5%	97.3%
MM12-118B	PHP-11	non-UDG	0.4	22.1%	192	42.5%	96.8%
MM12-QC-6	PHP-22	non-UDG	0.4	21.2%	143	42.5%	95.5%
LLII-12-217-8	PHP-9	non-UDG	0.3	18.5%	92	41.1%	97.0%
MM12-125b	PHP-17	non-UDG	0.3	20.3%	80	40.0%	96.8%
MM12-115b	PHP-14	non-UDG	0.2	17.1%	76	41.4%	96.1%
LL2S-253-D1	PHP-3	non-UDG	0.2	7.3%	85	43.3%	96.4%
LL2C-118-C	PHP-4	non-UDG	0.2	8.6%	86	44.6%	95.7%
MM12-QC-9	PHP-20	non-UDG	0.2	8.2%	82	45.5%	95.3%
LL2C-205-B	PHP-5	non-UDG	0.1	10.3%	51	39.8%	95.9%
MM12-QC-2	PHP-25	non-UDG	0.1	5.6%	47	44.1%	95.1%
MM12-QC-3	PHP-24	non-UDG	0.1	6.0%	42	44.5%	95.9%
MM12-QC-10	PHP-19	non-UDG	0.1	3.0%	52	48.8%	96.2%
MM12-QC-4	PHP-23	non-UDG	0.1	4.3%	35	47.8%	93.4%
MM12-QC-8	PHP-21	non-UDG	0.1	4.4%	30	41.7%	93.0%
LLII 12-170-6	PHP-8	non-UDG	0.1	4.4%	30	44.6%	94.5%
LL2C-243-A2	PHP-7	non-UDG	0.0	3.5%	26	43.9%	94.9%
LL2S-189-E	PHP-2	non-UDG	0.0	1.0%	9	41.0%	88.9%
Blanks		UDG + non-UDG	0.0	0.7%	4	43.1%	92.0%

Libraries with sufficient mapped read coverage (>3x) and percent coverage of the reference genome (>80%) are highlighted. Minimum size 24 bp, minimum map quality 30.

Table E6.3 Reads mapped to *Equus caballus* (NC_001640.1)

Core	SedaDNA ID	UDG vs. non-UDG	mean coverage	Ref seq coverage	# of reads	GC	Pairwise identity
BC-4-2B	**PHP-1**	**All reads (UDG + non-UDG)**	**49.7**	**98.6%**	**12870**	**42.3%**	**97.6%**
BC-4-2B	*PHP-1*	*UDG*	*41.3*	*98.6%*	*10429*	*42.2%*	97.7%
BC-4-2B	*PHP-1*	*non-UDG*	*8.3*	*97.3%*	*2442*	*42.7%*	97.1%
MM12-QC-6	**PHP-22**	**Non-UDG**	**3.0**	**91.7%**	**848**	**42.2%**	**97.6%**
MM12-117b	**PHP-15**	**Non-UDG**	**2.7**	**83.2%**	**872**	**42.2%**	**96.8%**
MM12-116b	PHP-13	Non-UDG	2.3	70.5%	802	43.2%	97.0%
MM12-QC-2	PHP-25	Non-UDG	1.5	73.9%	418	42.1%	97.7%
LL2C-243-A2	PHP-7	Non-UDG	1.0	59.8%	261	41.7%	97.8%
LLII-12-217-8	PHP-9	Non-UDG	0.9	58.5%	299	41.8%	97.7%
LLII-12-84-3	PHP-6	Non-UDG	0.8	30.3%	311	45.4%	97.8%
LL2C-205-B	PHP-5	Non-UDG	0.6	44.2%	208	41.7%	97.6%
MM12-119B	PHP-12	Non-UDG	0.6	22.4%	222	44.2%	96.3%
MM12-QC-4	PHP-23	Non-UDG	0.5	38.8%	145	41.3%	97.3%
LL2C-118-C	PHP-4	Non-UDG	0.4	25.1%	139	43.9%	96.2%
MM12-115b	PHP-14	Non-UDG	0.3	25.5%	99	41.5%	97.3%
MM12-QC-9	PHP-20	Non-UDG	0.3	17.7%	112	44.3%	96.5%
MM12-118B	PHP-11	Non-UDG	0.3	12.4%	141	44.7%	97.2%
LLII-12-170-6	PHP-8	Non-UDG	0.2	18.9%	85	44.1%	96.6%
MM12-132b	PHP-16	Non-UDG	0.2	9.3%	79	43.9%	96.3%
MM12-QC-3	PHP-14	Non-UDG	0.2	15.2%	78	43.8%	96.3%
LL2S-253-D1	PHP-3	Non-UDG	0.2	12.0%	71	44.3%	95.8%
MM12-125b	PHP-17	Non-UDG	0.1	8.8%	48	43.6%	96.0%
MM12-QC-10	PHP-19	Non-UDG	0.1	4.0%	59	48.0%	98.5%
MM12-QC-8	PHP-21	Non-UDG	0.0	3.4%	17	44.2%	95.9%
LL2S-189-E	PHP-2	Non-UDG	0.0	2.0%	20	47.2%	94.2%
Blanks		UDG + non-UDG	0.0	1.70%	1.7%	47.9%	47.9%

Libraries with sufficient mapped read coverage (>3x) and percent coverage of the reference genome (>80%) are highlighted. Minimum size 24 bp, minimum map quality 30.

Table E6.4 Reads mapped to *Bison priscus* (NC_027233.1)

Core	SedaDNA ID	UDG vs. non-UDG	mean coverage	Ref seq coverage	# of reads	GC	Pairwise identity
BC-4-2B	**PHP-1**	**All reads (UDG + non-UDG)**	**286.7**	**100.00%**	**76,953**	**39.70%**	**98.7%**
BC-4-2B	*PHP-1*	*UDG (Bison ssp.)*	*136.8*	*100.00%*	*38,256*	*39.40%*	98.9%
BC-4-2B	*PHP-1*	*UDG (PalaeoChip)*	*114.0*	*100.00%*	*28,572*	*39.90%*	98.7%
BC-4-2B	*PHP-1*	*non-UDG*	*35.9*	*100.00%*	*10,127*	*40.00%*	98.2%
MM12-116b	**PHP-13**	**Non-UDG**	**11.8**	**99.70%**	**3,637**	**40.00%**	**98.2%**
MM12-117b	**PHP-15**	**Non-UDG**	**10.2**	**99.90%**	**3,065**	**40.00%**	**98.0%**
MM12-132b	**PHP-16**	**Non-UDG**	**4.2**	**95.00%**	**1,153**	**39.00%**	**98.1%**
MM12-QC-6	**PHP-22**	**Non-UDG**	**3.2**	**93.30%**	**862**	**39.70%**	**97.4%**
MM12-119B	PHP-12	Non-UDG	2.0	70.10%	628	42.00%	95.7%
LLII-12-217-8	PHP-9	Non-UDG	1.1	65.20%	380	40.30%	97.3%
MM12-QC-3	PHP-24	Non-UDG	1.0	62.30%	362	40.60%	98.2%
MM12-115b	PHP-14	Non-UDG	1.0	57.90%	291	40.00%	97.5%
LLII-12-84-3	PHP-6	Non-UDG	1.0	36.10%	424	44.80%	95.2%
MM12-125b	PHP-17	Non-UDG	0.9	55.30%	264	39.80%	97.4%
MM12-118B	PHP-11	Non-UDG	0.9	47.90%	358	41.10%	94.8%
LL2C-118-C	PHP-4	Non-UDG	0.6	34.90%	203	41.50%	95.9%
LLII-12-170-6	PHP-8	Non-UDG	0.4	33.50%	163	40.80%	97.2%
MM12-QC-9	PHP-20	Non-UDG	0.4	24.30%	164	43.10%	95.5%
MM12-QC-2	PHP-25	Non-UDG	0.4	24.90%	141	41.70%	95.7%
LL2S-253-D1	PHP-3	Non-UDG	0.4	24.10%	141	41.80%	95.8%
LL2C-243-A2	PHP-7	Non-UDG	0.3	19.60%	89	41.60%	95.3%
MM12-QC-4	PHP-23	Non-UDG	0.2	13.60%	86	42.70%	95.4%
LL2C-205-B	PHP-5	Non-UDG	0.1	8.00%	66	42.00%	93.6%
MM12-QC-10	PHP-19	Non-UDG	0.1	4.10%	79	48.40%	96.4%
MM12-QC-8	PHP-21	Non-UDG	0.1	4.80%	39	44.30%	93.6%
LL2S-189-E	PHP-2	Non-UDG	0.0	1.90%	17	45.70%	92.1%
Blanks		UDG + non-UDG	0.0	1.60%	6	46.30%	96.4%

Libraries with sufficient mapped read coverage (>3X) and percent coverage of the reference genome (>80%) are highlighted. Minimum size 24 bp, minimum map quality 30.

Table E6.5 Library stats summary table

Site, core, age	Library ID	UDG	Enrichment target or Shotgun	Total reads sequenced	Reads *bwa* mapped at min24, MQ30			
					Equus	*Mammuthus*	*Bison*	*Homo*
Bear Creek BC 4-2B 30,000 BP	CSMii-1a-U-VI	UDG	PalaeoChip animals	1,303,874	1,919	633	4,331	161
	CSMii-1b-U-VI	UDG	PalaeoChip animals	2,061,905	924	397	2,667	133
	CSMii-1c-U-VI	UDG	PalaeoChip animals	2,819,701	1,210	368	4,098	153
	CSMii-1d-U-VI	UDG	PalaeoChip animals	3,890,546	213	96	859	39
	PHP-1-U-VI	UDG	PalaeoChip animals	7,256,963	41	24	0	19
	PHPii-1-AB-U-VII	UDG	PalaeoChip animals	1,727,494	2,604	707	6,394	271
	PHPii-1-CD-U-VII	UDG	PalaeoChip animals	1,921,777	1,336	793	3,983	138
	PHPii-1-EF-U-VII	UDG	PalaeoChip animals	3,974,493	2,181	1,759	6,239	9,941
	SET277-En-VIII		PalaeoChip animals	4,025,693	683	578	2,215	94
	SET278-En-VIII		PalaeoChip animals	3,290,498	256	98	852	60
	SET279-En-VIII		PalaeoChip animals	1,888,554	86	52	352	21
Bear Creek BC 4-2B 30,000 BP	CSMii-1a-U-I	UDG	*Bison bison* & *Bison priscus*	2,431,743	556	175	5,290	137
	CSMii-1a-U-II	UDG	*Bison bison* & *Bison priscus*	1,537,565	449	130	4,183	117
	CSMii-1b-U-I	UDG	*Bison bison* & *Bison priscus*	1,419,845	309	101	3,334	88
	CSMii-1b-U-II	UDG	*Bison bison* & *Bison priscus*	1,810,430	589	208	6,072	183
	CSMii-1c-U-I	UDG	*Bison bison* & *Bison priscus*	6,326,115	18	14	131	11
	CSMii-1c-U-II	UDG	*Bison bison* & *Bison priscus*	3,033,708	94	30	1,196	24
	CSMii-1d-U-I	UDG	*Bison bison* & *Bison priscus*	6,165,899	129	36	1,357	41
	CSMii-1d-U-II	UDG	*Bison bison* & *Bison priscus*	3,077,273	164	46	1,638	49
	PHP-1-U-I	UDG	*Bison bison* & *Bison priscus*	8,055,190	69	33	1,012	37
	PHP-1-U-II	UDG	*Bison bison* & *Bison priscus*	9,331,772	103	37	1,242	33
	PHPii-1-AB-U-III	UDG	*Bison bison* & *Bison priscus*	3,355,591	240	57	2,370	69
	PHPii-1-AB-U-IV	UDG	*Bison bison* & *Bison priscus*	3,654,777	375	101	3,913	120
	PHPii-1-CD-U-III	UDG	*Bison bison* & *Bison priscus*	1,234,076	210	91	2,399	73
	PHPii-1-CD-U-IV	UDG	*Bison bison* & *Bison priscus*	2,461,566	116	45	1,340	35
	PHPii-1-EF-U-III	UDG	*Bison bison* & *Bison priscus*	1,779,858	214	92	1,377	479
	PHPii-1-EF-U-IV	UDG	*Bison bison* & *Bison priscus*	4,846,102	176	93	1,401	613
	SET277-En-V		*Bison bison* & *Bison priscus*	4,383,245	116	78	1,461	50
Bear Creek BC 4-2B 30,000 BP	PHP-1		PalaeoChip plants/animals	1,619,859	280	165	1205	68
	SET-277		PalaeoChip plants/animals	1,235,759	428	311	1466	98
	SET-278		PalaeoChip plants/animals	1,275,219	338	131	1034	81
	SET-279		PalaeoChip plants/animals	1,519,972	370	221	1541	92
	SET-279_SG		**Shotgun**	8,442,733	7	6	17	15

Site, core, age	Library ID	UDG	Enrichment target or Shotgun	Total reads sequenced	Reads *bwa* mapped at min24, MQ30			
					Equus	*Mammuthus*	*Bison*	*Homo*
Lucky Lady II LL2S-189-E 10,220 BP	PHP-2		PalaeoChip plants/animals	63,685	2	2	3	3
	PHPii-2		PalaeoChip plants/animals	4,141,976	11	1	8	8
	PHPii-2cd		PalaeoChip plants/animals	4,461,835	6	5	5	11
Lucky Lady II LL2S-253-D1 10,340 BP	PHP-3		PalaeoChip plants/animals	*not sequenced*				
	PHPii-3		PalaeoChip plants/animals	5,445,860	26	24	48	30
	PHPii-3cd		PalaeoChip plants/animals	3,857,668	44	30	92	55
Lucky Lady II LL2C-118-C 13,105 BP	PHP-4		PalaeoChip plants/animals	1,619,858	57	31	99	40
	PHPii-4		PalaeoChip plants/animals	6,129,319	81	54	103	47
Lucky Lady II LL2C-205-B 13,150 BP	PHP-5		PalaeoChip plants/animals	1,126,060	79	26	34	30
	PHPii-5		PalaeoChip plants/animals	3,871,764	128	24	31	45
Lucky Lady II LLII 12-84-3 13,205 BP	PHP-6		PalaeoChip plants/animals	1,571,297	57	63	83	41
	PHPii-6		PalaeoChip plants/animals	4,287,316	94	90	106	91
	SET-271		PalaeoChip plants/animals	1,807,078	49	59	74	55
	SET-272		PalaeoChip plants/animals	1,322,559	59	67	82	55
	SET-273		PalaeoChip plants/animals	1,247,471	51	61	78	47
	SET-272-SG		**Shotgun**	2,086,749	5	3	9	17
Lucky Lady II LL2C-243-A2 13,870 BP	PHP-7		PalaeoChip plants/animals	1,449,830	24	9	14	17
	PHPii-7		PalaeoChip plants/animals	4,370,642	236	16	74	58
Lucky Lady II LLII 12-170-6 15,405 BP	PHP-8		PalaeoChip plants/animals	1,331,181	84	29	162	34
Lucky Lady II LLII 12-217-8 15,865 BP	PHP-9		PalaeoChip plants/animals	958,126	116	30	136	33
	SET-274		PalaeoChip plants/animals	845,348	58	17	89	21
	SET-275		PalaeoChip plants/animals	970,115	81	31	80	40
	SET-276		PalaeoChip plants/animals	341,707	43	13	74	15
	SET-274_SG		**Shotgun**	1,937,626	2	0	2	7
Upper Goldbottom MM12-118B 9685 BP	PHP-11		PalaeoChip plants/animals	79,090	1	3	9	5
	PHPii-11		PalaeoChip plants/animals	3,221,976	15	24	35	18
	SET-268		PalaeoChip plants/animals	1,678,166	47	44	103	40
	SET-269		PalaeoChip plants/animals	1,754,121	45	83	106	48
	SET-270		PalaeoChip plants/animals	1,249,732	32	37	104	39
	SET-268-SG		**Shotgun**	2,165,736	2	4	2	5
Upper Goldbottom MM12-119B	PHP-12		PalaeoChip plants/animals	*not sequenced*				
	PHPii-12		PalaeoChip plants/animals	61,637	0	0	0	0

Site, core, age	Library ID	UDG	Enrichment target or Shotgun	Total reads sequenced	Reads *bwa* mapped at min24, MQ30			
					Equus	*Mammuthus*	*Bison*	*Homo*
Upper Goldbottom MM12-119B 10,340 BP	CSMii-PHP-12a		PalaeoChip plants/animals	5,234,065	65	95	135	69
	CSMii-PHP-12b		PalaeoChip plants/animals	3,464,073	68	37	199	66
	CSMii-PHP-12c		PalaeoChip plants/animals	4,649,222	38	37	110	51
	CSMii-PHP-12d		PalaeoChip plants/animals	5,000,444	50	41	183	55
Upper Goldbottom MM12-116b 17,500 BP	PHP-13		PalaeoChip plants/animals	1,624,580	801	4997	3636	278
Upper Goldbottom MM12-115b 18,510 BP	PHP-14		PalaeoChip plants/animals	2,320,965	98	75	290	31
Upper Goldbottom MM12-117b 21,775 BP	PHP-15		PalaeoChip plants/animals	1,910,387	871	1699	3064	197
Upper Goldbottom MM12-132b 40,410 BP	PHP-16		PalaeoChip plants/animals	15,006	0	0	0	0
	PHPii-16		PalaeoChip plants/animals	1,741,823	78	138	1152	69
Upper Goldbottom MM12-125b 42,100 BP	PHP-17		PalaeoChip plants/animals	482	0	0	1	0
	PHPii-17		PalaeoChip plants/animals	2,382,657	47	79	262	44
Upper Quartz MM12-QC-10 5765 BP	PHP-19		PalaeoChip plants/animals	2,279,133	43	40	65	101
	PHPii-19		PalaeoChip plants/animals	6,965,795	15	11	13	18
Upper Quartz MM12-QC-9 5840 BP	PHP-20		PalaeoChip plants/animals	1,883,409	80	48	100	52
	PHPii-20		PalaeoChip plants/animals	4,030,038	31	33	63	37
Upper Quartz MM12-QC-8 5915 BP	PHP-21		PalaeoChip plants/animals	1,590,777	7	16	18	11
	PHPii-21		PalaeoChip plants/animals	3,551,677	9	13	20	12
Upper Quartz MM12-QC-6 12,805 BP	PHP-22		PalaeoChip plants/animals	1,135,493	299	70	434	93
	PHPii-22		PalaeoChip plants/animals	4,944,689	548	72	427	75
Upper Quartz MM12-QC-4 14,925 BP	PHP-23		PalaeoChip plants/animals	1,207,782	66	13	47	25
	PHPii-23a		PalaeoChip plants/animals	5,380,376	34	9	15	20
	PHPii-23b		PalaeoChip plants/animals	8,141,488	44	12	23	27
Upper Quartz MM12-QC-3 15,745 BP	PHP-24		PalaeoChip plants/animals	1,129,623	77	41	361	54
Upper Quartz MM12-QC-2 16,560 BP	PHP-25		PalaeoChip plants/animals	1,568,411	417	46	140	70

Site, core, age	Library ID	UDG	Enrichment target or Shotgun	Total reads sequenced	Reads *bwa* mapped at min24, MQ30			
					Equus	*Mammuthus*	*Bison*	*Homo*
Extraction blanks PHP batch	PHP-10-BK		PalaeoChip plants/animals	9,882	0	0	0	18
	PHP-18-BK		PalaeoChip plants/animals	1,495	1	0	7	9
	PHP-26-BK		PalaeoChip plants/animals	7,351	0	1	0	8
Library blanks PHP batch	LibBK-PHP_CL		PalaeoChip plants/animals	4,451	0	0	0	0
Extraction blanks PHPii batch	PHPii-BK27		PalaeoChip plants/animals	2,316	6	2	3	67
	PHPii-BK28		PalaeoChip plants/animals	4,045	0	0	0	3
	PHPii-BK29		PalaeoChip plants/animals	2,170	0	0	0	0
	CSMii-BK2		PalaeoChip plants/animals	8,681	0	0	1	13
Library blanks PHPii batch	PHPii-LB		PalaeoChip plants/animals	4,570	0	0	0	0
	CSMii-LB		PalaeoChip plants/animals	275	0	0	0	0
Extraction blanks SET batch	SET-BK22		PalaeoChip plants/animals	55,877	0	0	0	0
	SET-BK23		PalaeoChip plants/animals	852	0	0	0	14
	SET-BK23-SG		**Shotgun**	960,533	0	0	0	9
Library blanks SET batch	SET-BK24		PalaeoChip plants/animals	475	0	0	0	0
	SET-BK24-SG		**Shotgun**	1,538,205	0	0	0	3
Extraction and library blanks UDG PalaeoChip batch	PHP-10-BK-U-VI	UDG	PalaeoChip-Animals	2,321	0	0	0	0
	CSMii-BK2-U-VI	UDG	PalaeoChip-Animals	4	0	0	0	0
	PHP-CSM-LB-U-VI	UDG	PalaeoChip-Animals	335	0	0	0	0
	PHPii-BK29-U-VII	UDG	PalaeoChip-Animals	1,691	0	0	0	0
Extraction and library blanks UDG Bison batch	PHP-10-BK-U-I	UDG	*Bison bison* & *Bison priscus*	1,262	0	0	0	1
	CSMii-BK2-U-I	UDG	*Bison bison* & *Bison priscus*	5,647	1	1	1	4
	PHP-CSM-LB-U-I	UDG	*Bison bison* & *Bison priscus*	260	0	0	0	0
	PHPii-BK29-U-III	UDG	*Bison bison* & *Bison priscus*	191	0	0	0	0
	PHPii-LB-U-III	UDG	*Bison bison* & *Bison priscus*	30	0	0	0	0
	SETBK22-En-V		*Bison bison* & *Bison priscus*	1,709	0	0	0	0

*Shogtun reads from Chapter 2 included for comparison.

Table E6.6 UDG treatment and blunt end repair master mixes.

Blunt-End Repair with UDG: Step 1	
Component	Final Concentration
NE Buffer 2.1	1X
DTT	1 mM
dNTP mix	100 µM
ATP	1 mM
T4 polynucleotide kinase	0.4 U/µL
Uracil-DNA glycosylase	0.1 U/µL
Endonuclease VIII	0.4 U/µL
Blunt-End Repair with UDG: Step 2	
T4 DNA polymerase	0.2 U/µL
Polymerase added individually to each PCR well.	

A final volume of 40 µL per rxn was used for the master mixture and template DNA.
Nanopure Barnstead water was used to bring up the volume to the desired concentration.
Step 1: 3 hours at 37°C.
Step 2a: 15 min at 25°C.
Step 2b: 15 min at 12°C.

Table E6.7 PHP-1 human mapped *Mitomaster* output (Lott et al., 2013).

rCRS Position	Query Position	rCRS NT	Query NT	Mut type	Locus	Other	Freq % in T2b
709	707	G	A	transition	12S	rRNA	98.934 (835/844)
750	748	A	G	transition	12S	rRNA	99.763 (842/844)
930	928	G	A	transition	12S	rRNA	99.408 (839/844)
1888	1886	G	A	transition	16S	rRNA	97.867 (826/844)
2706	2704	A	G	transition	16S	rRNA	99.052 (836/844)
3826	3823	T	C	transition	ND1	ND1:L174L	3.791 (32/844)
4216	4213	T	C	transition	ND1	ND1:Y304H	99.408 (839/844)
4769	4766	A	G	transition	ND2	ND2:M100M	99.526 (840/844)
4917	4914	A	G	transition	ND2	ND2:N150D	100.000 (844/844)
7028	7025	C	T	transition	COI	COI:A375A	99.171 (837/844)
8860	8857	A	G	transition	ATPase6	ATPase6:T112A	99.289 (838/844)
9063	9060	A	G	transition	ATPase6	ATPase6:L179L	0.000 (0/844)
9948	9945	G	A	transition	COIII	COIII:V248I	0.118 (1/844)
11251	11248	A	G	transition	ND4	ND4:L164L	99.526 (840/844)
11719	11716	G	A	transition	ND4	ND4:G320G	99.645 (841/844)
11812	11809	A	G	transition	ND4	ND4:L351L	99.289 (838/844)
13368	13365	G	A	transition	ND5	ND5:G344G	99.171 (837/844)
14766	14763	C	T	transition	Cytb	Cytb:T7I	99.526 (840/844)
14905	14902	G	A	transition	Cytb	Cytb:M53M	98.934 (835/844)
15326	15323	A	G	transition	Cytb	Cytb:T194A	99.408 (839/844)
15452	15449	C	A	transversion	Cytb	Cytb:L236I	99.408 (839/844)
15607	15604	A	G	transition	Cytb	Cytb:K287K	99.526 (840/844)
16519	16516	T	C	transition	ATTCR:Control RegionCR:7S-like	non-coding	94.668 (799/844)

T2b5 haplogroup called at 86.99% quality as per HaploGrep 2 (Weissensteiner et al., 2016). PHP-1 Human mitogenome assembly statistics:
Sequences: 13,190
Coverage of 16,566 bases:
Mean: 56.2 Std Dev: 93.3
Minimum: 0 Maximum: 900
Forward: 28.0 Reverse: 28.2
Ref-Seq: 91.8% (15,213 bp)

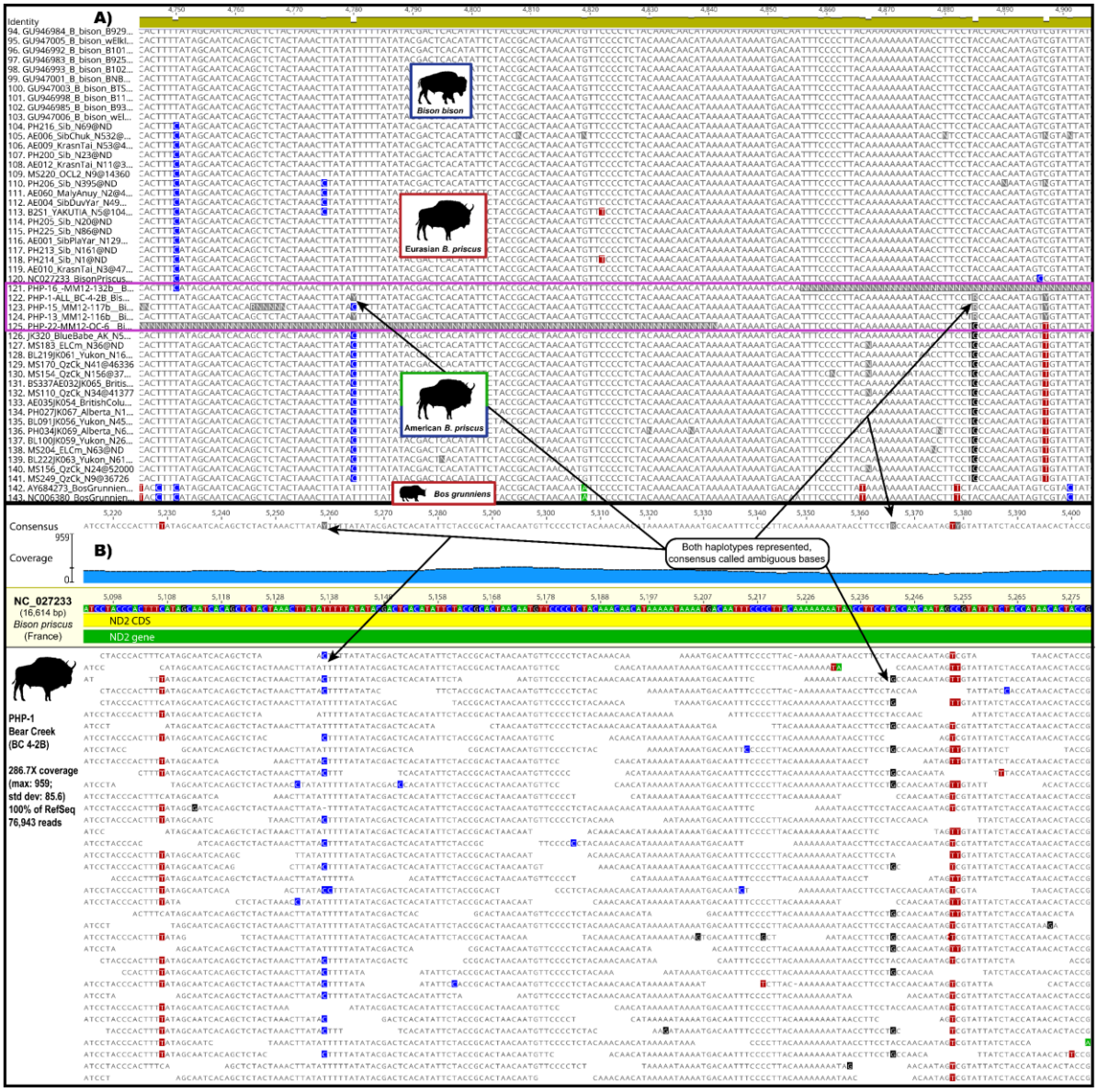

Fig. E6.7 Multi-allelic segregating sites of *B. priscus* mitogenomes.
A) Multiple alignment generated with *muscle* v3.8.425 (Edgar, 2004) and visualized in Geneious Prime (2019.2.3). Sequence order modified from *muscle*.
B) Mapped reads in the ND2 gene with allelic variability indicative of both Eurasian and American steppe bison.

Chapter 7 Conclusion

The research subsumed within this dissertation contributes to Quaternary science in five key areas. First and foremost, this work details a pair of methodological innovations that greatly enhances the accessibility of ancient environmental DNA. With the combination of our sedaDNA optimized extraction procedure (the cold spin technique) and the PalaeoChip Arctic-1.0 targeted enrichment bait-set, previously inaccessible molecules have become viable biomarkers for ancient DNA applications, revealing the unbeknownst microbiological, genomic, and evolutionary resolution possible with buried archives of sedaDNA—even in the total absence of identifiable macro-tissues. Second, this new biomolecular resolution of macro-taxa from palaeoecosystems enabled the reconstruction of environmental turnover over 30,000 years in central Yukon, identifying the synergistic collapse of the mammoth-steppe biome and its replacement with Holocene flora and fauna. Third, this work hints at a road towards disentangling anthropogenic and climatological factors through the enhanced resolution available with environmental DNA wherein we observe a decline in the sedaDNA of some megafaunal grazers (steppe bison and woolly mammoth) predating the Bølling–Allerød warming and woody shrub expansion. Further, the potential extended persistence of Pleistocene fauna in Beringia hints at understandings of how ice age megafauna may have adapted to previous glacial/interglacial transitions through high-latitude or high-altitude refugia, how humans may have influenced and responded to these extirpations, and how the seeming finality of extinction is itself also likely much more complex and gradational than we might otherwise assume.

Fourth, the introductory chapter contextualizes deep time human ecological interactions in terms of our modern ecological crises and conceptions of an *Anthropocene* epoch, highlights ecological theory with abundant cross-disciplinary applications in the social and life sciences, provides a relatively comprehensive synthesis of the peopling and palaeoecology of Beringia paired with debates surrounded the LQE, and recounts the history, strengths, and limitations of ancient environmental DNA methodologies. Fifth, by contextualizing the peopling of Beringia and LQE across a range of social and life science

disciplines, this work highlights the complex and likely synergistic nature of the Pleistocene-Holocene mass extinctions. This aids in shifting understandings of this 'event' of major environmental turnover away from single track, left cerebral hemispheric conceptions (McGilchrist, 2009) towards an emphasis on the importance of the holistic, interconnected, and complex combination of compounding factors that have synergistically molded our inheritance of the contemporary biosphere.

7.1 Accessing previously inaccessible ancient environmental DNA

The three manuscripts of this dissertation contribute towards Quaternary science primarily in methodological innovation. The only previously successful use of capture enrichment techniques as applied to sedaDNA was published by Slon et al. (2017). In this instance, the authors were targeting cave sediments across Eurasia, most notably at Denisova cave where both Neandertal and Denisovan remains have been recovered. Slon and colleagues utilized a bait-set designed to capture Eurasian megafaunal mitochondrial DNA (Slon et al., 2016). This was designed principally as a screening tool for undiagnostic faunal remains, but the authors also applied it to middle Pleistocene sediments from Qesem Cave in Israel. Their initial attempts with sediment enrichment were unsuccessful (Slon et al., 2016), which prompted a small experimental effort to refine sedaDNA extraction as detailed in the supplementary materials of Slon et al. (2017). This paralleled my own concurrent challenges attempting to library prepare sedaDNA with either relatively empty extracts, or those where our target DNA was not effectively isolated from inhibitory substances (detailed in Chapter 3). Sadoway (2014) (a former researcher in the McMaster Ancient DNA Centre) likewise encountered substantial challenges isolating sedaDNA from the organo-mineral matrices of the original sediments. Sadoway (2014) was successful in utilizing a PCR metabarcoding technique on the same extracts however, which parallels much of the continued success of metabarcoding in Quaternary science (Taberlet et al., 2018).

Despite the success of metabarcoding, this technique has many limitations in terms of genetic targets amenable to primer design with degraded aDNA (as discussed in section 2.2). Alternatively, the deep-shotgun sequencing approach of Pedersen et al.

(2016) has been shown to be a viable means of reconstructing palaeoenvironments, and which circumvents the limits of metabarcoding. These authors seem to have partially dealt with sedimentary inhibition using phenol:chloroform extractions as opposed to the silica-spin column based approaches (Tan and Yiap, 2009; Ali et al., 2017) that are typically used at the McMaster Ancient DNA Centre—in this case, principally for safety, but also because these techniques perform equally well in most situations. Pedersen et al. (2016) report few details regarding their extractions or difficulties with inhibition, other than mentioning needing to purify some darkly coloured extracts multiple times.

In terms of their targeting approach however, Pedersen et al. (2016) shotgun sequenced over 1 billion molecules to investigate faunal and floral turnover in the ice-free corridor. Only 0.02% of the data they generated was informative of macro-scale palaeo-ecosystems, with only 0.0003% being informative of genera level data (as reported in the extended supplementary data table for figure 4 of Pedersen et al. [2016]). Meaning that >99.9% of the data generated was uninformative for their primary research question, yet constituted significant laboratory, sequencing, and computational costs processing such immense datasets. Conversely, up to 15% (average 4.53%) of the sequence data from Chapter 5 was able to be assigned to ecologically informative ranks. While most reads are still prokaryotes or otherwise uninformative of macro-scale ecological questions, PalaeoChip enrichments in this case constitute an average 226-fold increase in on-target DNA compared with Pedersen et al. (2016)—two to three orders of magnitude more macro-ecological sedaDNA than shotgun sequencing. This is paralleled by similar results reported in Chapters 2 and 3 where we found that a shotgun approach was incredibly inefficient in sequencing eDNA from macro-scale organisms in open-air, sedimentary materials. The innovation of applying capture enrichment to sedimentary DNA can aid smaller labs in conducting palaeogenetic ecological analyses at a scale that has only been feasible for a very small set of the world's most highly-funded ancient DNA facilities. Capture enrichment with sedaDNA necessitates an effective aDNA isolation technique. Therein, the cold spin extraction technique detailed in Chapters 2 and 3 constitutes a novel contribution independently, but which when paired with capture enrichment

enables a powerful means recovering sedaDNA using silica-based purifications with far improved targeting capabilities compared with PCR metabarcoding.

At the onset of this dissertation, I was simply trying to assess which available extraction method would work best to a facilitate capture enrichment approach with sediment. I soon found that library preparation with our permafrost samples would not work effectively without an optimized extraction procedure, which prompted the multi-year experimental effort detailed in Chapter 3. Whilst experimenting with sedaDNA extraction, I also designed a novel capture enrichment bait-set to target a complex mixture of extinct and extant animal mitochondrial genomes, as well as three chloroplast loci from ~2100 arctic plants. This bait-set itself is a novel contribution towards ancient environmental DNA, being the first to simultaneously target vastly different organisms simultaneously (plant and animal organelle genomes). This is also the first successful application of capture enrichment to open-air sediments as compared to the cave contexts analyzed by Slon et al. (2017). This capture technique allows for the investigation of coeval changes in fauna and flora in a manner unparalleled with traditional palaeontological or archaeological techniques. When utilizing other proxy measures of micro-remains, shifts in plants and animals are interpreted independently (pollen grains and coprophilic fungal spores). Here though, we can observe micro-records of these organisms changing synonymously with the same biomolecule, and at a local scale.

The third methodological innovation of this thesis is the demonstration that the extraction and enrichment techniques reported here can retrieve complete organelle genomes from multiple organisms simultaneously, and in the total absence of macro biological tissues. Chapter 6 details the successful reconstruction of mitogenomes from *Mammuthus primigenius*, *Equus* sp., and *Bison priscus*. This genomic resolution facilitates phylogenetic investigations of haplotype variability when compared with genetic reference data retrieved from other palaeontological remains. Our mitogenomes do appear to include inputs from multiple diverse individuals, which while limiting some phylogenetic approaches, does allow for the investigation of genetic diversity among multiple animals simultaneously—solely from sediment. A logical extension of this

approach is to enrich for human sedaDNA from Beringian permafrost to independently assess the onset of human occupations in the area.

I have been working in parallel to enrich for eukaryotic parasite sedaDNA from archaeological contexts to serve as a proxy indicator of *Homo sapiens.* This parasite sedaDNA project, along with the direct targeting of human DNA in permafrost, will serve as a post-doctoral follow-up to the results reported in this dissertation.

7.2 The Pleistocene-Holocene transition in eastern Beringia

Chapter 4 is concerned with the ecological contributions of this research to our understandings of environmental turnover during the Pleistocene-Holocene transition. We observed a coeval decline in megafaunal sedaDNA tied with the transition to Holocene ecosystems. Challenges in understanding the late Quaternary extinction event is largely driven by unknowns concerning whether the loss of Pleistocene megafauna drove a decline in the mammoth-steppe biome, or whether changing climate resulted in floral turnover and the loss of critical Pleistocene niches. This data suggests that megafaunal declines partially preceded a decline of the mammoth-steppe in eastern Beringia. SedaDNA signals of *Mammuthus* followed by *Bison* appear to be the first megafauna to decline in abundance in the Klondike, followed thereafter by the rise of woody shrubs and the decline of *Equus*. This leads one to question what may have caused these initial declines, but more fundamentally: to what degree is signal decay in genetic abundance tied to palaeo-biomass? If this measure is at all correlated enough to draw the general conclusion that these animals appear to have been decreasing in overall abundance in central Yukon since the LGM, the next question becomes: to what degree were climatological factors responsible, and to what degree are humans implicated?

The evidence of humans in eastern Beringia prior to 14,000 BP is weak, although not entirely absent. Early drafts of Chapter 4 had a stronger emphasis on archaeology; my co-authors pushed me to remove much of this content (largely for good reasons). I remain skeptical though that climate can resolve the LQE debate alone, either regionally in eastern Beringia or globally. Archaeological visibility is especially poor in much of subarctic North America, but is also poor throughout the Pleistocene and for much of the

Holocene among nomadic hunter-gatherers. Growing (but controversial) evidence of humans in LGM Beringia may be reflective of an as yet poorly represented human presence in the Bering palaeo-Isthmus area (Cinq-Mars, 1979; Cinq-Mars and Morlan, 1999; Kuzmin and Keates, 2005; Fiedel and Kuzmin, 2007; Kuzmin, 2008; Harington, 2011; Vachula et al., 2020).

The degree to which this alleged human presence is ecologically significant is a separate, and perhaps more important question. If humans persisted in Beringia through the LGM, longer term and iterative niche construction practices as detailed in Chapter 1 (section 1.2) could explain the progressive declines in megafauna observed both palaeontologically and genetically prior to the Younger Dryas. Differentiating these declines from the LGM will require stronger anthropogenic evidence and longer-term palaeoecological reconstructions, both of which can be addressed through sedaDNA. The story is further complicated by controversial evidence of ET impacts at the onset of the Younger Dryas (Firestone et al., 2007; Wolbach et al., 2018; Pino et al., 2019; Moore et al., 2020). Regardless of the accuracy of the ET hypothesis, the Younger Dryas chronozone is temporally correlated in our dataset with the disappearance of the mammoth-steppe and functional extinction of grazing megafauna in central Yukon. It has also been argued that disease may have played a role in the severity of these declines (MacPhee and Greenwood, 2013). The relative degrees to which these alleged factors may have synergistically caused the ecological turnover associated with the Pleistocene-Holocene transition remains unclear. However, the sedaDNA data presented in this dissertation illuminates certain ways forward to address the debate. Ultimately, the data here suggest that the ecological reconfiguration had elements of both gradual changes in taxonomic composition over millennia, along with a punctuated, rapid shift during the Younger Dryas. This implies that competing climatological, ecological, and archaeological camps may yet each hold important pieces to revealing the LQE puzzle that has otherwise been obscured by a series of false dichotomous debates. Perhaps a synergistic combination of rapidly oscillating climate change, the expansion of peatlands, floral turnover towards taxa favorable to mesic/hydric-browsing as opposed to xeric-

grazing, iteratively refugial population contractions during inter-glacial periods, the decline of keystone megaherbivores necessary for maintaining the mammoth-steppe biome and for controlling woody vegetation, along with novel interventions of persistent hunter-forager niche construction practices, and potentially ET impacts and/or hyperdisease may have each created unique combination of conditions that was untenable for most giants of the ice age. In the same way as how most epidemic disasters throughout recorded history (such as the Black Death) are best understood as a complex synergy of microbial, cultural, and environmental factors (Crawford, 2007), it would be a mistake to assume that the seeming severity of mass extinctions during the Pleistocene–Holocene transition was only due to one or two factors. Whereas I suspect, in all likelihood, it was rather due to a similarly complex network of inter-compounding factors that only become visible through holistic, cross-disciplinary investigations.

7.3 Pleistocene ghosts

The ghost ranges observed here are of interest for palaeo-ecology and wildlife conservation. Palaeontological remains suggest that horses and mammoths had been extirpated from Beringia by ~13,000 BP, which would draw implications either towards the rise of archaeological sites at 14,000 BP, or towards climatological factors related to the Bølling–Allerød interstadial and Younger Dryas stadial (Fig. 4.9). However, when we take an eDNA perspective, there is evidence from Yukon, Alaska, and Russia that these animals survived until at least 10,000 BP and perhaps even as late as the mid-Holocene (Vartanyan et al., 2008; Haile et al., 2009; Graham et al., 2016; Pečnerová et al., 2017; Zazula et al., 2017b). This evidence needs further research, but these sedaDNA ghost ranges imply that the late Quaternary mass extinction event may have taken longer than palaeontological remains would otherwise indicate. This ghost range post-dates the major environmental turnover between 13,000–10,000 BP, including what would appear to be the functional extinction of grazing megafauna in the Klondike. If these animals did persist until 6000 BP, this may suggest a northern refugium for grazing megafauna through inter-glacial periods, as observed in MIS 5e with the persistence of arctic ground squirrel nests and disjunct steppe-like vegetation (Zazula et al., 2011). Much of our

understandings of previous glacial-interglacial transitions are sparse; Meltzer (2020) contends that there are reasons to suspect that not all previous transitions were alike, and that perhaps the transition to our current inter-glacial was more abrupt with uniquely rapid interstadial/stadial oscillations. As discussed in Chapter 1 (section 1.3.1) previous inter-glacials had many of the woody flora characteristic of our current epoch but are thought to have had more of a wood-pasture, mosaic character than the boreal today. The ghost ranges observed here may hint at the ability for megafauna to persist long-term in periods of suboptimal ecosystem composition during interglacials. These animals may have been able to rebound from major climate induced range restrictions, and may have otherwise rebounded following the Holocene interglacial if not for the seeming severity and potential novelty of this transition (Meltzer, 2020). As such, while whatever factors drove the extinctions in the Beringian cul-de-sac would appear to have been a mix of gradual and punctuated factors (as per Chapter 4), these animals may have otherwise persisted if not for the magnitude of ecological restructuring that culminated during the Younger Dryas.

In an analogous situation**,** Holarctic muskox (*Ovibos moschatus*) have especially low modern genetic diversity (Kolokotronis et al., 2007; MacPhee and Greenwood, 2007; Campos et al., 2010; Cuyler et al., 2020). Perhaps enough so that these animals would appear to be at risk of functional extinction from a genetics standpoint. Their dramatic population flux during the late Pleistocene, as well more recently during the 19th and 20th centuries, includes repeated mass population declines followed by impressive recoveries. The ability for severely pressured megafauna to rebound despite multiple bottleneck events suggests a level of resilience that a more absolutist view of endangerment, extirpation, and extinction may fail to appreciate. This may lend credence to Pleistocene fauna having survived similarly severe transitions during previous interglacials, with the lingering presence of humans and other uniquely Holocene factors (e.g. especially severe climate oscillations and perhaps substantial biomass burning from a meteor impact as per the Younger Dryas cosmic impact hypothesis) having synergistically culminated to deny population recovery. Ultimately, understanding the LQE will likely require increasingly

regionally specific studies to understand the local nuances of the event, but I suspect that a broader synergistic understanding may exist eventually at an *Earth System* scale.

The possible extended persistence of these animals for millennia after their seeming functional extinction is also of conceptual utility for conservation efforts. If such animals can persist in fragmented, non-ideal refugia for some 7000 years after they disappear palaeontologically, this would imply that organisms today that we might consider critically endangered—such as the black rhinoceros (*Diceros bicornis*), eastern gorilla (*Gorilla beringei*), many subspecies of tiger (*Panthera tigris*), and some other 32,000+ organisms that are threatened by extinction (https://www.iucnredlist.org/)—may not be beyond saving. There may be many more gradations on the descent into extinction than we are generally aware of. It likely remains situation specific as to when an organism is beyond recovery, but by taking a deeper time perspective, it may be that this precipice extends further out into the abyss than what we might otherwise perceive when viewing the situation from the immediacy of a human lifetime. Had Pleistocene grazers who persisted until the mid-Holocene in high-latitude refugia had the ability to expand their ranges into alternative niches, it seems plausible that these organisms may have been able to recover and expand again in a future glacial period. In this way, perhaps glacial and interglacial periods imposed a cyclical oscillation of expansion and contraction of faunal ranges and populations as observed during MIS-5e with mastodon (*Mammut* ssp.) (Karpinski et al., 2020) and other mix forest browsers such as western camels (*Camelops hesternus*) (Zazula et al., 2017a) moving into Beringia during interglacials only to become repeatedly extirpated with the return to glacial conditions.

In the uniquely severe case of our most recent transition (MIS-1/2), the continued expansion of anti-herbivory boreal flora left unimpeded by a distinct dearth of megafaunal engineers, compounded by the seeming rise in subarctic human populations after 6000 BP (Holmes, 2008), may have simply continually denied any possibility of population rebound in a counterfactual scenario. Contemporary circumstances may reflect an analogous situation today with the ratcheting decline of wilderness areas denying the possibility of population recovery in threatened and endangered species. In this instance

however, our knowledge of both long-term and punctuated factors that give rise to extinctions may enable us to gradually reverse the pressures on particularly vulnerable populations, enabling a long-term rebounding of their fitness despite seemingly having tread far beyond recovery from our limited vantage point.

7.4 Moving forward

This dissertation highlights several avenues in need of further research. First is an expansion of the PalaeoChip Arctic-1.0 bait-set. These baits target reference mitogenomes of primarily megafaunal taxa available as of 2017. However, many new megafaunal genomes have become available since then, including organisms such as saber-toothed cats (Machairodontinae). The plant component of these baits is also restricted to a small subset of the chloroplast genome (*trn*L, *rbc*L, and *mat*K) which could be improved in both loci and taxa. Nuclear loci are not currently targeted at all for any organisms. The shotgun data reported in Chapters 2 and 3 found a substantial component of nuclear loci, at least among animals. Many of these loci have limited taxonomic references, but over time these databases will continue to improve, allowing a broader targeting of taxonomically informative loci across entire nuclear and organelle genomes. This eDNA bait-set can also be expanded to include other organisms of interest, such as eukaryotic parasites, fungi, ecologically informative microbes, insects, and a variety of other organisms in both the Holarctic and in other geographic regions. I intentionally avoided targeting human DNA to avoid the scenario where modern contaminants overwhelm the sequence data. An effort intended to target human sedaDNA is feasible with careful research design and could very well re-conceptualize our understandings of the peopling of Beringia, the Americas, and the spatiotemporal nuances of human dispersals throughout the globe.

Second, the degree to which sedaDNA abundance reflects modern and palaeo-biomass is poorly understood. There is research demonstrating a continuity between eukaryotic eDNA and biomass (Takahara et al., 2012; Yoccoz et al., 2012; Doi et al., 2015; 2017; Cristescu and Hebert, 2018; Wei et al., 2018; Matesanz et al., 2019), although the degree to which this conforms to palaeo-ecologies is largely unknown, as it

is to the degree that terrestrial megafaunal biomass is reflected by sedaDNA abundance in open-air sediments, rather than potentially being driven more by local stochastic factors.

Third, means of taxonomically binning sequenced reads needs improvement. *BLASTn* is one of the main the limiting factors in these analyses wherein there are insufficient options for numerically prioritizing hits to species or genera rather than accessions (individually uploaded and curated sequences with widely varying metadata completeness and accuracy). Improvements here would aid in both reducing false positives and false negatives and could reduce computational resource needs wherein smaller outputs with more analytically relevant data could be used for downstream analyses as opposed to much of the bloat necessitated by public redundant databases.

Fourth, a concentrated effort to collect permafrost cores intended for sedaDNA could alleviate concerns raised of allochthonous biomolecules. Ideally, cores would be collected from aeolian sites of well understood erosional history (low energy environments), where both OSL and ^{14}C dating can be utilized, there is good permafrost DNA preservation, and there is a lengthy history of faunal use, floral turnover, and ideally nearby archaeological sites. Therein, sediments deposited as near to the last interglacial as possible, with continuous records into the middle and late Holocene, could rigorously address questions of long-term environmental turnover as well as evaluating the veracity of the ghost range evidence reported here. Sites from multiple regions would also help account for, and contextualize, local scale variation.

Fifth, the remarkable breadth of sedaDNA reported here is counter-balanced by the increasingly precarious situation of permafrost. Perennial frozen ground is poised to undergo widespread, accelerating, and irreversible thaw across much of the arctic and subarctic (Kokelj et al., 2015; 2017; Nitze et al., 2018; Lewkowicz and Way, 2019; Ward Jones et al., 2019). As this permafrost thaws it will lose its contextual association as it slumps, as well as undergoing mass degradation of the innumerable biomolecules that have been cold preserved therein for tens, to likely hundreds, of thousands of years. Utilizing these permafrost archives while they still exist will aid in understanding our most recent ‘near-time’ example of mass extinction and ecological turnover, which could

critically aid in contextualizing our own on-going ecological crises as anthropogenic pressures extend into our last surviving wild places. However, these genetic archives of the north's ecological heritage will not survive indefinitely given current projections of a warming arctic. Once metabolic, chemical, and physical processes reengage to silently obliterate these vast archives, we will become forever ignorant of what mysteries of life's past may have been unearthed with such immense biomolecular datasets. Analogously, our galactic local group (e.g. the Milky Way, Andromeda, Triangulum) will someday cease to receive information from the rest of the universe (Krauss and Starkman, 2000). Space between galactic bodies is expanding faster than their light can reach our corner of the cosmos. Eventually, the cosmological event horizon will be so absolute that any life in our local group will be forever ignorant of the rest of the universe. While this analogy is somewhat hyperbolic, we too will eventually become inescapably ignorant of the biomolecular information loss and associated understandings that may have been derived from those lost microscopic remnants left behind on ancient landscapes that otherwise could have helped us contextualize how humanity ended up in our current predicaments of zoological impoverishment and existential risk—all ultimately as a result of the irreversible thaw of perennially frozen ground across the globe. A growing awareness of both the information potential and limited time horizons of permafrost sedaDNA will hopefully spur both the increased collection of archival cores, and the continued refinement and analysis of these cryospheric records before they recede beyond taphonomic horizons.

7.5 Our human ecological legacy

I opened this dissertation with an epigraph from Nietzsche forewarning the death of God. This often-misunderstood story laments humanities' deicide, or more precisely, it warns of a coming nihilism as we increasingly realize that in a future where religious foundations of meaning and purpose are lost, we then become the sole arbiters of our value structures. The madman in this story does not rejoice in this newfound freedom but is gravely concerned with what this foundational erosion of meaning implies for the future of humanity.

> *But how did we do this? How could we drink up the sea? Who gave us the sponge to wipe away the entire horizon? What were we doing when we unchained this earth from its sun? Whither is it moving now? Whither are we moving? Away from all suns? Are we not plunging continually? Backward, sideward, forward, in all directions? Is there still any up or down? Are we not straying, as through an infinite nothing? Do we not feel the breath of empty space? Has it not become colder? Is not night continually closing in on us? Do we not need to light lanterns in the morning? Do we hear nothing as yet of the noise of the gravediggers who are burying God? Do we smell nothing as yet of the divine decomposition? Gods, too, decompose. God is dead. God remains dead. And we have killed him.*

Now, it is admittedly a stretch to compare modern existential crises of radical freedom with the terminal Pleistocene mass extinction of megafauna. But the comparison holds utility here to bookend this work by drawing attention to our growing recognition of the immense responsibility humanity holds to the contemporary biosphere, and to all future life on this planet. In some ways, the biblical story of Eden has things reversed. Perhaps we cast ourselves out of Eden. We began walling ourselves off from an innate, intimate connection with evolutionary realities at the onset of the Neolithic revolution. I do not suspect that life during the Pleistocene was any easier than the arduous existence most humans have experienced throughout recorded history. But once population growth, sedentism, and domestication were underway, we became increasingly locked into a lifeway sharply diverged from any other form of Earth-based life hitherto known. The knowledge, population size, and technological capabilities humanity possesses today are irreversibly, and increasingly, transforming nearly every ecosystem on the planet, as well influencing a growing range of non-biotic components of the *Earth System*.

We likely will not know beyond reasonable doubt for many years to what degree we are partly responsible for the mass extinction event that coincided with our ancestors' global dispersal. It seems to me preposterous to think that ancient humans played no part

in this environmental transformation given the prolific abundance of anthroecosystems we see throughout recorded history. But, even if it turns out to be the case that Pleistocene megafauna died out principally from some synergistic (or independently severe) combination of rapidly oscillating climate change, extra-terrestrial impacts, disease, or as yet other unknown factors, human actions throughout recorded history—especially now—are uniquely resonant in their ability to transform life on this planet. In some sense, perhaps the deity we slew was Gaia as former warden of the biosphere. The value in understanding our human ecological legacy in Beringia, or anywhere in the world, is to determine what set of factors led to such radical environmental change, how long it took to happen, and what might have reversed or mitigated what was lost. Today, intentionally or not, we are undertaking a planetary engineering experiment. How much can we alter the atmospheric composition of this planet? How many resources can we extract and transform from biotic and abiotic systems? How much can we reshape and resize biosphere to better meet our evolving needs? How much can we alter our own genetic lineages before we become fully decoupled from non-anthropogenic selective processes? Biotic and abiotic systems will continue to coevolve irrespective of our willingness to deliberately shape their trajectories. But if we can learn from the disasters of Earth's past, perhaps we can wisely steward both our future selves and some reasonably resilient cohort of biological lineages through this precipice into some future worth living in. If we did commit a kind of metaphorical deicide, our usurpatious auto-deification is not cause for celebration, but of grave foreboding for the responsibility humanity now bears.

References

Abramova, Z.A., 1989. Paleolit Severnoi Azii. In: Boriskovskii, P.I. (Ed.), Paleolit Kavkaza i Severnoi Azii. Nauka, Leningrad, pp. 145–243.

Abramova, Z.A., Astakhov, S.N., Vasil'ev, S.A., Ermolva, N.M., Lisitsyn, N.F., 1991. Paleolit Eniseya. Nauka, Leningrad.

Adobe Inc., 2020. Adobe Illustrator. doi:https://adobe.com/products/illustrator

Agarwala, R., Barrett, T., Beck, J., Benson, D.A., Bollin, C., Bolton, E., Bourexis, D., Brister, J.R., Bryant, S.H., Canese, K., Charowhas, C., Clark, K., Dicuccio, M., Dondoshansky, I., Federhen, S., Feolo, M., Funk, K., Geer, L.Y., Gorelenkov, V., Hoeppner, M., Holmes, B., Johnson, M., Khotomlianski, V., Kimchi, A., Kimelman, M., Kitts, P., Klimke, W., Krasnov, S., Kuznetsov, A., Landrum, M.J., Landsman, D., Lee, J.M., Lipman, D.J., Lu, Z., Madden, T.L., Madej, T., Marchler-Bauer, A., Karsch-Mizrachi, I., Murphy, T., Orris, R., Ostell, J., O'sullivan, C., Panchenko, A., Phan, L., Preuss, D., Pruitt, K.D., Rodarmer, K., Rubinstein, W., Sayers, E., Schneider, V., Schuler, G.D., Sherry, S.T., Sirotkin, K., Siyan, K., Slotta, D., Soboleva, A., Soussov, V., Starchenko, G., Tatusova, T.A., Todorov, K., Trawick, B.W., Vakatov, D., Wang, Y., Ward, M., Wilbur, W.J., Yaschenko, E., Zbicz, K., 2016. Database resources of the National Center for Biotechnology Information. Nucleic Acids Research 44, D7–D19. doi:10.1093/nar/gkv1290

Ahmed, E., Parducci, L., Unneberg, P., Ågren, R., Schenk, F., Rattray, J.E., Han, L., Muschitiello, F., Pedersen, M.W., Smittenberg, R.H., Yamoah, K.A., Slotte, T., Wohlfarth, B., 2018. Archaeal community changes in Lateglacial lake sediments: Evidence from ancient DNA. Quaternary Science Reviews 181, 19–29. doi:10.1016/j.quascirev.2017.11.037

Al-Soud, W.A., Radstrom, P., 1998. Capacity of nine thermostable DNA polymerases to mediate DNA amplification in the presence of PCR-inhibiting samples. Applied and Environmental Microbiology 64, 3748–3753.

Alaeddini, R., 2012. Forensic implications of PCR inhibition - A review. Forensic Science International: Genetics 6, 297–305. doi:10.1016/j.fsigen.2011.08.006

Ali, N., Rampazzo, R.D.C.P., Costa, A.Di.T., Krieger, M.A., 2017. Current Nucleic Acid Extraction Methods and Their Implications to Point-of-Care Diagnostics. BioMed Research International 2017. doi:10.1155/2017/9306564

Alley, R.B., 2000. The Younger Dryas cold interval as viewed from central Greenland. Quaternary Science Reviews 19, 213–226. doi:10.1016/S0277-3791(99)00062-1

Allison, S.D., 2006. Soil minerals and humic acids alter enzyme stability: Implications for ecosystem processes. Biogeochemistry 81, 361–373. doi:10.1007/s10533-006-9046-2

Alroy, J., 2015. Current extinction rates of reptiles and amphibians. Proceedings of the National Academy of Sciences 112, 13003–13008. doi:10.1073/pnas.1508681112

Alsos, I.G., Sjo gren, P., Edwards, M.E., Landvik, J.Y., Gielly, L., Forwick, M., Coissac, E., Brown, A.G., Jakobsen, L. V., Foreid, M.K., Pedersen, M.W., 2015. Sedimentary ancient DNA from Lake Skartjorna, Svalbard: Assessing the resilience of arctic flora to Holocene climate change. The Holocene. doi:10.1177/0959683615612563

Alsos, I.G., Sjögren, P., Edwards, M.E., Landvik, J.Y., Gielly, L., Forwick, M., Coissac, E., Brown, A.G., Jakobsen, L. V., Foreid, M.K., Pedersen, M.W., 2016. Sedimentary ancient DNA from Lake Skartjorna, Svalbard: Assessing the resilience of arctic flora to Holocene climate change. The Holocene. doi:10.1177/0959683615612563

Altschul, S.F., Gish, W., Miller, W., Myers, E.W., Lipman, D.J., 1990. Basic local alignment search tool. Journal of Molecular Biology 215, 403–410. doi:10.1016/S0022-2836(05)80360-2

Alvarez, A.J., Khanna, M., Toranzos, G.A., Stotzky, G., 1998. Amplification of DNA bound on clay minerals. Molecular Ecology 7, 775–778.

Andersen, K., Bird, K.L., Rasmussen, M., Halie, J., Breuing-Madsen, H., Kjaer, K.H., Orlando, L., Gilbert, M.T.P., Willerslev, E., 2012. Meta-barcoding of 'dirt' DNA from soil reflects vertebrate biodiversity. Molecular Ecology 21, 1966–1979. doi:10.1111/j.1365-294X.2011.05261.x

Anderson-Carpenter, L.L., McLachlan, J.S., Jackson, S.T., Kuch, M., Lumibao, C.Y., Poinar, H.N., 2011. Ancient DNA from lake sediments: bridging the gap between paleoecology and genetics. BMC evolutionary biology 11, 1–15. doi:10.1186/1471-2148-11-30

Anderson, D.D., 1968. A stone age campsite at the gateway to America. Scientific American 218, 24–33. doi:10.1038/scientificamerican0668-24

Anderson, D.D., 1970. Microblade traditions in northwestern Alaska. Arctic Anthropology 7, 2–16.

Anderson, D.D., 1984. Prehistory of North Alaska. In: Damas, D. (Ed.), Handbook of North American Indians: Vol. 5, Arctic. Smithsonian Institution Press, Washington, D.C., pp. 80–93.

Anderson, E.N., Pearsall, D.M., Hunn, E.S., Turner, N.J. (Eds.), 2011. Ethnobiology. Wiley-Blackwell, Hoboken, New Jersey.

Anderson, J.R., Nilssen, A.C., 1998. Do Reindeer Aggregate on Snow Patches to Reduce Harassment by Parasitic Flies or to Thermoregulate. Rangifer 18, 3–17.

Anderson, M.K., 2005. Tending the wild: Native american knowledge and the management of California's natural resources. University of California Press, Berkeley, CA.

Andrews, T.D., MacKay, G., 2012. The archaeology and Paleoecology of alpine ice patches: A global perspective. Arctic 65, iii–vi. doi:10.14430/arctic4181

Andrews, T.D., MacKay, G., Andrew, L., 2012. Archaeological investigations of alpine ice patches in the Selwyn Mountains, Northwest Territories, Canada. Arctic 65, 1–21. doi:10.14430/arctic4182

Arnold, L.J., Roberts, R.G., Macphee, R.D.E., Haile, J.S., Brock, F., Möller, P., Froese, D.G., Tikhonov, A.N., Chivas, A.R., Gilbert, M.T.P., Willerslev, E., 2011. Paper II - Dirt, dates and DNA: OSL and radiocarbon chronologies of perennially frozen sediments in Siberia, and their implications for sedimentary ancient DNA studies. Boreas 40, 417–445. doi:10.1111/j.1502-3885.2010.00181.x

Asner, G.P., Vaughn, N., Smit, I.P.J., Levick, S., 2016. Ecosystem-scale effects of megafauna in African savannas. Ecography 39, 240–252. doi:10.1111/ecog.01640

Baker, A.G., Bhagwat, S.A., Willis, K.J., 2013. Do dung fungal spores make a good proxy for past distribution of large herbivores? Quaternary Science Reviews 62, 21–31. doi:10.1016/j.quascirev.2012.11.018

Bakker, E.S., Ritchie, M.E., Olff, H., Milchunas, D.G., Knops, J.M.H., 2006. Herbivore impact on grassland plant diversity depends on habitat productivity and herbivore size. Ecology Letters 9, 780–788. doi:10.1111/j.1461-0248.2006.00925.x

Bakker, E.S., Pagès, J.F., Arthur, R., Alcoverro, T., 2016a. Assessing the role of large herbivores in the structuring and functioning of freshwater and marine angiosperm ecosystems. Ecography 39, 162–179. doi:10.1111/ecog.01651

Bakker, E.S., Gill, J.L., Johnson, C.N., Vera, F.W., Sandom, C.J., Asner, G.P., Svenning, J.C., 2016b. Combining paleo-data and modern exclosure experiments to assess the impact of megafauna extinctions on woody vegetation. Proceedings of the National Academy of Sciences 113, 847–855. doi:10.1073/pnas.1502545112

Banks, W.E., d'Errico, F., Peterson, A.T., Kageyama, M., Sima, A., S??nchez-Go??i, M.F., 2008. Neanderthal extinction by competitive exclusion. PLoS ONE 3. doi:10.1371/journal.pone.0003972

Barker, G., Odling-Smee, J., 2014. Integrating Ecology and Evolution: Niche Construction and Ecological Engineering. In: Barker, G., Desjardins, E., Pearce, T. (Eds.), Entangled Life: Organism and Environment in the Biological and Social Sciences. Springer, Dordrecht, The Netherlands, pp. 187–211. doi:10.1007/978-94-007-7067-6

Barnosky, A.D., Koch, P.L., Feranec, R.S., Wing, S.L., Shabel, A.B., 2004. Assessing the causes of late pleistocene extinctions on the continents. Science. doi:10.1126/science.1101476

Barnosky, A.D., Matzke, N., Tomiya, S., Wogan, G.O.U., Swartz, B., Quental, T.B., Marshall, C., McGuire, J.L., Lindsey, E.L., Maguire, K.C., Mersey, B., Ferrer, E.A., 2011. Has the Earth's sixth mass extinction already arrived? Nature 471, 51–57. doi:10.1038/nature09678

Barrera-Bassols, N., Toledo, V.M., 2005. Ethnoecology of the Yucatec Maya: Symbolism, knowledge and management of natural resources. Journal of Latin American Geography 4, 9–41. doi:10.1353/lag.2005.0021

Barrón-Ortiz, C.I., Avilla, L.S., Jass, C.N., Bravo-Cuevas, V.M., Machado, H., Mothé, D., 2019. What is Equus? Reconciling taxonomy and phylogenetic analyses. Frontiers in Ecology and Evolution 7. doi:10.3389/fevo.2019.00343

Barta, J.L., Monroe, C., Teisberg, J.E., Winters, M., Flanigan, K., Kemp, B.M., 2014. One of the key characteristics of ancient DNA, low copy number, may be a product of its extraction. Journal of Archaeological Science 46, 281–289. doi:10.1016/j.jas.2014.03.030

Bartam, A.K., Lynch, M.D.J., Stearns, J.C., Moreno-Hagelsieb, G., Neufeld, J.D., 2011. Generation of multimillion-sequence 16S rRNA gene libraries from complex microbial communities by assembling paired-end Illumina reads. Applied and Environmental Microbiology 77, 3846–3852.

Bayer, K., Moitinho-Silva, L., Brümmer, F., Cannistraci, C. V., Ravasi, T., Hentschel, U., 2014. GeoChip-based insights into the microbial functional gene repertoire of marine sponges (high microbial abundance, low microbial abundance) and seawater. FEMS Microbiology Ecology 90, 832–843. doi:10.1111/1574-6941.12441

Bellemain, E., Carlsen, T., Brochmann, C., Coissac, E., Taberlet, P., Kauserud, H., 2010. ITS as an environmental DNA barcode for fungi: an in silico approach reveals potential PCR biases. BMC microbiology 10, 189. doi:10.1186/1471-2180-10-189

Bellemain, E., Davey, M.L., Kauserud, H., Epp, L.S., Boessenkool, S., Coissac, E., Geml, J., Edwards, M., Willerslev, E., Gussarova, G., Taberlet, P., Haile, J., Brochmann, C., 2013. Fungal palaeodiversity revealed using high-throughput metabarcoding of ancient DNA from arctic permafrost. Environmental microbiology 15, 1176–89. doi:10.1111/1462-2920.12020

Benson, D.A., Cavanaugh, M., Clark, K., Karsch-Mizrachi, I., Lipman, D.J., Ostell, J., Sayers, E.W., 2013. GenBank. Nucleic Acids Research 41. doi:10.1093/nar/gks1195

Benson, D.A., Cavanaugh, M., Clark, K., Karsch-Mizrachi, I., Ostell, J., Pruitt, K.D., Sayers, E.W., 2018. GenBank. Nucleic Acids Research 46, D41–D47. doi:10.1093/nar/gkx1094

Berke, S.K., 2010. Functional groups of ecosystem engineers: A proposed classification with comments on current issues. In: Integrative and Comparative Biology. pp. 147–157. doi:10.1093/icb/icq077

Berkes, F., Colding, J., Folke, C., 2000. Rediscovery of Traditional Ecological Knowledge as adaptive management. Ecological Applications 10, 1251–1262. doi:10.1890/1051-0761(2000)010[1251:ROTEKA]2.0.CO;2

Bezanilla, M., Manne, S., Laney, D.E., Lyubchenko, Y.L., Hansma, H.G., 1995. Adsorption of DNA to Mica, Silylated Mica, and Minerals: Characterization by Atomic Force Microscopy. Langmuir 11, 655–659. doi:10.1021/la00002a050

Bigelow, N.H., Edwards, M.E., 2001. A 14,000 yr paleoenvironmental record from Windmill Lake, central Alaska: Lateglacial and Holocene vegetation in the Alaska range. Quaternary Science Reviews 20, 203–215. doi:10.1016/S0277-3791(00)00122-0

Binford, L.R., 1981. Bones: Ancient Men, and Modern Myths. Academic Press, New York.

Bird, D.W., Bird, R.B., Parker, C.H., 2005. Aboriginal burning regimes and hunting strategies in Australia's Western Desert. Human Ecology 33, 443–464. doi:10.1007/s10745-005-5155-0

Birky, C.W., 2008. Uniparental inheritance of organelle genes. Current Biology 18, 692–695. doi:10.1016/j.cub.2008.06.049

Black, L.T., 1987. Whaling in the Aleutians. Études/Inuit/Studies 11, 7–50.

Bliege Bird, R., Bird, D.W., Codding, B.F., Parker, C.H., Jones, J.H., 2008. The "fire stick farming" hypothesis: Australian Aboriginal foraging strategies, biodiversity, and anthropogenic fire mosaics. Proceedings of the National Academy of Sciences of the United States of America 105, 14796–14801. doi:10.1073/pnas.0804757105

Blum, S.A.E., Lorenz, M.G., Wackernagel, W., 1997. Mechanism of retarded DNA degradation and prokaryotic origin of DNases in nonsterile soils. Systematic and Applied Microbiology 20, 513–521. doi:10.1016/S0723-2020(97)80021-5

Bocherens, H., 2015. Isotopic tracking of large carnivore palaeoecology in the mammoth steppe. Quaternary Science Reviews 117, 42–71. doi:10.1016/j.quascirev.2015.03.018

Boivin, N.L., Zeder, M.A., Fuller, D.Q., Crowther, A., Larson, G., Erlandson, J.M., Denham, T., Petraglia, M.D., 2016. Ecological consequences of human niche construction: Examining long-term anthropogenic shaping of global species distributions. Proceedings of the National Academy of Sciences 113, 6388–6396. doi:10.1073/pnas.1525200113

Bond, W.J., Keeley, J.E., 2005. Fire as a global "herbivore": The ecology and evolution of flammable ecosystems. Trends in Ecology and Evolution 20, 387–394. doi:10.1016/j.tree.2005.04.025

Bonduriansky, R., 2012. Rethinking heredity, again. Trends in Ecology and Evolution 27, 330–336. doi:10.1016/j.tree.2012.02.003

Bonduriansky, R., Day, T., 2009. Nongenetic inheritance and its evolutionary implications. Annual Review of Ecology, Evolution, and Systematics 40, 103–125. doi:10.1146/annurev.ecolsys.39.110707.173441

Bonhommeau, S., Dubroca, L., Pape, O. Le, Barde, J., Kaplan, D.M., Chassot, E., Nieblas, A.E., 2013. Eating up the world's food web and the human trophic level. Proceedings of the National Academy of Sciences of the United States of America 110, 20617–20620. doi:10.1073/pnas.1305827110

Boom, R., Sol, C.J., Salimans, M.M., Jansen, C.L., Wertheim-Van Dillen, P.M., Noordaa, J. van der, 1990. Rapid and simple method for purification of nucleic acids. J.Clin.Microbiol. 28, 495–503. doi:10.1556/AMicr.58.2011.1.7

Bos, K.I., Schuenemann, V.J., Golding, G.B., Burbano, H. a., Waglechner, N., Coombes, B.K., McPhee, J.B., N.DeWitte, S., Meyer, M., Schmedes, S., Wood, J., Earn, D.J.D., Herring, D.A., Bauer, P., Poinar, H.N., Krause, J., 2011. A draft genome of Yersinia pestis from victims of the Black Death. Nature 480, 278–278. doi:10.1038/nature10675

Boulanger, M.T., Lyman, R.L., 2013. Northeastern North American Pleistocene megafauna chronologically overlapped minimally with Paleoindians. Quaternary Science Reviews 85, 35–46. doi:10.1016/j.quascirev.2013.11.024

Bourgeon, L., 2015. Bluefish Cave II (Yukon Territory , Canada): Taphonomic Study of a Bone Assemblage. PaleoAmerica 1, 105–108. doi:10.1179/2055556314Z.0000000001

Bourgeon, L., Burke, A., Higham, T., 2017. Earliest human presence in North America dated to the last glacial maximum: New radiocarbon dates from Bluefish Caves, Canada. PLoS ONE 12, e0169486. doi:10.1371/journal.pone.0169486

Bowman, D.M.J.S., Haberle, S.G., 2010. Paradise burnt: How colonizing humans transform landscapes with fire. Proceedings of the National Academy of Sciences of the United States of America 107, 21234–21235. doi:10.1073/pnas.1016393108

Bowman, D.M.J.S., Balch, J., Artaxo, P., Bond, W.J., Cochrane, M.A., D'Antonio, C.M., Defries, R., Johnston, F.H., Keeley, J.E., Krawchuk, M.A., Kull, C.A., Mack, M., Moritz, M.A., Pyne, S., Roos, C.I., Scott, A.C., Sodhi, N.S., Swetnam, T.W., 2011. The human dimension of fire regimes on Earth. Journal of Biogeography 38, 2223–2236. doi:10.1111/j.1365-2699.2011.02595.x

Bowman, D.M.J.S., Perry, G.L.W., Higgins, S.I., Johnson, C.N., Fuhlendorf, S.D., Murphy, B.P., 2016. Pyrodiversity is the coupling of biodiversity and fire regimes in food-webs. Philosophical transactions of the Royal Society of London. Series B, Biological sciences 371, 20150169. doi:10.1098/rstb.2015.0169

Boyd, R., Richerson, P.J., 1982. Cultural transmission and the evolution of cooperative behavior. Human Ecology 10, 325–351. doi:10.1007/BF01531189

Boyer, F., Mercier, C., Bonin, A., Bras, Y. Le, Taberlet, P., Coissac, E., 2016. obitools: A unix-inspired software package for DNA metabarcoding. Molecular Ecology Resources 16, 176–182. doi:10.1111/1755-0998.12428

Bradshaw, R.H.W., 1981. Modern Pollen-Representation Factors for Woods in South-East England. The Journal of Ecology 69, 45. doi:10.2307/2259815

Bradshaw, R.H.W., Hannon, G.E., Lister, A.M., 2003. A long-term perspective on ungulate-vegetation interactions. Forest Ecology and Management 181, 267–280. doi:10.1016/S0378-1127(03)00138-5

Braje, T.J., Erlandson, J.M., 2013. Human acceleration of animal and plant extinctions: A late pleistocene, holocene, and anthropocene continuum. Anthropocene 4, 14–23. doi:10.1016/j.ancene.2013.08.003

Brault, M.O., Mysak, L.A., Matthews, H.D., Simmons, C.T., 2013. Assessing the impact of late Pleistocene megafaunal extinctions on global vegetation and climate. Climate of the Past 9, 1761–1771. doi:10.5194/cp-9-1761-2013

Briggs, A.W., Stenzel, U., Meyer, M., Krause, J., Kircher, M., Pääbo, S., 2009. Removal of deaminated cytosines and detection of in vivo methylation in ancient DNA. Nucleic Acids Research 38, 1–12. doi:10.1093/nar/gkp1163

Briggs, D.E.G., Summons, R.E., 2014. Ancient biomolecules: Their origins, fossilization, and role in revealing the history of life. BioEssays 36, 482–490. doi:10.1002/bies.201400010

Brown, T.A., Barnes, I.M., 2015. The current and future applications of ancient DNA in Quaternary science. Journal of Quaternary Science 30, 144–153. doi:10.1002/jqs.2770

Bryant, J.P., Kuropat, P.J., 1980. Selection of Winter Forage by Subarctic Browsing Vertebrates: The Role of Plant Chemistry. Annual Review of Ecology and Systematics 11, 261–285. doi:10.1146/annurev.es.11.110180.001401

Bunbury, J., Gajewski, K., 2009a. Postglacial climates inferred from a lake at treeline, southwest Yukon Territory, Canada. Quaternary Science Reviews 28, 354–369.

Bunbury, J., Gajewski, K., 2009b. Postglacial climates inferred from a lake at treeline, southwest Yukon Territory, Canada. Quaternary Science Reviews 28, 354–369. doi:10.1016/j.quascirev.2008.10.007

Burney, D.A., Robinson, G.S., Burney, L.P., 2003. Sporormiella and the late holocene extinctions in Madagascar. Proceedings of the National Academy of Sciences of the United States of America 100, 10800–10805. doi:10.1073/pnas.1534700100

Bush, M.B., Mcmichael, C.H., Piperno, D.R., Silman, M.R., Barlow, J., Peres, C.A., Power, M., Palace, M.W., 2015. Anthropogenic influence on Amazonian forests in pre-history: An ecological perspective. Journal of Biogeography 42, 2277–2288. doi:10.1111/jbi.12638

Buvit, I., Terry, K., 2015. Last Glacial Maximum Human Occupation of the Transbaikal , Siberia. PaleoAmerica 1, 374–376. doi:10.1179/2055557115Y.0000000007

Buvit, I., Terry, K., 2016. Outside Beringia: Why the Northeast Asian Upper Paleolithic Record Does Not Support a Long Standstill Model. PaleoAmerica 5563, 1–5. doi:10.1080/20555563.2016.1238277

Cai, P., Huang, Q., Zhang, X., Chen, H., 2006. Adsorption of DNA on clay minerals and various colloidal particles from an Alfisol. Soil Biology and Biochemistry 38, 471–476. doi:10.1016/j.soilbio.2005.05.019

Camacho, C., Coulouris, G., Avagyan, V., Ma, N., Papadopoulos, J., Bealer, K., Madden, T.L., 2009. BLAST+: Architecture and applications. BMC Bioinformatics 10, 1–9. doi:10.1186/1471-2105-10-421

Campos, P.F., Willerslev, E., Sher, A., Orlando, L., Axelsson, E., Tikhonov, A., Aaris-Sørensen, K., Greenwood, A.D., Kahlke, R.-D., Kosintsev, P., Krakhmalnaya, T., Kuznetsova, T., Lemey, P., MacPhee, R., Norris, C. a, Shepherd, K., Suchard, M. a, Zazula, G.D., Shapiro, B., Gilbert, M.T.P., 2010. Ancient DNA analyses exclude humans as the driving force behind late Pleistocene musk ox (Ovibos moschatus) population dynamics. Proceedings of the National Academy of Sciences of the United States of America 107, 5675–5680. doi:10.1073/pnas.0907189107

Cappellini, E., Prohaska, A., Racimo, F., Welker, F., Pedersen, M.W., Allentoft, M.E., Barros Damgaard, P. De, Gutenbrunner, P., Dunne, J., Hammann, S., Roffet-Salque, M., Ilardo, M., Moreno-Mayar, J.V., Wang, Y., Sikora, M., Vinner, L., Cox, J., Evershed, R.P., Willerslev, E., 2018. Ancient Biomolecules and Evolutionary Inference. Annual Review of Biochemistry 87, 1029–1060. doi:10.1146/annurev-biochem-062917-012002

Carey, J., 2016. Rewilding. Proceedings of the National Academy of Sciences 113, 806–808. doi:10.1073/pnas.1522151112

Carlson, P.C., Tanner, G.W., Wood, J.M., Humphrey, S.R., 1999. Fire in key deer habitat improves browse, prevents succession, and preserves endemic herbs. The Journal of Wildlife Management 57, 914–928. doi:10.1016/0006-3207(94)90455-3

Carothers, T., O'Donohue, A., 2019. Democracies Divided: The Global Challenge of Political Polarization. Brookings Institution Press, Washington, D.C.

Carpenter, M.L., Buenrostro, J.D., Valdiosera, C., Schroeder, H., Allentoft, M.E., Sikora, M., Rasmussen, M., Gravel, S., Guillén, S., Nekhrizov, G., Leshtakov, K., Dimitrova, D., Theodossiev, N., Pettener, D., Luiselli, D., Sandoval, K., Moreno-Estrada, A., Li, Y., Wang, J., Gilbert, M.T.P., Willerslev, E., Greenleaf, W.J., Bustamante, C.D., 2013. Pulling out the 1%: Whole-Genome capture for the targeted enrichment of ancient dna sequencing libraries. American Journal of Human Genetics 93, 852–864. doi:10.1016/j.ajhg.2013.10.002

Carroll, L., 1871. Through the Looking-Glass. Macmillan, United Kingdom.

CBOL Plant Working Group, 2009. A DNA barcode for land plants. Proceedings of the National Academy of Sciences of the United States of America 106, 12794–7. doi:10.1073/pnas.0905845106

Ceballos, G., Ehrlich, P.R., Barnosky, A.D., García, A., Pringle, R.M., Palmer, T.M., 2015. Accelerated modern human-induced species losses: Entering the sixth mass extinction. Science Advances 1, 9–13. doi:10.1126/sciadv.1400253

Cerling, T.E., Wynn, J.G., Andanje, S.A., Bird, M.I., Korir, D.K., Levin, N.E., MacE, W., MacHaria, A.N., Quade, J., Remien, C.H., 2011. Woody cover and hominin environments in the past 6-million years. Nature 476, 51–56. doi:10.1038/nature10306

Chang, D., Knapp, M., Enk, J., Lippold, S., Kircher, M., Lister, A., Macphee, R.D.E., Widga, C., Czechowski, P., Sommer, R., Hodges, E., Stümpel, N., Barnes, I., Dalén, L., Derevianko, A., Germonpré, M., Hillebrand-Voiculescu, A., Constantin, S., Kuznetsova, T., Mol, D., Rathgeber, T., Rosendahl, W., Tikhonov, A.N., Willerslev, E., Hannon, G., Lalueza-Fox, C., Joger, U., Poinar, H., Hofreiter, M., Shapiro, B., 2017. The evolutionary and phylogeographic history of woolly mammoths: A comprehensive mitogenomic analysis. Scientific Reports 7, 1–10. doi:10.1038/srep44585

Chen, C., 2007. Techno-Typological Comparison of Microblade Cores from East Asia and North America. In: Kuzmin, Y. V., Keats, S.G., Shen, C. (Eds.), Origin and Spread of Microblade Technology in Northern Asia and North America.

Archaeology Press, Simon Fraser University, Burnaby, B.C., pp. 7–38.

Chen, J., Tauer, C.G., Huang, Y., 2002. Paternal chloroplast inheritance patterns in pine hybrids detected with trnL-trnF intergenic region polymorphism. Theoretical and Applied Genetics 104, 1307–1311. doi:10.1007/s00122-002-0893-5

Chen, Y., Qin, N., Guo, J., Qian, G., Fang, D., Shi, D., Xu, M., Yang, F., He, Z., Nostrand, J.D. Van, Yuan, T., Deng, Y., Zhou, J., Li, L., 2014. Functional gene arrays-based analysis of fecal microbiomes in patients with liver cirrhosis. BMC genomics 15, 753. doi:10.1186/1471-2164-15-753

Cinq-Mars, J., 1979. Bluefish Cave I: A late Pleistocene Eastern Beringian Cave Deposit in the Northern Yukon. Canadian Journal of Archaeology 3, 1–31.

Cinq-Mars, J., Morlan, R., 1999. Bluefish caves and old crow basin: a new rapport. Ice Age Peoples of North America. Environments, Origins, and Adaptations of the First Americans 200–212.

Clark, D., 2001. Microblade-culture systematics in the far interior Northwest. Arctic anthropology 38, 64–80.

Clark, D.W., 1983. Is There a Northern Cordilleran Tradition ? Canadian Journal of Archaeology 7, 23–48.

Clark, D.W., 1991. Western subarctic prehistory. Canadian Museum of Civilization, Hull, Quebec.

Clark, P.. U., Mix, A.. C., 2002. Ice sheets and sea level of the Last Glacial Maximum. Quaternary Science Reviews 21, 1–7.

Clark, P.U., 2009a. The Last Glacial Maximum. Science 325, 710–714. doi:10.1126/science.1172873

Clark, P.U., 2009b. The Last Glacial Maximum. Science 325, 710–714. doi:10.1126/science.1172873

Cleaves, H.J., Crapster-Pregont, E., Jonsson, C.M., Jonsson, C.L., Sverjensky, D.A., Hazen, R.A., 2011. The adsorption of short single-stranded DNA oligomers to mineral surfaces. Chemosphere 83, 1560–1567. doi:10.1016/j.chemosphere.2011.01.023

Clinchy, M., Zanette, L.Y., Roberts, D., Suraci, J.P., Buesching, C.D., Newman, C., Macdonald, D.W., 2016. Fear of the human “super predator” far exceeds the fear of large carnivores in a model mesocarnivore. Behavioral Ecology 27, arw117. doi:10.1093/beheco/arw117

Cohen, K.M., Gibbard, P.L., 2010. Global chronostratigraphical correlation table for the last 2 . 7 million years , v . 2010. Journal of Quaternary Science 2, 7. doi:10.1029/2001PA000725.Ding

Coles, B., 2006. Beavers in Britian’s Past. Oxbow Books, Oxford.

Comandini, O., Rinaldi, A.C., 2004. Tracing megafaunal extinctions with dung fungal spores. Mycologist 18, 140–142. doi:DOI: 10.1017/S0269915XO400401X

Conroy, K.J., Baker, A.G., Jones, V.J., Hardenbroek, M. van, Hopla, E.J., Collier, R., Lister, A.M., Edwards, M.E., 2020. Tracking late-Quaternary extinctions in interior Alaska using megaherbivore bone remains and dung fungal spores. Quaternary Research 1–12. doi:10.1017/qua.2020.19

Cook, J.P., 1969. The Early Prehistory of Healy Lake, Alaska. University of Wisconsin, Madison.

Cook, J.P., 1996. Healy Lake. In: West, F.H. (Ed.), American Beginnings: The Prehistory and Paleoecology of Beringia. University of Chicago Press, Chicago, pp. 323–327.

Cooley, D., Clarke, H., Graupe, S., Landry-Cuerrier, M., Lantz, T., Milligan, H., Pretzlaw, T., Larocque, G., Humphries, M.M., 2019. The seasonality of a migratory moose population in northern Yukon. Alces 55, 105–130.

Cooper, A., Poinar, H., 2000. Ancient DNA: Do It Right or Not At All. Science 289, 1139. doi:10.1126/science.289.5482.1139b

Crawford, D.H., 2007. Deadly companions: How microbes shaped our history. Oxford University Press, Oxford, U.K.

Creanza, N., Kolodny, O., Feldman, M.W., 2017. Cultural evolutionary theory: How culture evolves and why it matters. Proceedings of the National Academy of Sciences of the United States of America 114, 7782–7789. doi:10.1073/pnas.1620732114

Crecchio, C., Stotzky, G., 1998. Binding of DNA on humic acids: Effect of transformation of Bacillus subtilis and resistance to DNase. Soil Biology and Biochemistry 30, 1061–1067.

Cribdon, B., Ware, R., Smith, O., Gaffney, V., Allaby, R.G., 2020. PIA: More Accurate Taxonomic Assignment of Metagenomic Data Demonstrated on sedaDNA From the North Sea. Frontiers in Ecology and Evolution 8, 1–12. doi:10.3389/fevo.2020.00084

Cristescu, M.E., Hebert, P.D.N., 2018. Uses and misuses of environmental DNA in biodiversity science and conservation. Annual Review of Ecology, Evolution, and Systematics 49, 209–230. doi:10.1146/annurev-ecolsys-110617-062306

Croft, D.A., Su, D.F., Simpson, S.W. (Eds.), 2018. Methods in Paleoecology: Reconstructing Cenozoic Terrestrial Environments and Ecological Communities. Springer, Cham, Switzerland.

Cruikshank, J., 2005. Do Glaciers Listen? Local Knowledge, Colonial Encounters, and Social Imagination. University of British Columbia Press, Vancouver.

Crumley, C.L., 1987. Historical Ecology. In: Crumley, C.L., Marquardt, W.H. (Eds.), Regional Dynamics: Burgundian Landscapes in Historical Perspective. Academic Press, Inc., San Diego, California, pp. 237–264.

Crumley, C.L., 2006. Historical Ecology: Integrated Thinking at Multiple Temporal and Spatial Scales. In: Hornborg, A., Crumley, C.L. (Eds.), The World System and the Earth System: Global Socioenvironmental Change and Sustainability Since the Neolithic. Left Coast Press, Walnut Creek, CA, pp. 15–28.

Crutzen, P.J., Stoermer, E.F., 2000. The "Anthropocene." IGBP Global Change Newsletter 41, 17–18.

Cuyler, C., Rowell, J., Adamczewski, J., Anderson, M., Blake, J., Bretten, T., Brodeur, V., Campbell, M., Checkley, S.L., Cluff, H.D., Côté, S.D., Davison, T., Dumond, M., Ford, B., Gruzdev, A., Gunn, A., Jones, P., Kutz, S., Leclerc, L.M., Mallory, C., Mavrot, F., Mosbacher, J.B., Okhlopkov, I.M., Reynolds, P., Schmidt, N.M., Sipko, T., Suitor, M., Tomaselli, M., Ytrehus, B., 2020. Muskox status, recent variation, and uncertain future. Ambio 49, 805–819. doi:10.1007/s13280-019-01205-x

Cwynar, L.C., 1988. Late Quaternary vegetation history of Kettlehole Pond, southwestern Yukon. Canadian Journal of Forest Research 18, 1270–1279.

D'Costa, V.M., King, C.E., Kalan, L., Morar, M., Sung, W.W.L., Schwarz, C., Froese, D., Zazula, G., Calmels, F., Debruyne, R., Golding, G.B., Poinar, H.N., Wright, G.D., 2011. Antibiotic resistance is ancient. Nature 477, 457–61. doi:10.1038/nature10388

Dabney, J., Meyer, M., Pääbo, S., 2013a. Ancient DNA damage. Cold Spring Harbor Perspectives in Biology 5. doi:10.1101/cshperspect.a012567

Dabney, J., Knapp, M., Glocke, I., Gansauge, M.-T., Weihmann, A., Nickel, B., Valdiosera, C., Garcia, N., Paabo, S., Arsuaga, J.-L., Meyer, M., 2013b. Complete mitochondrial genome sequence of a Middle Pleistocene cave bear reconstructed from ultrashort DNA fragments. Proceedings of the National Academy of Sciences 110, 15758–15763. doi:10.1073/pnas.1314445110

Dahl-Jensen, D., Albert, M.R., Aldahan, a., Azuma, N., Balslev-Clausen, D., Baumgartner, M., Berggren, a.-M., Bigler, M., Binder, T., Blunier, T., Bourgeois, J.C., Brook, E.J., Buchardt, S.L., Buizert, C., Capron, E., Chappellaz, J., Chung, J., Clausen, H.B., Cvijanovic, I., Davies, S.M., Ditlevsen, P., Eicher, O., Fischer, H., Fisher, D. a., Fleet, L.G., Gfeller, G., Gkinis, V., Gogineni, S., Goto-Azuma, K., Grinsted, a., Gudlaugsdottir, H., Guillevic, M., Hansen, S.B., Hansson, M., Hirabayashi, M., Hong, S., Hur, S.D., Huybrechts, P., Hvidberg, C.S., Iizuka, Y., Jenk, T., Johnsen, S.J., Jones, T.R., Jouzel, J., Karlsson, N.B., Kawamura, K., Keegan, K., Kettner, E., Kipfstuhl, S., Kjær, H. a., Koutnik, M., Kuramoto, T., Köhler, P., Laepple, T., Landais, a., Langen, P.L., Larsen, L.B., Leuenberger, D., Leuenberger, M., Leuschen, C., Li, J., Lipenkov, V., Martinerie, P., Maselli, O.J., Masson-Delmotte, V., McConnell, J.R., Miller, H., Mini, O., Miyamoto, a., Montagnat-Rentier, M., Mulvaney, R., Muscheler, R., Orsi, a. J., Paden, J., Panton, C., Pattyn, F., Petit, J.-R., Pol, K., Popp, T., Possnert, G., Prié, F., Prokopiou, M., Quiquet, a., Rasmussen, S.O., Raynaud, D., Ren, J., Reutenauer, C., Ritz, C., Röckmann, T., Rosen, J.L., Rubino, M., Rybak, O., Samyn, D., Sapart, C.J., Schilt, a., Schmidt, a. M.Z., Schwander, J., Schüpbach, S., Seierstad, I., Severinghaus, J.P., Sheldon, S., Simonsen, S.B., Sjolte, J., Solgaard, a. M., Sowers, T., Sperlich, P., Steen-Larsen, H.C., Steffen, K., Steffensen, J.P., Steinhage, D., Stocker, T.F., Stowasser, C., Sturevik, a. S., Sturges, W.T., Sveinbjörnsdottir, a., Svensson, a., Tison, J.-L., Uetake, J., Vallelonga, P., Wal, R.S.W. van de, Wel, G. van der, Vaughn, B.H., Vinther, B., Waddington, E., Wegner, a., Weikusat, I., White,

J.W.C., Wilhelms, F., Winstrup, M., Witrant, E., Wolff, E.W., Xiao, C., Zheng, J., 2013. Eemian interglacial reconstructed from a Greenland folded ice core. Nature 493, 489–494. doi:10.1038/nature11789

Danchin, É., 2013. Avatars of information: Towards an inclusive evolutionary synthesis. Trends in Ecology and Evolution 28, 351–358. doi:10.1016/j.tree.2013.02.010

Darimont, C.T., Fox, C.H., Bryan, H.M., Reimchen, T.E., 2015. The unique ecology of human predators. Science 349, 858–860.

Daulton, T.L., Amari, S., Scott, A.C., Hardiman, M., Pinter, N., Anderson, R.S., 2017. Comprehensive analysis of nanodiamond evidence relating to the Younger Dryas Impact Hypothesis. Journal of Quaternary Science 32, 7–34. doi:10.1002/jqs.2892

Davic, R.D., 2002. Herbivores as keystone predators. Conservation Ecology 6, r8.

Davic, R.D., 2003. Linking Keystone Species and Functional Groups : A New Operational Definition of the Keystone Species Concept. Conservation Ecology 7, r11. doi:10.1161/STROKEAHA.108.536094

Davis, R.S., Ranov, V.A., 1999. Recent Work on the Paleolithic of Central Asia. Evolutionary Anthropology 8, 186–193. doi:10.1002/(sici)1520-6505(1999)8:5<186::aid-evan6>3.0.co;2-r

Dawkins, R., 1990. The extended phenotype: The long reach of the gene. Oxford University Press, Oxford.

Denevan, W.M., 1992. The Pristine Myth: The Landscape of the Americas in 1492. Annals of the Association of American Geographers 82, 369–385.

Diekert, F.K., Richter, A., Rivrud, I.M., Mysterud, A., Clark, W.C., 2016. How constraints affect the hunter's decision to shoot a deer. Proceedings of the National Academy of Sciences of the United States of America 113, 14450–14455. doi:10.1073/pnas.1607685113

Dietrich, O., Köksal-Schmidt, Ç., Notroff, J., Schmidt, K., 2013. Establishing a Radiocarbon Sequence for Göbekli Tepe. State of Research and New Data. Neo-Lithics 1, 36–41.

Dincauze, D.F., 2000. Environmental Archaeology: Principles and Practice. Cambridge University Press, Cambridge.

Dirzo, R., Young, H.S., Galetti, M., Ceballos, G., Isaac, N.J.B., Collen, B., 2014. Defaunation in the Anthropocene. Science 345, 401–406. doi:10.1126/science.1251817

Dods, R.R., 2002. The death of Smokey Bear: The ecodisaster myth and forest management practices in prehistoric North America. World Archaeology 33, 475–487. doi:10.1080/00438240120107486

Doi, H., Uchii, K., Takahara, T., Matsuhashi, S., Yamanaka, H., Minamoto, T., 2015. Use of droplet digital PCR for estimation of fish abundance and biomass in environmental DNA surveys. PLoS ONE 10, 1–11. doi:10.1371/journal.pone.0122763

Doi, H., Inui, R., Akamatsu, Y., Kanno, K., Yamanaka, H., Takahara, T., Minamoto, T., 2017. Environmental DNA analysis for estimating the abundance and biomass of stream fish. Freshwater Biology 62, 30–39. doi:10.1111/fwb.12846

Dolukhanov, P.M., Shukurov, A.M., Tarasov, P.E., Zaitseva, G.I., 2002. Colonization of Northern Eurasia by modern humans: Radiocarbon chronology and environment. Journal of Archaeological Science 29, 593–606. doi:10.1006/jasc.2001.0753

Dong, D., Yan, A., Liu, H., Zhang, X., Xu, Y., 2006. Removal of humic substances from soil DNA using aluminium sulfate. Journal of Microbiological Methods 66, 217–222. doi:10.1016/j.mimet.2005.11.010

Doughty, C.E., Wolf, A., Malhi, Y., 2013. The legacy of the Pleistocene megafauna extinctions on nutrient availability in Amazonia. Nature Geoscience 6, 761–764. doi:10.1038/ngeo1895

Doughty, C.E., Roman, J., Faurby, S., Wolf, A., Haque, A., Bakker, E.S., Malhi, Y., Dunning, J.B., Svenning, J.-C., 2015. Global nutrient transport in a world of giants. Proceedings Of The National Academy Of Sciences 113, 1–6. doi:10.1073/pnas.1502549112

Doughty, C.E., Faurby, S., Svenning, J.C., 2016. The impact of the megafauna extinctions on savanna woody cover in South America. Ecography 39, 213–222. doi:10.1111/ecog.01593

Driver, J., 2001a. A reply to Thomas. In: Albarella, U. (Ed.), Environmental Archaeology: Meaning and Purpose. Kluwer Academic Publishers, Dordrecht, The Netherlands, pp. 59–60.

Driver, J., 2001b. Environmental archaeology is not human palaeoecology. In: Albarella, U. (Ed.), Environmental Archaeology: Meaning and Purpose. Kluwer Academic Publishers, Dordrecht, The Netherlands, pp. 43–54.

Drucker, D.G., Naito, Y.I., Péan, S., Prat, S., Crépin, L., Chikaraishi, Y., Ohkouchi, N., Puaud, S., Lázničková-Galetová, M., Patou-Mathis, M., Yanevich, A., Bocherens, H., 2017. Isotopic analyses suggest mammoth and plant in the diet of the oldest anatomically modern humans from far southeast Europe. Scientific Reports 7, 1–10. doi:10.1038/s41598-017-07065-3

Dumond, D.E., 2001. The Archaeology of eastern Beringia: Some contrasts and connections. Arctic Anthropology 38, 196–205. doi:10.2307/40316730

Dumond, D.E., 2011. Technology, typology, and subsitence: a partly contrarian look at the peopling of Beringia. In: Goebel, T., Buvit, I. (Eds.), From the Yenisei to the Yukon: Interpreting Lithic Assemblage Variability in Late Pleistocene/Early Holocene Beringia. Texas A&M University Press, College Station, pp. 345–361.

Dunnell, R.C., 1978. Style and Function : A Fundamental Dichotomy. American Antiquity 43, 192–202.

Dyke, A.S., 2004. An outline of the deglaciation of North America with emphasis on central and northern Canada. Developments in Quaternary Sciences 2, 373–424. doi:10.1016/S1571-0866(04)80209-4

Dyke, A.S., 2005. Late Quaternary Vegetation History of Northern North America Based on Pollen, Macrofossil, and Faunal Remains. Géographie physique et Quaternaire 59, 211. doi:10.7202/014755ar

Edgar, R.C., 2004. MUSCLE: Multiple sequence alignment with high accuracy and high throughput. Nucleic Acids Research 32, 1792–1797. doi:10.1093/nar/gkh340

Edwards, M., Franklin-Smith, L., Clarke, C., Baker, J., Hill, S., Gallagher, K., 2015. The role of fire in the mid-Holocene arrival and expansion of lodgepole pine (Pinus contorta var. latifolia Engelm. ex S. Watson) in Yukon, Canada. Holocene 25, 64–78. doi:10.1177/0959683614556389

Edwards, M.E., Alsos, I.G., Yoccoz, N., Coissac, E., Goslar, T., Gielly, L., Haile, J., Langdon, C.T., Tribsch, A., Binney, H.A., Stedingk, H. Von, Taberlet, P., 2018. Metabarcoding of modern soil DNA gives a highly local vegetation signal in Svalbard tundra. Holocene 28, 2006–2016. doi:10.1177/0959683618798095

Eerkens, J.W., Lipo, C.P., 2005. Cultural transmission, copying errors, and the generation of variation in material culture and the archaeological record. Journal of Anthropological Archaeology 24, 316–334. doi:10.1016/j.jaa.2005.08.001

Eisenhofer, R., Minich, J.J., Marotz, C., Cooper, A., Knight, R., Weyrich, L.S., 2019. Contamination in Low Microbial Biomass Microbiome Studies: Issues and Recommendations. Trends in Microbiology 27, 105–117. doi:10.1016/j.tim.2018.11.003

Elias, S.A., Crocker, B., 2008. The Bering Land Bridge: a moisture barrier to the dispersal of steppe-tundra biota? Quaternary Science Reviews 27, 2473–2483. doi:10.1016/j.quascirev.2008.09.011

Ellis, E.C., 2015. Ecology in an anthropogenic biosphere. Ecological Monographs 85, 287–331. doi:10.1890/14-2274.1

Emiliani, C., 1993. Calendar reform. Nature Correspondence 366, 716. doi:10.1038/366716a0

Enk, J., Rouillard, J.M., Poinar, H., 2013. Quantitative PCR as a predictor of aligned ancient DNA read counts following targeted enrichment. BioTechniques 55, 300–309. doi:10.2144/000114114

Enk, J., Devault, A., Widga, C., Saunders, J., Szpak, P., Southon, J., Rouillard, J.-M., Shapiro, B., Golding, G.B., Zazula, G., Froese, D., Fisher, D.C., Macphee, R.D.E., Poinar, H., 2016. Mammuthus population dynamics in Late Pleistocene North America: Divergence, Phylogeogrpaphy and Introgression. Frontiers in Ecology and Evolution 4, 1–13. doi:10.3389/fevo.2016.00042

Epp, L.S., Gussarova, G., Boessenkool, S., Olsen, J., Haile, J., Schrøder-Nielsen, A., Ludikova, A., Hassel, K., Stenøien, H.K., Funder, S., Willerslev, E., Kjær, K., Brochmann, C., 2015. Lake sediment multi-taxon DNA from North Greenland records early post-glacial appearance of vascular plants and accurately tracks environmental changes. Quaternary Science Reviews 117, 152–163. doi:10.1016/j.quascirev.2015.03.027

Erickson, C.L., 2008. Amazonia: The Historical Ecology of a Domesticated Landscape. In: Silverman, H., Isbell, W.H. (Eds.), The Handbook of South American Archaeology. Springer, New York, pp. 157–183.

Erkens, J.W., Bettinger, R.L., 2001. Techniques for assessing standardization in artifact assemblages: Can we scale material variablity? American Antiquity 66, 493–504.

Ermolova, N.M., 1978. Teriofauna doliny Angary v pozdem antropogene. Nauka, Novosibirsk.

Estes, J.A., Duggins, D.O., 1995. Sea Otters and Kelp Forests in Alaska: Generality and Variation in a Community Ecological Paradigm. Ecological Monographs 65, 75–100.

Estes, J.A., Burdin, A., Doak, D.F., 2015. Sea otters, kelp forests, and the extinction of Steller's sea cow. Proceedings of the National Academy of Sciences of the United States of America 201502552. doi:10.1073/pnas.1502552112

Estévez, J., 2004. Vanishing carnivores: What can the disappearance of large carnivores tell us about the Neanderthal world? International Journal of Osteoarchaeology 14, 190–200. doi:10.1002/oa.755

Faith, J.T., Surovell, T.A., 2009. Synchronous extinction of North America's Pleistocene mammals. Proceedings of the National Academy of Sciences of the United States of America 106, 20641–20645. doi:10.1073/pnas.0908153106

Feeney, J.C., 2016. Land Management Among Hunter-Gatherers: Questioning the Ubiquity Claims. Hunter/Gatherer 1.

Fenn, M., Huntington, T., McLaughlin, S., Eagar, C., Gomez, A., Cook, R.B., 2006. Status of soil acidification in North America. Journal of Forest Science 52, 3–13.

Fiedel, S., 2009. Sudden Deaths: The Chronology of Terminal Pleistocene Megafaunal Extinction. In: Haynes, G. (Ed.), American Megafaunal Extinctions at the End of the Pleistocene. Springer Netherlands, Dordrecht, pp. 21–37. doi:10.1007/978-1-4020-8793-6_2

Fiedel, S.J., 2018. The spore conundrum: Does a dung fungus decline signal humans' arrival in the Eastern United States? Quaternary International 446, 247–255. doi:10.1016/j.quaint.2015.11.130

Fiedel, S.J., Kuzmin, Y. V., 2007. Radiocarbon date frequency as an index of intensity of Paleolithic occupation of Siberia: Did humans react predictably to climate oscillations? Radiocarbon 49, 741–756. doi:10.1017/S0033822200042624

Firestone, R.B., West, a, Kennett, J.P., Becker, L., Bunch, T.E., Revay, Z.S., Schultz, P.H., Belgya, T., Kennett, D.J., Erlandson, J.M., Dickenson, O.J., Goodyear, a C., Harris, R.S., Howard, G. a, Kloosterman, J.B., Lechler, P., Mayewski, P. a, Montgomery, J., Poreda, R., Darrah, T., Hee, S.S.Q., Smith, a R., Stich, A., Topping, W., Wittke, J.H., Wolbach, W.S., 2007. Evidence for an extraterrestrial impact 12,900 years ago that contributed to the megafaunal extinctions and the Younger Dryas cooling. Proceedings of the National Academy of Sciences of the United States of America 104, 16016–16021. doi:10.1073/pnas.0706977104

Fisher, C., 2020. Maize Politics and Maya Farmers' Traditional Ecological Knowledge in Yucatán, 1450–1600. Human Ecology 48, 33–45. doi:10.1007/s10745-020-00134-8

Flenniken, J.J., 1987. The Paleolithic Dyuktai Pressure Blade Technique of Siberia. Arctic anthropology 24, 117–132. doi:10.2307/40316147

Foley, S.F., Gronenborn, D., Andreae, M.O., Kadereit, J.W., Esper, J., Scholz, D., Pöschl, U., Jacob, D.E., Schöne, B.R., Schreg, R., Vött, A., Jordan, D., Lelieveld, J., Weller, C.G., Alt, K.W., Gaudzinski-Windheuser, S., Bruhn, K.C., Tost, H., Sirocko, F., Crutzen, P.J., 2013. The Palaeoanthropocene - The beginnings of anthropogenic environmental change. Anthropocene. doi:10.1016/j.ancene.2013.11.002

Fowler, C.S., Turner, N.J., 1999. Ecological/cosmological knowledge and land management among hunter/gatherers. In: Lee, R.B., Daly, R. (Eds.), The Cambridge Encyclopedia of Hunters and Gatherers. Cambridge University Press, Cambridge, UK, pp. 419–425.

Fox-Dobbs, K., Leonard, J.A., Koch, P.L., 2008. Pleistocene megafauna from eastern Beringia: Paleoecological and paleoenvironmental interpretations of stable carbon and nitrogen isotope and radiocarbon records. Palaeogeography, Palaeoclimatology, Palaeoecology 261, 30–46. doi:10.1016/j.palaeo.2007.12.011

Frison, G.C., 1978. Prehistoric Hunters of the High Plains. Academic Press, New York.

Froese, D., Westgate, J., Preece, S., Storer, J., 2002. Age and significance of the Late Pleistocene Dawson tephra in eastern Beringia. Quaternary Science Reviews 21, 2137–2142. doi:10.1016/S0277-3791(02)00038-0

Froese, D., Stiller, M., Heintzman, P.D., Reyes, A. V, Zazula, G.D., Soares, A.E.R., Meyer, M., Hall, E., Jensen, B.J.L., Arnold, L.J., Macphee, R.D.E., Shapiro, B., Grayson, D.K., 2017. Fossil and genomic evidence constrains the timing of bison arrival in North America. doi:10.1073/pnas.1620754114

Froese, D.G., Zazula, G.D., Reyes, A. V., 2006. Seasonality of the late Pleistocene Dawson tephra and exceptional preservation of a buried riparian surface in central Yukon Territory, Canada. Quaternary Science Reviews 25, 1542–1551. doi:10.1016/j.quascirev.2006.01.028

Froese, D.G., Zazula, G.D., Westgate, J.A., Preece, S.J., Sanborn, P.T., Reyes, A. V., Pearce, N.J.G., 2009. The Klondike goldfields and Pleistocene environments of Beringia. GSA Today 19, 4–10. doi:10.1130/GSATG54A.1

Fry, B., 2006. Stable Isotope Ecology, Encyclopedia of Ecology. Springer, New York.

Gajewski, K., Bunbury, J., Vetter, M., Kroeker, N., Khan, A.H., 2014. Paleoenvironmental studies in Southwestern Yukon. Arctic 67, 58–70. doi:10.14430/arctic4349

Galetti, M., Mole, M., Jordano, P., Pires, M.M., Paulo, R., Pape, T., Nichols, E., Hansen, D., Olesen, J.M., Munk, M., Mattos, J.S. De, Schweiger, A.H., Johnson, C.N., Marquis, R.J., 2017. Ecological and evolutionary legacy of megafauna extinctions. doi:10.1111/brv.12374

Gardner, C., Berger, M., Taras, M., 2007. Habitat assessment of potential wood bison relocation sites in Alaska. Arctic 1–30.

Gardner, C.M., Gunsch, C.K., 2017. Adsorption capacity of multiple DNA sources to clay minerals and environmental soil matrices less than previously estimated. Chemosphere 175, 45–51. doi:10.1016/j.chemosphere.2017.02.030

Garland, S., Baker, A., Phillott, A.D., Skerratt, L.F., 2010. BSA reduces inhibition in a TaqMan® assay for the detection of Batrachochytrium dendrobatidis. Diseases of Aquatic Organisms 92, 113–116. doi:10.3354/dao02053

Geel, B. van, Aptroot, A., Baittinger, C., Birks, H.H., Bull, I.D., Cross, H.B., Evershed, R.P., Gravendeel, B., Kompanje, E.J.O., Kuperus, P., Mol, D., Nierop, K.G.J., Pals, J.P., Tikhonov, A.N., Reenen, G. van, Tienderen, P.H. van, 2008. The ecological implications of a Yakutian mammoth's last meal. Quaternary Research 69, 361–376. doi:10.1016/j.yqres.2008.02.004

Geel, B. van, Fisher, D.C., Rountrey, A.N., Arkel, J. van, Duivenvoorden, J.F., Nieman, A.M., Reenen, G.B.A. van, Tikhonov, A.N., Buigues, B., Gravendeel, B., 2011. Palaeo-environmental and dietary analysis of intestinal contents of a mammoth calf (Yamal Peninsula, northwest Siberia). Quaternary Science Reviews 30, 3935–3946. doi:10.1016/j.quascirev.2011.10.009

Geel, B. Van, Fisher, D.C., Rountrey, A.N., Arkel, J. van, Duivenvoorden, J.F., Nieman, A.M., Reenen, G.B.A. van, Tikhonov, A.N., Buigues, B., Gravendeel, B., 2011. Palaeo-environmental and dietary analysis of intestinal contents of a mammoth calf (Yamal Peninsula, northwest Siberia). Quaternary Science Reviews 30, 3935–3946. doi:10.1016/j.quascirev.2011.10.009

Giguet-Covex, C., Pansu, J., Arnaud, F., Rey, P.-J., Griggo, C., Gielly, L., Domaizon, I., Coissac, E., David, F., Choler, P., Poulenard, J., Taberlet, P., 2014. Long livestock farming history and human landscape shaping revealed by lake sediment DNA. Nature communications 5, 3211. doi:10.1038/ncomms4211

Gilbert, M.T.P., Binladen, J., Miller, W., Wiuf, C., Willerslev, E., Poinar, H., Carlson, J.E., Leebens-Mack, J.H., Schuster, S.C., 2007a. Recharacterization of ancient DNA miscoding lesions: Insights in the era of sequencing-by-synthesis. Nucleic Acids Research 35, 1–10. doi:10.1093/nar/gkl483

Gilbert, M.T.P., Tomsho, L.P., Rendulic, S., Packard, M., Drautz, D.I., Sher, A., Tikhonov, A., Dalén, L., Kuznetsova, T., Kosintsev, P., Campos, P.F., Higham, T., Collins, M.J., Wilson, A.S., Shidlovskiy, F., Buigues, B., Ericson, P.G.P., Germonpré, M., Götherström, A., Iacumin, P., Nikolaev, V., Nowak-Kemp, M., Willerslev, E., Knight, J.R., Irzyk, G.P., Perbost, C.S., Fredrikson, K.M., Harkins, T.T., Sheridan, S., Miller, W., Schuster, S.C., 2007b. Whole-genome shotgun sequencing of mitochondria from ancient hair shafts. Science (New York, N.Y.) 317, 1927–1930. doi:10.1126/science.1146971

Gill, J.L., 2014a. Ecological impacts of the late Quaternary megaherbivore extinctions. New Phytologist 201, 1163–1169. doi:10.1111/nph.12576

Gill, J.L., 2014b. Ecological impacts of the late Quaternary megaherbivore extinctions. New Phytologist. doi:10.1111/nph.12576

Gill, J.L., Williams, J.W., Jackson, S.T., Lininger, K.B., Robinson, G.S., 2009. Pleistocene megafaunal collapse, novel plant communities, and enhanced fire regimes in North America. Science (New York, N.Y.) 326, 1100–1103. doi:10.1126/science.1179504

Gill, J.L., Williams, J.W., Jackson, S.T., Donnelly, J.P., Schellinger, G.C., 2012. Climatic and megaherbivory controls on late-glacial vegetation dynamics: A new, high-resolution, multi-proxy record from Silver Lake, Ohio. Quaternary Science Reviews 34, 66–80. doi:10.1016/j.quascirev.2011.12.008

Ginolhac, A., Rasmussen, M., Gilbert, M.T.P., Willerslev, E., Orlando, L., 2011. mapDamage: testing for damage patterns in ancient DNA sequences. Bioinformatics 27, 2153–2155. doi:10.1093/bioinformatics/btr347

Glen, J.W., 1955. The Creep of Polycrystalline Ice. Proceedings of the Royal Society of London. Series A, Mathematical and Physical Sciences 228, 519–538. doi:10.1002/2015JB012542

Godfrey-Smith, P., 2000. Niche construction in biological and philosophical theories. Behavioral and Brain Sciences 23, 153–154. doi:10.1017/S0140525X00312419

Goebel, T., 1999. Pleistocene Human Colonization of Siberia and Pepoling of the Americas: An Ecological Approach. Evolutionary Anthropology 8, 208–227. doi:10.1002/(SICI)1520-6505(1999)8:6<208::AID-EVAN2>3.0.CO;2-M

Goebel, T., 2002a. Siberian middle Upper Paleolithic. In: Peregrine, P.N., Ember, M. (Eds.), Encyclopedia of Prehistory. Vol 2: Arctic and Subarctic. Kluwer Academic Publishers, New York, pp. 192–196.

Goebel, T., 2002b. The "microblade adaptation" and recolonization of Siberia during the late Upper Pleistocene. In: Elston, R.G., Kuhn, S.L. (Eds.), Thinking Small: Global Perspectives on Microlithization. Archaeological Paper No. 12. American Anthropological Association, Washington, D.C., pp. 117–131.

Goebel, T., Buvit, I. (Eds.), 2011a. From the Yenisei to the Yukon: Interpreting Lithic Assemblage Variability in Late Pleistocene/Early Holocene Beringia. Texas A&M University Press, College Station.

Goebel, T., Buvit, I., 2011b. Introducing the Archaeological Record of Beringia. In: Goebel, T., Buvit, I. (Eds.), From the Yenisei to the Yukon: Interpreting Lithic Assemblage Variability in Late Pleistocene/Early Holocene Beringia. Texas A&M University Press, College Station, pp. 1–30.

Goebel, T., Powers, W.R., Bigelow, N.H., 1991. The Nenana Complex of Alaska and Clovis Origins, Clovis: Origins and Adaptations. Center for the Study of the First Americans, Oregon State University, Corvallis.

Goring, C.A.I., Bartholomew, W.V., 1952. Adsorption of mononucleotides, nucleic acids, and nucleoproteins by clays. Soil Science. doi:10.1097/00010694-195208000-00005

Gotthardt, R.M., 1990. The Archaeological Sequence in The Northern Cordillera.

Gowlett, J.A.J., 2016. The discovery of fire by humans: A long and convoluted process. Philosophical Transactions of the Royal Society B: Biological Sciences 371. doi:10.1098/rstb.2015.0164

Graf, K.E., 2005. Adandomment of the Siberian Mammoth-Steppe during the LGM: Evidence from the calibration of 14C-dated archaeological occupations. Current Research in the Pleistocene 22, 2–5.

Graf, K.E., 2008. Uncharted Territory: Late Pleistocene Hunter-Gatherer Dispersals in the Siberian Mammoth-Steppe. University of Nevada.

Graf, K.E., 2009. "The Good, the Bad, and the Ugly": evaluating the radiocarbon chronology of the middle and late Upper Paleolithic in the Enisei River valley, south-central Siberia. Journal of Archaeological Science 36, 694–707. doi:10.1016/j.jas.2008.10.014

Graf, K.E., 2010. Hunter-gatherer disperals in the Mammoth-Steppe: Technological provisioning and land-use in the Enisei River Valley, south-central Siberia. Journal of Archaeological Science 37, 210–23.

Graf, K.E., 2014. Siberian Odyssey. In: Graf, K.E., Ketron, C. V., Waters, M.R. (Eds.), Paleoamerican Odyssey. Texas A&M University Press, College Station, pp. 65–80.

Graf, K.E., Bigelow, N.H., 2011. Human response to climate during the Younger Dryas chronozone in central Alaska. Quaternary International 242, 434–451. doi:10.1016/j.quaint.2011.04.030

Graham, R.W., Belmecheri, S., Choy, K., Culleton, B.J., Davies, L.J., Froese, D., Heintzman, P.D., Hritz, C., Kapp, J.D., Newsom, L.A., Rawcliffe, R., Saulnier-Talbot, É., Shapiro, B., Wang, Y., Williams, J.W., Wooller, M.J., 2016. Timing and causes of mid-Holocene mammoth extinction on St. Paul Island, Alaska. Proceedings of the National Academy of Sciences 113, 9310–9314. doi:10.1073/pnas.1604903113

Grayson, D.K., 2001. The Archaeological Record of Human Impacts on Animal Populations. Journal of World Prehistory 15, 1–68. doi:10.1023/a:1011165119141

Greaves, M.P., Wilson, M.J., 1969. The adsorption of nucleic acids by montmorillonite. Soil Biology and Biochemistry 1, 317–323. doi:10.1016/0038-0717(69)90014-5

Greaves, M.P., Wilson, M.J., 1970. The degradation of nucleic acids and montmorillonite-nucleic-acid complexes by soil microorganisms. Soil Biology and Biochemistry 2, 257–268. doi:10.1016/0038-0717(70)90032-5

Green, R.E., Krause, J., Briggs, A.W., Maricic, T., Stenzel, U., Kircher, M., Patterson, N., Li, H., Zhai, W., Fritz, M.H.-Y., Hansen, N.F., Durand, E.Y., Malaspinas, A.-S., Jensen, J.D., Marques-Bonet, T., Alkan, C., Prüfer, K., Meyer, M., Burbano, H. a, Good, J.M., Schultz, R., Aximu-Petri, A., Butthof, A., Höber, B., Höffner, B., Siegemund, M., Weihmann, A., Nusbaum, C., Lander, E.S., Russ, C., Novod, N., Affourtit, J., Egholm, M., Verna, C., Rudan, P., Brajkovic, D., Kucan, Z., Gusic, I., Doronichev, V.B., Golovanova, L. V, Lalueza-Fox, C., la Rasilla, M. de, Fortea, J.,

Rosas, A., Schmitz, R.W., Johnson, P.L.F., Eichler, E.E., Falush, D., Birney, E., Mullikin, J.C., Slatkin, M., Nielsen, R., Kelso, J., Lachmann, M., Reich, D., Pääbo, S., 2010. A draft sequence of the Neandertal genome. Science (New York, N.Y.) 328, 710–22. doi:10.1126/science.1188021

Grootes, P.M., Stuiver, M., 1997. Oxygen 18/16 variability in Greenland snow and ice with 10-3- to 105-year time resolution. Journal of Geophysical Research: Oceans 102, 26455–26470. doi:10.1029/97JC00880

Guthrie, R.D., 2001. Origin and causes of the mammoth steppe: A story of cloud cover, woolly mammal tooth pits, buckles, and inside-out Beringia. Quaternary Science Reviews 20, 549–574. doi:10.1016/S0277-3791(00)00099-8

Guthrie, R.D., 2003. Rapid body size decline in Alaskan Pleistocene horses before extinction. Nature 426, 169–171.

Guthrie, R.D., 2006. New Carbon Dates Link Climatic Change with Human Colonization and Pleistocene Extinctions. Nature 441, 207–209. doi:10.1038/nature04604

Gutierrez, J.L., Jones, C.G., 2006. Physical Ecosystem Engineers as Agents of Biogeochemical Heterogeneity. BioScience 56, 227. doi:10.1641/0006-3568(2006)056[0227:PEEAAO]2.0.CO;2

Haile, J., 2008. Ancient DNA from Sediments and Associated Remains. University of Oxford.

Haile, J., Holdaway, R., Oliver, K., Bunce, M., Gilbert, M.T.P., Nielsen, R., Munch, K., Ho, S.Y.W., Shapiro, B., Willerslev, E., 2007. Ancient DNA Chronology within Sediment Deposits: Are Paleobiological Reconstructions Possible and Is DNA Leaching a Factor? Molecular Biology and Evolution 24, 982–989. doi:10.1093/molbev/msm016

Haile, J., Froese, D.G., MacPhee, R.D.E., Roberts, R.G., Arnold, L.J., Reyes, A. V., Rasmussen, M., Nielsen, R., Brook, B.W., Robinson, S., Demuro, M., Gilbert, M.T.P., Munch, K., Austin, J.J., Cooper, A., Barnes, I., Möller, P., Willerslev, E., 2009. Ancient DNA reveals late survival of mammoth and horse in interior Alaska. Proceedings of the National Academy of Sciences of the United States of America 106, 22352–22357. doi:10.1073/pnas.0912510106

Halffman, C.M., Potter, B.A., McKinney, H.J., Finney, B.P., Rodrigues, A.T., Yang, D.Y., Kemp, B.M., 2015. Early human use of anadromous salmon in North America at 11,500 y ago. Proceedings of the National Academy of Sciences 112, 12344–12348. doi:10.1073/pnas.1509747112

Handsley-Davis, M., Kowal, E., Russell, L., Weyrich, L.S., 2020. Researchers using environmental DNA must engage ethically with Indigenous communities. Nature Ecology and Evolution 1–3. doi:10.1038/s41559-020-01351-6

Handt, O., Krings, M., Ward, R.H., Pääbo, S., 1996. The retrieval of ancient human DNA sequences. American journal of human genetics 59, 368–76.

Hansen, A.J., Mitchell, D.L., Wiuf, C., Paniker, L., Brand, T.B., Binladen, J., Gilichinsky, D. a, Rønn, R., Willerslev, E., 2006. Crosslinks rather than strand breaks determine

access to ancient DNA sequences from frozen sediments. Genetics 173, 1175–9. doi:10.1534/genetics.106.057349

Harari, Y.N., 2016. Homo Deus: A brief history of tomorrow. Signal.

Hare, P.G., 1995. Holocene occupations in the southern Yukon: New perspectives from the Annie Lake site. Occasional Papers in Archaeology 5.

Harington, C.R., 2011. Pleistocene vertebrates of the Yukon Territory. Quaternary Science Reviews 30, 2341–2354. doi:10.1016/j.quascirev.2011.05.020

Harrison, J.W., Svec, T.A., 1998. The beginning of the end of the antibiotic era? Part I. The problem: abuse of the "miracle drugs". Quintessence international (Berlin, Germany : 1985) 29, 151–162.

Hart, C.J.R., Radloff, J.K., 1990. Geology of Whitehorse, Alligator Lake, Fenwick Creek, Carcross and part of Robinson map areas (105D/11, 6, 3, 2, & 7). Indian and Northern Affairs Canada, Northern Affairs, Yukon Region, Whitehorse, Yukon.

Hart, D., Sussman, R.W., 2009. Man the hunted, expanded edition: primates, predators, and human evolution. Routledge (first issue published by WestView Press), New York.

Haynes, G., 2002. The Early Settlement of North America: The Clovis Era. Cambridge University Press, Cambridge.

Haynes, G., 2013. Extinctions in North America's Late Glacial landscapes. Quaternary International 285, 89–98. doi:10.1016/j.quaint.2010.07.026

He, Z., Gentry, T.J., Schadt, C.W., Wu, L., Liebich, J., Chong, S.C., Huang, Z., Wu, W., Gu, B., Jardine, P., Criddle, C., Zhou, J., 2007. GeoChip: a comprehensive microarray for investigating biogeochemical, ecological and environmental processes. The ISME Journal 1, 67–77. doi:10.1038/ismej.2007.2

He, Z., Deng, Y., Nostrand, J.D. Van, Tu, Q., Xu, M., Hemme, C.L., Li, X., Wu, L., Gentry, T.J., Yin, Y., Liebich, J., Hazen, T.C., Zhou, J., 2010. GeoChip 3.0 as a high-throughput tool for analyzing microbial community composition, structure and functional activity. The ISME Journal 4, 1167–1179. doi:10.1038/ismej.2010.46

Heads, M., 2012. Bayesian transmogrification of clade divergence dates: A critique. Journal of Biogeography 39, 1749–1756. doi:10.1111/j.1365-2699.2012.02784.x

Hebsgaard, M.B., Phillips, M.J., Willerslev, E., 2005. Geologically ancient DNA: fact or artefact? Trends in Microbiology 13, 212–220.

Hebsgaard, M.B., Gilbert, M.T.P., Arneborg, J., Heyn, P., Allentoft, M.E., Bunce, M., Munch, K., Schweger, C., Willerslev, E., 2009. 'The Farm Beneath the Sand'- an archaeological case study on ancient "dirt" DNA. Antiquity 83, 430–444. doi:10.1017/S0003598X00098537

Heintzman, P.D., Froese, D., Ives, J.W., Soares, A.E.R., Zazula, G.D., Letts, B., Andrews, T.D., Driver, J.C., Hall, E., Gregory Hare, P., Jass, C.N., Mackay, G., Southon, J.R., Stiller, M., Woywitka, R., Suchard, M.A., Shapiro, B., Hare, P.G., Jass, C.N., Mackay, G., Southon, J.R., Stiller, M., Woywitka, R., Suchard, M.A., Shapiro, B., 2016. Bison phylogeography constrains dispersal and viability of the Ice

Free Corridor in western Canada. Proceedings of the National Academy of Sciences of the United States of America 113, 8057–8063. doi:10.1073/pnas.1601077113

Heintzman, P.D., Zazula, G.D., MacPhee, R.D.E., Scott, E., Cahill, J.A., McHorse, B.K., Kapp, J.D., Stiller, M., Wooller, M.J., Orlando, L., Southon, J., Froese, D.G., Shapiro, B., 2017. A new genus of horse from pleistocene North America. eLife 6, 1–43. doi:10.7554/eLife.29944

Henrich, J., McElreath, R., 2003. The Evolution of Cultural Evolution. Evolutionary Anthropology 12, 123–135. doi:10.1002/evan.10110

Higdon, J.W., 2002. Functionally dominant herbivores as keystone species. Conservation Ecology 6, r8.

Higuchi, R., Bowman, B., Freiberger, M., Ryder, O.A., Wilson, A.C., 1984. DNA Sequences from the Quagga, An Extinct Member of the Horse Family. Nature 312, 282–284.

Higuera, P.E., Brubaker, L.B., Anderson, P.M., Hu, F.S., Brown, T.A., 2009. Vegetation mediated the impacts of postglacial climate change on fire regimes in the south-central Brooks Range, Alaska. Ecological Monographs 79, 201–219. doi:10.1890/07-2019.1

Hill, K., Barton, M., Magdalena Hurtado, A., 2009. The emergence of human uniqueness: Characters underlying behavioral modernity. Evolutionary Anthropology 18, 187–200. doi:10.1002/evan.20224

Hoesel, A. Van, Hoek, W.Z., Pennock, G.M., Drury, M.R., 2014. The younger dryas impact hypothesis: A critical review. Quaternary Science Reviews 83, 95–114. doi:10.1016/j.quascirev.2013.10.033

Hoffecker, J.F., Elias, S.A., 2007. Human Ecology of Beringia. Columbia University Press, New York.

Hoffecker, J.F., Elias, S.A., Rourke, D.H.O., 2014. Out of Beringia? Science 343, 979–980.

Hofreiter, M., Mead, J.I., Martin, P., Poinar, H.N., 2003. Molecular caving. Current Biology 13, 693–695. doi:10.1016/j.cub.2003.08.039

Hofreiter, M., Collins, M., Stewart, J.R., 2012. Ancient biomolecules in Quaternary palaeoecology. Quaternary Science Reviews 33, 1–13. doi:10.1016/j.quascirev.2011.11.018

Holliday, V., Surovell, T., Johnson, E., 2016. A blind test of the Younger Dryas impact hypothesis. PLoS ONE 11, 4–8. doi:10.1371/journal.pone.0155470

Holliday, V.T., Surovell, T., Meltzer, D.J., Grayson, D.K., Boslough, M., 2014. The Younger Dryas impact hypothesis: A cosmic catastrophe. Journal of Quaternary Science 29, 515–530. doi:10.1002/jqs.2724

Hollingsworth, P.M., 2011. Refining the DNA barcode for land plants. Proceedings of the National Academy of Sciences 108, 19451–19452. doi:10.1073/pnas.1116812108

Hollingsworth, P.M., Graham, S.W., Little, D.P., 2011. Choosing and using a plant DNA barcode. PLoS ONE 6. doi:10.1371/journal.pone.0019254

Holly, D.H.J., 2002. Subarctic" Prehistory" in the Anthropological Imagination. Arctic anthropology 39, 10–26.

Holmes, C.E., 2001. Tanana River Valley archaeology circa 14,000 to 9000 BP. Arctic Anthropology 38, 154–170.

Holmes, C.E., 2008. The Taiga period: Holocene archaeology of the northern boreal forest, Alaska. Alaska Journal of Anthropology 6, 69–82.

Holmes, C.E., 2011. The Beringian and Transitional Periods in Alaska. In: Goebel, T.E., Buvit, I. (Eds.), From the Yenisei to the Yukon: Interpreting Lithic Assemblage Variability in Late Pleistocene/Early Holocene Beringia. Texas A&M University Press, College Station, pp. 179–191.

Holmsgaard, P.N., Norman, A., Hede, S.C., Poulsen, P.H., Al-Soud, W.A., Hansen, L.H., Sørensen, S.J., 2011. Bias in bacterial diversity as a result of Nycodenz extraction from bulk soil. Soil Biology and Biochemistry 43, 2152–2159.

Horn, S., 2012. Target enrichment via DNA hybridization capture. Methods in Molecular Biology 840, 177–188.

Höss, M., Pääbo, S., 1993. DNA extraction from Pleistocene bones by purification method. Nucleic Acids Research 21, 3913–3914.

Höss, M., Dilling, A., Currant, A., Pääbo, S., 1996. Molecular phylogeny of the extinct ground sloth Mylodon darwinii. Proceedings of the National Academy of Sciences 93, 181–185. doi:10.1073/pnas.93.1.181

Hu, A., Meehl, G.A., Otto-Bliesner, B.L., Waelbroeck, C., Han, W., Loutre, M.F., Lambeck, K., Mitrovica, J.X., Rosenbloom, N., 2010. Influence of Bering Strait flow and North Atlantic circulation on glacial sea-level changes. Nature Geoscience 3, 118–121. doi:10.1038/ngeo729

Hughes, O.L., 1990. Surficial geology and geomorphology, Aishihik Lake, Yukon Territory, Geological Survey of Canada. Energy Mines and Resources Canada.

Hunan Medical Institute, 1980. Study of an Ancient Cadaver in Mawangtui Tomb No. 1 of the Han Dynasty in Changsha. Beijin: Ancient Memorial Press 184–187.

Huntington, H.P., 2000. Using traditional ecological knowledge in science: Methods and applications. Ecological Applications 10, 1270–1274. doi:10.1890/1051-0761(2000)010[1270:UTEKIS]2.0.CO;2

Huson, D.H., Mitra, S., 2011. Comparative Metagenome Analysis Using MEGAN. Handbook of Molecular Microbial Ecology I: Metagenomics and Complementary Approaches 341–352. doi:10.1002/9781118010518.ch39

Huson, D.H., Auch, A.F., Qi, J., Schuster, S.C., 2007. MEGAN analysis of metagenomic data. Genome Research 17, 377–386. doi:10.1101/gr.5969107

Huson, D.H., Beier, S., Flade, I., Górska, A., El-Hadidi, M., Mitra, S., Ruscheweyh, H.J., Tappu, R., 2016. MEGAN Community Edition - Interactive Exploration and Analysis of Large-Scale Microbiome Sequencing Data. PLoS Computational Biology 12. doi:10.1371/journal.pcbi.1004957

Huson, D.H., Albrecht, B., Bağci, C., Bessarab, I., Górska, A., Jolic, D., Williams, R.B.H., 2018. MEGAN-LR: New algorithms allow accurate binning and easy interactive exploration of metagenomic long reads and contigs. Biology Direct 13, 1–17. doi:10.1186/s13062-018-0208-7

Huxley, J., 1942. Evolution. The modern synthesis. Allen & Unwin, London.

Ion, P.G., Kershaw, G.P., 1989. The selection of snowpatches as relief habitat by woodland caribou (Rangifer tarandus caribou), Macmillan Pass, Selwyn/Mackenzie Mountains, NWT, Canada. Arctic & Alpine Research 21, 203–211. doi:10.2307/1551633

IPBES, 2019. Global assessment report on biodiversity and ecosystem services of the Intergovernmental Science-Policy Platform on Biodiversity and Ecosystem Services. IPBES secretariat, Bonn, Germany.

IPCC, 2014. Climate Change 2014: Synthesis Report. Contribution of Working Groups I, II and III to the Fifth Assessment Report of the Intergovernmental Panel on Climate Change. IPCC, Geneva, Switzerland.

Irwin, H.T., Wormington, H.M., 1970. Paleo-Indian Tool Types in the Great Plains. American Antiquity 35, 24–34. doi:10.2307/278175

Ives, J.W., 1990. A theory of Northern Athapaskan prehistory. Westview Press and University of Calgary Press, Boulder, Colorado.

Izuho, M., 2014. Human Technological and Behavioral Adaptation to Landscape Changes around the Last Glacial Maximum in Japan: A Focus on Hokkaido. In: Graf, K.E., Ketron, C. V., Waters, M.R. (Eds.), Paleoamerican Odyssey. Texas A&M University Press, College Station, pp. 45–64.

Jaanusson, V., 1976. Faunal dynamics in the middle Ordovician (Viruan) of Balto-Scandia. In: The Ordovician System: Proceedings of a Palaeontological Association Symposium. pp. 301œ326. University of Wales Press and National Museum of Wales, Cardiff, pp. 301–326.

Jackson, S.T., 2012. Representation of flora and vegetation in Quaternary fossil assemblages: Known and unknown knowns and unknowns. Quaternary Science Reviews 49, 1–15. doi:10.1016/j.quascirev.2012.05.020

James, S.R., 1989. Hominid Use of Fire in the Lower and Middle Pleistocene. Current Anthropology. doi:10.2307/2743299

Jiménez-Hidalgo, E., Carbot-Chanona, G., Guerrero-Arenas, R., Bravo-Cuevas, V.M., Holdridge, G.S., Israde-Alcántara, I., 2019. Species Diversity and Paleoecology of Late Pleistocene Horses From Southern Mexico. Frontiers in Ecology and Evolution 7, 1–18. doi:10.3389/fevo.2019.00394

Johnson, C.N., 2002. Determinants of loss of mammal species during the Late Quaternary "megafauna" extinctions: life history and ecology, but not body size. Proceedings. Biological sciences / The Royal Society 269, 2221–2227. doi:10.1098/rspb.2002.2130

Johnson, C.N., 2009. Ecological consequences of Late Quaternary extinctions of megafauna. Proceedings. Biological sciences / The Royal Society 276, 2509–19. doi:10.1098/rspb.2008.1921

Johnson, L.M., 2000. "A place that's good," Gitksan landscape perception and ethnoecology. Human Ecology 28, 301–325.

Johnson, S.S., Hebsgaard, M.B., Christensen, T.R., Mastepanov, M., Nielsen, R., Munch, K., Brand, T., Gilbert, M.T.P., Zuber, M.T., Bunce, M., Rønn, R., Gilichinsky, D., Froese, D., Willerslev, E., 2007. Ancient bacteria show evidence of DNA repair. PNAS 104, 14401–14405. doi:10.1073/pnas.0710637105

Jones, K.E., Patel, N.G., Levy, M.A., Storeygard, A., Balk, D., Gittleman, J.L., Daszak, P., 2008. Global trends in emerging infectious diseases. Nature 451, 990–993. doi:10.1038/nature06536

Jones, R., 1969. Fire-stick Farming. Australian Natural History 16, 224–228.

Jónsson, H., Ginolhac, A., Schubert, M., Johnson, P.L.F., Orlando, L., 2013. MapDamage2.0: Fast approximate Bayesian estimates of ancient DNA damage parameters. Bioinformatics 29, 1682–1684. doi:10.1093/bioinformatics/btt193

Jørgensen, T., Haile, J., Möller, P.E.R., Andreev, A., Boessenkool, S., Rasmussen, M., Kienast, F., Coissac, E., Taberlet, P., Brochmann, C., Bigelow, N.H., Andersen, K., Orlando, L., Gilbert, M.T.P., Willerslev, E., 2012a. A comparative study of ancient sedimentary DNA, pollen and macrofossils from permafrost sediments of northern Siberia reveals long-term vegetational stability. Molecular Ecology 21, 1989–2003. doi:10.1111/j.1365-294X.2011.05287.x

Jørgensen, T., Kjær, K.H., Haile, J., Rasmussen, M., Boessenkool, S., Andersen, K., Coissac, E., Taberlet, P., Brochmann, C., Orlando, L., Gilbert, M.T.P., Willerslev, E., 2012b. Islands in the ice: Detecting past vegetation on Greenlandic nunataks using historical records and sedimentary ancient DNA Meta-barcoding. Molecular Ecology 21, 1980–1988. doi:10.1111/j.1365-294X.2011.05278.x

Kalendar, R., Lee, D., Schulman, A.H., 2011. Java web tools for PCR, in silico PCR, and oligonucleotide assembly and analysis. Genomics 98, 137–144. doi:10.1016/j.ygeno.2011.04.009

Kanagawa, T., 2003. Bias and artifacts in multitemplate polymerase chain reactions (PCR). Journal of Bioscience and Bioengineering 96, 317–323. doi:http://dx.doi.org/10.1016/S1389-1723(03)90130-7

Karpinski, E., Mead, J.I., Poinar, H.N., 2016. Molecular identification of paleofeces from Bechan Cave, southeastern Utah, USA. Quaternary International 443, 140–146. doi:10.1016/j.quaint.2017.03.068

Karpinski, E., Hackenberger, D., Zazula, G., Widga, C., Duggan, A.T., Golding, G.B., Kuch, M., Klunk, J., Jass, C.N., Groves, P., Druckenmiller, P., Schubert, B.W., Arroyo-Cabrales, J., Simpson, W.F., Hoganson, J.W., Fisher, D.C., Ho, S.Y.W., MacPhee, R.D.E., Poinar, H.N., 2020. American mastodon mitochondrial genomes suggest multiple dispersal events in response to Pleistocene climate oscillations. Nature Communications 11, 4048. doi:10.1038/s41467-020-17893-z

Keenan, T.J., Cwynar, L.C., 1992. Late Quaternary history of black spruce and grasslands in southwest Yukon Territory. Canadian Journal of Botany 70, 1336–1345.

Keesing, F., Young, T.P., 2014. Cascading consequences of the loss of large mammals in an African Savanna. BioScience 64, 487–495. doi:10.1093/biosci/biu059

Keith, G., 1890. Letters to Mr. Roderic McKenzie, 1807–1817. The Mackenzie River and Great Bear Lake Departments. In: Masson, L.R. (Ed.), Les bourgeois de la Compagine du Nord-Quest, Volume II. Imprimerie Générale A. Coté et Cie, Québec, pp. 5–132.

Khanna, M., Yoder, M., Calamai, L., Stotzky, G., 2005. X-ray diffractometry and electron microscopy of DNA from Bacillus subtilis bound on clay minerals. Sciences of Soils 3, 1–10. doi:10.1007/s10112-998-0001-3

Kienast, F., Wetterich, S., Kuzmina, S., Schirrmeister, L., Andreev, A.A., Tarasov, P., Nazarova, L., Kossler, A., Frolova, L., Kunitsky, V. V., 2011. Paleontological records indicate the occurrence of open woodlands in a dry inland climate at the present-day Arctic coast in western Beringia during the Last Interglacial. Quaternary Science Reviews 30, 2134–2159. doi:10.1016/j.quascirev.2010.11.024

King, C.E., Debruyne, R., Kuch, M., Schwarz, C., Poinar, H.N., 2009. A quantitative approach to detect and overcome PCR inhibition in ancient DNA extracts. BioTechniques 47, 941–949. doi:10.2144/000113244

Kircher, M., Sawyer, S., Meyer, M., 2012. Double indexing overcomes inaccuracies in multiplex sequencing on the Illumina platform. Nucleic Acids Research 40, 1–8. doi:10.1093/nar/gkr771

Klunk, J., Duggan, A.T., Redfern, R., Gamble, J., Boldsen, J.L., Golding, G.B., Walter, B.S., Eaton, K., Stangroom, J., Rouillard, J.M., Devault, A., DeWitte, S.N., Poinar, H.N., 2019. Genetic resiliency and the Black Death: No apparent loss of mitogenomic diversity due to the Black Death in medieval London and Denmark. American Journal of Physical Anthropology 169, 240–252. doi:10.1002/ajpa.23820

Knauth, S., Schmidt, H., Tippkötter, R., 2013. Comparison of commercial kits for the extraction of DNA from paddy soils. Letters in applied microbiology 56, 222–228.

Kobayashi, T., 1970. Microblade Industries in the Japanese Archipelago. Arctic Anthropology 7, 38–58.

Kohl, M.T., Stahler, D.R., Metz, M.C., Forester, J.D., Kauffman, M.J., Varley, N., White, P.J., Smith, D.W., MacNulty, D.R., 2018. Diel predator activity drives a dynamic landscape of fear. Ecological Monographs 88, 638–652. doi:10.1002/ecm.1313

Kokelj, S. V., Tunnicliffe, J., Lacelle, D., Lantz, T.C., Chin, K.S., Fraser, R., 2015. Increased precipitation drives mega slump development and destabilization of ice-rich permafrost terrain, northwestern Canada. Global and Planetary Change 129, 56–68. doi:10.1016/j.gloplacha.2015.02.008

Kokelj, S. V., Lantz, T.C., Tunnicliffe, J., Segal, R., Lacelle, D., 2017. Climate-driven thaw of permafrost preserved glacial landscapes, northwestern Canada. Geology 45, 371–374. doi:10.1130/G38626.1

Kolokotronis, S.O., MacPhee, R.D.E., Greenwood, A.D., 2007. Detection of mitochondrial insertions in the nucleus (NuMts) of Pleistocene and modern muskoxen. BMC Evolutionary Biology 7, 1–10. doi:10.1186/1471-2148-7-67

Koopal, L.K., Goloub, T.P., Davis, T.A., 2004. Binding of ionic surfactants to purified humic acid. Journal of Colloid and Interface Science 275, 360–367. doi:10.1016/j.jcis.2004.02.061

Krauss, L.M., Starkman, G.D., 2000. Life, the Universe, and Nothing: Life and Death in an Ever-expanding Universe. The Astrophysical Journal 531, 22–30. doi:10.1086/308434

Kreader, C.A., 1996. Relief of Amplification Inhibition in PCR with Bovine Serum Albumin or T4 Gene 32 Protein. Applied and Environmental Microbiology 62, 1102–1106.

Krehenwinkel, H., Fong, M., Kennedy, S., Huang, E.G., Noriyuki, S., Cayetano, L., Gillespie, R., 2018. The effect of DNA degradation bias in passive sampling devices on metabarcoding studies of arthropod communities and their associated microbiota. PLoS ONE 13, 1–14. doi:10.1371/journal.pone.0189188

Kress, W.J., Erickson, D.L., 2007. A two-locus global DNA barcode for land plants: the coding rbcL gene complements the non-coding trnH-psbA spacer region. PloS one 2, e508. doi:10.1371/journal.pone.0000508

Kuch, M., Rohland, N., Betancourt, J.L., Latorre, C., Steppan, S., Poinar, H.N., 2002. Molecular analysis of a 11 700-year-old rodent midden from the Atacama Desert, Chile. Molecular Ecology 11, 913–924. doi:10.1046/j.1365-294X.2002.01492.x

Kunz, M.L., Bever, M., 2003. The Mesa Site: Paleoindians Above the Arctic Circle, BLM-Alaska Open File Report 86, April. Department of the Interior. On file from the Bureau of Land Management-Alaska.

Kunz, M.L., Reanier, R.E., 1994. Paleoindians in Beringia: Evidence from arctic Alaska. Science. doi:10.1126/science.263.5147.660

Kunz, M.L., Reanier, R.E., 1995. The Mesa site: a Paleoindian hunting lookout in Arctic Alaska. Arctic Anthropology.

Kuzmin, Y. V., 2008. Siberia at the Last Glacial Maximum: Environment and archaeology. Journal of Archaeological Research 16, 163–221. doi:10.1007/s10814-007-9019-6

Kuzmin, Y. V., Keates, S.G., 2005. Dates are not just data: Paleolithic settlement patterns in Siberia derived from radiocarbon records. American Antiquity 70, 773–789. doi:10.2307/40035874

Kuzmina, S.A., Sher, A. V., Edwards, M.E., Haile, J., Yan, E. V., Kotov, A. V., Willerslev, E., 2011. The late Pleistocene environment of the Eastern West Beringia based on the principal section at the Main River, Chukotka. Quaternary Science Reviews 30, 2091–2106. doi:10.1016/j.quascirev.2010.03.019

Kuzyk, G.W., Russell, D.E., Farnell, R.S., Gotthardt, R.M., Hare, P.G., Blake, E., 1999. In pursuit of prehistoric caribou on Thandlät, southern Yukon. Arctic 52, 214–219.

Kylafis, G., Loreau, M., 2008. Ecological and evolutionary consequences of niche construction for its agent. Ecology Letters 11, 1072–1081. doi:10.1111/j.1461-0248.2008.01220.x

Lacourse, T., Gajewski, K., 2000. Late quaternary vegetation history of Sulphur Lake, southwest Yukon Territory, Canada. Arctic 53, 27–35. doi:10.14430/arctic831

Laland, K.N., Brown, G.R., 2002. Sense and Nonsense: Evolutionary Perspectives on Human Behaviour. Oxfo, Oxford.

Laland, K.N., O'Brien, M.J., 2010. Niche Construction Theory and Archaeology. Journal of Archaeological Method and Theory 17, 303–322. doi:10.1007/s10816-010-9096-6

Laland, K.N., Odling-Smee, J., Feldman, M.W., 2000. Niche construction, biological evolution, and cultural change. Behavioral and Brain Sciences 23, 131–175. doi:10.1017/s0140525x00002417

Lantis, M., 1938. The Alaskan Whale Cult and Its Affinities. American Anthropologist 40, 438–464. doi:10.1525/aa.1938.40.3.02a00070

Laundre, J.W., Hernandez, L., Ripple, W.J., 2010. The Landscape of Fear: Ecological Implications of Being Afraid. The Open Ecology Journal 3, 1–7. doi:10.2174/1874213001003030001

Lebart, L., Morineau, A., Tabard, N., 1977. Techniques De La Description Statistique Méthodes Et Logiciels Pour L'analyse Des Grands Tableaux. Dunod, Paris.

LeCompte, M.A., Goodyear, A.C., Demitroff, M.N., Batchelor, D., Vogel, E.K., Mooney, C., Rock, B.N., Seidel, A.W., 2012. Independent evaluation of conflicting microspherule results from different investigations of the Younger Dryas impact hypothesis. Proceedings of the National Academy of Sciences of the United States of America 109. doi:10.1073/pnas.1208603109

Leonard, W.R., Robertson, M.L., 1997. Comparative primate energetics and hominid evolution. American Journal of Physical Anthropology 102, 265–281. doi:10.1002/(SICI)1096-8644(199702)102:2<265::AID-AJPA8>3.0.CO;2-X

Lepofsky, D., Armstrong, C.G., 2018. Foraging New Ground: Documenting Ancient Resource and Environmental Management in Canadian Archaeology. Canadian Journal of Archaeology / Journal Canadien d'Archéologie 42, 57–73.

Lewkowicz, A.G., Way, R.G., 2019. Extremes of summer climate trigger thousands of thermokarst landslides in a High Arctic environment. Nature Communications 10, 1–11. doi:10.1038/s41467-019-09314-7

Li, H., Durbin, R., 2009. Fast and accurate short read alignment with Burrows-Wheeler transform. Bioinformatics (Oxford, England) 25, 1754–60. doi:10.1093/bioinformatics/btp324

Li, X., Rui, J., Xiong, J., Li, J., He, Z., Zhou, J., Yannarell, A.C., Mackie, R.I., 2014. Functional potential of soil microbial communities in the maize rhizosphere. PLoS ONE 9, 1–9. doi:10.1371/journal.pone.0112609

Lindahl, J.F., Grace, D., 2015. The consequences of human actions on risks for infectious diseases: a review. Infection Ecology & Epidemiology 5, 30048. doi:10.3402/iee.v5.30048

Lipo, C., 1997. Population Structure, Cultural Transmission, and Frequency Seriation. Journal of Anthropological Archaeology 16, 301–333. doi:10.1006/jaar.1997.0314

Lopes dos Santos, R.A., Deckker, P. De, Hopmans, E.C., Magee, J.W., Mets, A., Sinninghe Damsté, J.S., Schouten, S., 2013. Abrupt vegetation change after the Late Quaternary megafaunal extinction in southeastern Australia. Nature Geoscience 6, 627–631. doi:10.1038/ngeo1856

Lorenz, M.G., Wackernagel, W., 1987a. Adsorption of DNA to sand and variable degradation of adsorbed DNA. Applied and Environmental Microbiology 53, 2948–2952.

Lorenz, M.G., Wackernagel, W., 1987b. Adsorption of DNA to sand and variable degradation rates of adsorbed DNA. Applied and Environmental Microbiology 53, 2948–2952.

Lorenzen, E.D., Nogués-Bravo, D., Orlando, L., Weinstock, J., Binladen, J., Marske, K.A., Ugan, A., Borregaard, M.K., Gilbert, M.T.P., Nielsen, R., Ho, S.Y.W., Goebel, T., Graf, K.E., Byers, D., Stenderup, J.T., Rasmussen, M., Campos, P.F., Leonard, J.A., Koepfli, K.-P., Froese, D., Zazula, G., Stafford, T.W., Aaris-Sørensen, K., Batra, P., Haywood, A.M., Singarayer, J.S., Valdes, P.J., Boeskorov, G., Burns, J.A., Davydov, S.P., Haile, J., Jenkins, D.L., Kosintsev, P., Kuznetsova, T., Lai, X., Martin, L.D., McDonald, H.G., Mol, D., Meldgaard, M., Munch, K., Stephan, E., Sablin, M., Sommer, R.S., Sipko, T., Scott, E., Suchard, M.A., Tikhonov, A., Willerslev, R., Wayne, R.K., Cooper, A., Hofreiter, M., Sher, A., Shapiro, B., Rahbek, C., Willerslev, E., 2011. Species-specific responses of Late Quaternary megafauna to climate and humans. Nature 479, 359–64. doi:10.1038/nature10574

Lott, M.T., Leipzig, J.N., Derbeneva, O., Michael Xie, H., Chalkia, D., Sarmady, M., Procaccio, V., Wallace, D.C., 2013. MtDNA variation and analysis using Mitomap and Mitomaster. Current Protocols in Bioinformatics 44, 1.23.1-1.23.26. doi:10.1002/0471250953.bi0123s44

Lu, J., Salzberg, S.L., 2018. Removing Contaminants from Metagenomic Databases. PLoS computational biology 261859. doi:10.1101/261859

Lund, P.W., 1841. Blik paa Brasiliens Dyreverden för Sidste Jordomvaeltning. Trykt i B. Luno's bogtrykkeri, Copenhagen.

Lupo, K.D., Schmitt, D.N., 2016. When bigger is not better: The economics of hunting megafauna and its implications for Plio-Pleistocene hunter-gatherers. Journal of Anthropological Archaeology. doi:http://dx.doi.org/10.1016/j.jaa.2016.07.012

Lydolph, M.C., Jacobsen, J., Arctander, P., Gilbert, T.P., Gilichinsky, D. a, Hansen, A.J., Gilbert, M.T.P., Willerslev, E., 2005. Beringian Paleoecology Inferred from Permafrost-Preserved Fungal DNA. Applied and Environmental Microbiology 71, 1012–1017. doi:10.1128/AEM.71.2.1012

Lyman, R.L., VanPool, T.L., O'Brien, M.J., 2008. Variation in North American dart points and arrow points when one or both are present. Journal of Archaeological Science 35, 2805–2812. doi:10.1016/j.jas.2008.05.008

Lyons, S.K., Smith, F.A., Wagner, P.J., White, E.P., Brown, J.H., 2004. Was a "hyperdisease" responsible for the late Pleistocene megafaunal extinction? Ecology Letters 7, 859–868. doi:10.1111/j.1461-0248.2004.00643.x

Macias-Fauria, M., Jepson, P., Zimov, N., Malhi, Y., 2020. Pleistocene Arctic megafaunal ecological engineering as a natural climate solution? Philosophical Transactions of the Royal Society B: Biological Sciences 375. doi:10.1098/rstb.2019.0122

Mackelprang, R., Waldrop, M.P., DeAngelis, K.M., David, M.M., Chavarria, K.L., Blazewicz, S.J., Rubin, E.M., Jansson, J.K., 2011. Metagenomic analysis of a permafrost microbial community reveals a rapid response to thaw. Nature 480, 368–371. doi:10.1038/nature10576

MacNeish, R.S., 1959. A Speculative Framework of Northern North American Prehistory as of April 1959. Anthropologica 1, 7–23.

MacPhee, R.D.E., Greenwood, A.D., 2007. Continuity and Change in the Extinction Dynamics of Late Quaternary Muskox (OVIBOS): Genetic and Radiometric Evidence. Bulletin of Carnegie Museum of Natural History 39, 203–212. doi:10.2992/0145-9058(2007)39[203:cacite]2.0.co;2

MacPhee, R.D.E., Greenwood, A.D., 2013. Infectious Disease, Endangerment, and Extinction. International Journal of Evolutionary Biology 2013, 1–9. doi:10.1155/2013/571939

MacPhee, R.D.E., Marx, P.A., 1997. Humans, hyperdisease, and first-contact extinctions. In: Goodman, S.M., Patterson, B.D. (Eds.), Natural Change and Human Impact in Madagascar. Smithsonian Institution Press, Washington, D.C., pp. 169–217.

Mah, M.W., Memish, Z.A., 2000. Antibiotic resistance. An impending crisis. Saudi medical journal 21, 1125–1129.

Mahony, M.E., 2015. 50,000 years of paleoenvironmental change recorded in meteoric waters and coeval paleoecological and cryostratigraphic indicators from the Klondike goldfields, Yukon, Canada. University of Alberta. doi:10.1145/3132847.3132886

Malhi, Y., Doughty, C.E., Galetti, M., Smith, F.A., Svenning, J.-C., Terborgh, J.W., 2016. Megafauna and ecosystem function from the Pleistocene to the Anthropocene. Proceedings of the National Academy of Sciences 113, 838–846. doi:10.1073/pnas.1502540113

Mamanova, L., Coffey, A.J., Scott, C.E., Kozarewa, I., Turner, E.H., Kumar, A., Howard, E., Shendure, J., Turner, D.J., 2010a. Target-enrichment strategies for next-generation sequencing. Nature methods 7, 111–8. doi:10.1038/nmeth.1419

Mamanova, L., Coffey, A.J., Scott, C.E., Kozarewa, I., Turner, E.H., Kumar, A., Howard, E., Shendure, J., Turner, D.J., 2010b. Target-enrichment strategies for next-

generation sequencing. Nature methods 7, 111–118. doi:10.1038/nmeth.1419

Mann, D.H., Groves, P., Kunz, M.L., Reanier, R.E., Gaglioti, B. V., 2013. Ice-age megafauna in Arctic Alaska: Extinction, invasion, survival. Quaternary Science Reviews 70, 91–108. doi:10.1016/j.quascirev.2013.03.015

Mann, D.H., Groves, P., Reanier, R.E., VGaglioti, B., LKunz, M., BethShapiro, B., 2015. Life and extinction of megafauna in the ice-age Arctic. Proceedings of the National Academy of Sciences of the United States of America 112, 14301–14306. doi:10.1073/pnas.1516573112

Marciniak, S., Klunk, J., Devault, A., Enk, J., Poinar, H.N., 2015. Ancient human genomics: the methodology behind reconstructing evolutionary pathways. Journal of human evolution 79, 21–34. doi:10.1016/j.jhevol.2014.11.003

Maron, D.F., 2018. Under poaching pressure, elephants are evolving to lose their tusks. National Geographic.

Martin, P.S., 1967. Prehistoric overkill. In: Martin, P.S., Wright, H.E. (Eds.), Pleistocne Extinctions: The Search for a Cause. Yale University Press, New Haven, pp. 75–120.

Martin, P.S., 1973. The Discovery of America. Science 179, 969–974. doi:10.1038/100283a0

Martin, P.S., 1984. Prehistoric Overkill: The Global Model. In: Martin, P.S., Klein, R.G. (Eds.), Quaternary Extinctions: A Prehistoric Revolution. University of Arizona Press, Tucson, pp. 354–403.

Maschenko, E.N., Potapova, O.R., Vershinina, A., Shapiro, B., Streletskaya, I.D., Vasiliev, A.A., Oblogov, G.E., Kharlamova, A.S., Potapov, E., Plicht, J. van der, Tikhonov, A.N., Serdyuk, N. V., Tarasenko, K.K., 2017. The Zhenya Mammoth (Mammuthus primigenius (Blum.)): Taphonomy, geology, age, morphology and ancient DNA of a 48,000 year old frozen mummy from western Taimyr, Russia. Quaternary International 445, 104–134. doi:10.1016/j.quaint.2017.06.055

Matesanz, S., Pescador, D.S., Pías, B., Sánchez, A.M., Chacón-Labella, J., Illuminati, A., la Cruz, M. de, López-Angulo, J., Marí-Mena, N., Vizcaíno, A., Escudero, A., 2019. Estimating belowground plant abundance with DNA metabarcoding. Molecular Ecology Resources 19, 1265–1277. doi:10.1111/1755-0998.13049

Matheson, C.D., Gurney, C., Esau, N., Lehto, R., 2010. Assessing PCR Inhibition from Humic Substances. The Open Enzyme Inhibition Journal 3, 38–45.

Matsui, A., Ishiguro, N., Hongo, H., Minagawa, M., 2005. Wild pig? Or domesticated boar? An archaeological view on the domestication of Sus scrofa in Japan. In: Vigne, J.-D., Peters, J., Helmer, D. (Eds.), The First Steps of Animal Domestication: New Archaeological Approaches. Oxbow Books, Oxford, U.K., pp. 148–159.

McGilchrist, I., 2009. The Master and his Emissary: The Divided Brain and the Making of the Western World. Yale University Press, New Haven and London, UK.

McKay, N.P., Overpeck, J.T., Otto-Bliesner, B.L., 2011. The role of ocean thermal expansion in Last Interglacial sea level rise. Geophysical Research Letters 38, 4–9. doi:10.1029/2011GL048280

McKee, A.M., Spear, S.F., Pierson, T.W., 2015. The effect of dilution and the use of a post-extraction nucleic acid purification column on the accuracy, precision, and inhibition of environmental DNA samples. Biological Conservation 183, 70–76. doi:10.1016/j.biocon.2014.11.031

McMurdie, P.J., Holmes, S., 2014. Waste not, want not: why rarefying microbiome data is inadmissible. PLoS computational biology 10, e1003531. doi:10.1371/journal.pcbi.1003531

Meiri, M., Lister, A.M., Collins, M.J., Tuross, N., Goebel, T., Blockley, S., Zazula, G.D., Doorn, N. van, Guthrie, R.D., Boeskorov, G.G., Baryshnikov, G.F., Sher, A., Barnes, I., 2013. Faunal record identifies Bering isthmus conditions as constraint to end-Pleistocene migration to the New World. Proceedings of the Royal Society B: Biological Sciences 281. doi:10.1098/rspb.2013.2167

Meltzer, D.J., 2015. Pleistocene Overkill and North American Mammalian Extinctions. Annual Review of Anthropology 44, 33–53. doi:10.1146/annurev-anthro-102214-013854

Meltzer, D.J., 2020. Overkill, glacial history, and the extinction of North America's Ice Age megafauna. Proceedings of the National Academy of Sciences 1–9. doi:10.1073/pnas.2015032117

Meltzer, D.J., Holliday, V.T., Cannon, M.D., Miller, D.S., 2014. Chronological evidence fails to support claim of an isochronous widespread layer of cosmic impact indicators dated to 12,800 years ago. Proceedings of the National Academy of Sciences of the United States of America 111. doi:10.1073/pnas.1401150111

Mesoudi, A., 2011. Cultural Evolution: How Darwinian Theory can Explain Human Culture and Synthesize the Social Sciences. University of Chicago Press, Chicago.

Mesoudi, A., O'Brien, M.J., 2008. The Cultural Transmission of Great Basin Projectile-Point Technology I : An Experimental Simulation. American AAntiquity 73, 3–28.

Mesoudi, A., Whiten, A., Laland, K.N., 2006. Towards a unified science of cultural evolution. Behavioral and Brain Sciences 29, 329–347. doi:10.1017/S0140525X06009083

Mesoudi, A., Blanchet, S., Charmantier, A., Danchin, É., Fogarty, L., Jablonka, E., Laland, K.N., Morgan, T.J.H., Müller, G.B., Odling-Smee, F.J., Pujol, B., 2013. Is Non-genetic Inheritance Just a Proximate Mechanism? A Corroboration of the Extended Evolutionary Synthesis. Biological Theory 7, 189–195. doi:10.1007/s13752-013-0091-5

Meulendyk, T., Moorman, B.J., Andrews, T.D., MacKay, G., 2012. Morphology and development of ice patches in Northwest Territories, Canada. Arctic 65, 44–58. doi:10.14430/arctic4184

Meyer, M., Kircher, M., 2010. Illumina sequencing library preparation for highly multiplexed target capture and sequencing. Cold Spring Harbor Protocols 5. doi:10.1101/pdb.prot5448

Meyer, M., Kircher, M., Gansauge, M.-T., Li, H., Racimo, F., Mallick, S., Schraiber, J.G., Jay, F., Prüfer, K., Filippo, C. de, Sudmant, P.H., Alkan, C., Fu, Q., Do, R., Rohland, N., Tandon, A., Siebauer, M., Green, R.E., Bryc, K., Briggs, A.W., Stenzel, U., Dabney, J., Shendure, J., Kitzman, J., Hammer, M.F., Shunkov, M. V, Derevianko, A.P., Patterson, N., Andrés, A.M., Eichler, E.E., Slatkin, M., Reich, D., Kelso, J., Pääbo, S., 2012. A high-coverage genome sequence from an archaic Denisovan individual. Science (New York, N.Y.) 338, 222–6. doi:10.1126/science.1224344

Mills, L.S., Soulé, M.E., Doak, D.F., 1993. The Keystone-Species concept in ecology and conservation, Management and policy must explicitely consider the complexity of interactions in natural systems. BioScience 43, 219–224.

Mitchell, D., Willerslev, E., Hansen, A., 2005. Damage and repair of ancient DNA. Mutation research 571, 265–76. doi:10.1016/j.mrfmmm.2004.06.060

Mochanov, Y.A., Fedoseeva, S.A., 1996. Dyuktai Cave. In: West, C.F., Robinson, B.S. (Eds.), American Beginnings: The Prehistory and Palaeoecology of Beringia. University of Chicago Press, Chicago, pp. 164–173.

Moore, A.M.T., Kennett, J.P., Napier, W.M., Bunch, T.E., Weaver, J.C., LeCompte, M., Adedeji, A.V., Hackley, P., Kletetschka, G., Hermes, R.E., Wittke, J.H., Razink, J.J., Gaultois, M.W., West, A., 2020. Evidence of Cosmic Impact at Abu Hureyra, Syria at the Younger Dryas Onset (~12.8 ka): High-temperature melting at >2200 °C. Scientific Reports 10, 1–22. doi:10.1038/s41598-020-60867-w

Morlan, R.E., 1967. The Preceramic Period of Hokkaido: An Outline. Arctic Anthropology 4, 164–220.

Morrissey, E.M., McHugh, T.A., Preteska, L., Hayer, M., Dijkstra, P., Hungate, B.A., Schwartz, E., 2015. Dynamics of extracellular DNA decomposition and bacterial community composition in soil. Soil Biology and Biochemistry 86, 42–49. doi:10.1016/j.soilbio.2015.03.020

Muhs, D.R., Ager, T.A., Begét, J.E., 2001. Vegetation and paleoclimate of the last interglacial period, central Alaska. Quaternary Science Reviews 20, 41–61. doi:10.1016/S0277-3791(00)00132-3

Mullis, K.B., Faloona, F.A., 1989. Specific Synthesis of DNA in Vitro via a Polymerase-Catalyzed Chain Reaction. In: Selected Methods in Enzymology. Academic Press, pp. 189–204.

Murchie, T.J., 2015. Investigating the Antiquity of Inter-Regional Contact between Southern Yukon and the Northern Northwest Coast through an Ancient DNA Analysis of Cryogenic Wooden Biofacts Recovered from Alpine Archaeological Sites in the Northwestern Subarctic. University of Calgary.

Murchie, T.J., Monteath, A.J., Long, G.S., Karpinski, E., Cocker, S., Zazula, G., MacPhee, R., Froese, D., Poinar, H., 2021a. Ecological turnover and megafaunal ghost ranges as revealed by palaeoenvironmental DNA.

Murchie, T.J., Kuch, M., Duggan, A., Ledger, M.L., Roche, K., Klunk, J., Karpinski, E., Hackenberger, D., Sadoway, T., MacPhee, R., Froese, D., Poinar, H., 2021b. Optimizing extraction and targeted capture of ancient environmental DNA for reconstructing past environments using the PalaeoChip Arctic-1.0 bait-set. Quaternary Research 99, 305–328. doi:https://doi.org/10.1017/qua.2020.59

Nakajima, H., 1997. Emerging infectious disease: global response, global alert. Health for the millions 23, 19.

NCBI Resource Coordinators, 2018. Database resources of the National Center for Biotechnology Information. Nucleic Acids Research 46, 8–13. doi:10.1093/nar/gkx985

Nguyen, L.T., Schmidt, H.A., Haeseler, A. Von, Minh, B.Q., 2015. IQ-TREE: A fast and effective stochastic algorithm for estimating maximum-likelihood phylogenies. Molecular Biology and Evolution 32, 268–274. doi:10.1093/molbev/msu300

Nichols, R. V., Vollmers, C., Newsom, L.A., Wang, Y., Heintzman, P.D., Leighton, M., Green, R.E., Shapiro, B., 2018. Minimizing polymerase biases in metabarcoding. Molecular Ecology Resources 18, 927–939. doi:10.1111/1755-0998.12895

Nieblas, A.E., Bonhommeau, S., Pape, O. Le, Chassot, E., Dubroca, L., Barde, J., Kaplan, D.M., 2014. Reply to Roopnarine: What is an apex predator? Proceedings of the National Academy of Sciences of the United States of America 111, 2014. doi:10.1073/pnas.1324146111

Niemeyer, B., Epp, L.S., Stoof-Leichsenring, K.R., Pestryakova, L.A., Herzschuh, U., 2017. A comparison of sedimentary DNA and pollen from lake sediments in recording vegetation composition at the Siberian treeline. Molecular Ecology Resources 17, e46–e62. doi:10.1111/1755-0998.12689

Nikolskiy, P., Pitulko, V., 2013. Evidence from the Yana Palaeolithic site, Arctic Siberia, yields clues to the riddle of mammoth hunting. Journal of Archaeological Science 40, 4189–4197. doi:10.1016/j.jas.2013.05.020

Nitze, I., Grosse, G., Jones, B.M., Romanovsky, V.E., Boike, J., 2018. Remote sensing quantifies widespread abundance of permafrost region disturbances across the Arctic and Subarctic. Nature Communications 9, 1–11. doi:10.1038/s41467-018-07663-3

Odling-Smee, J.F., Laland, K.N., Fledman, M.W., 1996. Niche Construction. The American Naturalist 147, 641–648.

Odling-Smee, J.F., Laland, K.N., Fledman, M.W., 2003. Niche construction: The neglected process in evolution. Princeton University Press, Princeton.

Ogram, A., Sayler, G., Gustin, D., Lewis, R., 1988. DNA adsorption to soils and sediments. Environmental science and technology 22, 982–984.

Okasha, S., 2005. On Niche Construction and Extended Evolutionary Theory. Biology & Philosophy 20, 1–10. doi:10.1007/s10539-005-0431-3

Opel, K.L., Chung, D., McCord, B.R., 2010. A study of PCR inhibition mechanisms using real time PCR. Journal of forensic sciences 55, 25–33. doi:10.1111/j.1556-4029.2009.01245.x

Ord, T., 2020. The Precipice: Existential Risk and the Future of Humanity. Hachette Books, New York, NY.

Otto, W.H., Britten, D.J., Larive, C.K., 2003. NMR diffusion analysis of surfactant-humic substance interactions. Journal of Colloid and Interface Science 261, 508–513. doi:10.1016/S0021-9797(03)00062-6

Owen-Smith, N., 1987. Pleistocene extinctions: the pivotal role of megaherbivores. Paleobiology 13, 351–362. doi:10.2307/2400736

Owen-Smith, N., 1992. Megaherbivores: The influence of very large body size on ecology. Cambridge University Press, Cambridge.

Owen-Smith, R.N., 1988. Megaherbivores: the influence of very large body size on Ecology. Cambridge University Press, Cambridge.

Ozen, A.I., Ussery, D.W., 2015. Genome atlases, potential applications in study of metagenomes. In: Encyclopedia of Metagenomics: Genes, Genomes and Metagenomes: Basics, Methods, Databases and Tools. pp. 219–250. doi:10.1007/978-1-4899-7478-5

Ozga, A.T., Nieves-Colón, M.A., Honap, T.P., Sankaranarayanan, K., Hofman, C.A., Milner, G.R., Lewis, C.M., Stone, A.C., Warinner, C., 2016. Successful enrichment and recovery of whole mitochondrial genomes from ancient human dental calculus. American Journal of Physical Anthropology 160, 220–228. doi:10.1002/ajpa.22960

Pääbo, S., 1985a. Molecular cloning of ancient Egyptian mummy DNA. Nature 314, 644--645. doi:10.1038/314644a0

Pääbo, S., 1985b. Preservation of DNA in ancient Egyptian mummies. Journal of Archaeological Science 12, 411–417. doi:10.1016/0305-4403(85)90002-0

Pääbo, S., 1989. Ancient DNA: extraction, characterization, molecular cloning, and enzymatic amplification. Proceedings of the National Academy of Sciences of the United States of America 86, 1939–1943. doi:10.1073/pnas.86.6.1939

Paijmans, J.L.A., Barnett, R., Gilbert, M.T.P., Zepeda-Mendoza, M.L., Reumer, J.W.F., Vos, J. de, Zazula, G., Nagel, D., Baryshnikov, G.F., Leonard, J.A., Rohland, N., Westbury, M. V., Barlow, A., Hofreiter, M., 2017. Evolutionary History of Saber-Toothed Cats Based on Ancient Mitogenomics. Current Biology 27, 3330-3336.e5. doi:10.1016/j.cub.2017.09.033

Paine, R. t. T., 1995. A Conversation on Refining the Concept of Keystone Species. Conservation Biology 9, 962–964. doi:10.1046/j.1523-1739.1995.09040962.x

Paine, R.T., 1969a. A note on trophic complexity and community stability. The American Naturalist 103, 91–93. doi:10.1017/CBO9781107415324.004

Paine, R.T., 1969b. The Pisaster-Tegula interaction: prey patches, predator food preference, and intertidal community structure. Ecology 50, 950–961. doi:10.2307/1936888

Pala, M., Olivieri, A., Achilli, A., Accetturo, M., Metspalu, E., Reidla, M., Tamm, E., Karmin, M., Reisberg, T., Kashani, B.H., Perego, U.A., Carossa, V., Gandini, F., Pereira, J.B., Soares, P., Angerhofer, N., Rychkov, S., Al-Zahery, N., Carelli, V.,

Sanati, M.H., Houshmand, M., Hatina, J., MacAulay, V., Pereira, L., Woodward, S.R., Davies, W., Gamble, C., Baird, D., Semino, O., Villems, R., Torroni, A., Richards, M.B., 2012. Mitochondrial DNA signals of late glacial recolonization of europe from near eastern refugia. American Journal of Human Genetics 90, 915–924. doi:10.1016/j.ajhg.2012.04.003

Parducci, L., Bennett, K.D., Ficetola, G.F., Alsos, I.G., Suyama, Y., Wood, J.R., Pedersen, M.W., 2017. Ancient plant DNA in lake sediments. New Phytologist 214, 924–942. doi:10.1111/nph.14470

Pavelková Řičánková, V., Robovský, J., Riegert, J., 2014. Ecological structure of recent and last glacial mammalian faunas in northern Eurasia: the case of Altai-Sayan refugium. PloS one 9, e85056. doi:10.1371/journal.pone.0085056

Pearce, T., 2011. Ecosystem engineering, experiment, and evolution. Biology and Philosophy 26, 793–812. doi:10.1007/s10539-011-9282-2

Peck, T.R., 2011. Light from Ancient Campfires: Archaeological Evidence for Native Lifeways on the Northern Plains. AU Press, Athabasca University, Athabasca.

Pečnerová, P., Palkopoulou, E., Wheat, C.W., Skoglund, P., Vartanyan, S., Tikhonov, A., Nikolskiy, P., Plicht, J. van der, Díez-del-Molino, D., Dalén, L., 2017. Mitogenome evolution in the last surviving woolly mammoth population reveals neutral and functional consequences of small population size. Evolution Letters 292–303. doi:10.1002/evl3.33

Pedersen, M.W., Ginolhac, A., Orlando, L., Olsen, J., Andersen, K., Holm, J., Funder, S., Willerslev, E., Kjær, K.H., 2013. A comparative study of ancient environmental DNA to pollen and macrofossils from lake sediments reveals taxonomic overlap and additional plant taxa. Quaternary Science Reviews 75, 161–168. doi:10.1016/j.quascirev.2013.06.006

Pedersen, M.W., Ruter, A., Schweger, C., Friebe, H., Staff, R.A., Kjeldsen, K.K., Mendoza, M.L.Z., Beaudoin, A.B., Zutter, C., Larsen, N.K., Potter, B.A., Nielsen, R., Rainville, R.A., Orlando, L., Meltzer, D.J., Kjær, K.H., Willerslev, E., 2016. Postglacial viability and colonization in North America's ice-free corridor. Nature 537, 45–49. doi:10.1038/nature19085

Pennington, W., Tutin, T.G., 1980. Modern pollen samples from west greenland and the interpretation of pollen data fromt he british late-glacial (late Devesian). New Phytologist 84, 171–201. doi:10.1111/j.1469-8137.1980.tb00759.x

Percy, D.M., Argus, G.W., Cronk, Q.C., Fazekas, A.J., Kesanakurti, P.R., Burgess, K.S., Husband, B.C., Newmaster, S.G., Barrett, S.C.H., Graham, S.W., 2014. Understanding the spectacular failure of DNA barcoding in willows (Salix): Does this result from a trans-specific selective sweep? Molecular ecology 4737–4756. doi:10.1111/mec.12837

Perry, D.A., 1978. An estimate of the effective range of pollen dispersal in lodgepole pine (Pinus contorta Dougl.). Annals of Botany 42, 1001–1002. doi:10.1093/oxfordjournals.aob.a085512

Petaev, M.I., Huang, S., Jacobsen, S.B., Zindler, A., 2013. Large Pt anomaly in the Greenland ice core points to a cataclysm at the onset of Younger Dryas. Proceedings of the National Academy of Sciences of the United States of America 110, 12917–12920. doi:10.1073/pnas.1303924110

Piganeau, G., Eyre-Walker, A., Grimsley, N., Moreau, H., 2011. How and why DNA barcodes underestimate the diversity of microbial eukaryotes. PLoS ONE 6. doi:10.1371/journal.pone.0016342

Pigati, J.S., Latorre, C., Rech, J.A., Betancourt, J.L., Martínez, K.E., Budahn, J.R., 2012. Accumulation of impact markers in desert wetlands and implications for the Younger Dryas impact hypothesis. Proceedings of the National Academy of Sciences of the United States of America 109, 7208–7212. doi:10.1073/pnas.1200296109

Pimm, S.L., Jenkins, C.N., Abell, R., Brooks, T.M., Gittleman, J.L., Joppa, L.N., Raven, P.H., Roberts, C.M., Sexton, J.O., 2014. The biodiversity of species and their rates of extinction, distribution, and protection. Science (New York, N.Y.) 344, 1246752. doi:10.1126/science.1246752

Pina-Martins, F., Paulo, O.S., 2015. NCBI Mass Sequence Downloader–Large dataset downloading made easy. SoftwareX 5, 80–83. doi:10.1016/j.softx.2016.04.007

Pino, M., Abarzúa, A.M., Astorga, G., Martel-Cea, A., Cossio-Montecinos, N., Navarro, R.X., Lira, M.P., Labarca, R., LeCompte, M.A., Adedeji, V., Moore, C.R., Bunch, T.E., Mooney, C., Wolbach, W.S., West, A., Kennett, J.P., 2019. Sedimentary record from Patagonia, southern Chile supports cosmic-impact triggering of biomass burning, climate change, and megafaunal extinctions at 12.8 ka. Scientific Reports 9, 1–27. doi:10.1038/s41598-018-38089-y

Pinter, N., Fiedel, S., Keeley, J.E., 2011a. Fire and vegetation shifts in the Americas at the vanguard of Paleoindian migration. Quaternary Science Reviews 30, 269–272. doi:10.1016/j.quascirev.2010.12.010

Pinter, N., Scott, A.C., Daulton, T.L., Podoll, A., Koeberl, C., Anderson, R.S., Ishman, S.E., 2011b. The Younger Dryas impact hypothesis: A requiem. Earth-Science Reviews 106, 247–264. doi:10.1016/j.earscirev.2011.02.005

Pires, M.M., Guimarães, P.R., Galetti, M., Jordano, P., 2018. Pleistocene megafaunal extinctions and the functional loss of long-distance seed-dispersal services. Ecography 41, 153–163. doi:10.1111/ecog.03163

Pitulko, V. V., Nikolsky, P.A., Girya, E.Y., Basilyan, A.E., Tumskoy, V.E., Koulakov, S.A., Astakhov, S.N., Pavlova, E.Y., Anisimov, M.A., 2004. The Yana RHS site: humans in the arctic before the last glacial maximum. Science 303, 52–56.

Pitulko, V. V., Tikhonov, A.N., Pavlova, E.Y., Nikolskiy, P.A., Kuper, K.E., Polozov, R.N., 2016. Early human presence in the Arctic: Evidence from 45,000-year-old mammoth remains. Science 351, 260–263. doi:10.1126/science.aad0554

Poinar, H.N., Hofreiter, M., Spaulding, W.G., Martin, P.S., Stankiewicz, B.A., Bland, H., Evershed, R.P., Possnert, G., Pääbo, S., 1998. Molecular coproscopy: Dung and diet of the extinct ground sloth Nothrotheriops shastensis. Science 281, 402–406.

doi:10.1126/science.281.5375.402

Pop, E., Bakels, C., 2015. Semi-open environmental conditions during phases of hominin occupation at the Eemian Interglacial basin site Neumark-Nord 2 and its wider environment. Quaternary Science Reviews 117, 72–81. doi:10.1016/j.quascirev.2015.03.020

Potter, B.A., 2005. American Paleo-Arctic Tradition. In: Nuttall, M. (Ed.), Encyclopedia of the Arctic: Volumes 1, 2, and 3. Routledge, New York, pp. 76–78.

Potter, B.A., Baichtal, J.F., Beaudoin, A.B., Fehren-Schmitz, L., Haynes, C.V., Holliday, V.T., Holmes, C.E., Ives, J.W., Kelly, R.L., Llamas, B., Malhi, R.S., Miller, D.S., Reich, D., Reuther, J.D., Schiffels, S., Surovell, T.A., 2018. Current evidence allows multiple models for the peopling of the Americas. Science Advances 4, 1–9. doi:10.1126/sciadv.aat5473

Power, M.J., Marlon, J., Ortiz, N., Bartlein, P.J., Harrison, S.P., Mayle, F.E., Ballouche, A., Bradshaw, R.H.W., Carcaillet, C., Cordova, C., Mooney, S., Moreno, P.I., Prentice, I.C., Thonicke, K., Tinner, W., Whitlock, C., Zhang, Y., Zhao, Y., Ali, A.A., Anderson, R.S., Beer, R., Behling, H., Briles, C., Brown, K.J., Brunelle, A., Bush, M., Camill, P., Chu, G.Q., Clark, J., Colombaroli, D., Connor, S., Daniau, A.L., Daniels, M., Dodson, J., Doughty, E., Edwards, M.E., Finsinger, W., Foster, D., Frechette, J., Gaillard, M.J., Gavin, D.G., Gobet, E., Haberle, S., Hallett, D.J., Higuera, P., Hope, G., Horn, S., Inoue, J., Kaltenrieder, P., Kennedy, L., Kong, Z.C., Larsen, C., Long, C.J., Lynch, J., Lynch, E.A., McGlone, M., Meeks, S., Mensing, S., Meyer, G., Minckley, T., Mohr, J., Nelson, D.M., New, J., Newnham, R., Noti, R., Oswald, W., Pierce, J., Richard, P.J.H., Rowe, C., Sanchez Goñi, M.F., Shuman, B.N., Takahara, H., Toney, J., Turney, C., Urrego-Sanchez, D.H., Umbanhowar, C., Vandergoes, M., Vanniere, B., Vescovi, E., Walsh, M., Wang, X., Williams, N., Wilmshurst, J., Zhang, J.H., 2008. Changes in fire regimes since the last glacial maximum: An assessment based on a global synthesis and analysis of charcoal data. Climate Dynamics 30, 887–907. doi:10.1007/s00382-007-0334-x

Powers, W.R., Hoffecker, J.F., 1989. Late Pleistocene Settlement in the Nenana Valley, Central Alaska. American Antiquity 54, 263–287. doi:10.2307/281707

Prüfer, K., Racimo, F., Patterson, N., Jay, F., Sankararaman, S., Sawyer, S., Heinze, A., Renaud, G., Sudmant, P.H., Filippo, C. de, Li, H., Mallick, S., Dannemann, M., Fu, Q., Kircher, M., Kuhlwilm, M., Lachmann, M., Meyer, M., Ongyerth, M., Siebauer, M., Theunert, C., Tandon, A., Moorjani, P., Pickrell, J., Mullikin, J.C., Vohr, S.H., Green, R.E., Hellmann, I., Johnson, P.L.F., Blanche, H., Cann, H., Kitzman, J.O., Shendure, J., Eichler, E.E., Lein, E.S., Bakken, T.E., Golovanova, L. V, Doronichev, V.B., Shunkov, M. V, Derevianko, A.P., Viola, B., Slatkin, M., Reich, D., Kelso, J., Pääbo, S., 2014. The complete genome sequence of a Neanderthal from the Altai Mountains. Nature 505, 43–9. doi:10.1038/nature12886

Rabanus-Wallace, M.T., Wooller, M.J., Zazula, G.D., Shute, E., Jahren, A.H., Kosintsev, P., Burns, J.A., Breen, J., Llamas, B., Cooper, A., 2017. Megafaunal isotopes reveal role of increased moisture on rangeland during late Pleistocene extinctions. Nature

Ecology and Evolution 1, 1–5. doi:10.1038/s41559-017-0125

Rainville, R.A., Gajewski, K., 2013. Holocene environmental history of the Aishihik region, Yukon, Canada. Canadian Journal of Earth Sciences 50, 397–405.

Rasmussen, M., Anzick, S.L., Waters, M.R., Skoglund, P., DeGiorgio, M., Stafford, T.W., Rasmussen, S., Moltke, I., Albrechtsen, A., Doyle, S.M., Poznik, G.D., Gudmundsdottir, V., Yadav, R., Malaspinas, A.-S., White, S.S., Allentoft, M.E., Cornejo, O.E., Tambets, K., Eriksson, A., Heintzman, P.D., Karmin, M., Korneliussen, T.S., Meltzer, D.J., Pierre, T.L., Stenderup, J., Saag, L., Warmuth, V.M., Lopes, M.C., Malhi, R.S., Brunak, S., Sicheritz-Ponten, T., Barnes, I., Collins, M., Orlando, L., Balloux, F., Manica, A., Gupta, R., Metspalu, M., Bustamante, C.D., Jakobsson, M., Nielsen, R., Willerslev, E., 2014. The genome of a Late Pleistocene human from a Clovis burial site in western Montana. Nature 506, 225–9. doi:10.1038/nature13025

Rasmussen, S.O., Andersen, K.K., Svensson, A.M., Steffensen, J.P., Vinther, B.M., Clausen, H.B., Siggaard-Andersen, M.L., Johnsen, S.J., Larsen, L.B., Dahl-Jensen, D., Bigler, M., Röthlisberger, R., Fischer, H., Goto-Azuma, K., Hansson, M.E., Ruth, U., 2006. A new Greenland ice core chronology for the last glacial termination. Journal of Geophysical Research Atmospheres 111, 1–16. doi:10.1029/2005JD006079

Ratnasignham, S., Hebert, P.D., 2007. BARCODING BOLD: The Barcode of Life Data System. Molecular Ecology Notes 7, 355–364. doi:10.1111/j.1471-8286.2006.01678.x

Rawlence, N.J., Lowe, D.J., Wood, J.R., Young, J.M., Churchman, G.J., Huang, Y.T., Cooper, A., 2014. Using palaeoenvironmental DNA to reconstruct past environments: Progress and prospects. Journal of Quaternary Science 29, 610–626. doi:10.1002/jqs.2740

Reimer, P.J., Bard, E., Bayliss, A., Beck, J.W., Blackwell, P.G., Ramsey, C.B., Buck, C.E., Cheng, H., Edwards, R.L., Friedrich, M., Grootes, P.M., Guilderson, T.P., Haflidason, H., Hajdas, I., Hatté, C., Heaton, T.J., Hoffmann, D.L., Hogg, A.G., Hughen, K.A., Kaiser, K.F., Kromer, B., Manning, S.W., Niu, M., Reimer, R.W., Richards, D.A., Scott, E.M., Southon, J.R., Staff, R.A., Turney, C.S.M., Plicht, J. van der, 2013. IntCal13 and Marine13 Radiocarbon Age Calibration Curves 0–50,000 Years cal BP. Radiocarbon 55, 1869–1887. doi:10.2458/azu_js_rc.55.16947

Reitz, E.J., Schakley, M., 2012. Environmental Archaeology. Springer, New York.

Remane, J., Bassett, M.G., Cowie, J.W., Gohrbandt, K.H., Lane, H.R., Michelsen, O., Naiwen, W., 1996. Revised guidelines for the establishment of global chronostratigraphic standards by the International Commission on Stratigraphy (ICS). Episodes. doi:10.18814/epiiugs/1996/v19i3/007

Remmers, W., Gamerio, J., Schaberl, I., Clausnitzer, V., 2016. Elephant (Loxodonta africana) footprints as habitat for aquatic macroinvertebrate communities in Kibale National Park, south-west Uganda. African Journal of Ecology 1–10. doi:10.1111/aje.12358

Renaud, G., Stenzel, U., Kelso, J., 2014. LeeHom: Adaptor trimming and merging for Illumina sequencing reads. Nucleic Acids Research 42, e141. doi:10.1093/nar/gku699

Reumer, J.W.F., Rook, L., Borg, K. Van Der, Post, K., Mol, D., Vos, J. De, 2003. Late Pleistocene survival of the saber-toothed cat Homotherium in northwestern Europe. Journal of Vertebrate Paleontology 23, 260–262. doi:10.1671/0272-4634(2003)23[260:LPSOTS]2.0.CO;2

Richards, M.P., Pettitt, P.B., Stiner, M.C., Trinkaus, E., 2001. Stable isotope evidence for increasing dietary breadth in the European mid-Upper Paleolithic. Proceedings of the National Academy of Sciences of the United States of America 98, 6528–6532. doi:10.1073/pnas.111155298

Richerson, P.J., Boyd, R., 2005. Not by Genes Alone: How Culture Transformed Human Evolution. The University of Chicago Press, Chicago and London.

Richerson, P.J., Boydb, R., Henrichc, J., 2010. Gene-culture coevolution in the age of genomics. Proceedings of the National Academy of Sciences of the United States of America 107, 8985–8992. doi:10.1073/pnas.0914631107

Riede, F., 2011. Adaptation and niche construction in human prehistory: a case study from the southern Scandinavian Late Glacial. Philosophical transactions of the Royal Society of London 366, 793–808. doi:10.1098/rstb.2010.0266

Riede, F., 2012. Theory for the a-theoretical: Niche construction theory and its implications for environmental archaeology. In: Berge, R., Jasinski, M.E., Sognnes, K. (Eds.), N-TAG TEN. Proceedings of the 10th Nordic TAG Conference at Stiklestad, Norway 2009. Archaeopress, Oxford, pp. 87–98.

Ries, L., Fletcher, R.J.J., Battin, J., Sisk, T.D., 2004. Ecological responses to habitat edges: Mechanisms, models, and variability explained. Annual Review of Ecology, Evolution, and Systematics. doi:10.1146/annurev.ecolsys.35.112202.130148

Ripple, W.J., Valkenburgh, B. Van, 2010. Linking Top-down Forces to the Pleistocene Megafaunal Extinctions. BioScience 60, 516–526. doi:10.1525/bio.2010.60.7.7

Ripple, W.J., Wolf, C., Newsome, T.M., Betts, M.G., Ceballos, G., Courchamp, F., Hayward, M.W., Valkenburgh, B. Van, Wallach, A.D., Worm, B., 2019. Are we eating the world's megafauna to extinction? Conservation Letters 1–10. doi:10.1111/conl.12627

Roach, N.T., Venkandesan, M., Rainbow, M.J., Lieberman, D.E., 2013. Elastic energy storage in the shoulder and the evolution of high-speed throwing in Homo. Nature 498, 483–486. doi:10.1038/nature12267.Elastic

Robinson, G.S., Burney, L.P., Burney, D.A., 2005. Landscape paleoecology and megafaunal extinction in southeastern New York State. Ecological Monographs 75, 295–315. doi:10.1890/03-4064

Rodríguez-Rey, M., Herrando-Pérez, S., Gillespie, R., Jacobs, Z., Saltré, F., Brook, B.W., Prideaux, G.J., Roberts, R.G., Cooper, A., Alroy, J., Miller, G.H., Bird, M.I., Johnson, C.N., Beeton, N., Turney, C.S.M., Bradshaw, C.J.A., 2015. Criteria for

assessing the quality of Middle Pleistocene to Holocene vertebrate fossil ages. Quaternary Geochronology 30, 69–79. doi:10.1016/j.quageo.2015.08.002

Roebroeks, W., Villa, P., 2011. Reply to Sandgathe et al.: Neandertal use of fire. Proceedings of the National Academy of Sciences 108, E299–E299. doi:10.1073/pnas.1108129108

Roebroeks, W., Villa, P., Trinkaus, E., Roebroeks, W., Villabcd, P., 2011. On the earliest evidence for habitual use of fire in Europe Wil Roebroeksa,1 and Paola Villa. Proceedings of the National Academy of Sciences of the United States of America 108, 5209–5214. doi:10.1073/pnas.1018116108/-/DCSupplemental.www.pnas.org/cgi/doi/10.1073/pnas.1018116108

Roopnarine, P.D., 2014. Humans are apex predators. Proceedings of the National Academy of Sciences of the United States of America 111, 2014. doi:10.1073/pnas.1323645111

Roos, C.I., Zedeño, M.N., Hollenback, K.L., Erlick, M.M.H., 2018. Indigenous impacts on North American Great Plains fire regimes of the past millennium. Proceedings of the National Academy of Sciences 201805259. doi:10.1073/pnas.1805259115

Rothschild, B.M., Laub, R., 2006. Hyperdisease in the late Pleistocene: validation of an early 20th century hypothesis. Die Naturwissenschaften 93, 557–564. doi:10.1007/s00114-006-0144-8

Roux, E. le, Kerley, G.I.H., Cromsigt, J.P.G.M., 2018. Megaherbivores Modify Trophic Cascades Triggered by Fear of Predation in an African Savanna Ecosystem. Current Biology 28, 2493-2499.e3. doi:10.1016/j.cub.2018.05.088

Rowley-Conwy, P., Layton, R., 2011. Foraging and farming as niche construction: stable and unstable adaptations. Philosophical transactions of the Royal Society of London. Series B, Biological sciences 366, 849–862. doi:10.1098/rstb.2010.0307

Roy, I., Ranhotra, P.S., Shekhar, M., Bhattacharyya, A., Pal, A.K., Sharma, Y.K., Singh, S.P., Singh, U., 2018. Over-representation of some taxa in surface pollen analysis misleads the interpretation of fossil pollen spectra in terms of extant vegetation. Tropical Ecology 59, 339–350.

Rozas-Dávila, A., Valencia, B.G., Bush, M.B., 2016. The functional extinction of Andean megafauna. Ecology 97, 2533–2539. doi:10.1002/ecy.1531

Rozzi, F.V.R., D'Errico, F., Vanhaeren, M., Grootes, P.M., Kerautret, B., Dujardin, V., 2009. Cutmarked human remains bearing Neandertal features and modern human remains associated with the Aurignacian at Les Rois. Journal of Anthropological Sciences 87, 153–185.

Rule, S., Brook, B.W., Haberle, S.G., Turney, C.S.M., Kershaw, A.P., Johnson, C.N., 2012. The aftermath of megafaunal extinction: Ecosystem transformation in Pleistocene Australia. Science 335, 1483–1486. doi:10.1126/science.1214261

Sadoway, T.R., 2014. A Metagenomic Analysis of Ancient Sedimentary DNA Across the Pleistocene-Holocene Transition. McMaster University.

Saeki, K., Sakai, M., Wada, S.I., 2010. DNA adsorption on synthetic and natural allophanes. Applied Clay Science 50, 493–497. doi:10.1016/j.clay.2010.09.015

Saiki, R.K., Scharf, S., Faloona, F., Mullis, K.B., Horn, G.T., Erlich, H.A., Arnheim, N., 1985. Enzymatic Amplification of P-Globin Genomic Sequences and Restriction Site Analysis for Diagnosis of Sickle Cell Anemia. Science 230.

Saiki, R.K., Gelfand, D.H., Stoffel, S., Scharf, S.J., Higuchi, R., Horn, G.T., Mullis, K.B., Erlich, H.A., 1988. Primer-directed enzymatic amplification of DNA with a thermostable DNA polymerase. Science 239, 487–491. doi:10.1126/science.2448875

Sandgathe, D.M., Dibble, H.L., Goldberg, P., McPherron, S.P., Turq, A., Niven, L., Hodgkins, J., 2011. Timing of the Appearance of Habitual Fire Use. Proceedings of the National Academy of Sciences of the United States of America 108, E298; author reply E299. doi:10.1073/pnas.1106759108

Sandom, C., Faurby, S., Sandel, B., Svenning, J.-C., 2014a. Global late Quaternary megafauna extinctions linked to humans, not climate change. Proceedings of the Royal Society of London B: Biological Sciences 281, 20133254. doi:10.1098/rspb.2013.3254

Sandom, C.J., Ejrnæs, R., Hansen, M.D.D., Svenning, J.-C., 2014b. High herbivore density associated with vegetation diversity in interglacial ecosystems. Pnas 111, 4162–7. doi:10.1073/pnas.1311014111

Sano, K., 2007. Emergence and Mobility of Microblade Industries in the Japanese Islands. In: Kuzmin, Y. V., Keates, S.G., Shen, C. (Eds.), Origin and Spread of Microbalde Technology in Northeastern Asia and North America. Archaeology Press, Simon Fraser University, Burnaby, B.C., pp. 79–90.

Säterberg, T., Sellman, S., Ebenman, B., 2013. High frequency of functional extinctions in ecological networks. Nature 499, 468–470. doi:10.1038/nature12277

Sato, H., Tsutsumi, T., 2007. The Japanese microblade industries: technology, raw material procurement, and adaptations. In: Kuzmin, Y.V., Keates, S.G., Shen, C. (Eds.), Origin and Spread of Microblade Technology in Northern Asia and North America. Archaeology Press, Simon Fraser University, Burnaby, Canada, pp. 53–78.

Savelle, J.M., Dyke, A.S., 2002. Variability in palaeoeskimo occupation on south-western Victoria Island, Arctic Canada: Causes and consequences. World Archaeology 33, 508–522. doi:10.1080/00438240120107503

Savelle, J.M., Dyke, A.S., 2009. Palaeoeskimo Demography on Western Boothia Peninsula, Arctic Canada. Journal of Field Archaeology 34, 267–283.

Sawyer, S., Krause, J., Guschanski, K., Savolainen, V., Pääbo, S., 2012. Temporal patterns of nucleotide misincorporations and DNA fragmentation in ancient DNA. PloS one 7, e34131. doi:10.1371/journal.pone.0034131

Saylor, C.R., Alsharif, K.A., Torres, H., 2017. The importance of traditional ecological knowledge in agroecological systems in peru. International Journal of Biodiversity Science, Ecosystem Services and Management 13, 150–161. doi:10.1080/21513732.2017.1285814

Scherjon, F., Bakels, C., MacDonald, K., Roebroeks, W., 2015. Burning the Land. Current Anthropology 56, 299–326. doi:10.1086/681561

Schlager, B., Straessle, A., Hafen, E., 2012. Use of anionic denaturing detergents to purify insoluble proteins after overexpression. BMC Biotechnology 12. doi:10.1186/1472-6750-12-95

Schmidt, K., 2010. Göbekli Tepe - The Stone Age Sanctuaries. New results of ongoing excavations with a special focus on sculptures and high reliefs. Documenta Praehistorica 37, 239–256. doi:10.4312/dp.37.21

Schofield, E.J., Edwards, K.J., McMullen, A.J., 2007. Modern Pollen-Vegetation Relationships in Subarctic Southern Greenland and the Interpretation of Fossil Pollen Data from the Norse landnám. Journal of Biogeography 34, 473–488. doi:10.1111/j.1365-2699.2006.01607.x

Schuenemann, V.J., Bos, K., DeWitte, S., Schmedes, S., Jamieson, J., Mittnik, a., Forrest, S., Coombes, B.K., Wood, J.W., Earn, D.J.D., White, W., Krause, J., Poinar, H.N., 2011. PNAS Plus: From the Cover: Targeted enrichment of ancient pathogens yielding the pPCP1 plasmid of Yersinia pestis from victims of the Black Death. Proceedings of the National Academy of Sciences 108, E746–E752. doi:10.1073/pnas.1105107108

Schweger, C., Froese, D., White, J.M., Westgate, J.A., 2011. Pre-glacial and interglacial pollen records over the last 3 Ma from northwest Canada: Why do Holocene forests differ from those of previous interglaciations? Quaternary Science Reviews 30, 2124–2133. doi:10.1016/j.quascirev.2011.01.020

Seersholm, F. V., Werndly, D.J., Grealy, A., Johnson, T., Keenan Early, E.M., Lundelius, E.L., Winsborough, B., Farr, G.E., Toomey, R., Hansen, A.J., Shapiro, B., Waters, M.R., McDonald, G., Linderholm, A., Stafford, T.W., Bunce, M., 2020. Rapid range shifts and megafaunal extinctions associated with late Pleistocene climate change. Nature Communications 11, 1–10. doi:10.1038/s41467-020-16502-3

Shaban, I.S., Mikulaj, V., 1998. Impact of an Anionic Surfactant Addition on Solubility of Humic Acid in Acid-Alkaline Solutions. Chemical Papers 52, 753–755.

Shackleton, N.J., Sanchez-Goni, M.F., Pailler, D., Lancelot, Y., 2003. Marine isotope substage 5e and the Eemian interglacial. Global and Planetary Change 36, 151–155. doi:10.1016/S0921-8181(02)00181-9

Shah, N., Nute, M.G., Warnow, T., Pop, M., 2019. Misunderstood parameter of NCBI BLAST impacts the correctness of bioinformatics workflows. Bioinformatics 35, 1613–1614. doi:10.1093/bioinformatics/bty833

Shapiro, B., 2015. How to clone a mammoth: The science of de-extinction. Princeton University Press.

Shapiro, B., Drummond, A.J., Rambaut, A., Wilson, M.C., Matheus, P.E., Sher, A. V., Pybus, O.G., Gilbert, M.T.P., Barnes, I., Binladen, J., Willerslev, E., Hansen, A.J., Baryshnikov, G.F., Burns, J.A., Davydov, S., Driver, J.C., Froese, D.G., Harington, C.R., Keddie, G., Kosintsev, P., Kunz, M.L., Martin, L.D., Stephenson, R.O., Storer, J., Tedford, R., Zimov, S., Cooper, A., 2004. Rise and fall of the Beringian steppe

bison. Science (New York, N.Y.) 306, 1561–1565. doi:10.1126/science.1101074

Shen, Y.Y., Chen, X., Murphy, R.W., 2013. Assessing DNA Barcoding as a Tool for Species Identification and Data Quality Control. PLoS ONE 8, 1–5. doi:10.1371/journal.pone.0057125

Shimelmitz, R., Kuhn, S.L., Jelinek, A.J., Ronen, A., Clark, A.E., Weinstein-Evron, M., 2014. "Fire at will": The emergence of habitual fire use 350,000 years ago. Journal of Human Evolution 77, 196–203. doi:10.1016/j.jhevol.2014.07.005

Sidstedt, M., Jansson, L., Nilsson, E., Noppa, L., Forsman, M., Rådström, P., Hedman, J., 2015. Humic substances cause fluorescence inhibition in real-time polymerase chain reaction. Analytical Biochemistry 487, 30–37. doi:10.1016/j.ab.2015.07.002

Signor, P.W., Lipps, J.H., 1982. Sampling bias, gradual extinction patterns and catastrophes in the fossil record. GSA SPECIAL PAPERS 190, 291–296.

Sjögren, P., Edwards, M.E., Gielly, L., Langdon, C.T., Croudace, I.W., Merkel, M.K.F., Fonville, T., Alsos, I.G., 2017. Lake sedimentary DNA accurately records 20th Century introductions of exotic conifers in Scotland. New Phytologist 1–13. doi:10.1111/nph.14199

Slon, V., Glocke, I., Barkai, R., Gopher, A., Hershkovitz, I., Meyer, M., 2016. Mammalian mitochondrial capture, a tool for rapid screening of DNA preservation in faunal and undiagnostic remains, and its application to Middle Pleistocene specimens from Qesem Cave (Israel). Quaternary International 398, 210–218. doi:10.1016/j.quaint.2015.03.039

Slon, V., Hopfe, C., Weiß, C.L., Mafessoni, F., La Rasilla, M. De, Lalueza-Fox, C., Rosas, A., Soressi, M., Knul, M. V., Miller, R., Stewart, J.R., Derevianko, A.P., Jacobs, Z., Li, B., Roberts, R.G., Shunkov, M. V., Lumley, H. De, Perrenoud, C., Gušić, I., Kućan, Ž., Rudan, P., Aximu-Petri, A., Essel, E., Nagel, S., Nickel, B., Schmidt, A., Prüfer, K., Kelso, J., Burbano, H.A., Pääbo, S., Meyer, M., 2017. Neandertal and Denisovan DNA from Pleistocene sediments. Science 356, 605–608. doi:10.1126/science.aam9695

Smith, B.D., 2007. Niche construction and the behavioral context of plant and animal domestication. Evolutionary Anthropology 16, 188–199. doi:10.1002/evan.20135

Smith, B.D., 2009. Resource Resilience, Human Niche Construction, and the Long-Term Sustainability of Pre-Columbian Subsistence Economies in the Mississippi River Valley Corridor. Journal of Ethnobiology 29, 167–183. doi:10.2993/0278-0771-29.2.167

Smith, B.D., 2011. General patterns of niche construction and the management of 'wild' plant and animal resources by small-scale pre-industrial societies. Philosophical Transactions of the Royal Society B: Biological Sciences 366.

Smith, B.D., Zeder, M.A., 2013. The onset of the Anthropocene. Anthropocene 4, 8–13. doi:10.1016/j.ancene.2013.05.001

Smith, D., Ferguson, G., 2012. Decade of the Wolf, Revised and Updated: Returning The Wild To Yellowstone. Lyons Press, Guilford, USA.

Smith, F.A., Hammond, J.I., Balk, M.A., Elliott, S.M., Lyons, S.K., Pardi, M.I., Tomé, C.P., Wagner, P.J., Westover, M.L., 2015. Exploring the influence of ancient and historic megaherbivore extirpations on the global methane budget. Proceedings of the National Academy of Sciences 113, 201502547. doi:10.1073/pnas.1502547112

Smith, F.A., Doughty, C.E., Malhi, Y., Svenning, J.C., Terborgh, J., 2016. Megafauna in the Earth system. Ecography 39, 99–108. doi:10.1111/ecog.02156

Smith, F.A., Smith, R.E.E.E., Lyons, S.K., Payne, J.L., 2018. Body size downgrading of mammals over the late Quaternary. Science 360, 310–313. doi:10.1126/science.aao5987

Smith, J.A., Suraci, J.P., Clinchy, M., Crawford, A., Roberts, D., Zanette, L.Y., Wilmers, C.C., 2017. Fear of the human 'super predator' reduces feeding time in large carnivores. Proceedings of the Royal Society B: Biological Sciences 284. doi:10.1098/rspb.2017.0433

Søe, M.J., Nejsum, P., Seersholm, F.V., Fredensborg, B.L., Habraken, R., Haase, K., Hald, M.M., Simonsen, R., Højlund, F., Blanke, L., Merkyte, I., Willerslev, E., Kapel, C.M.O., 2018. Ancient DNA from latrines in Northern Europe and the Middle East (500 BC–1700 AD) reveals past parasites and diet. Plos One 13, e0195481. doi:10.1371/journal.pone.0195481

Soininen, E.M., Gauthier, G., Bilodeau, F., Berteaux, D., Gielly, L., Taberlet, P., Gussarova, G., Bellemain, E., Hassel, K., Stenoien, H.K., Epp, L., Schroder-Nielsen, A., Brochmann, C., Yoccoz, N.G., 2015. Highly overlapping winter diet in two sympatric lemming species revealed by DNA metabarcoding. PLoS ONE 10, 1–18. doi:10.1371/journal.pone.0115335

Sønstebø, J.H., Gielly, L., Brysting, A.K., Elven, R., Edwards, M., Haile, J., Willerslev, E., Coissac, E., Rioux, D., Sannier, J., Taberlet, P., Brochmann, C., Sonstebo, J.H., Gielly, L., Brysting, A.K., Elven, R., Edwards, M., Haile, J., Willerslev, E., Coissac, E., Rioux, D., Sannier, J., Taberlet, P., Brochmann, C., 2010. Using next-generation sequencing for molecular reconstruction of past Arctic vegetation and climate. Molecular Ecology Resources 10, 1009–1018. doi:10.1111/j.1755-0998.2010.02855.x

Spaulding, A.C., 1946. Northeastern Archaeology and General Trends in the Northern Forest Zone. In: Johnson, F. (Ed.), Man in Northeastern North America. Papers of the Robert S. Peabody Foundation for Archaeology, Vol. 3. Philips Academcy, Andover, pp. 146–167.

Speck, F.G., 1915. The family hunting band as the basis of Algonkian social organization. American Anthropologist 17, 289–305.

Speth, J.D., 2010. The Paleoanthropology and Archaeology of Big-Game Hunting: Protein, Fat, or Politics? Springer, New York. https://doi. org/10.1007/978-1-4419-6733-6, New York.

Sterelny, K., 2001. Niche construction, developmental systems, and the extended replicator. In: Oyama, S., Griffiths, P.E., Gray, R.D. (Eds.), Cycles of Contingency: Developmental Systems and Evolution. MIT Press, Cambridge, pp. 333–349.

Steven, B., Briggs, G., McKay, C.P., Pollard, W.H., Greer, C.W., Whyte, L.G., 2007. Characterization of the microbial diversity in a permafrost sample from the Canadian high Arctic using culture-dependent and culture-independent methods. FEMS Microbiology Ecology 59, 513–523. doi:10.1111/j.1574-6941.2006.00247.x

Stivrins, N., Soininen, J., Amon, L., Fontana, S.L., Gryguc, G., Heikkilä, M., Heiri, O., Kisielienė, D., Reitalu, T., Stančikaitė, M., Veski, S., Seppä, H., 2016. Biotic turnover rates during the Pleistocene-Holocene transition. Quaternary Science Reviews 151, 100–110. doi:10.1016/j.quascirev.2016.09.008

Stolzenburg, W., 2008. Where the Wild Things Were: Life, Death, and Ecological Wreckage In A Land Of Vanishing Predators. Bloomsbury Press, New York.

Strong, W.L., Hills, L. V., 2013. Holocene migration of lodgepole pine (Pinus contorta var. latifolia) in southern Yukon, Canada. Holocene 23, 1340–1349. doi:10.1177/0959683613484614

Stuart, A.J., 2015. Late Quaternary megafaunal extinctions on the continents: a short review. Geological Journal 50, 414–433. doi:10.1002/gj

Stuart, G.S.L., 1986. An Archaeological and paleoenvironmental correlation for the Kluane-Aishihik area, southwest Yukon, Canada. University of Calgary.

Stuiver, M., Reimer, P.J., 1993. Extended 14C data base and revised CALIB 3.0 14C age calibration program. Radiocarbon 35, 215–230. doi:10.2458/azu_js_rc.35.1561

Stuiver, M., Reimer, P.J., Reimer, R.W., 2020. CALIB 8.2.

Subramanian, M., 2019. Humans Versus Earth. Nature 572, 168–170. doi:http://dx.doi.org/10.1038/d41586-019-02381-2

Suraci, J.P., Clinchy, M., Zanette, L.Y., Wilmers, C.C., 2019. Fear of humans as apex predators has landscape-scale impacts from mountain lions to mice. Ecology Letters 22, 1578–1586. doi:10.1111/ele.13344

Surovell, T. a, Waguespack, N.M., 2009. Human Prey Choice in the Late Pleistocene and Its Relation to Megafaunal Extinctions. American Megafaunal Extinctions at the End of the Pleistocene 77–105.

Svenning, J.-C., Pedersen, P.B.M., Donlan, J., Ejrnaes, R., Faurby, S., Galetti, M., Hansen, D.M., Sandel, B., Sandom, C.J., Terborgh, J., Vera, F.W.M., 2015. Science for a wilder Anthropocene -synthesis and future directions for rewilding research. Pnas 113, 1–7. doi:10.1073/pnas.1502556112

Swadling, P., Hide, R., 2005. Changing landscape and social interaction: Looking at agricultural history from a Sepik-Ramu perspective. In: A. Pawley, R., Attenborough, J., Golson, J., Hide, R. (Eds.), Papuan Pasts: Cultural, Linguistic and Biological Histories of Papuan-Speaking Peoples. Australian National University, Research School of Pacific & Asian Studies, Canberra, Australia, pp. 289–327.

Swanson, M.E., Franklin, J.F., Beschta, R.L., Crisafulli, C.M., DellaSala, D.A., Hutto, R.L., Lindenmayer, D.B., Swanson, F.J., 2010. The forgotten stage of forest succession: early-successional ecosystems on forest sites. Frontiers in Ecology and the Environment 9, 117–125. doi:10.1890/090157

Swift, J.A., Bunce, M., Dortch, J., Douglass, K., Faith, J.T., Fellows Yates, J.A., Field, J., Haberle, S.G., Jacob, E., Johnson, C.N., Lindsey, E., Lorenzen, E.D., Louys, J., Miller, G., Mychajliw, A.M., Slon, V., Villavicencio, N.A., Waters, M.R., Welker, F., Wood, R., Petraglia, M., Boivin, N., Roberts, P., 2019. Micro Methods for Megafauna: Novel Approaches to Late Quaternary Extinctions and Their Contributions to Faunal Conservation in the Anthropocene. BioScience 69, 877–887. doi:10.1093/biosci/biz105

Sze, M.A., Schloss, P.D., 2019. The impact of DNA polymerase and number of rounds of amplification in PCR on 16S rRNA gene sequence data. bioRxiv 565598. doi:10.1101/565598

Taberlet, P., Coissac, E., Pompanon, F., Gielly, L., Miquel, C., Valentini, A., Vermat, T., Corthier, G., Brochmann, C., Willerslev, E., 2007. Power and limitations of the chloroplast trnL (UAA) intron for plant DNA barcoding. Nucleic Acids Research 35, e14. doi:10.1093/nar/gkl938

Taberlet, P., Coissac, E., Hajibabaei, M., Rieseberg, L.H., 2012. Environmental DNA. Molecular Ecology 21, 1789–1793. doi:10.1111/j.1365-294X.2012.05542.x

Taberlet, P., Bonin, A., Zinger, L., Coissac, E., 2018. Environmental DNA: For Biodiversity Research and Monitoring. Oxford University Press, Oxford, U.K.

Takahara, T., Minamoto, T., Yamanaka, H., Doi, H., Kawabata, Z., 2012. Estimation of fish biomass using environmental DNA. PLoS ONE 7, 3–10. doi:10.1371/journal.pone.0035868

Takahashi, Y., Tatsuma, T., 2014. Metal oxides and hydroxides as rechargeable materials for photocatalysts with oxidative energy storage abilities. Electrochemistry 82, 749–751. doi:10.5796/electrochemistry.82.749

Tan, S.C., Yiap, B.C., 2009. DNA, RNA, and protein extraction: The past and the present. Journal of Biomedicine and Biotechnology 2009. doi:10.1155/2009/574398

Tanford, C., 1980. The hydrophobic effect: formation of micelles and biological membranes, 2nd editio. ed. Wiley Interscience, New York.

Tarasov, P., Granoszewski, W., Bezrukova, E., Brewer, S., Nita, M., Abzaeva, A., Oberhänsli, H., 2005. Quantitative reconstruction of the last interglacial vegetation and climate based on the pollen record from Lake Baikal, Russia. Climate Dynamics 25, 625–637. doi:10.1007/s00382-005-0045-0

Taylor, B.R., Parkinson, D., 1988. Patterns of water absorption and leaching in pine and aspen leaf litter. Soil Biology and Biochemistry 20, 257–258. doi:10.1016/0038-0717(88)90047-8

Thomas, K., 2001. Environmental archaeology is dead: long live bioarchaeology, geoarchaeology and human palaeoecology. A comment on “Environmental archaeology is not human palaeoecology.” In: Albarella, U. (Ed.), Environmental Archaeology: Meaning and Purpose. Kluwer Academic Publishers, Dordrecht, The Netherlands, pp. 55–58.

Thomsen, P.F., Willerslev, E., 2015. Environmental DNA - An emerging tool in conservation for monitoring past and present biodiversity. Biological Conservation 183, 4–18. doi:10.1016/j.biocon.2014.11.019

Todd, N.E., 2006. Trends in proboscidean diversity in the African Cenozoic. Journal of Mammalian Evolution 13, 1–10. doi:10.1007/s10914-005-9000-4

Tomasello, M., 2014. Horizon The ultra-social animal. European Journal of Social Psychology 44, 187–194.

Tremblay, R., Landry-Cuerrier, M., Humphries, M.M., 2020. Culture and the social-ecology of local food use by indigenous communities in northern North America. Ecology and Society 25, 1–26. doi:10.5751/ES-11542-250208

Trigger, B.G., 2006. A History of Archaeological Thought. Cambridge University Press, Cambridge.

Tu, Q., Yu, H., He, Z., Deng, Y., Wu, L., Nostrand, J.D. Van, Zhou, A., Voordeckers, J., Lee, Y.J., Qin, Y., Hemme, C.L., Shi, Z., Xue, K., Yuan, T., Wang, A., Zhou, J., 2014. GeoChip 4: A functional gene-array-based high-throughput environmental technology for microbial community analysis. Molecular Ecology Resources 14, 914–928. doi:10.1111/1755-0998.12239

Turner, N., Deur, D., 2005. Keeping it living: Traditions of plant use and cultivation on the Northwest Coast of North America. University of Washington Press, Seattle, WA.

Turney, C.S.M., Jones, R.T., 2010. Does the Agulhas Current amplify global temperatures during super-interglacials? Journal of Quaternary Science 25, 839–843. doi:10.1002/jqs.1423

Uchida, K., Kamura, K., 2020. Traditional Ecological Knowledge Maintains Useful Plant Diversity in Semi-natural Grasslands in the Kiso Region, Japan. Environmental Management 65, 478–489. doi:10.1007/s00267-020-01255-y

Vachula, R.S., Huang, Y., Russell, J.M., Abbott, M.B., Finkenbinder, M.S., O'Donnell, J.A., 2020. Sedimentary biomarkers reaffirm human impacts on northern Beringian ecosystems during the Last Glacial period. Boreas 49, 514–525. doi:10.1111/bor.12449

Valen, L. Van, 1973. A new evolutionary law. Evol. Theor. 1, 1–30.

Valkenburgh, B. Van, Hayward, M.W., Ripple, W.J., Meloro, C., Roth, V.L., 2015. The impact of large terrestrial carnivores on Pleistocene ecosystems. Proceedings of the National Academy of Sciences 113, 1–6. doi:10.1073/pnas.1502554112

Valls, A., Coll, M., Christensen, V., 2015. Keystone species: Toward an operational concept for marine biodiversity conservation. Ecological Monographs 85, 29–47. doi:10.1890/14-0306.1

Vartanyan, S.L., Arslanov, K.A., Karhu, J.A., Possnert, G., Sulerzhitsky, L.D., 2008. Collection of radiocarbon dates on the mammoths (Mammuthus primigenius) and other genera of Wrangel Island, northeast Siberia, Russia. Quaternary Research 70, 51–59. doi:10.1016/j.yqres.2008.03.005

Velázquez-Rosas, N., Silva-Rivera, E., Ruiz-Guerra, B., Armenta-Montero, S., González, J.T., 2018. Traditional ecological knowledge as a tool for biocultural landscape restoration in northern Veracruz, Mexico: A case study in El Tajín region. Ecology and Society 23. doi:10.5751/ES-10294-230306

Vos, J.M. De, Joppa, L.N., Gittleman, J.L., Stephens, P.R., Pimm, S.L., 2015. Estimating the normal background rate of species extinction. Conservation Biology 29, 452–462. doi:10.1111/cobi.12380

Wales, N., Andersen, K., Cappellini, E., Ávila-Arcos, M.C., Gilbert, M.T.P., 2014. Optimization of DNA recovery and amplification from non-carbonized archaeobotanical remains. PLoS ONE 9. doi:10.1371/journal.pone.0086827

Wallace, A.R., 1876. The geographical distribution of animals, with a study of the relations of living and extinct faunas as elucidating past changes of the earth's surface, vol. 1. ed. Harper and Brothers, New York.

Wang, X.-C., Geurts, M.-A., 1991a. Late Quaternary pollen records and vegetation history of the southwest Yukon Territory: a review. Geographie Physique et Quaternaire 45, 175–193. doi:10.7202/032859ar

Wang, X.-C., Geurts, M.-A., 1991b. Post-glacial vegetation history of the Ittlemit Lake basin, southwest Yukon Territory. Arctic 44, 23–30. doi:10.14430/arctic1514

Wang, X., 1989. Post-Glacial Vegetation History of the Aishihik Basin and Its Vicinity, Southwest Yukon Territory: a Palynological Perspective. University of Ottawa, Ontario.

Ward Jones, M.K., Pollard, W.H., Jones, B.M., 2019. Rapid initialization of retrogressive thaw slumps in the Canadian high Arctic and their response to climate and terrain factors. Environmental Research Letters 14. doi:10.1088/1748-9326/ab12fd

Warinner, C., Speller, C., Collins, M.J., Lewis, C.M., 2015. Ancient human microbiomes. Journal of Human Evolution 79, 125–136. doi:10.1016/j.jhevol.2014.10.016

Waters, C.N., Zalasiewicz, J., Summerhayes, C., Barnosky, A.D., Poirier, C., Ga, A., Cearreta, A., Edgeworth, M., Ellis, E.C., Ellis, M., Jeandel, C., Leinfelder, R., Mcneill, J.R., Richter, D., Steffen, W., Syvitski, J., Vidas, D., Wagreich, M., Williams, M., Zhisheng, A., Grinevald, J., Odada, E., Oreskes, N., Wolfe, A.P., 2016. The Anthropocene is functionally and stratigraphically distinct from the Holocene. Science 351, 1–10. doi:10.1126/science.aad2622

Waters, M.R., Stafford Jr, T.W., 2007. Redefining the Age of Clovis : Science 315, 1122–1126. doi:10.1126/science.1137166

Waugh, J., 2007. DNA barcoding in animal species: Progress, potential and pitfalls. BioEssays 29, 188–197. doi:10.1002/bies.20529

Wei, N., Nakajima, F., Tobino, T., 2018. A Microcosm Study of Surface Sediment Environmental DNA: Decay Observation, Abundance Estimation, and Fragment Length Comparison. Environmental Science and Technology 52, 12428–12435. doi:10.1021/acs.est.8b04956

Weissensteiner, H., Pacher, D., Kloss-Brandstätter, A., Forer, L., Specht, G., Bandelt, H.J., Kronenberg, F., Salas, A., Schönherr, S., 2016. HaploGrep 2: mitochondrial haplogroup classification in the era of high-throughput sequencing. Nucleic Acids Research 44, W58–W63. doi:10.1093/nar/gkw233

Wentzel, W.F., 1889. Letters to the Hon. Roderic Mckenzie, 1807–1824. In: Masson, L.R. (Ed.), Les Bourgeois de La Compagine Du Nord-Quest, Volume I. Imprimerie Générale A. Coté et Cie, Québec, pp. 67–153.

Werdelin, L., Lewis, M.E., 2013. Temporal Change in Functional Richness and Evenness in the Eastern African Plio-Pleistocene Carnivoran Guild. PLoS ONE 8, 1–11. doi:10.1371/journal.pone.0057944

West, F.H., 1967. The Donnelly Ridge Site and the Definition of an Early Core and Blade Complex in Central Alaska. American Antiquity 32, 360–382. doi:10.2307/2694665

West, F.H., 1975. Dating Denali Complex. Arctic Anthropology 12, 76–81.

West, F.H., 1981. The Archaeology of Beringia. Columbia University Press, New York.

West, F.H., 1996. The Archaeological Evidence. In: West, F.H. (Ed.), American Beginnings: The Prehistory and Paleoecology of Beringia. University of Chicago Press, Chicago, pp. 537–559.

Westgate, J.A., Preece, S.J., Kotler, E., Hall, S., 2000. Dawson tephra: A prominent stratigraphic marker of Late Wisconsinan age in west-central Yukon, Canada. Canadian Journal of Earth Sciences 37, 621–627. doi:10.1139/e99-117

Weyrich, L.S., Dobney, K., Cooper, A., 2015. Ancient DNA analysis of dental calculus. Journal of Human Evolution 79, 119–124. doi:10.1016/j.jhevol.2014.06.018

Weyrich, L.S., Duchene, S., Soubrier, J., Arriola, L., Llamas, B., Breen, J., Morris, A.G., Alt, K.W., Caramelli, D., Dresely, V., Farrell, M., Farrer, A.G., Francken, M., Gully, N., Haak, W., Hardy, K., Harvati, K., Held, P., Holmes, E.C., Kaidonis, J., Lalueza-Fox, C., La Rasilla, M. De, Rosas, A., Semal, P., Soltysiak, A., Townsend, G., Usai, D., Wahl, J., Huson, D.H., Dobney, K., Cooper, A., 2017. Neanderthal behaviour, diet, and disease inferred from ancient DNA in dental calculus. Nature 544, 357–361. doi:10.1038/nature21674

Whiten, A., Hinde, R.A., Laland, K.N., Stringer, C.B., 2011. Culture evolves. Philosophical Transactions of the Royal Society B: Biological Sciences 366, 938–948. doi:10.1098/rstb.2010.0372

Whittmire, C.M., 2002. Vegetative and fire history of the area surrounding Keyhold Pond, Yukon Territory. University of Regina, Saskatchewan.

Whitworth, T.L., Dawson, R.D., Magalon, H., Baudry, E., 2007. DNA barcoding cannot reliably identify species of the blowfly genus Protocalliphora (Diptera: Calliphoridae). Proceedings. Biological sciences / The Royal Society 274, 1731–9. doi:10.1098/rspb.2007.0062

Willerslev, E., Cooper, A., 2005. Ancient DNA. Proceedings of the Royal Society of London Biological Series 272, 3–16.

Willerslev, E., Hansen, A.J., Binladen, J., Brand, T.B., Gilbert, M.T.P., Shapiro, B., Bunce, M., Wiuf, C., Gilichinsky, D.A., Cooper, A., 2003a. Diverse plant and animal genetic records from Holocene and Pleistocene sediments. Science (New York, N.Y.) 300, 791–5. doi:10.1126/science.1084114

Willerslev, E., Hansen, A.J., Binladen, J., Brand, T.B., Gilbert, M.T.P., Shaprio, B., Bunce, M., Wiuf, C., Gilichinsky, D.A., Cooper, A., 2003b. Diverse Plant and Animal Genetic Records from Holocene and Pleistocene Sediments. Science 300, 791–795. doi:10.1126/science.1084114

Willerslev, E., Hansen, A.J., Poinar, H.N., 2004a. Isolation of nucleic acids and cultures from fossil ice and permafrost. Trends in Ecology and Evolution 19, 141–147. doi:10.1016/j.tree.2003.11.010

Willerslev, E., Hansen, A.J., Rønn, R., Brand, T.B., Barnes, I., Wiuf, C., Gilichinsky, D., Mitchell, D., Cooper, A., 2004b. Long-term persistence of bacterial DNA. Current Biology 14, 13–14. doi:10.1016/j.cub.2003.12.012

Willerslev, E., Davison, J., Moora, M., Zobel, M., Coissac, E., Edwards, M.E., Lorenzen, E.D., Vestergard, M., Gussarova, G., Haile, J., Craine, J., Gielly, L., Boessenkool, S., Epp, L.S., Pearman, P.B., Cheddadi, R., Murray, D., Brathen, K.A., Yoccoz, N., Binney, H., Cruaud, C., Wincker, P., Goslar, T., Alsos, I.G., Bellemain, E., Brysting, A.K., Elven, R., Sonstebo, J.H., Murton, J., Sher, A., Rasmussen, M., Ronn, R., Mourier, T., Cooper, A., Austin, J., Moller, P., Froese, D., Zazula, G., Pompanon, F., Rioux, D., Niderkorn, V., Tikhonov, A., Savvinov, G., Roberts, R.G., MacPhee, R.D.E., Gilbert, M.T.P., Kjaer, K.H., Orlando, L., Brochmann, C., Taberlet, P., 2014. Fifty thousand years of Arctic vegetation and megafaunal diet. Nature 506, 47–51. doi:10.1038/nature12921

Wilson, E.O., Bossert, W.H., 1971. A primer of population biology. Sinauer Associates, Inc., Sunderland, Massachusetts.

Winterhalder, B., 1981. Optimal Foraging Strategies and Hunter-Gatherer Research in Anthropology: Theory and Models. In: Smith, E.A., Winterhalder, B. (Eds.), Hunter-Gatherer Foraging Strategies: Ethnographic and Archaeological Analyses. University of Chicago Press, Chicago, pp. 13–56.

Wolbach, W.S., Ballard, J.P., Mayewski, P.A., Parnell, A.C., Cahill, N., Adedeji, V., Bunch, T.E., Domínguez-Vázquez, G., Erlandson, J.M., Firestone, R.B., French, T.A., Howard, G.A., Israde-Alcántara, I., Johnson, J.R., Kimbel, D., Kinzie, C.R., Kurbatov, A., Kletetschka, G., LeCompte, M.A., Mahaney, W.C., Melott, A.L., Mitra, S., Maiorana-Boutilier, A., Moore, C.R., Napier, W.M., Parlier, J., Tankersley, K.B., Thomas, B.C., Wittke, J.H., West, A., Kennett, J.P., Mitra, S., Moore, C.R., Napier, W.M., Parlier, J., Tankersley, K.B., Thomas, B.C., Wittke, J.H., West, A., Kennett, J.P., 2018. Extraordinary Biomass-Burning Episode and Impact Winter Triggered by the Younger Dryas Cosmic Impact ∼12,800 Years Ago. 2. Lake, Marine, and Terrestrial Sediments. Journal of Geology 126, 185–205. doi:10.1086/695703

Worm, B., 2015. A most unusual (super)predator. Science 349, 784–785. doi:10.1126/science.aac8697

Worm, B., Paine, R.T., 2016. Humans as a Hyperkeystone Species. Trends in Ecology and Evolution 31, 600–607. doi:10.1016/j.tree.2016.05.008

Wrangham, R., 2008. Catching Fire: How Cooking Made Us Human. Basic Books.

Wright, J.P., Jones, C.G., 2006. The Concept of Organisms as Ecosystem Engineers Ten Years On: Progress, Limitations, and Challenges. BioScience 56, 203. doi:10.1641/0006-3568(2006)056[0203:TCOOAE]2.0.CO;2

Wright, J.P., Jones, C.G., Flecker, A.S., 2002. An ecosystem engineer, the beaver, increases species richness at the landscape scale. Oecologia 132, 96–101. doi:10.1007/s00442-002-0929-1

Wyatt, K.B., Campos, P.F., Gilbert, M.T.P., Kolokotronis, S.O., Hynes, W.H., DeSalle, R., Daszak, P., MacPhee, R.D.E., Greenwood, A.D., 2008. Historical mammal extinction on Christmas Island (Indian Ocean) correlates with introduced infectious disease. PLoS ONE 3. doi:10.1371/journal.pone.0003602

Wygal, B.T., 2011. Microblade/Non-Microblade Dichotomy: Climatic Implications, Toolkit Variability, and the Role of Tiny Tools in Eastern Beringia. In: Goebel, T., Buvit, I. (Eds.), From the Yenisei to the Yukon: Interpreting Lithic Assemblage Variability in Late Pleistocene/Early Holocene Beringia. Texas A&M University Press, College Station, pp. 234–254.

Wygal, B.T., 2018. The peopling of eastern Beringia and its archaeological complexities. Quaternary International 466, 284–298. doi:10.1016/j.quaint.2016.09.024

Yergeau, E., Hogues, H., Whyte, L.G., Greer, C.W., 2010. The functional potential of high Arctic permafrost revealed by metagenomic sequencing, qPCR and microarray analyses. The ISME Journal 4, 1206–1214. doi:10.1038/ismej.2010.41

Yoccoz, N.G., Bråthen, K.A., Gielly, L., Haile, J., Edwards, M.E., Goslar, T., Stedingk, H. Von, Brysting, A.K., COISSAC, E., Pompanon, F., Sønstebø, J.H., Miquel, C., Valentini, A., Bello, F. De, Chave, J., Thuiller, W., Wincker, P., Cruaud, C., Gavory, F., Rasmussen, M., Gilbert, M.T.P., Orlando, L., Brochmann, C., Willerslev, E., Taberlet, P., 2012. DNA from soil mirrors plant taxonomic and growth form diversity. Molecular Ecology 21, 3647–3655. doi:10.1111/j.1365-294X.2012.05545.x

Young, J.M., Rawlence, N.J., Weyrich, L.S., Cooper, A., 2014. Limitations and recommendations for successful DNA extraction from forensic soil samples: a review. Science & Justice 54, 238–244.

Zalasiewicz, J., Waters, C.N., Williams, M., Summerhayes, C.P., Head, M.J., 2019a. 7.9 The Epilogue and Forward Look for the Anthropocene. In: The Anthropocene as a Geologic Time Unit: A Guide to the Scientific Evidence and Current Debate. Cambridge University Press, Cambridge, U.K., pp. 285–286.

Zalasiewicz, J., Waters, C.N., Williams, M., Summerhayes, C.P. (Eds.), 2019b. The Anthropocene as a Geologic Time Unit: A Guide to the Scientfic Evidence and

Current Debate. Cambridge University Press, Cambridge, U.K.

Zazula, G.D., Froese, D.G., Schweger, C.E., Mathewes, R.W., Beaudoin, A.B., Telka, A.M., Harington, C.R., Westgate, J.A., 2003. Ice-age steppe vegetation in East Beringia. Nature 423, 603. doi:10.1038/423603a

Zazula, G.D., Froese, D.G., Westgate, J.A., Farge, C. La, Mathewes, R.W., 2005. Paleoecology of Beringian "packrat" middens from central Yukon Territory, Canada. Quaternary Research 63, 189–198. doi:10.1016/j.yqres.2004.11.003

Zazula, G.D., Schweger, C.E., Beaudoin, A.B., McCourt, G.H., 2006a. Macrofossil and pollen evidence for full-glacial steppe within an ecological mosaic along the Bluefish River, eastern Beringia. Quaternary International 142–143, 2–19. doi:10.1016/j.quaint.2005.03.010

Zazula, G.D., Froese, D.G., Elias, S.A., Kuzmina, S., Farge, C. La, Reyes, A. V., Sanborn, P.T., Schweger, C.E., Scott Smith, C.A., Mathewes, R.W., 2006b. Vegetation buried under Dawson tephra (25,300 14C years BP) and locally diverse late Pleistocene paleoenvironments of Goldbottom Creek, Yukon, Canada. Palaeogeography, Palaeoclimatology, Palaeoecology 242, 253–286. doi:10.1016/j.palaeo.2006.06.005

Zazula, G.D., Froese, D.G., Elias, S.A., Kuzmina, S., Mathewes, R.W., 2011. Early Wisconsinan (MIS 4) Arctic ground squirrel middens and a squirrel-eye-view of the mammoth-steppe. Quaternary Science Reviews 30, 2220–2237. doi:10.1016/j.quascirev.2010.04.019

Zazula, G.D., MacPhee, R.D.E., Metcalfe, J.Z., Reyes, A. V., Brock, F., Druckenmiller, P.S., Groves, P., Harington, C.R., Hodgins, G.W.L., Kunz, M.L., J Longstaffe, F., Mann, D.H., McDonald, H.G., Nalawade-Chavan, S., Southon, J.R., 2014. American mastodon extirpation in the Arctic and Subarctic predates human colonization and terminal Pleistocene climate change. Proceedings of the National Academy of Sciences of the United States of America 111, 18460–18465. doi:10.1073/pnas.1416072111

Zazula, G.D., MacPhee, R.D.E., Southon, J., Nalawade-Chavan, S., Reyes, A. V., Hewitson, S., Hall, E., 2017a. A case of early Wisconsinan "over-chill": New radiocarbon evidence for early extirpation of western camel (Camelops hesternus) in eastern Beringia. Quaternary Science Reviews 171, 48–57. doi:10.1016/j.quascirev.2017.06.031

Zazula, G.D., Hall, E., Hare, P.G., Thomas, C., Mathewes, R., Farge, C. La, Martel, A.L., Heintzman, P.D., Shapiro, B., 2017b. A middle holocene steppe bison and paleoenvironments from the versleuce meadows, Whitehorse, Yukon, Canada. Canadian Journal of Earth Sciences 54, 1138–1152. doi:10.1139/cjes-2017-0100

Zeckhausera, R., 2017. Human hunters and nonhuman predators: Fundamental differences. Proceedings of the National Academy of Sciences of the United States of America 114, 13–14. doi:10.1073/pnas.1617003114

Zhu, D., Ciais, P., Chang, J., Krinner, G., Peng, S., Viovy, N., Peñuelas, J., Zimov, S., 2018. The large mean body size of mammalian herbivores explains the productivity paradox during the Last Glacial Maximum. Nature Ecology & Evolution. doi:10.1038/s41559-018-0481-y

Zimov, S.A., 2005. Pleistocene park: Return of the mammoth's ecosystem. Science 308, 796–798. doi:10.1126/science.1113442

Zimov, S.A., Zimov, N.A., 2014. Role of megafauna and frozen soil in the atmospheric ch4 dynamics. PLoS ONE 9. doi:10.1371/journal.pone.0093331

Zimov, S.A., Chuprynin, V.I., Oreshko, A.P., Chapin, F.S., Reynolds, J.F., Chapin, M.C., 1995. Steppe-Tundra Transition: A Herbivore-Driven Biome Shift at the End of the Pleistocene. The American Naturalist 146, 765–794.

Zimov, S.A., Zimov, N.S., Tikhonov, A.N., Chapin, I.S., 2012a. Mammoth steppe: A high-productivity phenomenon. Quaternary Science Reviews 57, 26–45. doi:10.1016/j.quascirev.2012.10.005

Zimov, S.A., Zimov, N.A., Chapin, F.S.I., 2012b. The Past and Future of the Mammoth Steppe Ecosystem. In: Paleontology in Ecology and Conservation. pp. 1–7. doi:10.1007/978-3-642-25038-5_1

Zischler, H., Hoss, M., Handt, O., Haeseler, A. Von, Kuyl, A.C. Van der, Goudsmit, J., 1995. Detecting dinosaur dna. Science 268, 1192–1193.